PROBING THE HIV REVERSE-TRANSCRIPTASE ENZYME WITH NOVEL BIFUNCTIONAL HIV-1 RT INHIBITORS OF THE GENERAL FORMULA (NRTI)-SPACER-(NNRTI)

BY

Ebrahim Mohamed

Thesis Presented for the Degree of

DOCTOR OF PHILOSOPHY

In the Department of Chemistry

UNIVERSITY OF CAPE TOWN

March 2009

Supervisor: Professor Roger Hunter

Contents

Declaration

I declare that “Probing the HIV Reverse-Transcriptase enzyme with novel bifunctional HIV-1 RT inhibitors of the general formula (NRTI)-spacer-(NNRTI)” is my own work and that all sources that I have used or quoted have been indicated and acknowledged by means of complete references.

_____

Ebrahim Mohamed

Abstract

The high levels of resistance elicited by both nucleoside (NRTI) and non-nucleoside (NNRTI) reverse transcriptase inhibitors have prompted the design of double-drugs combining these two entities with the aim of addressing the emergence of resistance as well as searching for synergism between the two drug target sites on HIV reverse transcriptase (RT). The strategy involves combining two different inhibitors into a single chemical entity *via* a linker, with the aim of developing a mixed-site inhibitor combining the inhibitory actions of each drug.

This thesis describes the rational drug-design and synthesis of nine bifunctional drugs combining a nucleos(t)ide and a non-nucleoside reverse transcriptase inhibitor linked *via* different non-cleavable spacers. The C-5 position of the nucleos(t)ide portion of the bifunctional was used for attachment of the spacer throughout. However, the site of attachment on the non-nucleoside drug varies according to the inhibitor type.

Chapter Two describes the first series involving the synthesis of bifunctional HIV-drugs using d4U as the NRTI and UC-781 as the NNRTI. This resulted in two unthiated UC-781/d4U entities being synthesized in a convergent manner in 16 steps for the pentane-propyne target and 20 steps for the target bearing PEG-propyne units using Sonogashira coupling methodology as a key step.

Chapter Three describes the second series incorporating a new NNRTI in the form of 2- and 4-pyrimidinylarylamine motifs. Key features in this chapter include the synthesis of tri-substituted anilines, the library generation of 2- and 4-pyrimidinylarylamine derivatives as model NNRTIs, as well as Sonogashira coupling reactions to obtain three bifunctional targets.

The final part of this thesis describes the synthesis of a remarkable d4U/TMC120 bifunctional system, synthesized on the basis of molecular modeling. Biological results indicate that the d4U-4-PEG-TMC120 bifunctional has the lowest EC_{50} anti-HIV activity of any NRTI-spacer-NNRTI bifunctional inhibitor synthesized to date. The NRTI was also triphosphorylated and the product evaluated in an *in vitro* RT inhibition assay, which culminated in a ‘proof of principle’ of synergy existing between the substrate site and the allosteric binding pocket. Also presented, is work carried out to change the rigid d4U to a more flexible acyclic nucleotide phosphonate in a pronucleotide approach. A range of conclusions on the work are presented at the end.

Acknowledgements

I would like to thank the following people for their contribution to the preparation of this thesis:

My supervisor, Professor Roger Hunter for his guidance, enthusiasm and patience throughout the course of my PhD studies.

Professors Karen Anderson and William Jorgensen (Yale University, USA) for their assistance in the biological activity experiments and the molecular modelling, not forgetting all the useful discussions and suggestions.

Associate Professor David W. Gammon and Dr Eugene Sickle for their helpful discussions.

Colleagues past and present in the Hunter/Gammon/Sickle Organic research groups, Dr Gareth Arnott, Dr Philip Richards, Dr Theophilus Mudzunga, Dr Seanette Wilson, Dr Clare Muhanji, Dr Nashia Stellenboom, Dr Sophie Rees-Jones, Dr Hayley Haupt, Dr Henok Kinfe, Dr Vincent Zishiri, Dr Rajinder Singh, Dr Ian Hale, Dr Pieter Levecque, Yassir Younis, Ana Andrijevic, Myles Smith, Thozama Qwebani, Rudy Cozett, Aklilu Kidane, Dawid van der Merwe, Devendren Patten, Mlandzeni Boyce and Scebi Mkhize.

Noel Hendricks, Pete Roberts, Tommie van der Merwe (Mass spectrometry service, University of Witwatersrand) and Dr Marietjie Stander (Mass spectrometry service, Stellenbosch University) for their analytical services.

The National Research Foundation (NRF) and the Equity Development Program (EDP, University of Cape Town) for their financial support.

My parents, Sayed and Zubeira Mohamed, and my siblings (Kashief and Fazlin) for their constant love and encouragement during the course of this PhD. This thesis is dedicated to them.

Last but not least, my wife, Madeniah - shukran for all your constant support.

Abbreviations

ABC	(1*S*,4*R*)-4-[2-Amino-6-(cyclopropyl-amino)-9*H*-purin-9-yl]-2-cyclopentene-1-methanol succinate
AcBr	Acetyl bromide
AcOH	Acetic acid
AIDS	Acquired Immunodeficiency Syndrome
Amino Acids	A, Alanine; C, Cysteine; D, Aspartate; E, Glutamate; F, Phenylalanine; G, Glycine; H, Histidine; I, Isoleucine; K, Lysine; L, Leucine; M, Methionine; N, Asparagine; P, Proline; Q, Glutamine; R, Arginine; S, Serine; T, Threonine; V, Valine; W, Tryptophan; Y, Tyrosine
APY	Arylpyrimidine
α-APA	α-(2,6-Dichlorophenyl)-α-(2-acetyl-5-methylanilino)acetamide
APTS	8-Aminopyrene-1,3,6-trisulfonate
aq.	Aqueous
Ar	Aromatic
AZT	3'-Azido-2',3'-dideoxythymidine
B**:**	Generic base
BnBr	Benzyl bromide
Boc	*tert*-Butyl carbonate
BOP	Benzotriazol-1-yloxy-tris(dimethylamino)phosphonium hexafluoro phosphate
br	Broad
brs	Broad singlet
Bu_3SnH	Tributyltin hydride
$BuNH_2$	Butylamine
t-BuOK	Potassium *tert*-butoxide
BVDU	Bromovinyldeoxyuridine
CAN	Ceric ammonium nitrate
cat.	Catalytic
CD4	Cluster of differentiation 4
cDNA	Complemetary deoxynucleic acid
CF_3COOH	Trifluoroacetic acid
CH_2Cl_2	Dichloromethane / Methylene chloride

CH_3CN	Acetonitrile
CS_2	Carbondisulfide
δ	Chemical shift in ppm
d	Doublet
dd	Doublet of doublets
dt	Doublet of triplets
d_2U	2',3'-Dideoxyuridine
d_4T	2',3'-Didehydro-2',3'-dideoxythymidine
d_4U	2',3'-Didehydro-2',3'-dideoxyuridine
DABO	Dihydroalkoxybenzyloxopyrimidine
DAPY	Diarylpyrimidine
DATA	Diaryltriazine
DBU	1,8-Diazabicyclo[5.4.0]undec-7-ene
DCC	1,3-Dicyclohexylcarbodiimide
DCE	Dichloroethane
dCTP	Deoxycytidine triphosphate
ddC	2',3'-Dideoxycytidine
ddI	2',3'-Dideoxyinosine
Delavirdine	1-(5-Methanesulfonamido-1*H*-indol-2-yl-carbonyl)-4-[3-(1-methylethyl-amino)pyridinyl]piperazine monomethane sulfonate
DIA	(Diisopropylamino)phosphine
DIAD	Diisopropylazodicarboxylate
DIEA	Diisopropylethylamine
DMA	*N,N*-Dimethylacetamide
DMAP	*N,N*-Dimethylaminopyridine
DME	1,2-Dimethoxyethane
DMP	2,2-Dimethoxypropane
DMSO	Dimethylsulfoxide
DNA	Deoxyribonucleic acid
dGTP	Deoxyguanidine triphosphate
dNMP	Deoxyribonucleotide monophosphate
dNTP	Deoxyribonucleotide triphosphate
dsDNA	Double-stranded deoxyribonucleic acid
dTTP	Deoxythymidine triphosphate
EDC	Ethylene dichloride

Efavirenz	(-)-6-Chloro-4-cyclopropylethynyl-4-trifluoromethyl-1,4-dihydro-2*H*-3,1-benzoxazin-2-one
E1	Unimolecular elimination
E2	Bimolecular elimination
EDTA	Ethylenediaminetetraacetate monosodium
EI	Electron impact
Enfuvirtide	36-amino acid peptide
ES	Electron spray
Et_3N	Triethylamine
Et_2O	Diethyl ether
EtOAc	Ethyl acetate
EtOH	Ethanol
eq.	Equivalent
FAB	Fast atom bombardment
FDA	US Food and Drug Administration
FDU	5-Fluoro-2'-deoxyuridine
(-)-FTC	(-)-β-L-3'-thia-2',3'-dideoxy-5-fluorocytidine
(+)-FTC	(+)-β-D-3'-thia-2',3'-dideoxy-5-fluorocytidine
g	Grams
GALT	Gastrointestinal associated lymphoid tissue
gp	Glycoprotein
GR	Glutathion reductase
HAART	Highly active anti-retroviral therapy
HBY 097	(*S*)-4-Isopropoxycarbonyl-6-methoxy-3-(methylthiomethyl)-3,4-dihydroquinoxaline-2(1*H*)-thione
HCl	Hydrochloric acid
HCMV	Cytomegalovirus
HEPT	1-[(2-Hydroxyethoxy)methyl]-6-(phenylthio)thymine
HI-236	*N'*-(5-bromo-2-pyridyl)-*N*-[2-(2,5-dimethoxyphenyl)ethyl]thiourea
HIV-1	Human Immunodeficiency Virus type 1
HOPT	1-Hydroxybenzotriazole
HPLC	High-pressure liquid chromatography
hr.	Hour
HRMS	High-resolution mass spectrometry
Hz	Hertz

IDU	5-Iodo-2'-deoxyuridine (Idoxuridine)
IN	Integrase
IR	Infrared spectrometry
ITU	Imidoylthiourea
J	Coupling constant
LAH	Lithium aluminium hydride
Lit.	Literature
LTR	Long terminal repeat
m	Meta
m	Multiplet
M^+	Molecular ion
MA	HIV-1 matrix protein
MeOH	Methanol
mg	Milligram(s)
MHz	Mega hertz
MKC-442	6-Benzyl-1-(ethoxymethyl)-5-isopropyluracil
ml	Millilitre(s)
mmol	Millimole(s)
Mp	Melting point
mRNA	Messenger ribonucleic acid
MsCl	Methanesulfonyl chloride
m/z	Mass to charge ratio
NBS	*N*-Bromosuccinamide
NCp	Nucleocapsid protein
NEM	Nucleotide excision mechanism
Nevirapine	11-Cyclopropyl-5,11-dihydro-4-methyl-6*H*-dipyrido(3,2-b:2',3'-f)(1,4)diazepin-6-one
NMM	*N*-Methylmorpholine
NMR	Nuclear magnetic resonance
NNIBP	Non-nucleoside inhibitor binding pocket
NNIBS	Non-nucleoside inhibitor binding site
NNRTI	Non-nucleoside reverse transcriptase inhibitor
NNRTI-BP	Non-nucleoside reverse transcriptase inhibitor binding pocket
NRTI	Nucleoside reverse transcriptase inhibitor
o	Ortho

p	Para
PBS	Primer binding site
PG	Protecting group
$P(OEt)_3$	Triethyl phosphite
Pd/C	Palladium-on-carbon
Pet ether	Petroleum ether
PETT	Phenylethylthiazolylthiourea
PFA	Phosphonoformate
Phospho	Phosphonate
PI	Protease inhibitor
PLM (II)	Plasmepsin (II)
PMBCl	*p*-Methoxybenzyl chloride
PMEA	9-(2-phosphonylmethoxyethyl)adenine
PMPA	(*R*)-9-(2-Phosphonylmethoxypropyl)adenine
PPh_3	Triphenylphosphine
$(PPh_3)_4P$	Tetrakis(triphenylphosphine)palladium (0)
PQ	Primaquine
PR	Protease
RDDP	RNA-dependent DNA polymerase
Ribavirin	1-β-D-Ribofuranosyl-1*H*-1,2,4-triazole-3-carboxamide
RNA	Ribonucleic acid
RNase H	Ribonuclease H
RT	Reverse transcriptase
rt	Room temperature
s	Singlet
SATE	*S*-Acyl-2-thioethyl
S_N1	Unimolecular nucleophilic substitution
S_N2	Bimolecular nucleophilic substitution
ssRNA	Single-stranded ribonucleic acid
t	Triplet
TBDMSCl	*tert*-Butyldimethylsilyl chloride
TBDPS	*tert*-Butyldiphenylsilyl chloride
3TC	(-)-β-L-3'-Thia-2',3'-dideoxycytidine
td	Triplet of doublets

TFA	Trifluoroacetic acid
TFT	5-Trifluoromethyl-2'-deoxyuridine (Trifluorothymidine or Trifluridine)
THF	Tetrahydrofuran
THP	Tetrahydropyran
TIBO	(+)-(*S*)-4,5,6,7-Tetrahydro-8-chloro-5-methyl-6-(3-methyl-2-butenyl)imidazo[4,5,1jk][1,4]benzodiazepine-2(1*H*)-thione
TIPS	Triisopropylsilyl
TLC	Thin layer chromatography
TMSCl	Trimethylsilyl chloride
TSAO	2',5'-bis-*O*-(*tert*-Butyldimethylsilyl)-3'-spiro-5'-(4''-amino-1'',2''-oxathiole-2'',2''-dioxide)pyrimidine
p-TsOH	*para*-Toluenesulfonic acid
q	Quartet
UV	Ultra violet
w/v	Weight by volume
v/v	Volume by volume

INTRODUCTION

1.1 HUMAN IMMUNODEFICIENCY VIRUS (HIV)

The Human Immunodeficiency Virus (HIV) is an intracellular parasite, belonging to a class of viruses called retroviruses (viral family *Retroviridae*), and is the causative agent of Acquired Immunodeficiency Syndrome (AIDS). Retroviruses are ribonucleic acid (RNA) viruses, and in order to replicate they must make a deoxyribonucleic acid (DNA) copy of their RNA. It is the DNA genes that allow the virus to replicate. HIV exists as two distinct viruses: type-1 (HIV-1) and type-2 (HIV-2), which both have a similar molecular structure in that they contain a single-stranded RNA genome but which differ in origin and gene sequence. The difference between them is that HIV-1 carries a *vpu* gene whereas HIV-2 carries the *vpx* gene, and HIV-2 is more geographically restricted to West Africa compared to HIV-1. HIV-2 also tends to have slower rates of disease progression to AIDS than HIV-1, although when this occurs the symptoms are almost indistinguishable between the two types.[1,2]

1.2 THE STRUCTURE OF THE HIV-1 VIRION

The structure of HIV-1 involves outer and inner cores. The outer core consists of a lipid bilayer acquired from the host cell, while the inner core contains two proteins, p24 and p17, as matrix proteins surrounding the nucleocapsid containing the genetic material. A single virion has an icosahedral shape with a knobby-looking envelope. The knobs are comprised of the envelope glycoproteins gp-120 and gp-41. Beneath the envelope are the viral matrix proteins p17 and p24, which, aside from structural maintenance, houses the nucleocapsid containing the viral genome for transmission to the host nucleus. The HIV genome transcribes nine genes: *gag*, *pol*, *env*, *tat*, *rev*, *nef*, *vif*, *vpu* and *vpr*, which carry all the information needed to make new viruses (Fig. 1.1).[3,4]

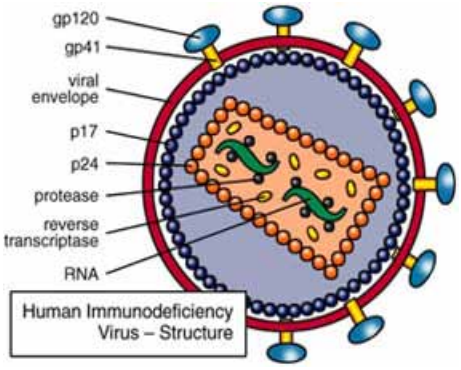

Figure 1.1 Structure of a HIV-1 virion.[5]

Copies of reverse transcriptase (RT), integrase (IN), and protease (PR) necessary for replication purposes are also housed together with the HIV viral RNA.

1.3 EPIDEMIOLOGY OF HIV/AIDS

According to statistics released by UNAIDS and WHO for July 2008, every day, over 6800 people become infected with HIV and over 5700 people die from AIDS. The estimated number of people having died from HIV/AIDS-related illnesses is around 2.1 million per annum for 2007. The annual number of new HIV infections (for 2008) stands at around 2.5 million, while the total number of people estimated to be living with HIV/AIDS is approximately 33.2 million [30.6-36.1 million]. Sub-Saharan Africa presents itself as the region most heavily affected by HIV with 22.0 million people living with HIV (Fig 1.2), accounting for 67% of all people living with HIV and 75% of global AIDS deaths. Of these, an estimated 5.7 million of these people live in South Africa.[6]

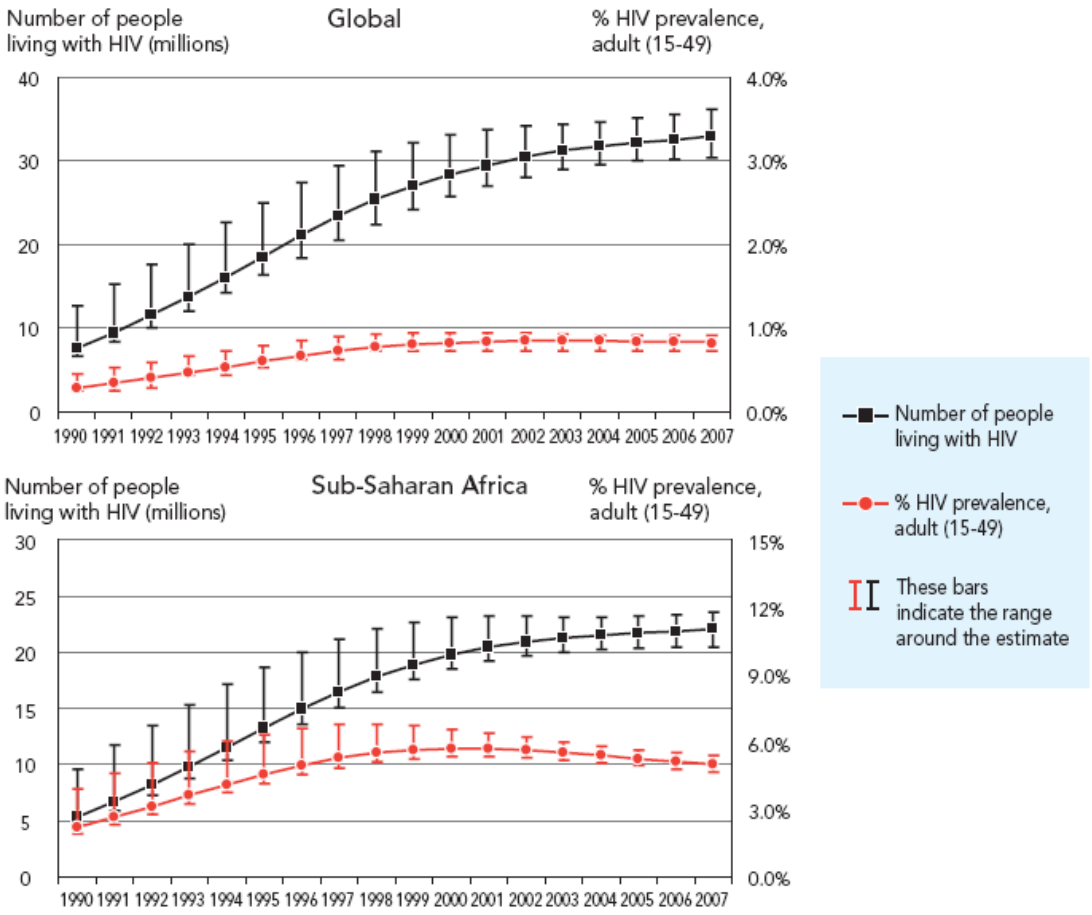

Figure 1.2 Estimated number of people living with HIV and adult HIV prevalence. Global HIV epidemic, 1990-2007, and HIV epidemic in Sub-Saharan Africa, 1990-2007 (2008 report on the global AIDS Epidemic).[6]

1.4 THE HIV LIFE-CYCLE

Like all viruses, HIV-1 needs a host-cell to proliferate itself, which it uses for replication, Figure 1.3.

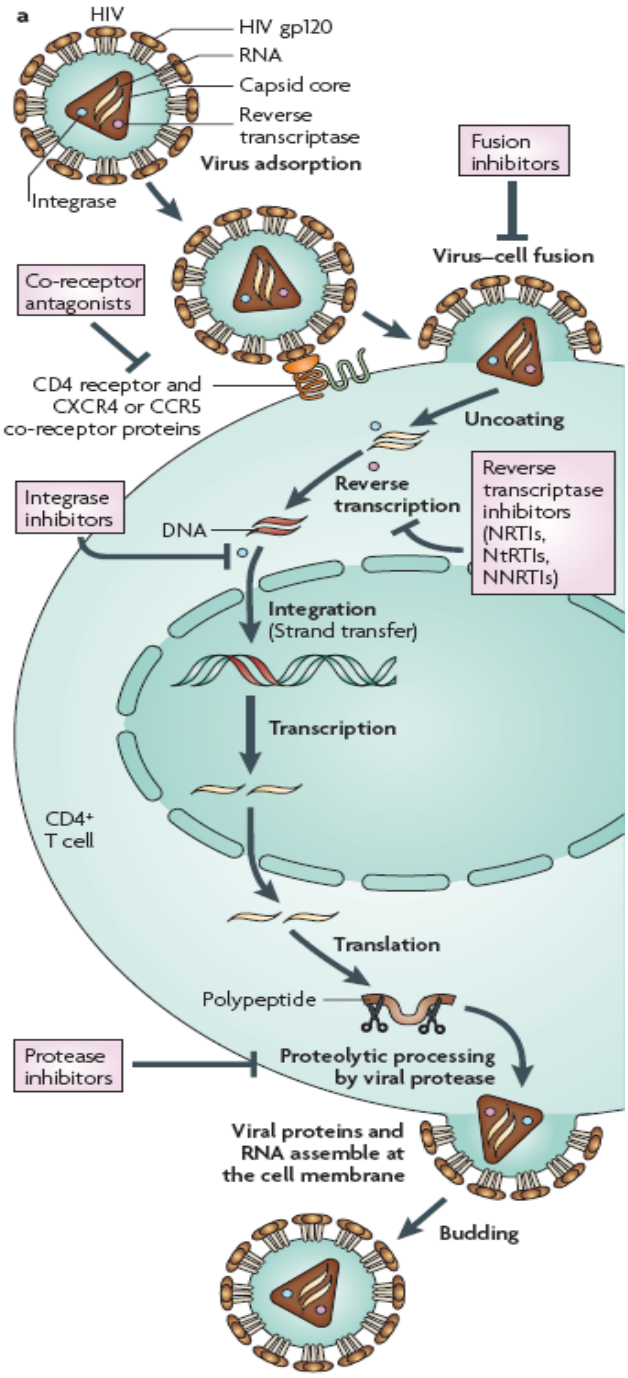

Figure 1.3 The Life-cycle of the HIV-1 virus.[7]

However, what differentiates HIV from other viruses and what makes it so lethal, is that HIV mostly infects cells of the immune system. HIV-1 will only infect a human cell that bears a CD4 surface marker.[8] Such cells include macrophages, some dendritic cells, and most importantly, CD4+ T-lymphocytes, also referred to as "T-helper cells", which play an important role in the body's immune-defence when foreign entities invade the body. HIV-1 entry into CD4+ cells involves several sequential steps (Fig. 1.4) that involve firstly the interaction of the HIV receptor gp-120 with the host CD4 receptor. This gp-120/CD4 complex leads to a loss of entropy (i.e. ordering) in gp-120, which is counteracted by a large enthalpy of formation (ΔH < 0). This interaction leads to conformational changes in gp-120, and to a lesser extent CD4, that enable the interaction of gp-120 with the CCR5 or CXCR4 co-receptor. Subsequently, the formation of a CD4-gp-120-CCR5/CXCR4 complex triggers conformational changes in the gp-41 that eventually allows fusion between the cellular and viral membranes leading to the viral core into the cytoplasm.[9,10,11,12]

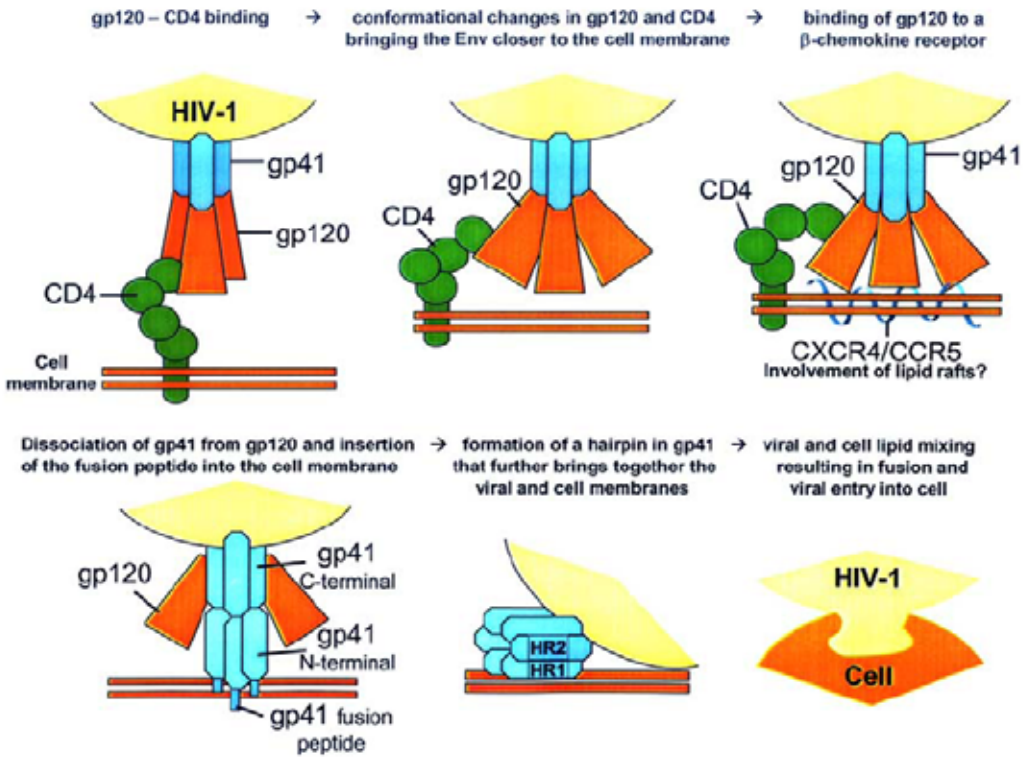

Figure 1.4 HIV-1 attachment and fusion to CD4+ cell.[12]

Viral entry thus involves the following three distinct steps: CD4 binding, chemokine receptor engagement and the structural changes in the viral envelope required for fusion between viral and cellular membranes. HIV-1 entry inhibitors thus encompass three mechanistically distinct classes of agents known as attachment inhibitors (PRO-452, PRO-2000), co-receptor inhibitors

such as Maraviroc™ (Met-RANTES, T-22, T-134), and the fusion inhibitor Fuzeon™ (Enfuvirtide, T-20).[14] Once the HIV nucleocapsid enters the cell (Fig. 1.3), partial uncoating of the viral core occurs to release the genetic material of the virus into the host cell cytoplasm, where the viral enzyme reverse transcriptase (RT) transforms the ssRNA genome to a dsDNA form.[14] RT promotes (catalyses) three types of reactions: RNA-directed DNA synthesis, DNA-directed DNA synthesis both of which are carried out by the polymerase moiety of RT, and RNA hydrolysis directed by ribonuclease (RNase H). The dsDNA is subsequently transported into the cell nucleus, where another virion-associated enzyme, HIV integrase, catalyses the integration of the viral DNA into the host-cell genome. Importantly though, the viral DNA lies dormant until called upon to transcribe, when, transcription of the integrated viral DNA leads to the production of genomic messenger RNA (mRNA) molecules that are transported back to the cell cytoplasm, where translation takes place leading to the production of Gag and Gag-Pol proteins. Immature Gag and fused Gag-Pol precursor are transported to the cell membrane, where viral progeny begin assembling and "budding" from the infected cells. Viral particles released following budding, however, do not contain the characteristic HIV condensed core and are not infectious. Virus infectivity is acquired after particle maturation, which is mediated by the virion-associated HIV aspartyl protease. This enzyme cleaves the immature Gag and Gag-Pol precursors into functional polypeptides.[15]

1.5 HIV PATHOGENESIS

AIDS results from selective depletion of CD4+ helper T-lymphocytes.[16a,b] Progressive CD4 cell depletion has been identified as the fundamental basis of AIDS, but the specific mechanism by which this cell death occurs is still not well understood. It is well accepted that in chronic disease less than 15% of all CD4 cells are infected. The proportional loss of CD4 cells in AIDS far exceeds this prevalence of cell infection, implying that a direct cytopathic effect of the virus cannot be the sole explanation of CD4 cell depletion. In recent years, it has been shown that during acute infection there is massive depletion of CD4 cells in the gastrointestinal associated lymphoid tissue (GALT) and other mucosal tissues. Importantly, CD4 cell depletion in these tissues appears to be significantly greater than that observed in peripheral blood.[16b]

The function of CD4 cells is to help CD8+ cytotoxic T-lymphocytes to destroy other cells that express foreign antigens and also to enhance antibody production by B-lymphocytes. Thus, CD4 cells represent a key component of the immune system. In a healthy individual, about 1200 CD4 cells circulate per µL blood; when CD4 counts drop below 400/ µL, opportunistic infections start to occur.[2] HIV eventually kills the helper T-cell that are vital for the immune system, and the decline in CD4+ T-cells eventually has a great effect on humoral response functions, specifically

the functioning of the B-cells. Helper T-cell depletion inhibits the B-cells from differentiating into plasma cells and memory cells, thus impairing the immune system's ability to fight against foreign antigens that have entered the body.[17] A person with a CD4 level below 200/ µL defines a state of AIDS.

1.6 THE REVERSE TRANSCRIPTASE ENZYME (RT)

HIV reverse transcriptase (RT) is a multifunctional enzyme (Fig. 1.5) responsible for catalytic transformation of single-stranded viral RNA into double-stranded DNA (dsDNA) that in turn gets integrated into host cell chromosomes by integrase.[18] In summary again, HIV-1 RT carries out reverse transcription by the following catalytic activities:

(i) RNA-dependent DNA polymerization to form an RNA-DNA hybrid.

(ii) RNase H degradation of the RNA strand from RNA-DNA hybrid.

(iii) DNA-dependent DNA polymerization to form a dsDNA.

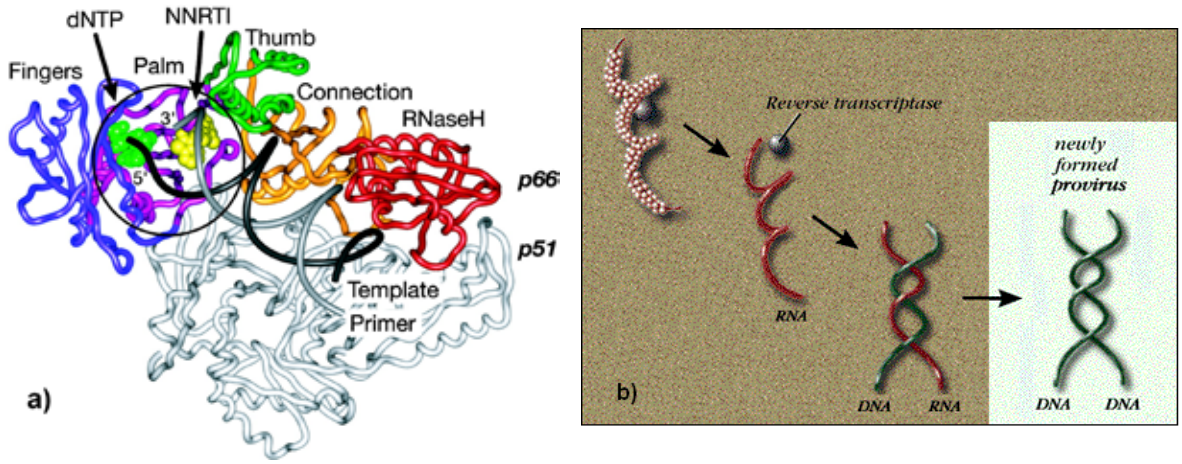

Figure 1.5 (a) Structure of the HIV-1 reverse transcriptase enzyme adapted from Pata *et al.*[19] (b) RNA-directed followed by DNA-directed synthesis.[18]

From a structural point of view, HIV-1 RT is a heterodimer consisting of two subunits: a 66 kDa one and a 51 kDa one (p66 and p51). The p66 subunit contains an N-terminal polymerase domain and a C-terminal RNase H domain. The p51 subunit is derived either from p66 or from a large gag-pol precursor by proteolytic cleavage with HIV-1 protease, and has the same amino acid sequence as the polymerase domain of p66. Crystal structures of RT have revealed the part of the p66 subunit responsible for transcription to resemble a right hand with fingers, palm, thumb, and connection subdomains. The p66 palm contains the polymerase active side that is defined by Asp110, Asp185, and Asp186 residues located in the β9-β10 sheet. These amino acids bind the divalent magnesium cations required for catalysis (more details later).[20,21,22]

The primary function of reverse transcriptase is to build a DNA strand from an RNA template, which is performed at the polymerase active site of the p66 subunit. This process is complex and requires the concerted function of two enzyme active sites in RT (Fig.1.6). Reverse transcription is initiated at the 3'-end of a cellular lysyl-tRNA^{Lys,3}, hybridized to the primer binding site (PBS) of the HIV RNA genome, by the RNA-primed RNA-dependent DNA polymerase activity (RDDP) of RT. This elongates to produce viral DNA until the 5'-end of the HIV-1 RNA is reached (Fig. 1.6, Step 1). The product formed from this reaction is termed the minus strand strong-stop DNA. RT ribonuclease H (RNase H) activity then hydrolyzes the HIV genomic RNA (step 2), to allow the nascent DNA to hybridize with the repeat sequence (R) at the 3'-end of the HIV genomic RNA (step 3). After this strand transfer, the nascent DNA strand is further elongated by RT DNA-primed RDDP activity. RNase H activity is again required to hydrolyze the rest of genome RNA except for a purine rich sequence, termed the polypurine tract (PPT), which serves as a primer for the initiation of second strand DNA synthesis (step 5). RNA-primed DNA-dependent DNA polymerase activity (DDDP) then elongates the PPT primer (step 6). Removal of the PPT and tRNA primers by RT RNase H activity (step 7) then allows second strand transfer to take place by interaction of the complementary PBS sequences (step 8).

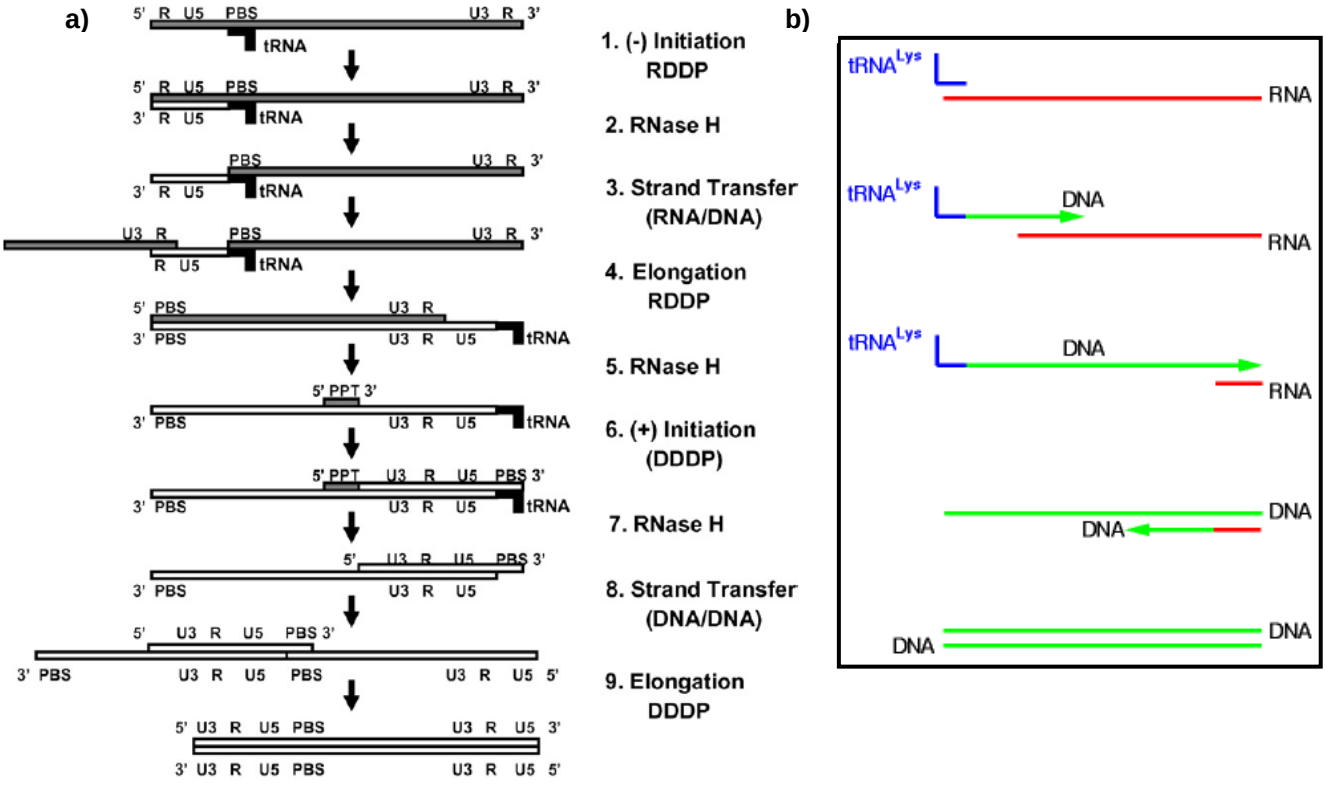

Figure 1.6 a) HIV reverse transcription mediated by the DNA polymerase, RNase H and the transfer activities of the viral RT.[22] b) Simplification of the transcription process.

HIV-1 RT DNA-primed DDDP activity including strand-displacement activity completes the synthesis of the double-strand proviral DNA precursor.

The final product of the complete reaction carries U3-R-U5 long terminal repeats (LTR) at both ends (step 9).[22] As a result, the reverse transcriptase enzyme has played a key role in the HIV-1 life-cycle, making it a primary target for development of new anti-HIV drugs used in the treatment of HIV/AIDS.[14,23]

1.7 DEVELOPMENTS IN ANTI-HIV CHEMOTHERAPY

With the onslaught of drug-resistant mutations, combination therapy comprising of at least three anti-HIV drugs, has become the standard treatment of HIV-infected patients.[23] Drugs used in Highly Active Anti-retroviral Therapy (HAART) fall into one of three categories: (i) nucleoside/nucleotide reverse transcriptase inhibitors (NRTIs), that following two phosphorylation steps (i.e. acyclic nucleotide phosphonates) or three phosphorylation steps (for nucleosides) act as chain terminators at the substrate binding site (Fig. 1.7) of RT; (ii) non-nucleoside RT inhibitors (NNRTIs) that are able to interact with reverse transcriptase at an allosteric, non-substrate binding site; and (iii) protease inhibitors (PIs) that inhibit the virus-associated protease.[23] Other clinically approved drugs include the fusion inhibitor Fuzeon, the integrase inhibitor Raltegravir and the CCR5 antagonist Maraviroc. Generally, drug combinations involve two NRTI's plus one NNRTI, or two NRTI's and one PI. Protease inhibitors will not be dealt with in any further detail.

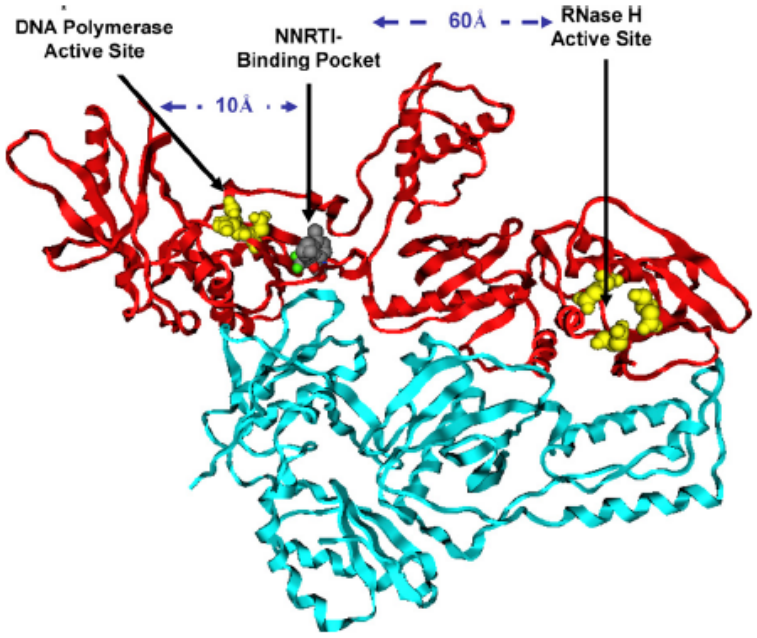

Figure 1.7 Ribbon representation of HIV-1 RT in complex with efavirenz. The p66 and p51 domains of RT is highlighted in red in blue respectively. The DNA active site and the RNase H active site is higglighted with yellow spheres.[22]

Recent studies have shown that the combination therapy of NRTIs, NNRTIs and PIs are able to significantly reduce the viral load, increase CD4 count, decrease mortality and delay disease progression.[23] This type of therapy has been shown to work particularly well in AIDS patients with advanced immune suppression.[24] In addition, there has been found to be a significant benefit in early aggressive anti-HIV chemotherapy, especially in patients showing no symptoms of the disease (asymptotic stage).[25] HAART is able to partially restore the immune system in patients with advanced HIV infection, but also exacerbates cryptococcal meningitis.[26] Thus, HAART has profound repercussions on various AIDS-associated diseases.

Therefore, almost all current HIV-drug candidates, either in preclinical or advanced clinical development, target well-defined steps in the HIV replicative life cycle. These drugs fall into categories associated with the life cycle such as (i) viral adsorption (gp-120) inhibitors; (ii) viral co-receptor antagonists; (iii) viral fusion (gp-41) inhibitors; (iv) nucleocapsid protein (NCp7) Zn finger-targeted agents; (v) reverse transcriptase and integrase inhibitors; (vi) transcription (transactivation) inhibitors and (vii) HIV protease inhibitors.[23]

The inhibitors that lie at the core of this project are the *reverse transcriptase inhibitors*.

1.8 NUCLEOSIDE REVERSE TRANSCRIPTASE INHIBITORS (NRTIs)

The substrate (dNTP) binding site of HIV-1 reverse transcriptase is the obvious target for a large variety of NRTI analogues,[23] and the HIV-1 binding site has been targeted for many years now as an efficient way of combatting HIV. In 1987, zidovudine (AZT), a nucleoside RT inhibitor (NRTI), was approved in the USA as the first chemotherapeutic agent against HIV/AIDS.[23] However, resistance to anti-HIV compounds develops rapidly, sometimes within a few days of initiating treatment. Errors made by the viral enzyme RT and cellular RNA polymerase II result in about one mutation per viral replication (1 base change in 10 000 RNA nucleotides), which, together with the rapid replication of the virus, is responsible for rapid emergence of drug resistant mutants. This problem led many in pursuit of developing other NRTIs, and over 21 years of research has culminated in seven US Food and Drug Administration (FDA) approved NRTIs. Examples of such NRTIs are zidovudine[27] (AZT, 1987), didanosine[28] (ddI, 1991), zalcitabine[29] (ddC, 1992), stavudine[30] (d4T, 1994), lamivudine[31] (3TC, 1995), abacavir[32] (ABC, 1998) and emtricitabine[33] (racemic FTC, 2000) all of which are FDA clinically approved drugs (Fig. 1.8).

These NRTIs are pro-drugs and need to firstly be phosphorylated by cell-derived kinases to their 5'-triphosphate forms, before they can halt the chain propagation step at the reverse transcriptase level as illustrated in Figure 1.9. The active metabolites then act as competitive

inhibitors (alternative substrates) with respect to the normal substrates (dATP, dGTP, dCTP or dTTP), and lead to the termination of chain elongation.[23]

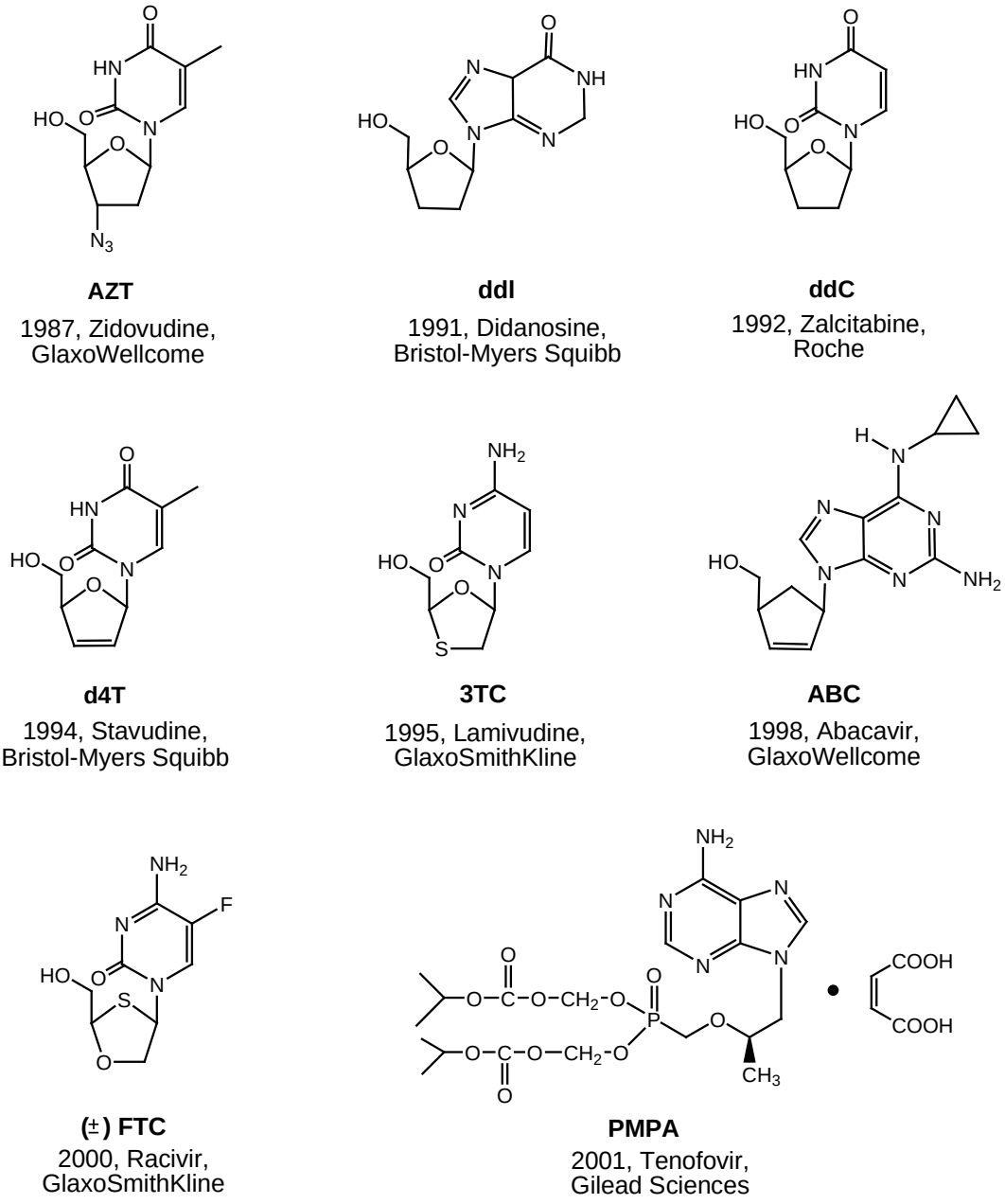

Figure 1.8 Nucleoside reverse transcriptase inhibitors and Tenofovir (PMPA).

D4T shows selective anti-HIV activity comparable to that of AZT *in vitro*. However, d4T is more toxic overall and less inhibitory to mitochondrial DNA replication than AZT.[34a] Together with the early PI's, d4T is known to promote severe lipoatrophy and other body composition changes associated with antiretroviral therapy. However, there is some evidence that reducing or stopping the drug can slow or halt the changes in body composition and metabolism. Lowering

the dose of d4T has also been shown to help to alleviate peripheral neuropathy, another side effect of the drug. The World Health Organization recommended in 2007 that d4T dosing should be reduced to 30mg twice a day in order to counter toxicity. [34b]

It has also been shown that under physiological conditions, RT can remove these chain-terminators, thus unblocking the primer terminus with great efficiency and thus restoring DNA synthesis and viral replication.[35]

In contrast to the nucleoside analogues, the nucleotide analogues (NtRTIs), e.g. PMPA, are mono-phosphorylated pro-drugs in the form of phosphonates (Fig. 1.8), and thus only require a further two phosphorylation steps by cellular kinases in order to be transformed into the active metabolite. NtRTIs can therefore by-pass the nucleoside-kinase reaction, the latter being well documented as generally the rate-determining step en route to the active triphosphate resulting in limitation of the activity of the dideoxynucleoside analogues.[7] An included bonus is that the phosphonate, unlike the phosphate, cannot be cleaved by phosphatases that would normally convert nucleoside monophosphates back to their parent nucleoside.

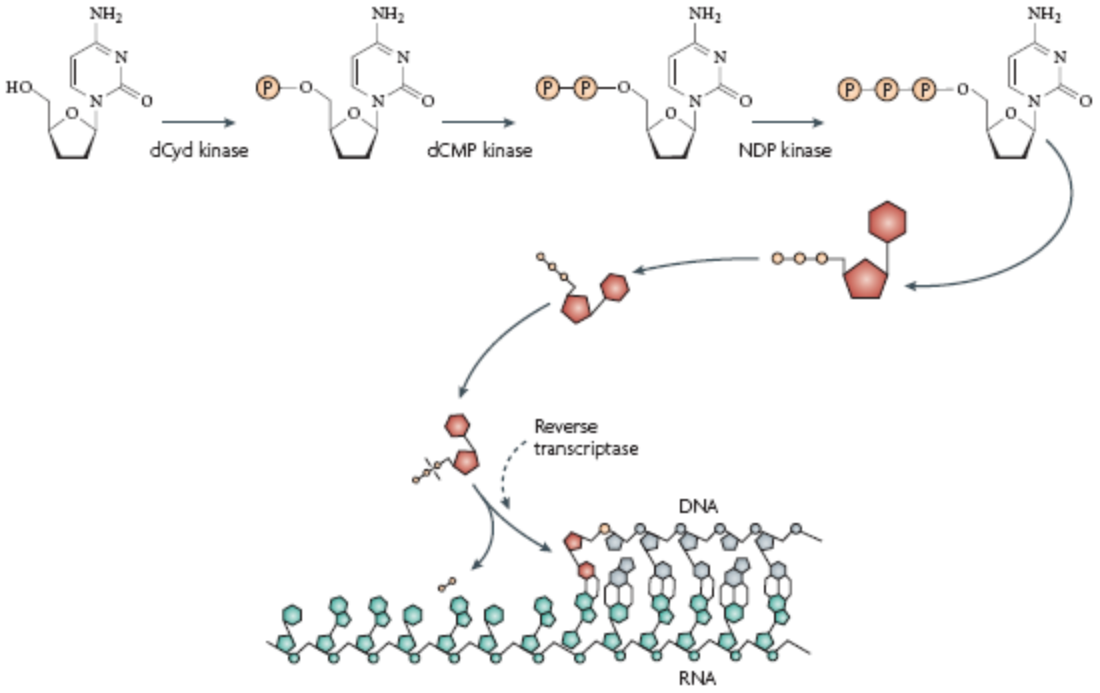

Figure 1.9 Mechanism of anti-HIV action of 2', 3'-deoxynucleoside analogues- shown for 2,3'-dideoxycytidine.[7]

Tenofovir[36], which is FDA clinically approved, has proven to be antivirally active and has showed favourable activity/resistance profiles. It is currently the only approved NtRTI for treatment in HIV

chemotherapy. It is scarcely affected by HIV-1 RT mutations while at the same time retains its full potency as an antiretroviral.

At present, the existing drugs still find it remarkably difficult to comply with the ever- increasing demands of higher activity (potency), lower toxicity (side-effects) and favorable resistance profiles required for anti-HIV drugs. As a result, several new NRTIs are in clinical development.[37] Racivir, also known as (±) FTC, is one such inhibitor. Its mechanism of action is precisely the same as that of zidovudine[38], in that after successful phosphorylation to the active metabolite, the ddNTP competes with the normal substrates. Upon expulsion of the β, γ-diphosphate following nucleophilic substitution by the HIV DNA 3'-hydroxyl (attached to the primer terminus) with an incoming ddNTP, ddNMP is incorporated at the 3'-end of the DNA chain, leading to chain termination since the decoy inhibitor does not possess the necessary 3'-hydroxyl functionality for further elongation (Fig. 1.9). Racivir comprises a 50:50 racemic mixture of two enantiomers[39a] and is thus considered a form of combination therapy in which (-)-FTC is moderately more potent than (+)-FTC.[39b] Pharmacokinetic studies carried out by Anderson and co-workers[39b] revealed that compared to the (+)-isomer, (-)-FTC is more efficiently taken up into the cell and phosphorylated to its active triphosphate form. Also, by serving as a much poorer substrate of cytidine deaminase than the (+)-isomer, (-)-FTC is not degraded back to its parent nucleoside. FTC has also shown diminished resistance profiles.

Further successes have come in the form of NtRTI prodrugs. [40,41, 42] Attempts have been made to synthesize 2', 3'-dideoxynucleotide (ddNMP) prodrugs, as well as other forms of prodrugs that are taken up into the cell immediately in the nucleotide form. Successes have been achieved using this approach for a number of NRTIs such as d4T (more later).

1.9 THE STRUCTURE OF HIV-1 RT IN COMPLEX WITH NUCLEOSIDE INHIBITORS

Nucleotide analogues bind at the dNTP-binding site (Fig. 1.10), adjacent to the 3' terminus of the primer strand that is located in the palm subdomain of the p66 subunit.[43] The catalytic triad of aspartic acids, (Asp110, Asp185 and Asp186), which are conserved in most polymerases are also located at this site. The nucleotide analogue binding site is composed of both protein and nucleic acid. The nucleic acid part of the binding site is made up of the 3'-primer terminus, which possesses the 3'-OH group that is the site for the covalent attachment of the incoming substrate. The base of the 3'-primer terminal nucleotide also helps to bind incoming substrate *via* base-stacking interactions. The first base in the template overhang contributes base-specific H-bond donor and acceptor groups that guide dNTP selection based on Watson-Crick base pairing

rules. Based on modelling experiments, residues Asp185 and Asp186 of the conserved Tyr-Met-Asp-Asp motif and Asp110 are believed to bind the triphosphate moiety of the incoming dNTP *via* two chelated Mg^{2+} ions (Fig. 1.11).[43] Once again, substitution with expulsion of the diphoshate (as described before) leads to incorporation of the resulting dNMP at the 3'-end of the DNA chain.

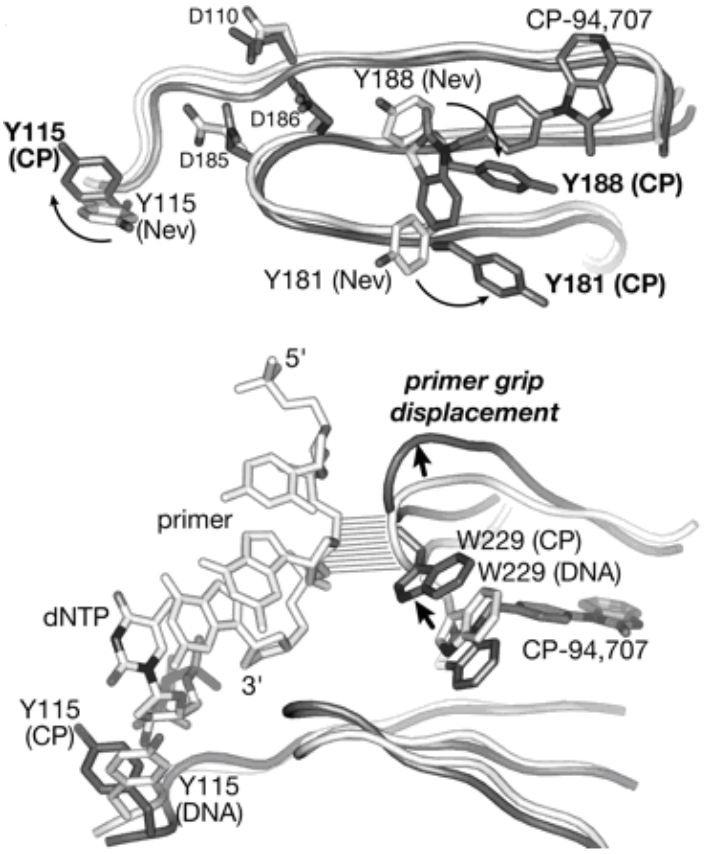

Figure 1.10 Superposition of HIV-1 RT in complex with an inhibitor and in ternary complex with primer template DNA and incoming dNTP. Displacement of TRP-229 and concomitant displacement of the primer grip are indicated with arrows. Nonspecific contacts between the primer grip and the primer strand DNA are indicated with parallel lines.[44]

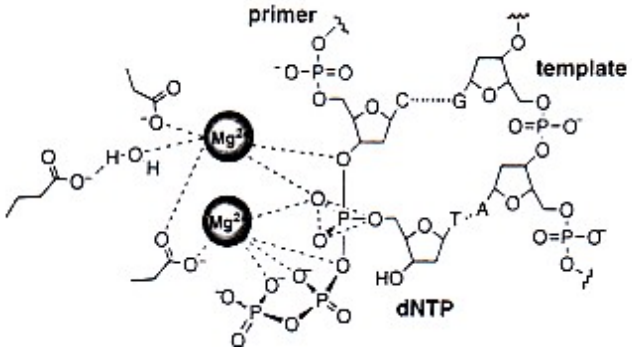

Figure 1.11 Proposed transition state of DNA polymerase-catalyzed nucleotide insertion.[45]

1.10 NUCLEOTIDE REVERSE TRANSCRIPTASE INHIBITORS (NtRTIs)

In most cases the ultimate bottleneck in the metabolic pathway leading from 2',3'-dideoxynucleoside (ddN) analogues to their active 5'-triphosphate form is the first phosphorylation step.[23] Unlike adefovir dipivoxil [9-(2-phosphonylmethoxyethyl)adenine (PMEA)] and tenofovir disoproxil [(*R*)-9-(2-phosphonylmethoxypropyl)adenine (PMPA)] (Fig. 1.12) which are already equipped with a phosphonate group and therefore only require two more phosphorylations to be converted to their active metabolites (PMEApp and PMPApp, respectively), nucleoside analogues lack this advantage.

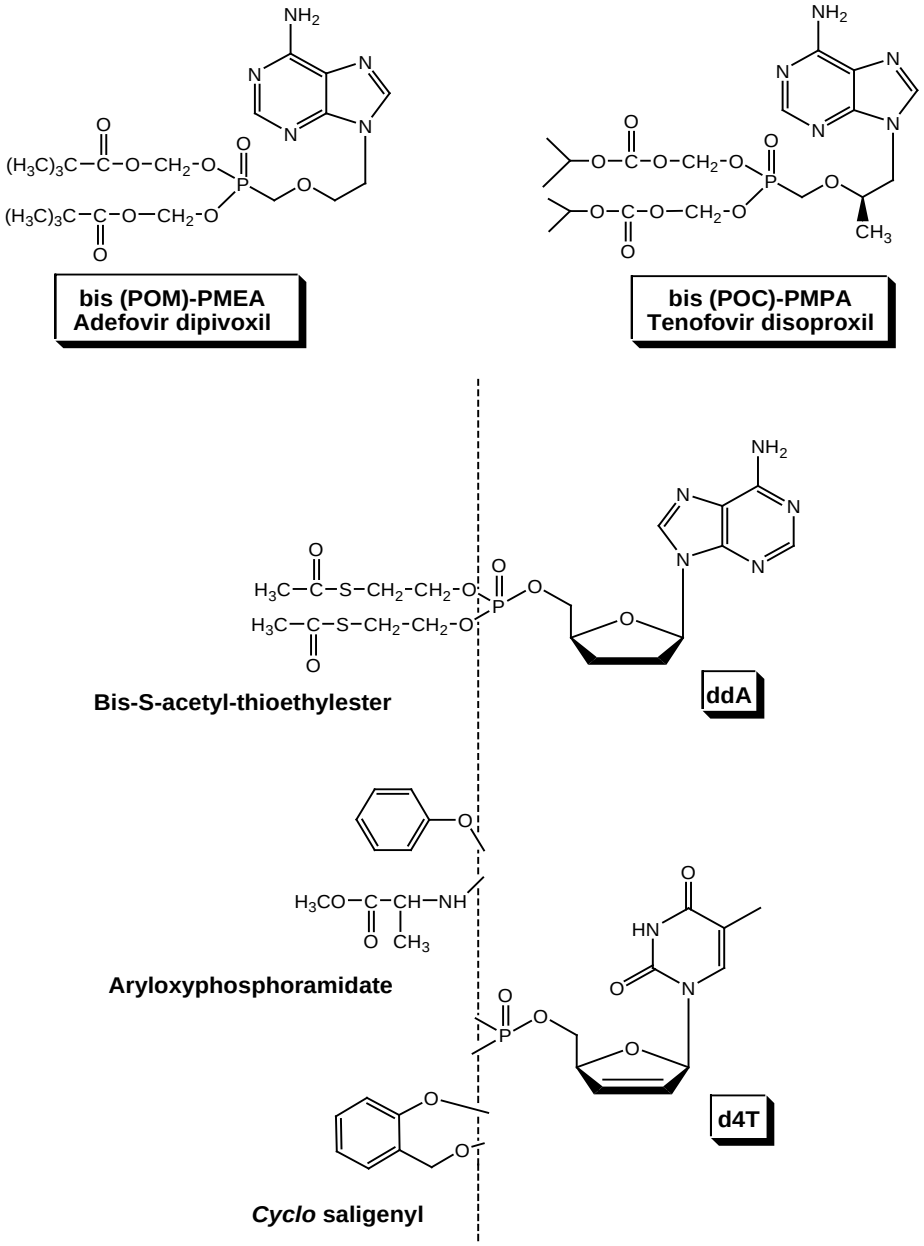

Figure 1.12 Acyclic nucleotides phosphonates: PMEA and PMPA in their prodrug forms. Prodrugs of ddNMPs.[23]

Figure 1.12 depicts various known versions of mono-phosphorylated nucleotide pro-drugs, which will be discussed.

Many research groups have focused their attention on constructing 2',3'-dideoxynucleotide (ddNMP) prodrugs as esters or amides, that once taken up by the cells, deliver the nucleotide (ddNMP) form. This so-called pronucleotide or prodrug approach (discussed in detail later) has proven successful for a number of NRTIs such as 2',3'-dideoxyadenosine (ddA) and d4T (Fig. 1.12). The bis(S-acetyl-2-thioethyl)phosphotriester of ddA [bis(SATE)ddAMP] was synthesized by Imbach and co-workers[46] and found to be 1000-fold more potent than the parent nucleoside. This increase in potency can be attributed to direct delivery of bis(SATE)ddAMP into the cells, which circumvents adenosine deaminase enzymes rapidly degrading ddA to ddI.[46]

Similarly, McGuigan and co-workers[47,48,49] have over a number of years synthesized and evaluated the highly potent arylphosphoramidate derivatives of d4T, AZT and ddU as prodrugs (Fig. 1.12). This prodrug comprises a phosphate derivative bearing aryloxy and alaninyl (methyl ester) O- and N-based groups respectively as a phosphoramidate derivative. Direct intake of aryloxyphosphoramidate derivatives of d4T, d4A and ddA intracellularly (via the alaninyl nucleoside-MP intermediate[50]) have provided anti-HIV activities that are 25- to 625-fold greater than the parent nucleosides.[51]

Similarly, Meier and co-workers[52,53] have introduced the cyclic saligenyl group (Fig. 1.12), which by-passes the rate-determining, thymidine kinase (in the case of d4T) and adenosine deaminase (in the case of ddA) enzymatic step. *Cyclo*Saligenyl pronucleotides deliver the monophosphate nucleotides of d4T and ddA exclusively under intracellular conditions of pH.[54,55] To fully understand how this works, 'the Prodrug Approach' will now be discussed in detail.

1.10.1 THE PRODRUG APPROACH (The Pronucleotide Approach)

The first introduction of prodrugs to the field of medicinal chemistry is kindly attributed to Albert[56] in 1951 who wrote: "A prodrug is a molecule which does not have any intrinsic biological activity but which is capable during the different phases of its metabolism to generate a biologically active drug". Furthermore, a potent suitable prodrug should overcome the crucial paradox: to be lipophilic enough to by-pass a membrane or metabolic barrier and to be hydrophilic enough to fulfill solubility, bioavailability or transport criteria.[57] The systematic enzymatic cleavage of the chemical bond allowing efficient prodrug-to-drug conversion is of particular interest since it depends on the type of cleavable linkage: -carbonate, -ester, -amide, carbamate, -phosphate, -phosphonate, -phosphoramidate, or –amidine.[57] The enzymatic stability of the resulting prodrug is characterized by its half-life, which can vary from a few minutes to several weeks.

All of the above is schematically depicted in Figure 1.13 for d4T.

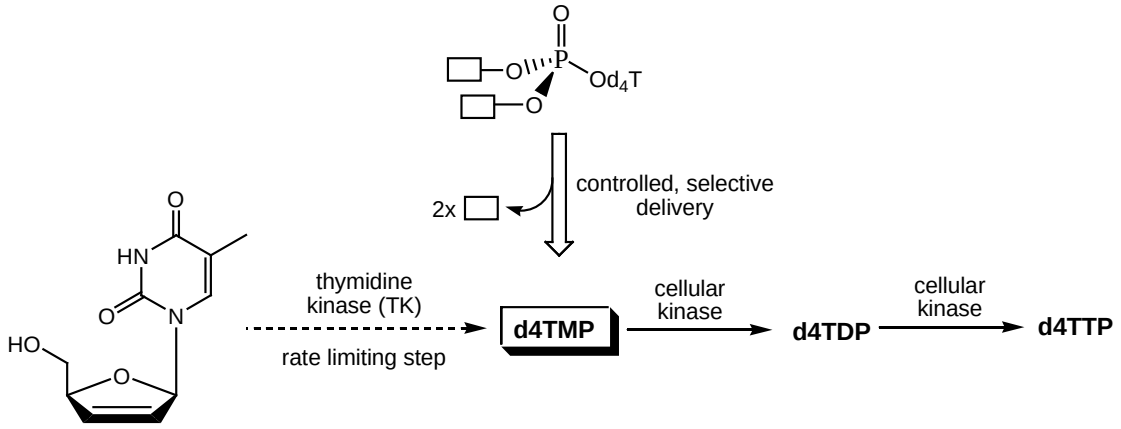

Figure 1.13 Metabolic transformation of d4T into active ddNTPP, after controlled selective delivery, i.e. the prodrug approach.[58]

In contrast to d4T, the fate of the majority of nucleoside analogues has not yet been studied in detail. After being tested, many parent nucleosides are discarded after not displaying any biological activity. Thus, it is likely that such a lack of understanding of the metabolic blockade has prevented the successful development of certain nucleosides into active nucleotide prodrugs.[58]

Nucleotides are very polar molecules that do not easily pass through cellular membranes and are dephosphorylated in the serum by non-specific phosphatases.[58] However, this problem can be overcome by masking the phosphate or phosphonate moiety of the nucleotide with degradable lipophilic carrier groups as illustrated in Figure 1.13. This leads to neutral, membrane-permeable nucleotide delivery systems, which is known as the pronucleotide approach.

Under physiological conditions, nucleotides are charged species (phosphate monoester pK_a values are about 1.6 and *ca*. 6.6). Therefore, as reported by Meier, one requires two masking groups to obtain a neutral lipophilic phosphate triester.[58]

Several methods with corresponding mechanisms for achieving this have been employed. Strategies involving pure chemical hydrolysis of dialkyl, dibenzyl and diphenyl phosphate triesters have proven to be successful in *in vitro* and *in vivo* studies.[59] However, recent pronucleotide approaches are based on enzymatic or chemical activation of the masking groups. These approaches use enzymatic activity and specific pH conditions.[59,60]

An example of this is the neutral lipophilic phosphotriesters using pivaloyloxymethyl (POM) phosphate-masking groups (Fig. 1.14), which can penetrate into cells *via* passive diffusion.[61]

Cleavage of one of the POM groups by non-specific cellular carboxyl esterases yields the hydroxymethyl analogue which is inherently chemically labile and spontaneously dissociates with elimination of formaldehyde to give the phosphodiester.[61]

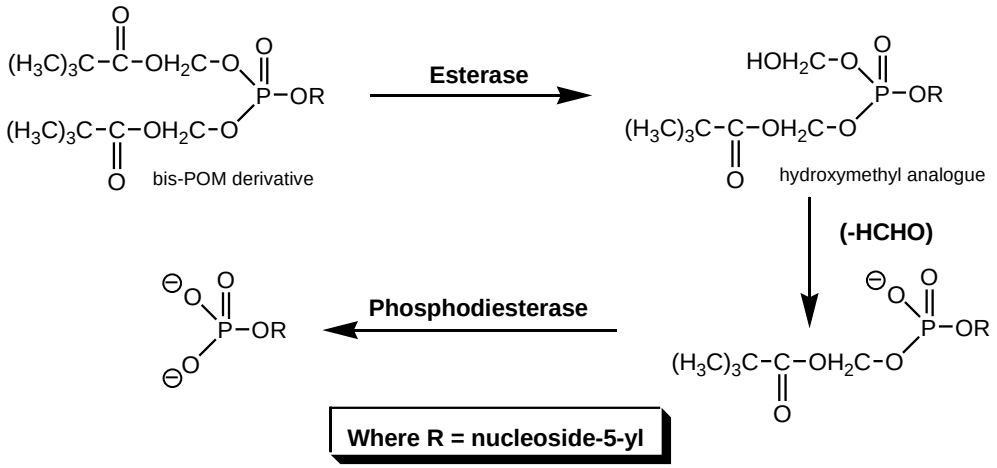

Figure 1.14 Biotransformation of POM2 nucleoside 5'-monophosphate prodrugs.[61]

Cleavage of the second POM group by cellular phoshodiesterases regenerates the desired parent nucleoside 5'-monophosphate. These enzyme-triggered approaches on POC and POM phosphate-masking groups have proven very successful in *in vitro* intracellular delivery systems.[61]

However, thus far, the only successful intracellular pH-driven nucleotide delivery strategy is the *cyclo*Sal approach.[62,63] This designed chemically induced coupling, follows a cascade mechanism[62-63], and goes as follows (Fig. 1.15): following nucleophilic attack of hydroxide at the phosphorus atom of *cyclo*Sal triester **1**, the phenolate is displaced preferentially in an S_NP reaction, since it is the best leaving group of the three OR groups. This leads to 2-hydroxybenzylphosphate diester **2** *via* proton transfer. The resulting *ortho* substituent of the benzyl ether is changed from a very weak electron-donating group (phosphate) to a strong electron-donating group (hydroxy). This electronic change activates the remaining masking group and induces a spontaneous rupture of diester **2** to yield the nucleotide and salicyl alcohol **8** (cascade reaction; steps b_1 and b_2). The bond cleavage proceeds after intramolecular proton transfer (intermediate **4**) via zwitterion **5** or 2-quinone methide **6**.[58]

The disfavoured pathway involves cleavage of the benzyl ester bond (step c), in which cation **3** is rapidly trapped by water to yield phenyl phosphate diester **7**. However, no further chemical hydrolysis of the phosphate diester takes place at physiological pH and **7** comes to a dead end. Thus, the pathway *via* step c does not occur .[58]

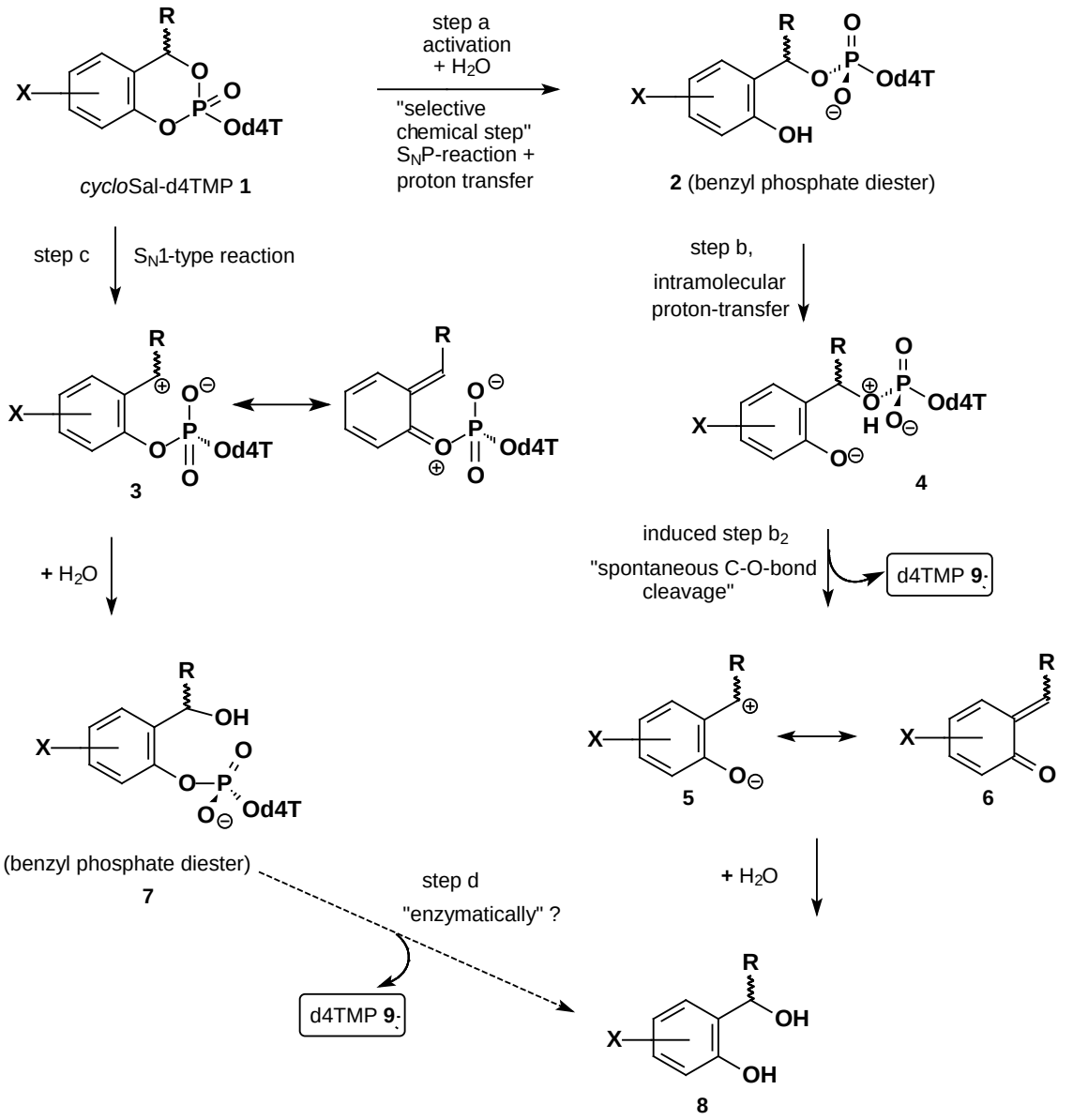

Figure 1.15 Two possible cascade hydrolysis of *cyclo*Sal-d4TMP triester 1.[58]

In summary, the *cyclo*Sal strategy requires one bifunctional masking group per equivalent nucleotide and is chemically triggered intracellularly at physiological pH to render the desired parent nucleotide-MP.

1.10.2 THE ACYCLIC NUCLEOTIDE PHOSPHONATES (ANPs)

The acyclic nucleotide phosphonates (ANPs) represent a new dimension for the treatment of DNA virus and retrovirus infections.[64] These ANPs encompass three compounds that have been formally licensed for the treatment of (i) HCMV (human cytomegalovirus) infections (i.e. HCMV retinitis) in AIDS patients (cidofovir, Vistide ®) (Fig. 1.16), (ii) chronic HBV (hepatitis B virus)

infections (adefovir dipivoxil, Hepsera ®), and (iii) HIV (human immunodeficiency virus) infections (AIDS) [tenofovir disoproxil fumarate (TDF), Viread ®].[40]

ANPs have therefore proved to be the cornerstone of anti-viral therapy. The question would therefore be: What is the significance of an acyclic nucleoside 'phosphonate'? In regular nucleotides (or nucleoside phosphates), the phosphate group is attached to the 5'-oxygen as an ester sugar bound to the nucleoside.[40]

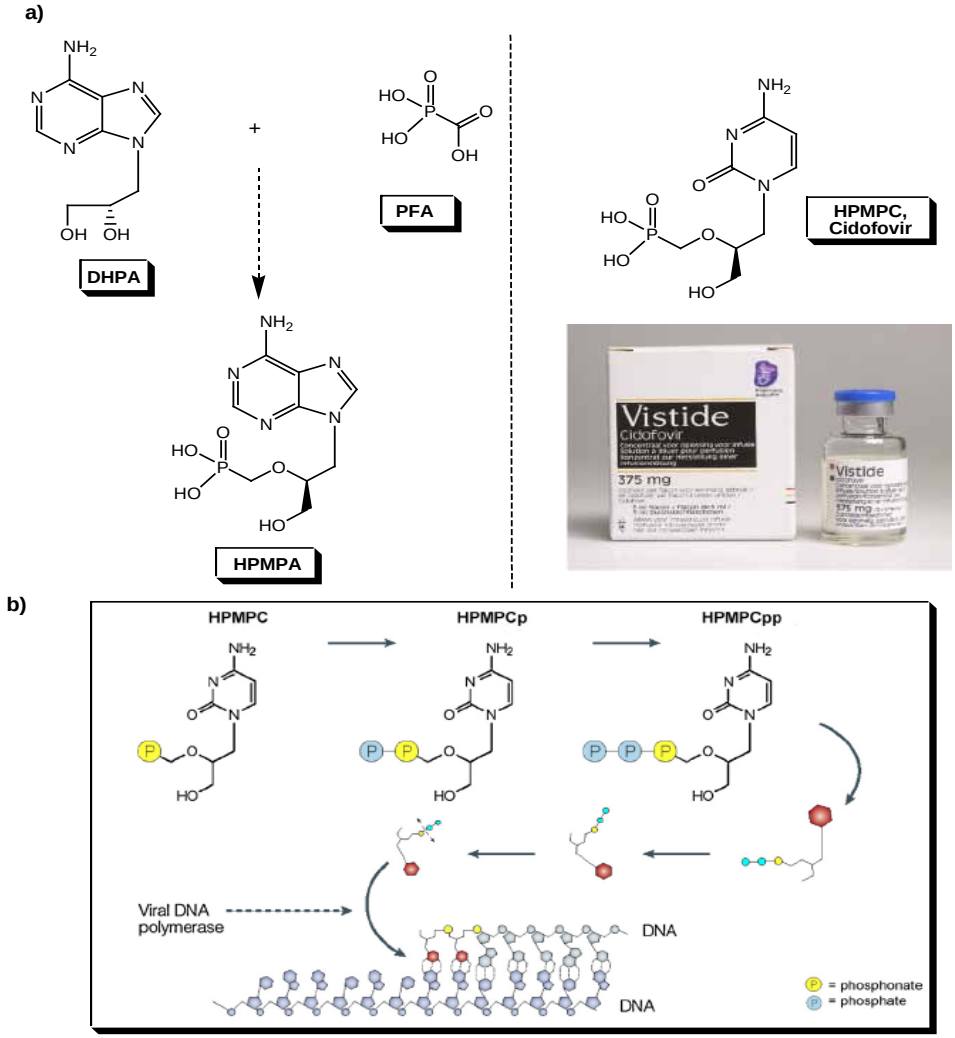

Figure 1.16 a) Broad spectrum of acyclic nucleotide phosphonates (ANPs); b) Mechanism of action of cidofovir.[40]

In the ANPs, the phosphate group, is attached to the nucleoside *via* a phosphonomethyl ether phosphonate grouping, which, unlike the phosphate ester linkage, should resist any attack from esterases, or any catabolic enzymes at large, by virtue of it having a more stable P-C bond over a P-O bond.

The concept of ANPs was born in 1986 with the discovery of the ANP prototype, (*S*)-9-(3-hydroxyl-2-phosphonylmethoxypropyl)adenine (HPMPA) (Fig. 1.16), as a broad spectrum anti-DNA virus agent.[65] HPMPA itself could be envisaged as a kind of construct resulting from the replacement of the carboxylate group of phosphonoacetic acid [PAA, the predecessor of the antiviral agent phosphonoformic acid (foscarnet, Foscavir ®] by the acyclic nucleoside analogue DHPA [(*S*)-9-(2,3-dihydroxypropyl)adenine], which was described in 1978 an an acyclic nucleoside analogue with broad spectrum antiviral activity.[66]

Cidofovir, adefovir, tenofovir and several others show high potential as therapeutic agents. According to their activity spectrum, the ANPs can be classified into two categories: (i) the 'HPMP' derivatives, represented by HPMPC (cidofovir), which are active against a broad variety of DNA viruses (polyoma-, papilloma-, adeno-, herpes- and poxvirus, and (ii) the 'PME' and 'PMP' derivatives, represented by PMEA (adefovir) and PMPA (tenofovir) (Fig. 1.12, pg. 14), which are primarily active against hepadna- and retroviruses. Their clinical usages, approved and potential are represented in Table 1.1.

Table 1.1 Clinical applications of acyclic nucleotide phosphonates.[40]

Compound *Commercially available*	***Dosage and route of administration***	***Approved clinical use***	***Off-label (potential) clinical use***
Cidofovir (Vistide®)	Intravenous (5 mg/kg weekly or two-weekly) Topical (gel/cream) 1%	CMV retinitis in AIDS patients	- Severe polyoma-, papilloma-, adeno-, herpes- and pox-virus infectious - HPV-, HSV-1-, HSV-2-, MCV-, and poxvirus
Adefovir dipivoxil (Hepsera ®)	Oral (10 mg daily)	Chronic hepatitis B (HBV infection)	
Tenofovir disoproxil fumarate (TDF) (Viread ®)	Oral (300 mg daily)	AIDS (HIV infection)	Chronic hepatitis B (HBV infection)
TDF in fix-dose combinations with emtricitabine (Truvada ®)	Oral (300 mg TDF daily) (200 mg emtricitabine daily)	AIDS (HIV infection)	Chronic hepatitis B (HBV infection)
TDF in fix-dose combinations with emtricitabine and efavirenz (Atripla ®)	Oral (300 mg TDF daily) (200 mg emtricitabine daily) (600 mg efavirenz daily)	AIDS (HIV infection)	

1.11 NRTI RESISTANCE

HIV-1 RT is very tolerant to non-standard base pairs and modified sugars which has advantages for chemotherapy. However, one drawback is the resultant mutations (no proof-reader), due to misincorporations ranging from 1/1700 to 1/4000 nucleotides. One estimate suggests about 10 base changes in the HIV genome per replication cycle, and the resultant mutant strains can exhibit NRTI resistance. There are two currently known biochemical mechanisms of NRTI drug resistance. The first is mediated by mutations in the RT enzyme that allow it to discriminate against NRTIs during DNA synthesis, thereby preventing their addition to the growing DNA chain. The second mechanism (NEM) involves an increase in nucleotide excision rate in the mutant strain, resulting in continued DNA synthesis.[67,68] In the second mechanism, the oxygen anion of a nucleoside diphosphate or triphosphate is used as a pyrophosphate nucleophile to attack and cleave the 3'/5'-phosphate bond of the primer, producing an unblocked primer and a dinucleoside tri- or tetraphosphate containing the dideoxynucleoside monophosphate from the primer terminus linked through its phosphate group to the distal phosphate of the free nucleoside di- or triphosphate (Fig. 1.17).[68]

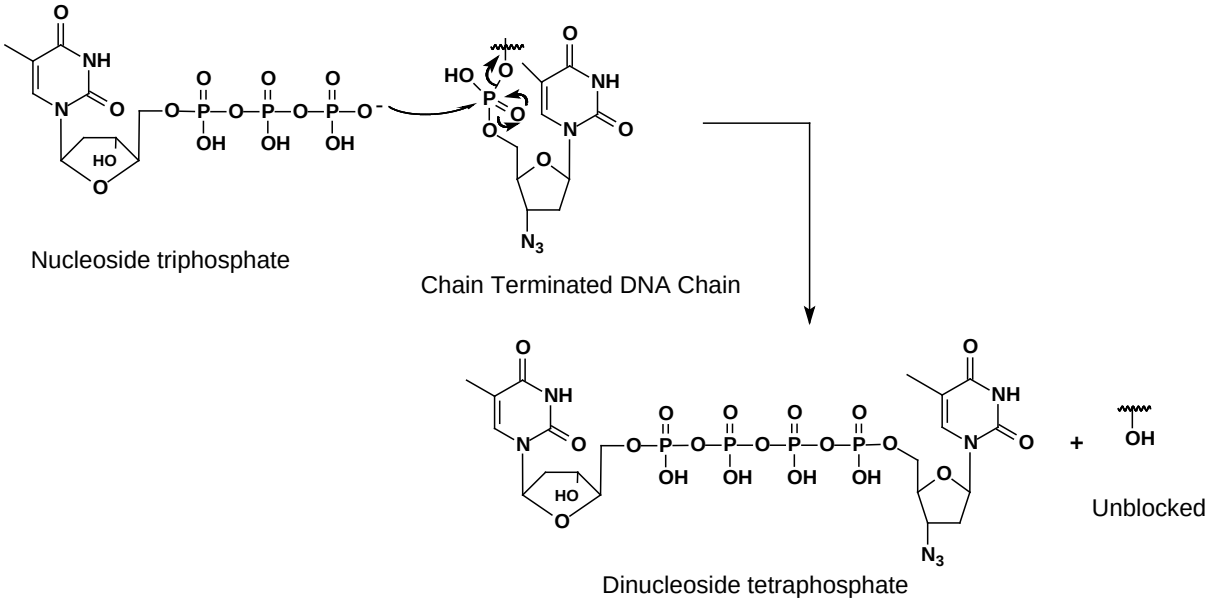

Figure 1.17 Removal of NRTI from the primer terminus through dinucleoside polyphosphate synthesis

Biochemical and modelling studies suggest that incorporation of AZT results in steric strain between the azido group and Asp185 of the mutant, resulting in an enhanced excision rate (Fig. 1.18). This explains why NEMs cause the highest levels of phenotypic resistance to AZT.

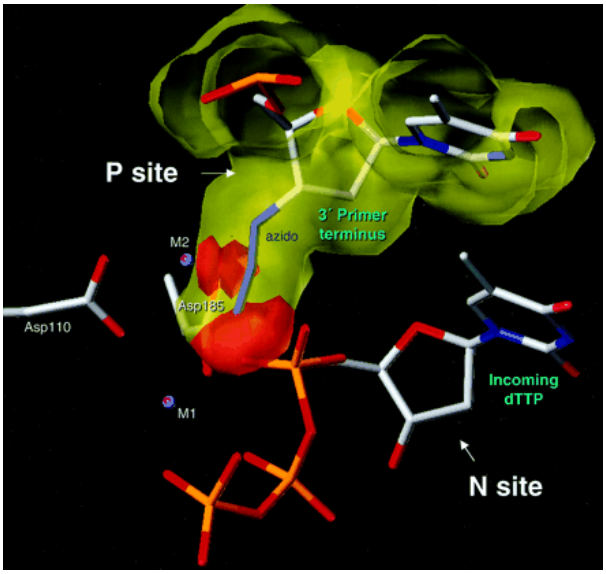

Figure 1.18 Steric hindrance when an AZT-terminated primer is bound to RT at the P site. The figure, based on the structure of the ternary RT-DNA-dNTP complex, shows that the distance between the azido of AZT and D185 (mutant) would cause steric conflict; the distance between D185 and the first and second azido nitrogens is less than the sum of the van der Waals radii.

The M184V mutation causes the high-level of lamivudine resistance observed and emerges rapidly in patients receiving lamivudine monotherapy. This mutation (M184V) and other NRTI resistance mutations interfere with the effects of the NEMs. The mutational antagonism between the NEMs and several of the mutations that act by allowing RT to discriminate against NRTIs explains the clinical synergism observed with dual NRTI combinations such as Zidovudine/Lamivudine, Stavudine/Lamivudine, Zidovudine/didanosine and Stavudine/didanosine.[67]

1.12 NON-NUCLEOSIDE REVERSE TRANSCRIPTASE INHIBITORS (NNRTIs)

More than 30 structurally different classes of NNRTIs (Fig. 1.19) have been synthesized, [69,70] since the well known TIBO derivatives[71] were first discovered by the Janssen group in 1987. NNRTIs are a chemically diverse set of compounds, largely specific for HIV-1 RT and, unlike the NRTIs, they do not require intracellular metabolism for activity.

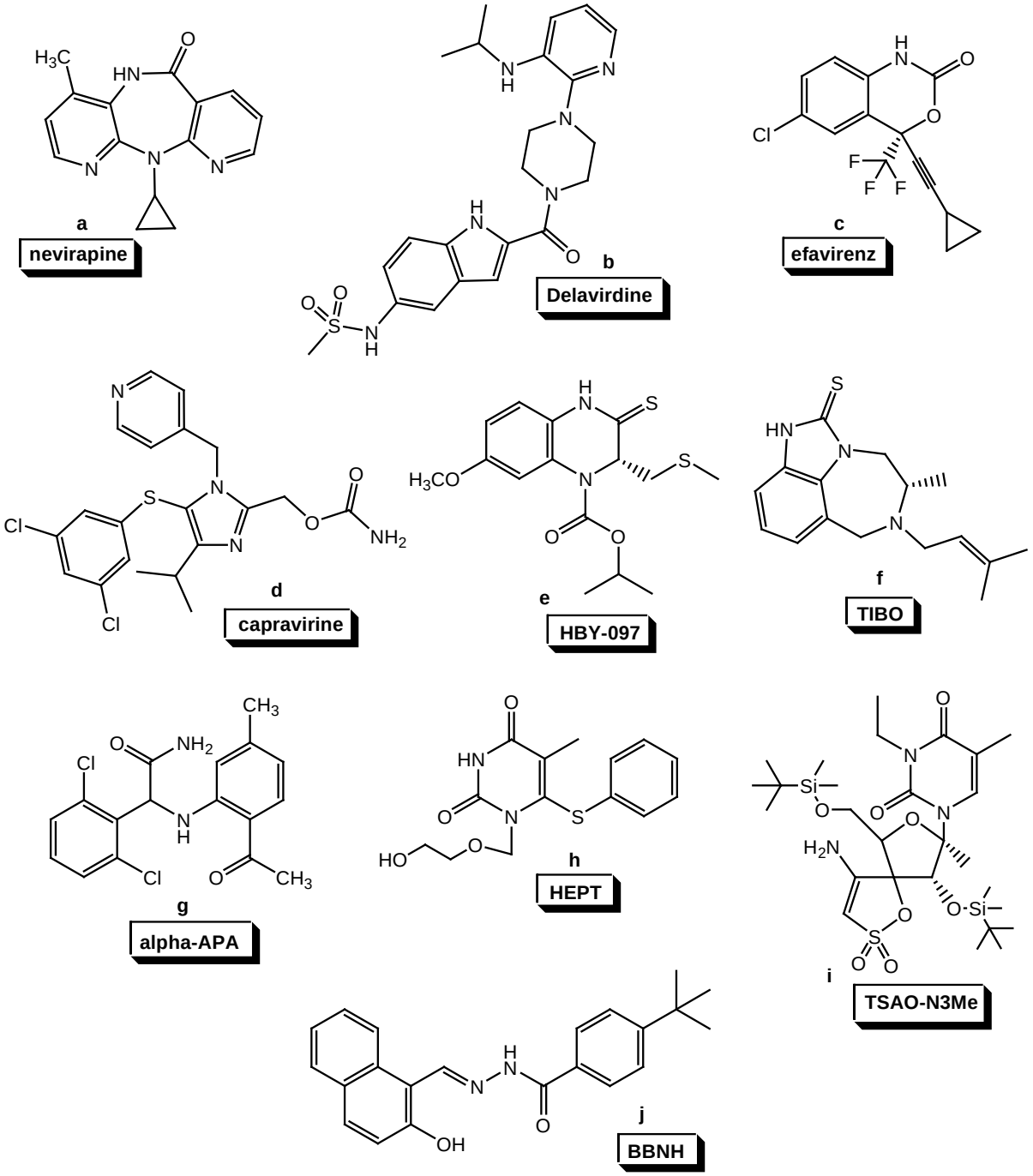

Figure 1.19 Non-nucleoside reverse transcriptase inhibitors.[70]

In general, NNRTIs are a group of small (< 600 Da) hydrophobic compounds with diverse structures, as can be seen in Figure 1.19. They specifically inhibit HIV-1, but not HIV-2 RT, which is unable to form the required pocket for binding.

By far the chief pioneer for nearly 17 years in NNRTI development is the late Dr. Paul Janssen. Beginning in 1987, Janssen and his co-collaborators (Das, Clark, Arnold, De Corte, de Clercq, Pauwels, Lewi, Kukla and others) engineered the field of non-nucleoside reverse transcriptase inhibition of HIV-1 RT. Figure 1.20 provides crucial insight in the form of a historical synopsis of their developments that ultimately led to the discovery of TMC278.[72]

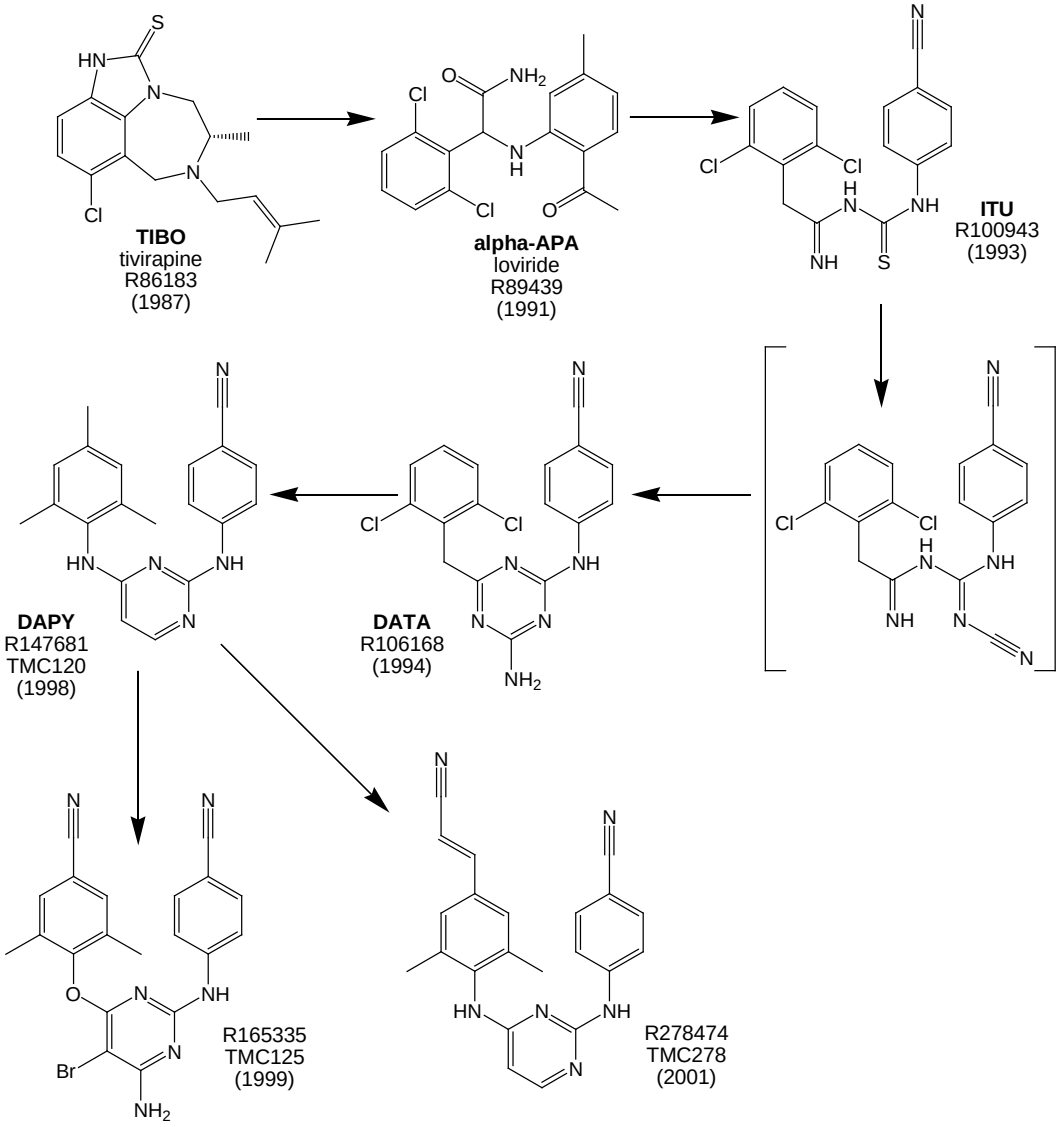

Figure 1.20 Chemical evolution from TIBO to TMC278, starting in 1987.[72]

TIBO (***t***etrahydro***i***madazo***b***enzodiazepin***o***ne) analogues were discovered by screening a subset of a Janssen compound library in a cell-based anti-HIV test at the Rega Institute.[71] Subsequent screening of the Janssen compounds led to the discovery (2nd lead series) of the α-APA (α-***a***nilino***p***henyl***a***cetamide) class of NNRTIs.[73] Further chemical modification led to the class of potent ITU (***i***mino***t***hio***u***rea) NNRTIs.[74] In an attempt to synthesize the corresponding imino-*N*-cyanoguanidine derivatives of ITU, an unexpected ring closure occurred, producing the first compound of the DATA (***d***i***a***ryl***t***ri***a***zine) class of NNRTIs.[75]

Molecular modeling studies suggested in 1996 that replacing the central aminotriazine ring of DATA with a pyrimidine ring would lead to greater activity. This was the birth of the DAPY (***d***i***a***ryl***py***rimidine) NNRTIs, of which TMC120 (R147681) is the prototype. TMC120 and TMC125 have subsequently proved to be highly active in reducing viral loads.[76]

Further collaborative work among medicinal chemists, crystallographers, and molecular modelers led in 2001 to the discovery of the cyanovinyl DAPY compounds, of which the *E*-isomer TMC278 (R278474) is the prototype. The potency of TMC278 against wild-type and mutant HIV-1 RTs are compared in Table 1.2 below with those of two other DAPY compounds (TMC120 and TMC125), as well as with three approved NNRTI drugs.[77]

Table 1.2 Potency data (EC_{50} μM) in of DAPY compounds and the three approved NNRTIs against HIV resistant strains.[77]

Compound	*Wild-type*	*K103N*	*Y181C*	*K103N/Y181C*	*L100I*	*L100I/K103N*
TMC278	0.0004	0.0003	0.0001	0.0008	0.0005	0.008
TMC125	0.002	0.001	0.006	0.005	0.003	0.01
TMC120	0.001	0.004	0.008	0.044	0.016	>10
Efavirenz	0.001	0.039	0.002	0.04	0.038	>10
Delavirdine	0.016	>1	>1	>10	>1	N/A
Nevirapine	0.085	>1	>1	>100	0.6	N/A

** EC_{50} is defined as the concentration of compound required to inhibit syncytia formation in HIV-1 infected cells to 50%.

Table 1.2 reveals how first-generation NNRTIs (Nevirapine and Delavirdine) are effective in inhibiting wild-type HIV-1 RT, but are poor at overcoming single and double point mutations because of their rigidity. Efavirenz on the other hand, often referred to as a second-generation

NNRTI, is very good (1 nM range) at inhibiting wild-type HIV-1 RT, as well as being capable of inhibiting single point mutations. The flexible third-generation DAPY compounds, especially TMC125 and TMC278, display an outstanding anti-HIV profile for inhibition against all single point mutations as well as a remarkable 8 nM activity for TMC278 against the double point mutation of L100I/K103N. The mechanism by which this works will be discussed later.

1.12.1 THE NNRTI-BINDING POCKET

All NNRTIs bind to a single site on the p66 subunit of the HIV-1 RT p66/p51 heterodimer termed the NNRTI binding pocket (NNRTI-BP) (see Fig. 1.7 again), despite being a heterogeneous class of inhibitors with diverse chemical structures. The NNRTI-BP is situated between the β6-β10-β9 and β12-β13-β14 sheets in the palm subdomain of the p66 subunit. This is also approximately 10Å away from the RT DNA polymerase aspartic acid catalytic triad.[20] The NNRTI-BP is predominantly hydrophobic in nature with substantial aromatic character (Y181, Y188, F227, W229 and Y232), but also contains hydrophilic residues (K101, K103, S105, D192, and E224 of the p66 subunit and E138 of the β7-β8 loop of the p51 subunit). A likely entrance to the NNRTI-BP is located at the p66/p51 interface, ringed by residues L100, K101, K103, V179, and Y181 (p66 subunit) and E138 (p51 subunit).[78] In the absence of ligand, the side chains of Y181 and Y188 of p66 point into the hydrophobic core, and thus, the NNRTI-BP does not exist in the free 'apo'-enzyme (Fig. 1.21).[78,79] NNRTI-binding to HIV-1 RT causes the Y181 and Y188 to rotate away from their positions in the hydrophobic core thereby creating space for ligand accommodation.[78] Effectively, this equates to an approx. 30^{o} twisting of the β12-β13-β14 sheet, which leads to an expansion of the NNRTI-BP.[70]

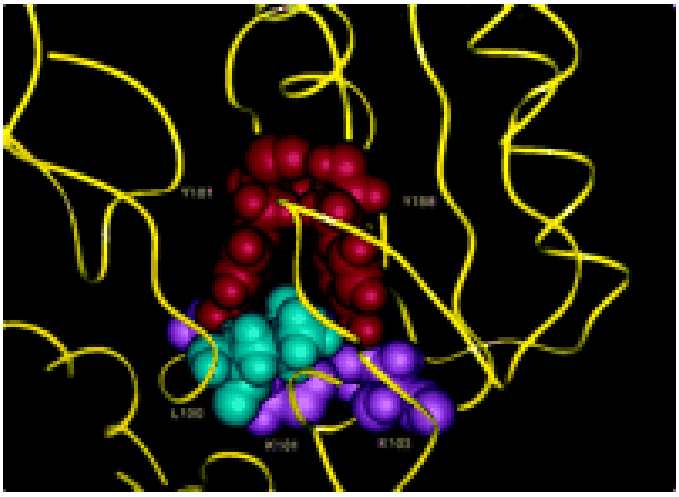

Figure 1.21 Close-up of the future binding pocket area in unliganded RT. Amino acid residue 100 (shown in blue) makes contact with residues Y181 and Y188 (shown in red) which undergo major structural rearrangement prior to non-nucleoside inhibitor binding. L100 also makes contact with K101 and K103 (purple) in the uncomplexed state.[80]

In NNRTI-bound RT, the p66 fingers and RNase H domain fluctuate in opposite directions (anti-correlated motions), giving rise to open and close conformations (Fig. 1.22).[70] The p66 palm and connection serve as a rigid support for the flexible regions. The p66 thumb, on the other hand, is subject to orthogonal, but cooperative motions, with respect to the p66 fingers and RNase H. Thus, the net effect of NNRTI-binding to RT is to change the direction of domain movements.[81] To understand this, the mechanism of NNRTI-RT inhibition will be discussed in detail.

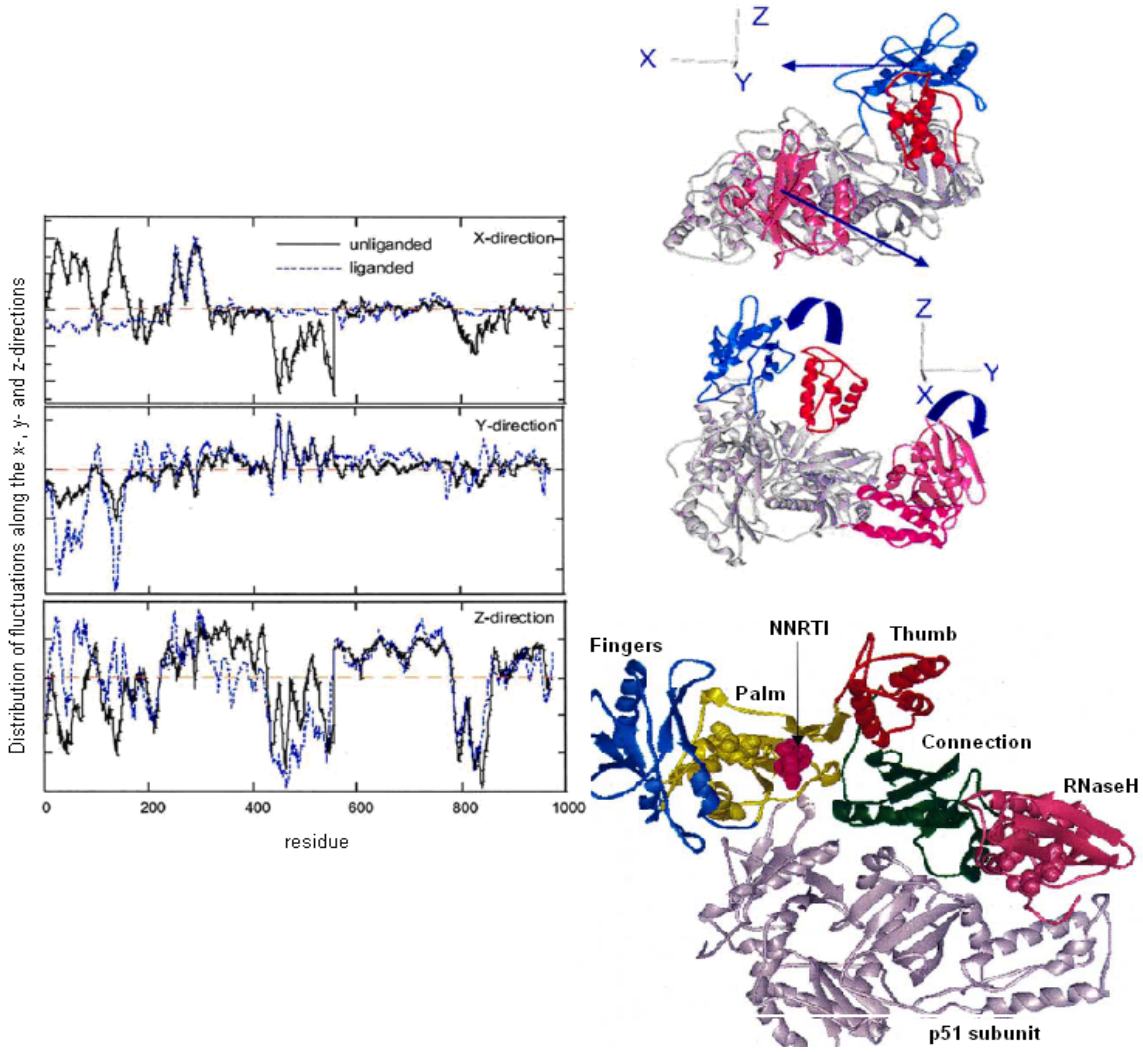

Figure 1.22 Residue fluctuations along the x-, y- and z-directions for unliganded (black line) and nevirapine-bound (blue line) RT. The X axis coincides with the out-of-plane direction; the Y and Z axis lie along the in-plane directions. The ribbon diagrams on the right represent the p66 fingers, thumb, RNase H, and the p51 thumb are coloured blue, red, pink and magenta, respectively.[70]

1.12.2 THE NNRTI BINDING MODE AND MECHANISM OF RT INHIBITION

A number of different mechanisms for NNRTI inhibition of RT have been proposed. In 1992, Kohlstaedt and co-workers[20] suggested that binding of nevirapine induces so called 'molecular

arthritis' whereby relative domain movements, similar to Figure 1.22 above, thought to be necessary for the catalytic cycle of the enzyme, are inhibited. Generally, crystal structures of RT with bound NNRTIs have the p66 thumb subdomain in an extended position. For unliganded RT, the thumb subdomain can either be folded down into the DNA-RNA cleft[79a] or can adopt a more extended position.[79b] Examination of various crystal forms of RT with different NNRTIs bound showed significant variations in relative domain positioning.[79c] Thus, there is no clear evidence that NNRTI binding induces a single positioning of the p66 thumb subdomain. Comparing the NNRTI bound and free forms of RT indicated a significant and consistent movement of strands β2-β3 containing the critical Asp110, Asp185 and Asp186 active site triad[79b], which ultimately explains the inhibition of RT by NNRTIs (Figure 1.23).

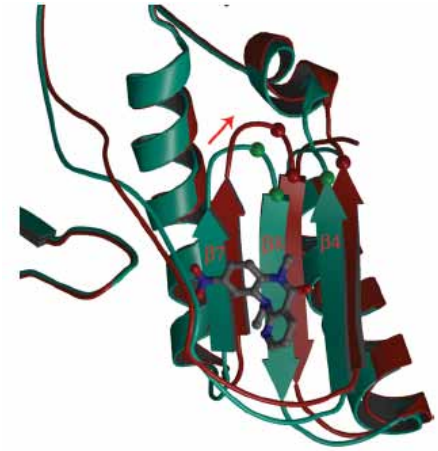

Figure 1.23 Diagram comparing the NNRTI site and polymerase active site in RT for the apo enzyme (in green) and for inhibitor-bound form (1051U91, shown in grey as ball and stick representation) in brown. The three key aspartic acid residues in the polymerase active site (110, 185 and 186) are shown as small spheres which mark their Cα atoms. The three-stranded β-sheet (strands β4, β7 and β8) moves as a rigid body on binding an NNRTI, thereby causing inhibition of the enzyme. The direction of movement is indicated by the arrow; Cα atom of Asp186 is displaced by 1.9 Å.[79b]

Parallel rapid reaction kinetic experiments showed that the rate limiting step inhibited was the chemical bond formation, in line with the proposed structural mechanism.[79c] An alternative to the active site displacement mechanism was proposed by Das and co-workers in 2007, in which the NNRTI distorts the catalytic triad position into a conformation incompatible with the binding of the divalent cations Mn^{2+}/Mg^{2+}.[79d] This idea was built on the back of an RT crystal structure determined in the absence of NNRTI and with ATP bound but in a mode significantly different to dNTP binding in the catalytic complex. The loss of Mn^{2+} or Mg^{2+} counter ion would be expected to significantly weaken the binding of dNTPs, since charge repulsion between the nucleotide phosphate groups and the catalytic aspartates would result. In fact, the opposite is the case as kinetic data shows that the presence of an NNRTI in fact significantly strengthens the binding of deoxynucleoside triphosphate in the initial collision complex for the quaternary complex.[79e]

Additionally, there is a metal-ion dependency of dTTP binding in the complexes of nevirapine/delavirdine or efavirenz present, giving further evidence that the cations remain in place after an NNRTI is bound. These data hence argue against the proposal of the NNRTI-shifted aspartates being unable to bind divalent cations.

An alternative mechanism of NNRTI inhibition has been described which relates to movement of residues in the region of the primer grip.[78] This region, containing residue Pro236, is however extremely flexible taking up very variable conformations which are unrelated to NNRTI potency. Interference of the catalytic step of the polymerase would thus be via an indirect route involving perturbations of the primer position. The effects of NNRTIs on the stability of RT heterodimer formation do not appear to significantly contribute to the mechanism of inhibition of the enzyme.[79f,79g] The status quo in 2009, on the NNRTI mechanism of RT inhibition, is that any of the above mechanisms are acceptable and that the precise mechanism is still not known.

1.12.3 FIRST- AND SECOND-GENERATION NNRTIs: DIFFERENCES IN THE MODE OF BINDING TO HIV-1 RT

NNRTIs can be broadly categorized into first- and third-generation compounds. Efavirenz appears to be the odd one out as a bridging second-generation type. First- generation NNRTIs such as nevirapine, delavirdine, TIBO and loviride were mainly discovered by random screening but are associated with rapid development of mutations due to their inherit rigidity. By comparison, third-generation NNRTIs, such as the DAPY compounds in view of their flexibility and hydrogen bonding ability to K101, were developed with 'rational drug-design' strategies in mind. These strategies include molecular modeling, rational-based drug synthesis and biological and pharmacokinetic evaluations. In general, third-generation NNRTIs tend to be more potent than first-generation counterparts and are more active against a broader spectrum of drug-resistant strains of HIV-1.[82]

The common pharmacophores[83,84] that are crucial for tight and specific binding to the RT NNRTI-BP include an aromatic ring capable of π-stacking interactions at the back of the pocket, NH-C=O or NH-C=S groups able to participate in hydrogen-bonding, and a few more hydrocarbon-rich regions for hydrophobic contacts.[70] The X-ray crystal structure analysis of HIV-1 RT has demonstrated similarities in the geometry of the binding modes of both generation types.[85] Generally, the binding of first-generation NNRTIs in the pocket resembles a 'butterfly' (Fig. 1.24) resting on the β6-β10-β9 sheet.

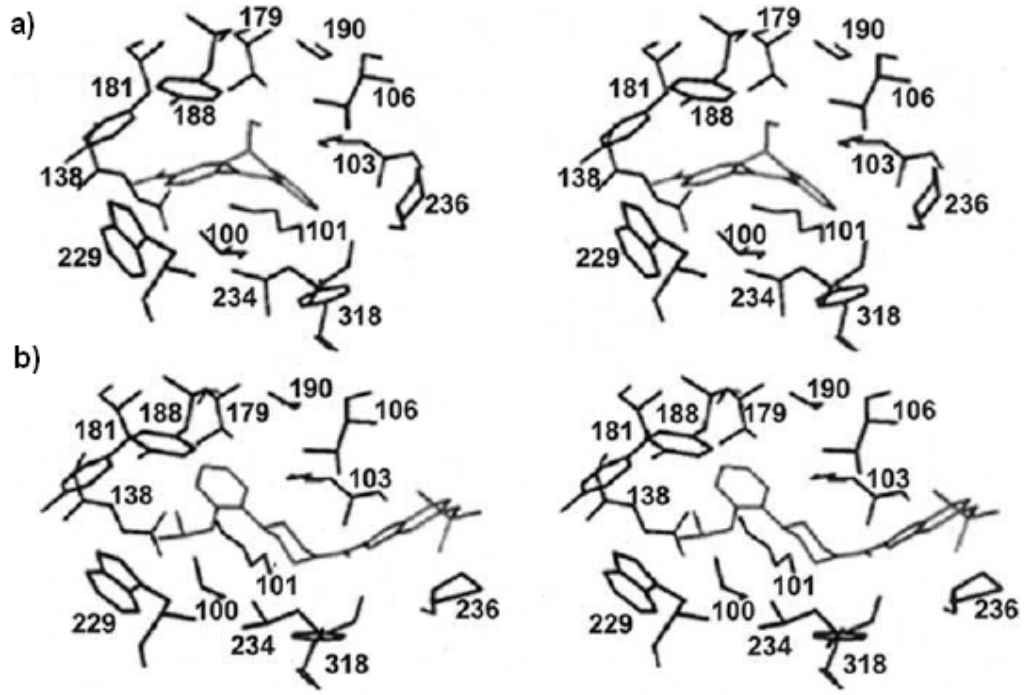

Figure 1.24 Stereoview of a) nevirapine and b) delavirdine in a clear butterfly binding mode in the NNRTI-BP.[70]

This butterfly-like mode is defined by Wing I, Wing II and the body/linker modular segments to which specific pharmacophores bind. The Wing II region is lined with aromatic amino acid residues Y181, Y188 and W229 at the back of the pocket that have favourable π-π interactions. Wing I has fewer hydrophobic interactions compared to Wing II and involves the side chains of K101, K103, V106, V179 and Y318. The body of the 'butterfly' has interactions with the main chain atoms of Y188, Y189 and G190, and with the side chains of V106 and V179. The back of the 'butterfly' is flanked with residues L100 and L234, which interact with both wings.[70]

Recent studies, including crystallographic analysis and computational modeling, have made it possible to develop drugs based on a deeper understanding of the structural features required for anti-HIV activity as well as conformational changes that may help in minimizing the drug resistance. The thiocarboxanilide UC-781 is one of these prototype anti-HIV drugs and also a member of a series of carboxanilide derivatives (Figure 1.25).[14] Although it failed at an advanced stage of clinical trials, it has been identified as a potent inhibitor of HIV-1 replication. Further studies have shown it to be a useful microbicide.[86]

Table 1.3 shows the effectiveness of UC-781 in terms of treatment on HIV-1-infected cells. It has been shown to have a favourable combination of both high potency (EC_{50} = 9 nM) as well as resistance to single point mutations such as L100I, K103N, Y181C and V106A.[14] These mutations are of serious concern for many NNRTIs.

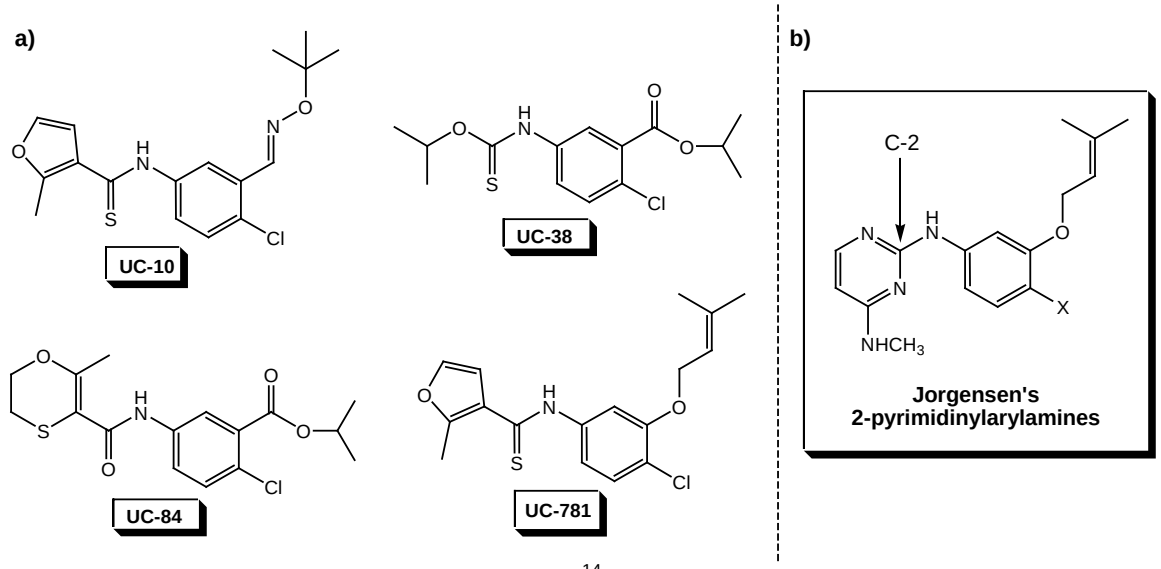

Figure 1.25 a) Series of carboxanilide derivatives[14], b) Jorgensen's 2-pyrimidinylarylamines with the incorporated UC-781 pendent ring at the C-2 position.

Table 1.3 Potency of Carboxanilide compounds against HIV-1 RT Wild Type and Mutants[14]

	EC_{50} (μM) {fold resistance}			
HIV-1 strain	*UC-10*	*UC-38*	*UC-84*	*UC-781*
L100I	0.242 {2}	2.06 {71}	>112 {>2700}	0.024 {3}
K103N	1.140 {8}	-	-	0.069 {8}
V106A	0.370 {3}	2.06 {71}	>61 {>1500}	0.015 {2}
Y181C	0.214 {2}	1.9 {66}	42 {1000}	0.033 {4}
Wild type	0.142 {1}	0.029 {1}	0.042 {1}	0.009 {1}

The results in Table 1.3 also show how UC-781 is far superior to all its counterparts. It has been reported that UC-781 is a rapid tight-binding inhibitor of RT (Figure 1.26). Crystallographic studies have attributed partial evidence for this. The UC-781 inhibitor is able to form a strong hydrogen bond between its thioamide sulfur (pharmacophore amide hydrogen) and the main-chain carbonyl oxygen of Lys101 (Figure 1.27a). This hydrogen bond is believed to form an anchor around which the carboxanilide inhibitor can pivot itself.[14] Thioamides orientate in the *s-trans*-configuration, while amide bonds adopt an *s-cis*-configuration according to IUPAC prioritization. Using biochemistry nomenclature these designations are swopped (Fig. 1.27b) to just '*cis*' for the thioamide and '*trans*' for the amide as defined by the relative orientatation of the R groups. Using biochemistry nomenclature it can be seen that the UC-781 thioamide adopts the preferred '*cis*' conformation for optimal tight and specific binding in the NNRTI-BP.

Very recently, Jorgensen[87] has demonstrated the use of 2-pyrimidinylarylamines as potential NNRTI's. His 2-pyrimidinylarylamines (Fig. 1.25) showed excellent biological activities (5 nM for X = CN; 6 nM for X = Cl) supporting the motif in Figure 1.29b with the aromatic ring firmly embedded into Wing 2. These inhibitors presented a very good structural activity study on what is essential for good binding in the NNRTI-BP without having to go through the more exotic synthesis of the DAPY compounds.

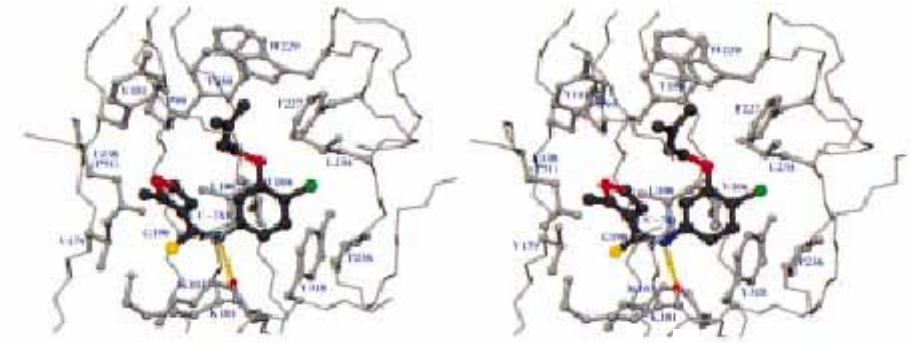

Figure 1.26 Stereo view of UC-781 in the NNRTI-BP. The H-bond is shown as the yellow line.[14]

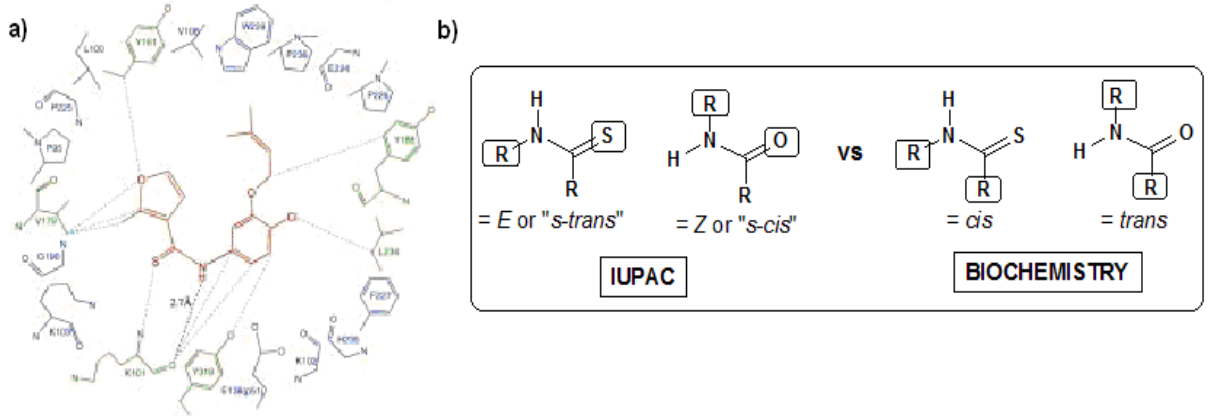

Figure 1.27 a) Schematic representation of the NNRTI-residues interaction, exemplifying the Lys101-thioamide H-bond.[14] b) IUPAC and Biochemistry nomenclature for *cis* and *trans* assigments around thioamides.

The crystal structures of third-generation NNRTIs (ITU, DATA and DAPY compounds) bound to HIV-1 RT show a different, unique 'horseshoe' or 'U' mode[88] compared to the butterfly-like nevirapine above. DAPY derivatives can adapt to changes in the NNRTI-BP, which plays a crucial role in overcoming point mutations in the pocket. The torsional flexibility of the DAPY structure permits access to numerous conformational variants, and their compact structure permits repositioning and reorientation (Fig. 1.28) when mutations are present in the NNRTI-BP.[89,90] The ability of etravirine (TMC125) to bind the RT enzyme in more than one

conformationally distinct mode explains the exceptional spectrum of activity observed for this compound (Table 1.2).[89]

Depicted in Figure 1.29a, the proposed docking of TMC125 and X-ray structure of TMC120, sees the pyrimidine-unit firmly embedded into the Wing I compartment of RT, together with the less-substituted phenyl ring (attached to C-2 of the pyrimidine) into the hydrophobic Wing II (interacting with Lys101 and Tyr318). However, the more substituted phenyl ring (attached to C-4 of the pyrimidine) clearly exits the 'front' entrance of the pocket through its '*ortho*-position' and leads off towards Glu188 and the p66 subunit of RT. The '*para*'-position of the C-4 phenyl ring points towards W229 which will become important later as a crucial interaction.

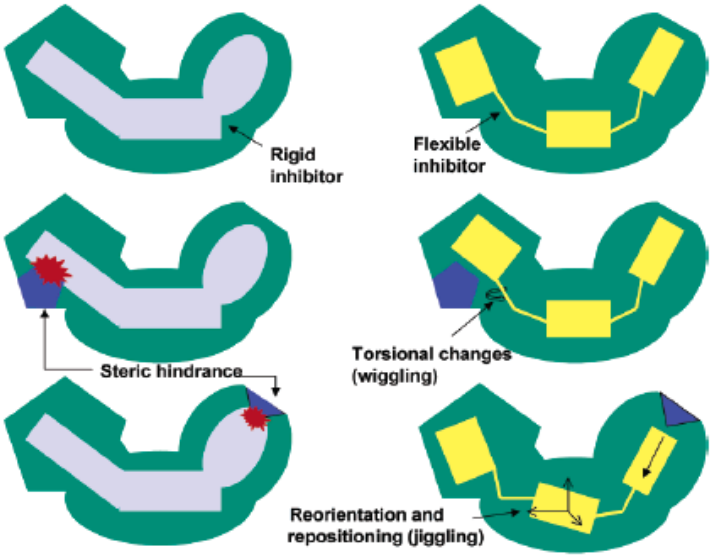

Figure 1.28 Schematic representation depicting how flexibility of an inhibitor can assist in overcoming resistant mutations.[90]

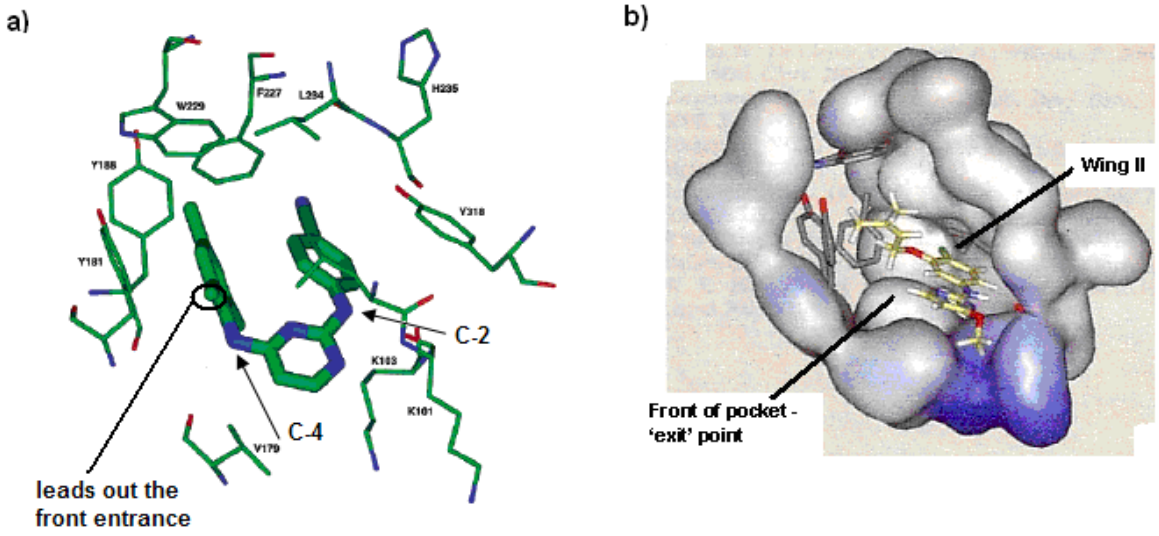

Figure 1.29 a) Proposed docking site for TMC125 at the entrance of NNRTI binding pocket of HIV-1 RT,[72,91] b) Proposed docking of 2-pyrimidinylarylamines at the entrance of the NNRTI-BP of HIV-1 RT.[87]

1.13 NNRTI RESISTANCE

Resistance mutations associated with NNRTI treatment failure occur primarily in and around the NNRTI-BP. The most common NNRTI-resistance mutations include Leu100Ile, Lys103Asn, Tyr181Cys, Tyr 188Leu, and Gly190Ala.[92,93] Structural and molecular modeling studies of drug-resistant HIV-1 mutants[94], both in the presence and in the absence of bound NNRTIs, have suggested possible mechanisms by which key mutations confer resistance to NNRTIs.

The Gly190Ala mutation, which causes high-level resistance to loviride and HBY-097, has no significant effect on the ITU, DATA, and the DAPY inhibitors. The resistance was proposed to be caused by filling the area of the binding pocket that would otherwise be occupied by the linker/body portion of the butterfly-shaped NNRTIs like loviride or by the quinoxaline ring of HBY-097.[95] The ITU, DATA, and DAPY inhibitors are not affected by the mutation, since a Cβ atom introduced by the Gly190Ala mutation would point toward the central part of the inhibitors (a thiourea, triazine or pyrimidine group). A minimum distance of 6Å between the Cα atom of Gly190 and the central part of these inhibitors suggests that there would be no serious steric conflict between the alanine at position 190 and the bound NNRTI.[90]

Leu100,[96] Tyr181,[97] and Tyr188[98] amino acid residues form a portion of the hydrophobic core of the binding pocket that interacts with Wing I of the ITU, DATA, and DAPY NNRTIs. Mutations of one or more of these amino acids can affect inhibitor-protein interactions and the size, shape, and chemical environment of the binding pocket.[90] Previous studies have shown that the Tyr181Cys[98] and Tyr188Leu[95] mutation affect the binding of an NNRTI by loss of favorable aromatic ring interactions. The Lys103Asn mutation possibly affects the kinetics of inhibitor-binding by stabilizing the unbound state of RT *via* the generation of an additional hydrogen bond between the Tyr188 phenoxyl group and the Asn103 side chain.[95]

As has been already discussed, the DAPY NNRTIs have improved potency when compared to other NNRTIs. Crystal structure analysis and molecular modeling studies have suggested a role for conformational flexibility in compensating for the effects of NNRTI-resistance mutations. To explain this, TMC128 complexed with RT will be discussed.

1.13.1 HIGH RESOLUTION STRUCTURES OF HIV-1 RT/TMC278 COMPLEXES

TMC278 (Fig. 1.30) is a diarylpyrimidine (DAPY) NNRTI that is highly effective in treating wild-type and drug-resistant HIV-1 infections in clinical trials at doses of ~25-75 mg/day.[77] In a recent PNAS[77] communication, Arnold and co-workers determined the structure of wild-type HIV-1 RT complexed with TMC278 at an 1.8 Å resolution (Fig. 1.30), using an RT crystal form engineered

by systematic RT mutagenesis. This was a remarkable feat considering that the underlying difficulty associated with crystallization of DAPY compounds lies in its effectiveness (position wiggling and jiggling) as an anti-HIV drug. Thus, the flexibility of the drug, and its binding mode, introduces heterogeneity into the periodic arrangement of RT/drug complexes in the crystal lattice.[88] Literally thousands of crystallization attempts failed and the 'best' crystals diffracted X-rays to only ~6.0Å resolution before crystal engineering strategies were employed. This high-resolution crystal structure revealed that the cyanovinyl group of TMC278 is positioned in a hydrophobic tunnel (Fig. 1.30) connecting the NNRTI-binding pocket to the nucleic acid-binding cleft,[77] this discovery being a vital component of this thesis.

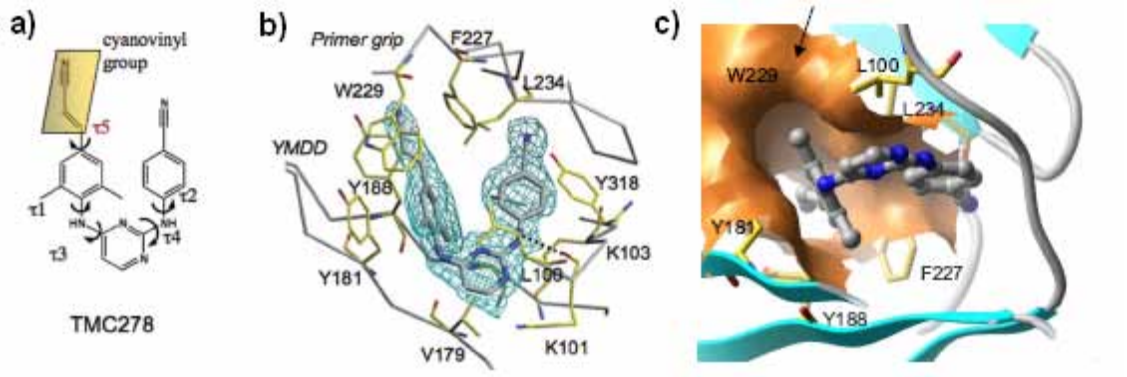

Figure 1.30 a) Chemical structure of TMC278. The τ angles define the torsional flexibility of TMC278, b) The position of TMC278 and conformation in complex with wild-type HIV-1 RT. The position and conformation were defined by the difference ($|F_o| - |F_c|$) electron density calculated at 1Å , c) The molecular surface (orange) defines the hydrophobic tunnel that accommodates the cyanovinyl moiety of TMC278.[77]

The crystal structures of TMC278 in complexes with the double mutant K103N/Y181C (2Å) and L100I/K103N HIV-1 RTs (2.9 Å) demonstrated that TMC278 adapts to bind mutant RTs. In the K103N/Y181C RT/TMC278 structure, loss of the aromatic ring interaction caused by the Y181C mutation is counter-balanced by interactions between the cyanovinyl group of TMC278 and the aromatic side chain of Y183.

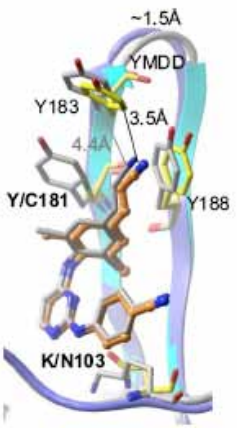

Figure 1.31 Superposition of K103N/Y181C mutant RT (cyan ribbon, yellow side chains)/TMC278 (orange) complex on wild-type RT (blue ribbon and gray side chain)/TMC278 (gray) complex.[77]

Furthermore, superposition of this structure onto the wild-type RT/TMC278 structure revealed moderate conformational changes for the bound TMC278, thus exemplifying its ability to adapt to mutations (Fig. 1.31).[77] The number of distances < 4.5 Å between pairs of atoms, one from RT and the other from TMC278, acts as an indicator of the extent of the hydrophobic interactions between RT and TMC278. In the K103N/Y181C mutant RT/TMC278 complex, the numbers of these distances tally 51, where as in the wild-type, it tallies 52. This clearly shows that the mutation has a negligible effect on tight and specific binding. A moderate tilting of the angle of τ3 by 5^{o} results in displacement of the dimethylphenyl-4-cyanovinyl group away from the mutated Y181C side chain. The once crucial aromatic interaction between the dimethylphenyl ring of TMC278 and the aromatic side chain of Y181 is lost, and a void is created by the mutation. Regardless of these mutations, TMC278 is still capable of inhibiting K103N, Y181C mutants, and the K103N/Y181C double mutant at an EC_{50} < 1 nM.[77]

In the L100I/K103N RT/TMC278 structure, the binding mode is significantly altered so that the drug conforms to changes in the binding pocket primarily caused by the L100I mutation. TMC278 inhibits the double mutant at an EC_{50} of ~8 nM. L100 is near the centre of the pocket and by default interacts with the pyrimidine ring in wild-type RT/TMC278 complexes; K103 is located on the other side of the pyrimidine ring (Fig. 1.30). When TMC278 binds to the mutant L100I/K103N mutant RT (Fig. 1.32), the drug undergoes major structural rearrangements compared to its wild-type RT binding. To avoid steric conflict with the L100I mutation, TMC278 shifts away from I100 and towards N103 and the entire molecule is displaced by 1.5 Å in the pocket.

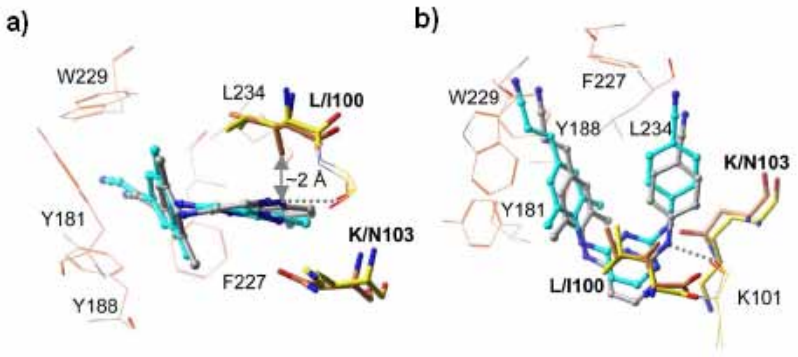

Figure 1.32 Comparison of L100I/K103N mutant RT/TMC278 (cyan) structure with the wild-type RT (yellow side chains)/TMC278 (gray) structures reveals wiggling (A) and jiggling (B) of TMC278.[77]

The number of distances < 4.5 Å between TMC278 and I100 is 12 in the complex with L100I/K103N mutant RT, which is appreciably less than the 28 and 30 distances in wild-type and the K103N/Y181C mutant. This is compensated by the number of protein-ligand distances < 4.5

Å for the residue 103. This increases from 16 and 17 in the wild-type and K103N/Y181C mutant structures, respectively, to 27 in the L100I/K103N mutant RT/TMC278 structure.[77]

Very importantly though, the recent discovery by Arnold of the opening to a tunnel connecting the NNRTI pocket and the NRTI substrate site has offered powerful support for the double-drug concept, a suggestion previously proposed by both Arnold[99] *et al* and Anderson[79e] *et al*. The first suggestion came from Arnold[99] *et al* in 1993 who wrote: "An interesting approach that would take optimal advantage of the currently available structural information would be to *design and synthesize inhibitors that would incorporate structural features from both nucleoside analogue and non-nucleoside inhibitors*…… Synthesis of these agents would be challenging, but there are a number of substituent positions that could be used for the linkage. Sites of attachment for the linkers to nucleoside analogues include sugar ring positions (e.g. 2', 3' and 5'-substitutions), extensions of mono-, di- and tri-phosphate esters, and positions on the nucleoside bases (e.g. the 5-position of pyrimidine rings). Selection of sites of attachment on the non-nucleoside moieties would vary according to the inhibitor type."

This was followed by a Science article in 1995 in which Anderson[79e] wrote: "We have established the mechanism of inhibition of RT by the three (clinically approved) NNRTIs. Athough the long-term inhibition of RT is limited by the high frequency of mutation of the enzyme, this detailed understanding of the action taken by RT when presented with these inhibitors (i.e. that binding of a NNRTI does not stop the binding process of a NRTI) should assist in the search for effective drugs to attenuate the AIDS virus. In particular, the interaction of the nucleotide binding site and the non-nucleoside inhibitor site may provide a means to increase the effectiveness of drugs used in combination therapy. *A single drug combining the functionalities of a nucleotide analogue and a non-nucleoside inhibitor would bind much more tightly because of the cooperative interactions between the sites.*" These two research contributions effectively gave birth to the field of HIV bifunctional double-drugs.

1.14 THE DOUBLE-DRUG STRATEGY

The double-drug strategy involves a chemotherapeutic approach which combines two different classes of inhibitor into a single molecular entity *via* a linker, with the aim of improving the physicochemical characteristics of the individual compounds.[100] Apart from HIV, the double-drug strategy has been employed in the synthesis of cancer,[101,102,103,104] malaria,[105,106,107] anti-inflammatory and cholinesterase[108] inhibitors, as well as in Alzheimers's[109] disease, for catechol-*O*-methyl transferase inhibitors[110] and bifunctional compounds targeted at thrombotic disorders.[111]

1.14.1 DOUBLE-DRUGS IN CANCER AND MALARIA

5-Fluoro-2'-deoxyuridine (FDU) either as its 5'-*O*-butanoate or as its 5'-*O*-butanoate-3'-*O*-retinoate (from retinoic acid) diester (Fig. 1.33) have been synthesized to act as anti-cancer double prodrugs that would serve as a means of releasing at least two active drugs that act through different mechanisms. The FDU, once released and phosphorylated, could act as a competitive inhibitor for thymidylate synthase whereas retinoic acid and butyric acid once released were expected to induce cell differentiation. The ester derivatives exhibited comparable activity to FDU.[101]

Retinoids have been reported to induce differentiation and arrest proliferation in a wide spectrum of cancer cells and are currently used for treatment of promyelocytic leukaemia. Butyric acid is an effective inhibitor of cell proliferation and inducer of cytodifferentiation. In the case of 5'-*O*-butanoate-3'-*O*-retinoate, a mutual prodrug combining butyric acid and *all-trans*-retinoic acid into FDU was evaluated for anticancer activity and was found to be more potent than the parent drugs.[102] Furthermore, the differentiation activity elicited by the double-drug was greater than that of the combined parent acids. The large increase in activity was attributed to two factors:

(i) The *all-trans*-retinoic acid fragment imparted lipophilicity and facilitated the penetration of butyric acid to the cellular target site.

(ii) The intracellularly released *all-trans*-retinoic acid and butyric acid affected the cells synergistically.

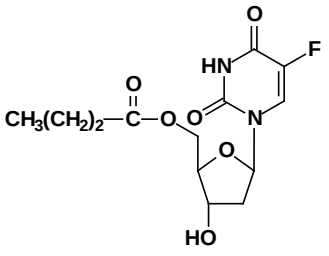

FDU-5'-*O*-butanoate

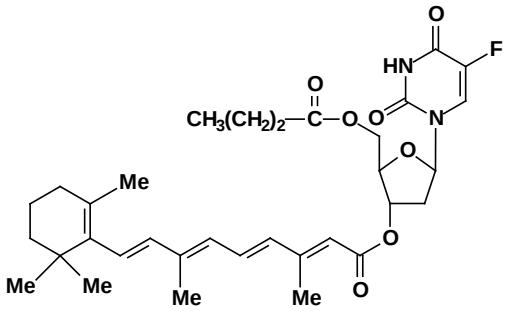

FDU-3'-*O*-retinoate-5'-*O*-butanoate

Figure 1.33 Examples of 5-Fluoro-2'-deoxyuridine (FDU) either as its 5'-*O*-butanoate or as its 5'-*O*-butanoate-3'-*O*-retinoate diester.

Similarly, the statine-based inhibitor of Plasmepsin (II) (PLM II) was linked to the antimalarial drug Primaquine (PQ) using a dicarboxylic acid linker (Fig. 1.34). PLM II is one of the aspartic proteases involved in the degradation of haemoglobin during the intraerythrocytic cycle of *Plasmodium falciparum*. Primaquine is highly active against all malaria species infecting

humans. Its toxicity levels can be minimised and its activity increased by converting it into a peptide prodrug. The PQ-Statine double-drugs showed remarkable improvement in the inhibition of both PLM II and *P. falciparum* growth in vitro. The double drugs kill the parasites mainly by inhibiting PLM II together with the digestion of haemoglobin that is essential for the survival of the parasite.[105]

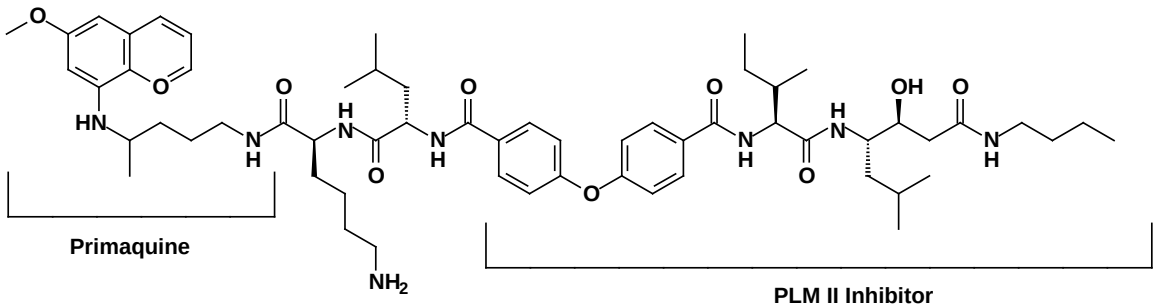

[Primaquine]-4,4'-oxy-bis(benzoic acid)-[PLM II]

Figure 1.34 [Primaquine]-4,4'-oxy-bis(benzoic acid)-[PLM II].

Biot *et al*.[106,107] synthesized double-headed antimalarial prodrugs (Fig. 1.35) that target two essential functions of the malarial parasite, namely glutathione regeneration and heme detoxification, with the aim of exploring their synergistic or additive effects. The double drugs combined a glutathione reductase (GR) inhibitor to a 4-aminoquinoline moiety with a bioreversible linker. However, these double-drugs exhibited poor inhibition activity.

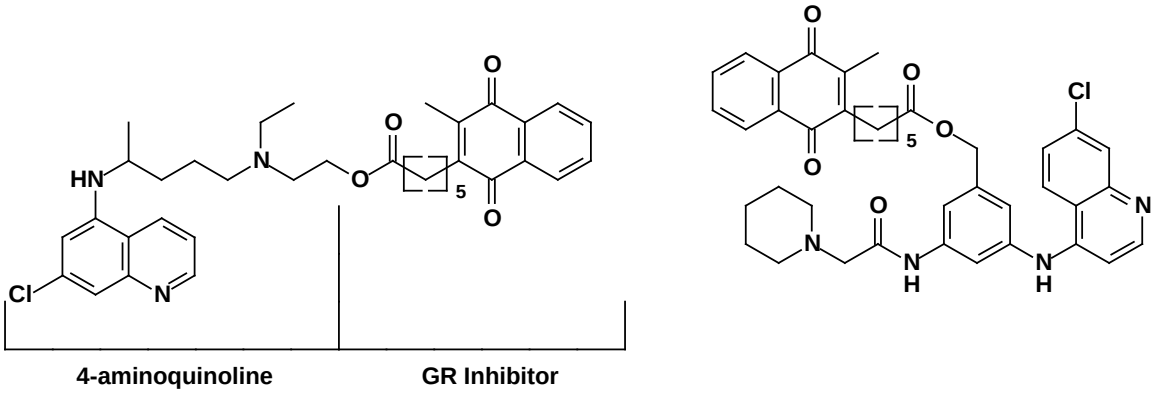

[4-aminoquinoline]-[GR Inhibitor]

Figure 1.35 Examples of double-headed antimalarial prodrugs.

1.14.2 DOUBLE-DRUGS IN HIV

Several strategies have been employed in the chemotherapy and chemoprophylaxis of HIV infections. The most effective current strategies involve the following targets: (i) CD4 as primary

cell receptor for viral entry into the cell; (ii) gp-120 as the viral glycoprotein involved in virus adsorption to the cells; (iii) CXCR4 and CCR5 as co-receptors for viral entry; (iv) gp-41 as viral glycoprotein required for virus-cell fusion; (v) NRTI binding site of the HIV reverse-transcriptase (RT) enzyme; (vi) NNRT binding site of RT; (vii) integration of the proviral DNA into the host genome by the HIV integrase; (viii) proviral DNA expression (ix) HIV protease as mentioned in Section 1.7.[23] Based on a combination of inhibitors for these targets, double-drug inhibitors of HIV can be divided into the following classes:

(A) *Fused:* Two drugs fused together to create a single entity that is active on each drug-target corresponding to the individual drugs.
(B) *Cleavable:* Two drugs joined by a cleavable (*via* hydrolysis) linker (spacer) that can target either the same or different drug-target. The cleavable linkers are stable outside the target cell, but are cleaved to individual drugs once in the cell cytoplasm.
(C) *Non-cleavable:* Stable (to hydrolytic cleavage) bifunctional entity ("mixed-site inhibitors") whose rationale is to bind the drug entities simultaneously at distinct binding sites that are in close proximity on the same drug target.

(A) FUSED DOUBLE-DRUG INHIBITORS FOR RT AND INTEGRASE (IN)

Vince and co-workers synthesized fused double-drug inhibitors, also referred to as "*portamanteau inhibitors*" based on the fusion of a non-nucleoside reverse transcriptase (RT) inhibitor (NNRTI) with a diketoacid (DKA) integrase (IN) inhibitor pharmacophore.[112] The best double-drug (Fig. 1.36) had a low cytotoxicity (EC_{50}: 24 nM against RT; 4.4 µM against IN; 10 nM against HIV-1 in a cell-based assay; CC_{50} = > 10 µM; SI = > 1000).[113]

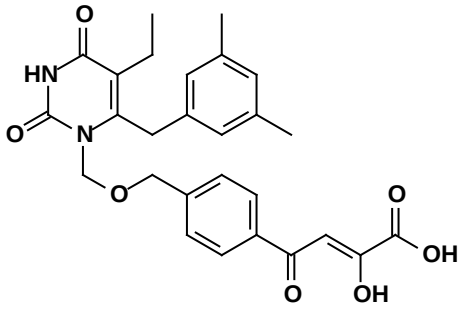

Figure 1.36 Structure of a portamanteau inhibitor combining an RT inhibitor with an IN inhibitor.

(B) CLEAVABLE DOUBLE-DRUG INHIBITORS

These have been by far the most common type studied with the emphasis on the synergistic effects of the two drugs released in combination.

(i) NRTI / Co-receptor antagonist as double-drugs

A combination of an HIV protease inhibitor and AZT into a single molecule has also been successfully used to improve poor membrane permeation. The protease inhibitor, KNI-727, unable to penetrate the cell membrane, was linked to AZT by a cleavable linker (Fig. 1.37) resulting in a boost in potency according to a MTT-cell assay by virtue of the parent components being released intracellularly (EC_{50} = 5.3 nM for the double drug, compared to 92.0 nM for KNI-727 and 6.2 nM for AZT).[114]

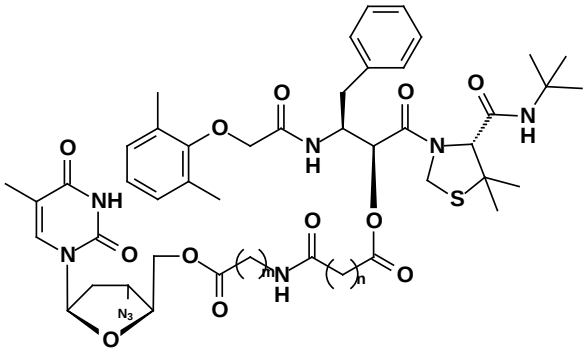

m=1, n=2

[AZT]-succinic-[KNI-727] conjugate

Figure 1.37 Structure of the [AZT]-succinic-[KNI-727] conjugate.

Similarly, Tamamura *et al.*[115] employed the double-drug strategy to synthesize a bifunctional drug that incorporated a CXCR4 inhibitor (T140) as a co-receptor antagonist with an NRTI (AZT) linked by succinate. T140 is a 14-amino acid peptide which inhibits infection of target cells by T cell-line-tropic strains of HIV through specific binding to its chemokine receptor, CXCR4. An equimolar mixture of AZT and T140 caused a significant increase in anti-HIV activity compared to the single compounds (Fig. 1.38). This result led to the synthesis of conjugated compounds which combined each entity into a single molecule. The conjugated drug exhibited a synergistic effect for anti-HIV in vitro (EC_{50} = 4.6 nM in MT-4 cells with HIV-1, SI = > 4300; AZT = 20 nM; T140-succinic acid = 310 nM). The mechanism of action is based on the hydrolysis of the enzymatically labile ester 5'-*O*-bond between the NRTI and the spacer.

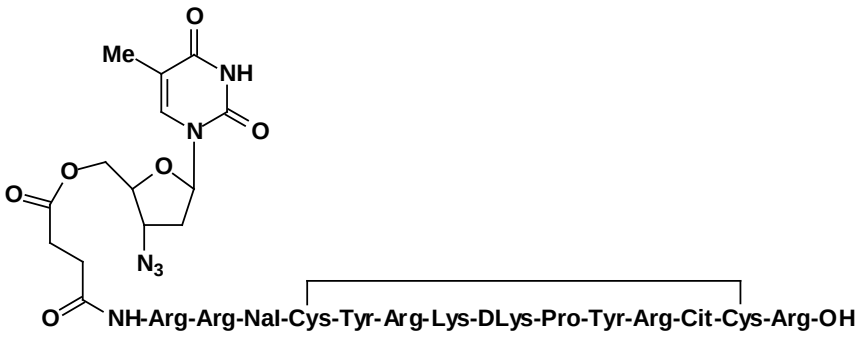

[AZT]-succinate-[T140]

Figure 1.38 Structure of the [AZT]-succinate-[T140] conjugate.

Daoudi *et al*.[116] synthesized bifunctional compounds combining bicyclam AMD3100 and a galactosylceramide (GalCer) analogue in a single molecule with the aim of inhibiting several steps of the complex virus/cell cascade interactions (virus-cell adsorption/fusion processes). The double-drug [Gal]-[AMD3100] conjugate (Fig. 1.39) exhibited superior potency to that of AMD3100 (EC_{50} = 0.065 μM in MT-4 cells with HIV-1; AMD3100 = 2.9 μM; GalSer = > 100 μM). AMD3100 is a CXCR4 antagonist and interferes with viral binding to the cellular co-receptors, whereas GalCer provides an attachment platform (alternative receptor in $CD4^-$ cells) for the virus (through its gp-120 and/or gp-41) onto the cell. When compared to the activity of GalSer, the bipharmacophore conjugate moderately increased its anti-HIV activity.

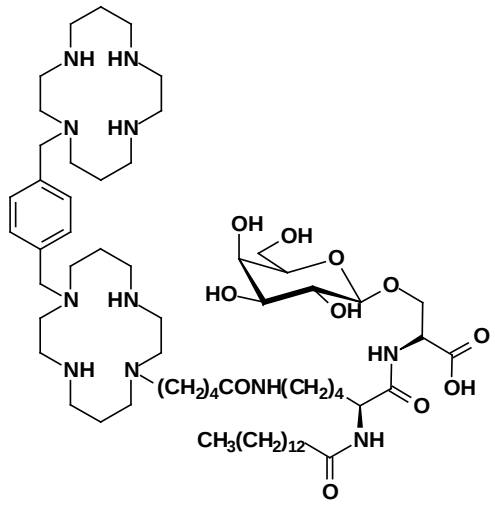

Gal-AMD3100 Conjugates

Figure 1.39 Structure of the Gal-AMD3100 conjugates.

Similarly, AZT coupled onto k-carrangeenan using a succinate diester spacer (Fig. 1.40) was synthesized with the aim of enhancing AZT intracellular uptake as well as to test the synergism of the prodrug.[117] Carrageenans are naturally occurring sulphated polysaccharides extracted

from different species of red seaweed that have a common structural backbone of D-galactose residues. The k-form is characterised by a repeating unit of 4-sulfate-b-D-galactopyranose linked 1® 3 and 3,6-anhydro-a-D-galactopyranose linked 1® 4.

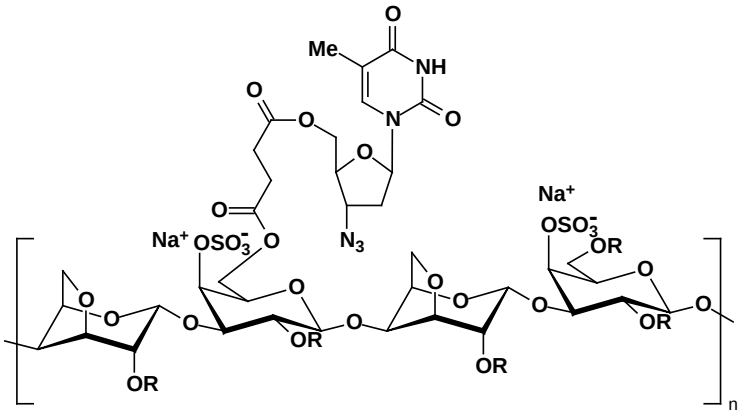

R = H or 5'-O-(succinate)-AZT

[AZT]-succinate-[k-carrageenan]

Figure 1.40 Structure of [AZT]-succinate-[k-Carrangeenan Conjugates].

The k-carrangeenan was expected to act not only as a drug-delivery carrier for AZT, but also as an anti-HIV agent which would act synergistically with AZT. Carrangeenans possess anti-HIV activity and inhibit the binding of the virions to the cell as gp-120 adsorption inhibitors, as well as cell-to-cell fusion inhibition. The [k-carrangeenan]-succinate diester-[AZT] conjugate inhibited the binding of the virions to the MT-4 cells and concomitantly delivered AZT to these cells to further inhibit the RT (EC_{50} = 6.8 nM, SI = 3000; AZT = 25 nM).

(ii) Reverse Transcriptase Double-Drugs

- NRTI homo/heterodimers

Several NRTI homo- and heterodimers targeting the HIV reverse transcriptase enzyme have been synthesized by attaching the linker at the 5', 5 or N-3 positions of the nucleosides. Ijichi *et al*.[118] have reported the synthesis of nucleotide heterodimers of AZT, ddI and Ribavirin. The dimers were formulated as a mixed phosphate diester via the 5'-hydroxyl groups of the nucleoside, with the aim of releasing two nucleosides at the active site. Thus, 5'-*O*-phosphorylation of AZT gave AZT cyanoethyl phosphate **1**, which condensed with ddI **2** in the presence of *p*-toluenesulfonyl chloride to afford heterodimer [AZT]-cyanoethylphosphate-[ddI] **3**. Deprotection of the cyanoethyl group with 1N NaOH led to the heterodimer **4** (Scheme 1.1). Similarly, [ddI-phospho-Ribavirin] **5** (EC_{50} > 17.5 mM) and [AZT-phospho-Ribavirin] **6** (EC_{50} = 0.004 mM) heterodimers (Fig. 1.41) were synthesized using the same procedure. The

heterodimers **4** and **6** showed enhanced anti-HIV activity relative to their monomers. Furthermore, AZT-P-ddI **4** (EC_{50} = 0.002 mM, CC_{50} = 18.2 mM) was ~2-fold more toxic than AZT to human granulocytes macrophage progenitor cells (EC_{50} = 0.002 mM, CC_{50} =10.7 mM) for AZT; EC_{50} = 13.3 mM, CC_{50} = 226 mM for ddI).

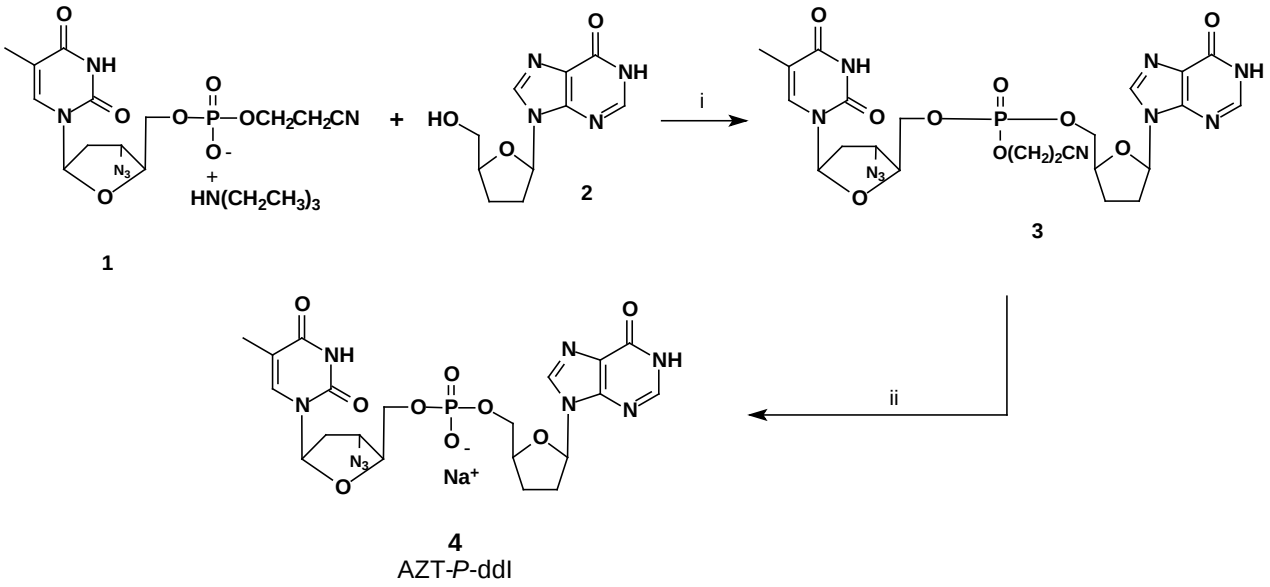

Scheme 1.1 *Reagents and Conditions*: (i) *p*-TsCl, CH_2Cl_2 (ii) NaOH.

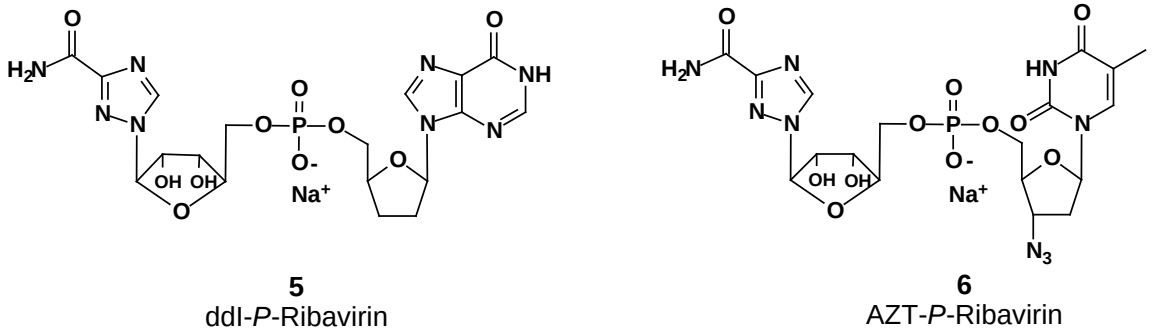

Figure 1.41 Structures of AZT, ddI, Ribavirin and HEPU heterodimers.

In a similar fashion, homo- and heterodimers of ddI, AZT and d4T have been synthesized by Mohamed *et al*.[119] with the aim of enhancing the antiviral activity of their components (Scheme 1.2). An ester linkage was used to link to a glutaric acid spacer. The synthetic strategy involved converting d4T **7** into half ester **8** by treatment with glutaric anhydride in methylene chloride, followed by an EDC-promoted esterification of the glutarate with ddI to form the heterodimer **9** in good yield (Scheme 1.2). AZT-ddI and ddI-ddI heterodimers bearing an ester linkage were also synthesized using this methodology. Other spacers used in this class of compounds were carbonate and carbamate-based to form AZT and d4T homo- and heterodimer carbonates **10**

and carbamates **11**, respectively (Fig. 1.42). Following intracellular hydrolysis of the carbonate or carbamate, the two nucleosides would be regenerated in the cytoplasm. The carbonates displayed anti-HIV activity comparable to AZT, while the carbamates displayed low anti-HIV activities. No synergistic effects on the inhibition of HIV replication was detected for either the carbonates **10a-c** and carbamates **11a-c**.

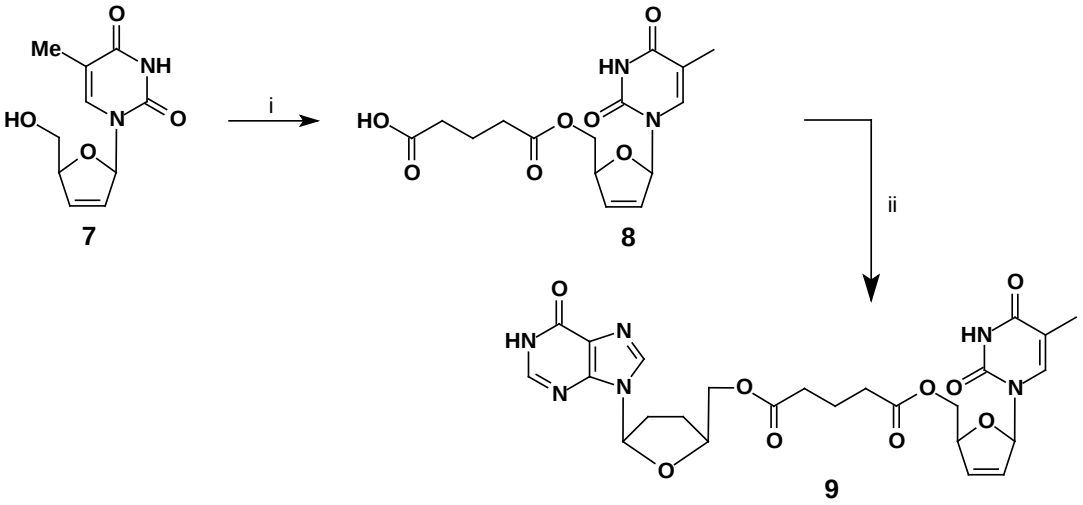

Scheme 1.2 R*eagents and Conditions*: (i) Glutaric anhydride, Et_3N, CH_2Cl_2; 85%. (ii) ddI/DMAP/EDC, HCl, CH_2Cl_2/DMF; 80%.

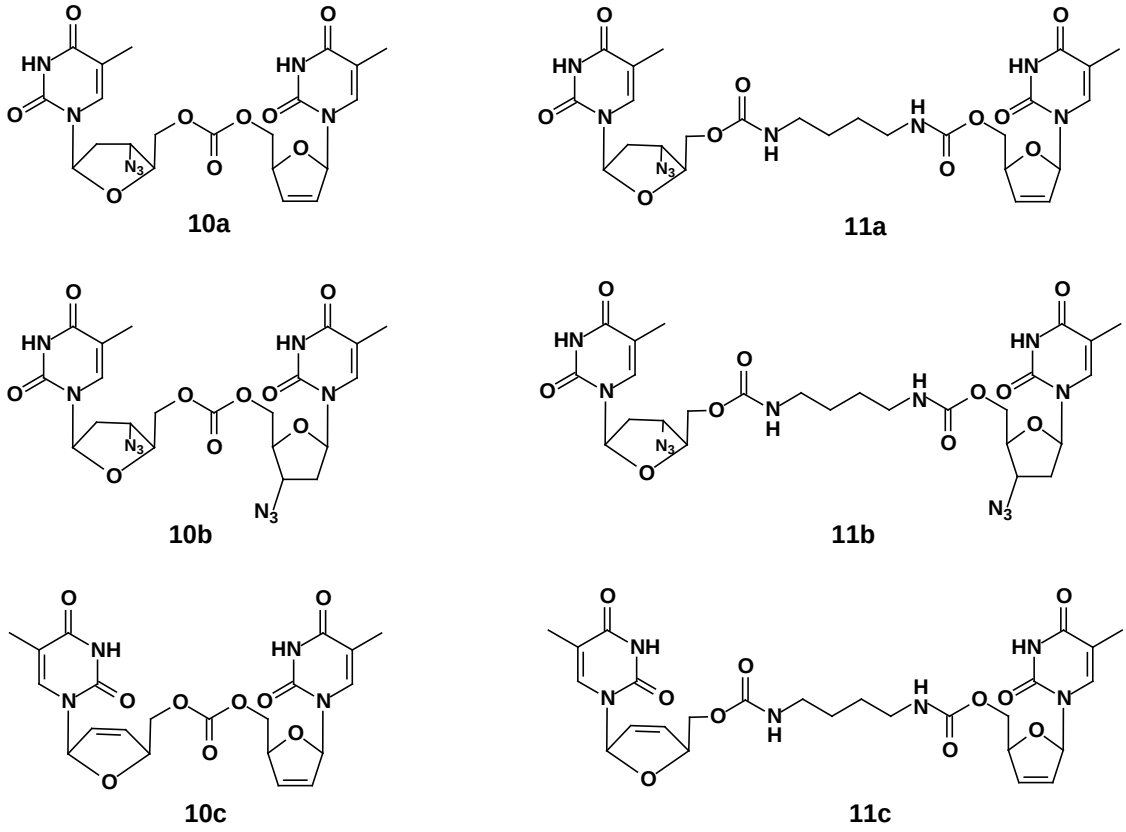

Figure 1.42 Structure of AZT/d4T homo- and heterodimer linked by a carbonate or carbamate spacer.

Similarly, the Ladurée group has reported the synthesis of a NRTI/NNRTI heterodimer of the formula [NRTI]-Glycyl-Succinyl-[Trovirdine].[120] Nucleosides d4U, d2U and d4T were varied as the NRTI and spacer linking was achieved via the C-5' hydroxyl group of NRTI with the *N*-piperazine of trovirdine. A succinyl-glycine moiety was chosen as a spontaneously cleavable linker, and introduced via coupling of the NRTIs with Boc-gly-OH using DCC in the presence of DMAP in DMF to give the 5'-esters **12**. Deprotection of Boc using 4M HCl/dioxane afforded the amine hydrochlorides **13** which were condensed with trovirdine analogue derivatives **14** using BOP/HOBt in the presence of triethylamine in DMF to afford the heterodimers **15 a-c** in 35-45% yield. The heterodimers were unfortunately devoid of antiviral activity at non-toxic concentrations (Scheme 1.3).

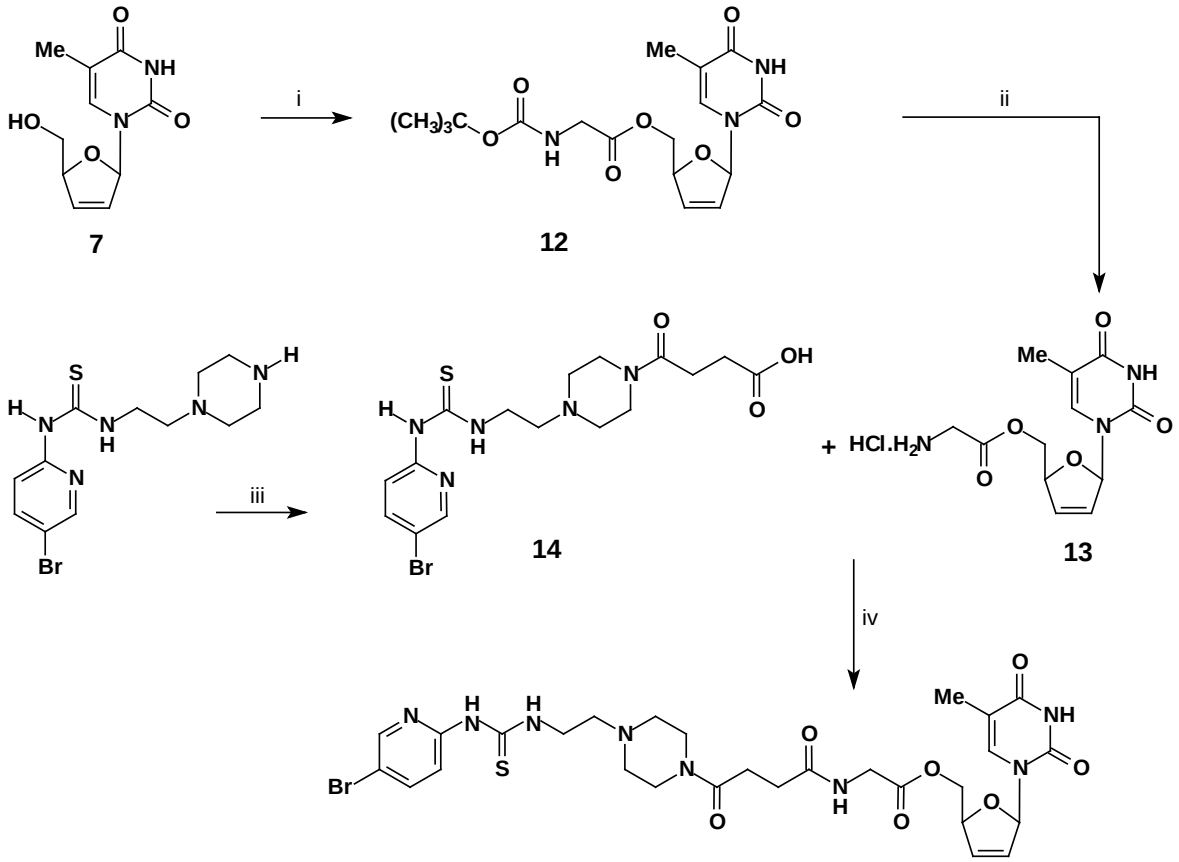

Scheme 1.3 *Reagents and Conditions*: (i) HOOC–CH_2–NHBoc, DCC, DMAP, DMF; 78%. (ii) 4M HCl/Dioxane; 87%. (iii) succinic anhydride, CH_2Cl_2; 64%. (iv) Et_3N, HOBt, BOP, DMF; 35-45%.

The synthesis of an analogous system using C-5/NRTI as the attachment point[121,122] (Scheme 1.4) was accomplished employing a Sonogashira reaction. Pd(0)-mediated Sonogashira coupling at C-5 of **16** with a C-3 propynyloxy spacer protected as its THP ether produced **17**.

Deprotection of THP using CF_3COOH in CH_2Cl_2 followed by condensation of the resultant alcohol with Boc-Gly-OH using DCC in the presence of DMAP and subsequent deprotection of the Boc group using 4M HCl in dioxane afforded the amine hydrochloride **18**. Condensation of amine **18** with trovirdine derivative **14** followed by deprotection of the acetate group with cyanide ion gave the heterodimer **20** in 35-45% yield for the last step. The heterodimers displayed inferior anti-HIV activity (compound **20** displayed an IC_{50} > 20 mM) compared to the parent compounds. The lack of activity was attributed to the wrong positioning of the linker to either NRTI or NNRTI with respect to their active sites in the enzyme.

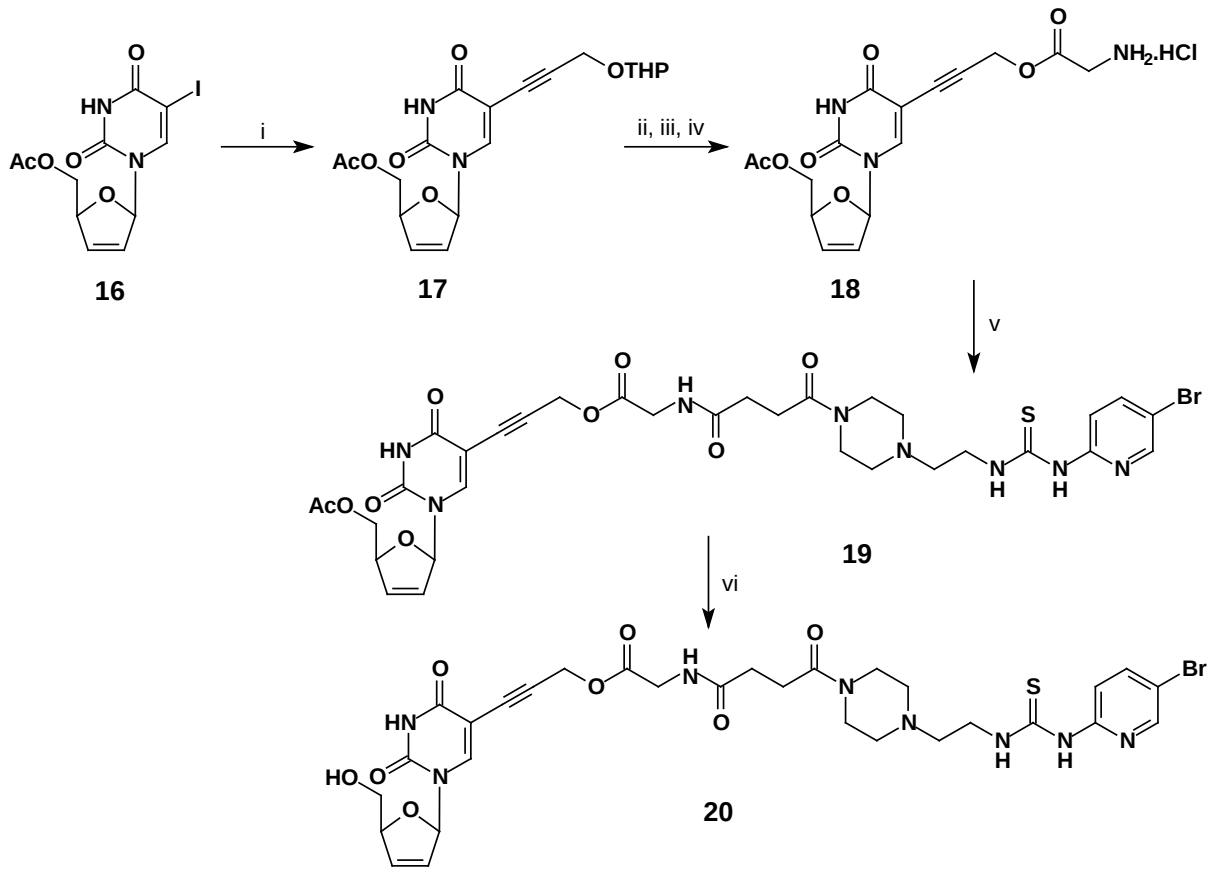

Scheme 1.4 *Reagents and Conditions*: (i) alkyne, $(PPh_3)_4Pd$, CuI, Et_3N, DMF; 67%. (ii) CF_3COOH, CH_2Cl_2, CH_3OH (iii) $HOOC–CH_2–NHBoc$, DCC, DMAP, DMF (iv) 4M HCl/Dioxane (v) **14**, Et_3N, HOBt, BOP, DMF; 48%. (vi) NaCN, MeOH; 38%.

Pederson *et al*.[123] has been recently reported the synthesis and antiviral activities of cleavable NRTI/ NNRTI double-prodrugs against HIV based on the mixed S-acyl-2-thioethyl (SATE) prodrug approach. The SATE prodrugs were first introduced in 1993 by Imbach. *et al*.[124] as a carboxyesterase-labile protecting group for the ddU nucleotide. The double pro-drug in question incorporated d4T as a 5'-phosphate and as a SATE ester linking through the phosphate to N-3 of MKC-442 (a HEPT derivative) via a cleavable *p*-hydroxybenzoyl linker. The double-prodrug

(fig 1.4) had good activities against HIV-1 (EC_{50} = 0.03 µM) and the Y181C mutant strain (EC_{50} = 2.7 µM). The activity was attributed to the NNRTI (MK-442) part of the molecule (Fig. 1.43).

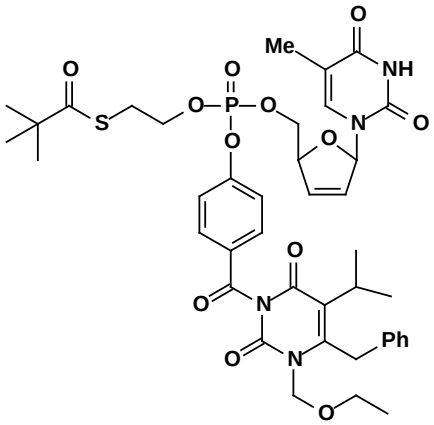

Figure 1.43 Structure of Pedersen's SATE-prodrug.[123]

(C) NON-CLEAVABLE DOUBLE-DRUG INHIBITORS (MIXED-SITE INHIBITORS)

- NRTI/NNRTI heterodimers

The combination of a nucleoside and a non-nucleoside RTI into a single molecular entity was advocated by Nanni *et al* in 1993.[99] This was supported by structural[99] and biochemical[125] studies which indicated that linking the compounds with an appropriate spacer might result in an improved inhibitory capacity. The first heterodimers incorporating an NRTI with an NNRTI were synthesized by the Camarasa group in 1995.[126] They reported the synthesis of a family of anti-HIV heterodimers based on combining AZT with either TSAO-T or HEPT via a polymethylene spacer between the N-3 of the thymine base of both compounds (Scheme 1.5). TSAO derivatives were first synthesized in 1992 and represent a unique structural class of NNRTI as they specifically interact at the interface between the p51 and p66 subunits of HIV-1 RT. The prototype compound of this family is the thymine derivative designated TSAO-T and the most selective compound is its 3-*N*-methyl substituted derivative TSAO-m^3T. The synthetic strategy for formation of **22** and **23** involved selective N-3 alkylation of AZT with a dibromoalkyl reagent followed by N-alkylation of the N-3-bromoalkyl AZT intermediate with TSAO-T or HEPT. The polymethylene spacer was varied in length from n = 3-6. Thus, treatment of AZT with 2 equiv of 1,3-dibromopropane in dry acetone:DMF (1:1) in the presence of K_2CO_3 gave the N-3 substituted derivative **21**. Subsequent reaction of **21** with TSAO-T or HEPT under basic conditions gave heterodimers **22** and **23** in 50-60% yield.

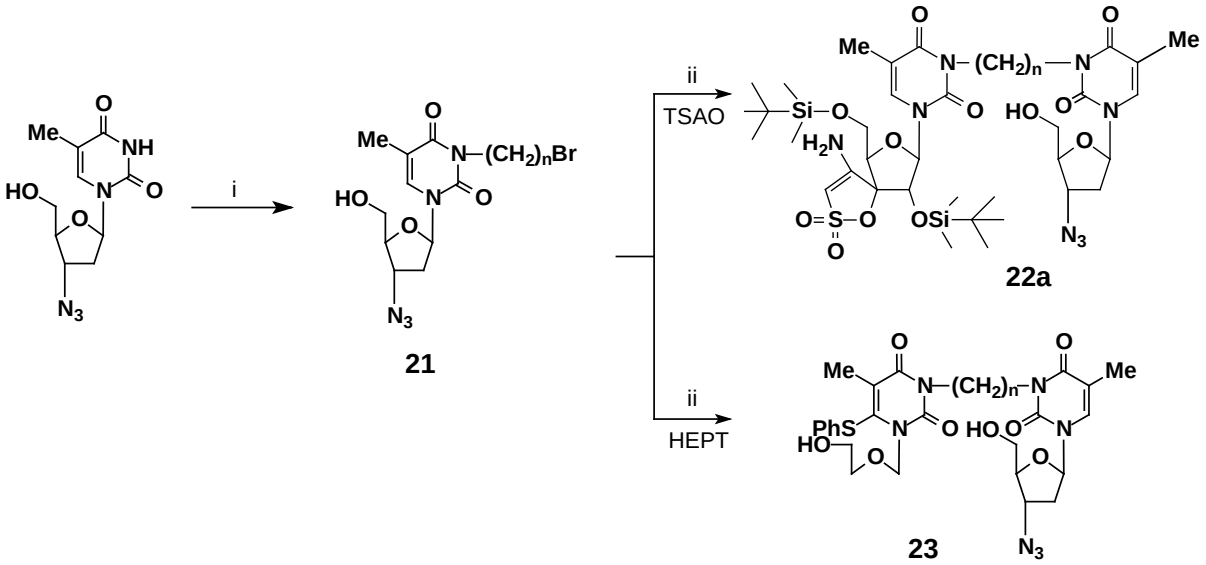

Scheme 1.5 *Reagents and Conditions*: (i) $(CH_2)_nBr_2$ (n = 3-9), K_2CO_3, acetone, DMF (1:1). (ii) K_2CO_3, acetone, DMF (1:1).

The most active compound in the series was [TSAO-T]-$(CH_2)_3$-[AZT] **22a** (EC_{50} = 0.10 mM; TSAO-T = 0.06 mM; AZT = 0.006 mM) incorporating a short spacer. Heterodimers bearing polymethylene linkers [-$(CH_2)_n$-] with n = 4-6 showed good antiviral activity, while longer spacers with n > 7 showed diminished activity. The precursors to the dimers were also tested. Specifically, AZT derivatives such as **21** proved inactive irrespective of the chain length of the methylene spacer. The activity of the TSAO-T-spacer derivatives **22d** decreased with increasing length of the spacer. Replacement of AZT with d4T resulted in improved anti-HIV activity. No marked differences in activity were observed when the spacer consisted of 1-butynyl, 1-butenyl or ethoxyethyl moieties. Similarly, heterodimers **22b**,**c** were synthesized using the C-5 of the NRTI for attachment, and these showed comparable activities to that of **22a**, whereas the corresponding d4T analogue of **22b** led to a 5-fold decrease in anti-HIV potency.

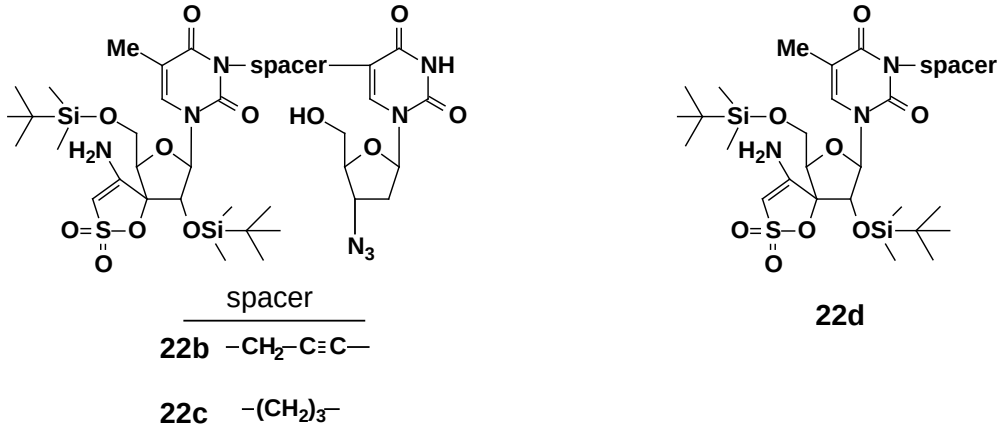

Figure 1.44

Spacer rigidity in the C-5 series did not markedly influence the antiviral potency since the heterodimer **22c** bearing a flexible propyl group as spacer was endowed with anti-HIV-1 activity comparable to that of the corresponding propynyl analogue **22b** (Fig. 1.44). Converting AZT, d4T and thymidine heterodimers to phenoxyphosphoramidate[127] prodrug heterodimers had no improved activity over the corresponding non-phosphorylated analogues. Overall, the d4T heterodimers had better inhibitory efficacy than the AZT ones.

By comparison, combinations of TSAO-m^{3}T and foscarnet (PFA) (Fig. 1.45) also synthesized by the Camarasa group as individual entities at a variety of concentrations revealed that these compounds displayed additive antiviral activity.[128] These results inspired the synthesis of a single molecule combining a TSAO derivative with foscarnet through a labile phosphate ester bond. PFA is an effective antiviral agent approved for intravenous treatment of Human Cytomegalovirus (HCMV) Retinitis in patients with AIDS.[129] It is also effective against HIV replication and inhibits HIV-1 RT by blocking the pyrophosphate binding site.[130]

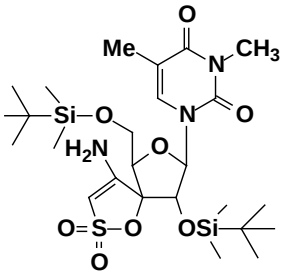

TSAO-m^{3}T

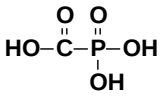

Phosphonoformate (PFA)

Figure 1.45 Structure of TSAO-m^{3}T and Foscarnet.

Thus, treatment of TSAO derivative **24** with the foscarnet-based phosphorylating reagent **25** in the presence of triethylamine led to the formation of the PFA diester **17** in moderate yield. Catalytic hydrogenolysis of **26** yielded the [TSAO-T]-[PFA] conjugate **27** in 60% yield (Scheme 1.6). Unfortunately, conjugate **27** was less active than the parent compound **24**, displaying no additive or synergistic anti-HIV activity and thus indicating the activity to be due to the TSAO part of the molecule and not the PFA part.

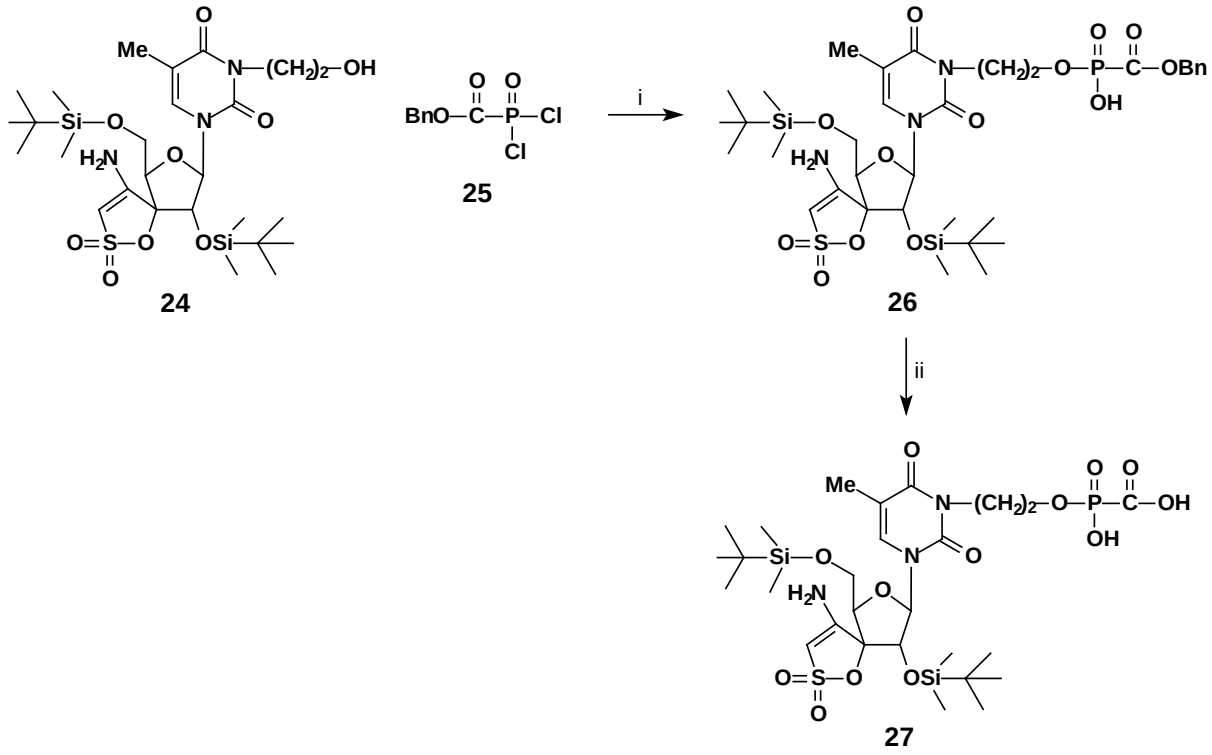

Scheme 1.6 *Reagents and Conditions*: (i) (a) **25**, Et_3N, CH_2Cl_2, -20 °C (b) H_2O; 54%. (ii) H_2, Pd/C, MeOH; 60%.

The design, synthesis and anti-HIV-1 evaluation of several non-cleavable heterodimers of the general formula [d4T]-NH$(CH_2)_n$–NH-[imidazo[1,5-b]pyridazine] (n = 6-12) involving a C-5 linkage to d4T was reported by Ladurée *et al*.[131] in 1998. Imidazo[1,5-*b*]pyridazine was chosen as the NNRTI due to its exceptional potency. The synthetic strategy involved synthesis of the NNRTI linked to a 1,n-diaminoalkyl spacer followed by substitution onto d4T via a C-5 chloromethyl group. The synthesis of the d4T coupling derivative (Scheme 1.7) involved C-5 hydroxymethylation of protected uridine **29** to give **30** in good yield followed by C-2'/3' double-bond introduction to afford **31** and selective chlorination of the hydroxymethyl group in the presence of the C-5' hydroxyl group of **31** to give **32**.

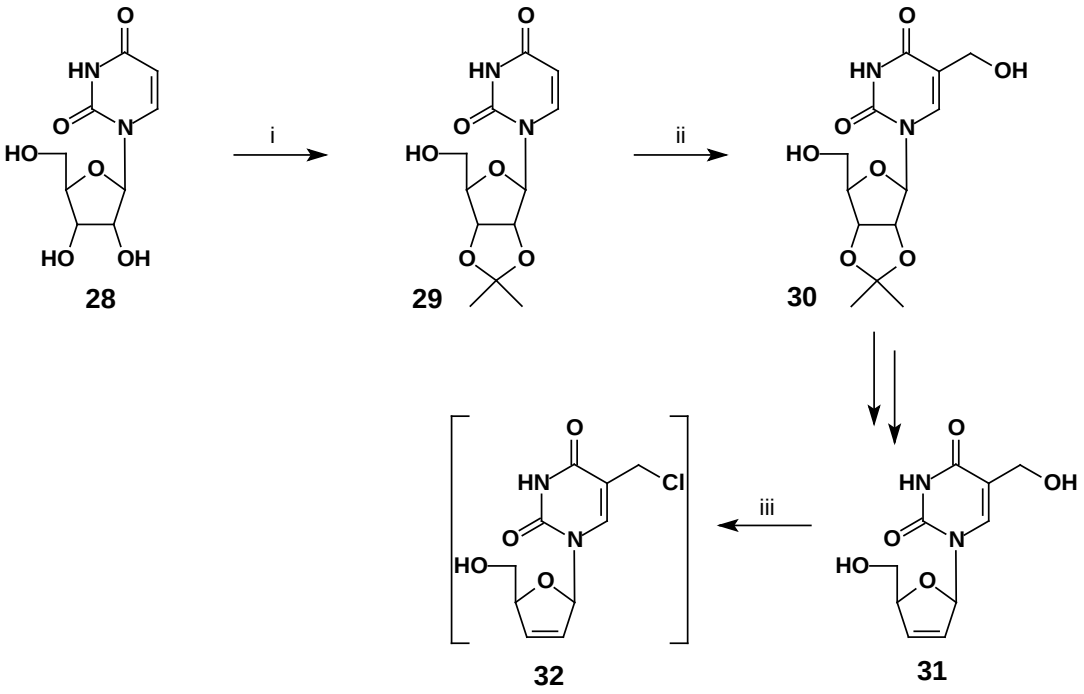

Scheme 1.7 *Reagents and Conditions*: (i) 2,2-DMP, APTS, MeCOMe. (ii) CH_2O, Et_3N, 60 °C; 93%. (iii) TMSCl, 1,4-dioxane, 60 °C.

Imidazo[1,5-*b*]pyridazine **33** was synthesized in seven steps from alanine, and was heated with a 1,n-diaminoalkane at 120 °C to give monomers **34a-d** via aromatic nucleophilic substitution. Condensation of **34a-d** with **32** in DMF gave heterodimers **35a-d** in 72-85% yield (Scheme 1.8). The anti-HIV activity of the NNRTI linked to its spacer **34a-d** was evaluated independently and the results revealed a decrease in activity compared to the unsubstituted NNRTI. The activity of the heterodimers **35a-d** was comparable to that of d4T and thus mainly due to the nucleoside part of the molecule.

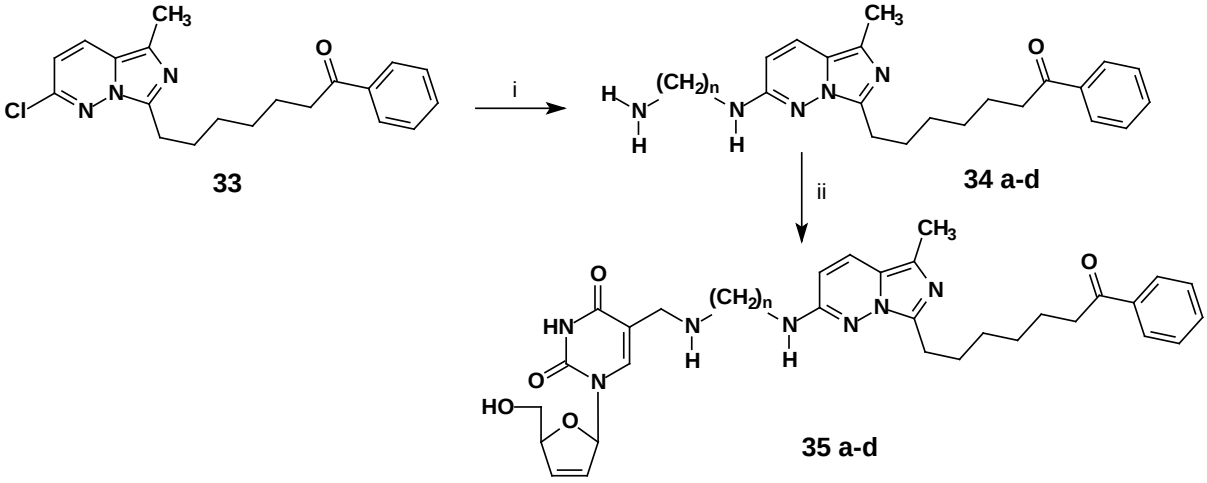

Scheme 1.8 *Reagents and Conditions*: (i) $H_2N–(CH_2)_n–NH_2$; a: n=6, b: n=8, c: n=10, d: n=12. (ii) d_4ClMUrd **32**, DIEA, DMF.

Similarly in 2000, Monneret and co-workers[132] synthesized a variety of (N-3 and C-5)AZT -HEPT bifunctional conjugates displaying anti-HIV activity ranging between 2-5 μM. In the same report, a non-cleavable ddC-HEPT conjugate was found to exhibit an anti-HIV potency of 0.45 μM against HIV-1 (wild-type and the Y181C nevirapine-resistant strain) and HIV-2 in cell culture. The ddC component in the mixed inhibitor **38** (Scheme 1.9) was prepared in a one-pot procedure (33% yield), involving reaction of 5'-*O*-acetyl-2',3'-dideoxyuridine **36** with triisopropylbenzenesulfonyl (TPS) chloride, followed by treatment with 1,12-diaminododecane. Coupling of amino derivative **37** with **37a** using *N*-methylmorpholine (NMM) and 2-chloro-4,6-dimethoxy-1,3,5-triazine (CMDT) provided **38** in good yield.

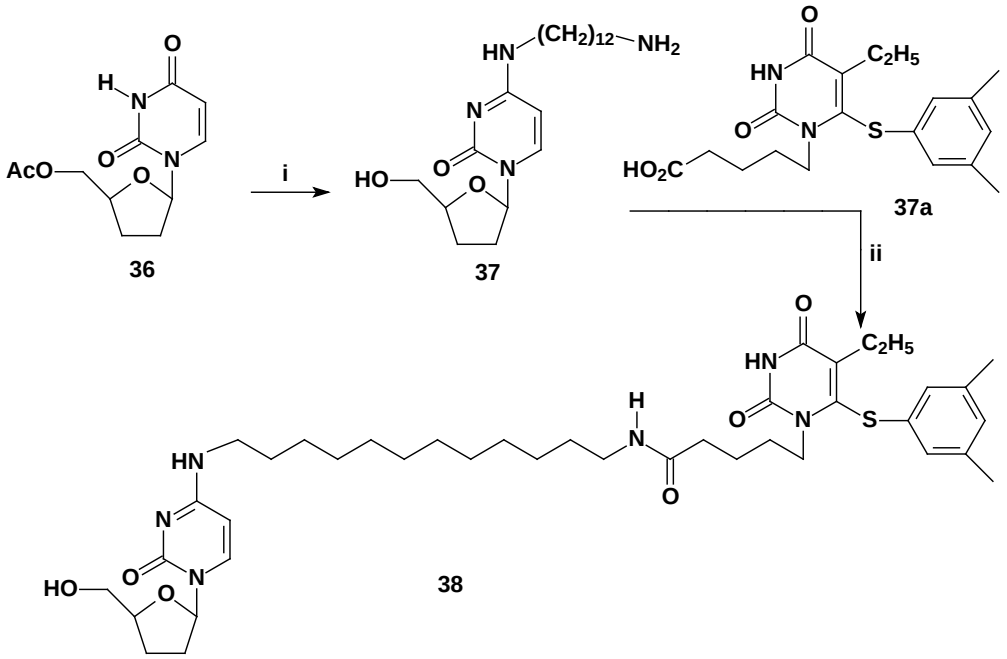

Scheme 1.9 *Reagents and Conditions*: (i) TPSCl, Et_3N, DMAP, DCM, then $NH_2(CH_2)_{12}NH_2$ (33%); (ii) CDMT, NMM, DMF, then **37a** (69%).

No synergistic effects were observed, and **38** appeared to inhibit RT through interaction of only one component (NNRTI) in its bis-substrate structure. A plausible reason offered by the authors is that the tethering arm is poorly adapted to permit the nucleoside and the NNRTI motifs to communicate simultaneously with their respective sites.

In 2006, Hunter and co-workers[100] reported the synthesis of [d4U]-butyne-[HI-236] as a non-cleavable, bifunctional NRTI/NNRTI HIV-1 reverse transcriptase inhibitor. The Sonogashira coupling partner **40** was synthesized by iodinating 5'-*O*-benzoyl d4U **39,** which was prepared in four steps from uridine according to the Bristol-Myers Squibb procedure for producing d4T from 5-methyluridine. Iodination of **39** was accomplished using elemental iodine and ceric ammonium

nitrate (CAN) in acetonitrile at 60°C in 80% yield (Scheme 1.10) to afford **40**, which underwent Sonogashira coupling with alkyne **41** to yield the desired coupled product **42** in 69% yield. With **42** in hand, benzoyl deprotection, Boc removal and thiourea installation remained for completion of the synthesis, and a number of permutations were tried out. Eventually, it was established that debenzoylation as the final step worked best, as the protected alkylated d4U moiety appeared to be less prone to acid-catalysed anomeric cleavage with the trifluoroacetic acid used to deprotect the Boc group. Thus deprotection of the Boc group of **42** using trifluoroacetic acid in methylene chloride at 0 °C furnished the crude amine as a trifluoroacetate salt. Processing involved adding Hünig's base to liberate the amine, and condensing directly with thiocarbonyl derivative **43** at rt overnight in THF. This contrasted with the much harsher conditions used by Bell and co-workers of heating in DMF at 100 °C. In this fashion, bifunctional benzoate **44** was produced in 60% for the two steps.

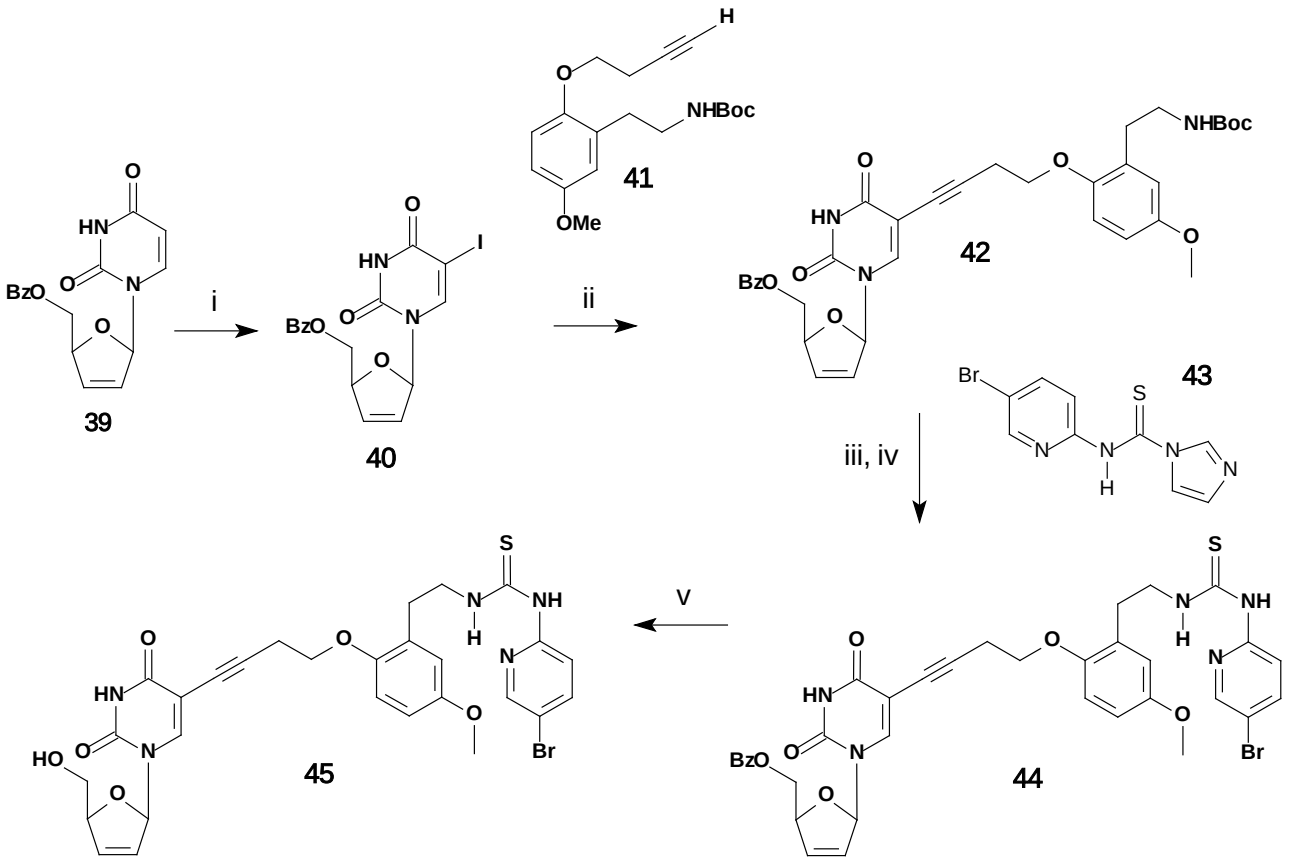

Scheme 1.10 *Reagents and Conditions:* (i) I_2, CAN, CH_3CN, 60 °C, 1 h (80%); (ii) alkyne **38**, $(PPh_3)_4Pd$ (10%), CuI (50%), Et_3N (2 eq.), DMF:THF (1:2), rt, 4 h (69%); (iii) CF_3COOH, CH_2Cl_2, 0 °C; (iv) $EtN(i\text{-}Pr)_2$ followed by **40**, THF, rt / overnight (60% for 2 steps); (v) NaOMe (cat), MeOH, 0 °C, 20 min (51%).

Final deprotection with catalytic methoxide in methanol furnished the target **45** in 51% yield and in an acceptable level of purity after chromatography. The inhibition of viral replication in HIV-

infected cells of the prototype bifunctional compound **45** was found to be 0.25 μM. The biological results (EC_{50} = 0.0048 μM for HI-236; d4T = 1 μM) led to the conclusion that the prototype compound **45**, as with the Monneret compound **38** in Scheme 1.9, behaves as an extended NNRTI with no synergistic effects.

In conclusion, most approaches have pursued the easier synthetic option of connecting the tether via the C-5' OH or N-3 of the nucleoside base. For the C-5 heterodimers, linker attachment has been achieved via a Pd(0) Sonogashira coupling (compound **20**) or hydroxymethylation of uridine (compound **35a-d**). Most of the heterodimers were designed as prodrugs linked with a cleavable tether, with the aim of regenerating the parent drugs once in the cell cytoplasm. Non-cleavable systems have as yet not demonstrated the mixed-site synergistic principle, probably as a result of inappropriate choice of the positioning of the spacer attachment.

Crucial to this thesis, was the use of either d4T or d4U as the NRTI Sonogashira coupling partner used in most of the syntheses covered above, thus strategies towards this important coupling partner will be discussed in next.

1.15 STRATEGIES USED IN THE SYNTHESIS OF D4T

Horwitz *et al*.[133] reported the first synthesis of d4T **7** in 1964 as a potentially novel anti-cancer drug. The strategy involved conversion of 3',5'-anhydrothymidine **47** to d4T by a base-mediated elimination reaction. Thus, 2'-deoxythymidine **46** was readily converted into 1-(3',5'-anhydro-2-deoxy-b-D-threo-pentofuranosyl)-thymine **47** by converting it first into its 3',5'-di-*O*-mesyl derivative, and then by heating the crude product under reflux with an excess of aq. sodium hydroxide. Formation of oxetane **47** from the dimesylate of **46** proceeded via intermediacy of the pyrimidine base with the ring closing step as shown. Eliminative opening of oxetane **47** was achieved by treatment with *t*-BuOK in DMSO (Scheme 1.11).

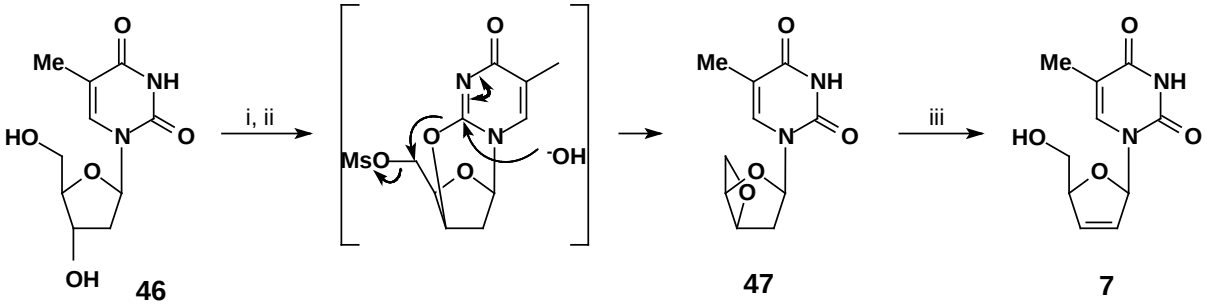

Scheme 1.11 *Reagents and Conditions*: (i) $MeSO_2Cl$, C_6H_5N (ii) aq. NaOH, reflux (iii) *t*-BuOK, DMSO; 57%.

Prolonged exposure of d4T to strong base at high temperature led to decomposition to give thymine as an undesired product thereby decreasing the overall yield.

In an attempt to overcome the decomposition of d4T just mentioned, Mansuri *et al*. [134] precipitated the 5'-alkoxide potassium salt of d4T by adding solvents such as toluene and acetone during work-up. Skonezny *et al*,[135] in a US patent, disclosed an improved process for producing d4T from the oxetane intermediate **47** by eliminating with potassium hydroxide in isopropanol.

In a modified procedure of Horwitz, Reese *et al*. (Scheme 1.12) converted 2'-deoxythymidine **46** directly in one step into anhydro derivative **48** in 68% yield via a 3'-sulfite ester leaving group. The key elimination reaction to form d4T in 76% yield was achieved by reacting anhydro compound **48** with NaH in *N*,*N*-dimethylacetamide at 100 °C.[136]

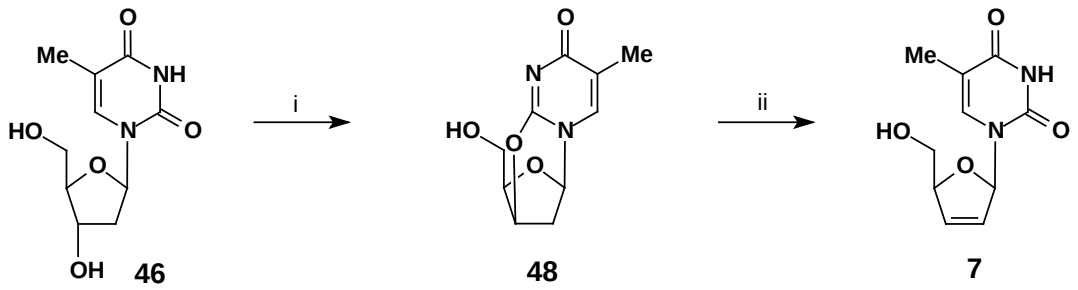

Scheme 1.12 *Reagents and Conditions*: (i) $(PhO)_2SO$, 1-methylimidazole, DMA; 65%. (ii) NaH, DMA, 100 °C; 81%.

Chen *et al*. (Scheme 1.13) from the Bristol-Myers Squibb group synthesized d4T from 5-methyluridine. This was achieved by base-mediated conversion of the trimesylate of **49** into epoxide **51** via intermediate **50,** which opened with acetyl bromide to afford a regioisomeric mixture of *trans* bromoacetates **52a-b**. *b*-Elimination with a Zn/Cu couple afforded 5'-mesyl d4T **53** under mild reductive elimination conditions, without significant nucleoside bond cleavage[137] as a result of superior *trans* stereoelectronic alignment in the elimination step.

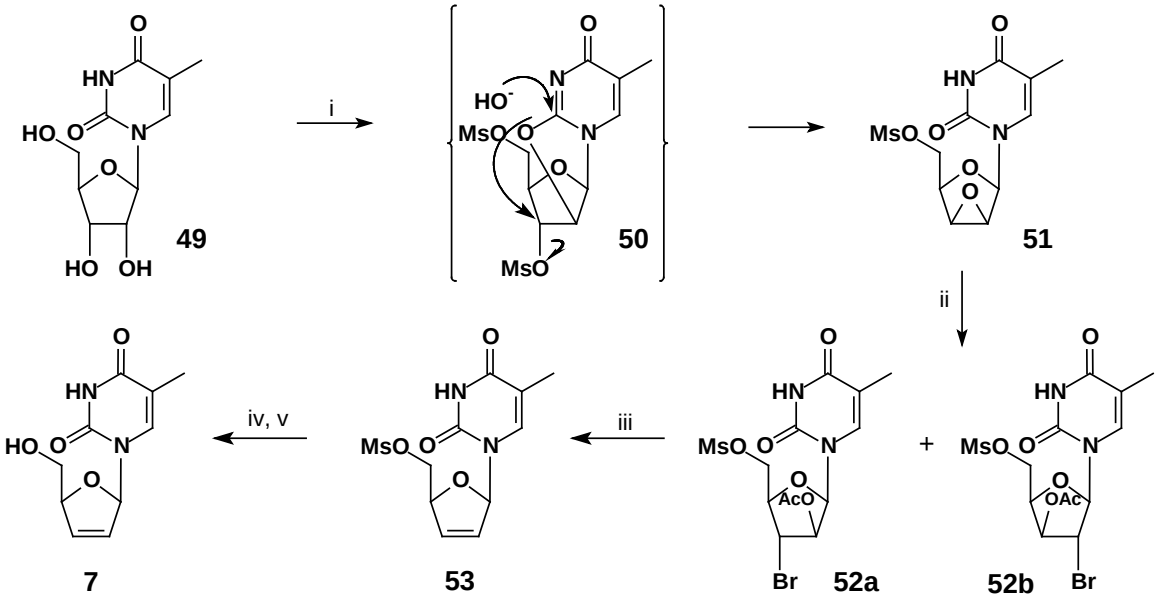

Scheme 1.13 *Reagents and Conditions*: (i) (1) MsCl, NMM, acetone (2) 1N NaOH/H_2O; 82%. (ii) (1) AcBr, MeOH (2) AcBr, CH_2Cl_2; 92%. (iii) Zn/Cu, MeOH; 88%. (iv) $PhCO_2Na$, DMF; 91%. (v) $BuNH_2$; 90%.

Alternatively, the use of a sulfonyl group at the 3'-position of 5-methyluridine instead of an acetyl group in the *syn*-bromomesylate **56** completely avoided the undesired cleavage of the thymine base (Scheme 1.14). D4T was prepared employing this methodology in 75% overall yield starting from the readily available ribonucleoside 5-methyluridine.[138]

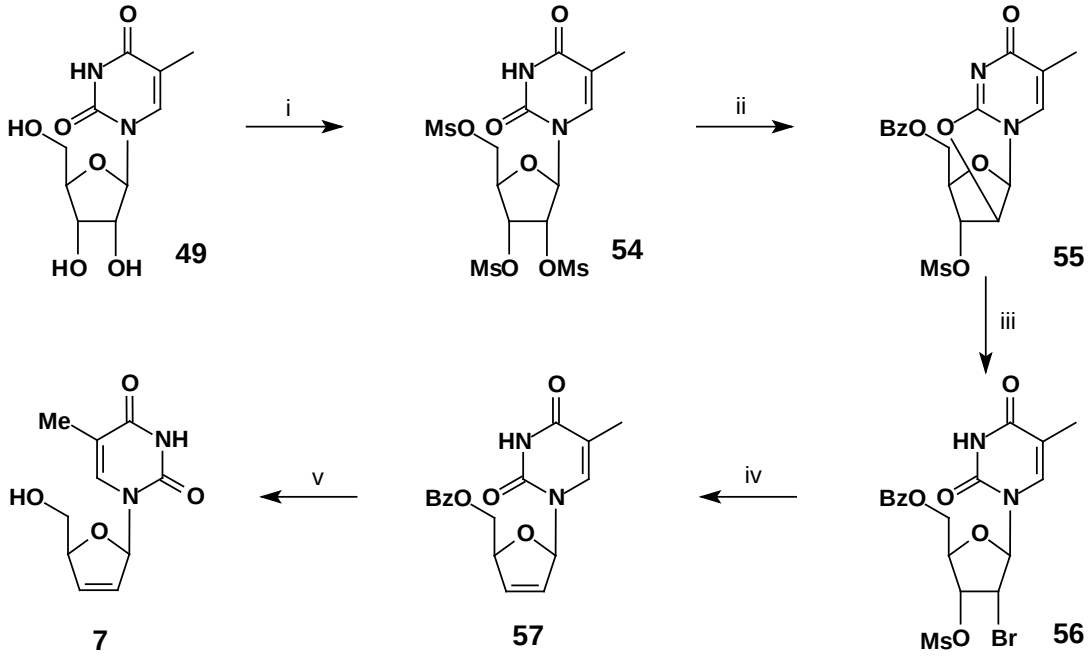

Scheme 1.14 *Reagents and Conditions*: (i) MsCl, NMM, acetone; 97%. (ii) $PhCO_2Na$, CH_3CONH_2; 90%. (iii) AcBr, MeOH, EtOAc; 98%. (iv) Zn, EtOAc/MeOH, cat. AcOH; 97%. (v) $BuNH_2$, 70 °C; 90%.

The key step in the synthesis was the zinc-induced reductive elimination of bromomesylate **56**, which afforded d4T without nucleoside bond cleavage. Sodium benzoate acted as a base to form anhydro ring **55** as well as a nucleophile to displace the 5'-mesyl group, preparing the way for the final facile deprotection with butylamine.

1.16 OBJECTIVE OF THE STUDY

The use of combinations of different drugs is designed to prevent resistant HIV strains by effectively suppressing viral replication overall, thus denying HIV the opportunity to produce new mutations. This principle holds provided there is minimised cross-resistance between the drugs. NNRTIs act by slowing down the chemical step catalyzed by RT, and this retardation allows the two-step binding of NRTI to come to equilibrium leading to tighter binding of the nucleotide. The research in this thesis aimed to:

(i) Synthesize and evaluate the anti-HIV activity of heterodimers of the general formula [NRTI]-spacer-[NNRTI] involving a biologically non-cleavable spacer, in the search for evidence of synergism between the two drugs and hence sites. The NRTI chosen initially was d4U, but was later evaluated as a acyclic nucleoside in an attempt to accommodate phosphorylation problems. The NNRTI employed moved from the second-generation UC-781[139] to the third-generation TMC120.[140]

(ii) Evaluate a structure-activity relationship by synthesizing different length linkers, as well as to probe the exact/minimum components of the NNRTI required to achieve good biological activity. In this study the possibility existed for finding new exciting lead compounds/derivatives for further exploration.

(iii) Synthesize and evaluate the anti-HIV activity of all compounds synthesized.

UC-781 and TMC120 were selected due to their potency against wild-type and NNRTI resistant HIV-1 strains (carrying the NNRTI resistant mutations K103N, V106A and Y181C). D4T is currently used to treat HIV, and was chosen owing to its higher inhibitory effect compared to AZT.

As proposed by Arnold, the attachment for the linkers to nucleoside analogues include sugar ring positions (e.g. 2', 3' and 5'-substitutions), extensions of mono-, di- and tri-phosphate esters, and positions on the nucleoside bases (e.g. the 5-position of pyrimidine rings). Selection of sites of attachment on the non-nucleoside moieties would vary according to the inhibitor type. These attachment points and the rational behind it will be discussed in detail in the results and discussion chapters before the onset of the syntheses.

SYNTHESIS OF d4U-SPACER-UC-781 DOUBLE-DRUGS

2.1 Strategy for the synthesis of [d4U]-spacer-[UC-781]

The bifunctional molecules **58** and **59** targeted in this chapter are shown in Fig. 2.1 below. The C-5 position on the pyrimidine moiety (base) of d4U was chosen as the appropriate attachment point for the tether following a report by Ruth and Cheng in the early 1980's, which demonstrated that a chain extension at the C-5 position caused minimum steric hindrance with DNA base-pairing.[141] Furthermore, it has been reported[142] that tethering at the C-5 position with a flexible chain of about 10Å still allows 5'-triphosphate generation leading to incorporation into nucleic acids. In our study, two variations were explored in the physiochemical composition of the spacer. Target **58** was chosen containing a simple aliphatic tether joined to an alkynyl segment, whilst target **59** incorporated ethylene glycol units in view of their anticipated water solubility.

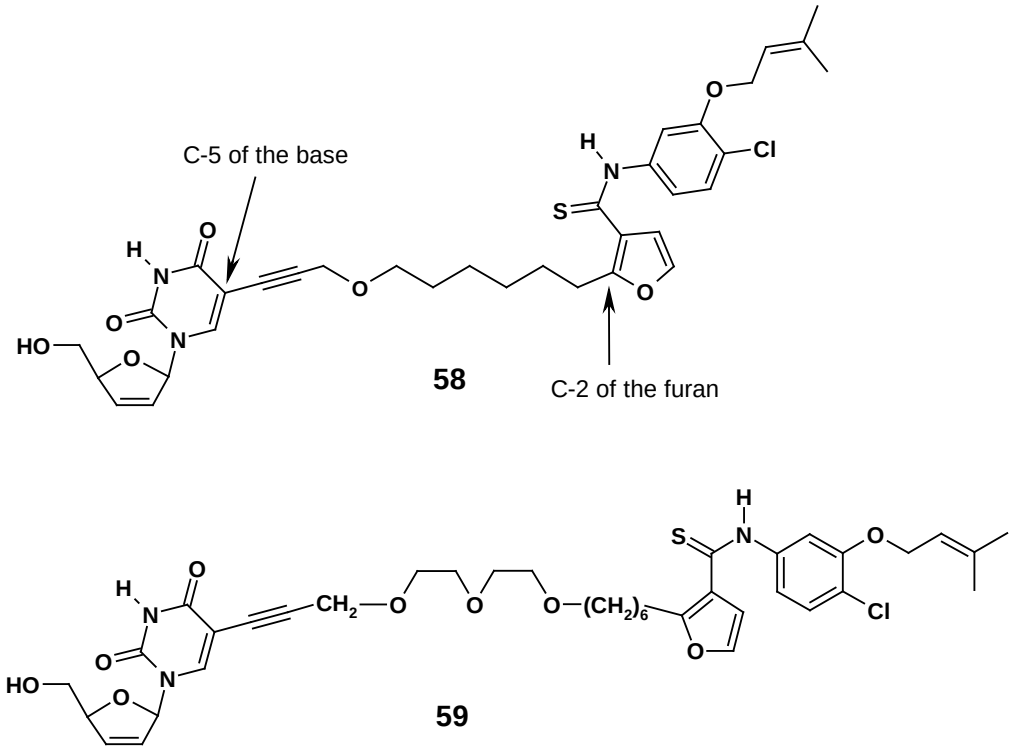

Figure 2.1 Structures of the target molecules.

Very recently, the Jorgenson group has provided excellent insight into the attachment point of the tether to d4U through their modeling studies.[143] At the time of project inception, no computer modeling studies had been reported, though, in the bifunctional setting. Over the years, many groups have been involved in modeling individual inhibitors (NRTIs as well as NNRTIs) in search

of understanding the mechanism through which these inhibitors operate, including key residue binding interactions in their respective sites and their ability or lack thereof to combat drug resistant mutations. Crystal structure information was available, but none dealing with issues relating to synergy between the substrate binding site and the NNRTI-BP. Therefore, our C-5 connection to d4U was based on a rudimentary molecular modeling interpretation of the growing DNA chain at the substrate active site. Work done by Uckun and co-workers[143] in 2000 depicted in Figure 2.2 clearly shows how a C-5 connection to the base (in this instance a 5-methyluracil moiety of a 5'-phosphorylated thymidine unit in the DNA chain) with an appropriately long spacer might 'exit' the substrate site with low interference to DNA base-pairing, leading to the NNRTI-BP. The NNRTI-BP is referred to as the 'NNI' in the Uckun paper, and so also in Figure 2.2.

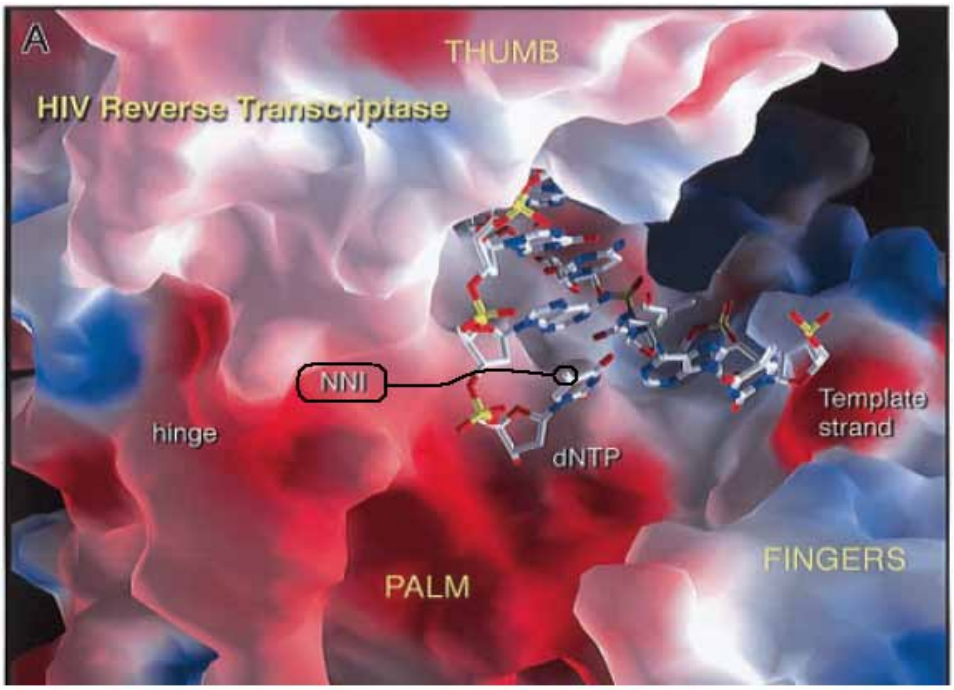

Figure 2.2 Modeling studies of the C-5 extension point of d4U.[143]

Structural studies carried out by Stammers and co-workers[14] on UC-781 in complex with HIV-1 RT, have revealed that elongation at the C-2 or C-5 positions of UC-781 could lead past Trp229 towards Glu138 and the p66 subunit, which in theory might access the NRTI binding site (Fig. 2.3). The C-2 position was chosen as the attachment point to the spacer (tether) based on the synthetic promise for C-2-alkylation of the furan moiety of UC-781. Again, it is well worth mentioning that at the time of our study we were not aware of the hydrophobic tunnel that could plausibly exist (connecting the NNRTI-BP to the nucleic acid-binding cleft) upon binding of an NNRTI as described by Arnold[77] in his recent TMC-278 work (Fig. 2.3), and all our attachment choices were based merely on extensive structural/crystal studies. To the best of our knowledge,

rational in-depth considerations were made regarding both the attachment points of the NRTI and the NNRTI in view of the difficulty previous groups had in understanding these issues.

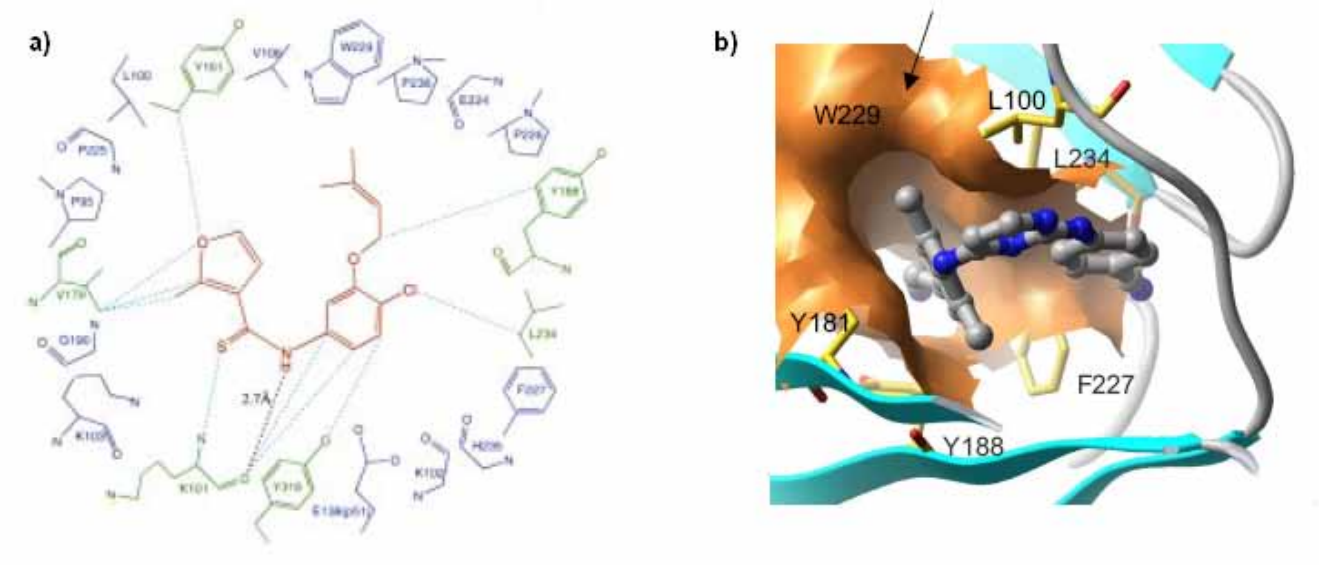

Figure 2.3 a) Schematic drawing of UC-781 in the NNRTI-BP. b) Hydrophobic exit tunnel as illustrated by Arnold and co-workers for TMC278.

Attachment of the linker to the C-5 position of the nucleoside was thought to be accessible *via* a Sonogashira[144] palladium cross-coupling reaction of a terminal alkyne with a 5-iodo nucleoside. This particular method has been used extensively by the Ladurée[129,130] group in preparation of C-5 tethered heterodimers. Furthermore, C-5 substituted pyrimidine nucleosides constitute a class of biologically significant molecule and the C-5 alkenyl and alkynyl-substituted ones have shown various antiviral activities. For example, (*E*)-5-(2-bromovinyl)-2'-deoxyuridine (BVDU) (Fig.2.4) is a highly potent and selective anti-Herpes agent currently in limited clinical use for Herpes Simplex virus type 1 (HSV-1).[145] Also, 5-iodo-2'-deoxyuridine (IDU) and 5'-trifluoromethyl-2'-deoxyuridine (TFT) are both administered as eye drops or ophthalmic cream in the treatment of Herpes virus.[146]

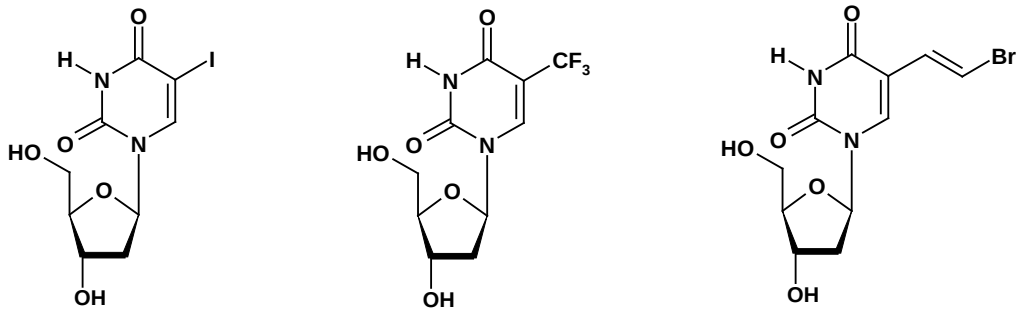

Idoxuridine (IDU) **Trifluridine (TFT)** **Brivudine (BVDU)**

Figure 2.4 C-5 substituted nucleosides in clinical use.

2.1.1 Retrosynthetic analysis of [d4U]-spacer-[UC-781]

The total synthesis of targets **58** and **59** was conceived as achievable *via* a convergent strategy involving the coupling of 5'-iodo d4U **60** to an alkyne of type **A** followed by deprotection of the benzoyl group to render the target compounds directly.

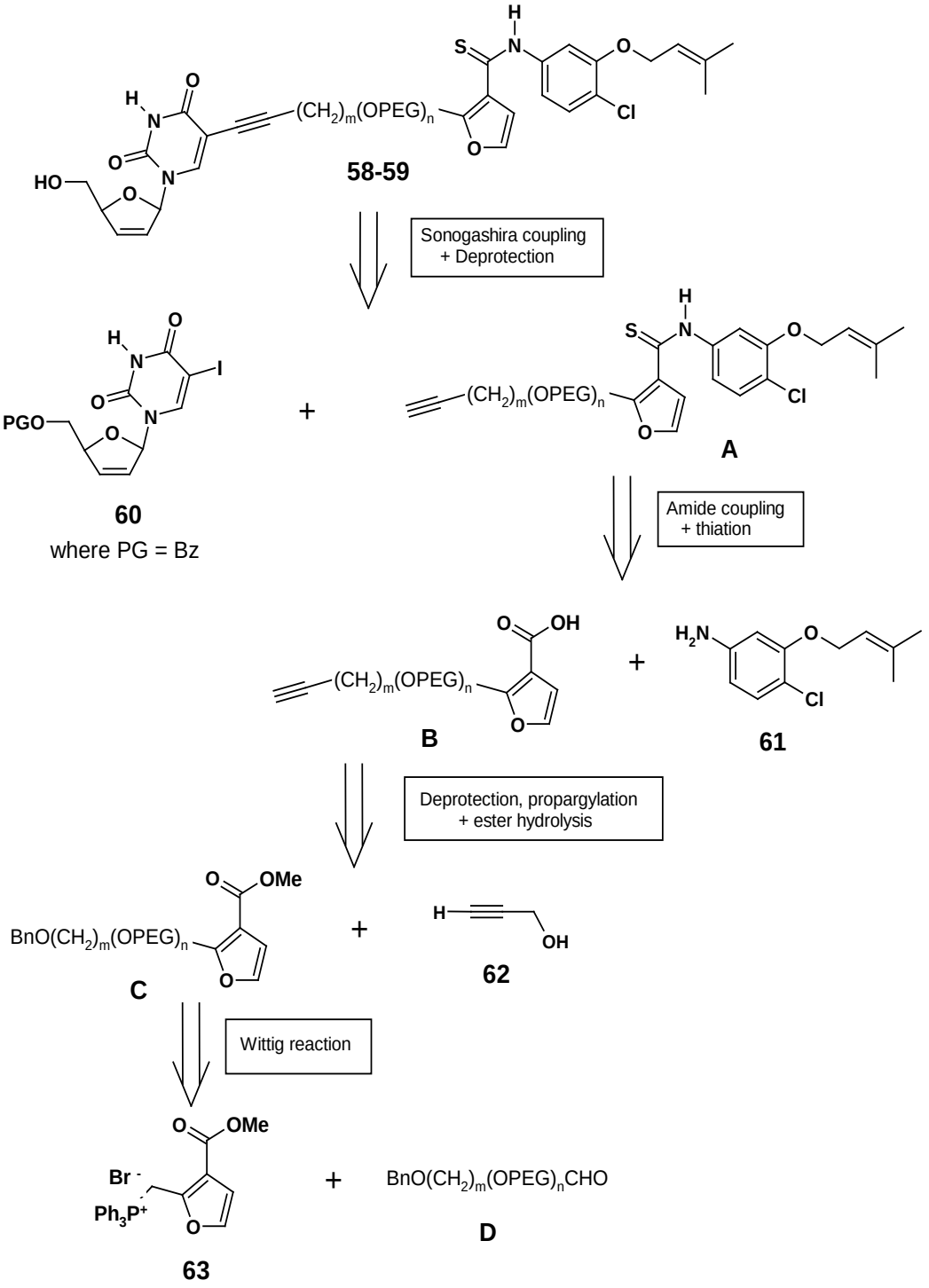

Figure 2.5 Retrosynthetic analysis of the synthetic strategy used towards the target molecules.

It was anticipated that sodium methoxide would be used to deprotect the benzoyl group without promoting nucleoside base cleavage. However, there was some concern regarding the reactivity and potential interference of the thioamide group in **A** under Sonogashira coupling conditions. Alkyne **A** would be obtained from amide coupling of furanoic acid **B** with substituted arylamine **61**, whose synthesis is discussed in Chapter 3. The development of new Wittig carbon-carbon bond-forming methodology for the 2-alkylation of phosphonate salt **63** with aldehyde **D** to furnish **C** was planned as new methodology for the 2-alkylation of 3-furoates.[147]

The key 5-iodo d4U **60** would be synthesized according to the Bristol-Myers-Squibb[138] methodology for d4T (Stavudine) production as outlined in Scheme 1.14.

2.1.2 Literature overview on Sonogashira Coupling

The Sonogashira coupling of 5-iodouridine with terminal alkynes has been extensively studied,[148] and the mechanism of this reaction involves oxidative insertion of Pd (0) into the aryl/alkenyl-halide bond. CuI activates the alkyne by forming a copper acetylide, which undergoes transmetallation with the palladium complex to form the alkynyl-Pd-R intermediate. Reductive elimination of Pd(0) leads to the coupled product (Fig. 2.6).

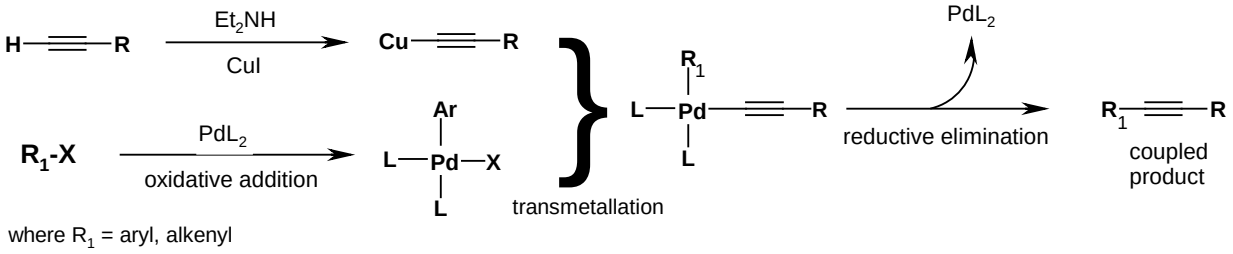

Figure 2.6 Sonogashira reaction mechanism.

Regarding literature precedent for our approach, Crisp and Flynn[149] have demonstrated that the C-5 alkynyl derivatives **66** could be obtained in high yield (70-90%) by cross-coupling of acetylated uridine triflate **64** with a range of terminal alkynes **65** (Scheme 2.1) using tetrakis(triphenylphosphine)palladium(0) as a catalyst. A slight elevation of reaction temperatures from ambient to 45 ^{o}C increased the rate of coupling. In this case, furanopyrimidine by-products **67** were isolated in low yield (7%) or in trace amounts.

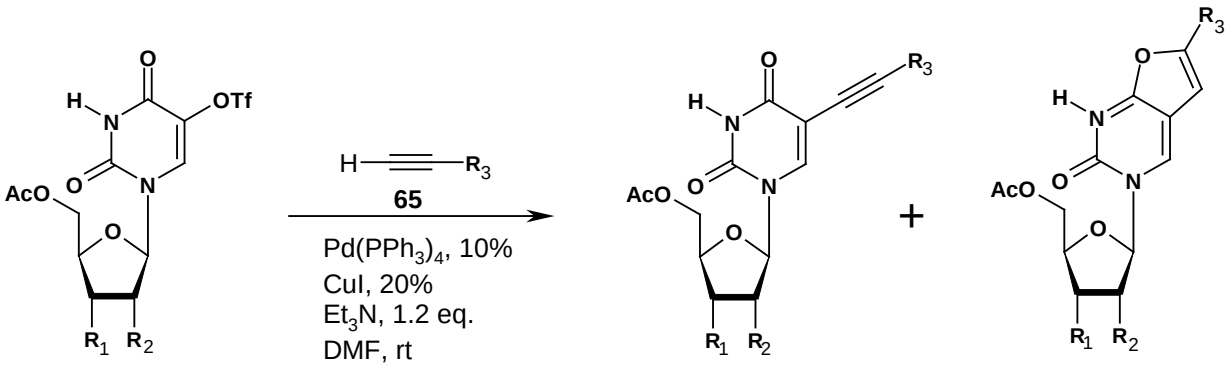

$R_1 = R_2 = OAc$
$R_1 = OAc \quad R_2 = H$
$R_1 = OH \quad R_2 = H$
$R_3 = Me_3Si$, Ph, 4-$MeOC_6H_4$, 3,5-$(CF_3)_2C_6H_4$, 3,5-F_2-C_6H_4, 4-$CF_3C_6H_4$, 4-FC_6H_4, C_6F_5

Scheme 2.1

Similarly, Robins *et al*[150] applied the Sonogashira reaction to couple protected 2'-deoxythymidine derivatives **68** with several alkynes **69** in triethylamine at 50 °C in the presence of bis(triphenylphosphine)palladium (II) chloride and copper (I) iodide (Scheme 2.2).

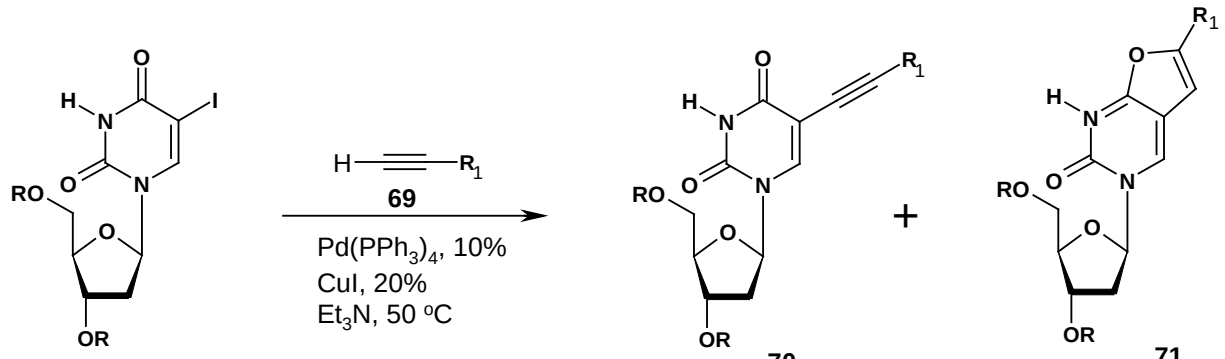

R_1

C_2H_5, C_3H_7, *n*-C_4H_9, *n*-C_5H_{11}, $C(CH_3)_3$, C_6H_5, $Si(CH_3)_3$, H, CH_2OTHP, CH_2OH, CH_2CH_2OTHP, CH_2CH_2OTol, CH_2CH_2OTs

Scheme 2.2

In this case, the extent of cyclization to form **71** was dependent on the reactants. Thus, coupling of **68a** with (trimethylsilyl)acetylene gave the target product **70** in 80% yield, whereas the use of 1-hexyne, 4-(*p*-toluyloxy)butyne, 4-tetrahydropyranyloxybutyne or 4-(trityloxy)butyne under the

same conditions gave the cyclized furanopyrimidin-2-one compound **71** as the major product. Conversely, coupling reactions with the same range of alkynes but using the nucleoside protected as its *p*-toluyl ester proceeded smoothly with minimal formation of deiodinated and furanopyrimidin-2-one by-products.[150]

Hobbs[151] (Scheme 2.3) attempted to use conditions optimized by Robins *et al* to couple propargylamine derivative **73** with unprotected 5-iodouridine **72** but failed owing to the nucleoside's insolubility in triethylamine. Successful coupling was achieved to form the coupled products **74** in good yields (70-90%) by using DMF as a solvent and tetrakis(triphenylphosphine)palladium as a catalyst instead of the Pd(II) used by Robins. He concluded that the successful coupling by Robins revealed that the use of DMF significantly improved the coupling rate and not the Pd(0).[152]

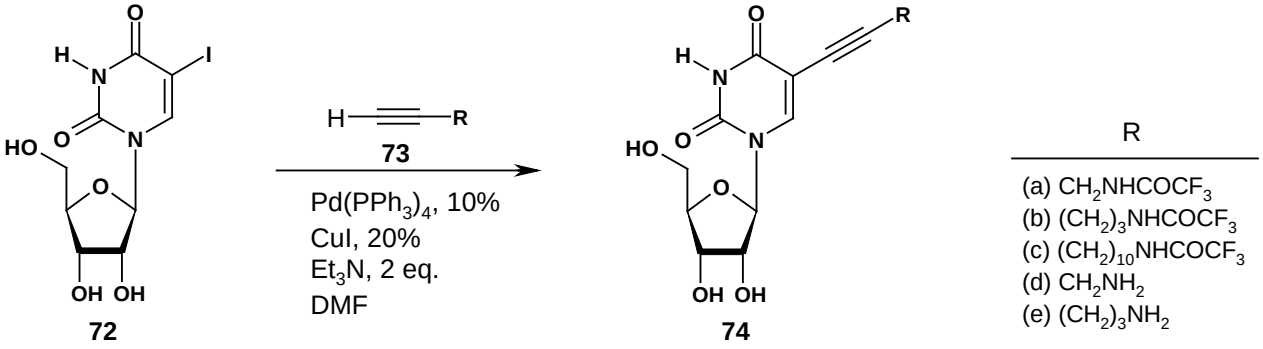

Scheme 2.3

Sonogashira coupling of protected propargylamine **73a** with 2'-deoxynucleoside **75** by the Robins group in the presence of triethylamine as a base furnished the target nucleoside **76** together with triethylammonium salts that were difficult to separate. To improve the purification of these nucleosides, Garg *et al.*[153] developed a heterogeneous protocol that employed a palladium-on-carbon catalyst and a resin-bound tertiary amine (Amberlite IRA-67) as a base. These conditions furnished the coupled product **76** in good yield (Scheme 2.4). The study involved a cross-coupling reaction of nucleoside **75** in the presence of Amberlite IRA-67 and Pd(0) (10 mol%), which resulted in the coupled compound **76** in 79% yield after filtration of the reaction media and purification by column chromatography. The authors then substituted Pd(0) with a heterogeneous transition-metal catalyst (Pd/C) to further simplify the purification process.

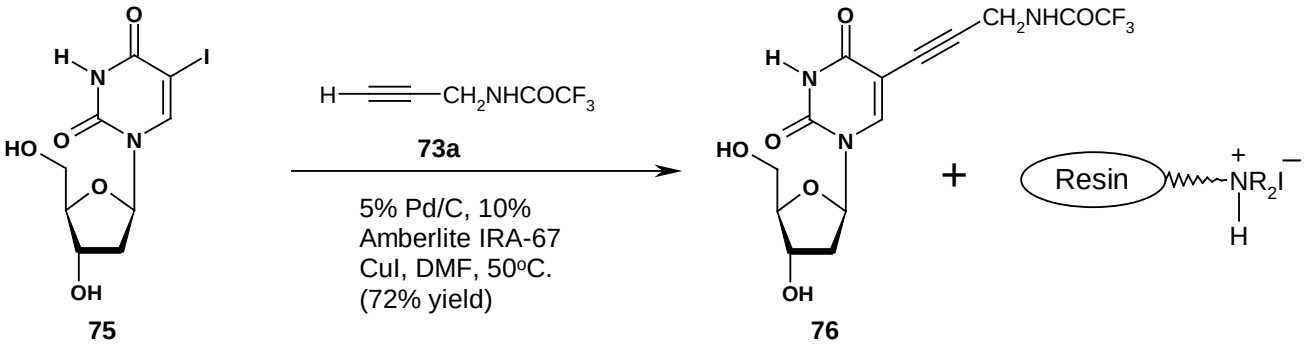

Scheme 2.4

C-5 alkynylated d4U analogues **79** and **81** have been synthesized *via* the smooth and efficient coupling of alkynes **78** and **80** with 5'-*O*-acetyl-5-iodo d4U **77** in DMF under co-catalysis of Pd and CuI (Scheme 2.5). Reaction with unprotected alkynes **80** gave the coupled compounds **81** after 22-24 hrs in low yields (35-45%), whereas the protected alkynes **78** gave the target compounds in good yields (70-76%).[154]

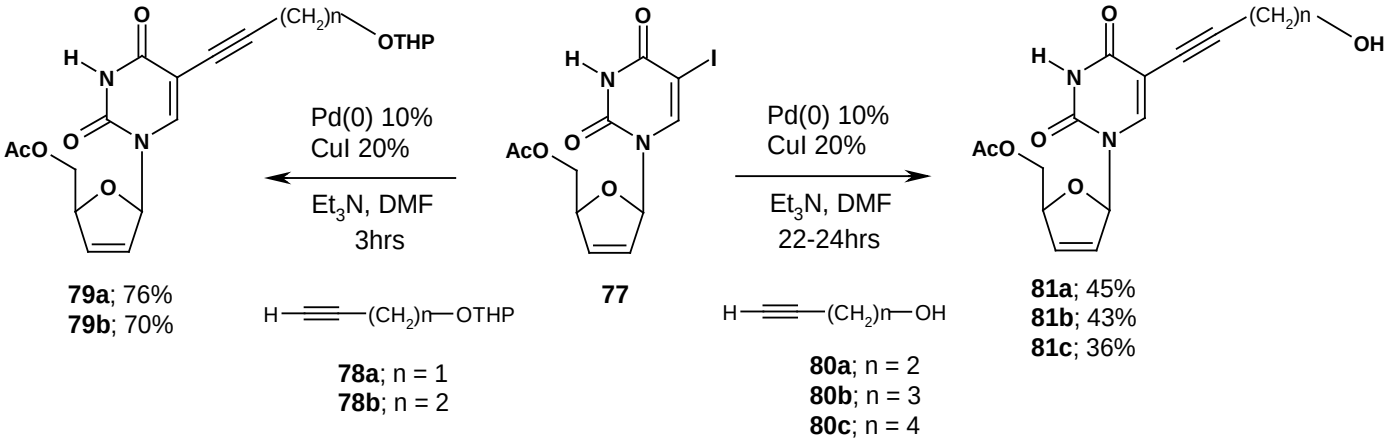

Scheme 2.5

In summary, the use of CuI as a co-catalyst has been shown to give better results. A mole ratio of 2:1 copper to palladium has been shown to offer the best coupling conditions for alkynes, leading to the minimization of side products (cyclic furanopyrimidine). It is noteworthy that performing the reaction in the presence of CuI has also been reported to increase the conversion rate to by-products. The choice of solvent has been reported to be an important determinant for the successful coupling of terminal alkynes with iodonucleosides,[152] and the use of DMF has been shown to reduce the percentage of cyclic by-product. A considerable

percentage of cyclized by-product was isolated when longer reaction times were employed or when an electron-withdrawing group on the nucleoside was present. In general, optimal conditions have been found to be 2.0-2.5 eq of terminal alkyne, 10% $Pd(PPh_3)_4$, 20% CuI and 1.2 eq Et_3N in DMF. Pd(0) has been reported to give better results than Pd (II).[148]

2.2 Synthesis of Target double-drug compounds

2.2.1 Synthesis of [d4U]-pentane-propyne-[UC-781]

2.2.1.1 Synthesis of 5'-iodo d4U

The 5'-O-benzoyl d4U derivative **86** was synthesized in four steps according to the Bristol-Myers Squibb procedure outlined in Scheme 2.6.[138] Thus, reaction of uridine with methanesulfonyl chloride (3.0 eq.) in pyridine yielded trimesylate **83** in good yield. Isolation of the product was achieved by adding the reaction mixture to ice-cold water and allowing for the product to precipitate out. Filtration of the precipitate followed by extensive washing (H_2O) and drying on the pump gave the desired **83** as evidenced by its ^{1}H NMR spectrum, which revealed the presence of three mesylate singlets resonating at δ_H 3.22, δ_H 3.33 and δ_H 3.35. Its ^{13}C NMR spectrum displayed resonances at δ_C 37.9, 37.9 and 36.9 for the three methyl groups together with the other (uridine) signals.

The next step involved a chemoselective substitution reaction at the C-5' centre as well as a C-2,2'-anhydro ring-closure required for subsequent bromination. To this end, trimesylate **83** was reacted with sodium benzoate in molten acetamide at 140 ^{o}C. After 1 hr, the reaction mixture was poured into ice-cold water, the precipitate stirred at 0 ^{o}C for 15 min and the desired (Baldwin's rules favours 5-*exo-tet*) solid product **84** was filtered off in 75% yield. Its ^{1}H NMR spectrum displayed the absence of an NH singlet at δ_H 11.51 present in **83** as well as the appearance of additional resonances in the downfield region for the aromatic protons of the benzoyl group. Its ^{13}C NMR spectrum displayed the appearance of a second carbonyl carbon at δ_C 170.6 as well as aromatic carbons, further confirming the presence of the benzoyl group, which could be assigned as being on the C-5' oxygen in view of the relative deshielding of the diastereotopic H-5' protons. There was also a significant downfield shift in the C-2' carbon from δ_C 76.0 in **83** to δ_C 86.0 in **84**, thus confirming that displacement of the mesylate and formation of the anhydro ring had taken place at this carbon. C-2' over C-3' attack by the pyrimidine base is favoured in agreement with Baldwin's rules that state that a 5-*exo-tet* cyclization should be kinetically faster than a 6-*exo-tet* process. A further factor, possibly even more dominant, is the preference for a [3.3.0] bicyclic over formation of a [3.2.1] bridged system.

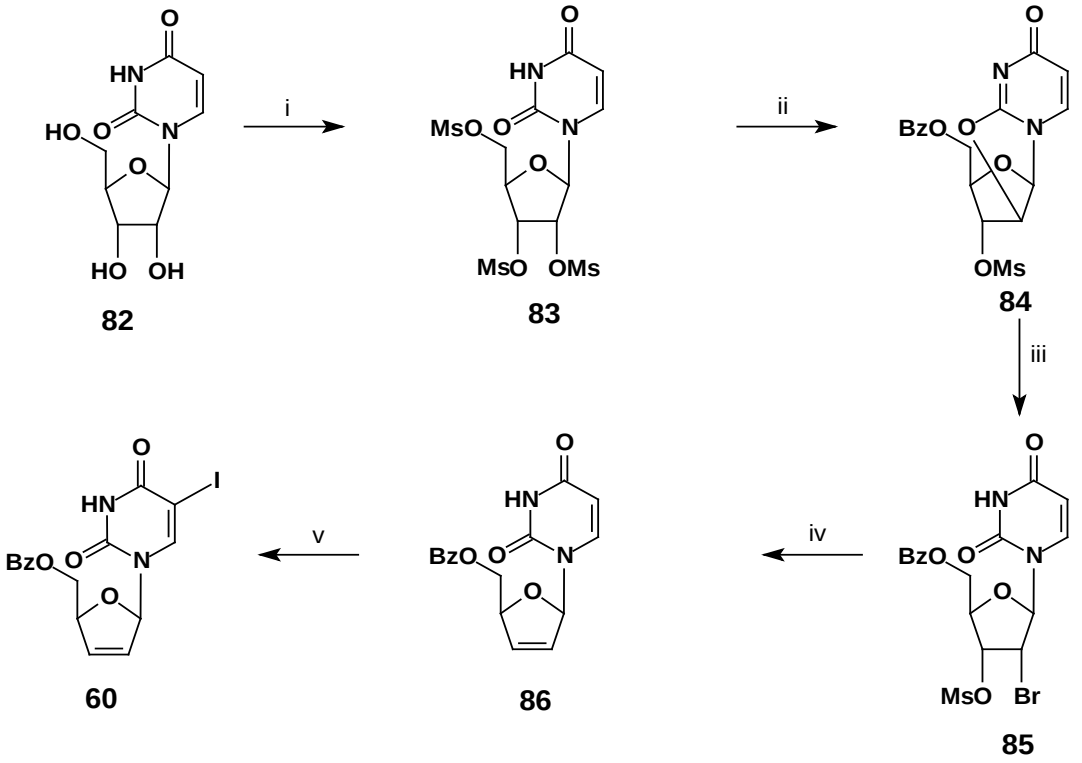

Scheme 2.6 *Reagents and Conditions*: (i) (1) MsCl, pyr, 0 ^{o}C, 5 hrs (71 %); (ii) NaOBz, CH_3CONH_2, 140 ^{o}C, 1 hr (75%); (iii) AcBr, EtOAc/MeOH (10:1), reflux, 1 hr (97%); (iv) Zn, EtOAc/MeOH; rt (89%); (v) I_2, CAN, CH_3CN, 35 ^{o}C, 3 hrs (80%).

Acid-catalyzed anhydro-ring opening of **84** by bromide ion generated as HBr *in situ* from the reaction between acetyl bromide with MeOH in EtOAc (1:10) gave the C-2' substituted *cis*-bromomesylate **85** in an excellent yield of 97%. The presence of the bromine atom in product **85** was evident in the ^{1}H NMR spectrum which displayed an upfield shift in the H-2' protons from δ_H 5.69 in **84** to δ_H 4.67 in **85**. The ^{13}C displayed a similar trend for the C-2' resonance moving upfield from δ_C 86.0 in **84** to δ_C 47.5 in **85**, consistent with a bromide substitution. The mechanism of the reaction involves an S_N2 displacement by bromide at the C-2' position *via* a protonated pyrimidine moiety acting the role of the leaving group. The resultant effect is inversion of configuration at C-2' to afford the *syn* stereochemistry shown in **85**.

Reductive elimination of bromomesylate **85** using zinc metal in ethyl acetate and methanol containing acetic acid afforded the 5'-*O*-benzoate ester of d4U **86** in 89% yield. A downfield shift was observed for the C-2' and C-3' carbons in the ^{13}C spectrum of **86** from δ_C 75.6 and δ_C 47.5 in **85** to δ_C 133.6 and δ_C 127.2 respectively, confirming the introduction of the double bond via elimination of the bromine and mesylate groups. The disappearance of the mesylate carbon at δ_C 38.8 in **85** further confirmed the elimination to have occurred. It is important to note that the

trans-elimination of bromine and the uracil base at C-1' was not observed, in spite of the preference of *anti* over *syn* on stereoelectronic grounds. This was undoubtedly due to the superior leaving ability of mesylate, an issue well thought out by the Bristol-Myers-Squibb group.

As mentioned before, halogen-substituted nucleosides exhibit interesting antiviral properties.[145,155] Prusoff *et al* described the first 5-iodination of uridine using an iodine/nitric acid combination.[156] Dale *et al* subsequently reported the iodination of 5-mercuriuridine derivatives using elemental iodine in aqueous alcohol.[157] The CAN-mediated C-5 halogenation of uracil derivatives was first reported by Asakura, *et al* in 1990, in which either molecular iodine, NaI or LiI were used as the source of iodine.[155] In this project the CAN-mediated strategy for conversion of **86** to its 5-iodo d4U **60** derivative using elemental iodine and CAN at 35 ^{o}C was chosen. The reaction was very much time and temperature sensitive. Excessive heating over 35 ^{o}C or long reaction times (over 4 hrs) resulted in the migration of the benzoyl group from the C-5'-hydroxyl to the pyrimidine nitrogen. However, one could obtain a high yield (80%) running the reaction at 35 ^{o}C for 3 hrs. The ^{1}H NMR spectrum supported iodination by virtue of the disappearance of the two uracil doublets for H-5 and H-6, and the appearance of a singlet for H-6 at δ_H 7.86.

2.2.1.2 Synthesis of tethered UC-781, Sonogashira coupling and Deprotection

2,3-Disubstituted furans constitute a widely encountered sub-unit in a range of natural and synthetic products. The 2-alkylation of 3-furoic acids has been a commonly employed strategy for entry[158] into this sub-unit with two carbanionic methodologies standing out as versatile options. Knight was the first person to demonstrate[159] that treatment of 3-furoic acid with two equivalents of LDA (THF / -78°C) regioselectively furnishes the dianion **87** (Figure 2.7), which can be C-2 alkylated with a range of reactive electrophiles. However, with less reactive electrophiles, *e.g.* ethyl iodide, yields were low. Keay and co-workers subsequently demonstrated[160] that 2-methyl-3-furoic acid reacts with two equivalents of *n*-BuLi at -20°C to furnish the 2-lithiomethyl dianion **88** which is more stable than **87**, giving higher yields with less reactive electrophiles. Development of **88** followed pioneering work by Tada *et al*[161] on use of the 2-dianion of 2,4-dimethyl-3-furoic acid **89** in natural product synthesis, (Figure 2.7).

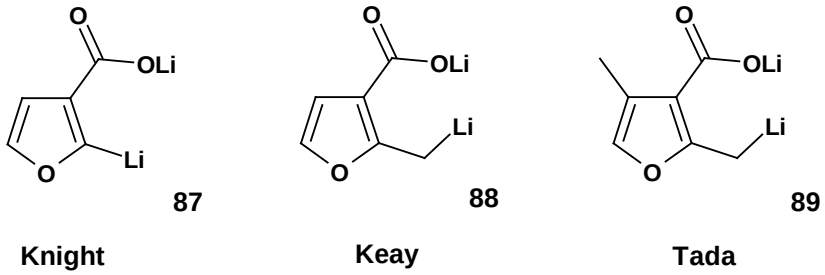

Figure 2.7 Well known strategies for 2-alkylation of 3-furanoic acids.

In view of both the need for access to reasonable quantities of 2-alkylated-3-furoates in conjunction with incorporation of the non-nucleoside inhibitor UC-781 into the bifunctional inhibitor, and the unattractive prospect of using large quantities of *n*-BuLi, we embarked on a study to identify a large-scale alternative. It occurred to us that Wittig methodology based on the 3-methoxycarbonyl-2-furanylmethylphosphonium salt (see **90** in Scheme 2.7) might provide the answer in view of the option of using a mild base to generate the stabilized ylide. Although 2-furanylmethylphosphonium salts[162] have been known and used in synthesis for some time, the corresponding 3-furoates were hitherto unknown before our study.

To this end, radical bromination of commercially available methyl 2-methyl-3-furoate using conditions reported by Khatuya[163] furnished methyl 2-bromomethyl-3-furoate in high yield, which, following evaporation of solvent and addition of triphenylphosphine in toluene furnished (rt, overnight) the desired and novel triphenylphosphonium salt **90** by filtration. Isolation of product involved no chromatography, with a single crystallization from methanol returning analytically pure material in 80% overall yield.

Pleasingly, reaction of **90** in methanol with sodium methoxide as base at room temperature followed by addition of hexanal (1.2 eq) as a model aldehyde resulted in rapid transformation to the Wittig product **91a** in high yield (92%) as a mixture (~1:1) of *E/Z* stereoisomers. Carrying the reaction out in THF using sodium hydride as base gave a significantly lower yield (~50%) of the Wittig product in a higher *E/Z* ratio to that obtained using sodium methoxide. Subsequent hydrogenation (H_2 / Pd-C) gave the anticipated 2-alkylated product **91b** in high yield (80%). A small percentage (~10%) of the 4,5-dihydro-2-alkylated product[164] was also obtained, which could be minimised by varying the reaction conditions, but not completely eliminated, (Scheme 2.7).

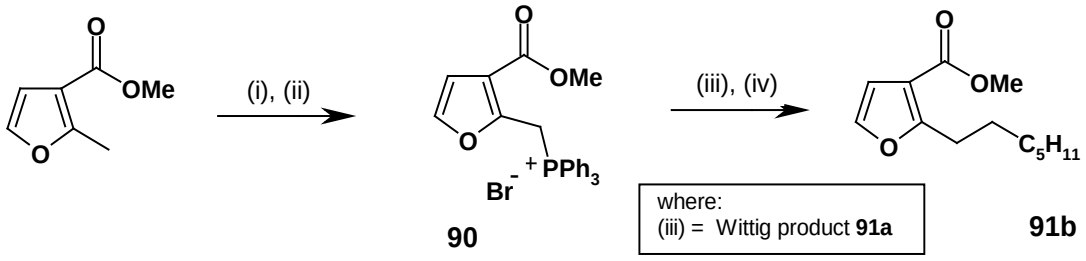

Scheme 2.7 *Reagents and conditions:* (i) NBS, $(BzO)_2$ (cat), CCl_4, Δ; (ii) PPh_3, toluene rt, (80% over two steps); (iii) NaOMe (1.1 eq), MeOH, $C_5H_{11}CHO$ (92%); (iv) H_2, Pd-C, EtOH (80%).

A range of aldehydes appropriate to producing alkylated side chains were subjected to the olefination/hydrogenation sequence and the results are presented in Table 2.1. Reactions involving formaldehyde, ethanal and 5-benzyloxypentanal all underwent smooth Wittig reactions in high yield as with the model reaction and, where appropriate, similarly gave products with about an equal *E/Z* isomer ratio. Subsequent hydrogenation of each one gave a small percentage of the 4,5-dihydro derivative as in the hexanal case, which could be separated from the desired alkylated product by careful silica-gel column chromatography. This new methodology culminated in a Tetrahedron Letters communication[147] being published in 2005. The Wittig product of interest for the synthesis of the tethered UC-781 was **92d** which was obtained in a 91% yield. The ^{1}H NMR spectrum of **92d** displayed a characteristic *E:Z* ratio of 1:1 best evaluated using the allylic H-3' quartet of doublets signals resonating at δ_H 2.62 and δ_H 2.28 for the *E*- and *Z*-isomers respectively (Fig. 2.8). This ratio (1:1) was further supported by the appearance of the vinyl H-2' doublet of triplets resonating at δ_H 6.51 (*J* = 16.0, 7.1 Hz, *E*-2') and δ_H 5.84 (*J* = 12.0, 7.6 Hz, *Z*-2'). Finally, a correct HRMS evaluation (*m/z* HRMS (EI) 314.1511, $C_{19}H_{22}O_4$ requires *m/z* 314.1518), confirmed the structure of **92d** as shown in Scheme 2.8.

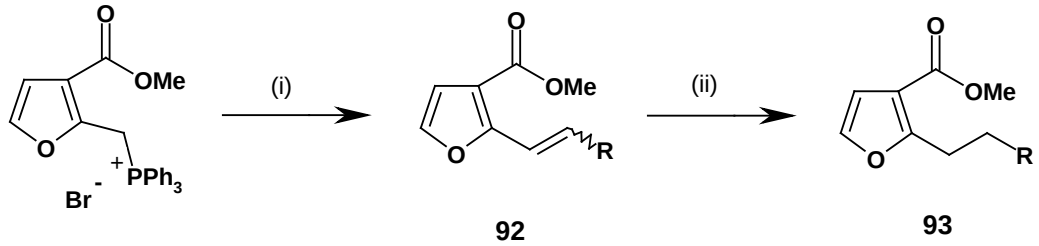

Scheme 2.8 *Reagents and conditions:* (i) NaOMe, MeOH, RCHO; (ii) H_2, Pd-C, EtOH.

Table 2.1 Wittig olefination and hydrogenation of **90** with various aldehydes

R of RCHO	% Yield of **92**	% Yield of **93**
a) H	92	80
b) CH_3	90	61
c) C_5H_{11}	92	80
d) C_4H_9OBn (**90a**)	91	94

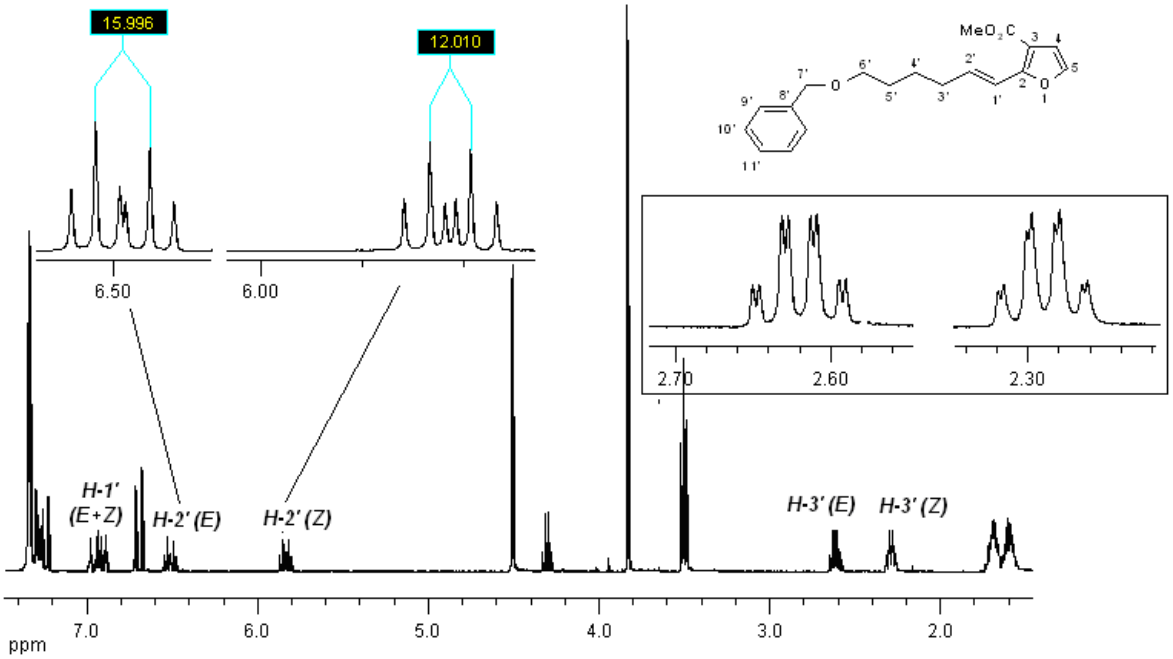

Figure 2.8 ^{1}H NMR spectrum of **92d** displaying the *E:Z* ratio of 1:1.

Hydrogenation of alkene **92d** resulted in concomitant hydrogenolysis of the benzyl ether (Scheme 2.8), which will be the only derivative further discussed because the others (i.e. **92a-92c**) were all model reactions. To this end, hydrogenolysis of **93d** *in situ* rendered the desired alcohol **94** in 94% yield. Key spectroscopic assignments in its ^{1}H NMR spectrum were the disappearance of the benzyl ether aromatic signals at δ_H 7.20 - δ_H 7.40 in **92d** as well as the benzyl ether methylene signal at δ_H 4.52. This was further supported by the absence of the double bond signals at δ_H 6.53 and δ_H 5.82. Subsequent tosylation of **94** using *p*-toluenesulfonyl chloride and triethylamine in dichloromethane with a catalytic amount of *N,N*-dimethylaminopyridine furnished **95** in 94% yield after silica-gel chromatography. Diagnostic peaks in the ^{1}H NMR spectrum of **95** were the methyl singlet at δ_H 2.42 integrating for the three hydrogens of the aromatic methyl, together with the appearance of the typical aromatic *AB* doublet system at δ_H 7.76 and δ_H 7.34 expected for the tosyl group aromatic protons. The ^{13}C

NMR spectrum of **95** clearly displayed new aromatic signals at δ_C 129.7 and δ_C 127.8 for the aromatic carbons bearing hydrogens. Substitution of tosylate **95** with propargyloxy anion, formed *in situ* from the reaction of sodium hydride and propargyl alcohol in tetrahydofuran at room temperature furnished the propargyl ether **96**. Interestingly, the substitution proceeded more efficiently this way round, *i.e.* was superior than propargylation of the alkoxide of **94** with propargyl bromide. The propargyl ether 3-furoate **96** was never isolated because TLC always revealed a considerable amount of hydrolysis to the furoic acid **97**. Thus, a one-pot base-mediated ester hydrolysis with potassium hydroxide dissolved in ethanol was developed to yield furoic acid **97** in 98% yield over two steps. Conversion to the acid chloride **98** with an excess of thionyl chloride was achieved in 1 hr at 40 ^{o}C, after which the excess thionyl chloride was removed under reduced pressure. The crude product was redissolved in dichloromethane and subsequent addition of dry pyridine at 0 ^{o}C followed by the substituted aniline **61** (Figure 2.5) furnished amide **99** in a high overall yield (78%; 2 steps) from the acid. The ^{1}H NMR spectrum of **99** confirmed that a successful amide coupling had taken place with the appearance of a broad amide NH signal at δ_H 7.36 (Fig. 2.9). The dimethylallyl (DMA) substituent peaks at δ_H 5.50 (olefin H-9'), δ_H 4.58 (methylene H-8'), δ_H 1.74 and δ_H 1.78 (two methyl groups H-10', 11'), as well as an increase in aromatic peaks (see details in Fig. 2.9) also supported the formation of **99**. ^{13}C NMR analysis supported amide formation further with the presence of a carbonyl signal resonating at δ_C 161.9. HRMS evaluation (*m/z* HRMS (EI) 443.1786, $C_{25}H_{30}O_4NCl$ requires *m/z* 443.1791) returned the correct molecular ion for **99**.

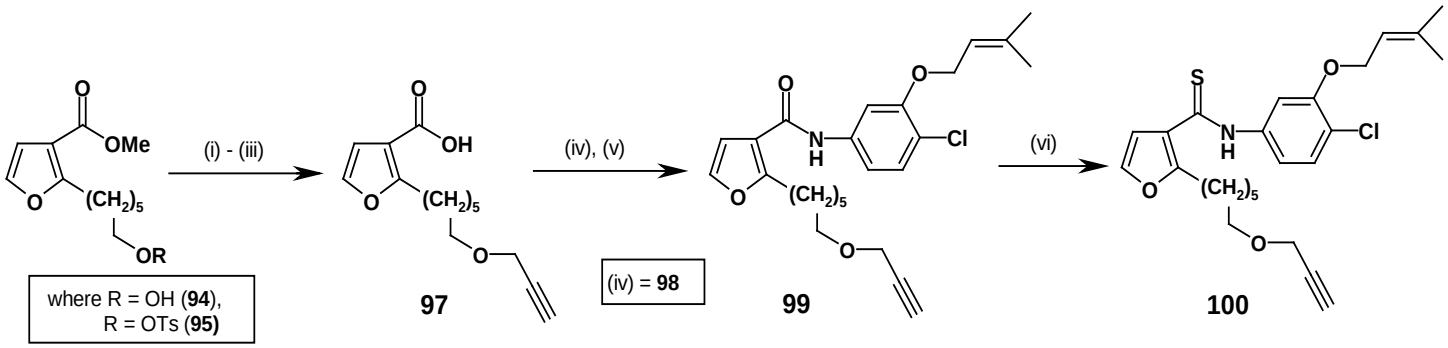

Scheme 2.9 *Reagents and conditions:* (i) *p*-TsCl, NEt_3, CH_2Cl_2, DMAP (cat) (94%); (ii) propargyl alcohol (10 eq), NaH (10 eq), THF, Δ; (iii) KOH, EtOH, (98%, 2 steps); (iv) $SOCl_2$, Δ; (v) RNH_2 **61**, pyr, (78%, 2 steps to give amide **99**); (vi) Lawesson's reagent, $NaHCO_3$, toluene, Δ, (70%).

Finally, thiation of amide **99** with Lawesson's reagent[165] in toluene at 90 ^{o}C with an equivalent of sodium hydrogen carbonate produced the C-2 elongated UC-781 derivative **100** for biological probing of substituent effects in the HIV reverse-transcriptase pocket, (Scheme 2.9). This reaction proved to be more problematic than was initially anticipated. Great care needed to be

taken with the amount of Lawesson's reagent added to the reaction mixture, keeping in mind a possible conversion of the furan ring into its corresponding thiophene.

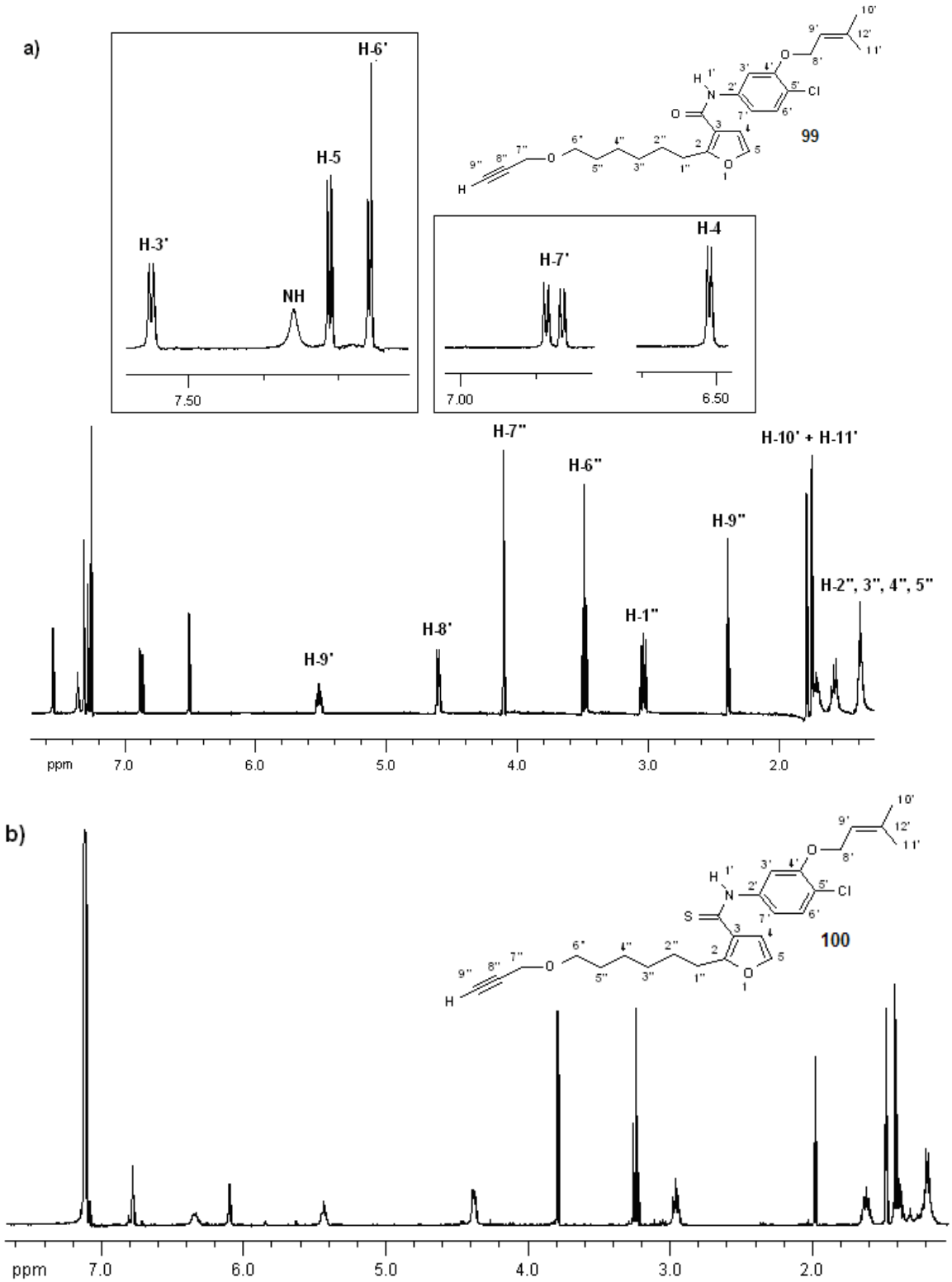

Figure 2.9 ^{1}H NMR spectra of a) amide **99**, b) thioamide **100**.

The partial double-bond character of an amide renders the oxygen atom of the amide nucleophilic character, and the latter is thus more nucleophilic than the furan oxygen. Hence, no thiophene formation was observed and the C-2 tethered UC-781 derivative was isolated in 70% yield after purification. Chromatographic success was only secured after the numerous failures on silica-gel columns were replaced by using flash-purification over neutral alumina. The thioamide **100** seemed to be very sensitive to the acidity of silica-gel columns, although the product could be obtained in lower yields (between 50-70%) on silica-gel after spiking the column with 5% triethylamine before loading commenced. Very importantly though, the reaction was only stopped after TLC confirmed the complete consumption of starting material, as the thioamide **100** had a very similar R_f to that of amide **99** on the plates. Evaluation of the products' ^{1}H and ^{13}C NMR spectra provided sufficient evidence for establishing the formation of thioamide **100**. The ^{1}H NMR spectrum of thioamide **100** revealed a similar pattern to that of amide **99** (Fig. 2.9) but with some significant shifts. However, confirmatory evidence was to come from infrared and mass spectrometry analysis. A distinguishing feature was the lack of a shift for the C-5 hydrogen (normally < 7 ppm for thiophenes) in the ^{1}H NMR spectrum indicating that thiophene conversion had not taken place as the H-5 signal resonated at δ_H 7.15 in **100**, relative to δ_H 7.32 in **99**. This was further confirmed in the ^{13}C NMR spectrum with the C-2 signal resonating steadily at δ_C 141.1 in **100**, compared to δ_C 140.9 in **99**. One surprise was that there was no visible shift in the ^{13}C NMR spectrum for the carbonyl signal of the thioamide, with the most deshielded signal resonating at δ_C 160.0. Literature precedence suggested that the thioamide signal should be very deshielded at around δ_C 200.0. Infrared spectroscopy (Fig. 2.10) finally provided positive results with the disappearance of the amide carbonyl stretching band at 1674 cm^{-1} in **99** (insert **b**, Fig. 2.10), and the appearance of thioamide stretching bands at 1162 and 1389 cm^{-1} in **100**. Finally, a correct HRMS evaluation (*m/z* HRMS (EI) 459.1634, $C_{25}H_{30}O_3NSCl$ requires *m/z* 459.1634), confirmed the structure of **100** as shown in Scheme 2.9.

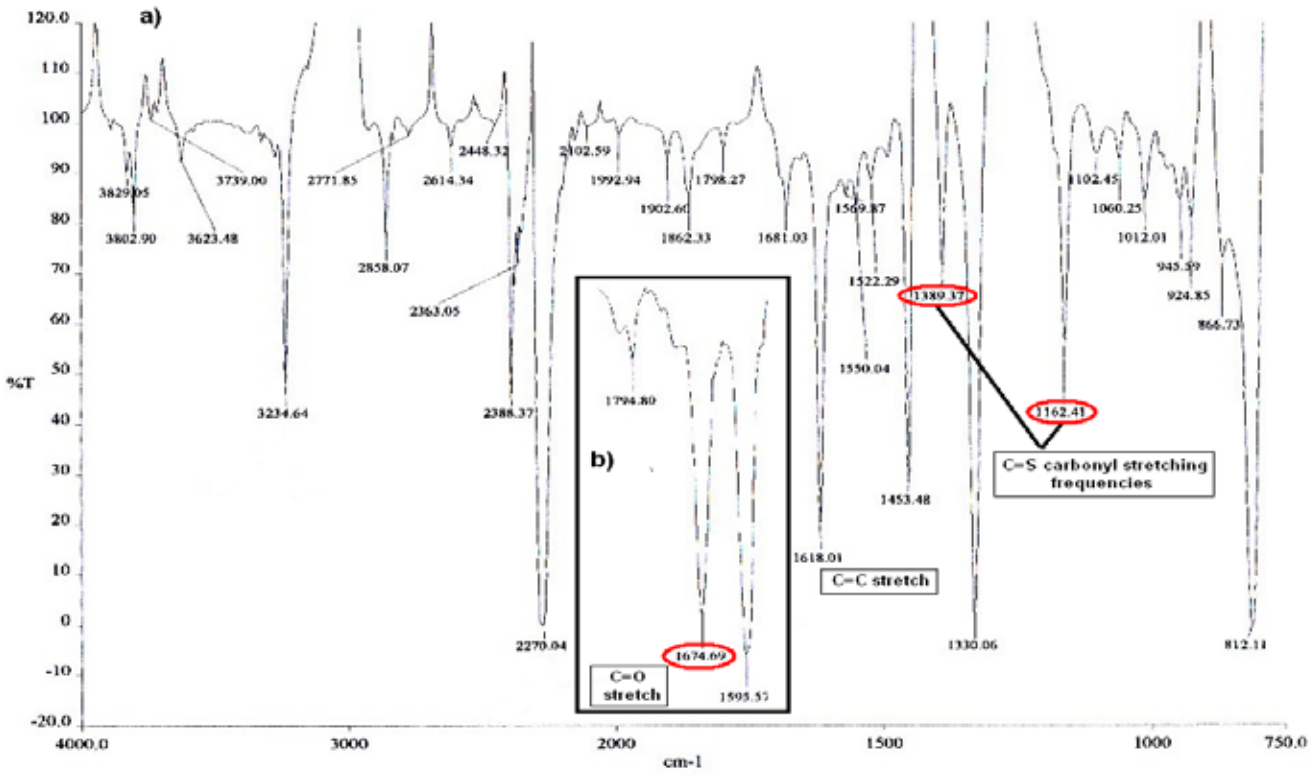

Figure 2.10 Infrared spectroscopy of a) thioamide **100**, and insert b) of amide **99**.

The next and penultimate step in the total synthesis of bifunctional target **58** was the Sonogashira coupling reaction of thioamide **100** to 5'-*O*-benzoyl-5-iodo-d4T **60**. Careful degassing of the tetrahydrofuran and dimethylformamide solvent mixture was carried out by bubbling pure crystal argon (~99.9% pure) through the solvents for ~1 hr in the presence of triethylamine to ensure complete de-oxygenation. This was vitally important in preventing oxidation of the Pd(0) and Cu(I) salts to be added. Thereafter, the dual-catalyst system was introduced after an hour and the mixture allowed to stir at room temperature. Unfortunately, every single attempt at this reaction failed to work. Reaction conditions were modified by increasing reaction temperatures, or changing the molar equivalents of catalysts added, yet no reaction occurred. It was assumed that the lack of reactivity was very likely due to the thioamide interfering in the Sonogashira reaction. The sulphur atom of the thioamide is a strong donor ligand capable of preventing oxidative insertion of R-X with Pd(0), ultimately terminating the mechanistic cycle of the Sonogashira reaction. To support this theory, we embarked on coupling amide **99** lacking the sulphur atom to see if a successful coupling could be obtained.

To this end, alkyne **99** was also subjected to a Sonogashira reaction with the nucleoside reverse transcriptase inhibitor derivative, 5'-O-benzoyl-5-iodo-d4T **60**, to afford benzoyl protected conjugate **101** (Scheme 2.10). As expected, under the identical conditions as mentioned above

for thioamide **99**, the reaction progressed smoothly and **101** was isolated in 61% yield after column chromatography. The ^{1}H NMR spectral data for **101** revealed signals for both **99** and d4U moieties in the ratio of 1:1 (Fig. 2.11). A successful coupling was further confirmed by the absence of a terminal alkyne proton at around δ_H 2.02 ppm. The ^{13}C NMR spectrum of **101** displayed diagnostic resonances at δ_C 144.0 (C-9), 90.6 (C-5), 58.8 (C-12) thus further confirming the presence of both the nucleoside and the alkyne. The structure was further confirmed by 2D NMR correlation.

Subsequent benzoyl group deprotection using 1M sodium methoxide in methanol yielded the unthiated bifunctional conjugate **102** in 51% yield. Debenzoylation was confirmed by an upfield shift in the diastereotopic protons at C-1 from δ_H 4.58 (multiplet) in **101** to δ_H 3.88 (dd, *J* 2.7, 12.4 *Hz*) and δ_H 3.78 (dd, *J* 2.7, 12.4 *Hz*) in **102**, respectively (see Fig. 2.11).

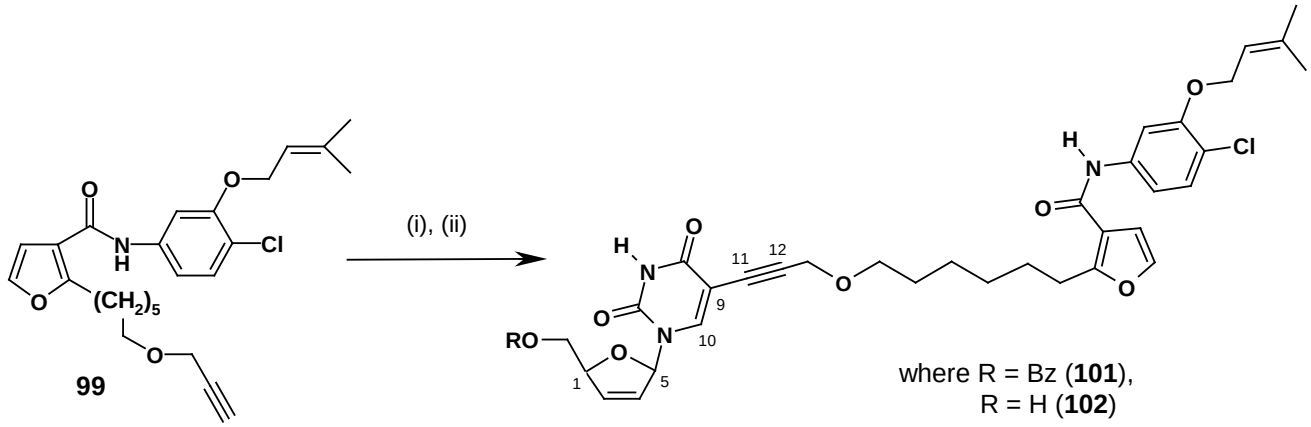

Scheme 2.10 *Reagents and conditions*: (i) 5'-Benzoyl-5-iodo-d4T, $Pd(PPh_3)_4$ (10%), CuI (50%), NEt_3 (2 eq), DMF/THF (1:2), rt, (61%); (ii) NaOMe, MeOH, rt, (51%).

The presence of a broad hydroxyl singlet at δ_H 2.80, as well as the absence of aromatic protons for the benzoyl group also confirmed the loss of the benzoyl group. The absence of the carbonyl carbon resonating at δ_C 166.3 as well as carbons for the aromatic group further confirmed that debenzoylation had taken place. Importantly, the olefinic protons of the ribose ring integrated correctly in the ^{1}H NMR spectrum. Other signals were intact indicating that no other tranformations had taken place.

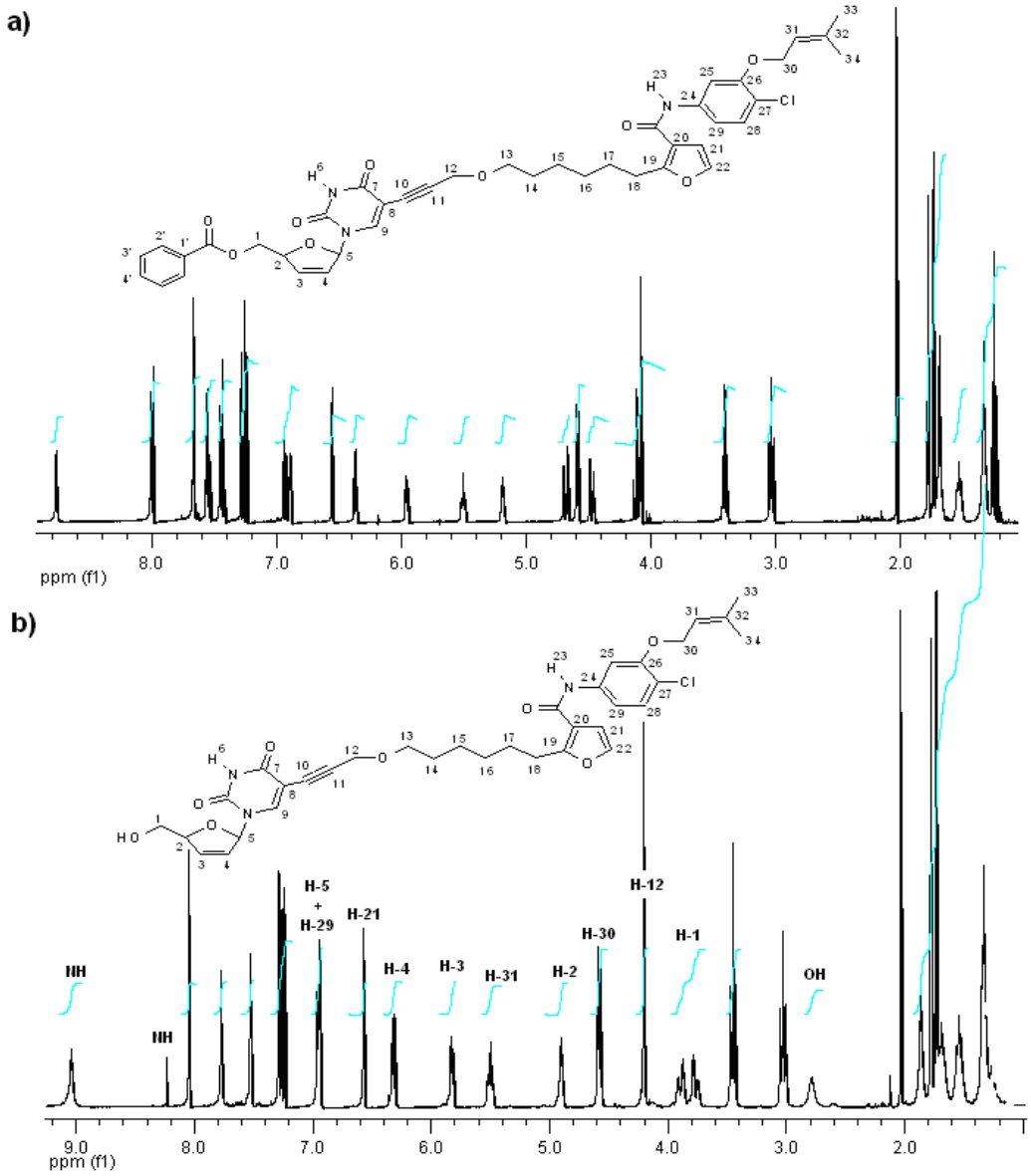

Figure 2.11 ^{1}H NMR spectra of a) **101** and b) **102**.

Unfortunately, all attempts at thiation of **101** or **102** using Lawesson's reagent failed. Compound **102** is the first example of a UC-781-derived conjugate (unthiated) as a result of developing this methodology.

The inhibition of viral replication in HIV-infected cells of the prototype tethered UC-781 compounds **99** and **100**, as well as unthiated bifunctional entity **102** were measured against HIV-1 (IIIB) replication in MT-2 cell culture using an MTT assay (Appendix I). Compound **100** had an EC_{50} value of 900 nM against 9 nM for UC-781, whilst compounds **99** and **102** showed no anti-HIV activity.

An examination of the inhibitory properties for these compounds offers insight into the design of a prototypical bifunctional compound, as well as offering valuable information regarding structure-activity relationships. Firstly, the fact that thioamide **100** is active and amide **99** not, suggests that the configuration around the thioamide is crucial for biological activity. Thioamides orientate in the *s-trans*-configuration (S larger than R), while amide bonds adopt an *s-cis*-configuration (R larger than O) according to IUPAC prioritization. Using biochemistry nomenclature, these designations are swopped (Fig. 2.12) to just '*cis*' for the thioamide and '*trans*' for the amide as defined by the relative orientation of the R groups. Here we will use the biochemistry nomenclature.

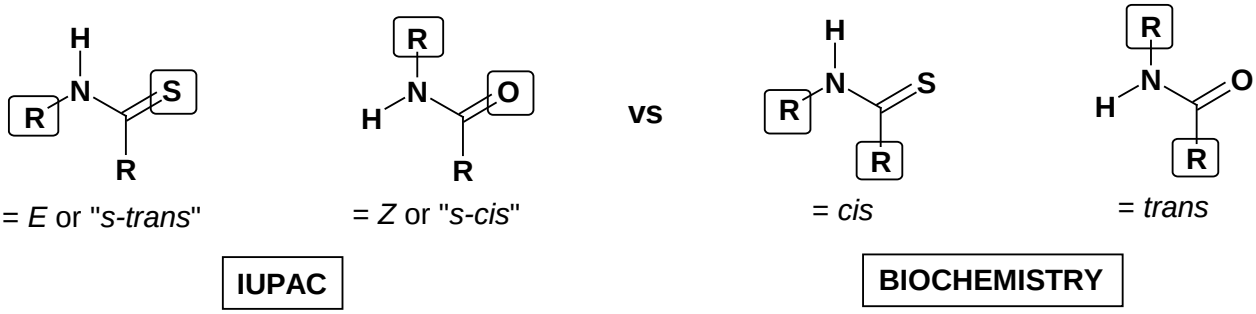

Figure 2.12 IUPAC and Biochemistry preferred configurations and nomenclature.

This configurational preference is easily understood by evaluating the size difference of a sulphur *vs* oxygen atom. In the *cis*-configuration, thioamide **100** is able to bind tightly and specifically to key residues in the NNRTI-BP such as Lys101 through two important hydrogen bonds as depicted in Figure 2.3. An important Wing II hydrophobic interaction between the DMA group and Tyr188 further cements the docking into the pocket. Thus, the incorrect *trans*-configuration of the amide **99** renders the molecule ineffective at binding to important pharmacophores residing in the NNRTI-BP. This may explain why bifunctional **102** showed no anti-HIV activity. In summary, the 100 fold reduction in potency, which casted doubt regarding the choice of tether attachment to the drug, together with the difficulties encountered in carbonyl group thiation, led us to ultimately change the NNRTI.

2.2.2 Synthesis of [d4U]-pentane-diPEG-propyne-[UC781]

2.2.2.1 Synthesis of the elongated spacer

The first priority in the synthesis of the elongated bifunctional target **59**, was to develop efficient strategies towards the synthesis of the spacer. It should be noted that this work was done

concurrently with the synthesis of target **58** and we were thus unaware of the end-game problems as described above in the synthesis of target **58**. Key to the spacer of **59** are two fragments **A** and **B** that are simplified in Figure 2.13.

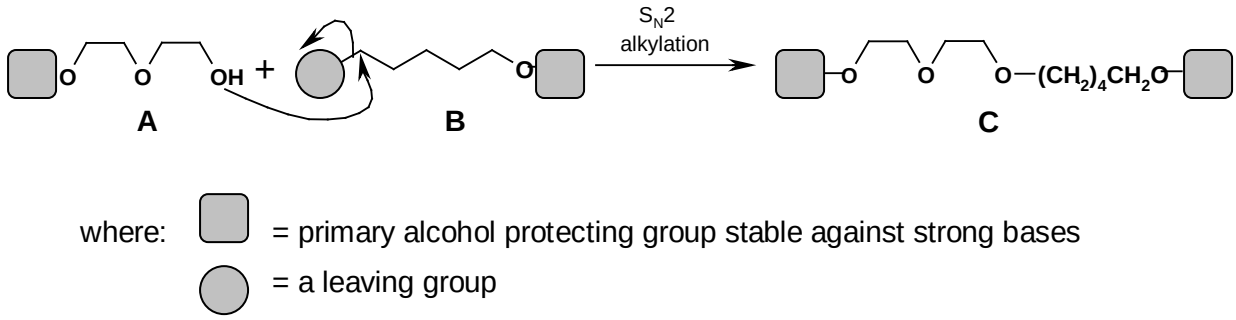

Figure 2.13 Illustration of two key fragments (A and B) required for the development of the spacer. Also included are the relevant functional groups which are essential in the synthetic route.

Therefore, the starting point in the synthesis of the spacer was to develop two key building blocks as: (i) a *mono-protected diethylene glycol unit* **A**, and (ii) a *linear 5-carbon chain unit* **B**, bearing both the functionalities of a leaving group and a protected alcohol, respectively, at the termini. The diethylene glycol unit **A** was introduced to overcome expected solubility issues in cell-culture testing.

Thus, the synthesis began with mono-protection of diethylene glycol *via* alkylation with benzyl bromide in tetrahydrofuran at room temperature (Scheme 2.11) using sodium hydride as base. An excess of diethylene glycol was used to avoid dialkylation, which could be separated in the extraction because of its water-solubility. The reaction was complete after 6 hours, and following work-up, the crude product was distilled to produce **103** in 70% yield.

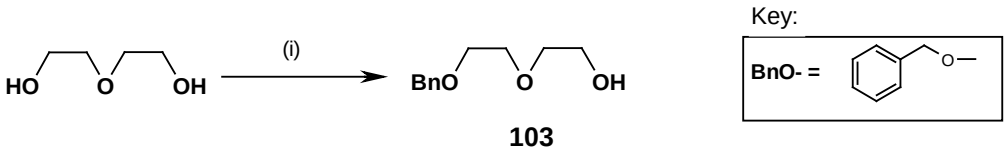

Scheme 2.11 *Reagents and conditions*: (i) BnBr, NaH, THF, rt (70%).

Much more challenging and time consuming, was the synthesis of the 5-carbon chain intermediate. The project explored two different hydroxyl protecting groups as tetrahydropyranyl (THP) and *p*-methoxyphenyl (PMP), as well as changing the leaving group from a bromide to a mesylate.

To this end, the transformation of commercially available 1,5-pentanediol **104** into intermediates **104b, c** and **e** was carried out *via* either a two or three-step conversion (Scheme 2.12). The first step, common to all, was the conversion of 1,5-pentanediol **104** into 5-bromo-1-pentanol **104a**

using hydrogen bromide (1.2 equivalents) and toluene at refluxing temperatures. A 55% yield was obtained after 10 hours without the azeotropic removal of water as reported in the literature procedure.[166] A small amount of the dibromide product was observed on TLC but was not isolated. The dibromide is a consistent by-product associated with this reaction,[166] but the bromopentanol **104a** could easily be purified by column chromatography.

Of the three routes undertaken to synthesize the 5-carbon chain intermediate (Scheme 2.12), two (**104b** and **104c**) required only one further step and so this was attempted first. The bromide leaving group was in place and all that remained was to protect the alcohol with a base-stable protecting group.

The first protecting group selected was the THP ether which was prepared using 3,4-dihydro-2H-pyran and Amberlite® in dichloromethane (Scheme 2.12, **104a** to **104b**) to afford compound **104b** in 82% yield. Although the yield was excellent, alternative protecting groups were explored because of difficulties experienced in the subsequent S_N2 alkylation described later.

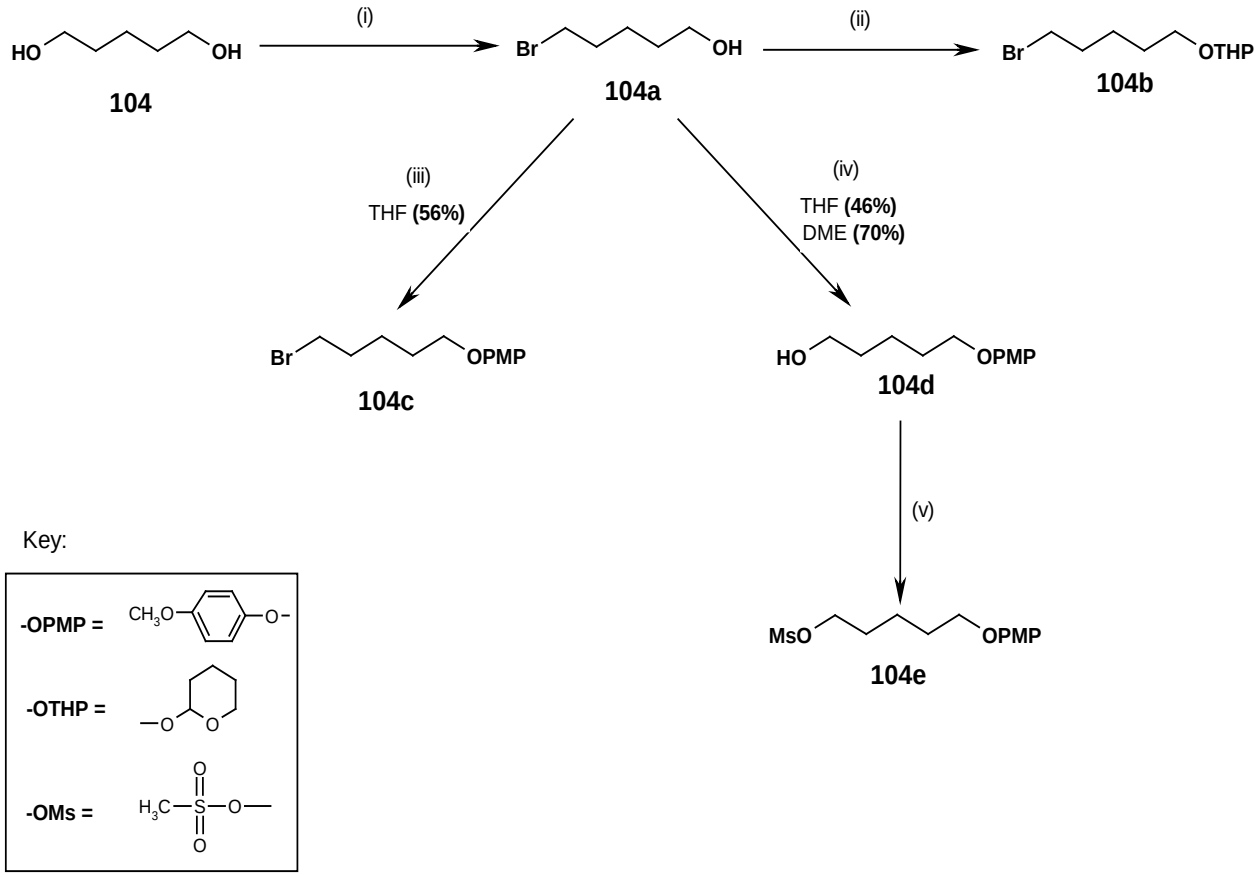

Scheme 2.12 *Reagents and conditions*: (i) HBr, H_2O, toluene, Δ (55%); (ii) DHP, Amberlite®, CH_2Cl_2 (82%); (iii) *p*-methoxyphenol, PPh_3, DIAD, THF (56%); (iv) *p*-methoxyphenol, NaH, solvent, Δ (THF-46%, DME-70%); (v) MsCl, pyr, CH_2Cl_2, DMAP, rt (93%).

The second protecting group studied was the *p*-methoxyphenyl group. This was introduced *via* two methods. In the first approach, a Mitsunobu reaction (Scheme 2.12, **104a** to **104c**) was used, in which the hydroxyl group is activated to an oxyphosphonium salt *via* the Mitsunobu reagents (triphenylphosphine and diisopropyl azodicarboxylate).[167] Subsequent substitution occurs *via* the phenoxide ion of *p*-methoxyphenol (or 4-hydroxyanisole) accompanied by an inversion of configuration, which has no stereochemical significance in this case. The procedure was carried out by adding *p*-methoxyphenol, triphenylphosphine and diisopropyl azodicarboxylate (DIAD) together in tetrahydrofuran (THF) to **104a**. Even though the reaction proceeded to completion in 2 hours at room temperature, enormous difficulty was experienced in trying to separate the desired product **104c** from the hydrogenated DIAD. Silica-gel TLC showed a small separation of the two components using pure hexane as solvent. However, column chromatography using the same solvent gave poor separation and the hydrogenated DIAD consistently co-eluted with **104c**. A 56% yield of product mixed with DIAD was finally obtained. The resulting ^{1}H NMR spectrum displayed diagnostic signals for the methoxy peak at δ_H 3.77, as well as an aromatic singlet at δ_H 6.83.

The second method used (Scheme 2.12, **104a** to **104d** to **104e**) for *p*-methoxyphenyl introduction involved a longer but less problematic sequence involving nucleophilic substitution of the bromide end of **104a**.[168] Thus, *p*-methoxyphenol was added to a suspension of sodium hydride in THF or dimethoxyethane (DME) as solvent, at 0^{o}C. To the resulting alkoxide anion, *in situ*, was added **104a** and the reaction mixture refluxed. After 24 hours, following work-up and column chromatography, a crystalline compound **104d** was obtained in variable yields (Table 2.2) depending on the solvent. A significantly improved yield for **104d** was obtained when the reaction was performed in DME (70%), rather than THF (46%). This effect can be attributed to the sodium ion's ability to chelate to the higher boiling solvent. Elemental analysis returned good combustion data for **104d**. Diagnostic signals in the ^{1}H NMR spectrum were the methoxy peak at δ_H 3.77 and the aromatic singlet at δ_H 6.82, integrating correctly against the polymethylene groups of the chain. Further confirmation was gained using infrared spectroscopy with a broad diagnostic stretch at 3617 cm^{-1} characteristic of a free hydroxyl group.

Table 2.2 Percentage yield of protection of **104a** in different solvents

	Solvent		
Compound	*Dichloromethane (DCM)*	*Tetrahydrofuran (THF)*	*Dimethoxyethane (DME)*
104b	82%	-	-
104c	-	56%	-
104d	-	46%	70%

The last step involved conversion of the hydroxyl group of the alcohol **104d** into a better leaving group. The mesylate was chosen for this purpose using methanesulfonyl chloride and pyridine as base in dichloromethane, with catalytic amounts of 4-dimethylaminopyridine (DMAP) added. The desired mesylate **104e** was obtained in 93% yield after column chromatography. The appearance in the ^{1}H NMR spectrum of a methyl singlet at δ_H 3.00, as well as the strong sulfonyl stretches at 1356 and 1175 cm^{-1} in the infrared spectrum supported the formation of **104e**.
This concluded the synthesis of the 5-carbon intermediate chain.

The next step in the synthesis of the spacer was the alkylation of **103** *via* an S_N2 reaction (as illustrated in Figure 2.12), with each of the three 5-carbon chain intermediates **104b**, **c** and **e** (Scheme 2.13), in order to identify the best coupling partner.

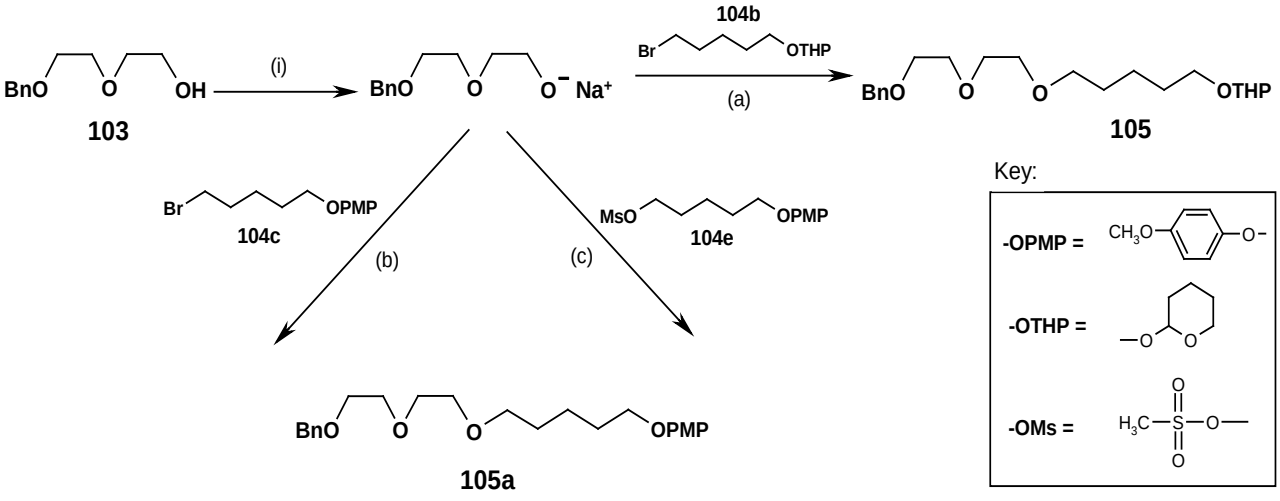

Scheme 2.13 *Reagents and conditions*: (i) NaH, solvent, Δ (**a** = THF = 41%); (**b** = THF = 37%); (**c** = THF = 72%, DME = 74%).

Each reaction of **103** was carried out with sodium hydride suspended in THF or DME at 0^{o}C in order to deprotonate **103** to its alkoxide anion, before subjecting **104b**, **c** and **e** to the mixture in

separate reactions. Furthermore, each reaction was performed in different solvents, as above, and at different temperatures. The reaction between **103** and **104b** gave low yields (41%) of compound **105** in THF at 0°C, in which the starting material decomposed at elevated temperatures. From the observed results it was concluded that the tetrahydropyranyl group was unstable and this was therefore eliminated as a synthetic option.

The reaction between **103** and **104c** also gave low isolated yields (37%) of **105a**, following refluxing in THF, even though the reaction proceeded to completion after just 2 hours. When taking into account the difficulties encountered in purifying **104c**, it was eliminated as the synthetic route to follow.

Most impressive was the reaction between **103** and **104e**. The alkylation produced good yields of **105a** following refluxing the reaction. Also discovered, very importantly, was that the reaction was solvent dependent. A summary of all the results is given in Table 2.3.

Table 2.3 Percentage yields for formation of **105a** from the alkylation reaction using three different 5-carbon chain intermediates in different solvents

	Solvent			
5-carbon intermediate	*Tetrahydrofuran (THF)*	*Dimethoxyethane (DME)*	*Temperature (°C)*	*Time (hrs)*
104b	41%	-	69	24
104c	37%	-	69	2
104e	72%	74%	69 and 102	20 (THF), 5 (DME)

Table 2.3 shows how much more effective the alkylation proceeded using the mesylate **104e** compared to the bromide **104c** as the leaving group. Also, importantly, the reaction using a higher boiling solvent, such as DME, went to completion much faster than with THF. This significant reduction in time may also be attributed to the sodium ions chelating to DME, lowering the activation energy barrier of the reaction and thereby going to product formation faster.

Evidence that coupling to compound **105a** had taken place was provided by its ^{1}H NMR spectrum, in which two aromatic peaks at δ_H 6.82 and δ_H 7.35, together with the methoxy singlet at δ_H 3.76 and the benzyl methylene at δ_H 4.57, in the correct relative integration, could be observed. The ^{13}C spectrum returned the correct number of signals (19 as 8:8:3). Preparation of mesylate **104e** was subsequently scaled-up as this was chosen as the synthetic intermediate of choice.

In the next step, deprotection of the *p*-methoxyphenyl protecting group of **105a** was achieved using cerium(IV) ammonium nitrate (CAN), at 0°C, in a 4:1 (v/v) mixture of acetonitrile/water as

originally reported[169,170] (Scheme 2.14). The mechanism of the reaction is thought to proceed[170] *via* a single-electron radical oxidation and occurs very rapidly. Careful monitoring of the reaction was required to avoid unwanted by-products or possible decomposition of the starting material.

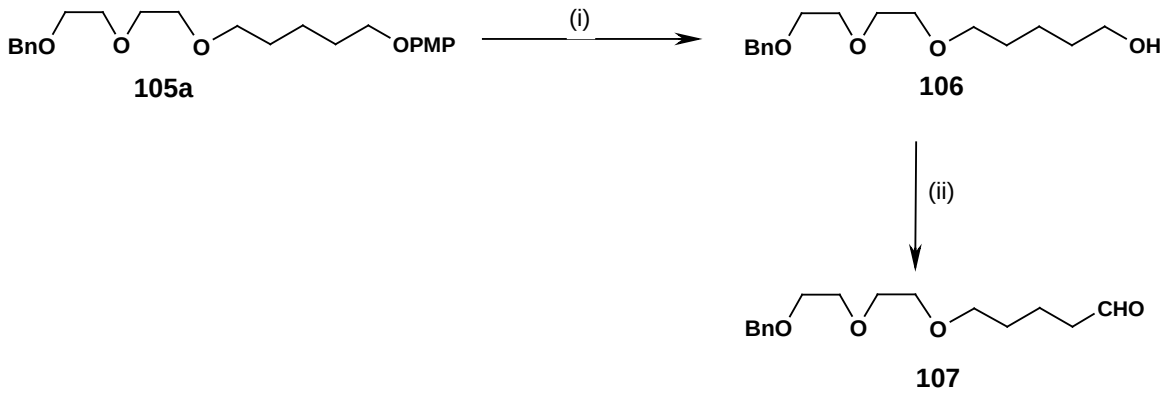

Scheme 2.14 *Reagents and conditions*: (i) CAN, CH_3CN:H_2O (4:1), 0 ^oC (86%); (ii) DMSO, $(COCl)_2$, NEt_3, CH_2Cl_2, -78 ^oC (98%).

The reaction was found to go to completion after only 10 minutes. Observing colour changes of the reaction mixture from start to finish was also a very reliable way to monitor the reaction progress. CAN was always added last to the reaction mixture, and after its addition the solution turned an immediate dark purple colour. The dark colour then slowly faded until completion when the solution became a clear orange colour.

CAN is a very harsh oxidising agent and it was found that leaving the reaction to go for any longer than 10 min resulted in the formation of undesirable by-products. It was suspected that the low pH of the reaction was also not favourable. Column chromatography purification following extractive work-up yielded the alcohol **106** in 86% yield. The key spectroscopic indicators in the ^1H NMR spectrum of **106** were the broad -OH singlet at δ_H 1.96, together with the disappearance of the aromatic peak around δ_H 6.82, as well as the methoxy peak around δ_H 3.76, confirming that deprotection had taken place. The ^{13}C NMR spectrum returned the correct number of resonances, i.e. 14.

The final reaction carried out, before coupling of the inhibitor building blocks commenced, was to transform alcohol **106** into aldehyde **107** *via* a Swern oxidation (Scheme 2.14). Dimethyl sulfoxide was thus added to dichloromethane and to the suspension was added oxalyl chloride at -78^{o}C. Addition of the alcohol **106** was followed by stirring for 15 min and the reaction mixture finally treated with triethylamine and allowed to warm to room temperature. The desired aldehyde **107** was obtained in 98% yield following work-up and column chromatography. The

diagnostic signal in the ^{1}H NMR spectrum of **107** was the singlet at δ_H 9.73 for the aldehyde proton. Infrared spectroscopy supported this with a strong stretching frequency at 1710 cm^{-1} characteristic of an aldehyde.

2.2.2.2 Synthesis of the tethered UC-781

In line with the retrosynthetic analysis proposed, a *Wittig* and subsequent hydrogenation *reaction* was employed to be a versatile method for C-2 chain elongation. Thus, it was decided to directly apply the methodology to aldehyde **107**.

To this end, phosphonium salt **90** was first reacted in dry methanol with 1.1 equivalents of a concentrated sodium methoxide/methanol mixture (4.63 M). The resultant concentration was about 0.10 M in methanol, at 0^{o}C (Scheme 2.15). The resulting ylide is stabilized because of the conjugation of the ylid carbanion into the ester, and therefore the reaction was expected to be *E*-selective and under thermodynamic control. Once again, colour was a very effective manner of monitoring the reaction progress. After addition of aldehyde **107** to the reaction mixture, the solution turned an immediate dark-red colour, which changed to light-orange at around 50% completion by TLC. Completion of the reaction was indicated by an almost clear solution within 3 hours. The same colour-changing pattern was observed in the model study carried out using hexanal and formaldehyde with the same phosphonium salt **90** above.

Surprisingly though, the experimentally observed ratio of E:Z isomers was found to be 3:2 after repeated attempts at the reaction, with yields for **108** consistently fluctuating at around 80%. A 3:2 ratio suggests a more kinetically controlled reaction preventing equilibration to the more stable product. Key spectroscopic indicators in the ^{1}H NMR spectrum of **108** were the two allylic methylene peaks at δ_H 2.27 and δ_H 2.60, which could be seen in a 3:2, E:Z ratio. The 3:2 ratio, however, was not detrimental because of the hydrogenation reaction which was to follow.

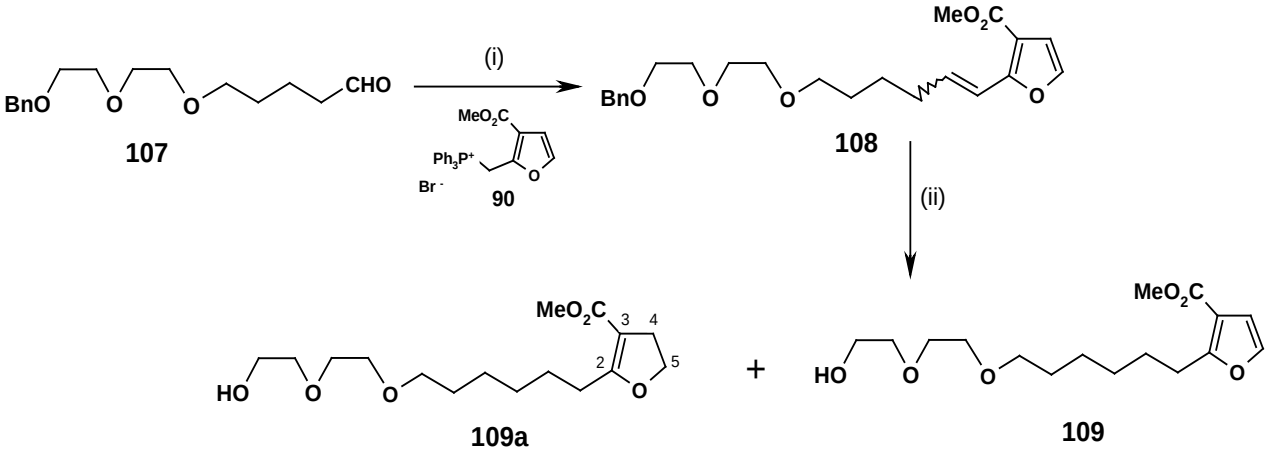

Scheme 2.15 *Reagents and conditions*: (i) phosphonium salt **90**, NaOMe, MeOH, rt (81%); (ii) H_2, Pd/C, EtOH, rt.

The hydrogenation reaction (Scheme 2.15) was intended to hydrogenate the double bond with concomitant hydrogenolysis of the benzyl group. The reaction was carried out by dissolving the tethered furan ester **108** in absolute ethanol with catalytic amounts of palladium-on-carbon added. The reaction vessel was then exposed to a constant atmosphere of hydrogen gas at room temperature and then carefully monitored at 10 min intervals by TLC. After ½ hr, TLC showed that the starting material had disappeared to form two spots running very close to each other. One spot ran slightly higher (i.e. less polar) than the starting material and sprayed red on TLC, while the other spot ran slightly lower (i.e. more polar) than the starting material and sprayed a bright-yellow colour on TLC. It was tentatively concluded that the less polar spot involved over-reduction of the furan ring to form the tethered dihydrofuran product **109a**, which formed simultaneously (see next paragraph) with the desired product **109**.

After a further ½ hr the deprotection of the benzyl group was complete, marked by a significantly more polar product on TLC. Unfortunately, no solvent system was able to separate the undesired dihydro-product **109a** from the desired product **109**. No yields were thus reported for this step. As before in the model study, TLC suggested after 10 min that the external olefinic bond is reduced first, after which over-reduction of the furan ring (according to ^{1}H NMR the 4,5-bond is reduced, not the 2,3-bond on the furan ring) starts. Debenzylation was slower and there seemed to be no difference in deprotection of the benzyl group between the two intermediates, with simultaneous debenzylation being observed after numerous attempts. The events can be reasoned as follows: the external olefin is reduced first because of its lower activation energy compared to stability associated with the heteroaromatic ring, although furan is notorious for having a much lower resonance energy (furan = 65 kJ/mol compared to benzene = 150 kJ/mol). The reason why only the dihydro-product is observed and not the tetrahydrofuran product is

probably because of the steric difficulty associated with reduction of a tetra-substituted double bond compared to a di-substituted double bond.

For chain extension, the tethered furan alcohol **109** was then converted into a tosylate as a leaving group for the propargylation step (Scheme 2.16), which involved *p*-toluenesulfonyl chloride together with triethylamine in dichloromethane. A catalytic amount of DMAP was added to speed up the reaction. The desired tosylated tether **110** was thus obtained in 76% yield after column chromatography. It was also possible to separate the over-reduced tosylated compound in 12% yield, which revealed the reduction of the 4,5-double bond as expected. Diagnostic signals in the ^{1}H NMR spectra of **110** were the tosyl group methyl peak at δ_H 2.41 and the aromatic peaks at δ_H 7.31 and δ_H 7.79. Infrared spectroscopy also showed two strong peaks at 1177 and 1369 cm^{-1} characteristic of a sulfonyl (S=O) stretch and this supported the formation of **110**. The ^{13}C NMR spectrum revealed the correct number of resonances, i.e. 21.

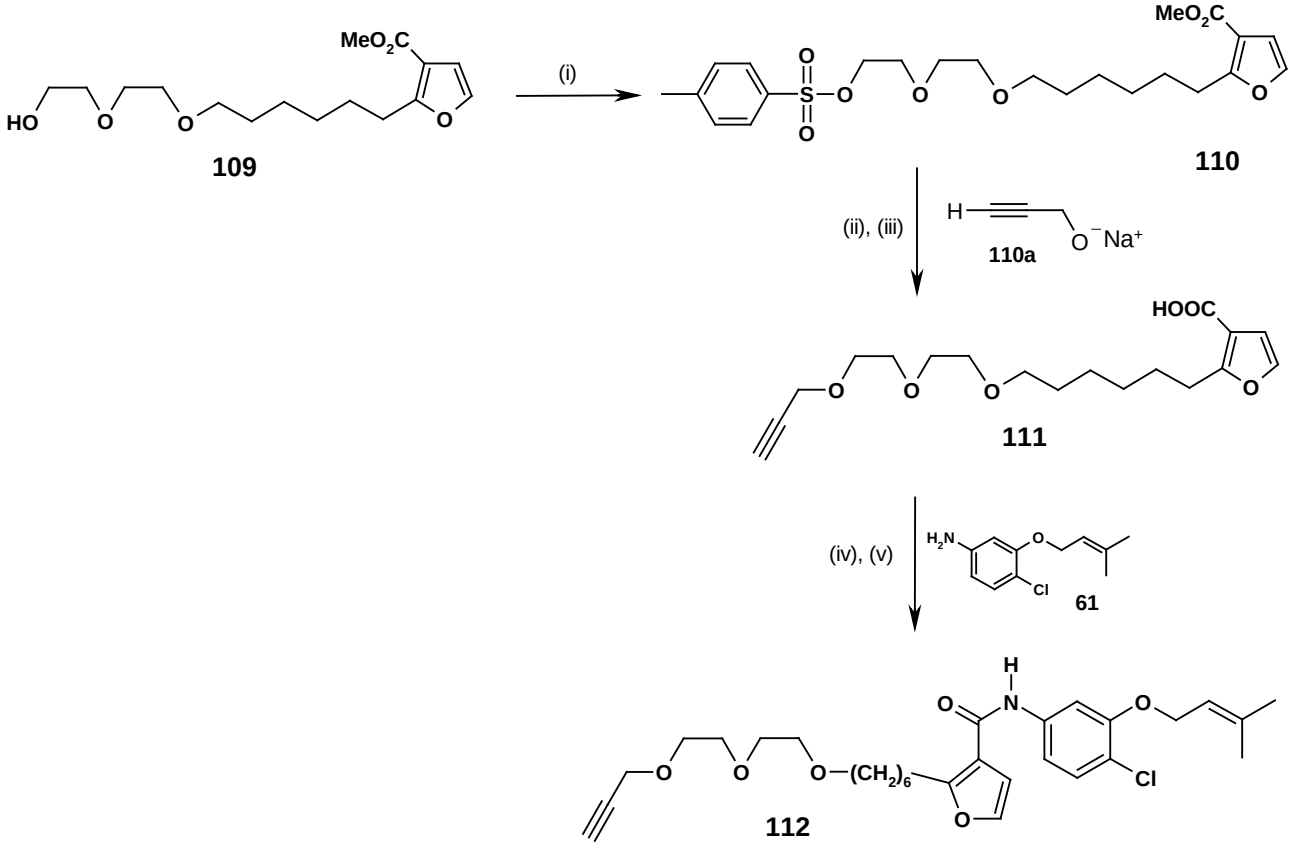

Scheme 2.16 *Reagents and conditions*: (i) *p*-TsCl, NEt_3, CH_2Cl_2, DMAP (cat) (76%); (ii) propargyl alcohol (10 eq), NaH (10 eq), THF, Δ; (iii) KOH, EtOH, (95%, 2 steps); (iv) $SOCl_2$, Δ; (v) RNH_2, **61**, pyr, (78%, 2 steps to give amide **112**).

A significant feature of the ^{1}H NMR spectrum of **110** (Figure 2.14) were the protons between δ_H 3.49 - δ_H 3.68 (3 peaks), as well as the peak at δ_H 4.15 assigned to the methylene protons connected to the glycol. Unlike previous spectra, these resonances were separated owing to the strong deshielding effect of the tosylate. The ^{13}C NMR was completely assigned using HSQC and HMBC 2-D techniques.

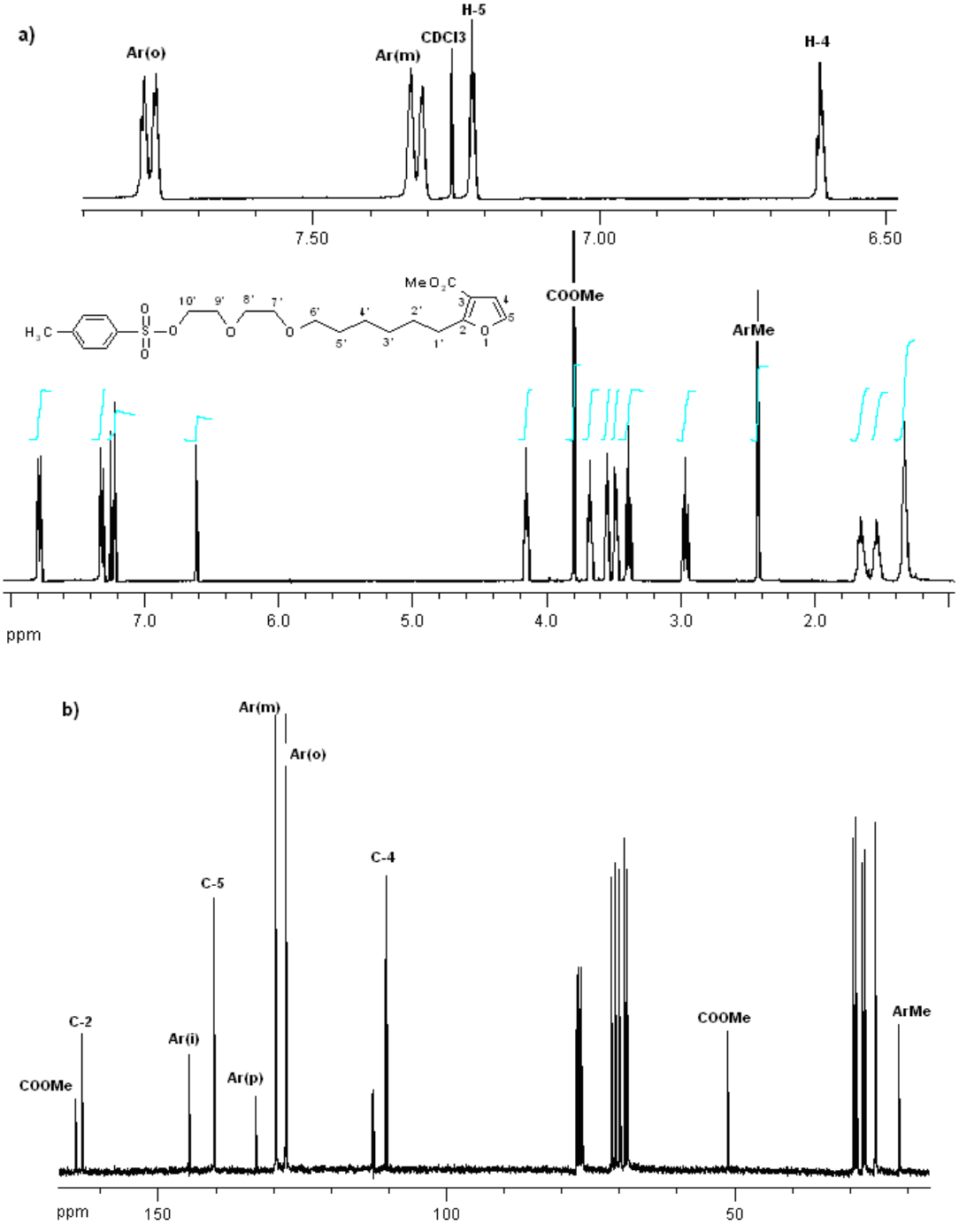

Figure 2.14 a) ^{1}H and b) ^{13}C NMR spectra of the tosylated tether **110**.

The subsequent propargylation reaction (Scheme 2.16), was achieved by firstly forming an alkoxide **110a** (in large excess) from the reaction between propargyl alcohol and sodium hydride in THF at 0°C. The tosylated tether **110** was subsequently added at refluxing temperature, and after an hour, all starting material had disappeared on TLC. The mechanism is presumably S_N2. A few drops of 1M NaOH were added to the reaction mixture to hydrolyse the ester to the corresponding carboxylic acid and the mixture refluxed for a further hour. Carboxylic acid **111** was thus obtained in 95% yield after column chromatography. The appearance in the ^{1}H NMR spectrum of an alkyne proton at δ_H 2.41 and an alkyne methylene doublet at δ_H 4.20 supported the formation of **111** (Figure 2.15). Infrared spectroscopy also confirmed the presence of a carboxylic acid with a strong absorption at around 1683 cm^{-1} characteristic of an acid carbonyl group.

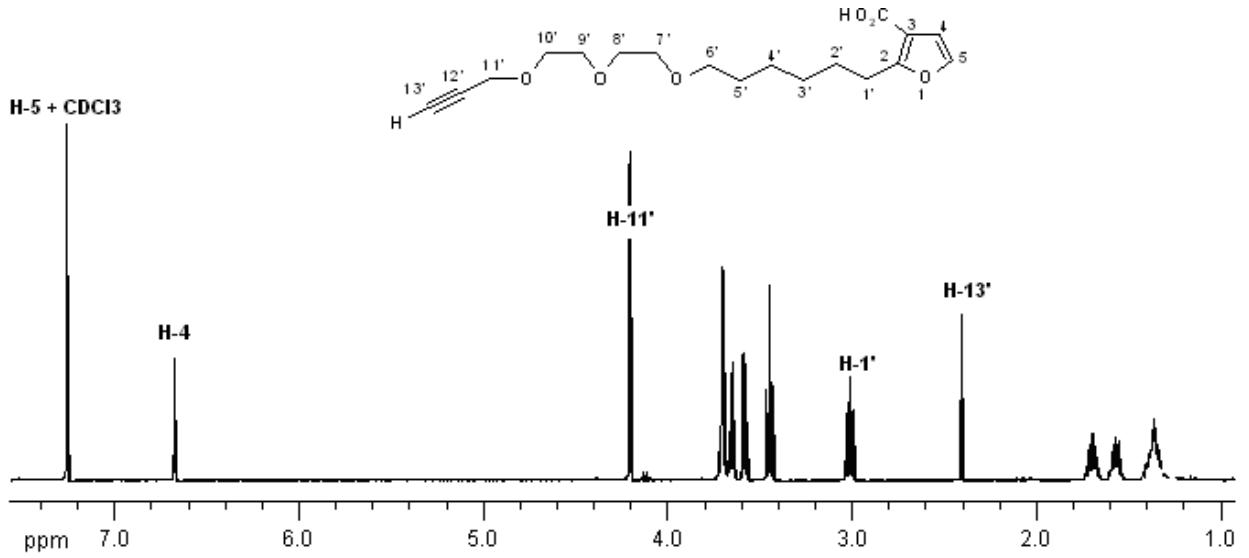

Figure 2.15 ^{1}H NMR spectrum of the alkyne tether **111**.

It is important to note from Figure 2.15 that the cluster of peaks between δ_H 3.58 - δ_H 3.70 designated to the methylenes of the glycol had now coalesced. Interestingly, previous studies on analogous systems had shown that the propargylation reaction worked best this way round, i.e. better than using the alkoxide of **109** with propargyl bromide. This may have something to do with the softness of the propargyloxy anion.

The first compound to be synthesized for anti-HIV testing was the *amide* **112** (Scheme 2.16). To this end, alkyne tether **111** was dissolved in excess thionyl chloride and heated to 40°C for 1 hour, whereafter the excess reagent was removed *in vacuo*. Pyridine was then added to the crude mixture together with dichloromethane at 0°C, followed by arylamine **61** and the mixture

left at room temperature. The reaction went to completion within 30 min (TLC) and amide **112** was obtained in 78% yield after column chromatography. Definitive spectroscopic signals in the ^{1}H NMR spectra of **112** were the amide NH signal at δ_H 7.58, together with the two methyl peaks at δ_H 1.74 and δ_H 1.78. A strong peak at 3304 cm^{-1} in the infrared spectrum further confirmed the formation of the amide.

2.2.2.3 Sonogashira coupling and final deprotection

The final reaction carried out in this part of the project was a Sonogashira coupling of a 5'-iodo-d4U derivative **60** to the amide **112** (Scheme 2.17).

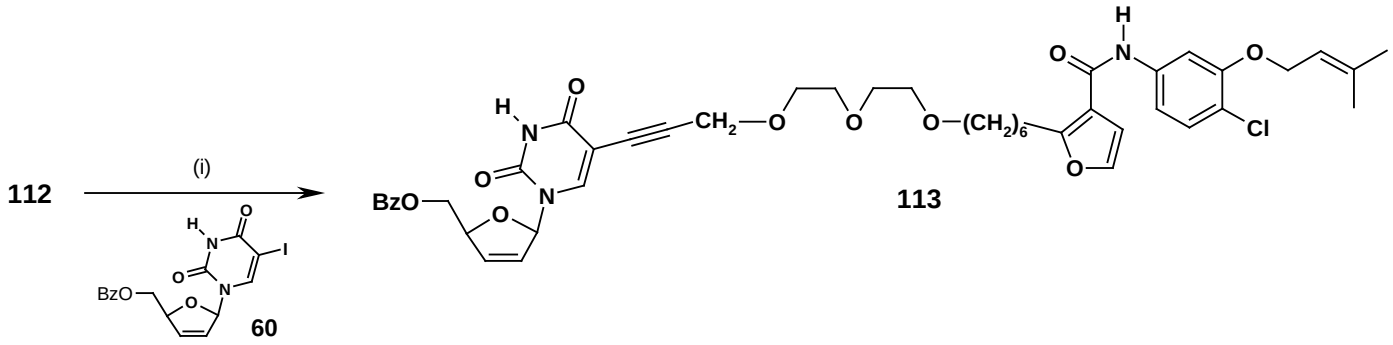

Scheme 2.17 *Reagents and conditions*: (i) 5'-Benzoyl-5-iodo-d4T, $Pd(PPh_3)_4$ (10%), CuI (50%), NEt_3 (2 eq), DMF/THF (1:2), rt, (61%).

The Sonogashira coupling reaction conditions involved adding triethylamine and reactants to a mixture of dimethylformamide and tetrahydrofuran (1:2, v/v), which was thoroughly degassed before the onset of the reaction to avoid unwanted oxidation of the palladium(0) catalyst. Introduction of the catalyst combination of Pd(0) / CuI in the form of solids resulted in product **113** formation after 2 hrs in 61% yield after column chromatography. Inherant to Sonogashira reactions are the undesirable Glaser-Edlington coupling of two molecules of alkyne leading to a homodimer. Fortunately, none of this undesired by-product was observed though. Key spectroscopic indicators in the ^{1}H NMR spectra (Fig. 2.16) of **113** were the d4U anomeric proton at δ_H 6.93, the imide proton at δ_H 8.63 as well as the UC-781 amide proton at δ_H 8.03. The appearance of a benzoyl aromatic multiplet between δ_H 7.45-7.55 was also diagnostic and the resonances from each fragment integrated correctly. The ^{13}C NMR returned the correct number of resonances of 44.

Again, every effort was put into conversion of **113** to the thioamide using Lawesson's reagent varying all of the reaction parameters, but without success. All of the material was consumed unfortunately in the myriad of attempts to synthesize the thioamide and no deprotection of the

benzoyl group of **113** was thus attempted. As expected, amide **112** had no anti-HIV activity, presumably for the same reasons as outlined before. Compound **113** was not tested for anti-HIV activity.

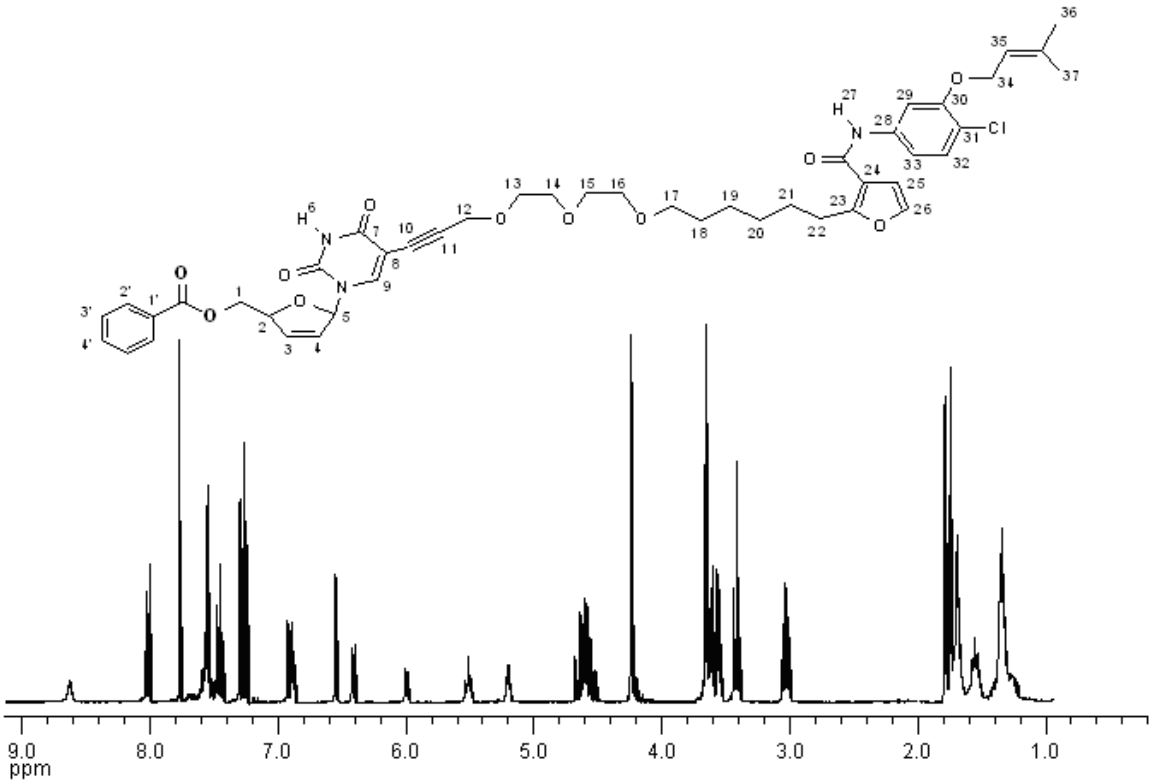

Figure 2.16 ^{1}H NMR spectrum of the alkyne tether **113**.

In summary, new methodology applicable to large-scale work has been developed for C-2 alkylation of 3-furoates of interest to both natural product synthesis and medicinal chemistry. Thiation of **102** and **113** was crucial in trying to probe the RT enzyme, and failure to do so led us to replace the NNRTI, thus creating a new bifunctional target for studying possible synergy between the substrate binding site and the NNRTI-BP.

SYNTHESIS OF d4U-SPACER-PYRIMIDINYLARYLAMINE DOUBLE-DRUGS

3.1 Strategy for the synthesis of [d4U]-spacer-[pyrimidinylarylamine]

A replacement NNRTI for UC-781 (Chapter 2) was identified as TMC120 based on the clinically approved TMC125 (Fig. 3.1) belonging to the family of diarylpyrimidines (DAPY's). These so-called third-generation NNRTI's were chosen for their remarkable anti-HIV potency against wild-type (2 nM for TMC125 and 1 nM for TMC120), as well as against single- and double-point mutations found in the NNRTI-BP upon binding of an NNRTI.[72]

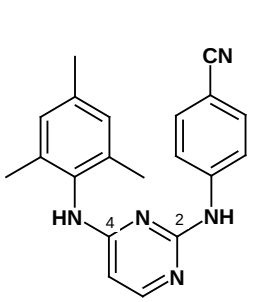

TMC120

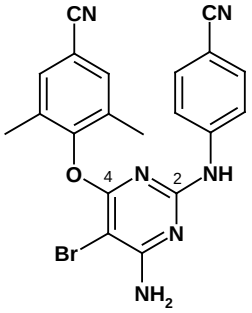

TMC125

Figure 3.1 Structures of TMC120, TMC125 and TMC278 belonging to the family of DAPY's.

Thus, the initial objective of this part of the project became the synthesis of bifunctional compounds of the general formula [d4U]-spacer-[DAPY] in search of synergism between the two inhibitors. Molecular modeling studies published independently by Balzarini[91] (Fig. 3.2 a) and Pauwels[73] (Fig. 3.2 b) on the binding of the DAPY derivative, TMC125, were used to ascertain the optimal connecting point for spacer elongation from the NNRTI. According to the Pauwels modeling interpretation depicted in Figure 3.2 (b), the proposed docking of TMC125 sees the pyrimidine unit firmly embedded into WING I of the RT NNRTI pocket, together with the less-substituted phenyl ring (attached to C-2 of the pyrimidine) bound in the hydrophobic WING II (interacting with Lys101 and Tyr318). The more substituted phenyl ring (attached to C-4 of the pyrimidine) snuggles in towards the back of WING II near to Tyr188 and Tyr181 but its *ortho*-methyl group offers the possibility of exiting the 'front' of the pocket towards Glu138 and the p66 subunit of RT. By comparison, the *para*-methyl group of the C-4 phenyl ring points towards Trp229, newly described by Arnold as the 'back exit tunnel' which in theory might access the NRTI binding site.[171] It should be noted though, that at the start of this part of the project, this so-called 'back exit tunnel' was unknown to all and thus the *para*-methyl group was not considered for spacer elongation. Importantly therefore, for the purpose of a complete structure-activity

relationship study, both the *ortho*- and *meta*-positions of the C-4 aromatic ring were identified for spacer extension.

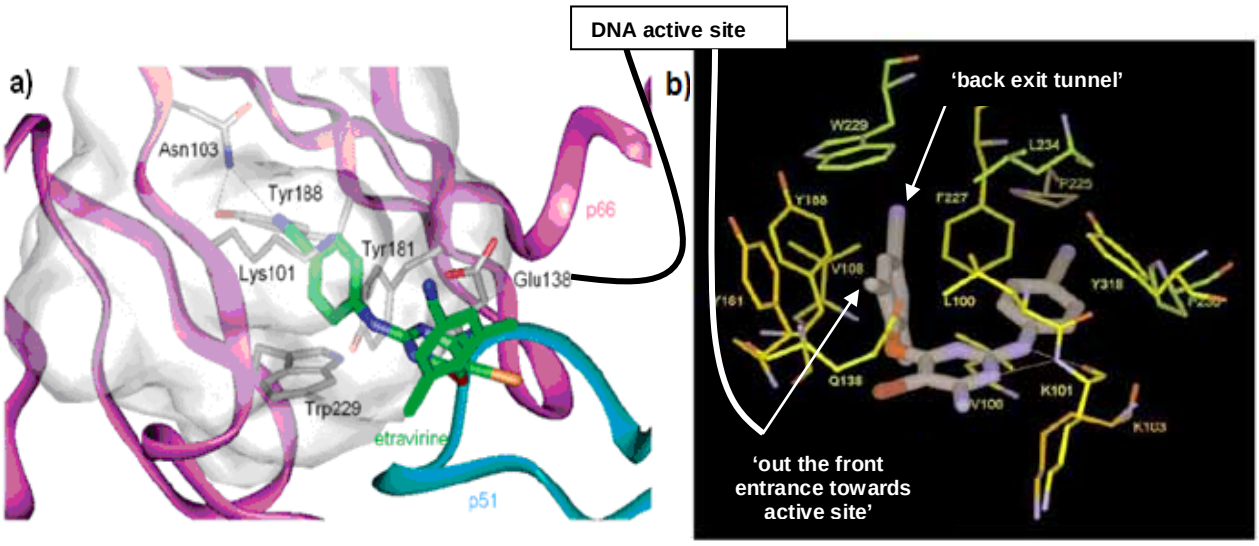

Figure 3.2 a) Proposed docking[91] site for TMC125 at the entrance of NNRTI-BP of HIV-1 RT, b) Proposed docking of 2-pyrimidinylarylamines at the entrance of the NNRTI-BP of HIV-1 RT.[73]

Recently, Jorgensen[87,172,173] has demonstrated the use of both 2-pyrimidinylarylamines and 2-thiazolylarylamines as potential NNRTI's (Fig. 3.3). Of interest to us were his 2-pyrimidinylarylamines of general formula (Het-NH-ArX), where Het is a pyrimidine heterocycle and X a substituent of the phenyl (Ar) ring, which showed excellent biological activities (5 nM for X = CN; 6 nM for X = Cl) supporting the motif in Figure 3.3 (b) with the C-2 aromatic ring firmly embedded into WING II. Jorgensen's simplified motif thus strips off the C-4 aromatic ring, in comparison to a full DAPY, and still retains excellent biological activity.

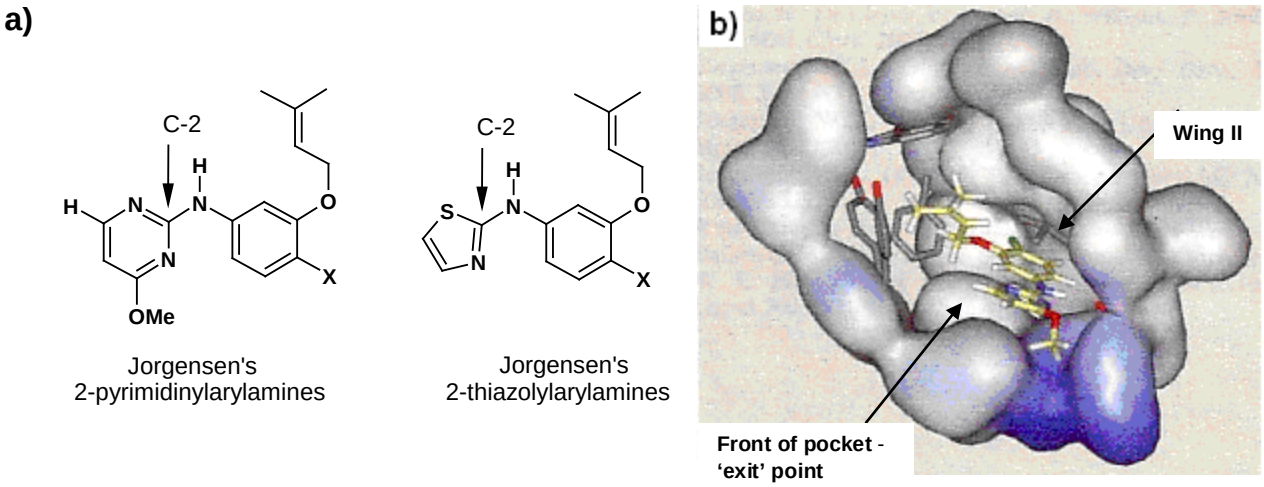

Figure 3.3 a) Jorgensen's potent NNRTIs, (b) Proposed docking of 2-pyrimidinylarylamines at the entrance of the NNRTI-BP of HIV-1 RT.[87]

Therefore, in view of the synthetic challenges of constructing a TMC120 bifunctional, initially a ***prototype*** [d4U]-spacer-[pyrimidinylarylamine] heterodimer system was chosen, with one aromatic ring of TMC120 removed and the other arylamine, at either the C-2 or C-4 position of the pyrimidine intended by us for linking the NNRTI binding pocket with the NRTI substrate binding site. Both the C-2 and C-4-substituted pyrimidines needed to be explored regarding tethering from the aromatic ring, in view of the multiple conformations of TMC compounds, although a spacer elongation from the C-4 aromatic ring was considered to be the more likely bifunctional prototype system to return biological activity.

Therefore, the bifunctional molecules **114, 115** and **116** shown in Figure 3.4 were selected as targets. As in Chapter 2, the C-5 position on the pyrimidine moiety (base) of d4U was chosen as the appropriate attachment point for the tether. Also, ethylene glycol units in the spacer were chosen in view of their anticipated water solubility. The *meta*-position on the C-2 or C-4 aromatic ring of the pyrimidinylarylamine was chosen as the spacer extension point in view of us being in possession of an appropriate *meta*-extended aniline building block from the UC-781 synthesis.

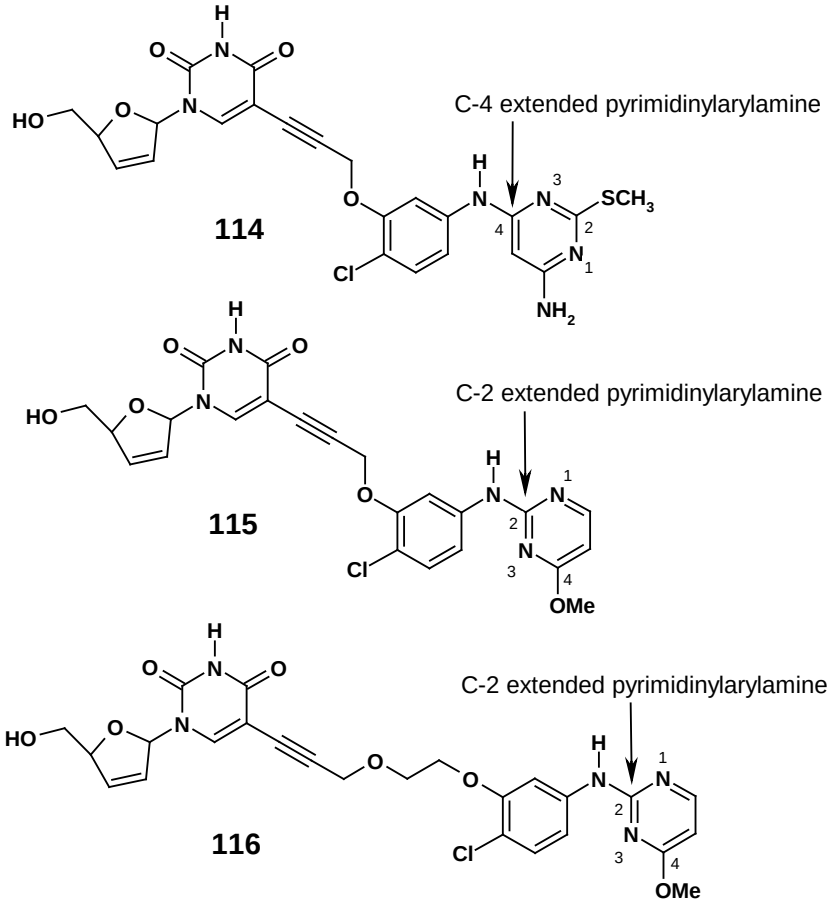

Figure 3.4 Structures of the target molecules.

3.1.1 Retrosynthetic analysis of [d4U]-spacer-[2- or 4-Pyrimidinylarylamines]

The total synthesis of targets **114-116** was conceived as achievable *via* a convergent strategy, involving the coupling of protected 5'-iodo d4U **60** to a 2- or 4-pyrimidinylamine of type **A** or **B** followed by deprotection of the benzoyl group to render the target compounds directly (Fig. 3.5). Synthesis of 2- or 4-pyrimidinylarylamines of type **A** and **B** was envisaged possible from the coupling of commercially available pyrimidines **117** and **118** with a common arylamine intermediate of type **C**.

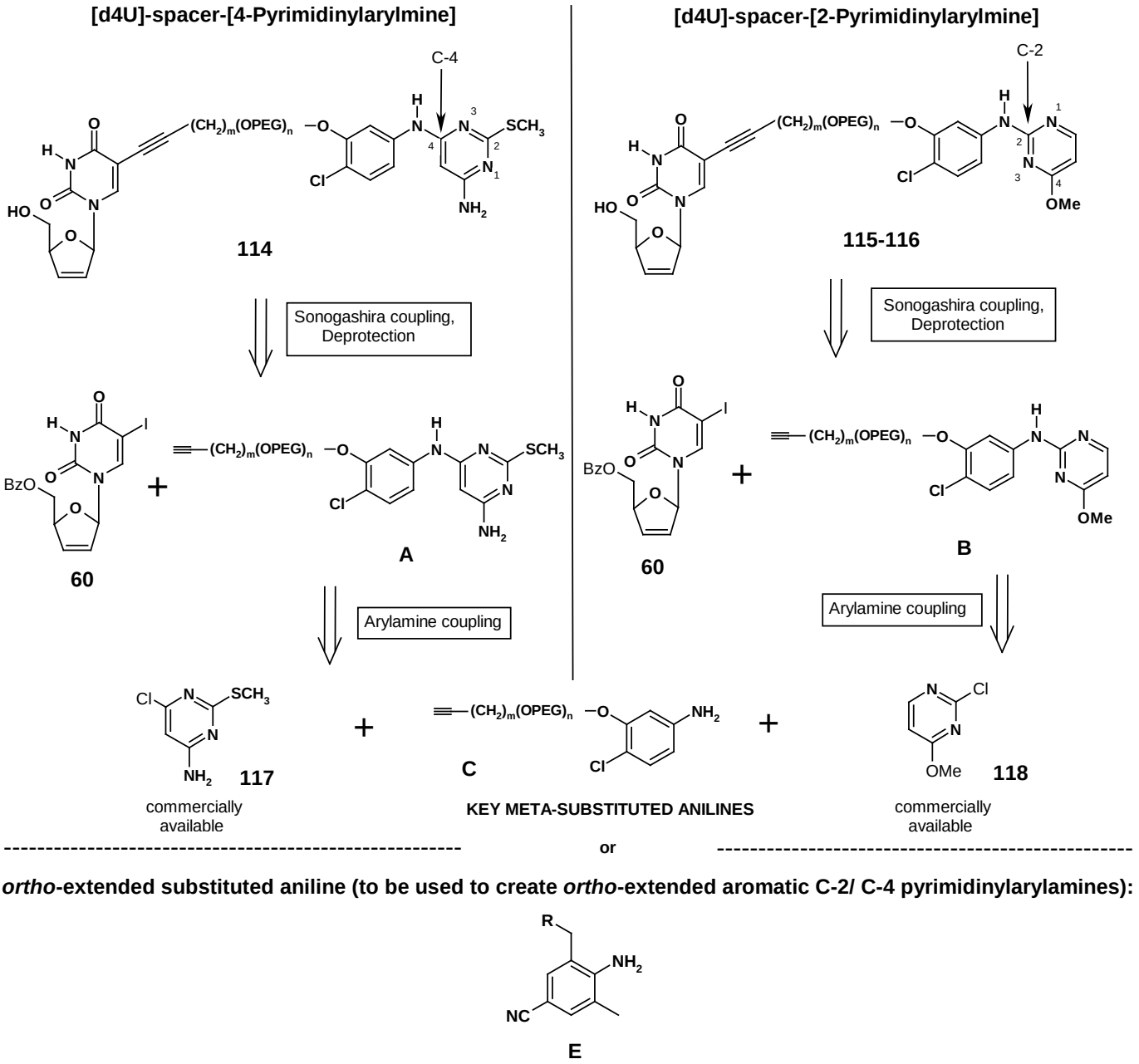

Figure 3.5 Retrosynthetic synopsis of the synthetic strategy towards the target molecules.

It was also well understood that 2- and 4-pyrimidinylarylamine derivatives of type **A** and **B** would have to be undertaken and synthesized, in which the substitution pattern of the aniline was varied to accommodate an *ortho*-extended arylamine component of type **E**, in order to achieve a successful SAR study. Since the molecular modeling studies by Pauwels (reviewed earlier) suggested that it was plausible to consider a spacer extension from both the *ortho*- and *meta*-positions on the key substituted aniline, it was also planned to couple various *ortho*- and *meta*-extended substituted arylamines to commercially available pyrimidines **117** and **118**, and the respective 2- and -4-pyrimidinylarylamine derivatives obtained tested for their anti-HIV activity.

2-Chloro-4-methoxy-1,3-pyrimidine **118** was chosen as the pyrimidine partner on the grounds that Jorgenson had identified activity with this template for his 2-pyrimidinylarylamines.[87] 4-Amino-6-chloro-2-methylthio-1,3-pyrimidine **117** was chosen because of its close resemblance to TMC125 in the substitution pattern on its pyrimidine ring.

3.2 Synthesis of the substituted anilines

3.2.1 Synthesis of the *meta-extended* substituted anilines

Synthesis of the arylamine subunit of the bifunctional targets **115** and **116** started from commercially available 2-amino-5-nitrophenol and involved a two-step procedure.[175] The first step was a Sandmeyer diazonium-promoted amino substitution to the chloride **119a** (Scheme 3.1). This was achieved by charging a reaction flask with concentrated hydrochloric acid at 0 ^{o}C and adding to this a mixture of 2-amino-5-nitrophenol and sodium nitrite in water. After maintaining this temperature for 3 hrs, sulfamic acid (H_2NSO_3H) was added slowly and the mixture poured carefully into a solution of 20% aqueous hydrochloric acid containing copper (I) chloride over 1hr. TLC confirmed reaction completion after stirring at room temperature for a further 1 hr and **119a** as a yellow solid was isolated in 73% yield after silica-gel purification.

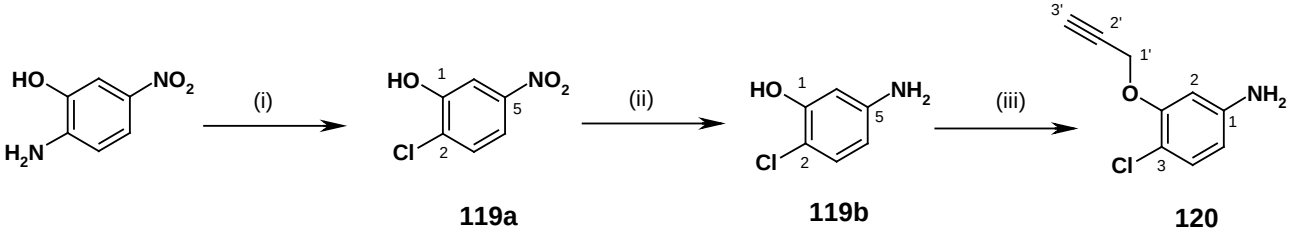

Scheme 3.1 *Reagents and conditions:* (i) HCl (conc), $NaNO_2$, CuCl (73%); (ii) Fe mesh, HCl, Δ (73%); (iii) propargyl bromide, K_2CO_3, *n*-Bu_4NI, acetone, r.t (79%).

The mechanism of the reaction involves an S_N1 nucleophilic aromatic substitution as depicted in Figure 3.6. The first stage (Figure 3.6) involves formation of the reactive NO^+ species formed

from the reaction between sodium nitrite and a strong acid, for example hydrochloric acid. It should be noted, though, that in dilute acid the actual species is N_2O_3, which acts as a carrier of NO^+. At high acidities, NO^+ is formed as depicted in Figure 3.6.

(a) Formation of reactive NO^+ species:

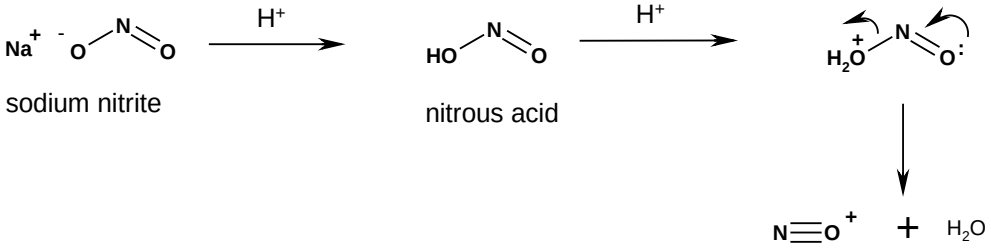

(b) Formation of the diazonium salt:

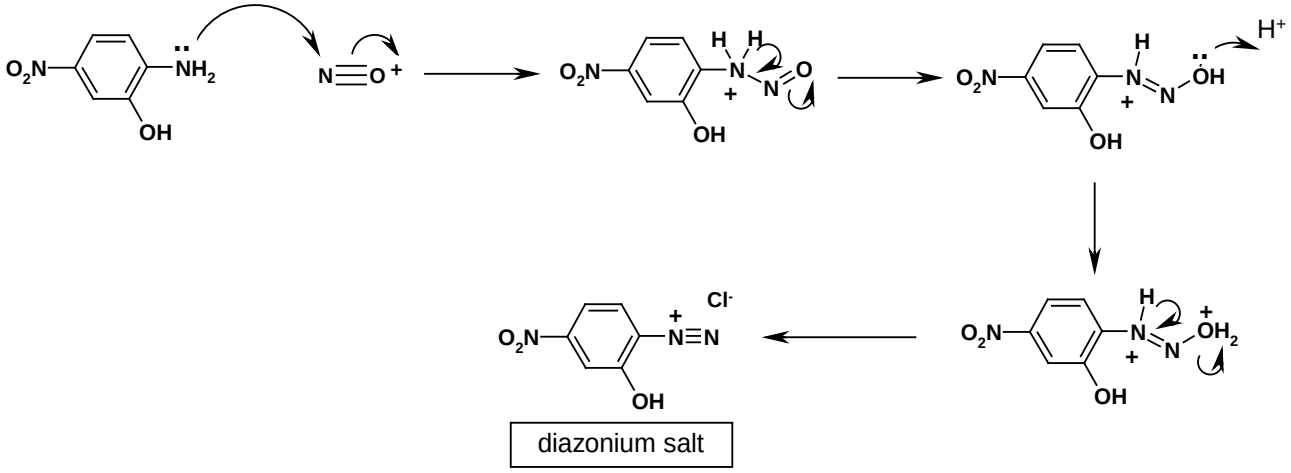

(c) S_N1 nucleophilic aromatic substitution:

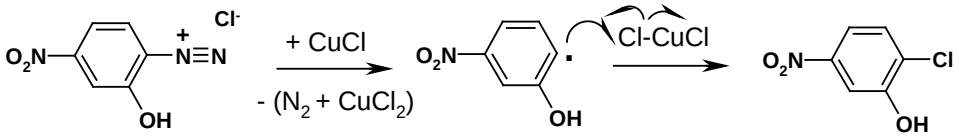

Figure 3.6 Mechanism for diazonium S_N1 nucleophilic aromatic substitution.

The NO^+ cation is then attacked by the lone pair of the amine and dehydration follows after a succession of proton transfers to yield the diazonium salt. The penultimate step involves a reduction of the diazonium ion by the cuprous ion, which results in the formation of an aryl radical. Finally, the aryl radical abstracts a halogen radical from cupric chloride, reducing it. CuCl is regenerated and is thus a true catalyst. Apart from NO^+, other attacking species can be NOCl

and $H_2NO_2^+$. Nucleophiles (e.g. Cl^-, SCN^-, thiourea) catalyze the reaction by converting HONO to a better electrophile (e.g. $HNO_2 + Cl^- + H^+ \rightarrow NOCl + H_2O$). A key diagnostic feature in the ^1H NMR spectrum of **119a** was the absence of the amino group hydrogens from the starting material integrating for two protons. The ^{13}C NMR spectrum of **119a** displayed a new downfield signal at δ_C 130.9 for the halogen bearing C-2. Infrared spectroscopy provided further evidence for conversion with the appearance of a strong carbon-halogen stretching band at 738 cm^{-1} for **119a**. Subsequent nitro-group reduction using iron mesh in refluxing ethanol with hydrochloric acid yielded key intermediate **119b** in a good yield of 73% after column chromatography. Its ^1H NMR spectrum revealed signals at δ_H 4.62 (integrating for two protons) and 8.06 (integrating for one proton) for the amine and hydroxyl groups respectively.

In anticipation of using a Sonogashira coupling strategy for linking the two drugs, **119b** was propargylated using propargyl bromide, potassium carbonate and a catalytic amount of *tetra*-butylammonium iodide in acetone at room temperature to afford **120** in a good yield of 79% after column chromatography (Scheme 3.1). The ^1H NMR spectrum of **120** displayed a signal for the alkyne proton (H-3') at δ_H 2.54 which appeared as a triplet of *J* 2.4 Hz, due to allylic coupling with the H-1' methylene protons (Fig. 3.7). Additional signals in the spectrum at δ_H 4.71 for H-1' and δ_H 3.75 for the amino group confirmed the formation of **120**. The ^{13}C NMR spectrum displayed diagnostic signals at δ_C 76.0 and δ_C 78.2 for C-3' and C-2' respectively.

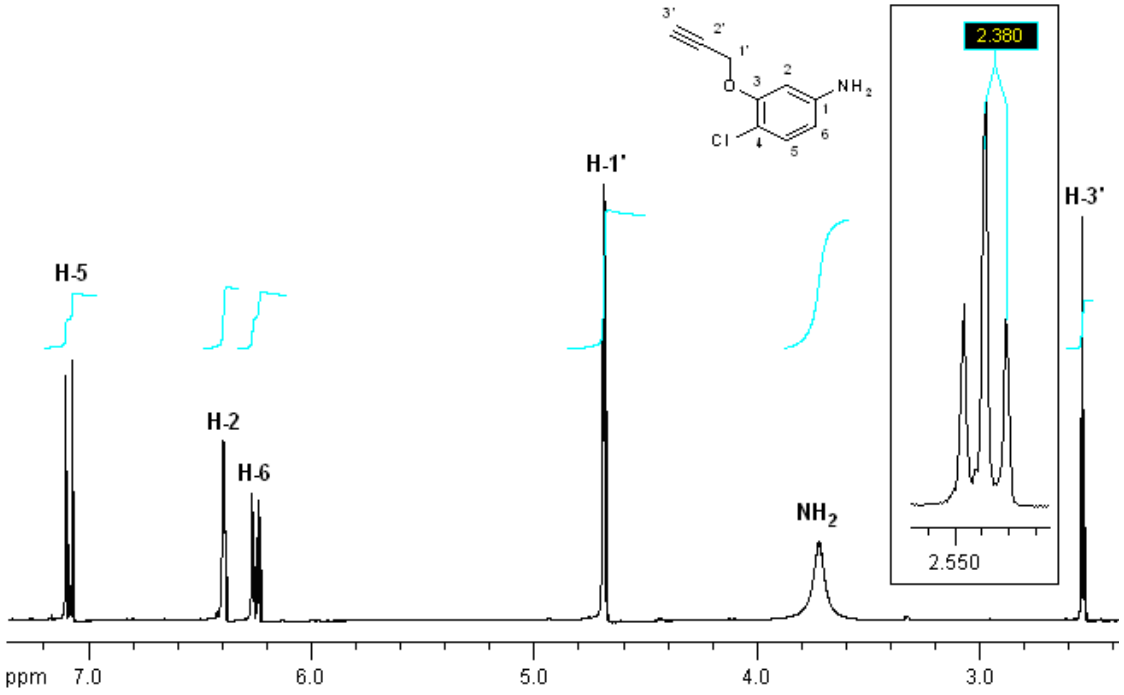

Figure 3.7 ^1H NMR spectrum of **120**.

Similarly, the UC-781 arylamine subunit **61** was prepared in two steps (Scheme 3.2) from the common intermediate **119a**. Alkylation of **119a** was carried out using 4-bromo-2-methyl-2-butene, potassium carbonate and *tetra*-butylammonium iodide in methylethylketone to afford **119c** in 94% yield after column chromatography. The ^{1}H NMR spectrum of **119c** confirmed the formation of the ether with the absence of the OH singlet at δ_H 9.73 in **119a**, and the appearance of two methyl signals at δ_H 1.80 and δ_H 1.81. The allylic methylene doublet at δ_H 4.70, and the vinylic proton signal at δ_H 5.49 further supported the formation of **119c**.

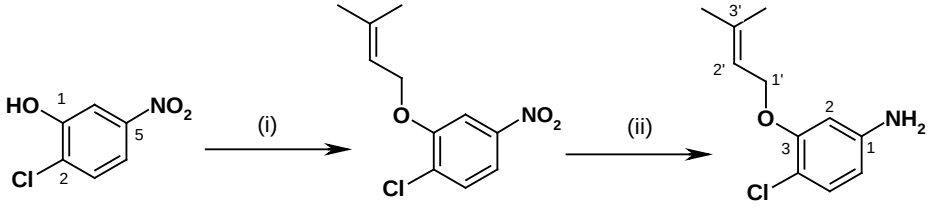

119a **119c** **61**

Scheme 3.2 *Reagents and conditions:* (i) 4-bromo-2-methyl-2-butene, K_2CO_3, *n*-Bu_4NI, MEK, r.t (94%); (ii) Fe mesh, HCl, Δ (88%).

Iron-mesh reduction of **119c** using the same conditions as described above for **119b**, rendered the desired arylamine **61** in 88% yield after chromatographic purification over silica-gel. The ^{1}H NMR spectrum of **61** displayed the appearance of an NH_2 singlet at δ_H 3.62. The ^{13}C NMR spectrum of **61** displayed a slight upfield shift in the C-1 carbon from δ_C 148.2 in **119c** to δ_C 146.2 in **61**, in agreement with the formation of **61**. The integrity of all the other signals remained the same with signals at δ_C 65.9 (C-1'), δ_C 101.5 (C-2), δ_C 107.9 (C-6), δ_C 112.1 (C-4), 119.5 (C-2'), 130.4 (C-5) and 154.9 (C-3). Finally, a correct HRMS evaluation (*m/z* HRMS (EI) 211.07668, $C_{11}H_{14}NOCl$ requires *m/z* 211.07652), confirmed the structure of **61**.

3.2.2 Synthesis of the *ortho-extended* substituted anilines

In keeping with our objective of preparing pyrimidinylarylamine derivatives, the next challenge was to generate methodology for *ortho*-extended anilines to be used as the aryl component in the Het-NH-*ArX* motif of the pyrimidinylarylamine derivatives. Literature methodologies for accessing *ortho*-extended anilines are quite scarce, with directed-ortho-metallation (DOM) and photo-Fries rearrangement methodologies as the principal options. However, with the success of the Wittig C-2 extension in the UC-781 series (Chapter 2), our minds once again shifted towards this reliable carbon-carbon bond-forming methodology. To this end, radical bromination (Scheme 3.3) of commercially available 2-nitro-*m*-xylene was performed using *N*-bromosuccinimide and azo*bis*isobutyronitrile in dry carbon tetrachloride to obtain benzylic bromide **121** in 70% yield as reported independently by both Weaver[176] and Makhija.[177] The

phosphonium salt **122** was subsequently prepared in 89% yield after reaction of **121** with triphenylphosphine in toluene (Scheme 3.3). Recrystallization from methanol/ethyl acetate (1:1) secured analytically pure material (99% recovery). The ^{1}H NMR spectrum of **122** displayed the enantiotopic methylene protons α to the phosphorus centre as a doublet at δ_H 5.21 due to phosphorus coupling (2H, d, $J_{P\text{-}H}$ = 15.0 Hz, CH_2P), as well as multiplets for the three new phenyl moieties at δ_H 7.65 and δ_H 7.90. Microanalysis returned good combustion data as: Found C, 63.17; H, 4.70; N, 2.74%; $C_{26}H_{23}O_2NPBr$ requires C, 63.17; H, 4,75; N, 2.85%.

Gratifyingly, reaction of **122** in methanol with sodium methoxide as base (2M in MeOH, 1.1 eq.) at room temperature followed by addition of acetaldehyde (2 eq.) resulted in rapid transformation to the Wittig product **122a** after 30 min. The crude alkene was put through an aqueous work-up and after removing the solvent was used in the next step without purification, in which nitro group reduction of crude **122a** in refluxing ethanol with iron mesh and hydrochloric acid, rendered the desired *ortho*-alkenylated aniline **122b**. Filtration of excess iron followed by evaporation of solvent and direct hydrogenation of **122b** using palladium-on-carbon in alcoholic hydrogenated solvent gave the anticipated *ortho*-alkylated product **123** in an excellent yield of 77% over the three steps.

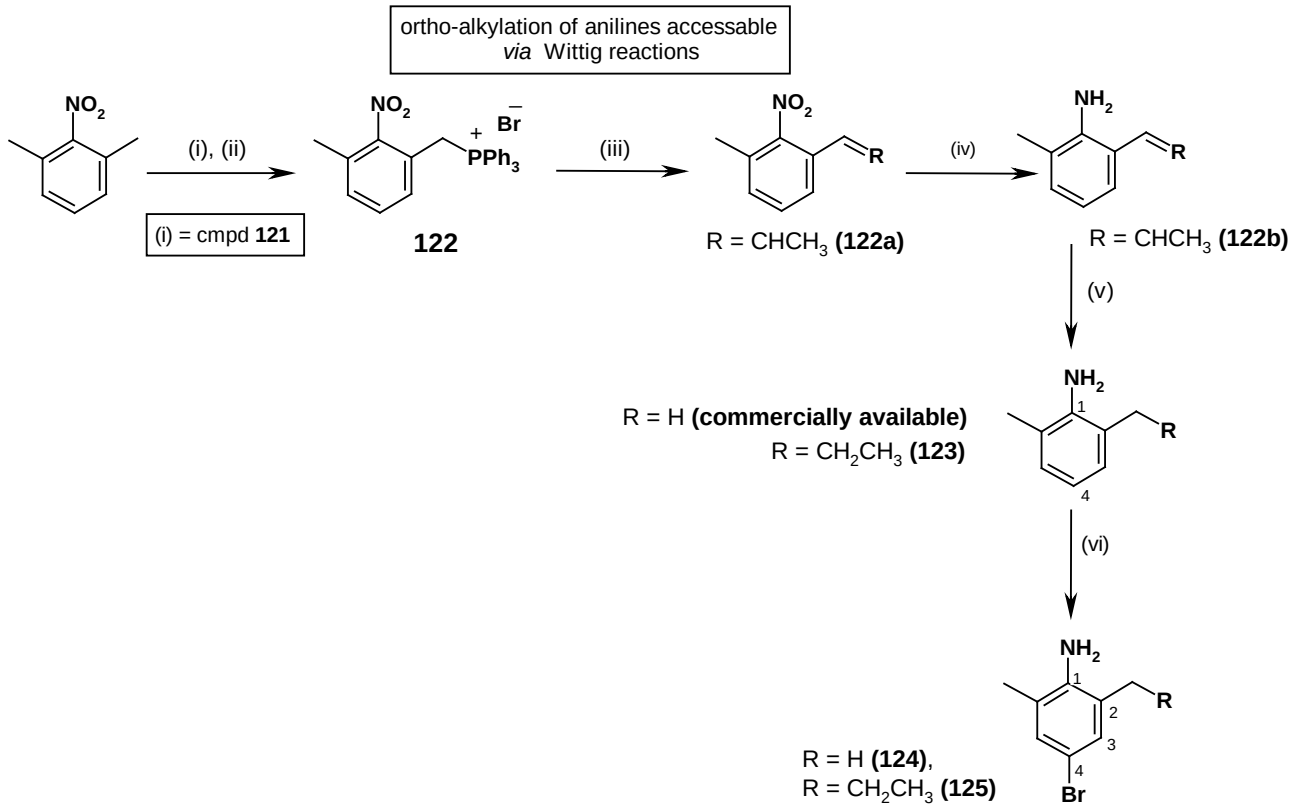

Scheme 3.3 *Reagents and conditions:* (i) NBS, AIBN, CCl_4, Δ (70%); (ii) PPh_3, Toluene, Δ (89%); (iii) NaOMe, acetaldehyde, MeOH, r.t; (iv) Fe mesh, HCl, Δ; (v) H_2, Pd-C, MeOH,THF (1:1) (77% over 3 steps); (vi) NH_4Br, H_2O_2, AcOH, 0°C - r.t (**124**-49%, **125**-53%).

Diagnostic signals in the ^{1}H NMR spectrum of **123** were the appearance of the NH_2 (2H) singlet at δ_H 3.61 confirming the reduction of the nitro moiety, and an increase in aliphatic proton signals.

The last transformation in the synthesis of the ortho-extended arylamine subunit was the incorporation of a halogen at the *para*-position relative to the amino group of **123** (Scheme 3.3). It was decided to include a cyano-functionality in this position because of the excellent biological data for TMC125. To this end, *para*-cyanation of the arylamine was accomplished *via* a two-step procedure. The first step involved regioselective and environmentally friendly bromination[178] of substituted aniline **123**. The study also included 2,6-dimethylaniline as a model arylamine. This was carried out using ammonium bromide as a bromine source and hydrogen peroxide (as oxidant) in acetic acid at room temperature. In this reaction, it is assumed that hydrogen peroxide oxidizes the Br^- (ammonium bromide) to Br^+ (HOBr), which reacts in the presence of acetic acid (Bronsted acid) with anilines to give the desired electrophilic substitution product (Fig. 3.8).[178] TLC confirmed completion of the electrophilic substitution after 2 hrs furnishing **124** (model) and **125** in moderate yields of 49% and 53% respectively.

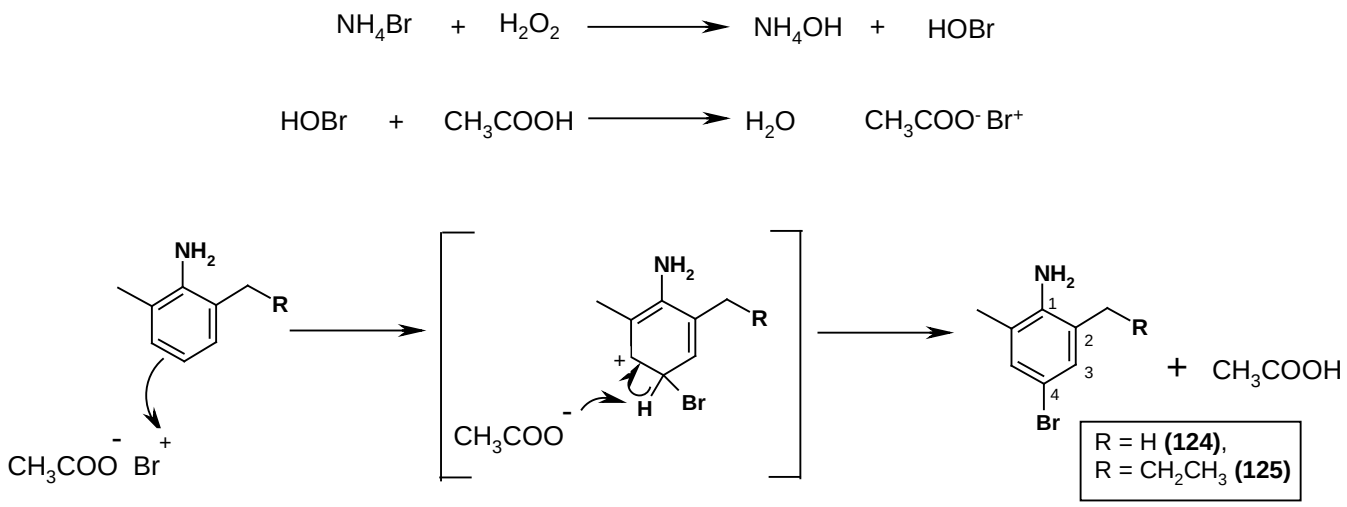

Figure 3.8 Mechanism of bromination of anilines.

The ^{1}H NMR spectrum of **124** revealed the absence of a singlet at δ_H 7.14 for the H-4 proton (Scheme 3.3) as well as the appearance of H-3/5 as a singlet at δ_H 7.15, implying that substitution had taken place. The ^{13}C NMR spectrum of **124** recorded the correct number of resonances as 5. The C-4 quaternary carbon bearing the halogen resonated at δ_C 113.7 consistent with a C-Br moiety. The same pattern was observed for aryl bromide **125** in the ^{13}C

and ^{1}H NMR spectra. For example, in **125**, the C-4 carbon bearing the halogen resonated at δ_C 112.9.

Palladium-catalyzed cyanations of aryl halides dominate the literature.[179-181] A major disadvantage of such procedures is the relatively expensive palladium-catalyst combinations employed, although the use of non-toxic sources of cyanide such as potassium hexacyanoferrate (II), $K_4[Fe(CN)_6]$, and ligand-free reaction conditions provide significant advantages.

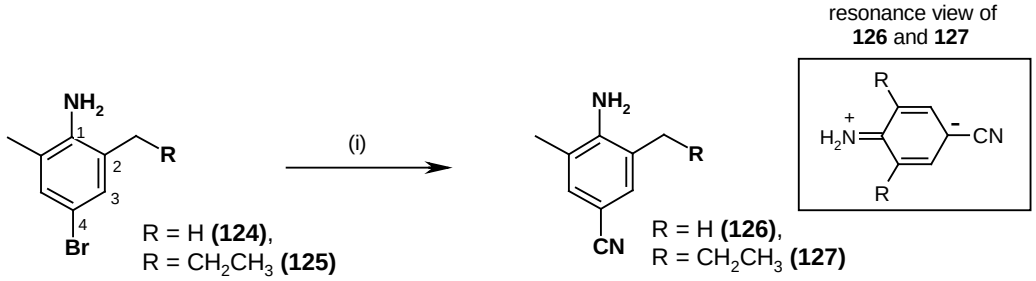

Scheme 3.4 *Reagents and conditions:* (i) CuCN, DMF, Δ (**126**-47%, **127**-84%).

The Pd(0) methodology was first attempted on aryl bromides **124** and **125** using $K_4[Fe(CN)_6]$ in dimethylacetamide without any success. Harsher cyanation conditions were then tried out as described by Mayr and co-workers[182] by subjecting aryl bromides **124** and **125** to cuprous cyanide (CuCN) in refluxing dimethylformamide for 6 hrs to produce *para*-cyanated products **126** and **127** after column purification (Scheme 3.4). The respective ^{1}H NMR spectra of **126** and **127** looked identical to that of their aryl bromide counterparts. However, the ^{13}C NMR spectrum supported the formation of **126** with the appearance of a C-4 upfield shift (due to resonance - see boxed Figure) from δ_C 113.7 in **124** to δ_C 99.1 in **126**. Also, a new signal indicative of a quaternary cyanide carbon (relaxed) resonated at δ_C 120.4. Once again, the same trends were observed in the ^{13}C NMR spectrum of **127**.

3.3 Synthesis of [d4U]-propyne-[4-pyrimidinylarylamines]

3.3.1 Synthesis of the 4-pyrimidinylarylamine derivatives

With the substituted anilines now in hand, attention focused on synthesizing the 4-pyrimidinylarylamine derivatives. Commercially available 4-amino-6-chloro-2-methylthio-pyrimidine **117** was thus coupled to the different *meta*- and *ortho*-extended arylamines under a variety of reaction conditions to furnish a range of new model 4-pyrimidinylarylamine derivatives to probe for anti-HIV activity.

For the aromatic *meta*-substituted 4-pyrimidinylarylmine derivatives, pyrimidine **117** was first condensed with arylamine **119b** in 1,4-dioxane at 100 ^{o}C (Scheme 3.5). The reaction required a

molar equivalent of anhydrous *p*-toluenesulfonic acid to be added to the pyrimidine starting material in 1,4-dioxane first, suggesting the condensation to occur *via* a protonated pyrimidine ring, after which an addition-elimination reaction results in formation of the desired compound **128** in 47% yield after silica-gel purification. As expected, the amine functionality won the chemoselective battle with the less nucleophilic hydroxyl group on the arylamine **119b**.

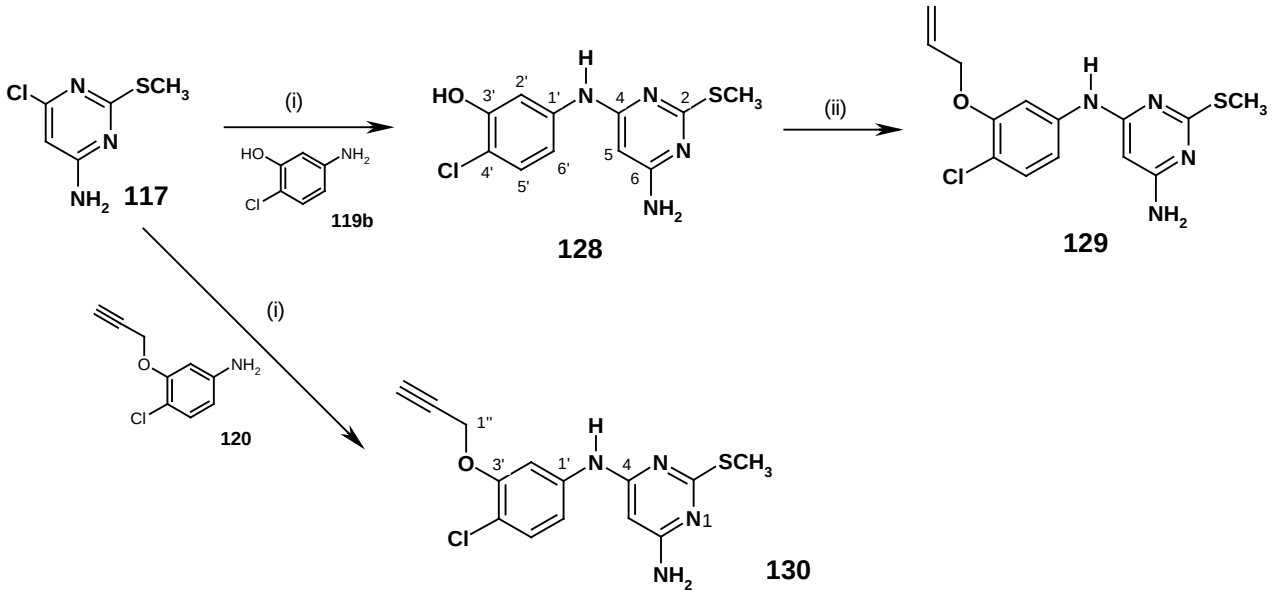

Scheme 3.5 *Reagents and conditions:* (i) 4-amino-6-chloro-2-(methylthio)pyrimidine, arylamine, *p*-TsOH, 1,4-dioxane, 100^{o}C (**128**-47%, **130**-49%); (ii) allyl bromide, K_2CO_3, *n*-Bu_4NI, acetone, r.t (46%).

The ^{1}H NMR spectrum of **128** revealed a thiomethyl singlet at δ_H 2.43, a singlet for the pyrimidine H-5 proton at δ_H 5.65 and a broad singlet NH_2 at δ_H 5.76. The bridging NH signal resonated at δ_H 8.08 in close proximity to the free OH signal at δ_H 8.58. The ^{13}C NMR spectrum displayed the vital C-4 and C-1' signals resonating at δ_C 164.3 and δ_C 141.1 respectively, assigned with the aid of 2-D NMR.

Compound **128** was then O-allylated by treatment with allyl bromide in acetone with potassium carbonate as a mild base to yield the model NNRTI derivative **129** in a moderate yield of 46% after column purification. Key diagnostic signals in the ^{1}H NMR spectrum of **129** were the allylic methylene protons signal at δ_H 4.65 and the disappearance of the OH signal at δ_H 8.58 in **128**. Finally, a correct HRMS evaluation (*m/z* HRMS (ES) 323.0732 $[M+H]^+$, $C_{14}H_{16}N_4OSCl$ requires *m/z* 323.0735 $[M+H]^+$), confirmed the structure of **129**. 4-Pyrimidinylarylamine **129** was synthesized in order to do a comparative study with that of Jorgensen's on the activity of 2-vs 4-pyrimidinylarylamines, and to expand on building a library of 4-pyrimidinylarylamines.

The Sonogashira coupling partner, 4-pyrimidinylarylamine **130** was next synthesized employing identical reaction conditions to that used in making **128**, except using the propargylated intermediate **120**. A 49% yield was obtained after column chromatography. The ^{1}H NMR spectrum of **130** (Fig. 3.9) displayed the typical alkyne triplet at δ_H 2.46 for H-3''. The ^{13}C NMR spectrum complemented this well (Fig. 3.9) with three distinct propargyloxy signals at δ_C 56.9 (C-1''), δ_C 76.4 (C-3'') and δ_C 77.9 (C-2'').

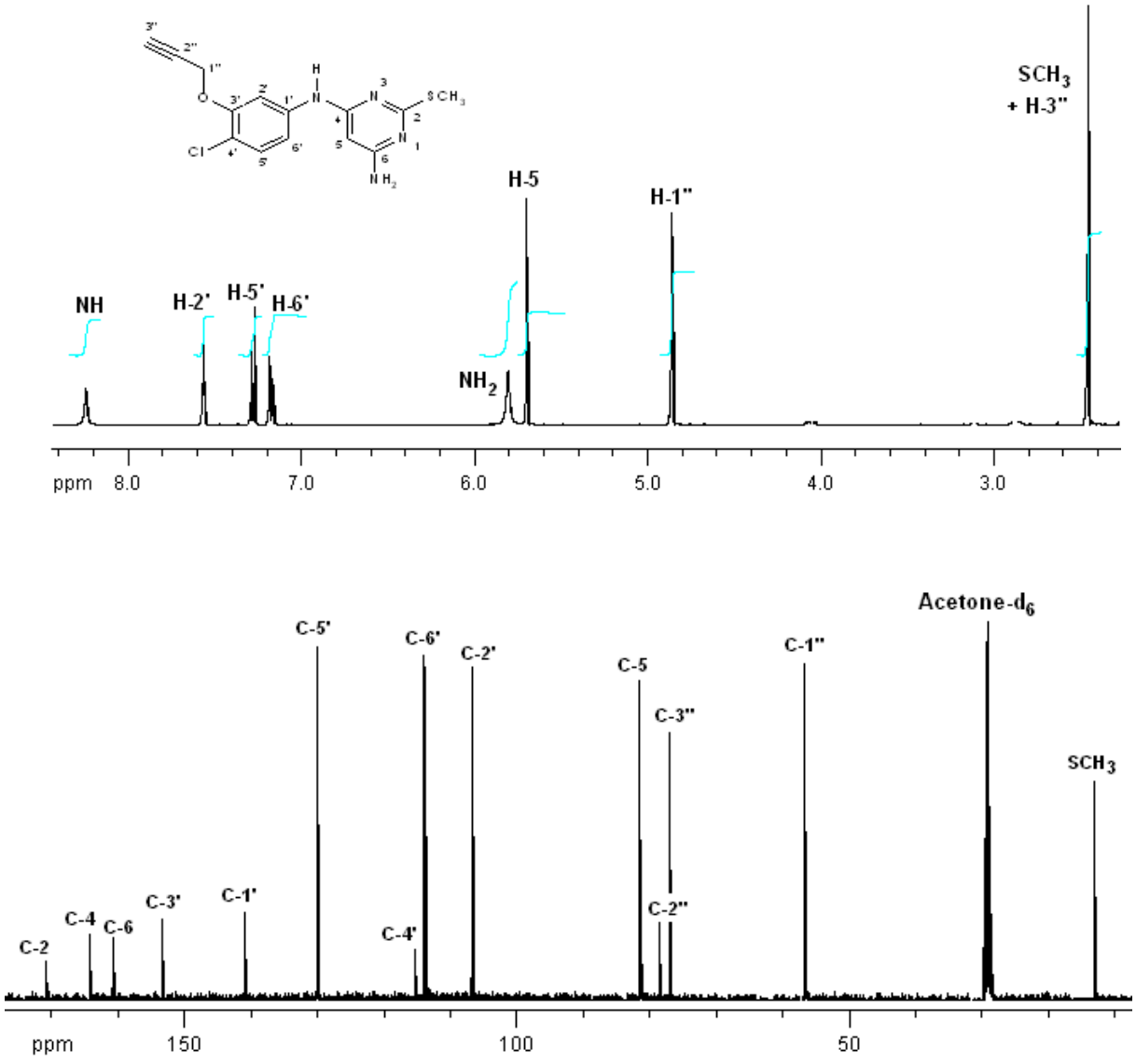

Figure 3.9 ^{1}H and ^{13}C NMR spectra of 4-pyrimidinylarylamine **130**.

Finally, condensation of the *ortho*-extended arylamines to 4-amino-6-chloro-2-methylthiopyrimidine **117** was undertaken in order to evaluate the affect of extended ortho-substituents as a possible spacer extention on the 4-pyrimidinylarylamines. Our initial focus was

simply to synthesize these aromatic ortho-extended model 4-pyrimidinylarylamine derivatives for anti-HIV probing, and not to generate bifunctional entities. To this end, different arylamines were all reacted in each case as a melt with 4-amino-6-chloro-2-methylthiopyrimidine **117** without the need for solvent, and the desired 4-pyrimidinylarylamine products (**131**-**134**) were isolated in low yields, 28-35% (Scheme 3.6).

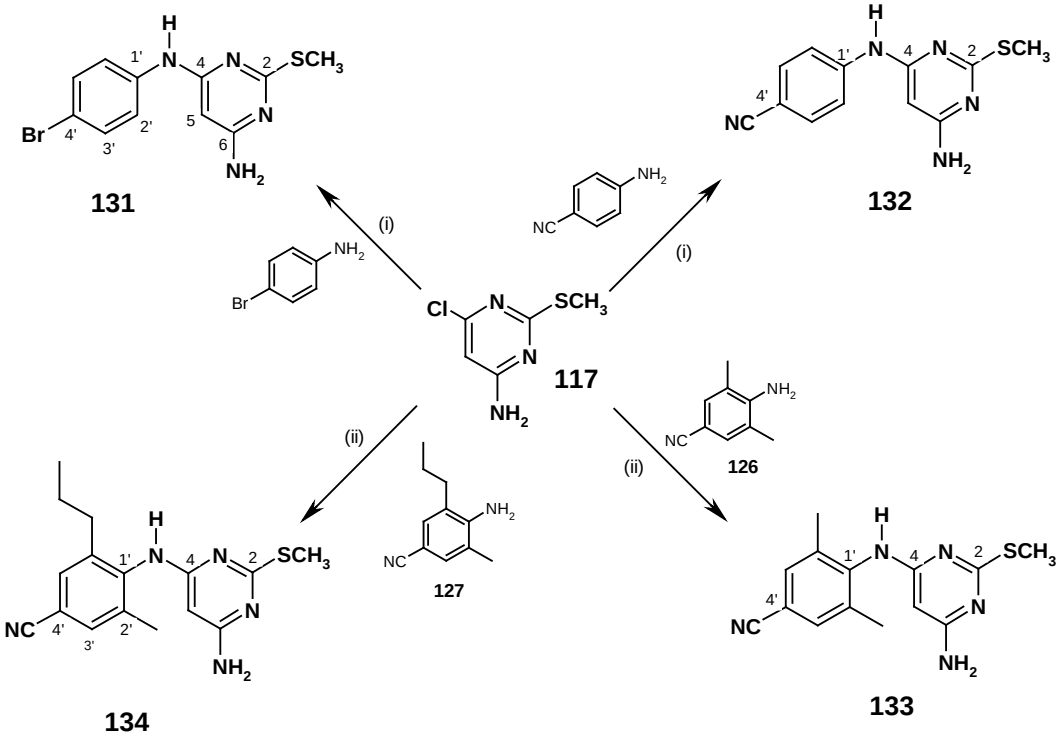

Scheme 3.6 *Reagents and conditions:* (i) melt neat with arylamine at 160 ^{o}C (**131**-28%, **132**-35%); (ii) melt neat with arylamine at 220 ^{o}C (**133**-35%, **134**-35%).

The low yields were never optimized as the primary objective was to get the derivatives tested and to evaluate the feasibility of an *ortho*-extended aromatic ring attached to the C-4 position on the pyrimidine. The ^{1}H NMR spectra of **131**-**134** displayed the characteristic pyrimidine and arylamine signals in a 1:1 ratio (see Table 3.1). A fair degree of consistency for the ^{13}C signals in the ^{13}C NMR spectra for **132**-**134** was observed as revealed in Table 3.2 for selected resonances.

Table 3.1 Some ^{1}H chemical shifts for 4-pyrimidinylarylamine derivatives **131**-**134**

Position	***131***	***132***	***133***	***134***
SCH_3	2.39	2.41	2.39	2.38
H-5	5.50	5.60	6.16	6.14
NH_2	6.38	6.54	5.50	5.56

NH	9.01	9.46	7.22	7.25
H-3'	7.49	7.75	7.18	7.15

Table 3.2 Some ^{13}C chemical shifts for 4-pyrimidinylarylamine derivatives **131**-**134**

Position	***131***	***132***	***133***	***134***
2	170.1	170.5	172.1	172.1
4	164.3	164.7	165.2	166.8
5	82.1	83.2	98.5	99.6
6	160.8	160.2	158.4	160.5
1'	140.9	146.1	149.8	151.7
2'	131.9	133.7	131.4	130.9
3'	121.9	119.2	120.9	125.4
4'	113.2	102.5	95.9	99.1
C≡N	-	120.2	120.2	120.6

3.3.2 Sonogashira coupling and final deprotection

For bifunctional generation (Scheme 3.7), the 4-pyrimidinylarylamine derivative **130** was subjected to a Sonogashira reaction with 5'-*O*-benzoyl-5-iodo-d4U **60**, which was prepared in 4 steps from uridine according to the Bristol-Myers Squibb procedure. The coupling used conditions described previously for UC-781 and was complete in 2 hrs to afford **135** in 83% yield following chromatography. Its ^{1}H NMR spectrum revealed signals for both the arylpyrimidinyl and d4U moieties in the ratio of 1:1. A successful coupling was further supported by the absence of a terminal alkyne proton at around δ_H 2.46. The ^{13}C NMR spectrum of **135** displayed diagnostic resonances at δ_C 144.1 (C-12), 90.9 (C-5), 57.3 (C-15), thus confirming the presence of both the nucleoside and the alkyne. The structure was further confirmed by 2D NMR.

Finally, **135** was deprotected with sodium methoxide in methanol to furnish **114** in 76% yield (Scheme 3.7). The ^{1}H NMR spectrum of **114** (Fig. 3.10) revealed resonances for both inhibitors, notably the d4U double bond signals and the H-12 uracil singlet at δ_H 8.28, as well as a characteristic set of aromatic and heteroaromatic signals for the APY unit together with the thiomethyl singlet at δ_H 2.45. Signals from both drug fragments integrated correctly. Its ^{13}C spectrum returned the correct number of singlets (23) and 2D-NMR techniques (HSQC, HMBC) were utilized to make a full structural assignment. Finally, a correct HRMS evaluation (*m/z*

HRMS (ES) 529.1073, $C_{23}H_{22}N_6O_5SCl$ requires *m/z* 529.1061), confirmed the structure of **114** as shown in Scheme 3.6. Compound **114** illustrates the first example of a prototype d4U / 4-pyrimidinylarylamine bifunctional heterodimer that culminated in an Afinidad communication published in 2007.[171]

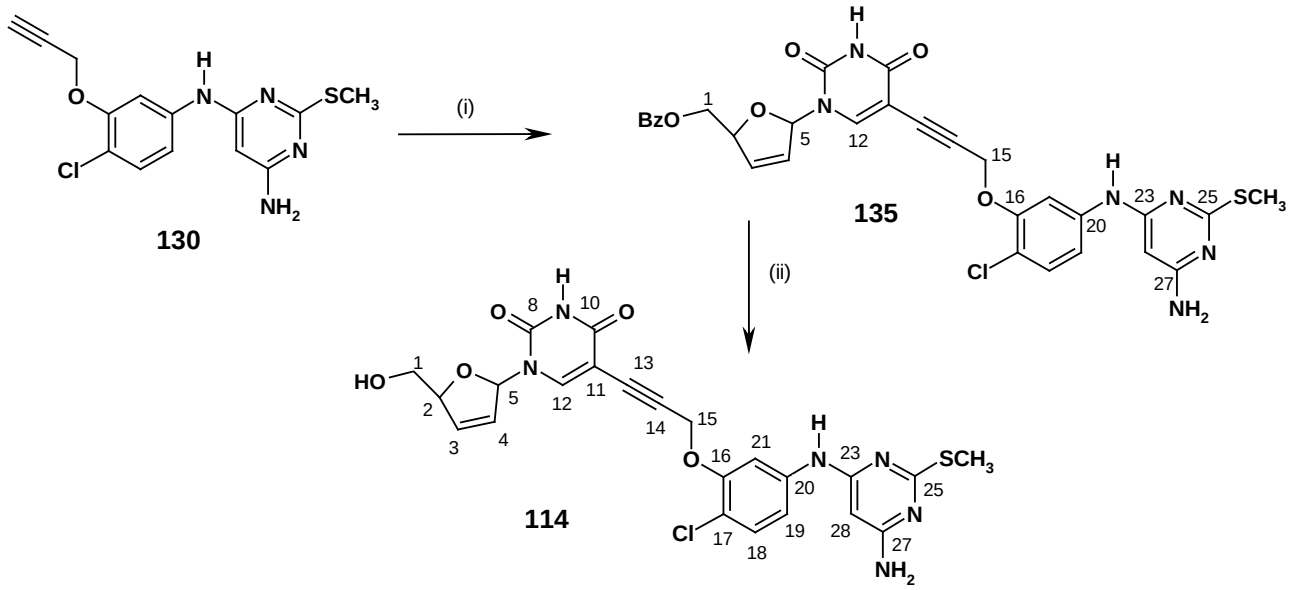

Scheme 3.7 *Reagents and conditions:* (i) 5'-Benzoyl-5-iodo-d4U, $Pd(PPh_3)_4$ (10%), CuI (50%), NEt_3 (2 eq), DMF/THF (1:2), rt, (83%); (ii) NaOMe, MeOH, rt, (76%).

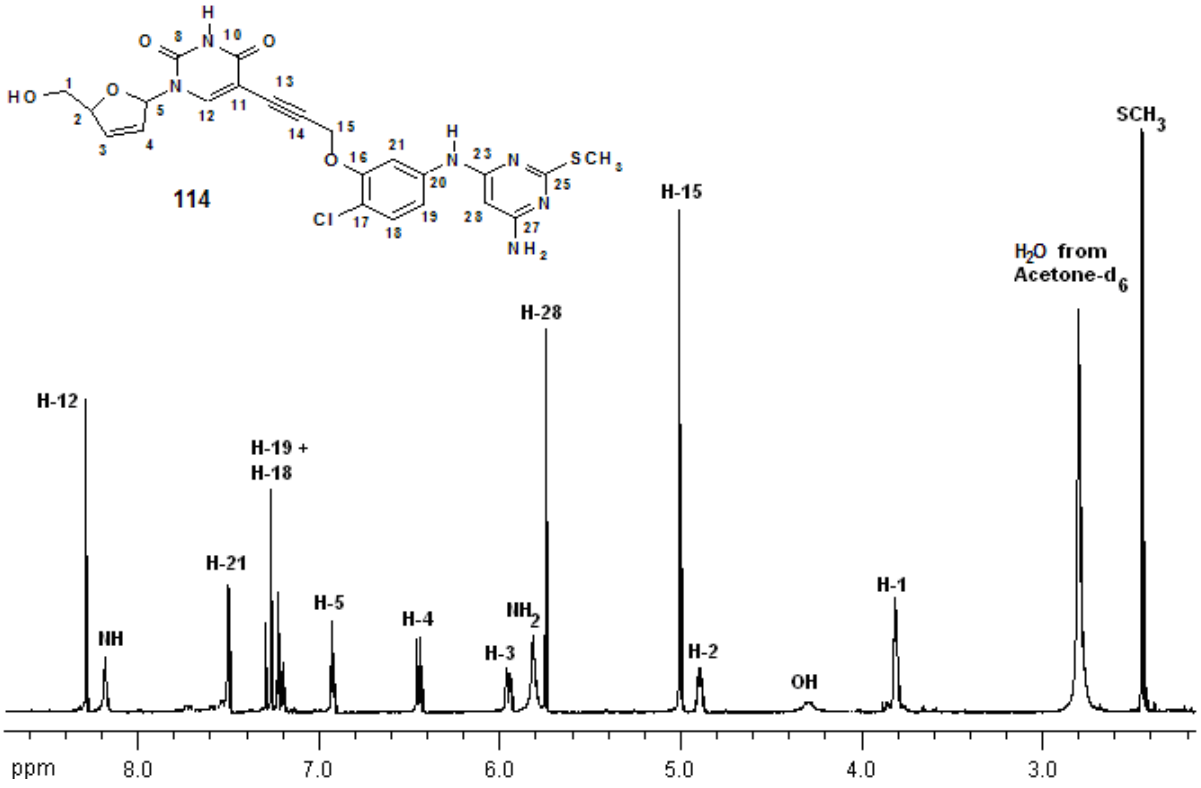

Figure 3.10 ^{1}H NMR spectrum of **114**.

3.4 Synthesis of [d4U]-spacer-[2-pyrimidinylarylamines]

3.4.1 Synthesis of the [d4U]-propyne-[2-pyrimidinylarylamines]

3.4.1.1 Synthesis of the 2-pyrimidinylarylamine derivatives

For the 2-pyrimidine substituted bifunctionals tethered at the *meta*-position of the aromatic ring, commercially available 2-chloro-4-methoxy-1,3-pyrimidine **118** was coupled to different *meta*-extended arylamines under a variety of reaction conditions to furnish a range of new model 2-pyrimidinylarylamine derivatives to either probe for anti-HIV activity as model NNRTIs (also extending the library of Jorgensen's derivatives), or to be used to generate double-drug entities. Thus, condensation of **118** with arylamine **119b** in the presence of *p*-toluenesulfonic acid in 1,4-dioxane yielded 2-pyrimidinylarylamine **136** in 95% yield after column purification (Scheme 3.8). The ^{1}H NMR spectrum of **136** displayed two aromatic signals at δ_H 6.23 (d, J = 5.7 Hz) and δ_H 8.16 (d, J = 5.7 Hz) corresponding to H-5 and H-6 respectively (Scheme 3.7). The pyrimidine methoxy singlet at δ_H 3.93, the bridging NH at δ_H 8.46 and the OH signal at δ_H 2.85 further confirmed formation of **136**. The ^{13}C NMR spectrum of **136** revealed corresponding resonances at δ_C 99.2 (C-5), δ_C 158.3 (C-6), δ_C 53.3 (OCH_3). The crucially important resonances for C-2 and C-1' were found at δ_C 170.2 and δ_C 141.0 respectively.

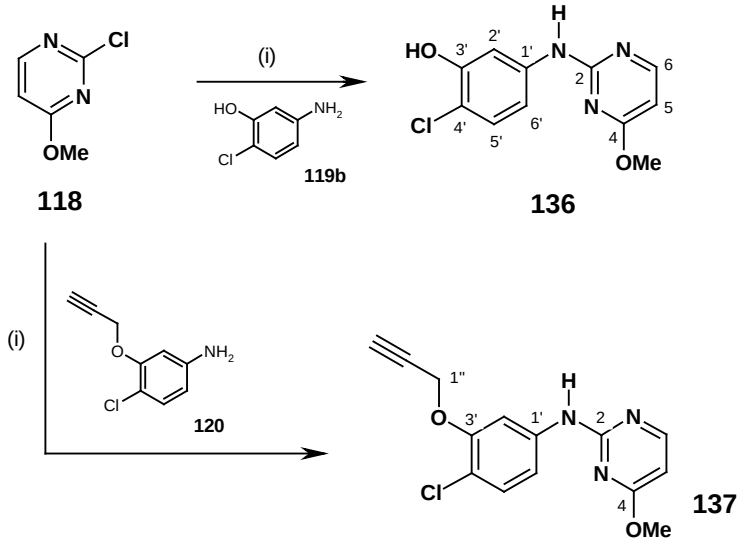

Scheme 3.8 *Reagents and conditions:* (i) p-TsOH, 1,4-dioxane, 100^{o}C (**136**-95%, **137**-73%).

Similarly, the Sonogashira coupling partner **137** was prepared in an identical manner to that for **136** and obtained in a 73% yield after column purification. The key diagnostic signals in its ^{1}H NMR spectrum were the alkyne proton at δ_H 3.10 and the propargylic methylene protons at δ_H 4.87 integrating correctly against the pyrimidine AB doublet pair for H-5/H-6. The ^{13}C NMR spectrum of **137** confirmed the incorporation of the propargyloxy moiety with signals at δ_C 56.6

(C-1''), δ_C 76.8 (C-3'') and δ_C 78.7 (C-2''). Combustion microanalysis returned good data: Found C, 58.00; H, 4.40; N, 14.64%; $C_{14}H_{12}N_3O_2Cl$ requires C, 58.04; H, 4.17; N, 14.50%.

3.4.1.2 Sonogashira coupling and final deprotection

The Sonogashira coupling of **137** with 5'-*O*-benzoyl-5-iodo-d4U **60** using identical conditions to those for forming bifunctional **114** was carried out and after silica-gel purification bifunctional **138** was isolated in a moderate 55% yield (Scheme 3.9). Its ^{1}H NMR spectrum revealed resonances for both inhibitor moieties in a 1:1 ratio, key being the disappearance of a terminal alkyne proton at δ_H 3.10. Its ^{13}C NMR spectrum returned the correct number of resonances as 28 for 30 carbons (revealing the characteristic appearance of only 4 singlets for the 6 carbons of the benzoyl phenyl) and was assigned using 2-D techniques such as HSQC and HMBC. The final benzoyl group deprotection (Scheme 3.9) was achieved under basic conditions with sodium methoxide in methanol at room temperature, with TLC confirming reaction completion after 2 hrs. Direct flash chromatography afforded bifunctional **115** in an excellent yield of 88% of sufficient purity as judged by spectroscopic analysis for biological testing.

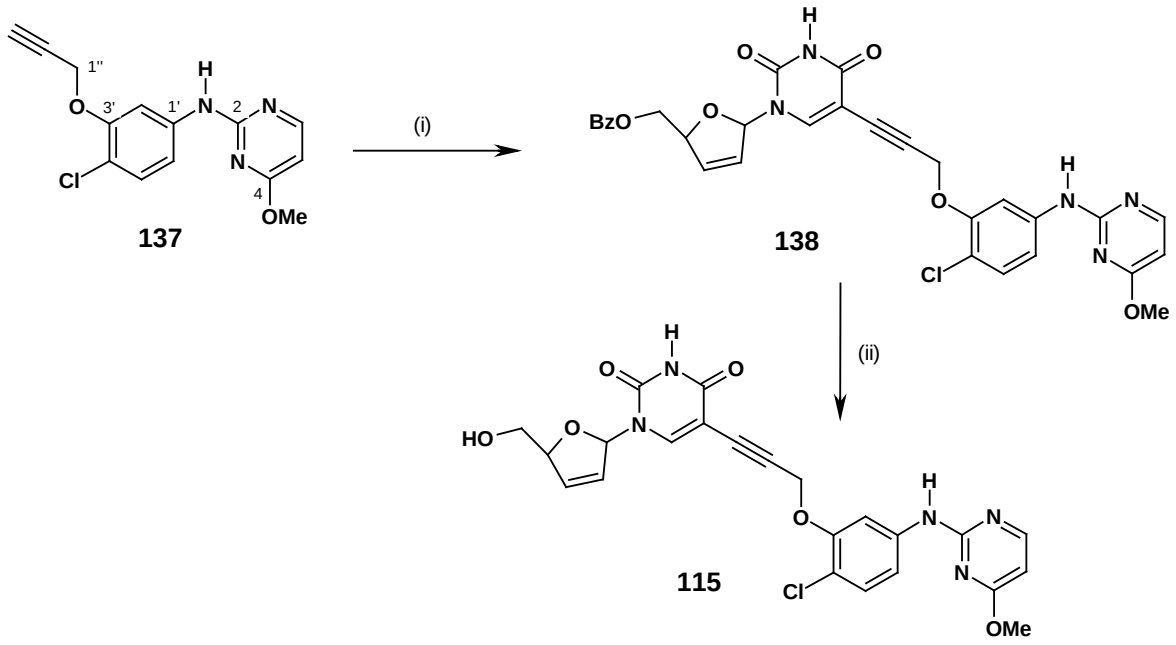

Scheme 3.9 *Reagents and conditions:* (i) 5'-Benzoyl-5-iodo-d4U, $Pd(PPh_3)_4$ (10%), CuI (50%), NEt_3 (2 eq), DMF/THF (1:2), rt, (55%); (ii) NaOMe, MeOH, rt, (88%).

Thus, the ^{1}H NMR spectrum of **115** (see Figure 3.11) revealed the disappearance of the aromatic signals integrating for the benzoyl group. Once again, the ^{13}C NMR spectrum of **115** returned the correct number of singlet resonances for 23 carbons. Finally, a correct HRMS

evaluation (*m/z* HRMS (ES) 498.1184 $[M+H]^+$, $C_{23}H_{21}N_5O_6Cl$ requires *m/z* 498.1180 $[M+H]^+$), confirmed the structure of **115**.

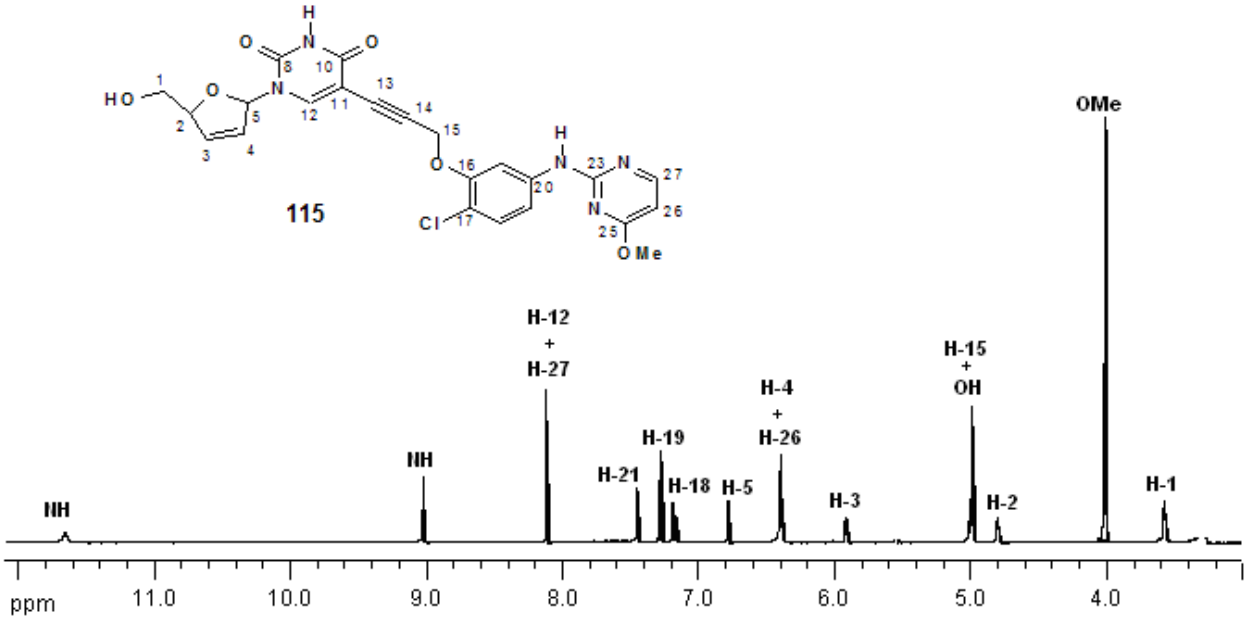

Figure 3.11 ^{1}H NMR spectrum of **115**.

3.4.2 Synthesis of the [d4U]-monoPEG-propyne-[2-pyrimidinylarylamines]

3.4.2.1 Synthesis of the 2-pyrimidinylarylamine derivatives

With a plausible route developed for the prototype propyne heterodimers, attention was turned towards synthesizing heterodimers with longer spacers for structure-activity purposes. A polyethylene (PEG) unit was chosen as the repeating unit in view of its synthetic accessibility as well as its promotion of water solubility. It was envisaged that a counterpart 2-pyrimidinylarylamine derivative of **137** would be prepared with a modified spacer for Sonogashira coupling as described previously. The overall synthetic scheme for the initial phase of the synthesis is shown in Scheme 3.10. Following the method described by Marshall *et al.*,[183] 1,2-ethanediol **139** was mono-protected as its monobenzyl ether **140** in 53% yield with benzyl bromide and sodium hydride in THF. The product was easily isolated by distillation, and although obtained only in moderate yield, the mono-benzylation could be carried out on a large scale. The presence of a benzyl group in the product was confirmed by the ^{1}H NMR spectrum, which revealed aromatic protons integrating for 5 protons resonating at δ_H 7.34 as well as methylene protons resonating at δ_H 4.56. The ^{13}C NMR spectrum displayed a methylene carbon at δ_C 73.3.

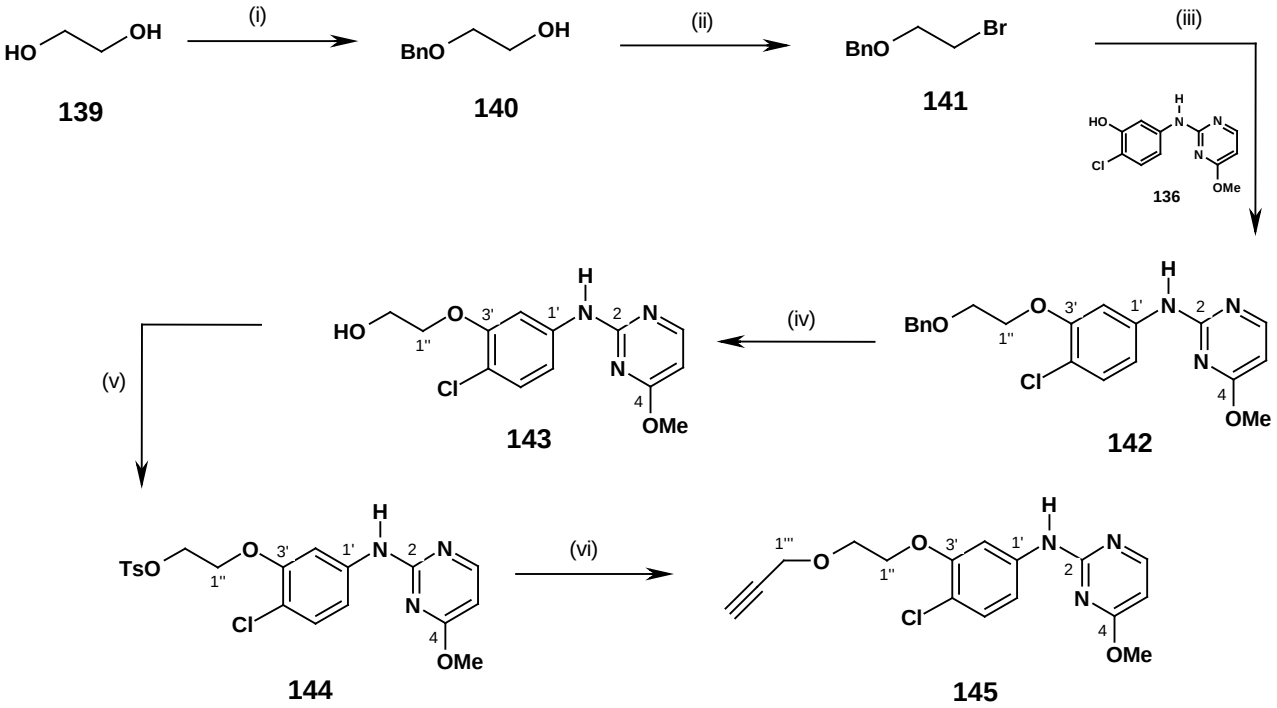

Scheme 3.10 *Reagents and conditions:* (i) BnBr, NaH, THF, reflux, 20 hrs (53%); (ii) PPh_3, CBr_4, CH_2Cl_2, 0 ^oC, 30 min (95%); (iii) **136**, K_2CO_3, *n*-Bu_4NI, acetone, r.t (100%); (iv) H_2, Pd/C, EtOH, rt (70%); (v) *p*-TsCl, NEt_3, CH_2Cl_2, DMAP (cat) (70%); (vi) propargyl alcohol, NaH, THF, Δ (98%).

Treatment of alcohol **140** with carbon tetrabromide and triphenylphosphine in dichloromethane (Scheme 3.10) smoothly yielded the bromide **141** in 95% yield. Work-up involved evaporating the solvent and purifying the crude product directly by column chromatography. Mechanistically, the reaction of triphenylphosphine with carbon tetrabromide generates a bromophosphonium ion *in situ* which then reacts with the alcohol to give an alkoxyphosphonium ion (Fig. 3.12). The phosphonium ion intermediate then undergoes nucleophilic attack by the bromide ion, with the expulsion of triphenylphosphine oxide. The driving force for the cleavage of the C-O bond is the formation of the strong phosphine oxide bond (P=O), and the process is overall neutral as the other by-product formed is bromoform ($CHBr_3$).

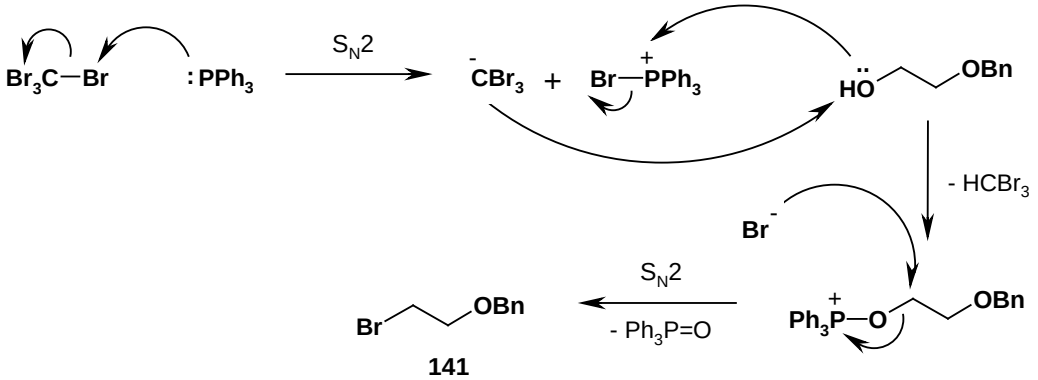

Figure 3.12 Mechanism of formation of bromide **141**.

The ^{1}H NMR spectrum of bromide **141** revealed the absence of a hydroxyl proton at δ_H 2.52, while its ^{13}C NMR spectrum revealed an upfield shift of the carbon at C-1 from δ_C 61.8 in alcohol **140** to δ_C 30.4, thus confirming that substitution by bromine had taken place.

The next step in the reaction sequence was the nucleophilic substitution of **141** by 2-pyrimidinylarylamine intermediate **136** to give **142**. The alkylation proceeded smoothly using potassium carbonate as a base in acetone to afford the desired compound **142** in 100% isolated yield. The ^{1}H NMR spectrum of **142** revealed a downfield shift of the protons α to bromine at δ_H 3.50 for the bromide **141** to δ_H 4.29 in **142**, as well as the presence of signals for the phenolic moiety, thus confirming that the alkylation had occurred.

Catalytic hydrogenation of **142** using palladium-on-carbon catalyst in ethanol furnished **143** in 70% yield (Scheme 3.10). The appearance of a hydroxyl proton as a broad singlet resonating at δ_H 2.25 and the absence of the characteristic benzylic methylene singlet at δ_H 4.67 for **142** provided sufficient evidence that debenzylation had taken place.

Subsequently, for O-propargylation, the same two-step sequence was used as with the UC-781 bifunctionals. Thus, the hydroxyl group of **143** was converted to its tosylate **144** in 70% yield by reacting it with *p*-toluenesulfonyl chloride in the presence of triethylamine and a catalytic amount of DMAP in dichloromethane. The ^{1}H NMR spectrum of **144** displayed pyrimidine aromatic protons with AB coupling (J_{AB} = 8.6 Hz) resonating at δ_H 7.45 and δ_H 7.84 as well as a methyl singlet at δ_H 2.43. The presence of additional aromatic signals in the ^{13}C NMR spectrum further confirmed the presence of a tosylate group.

Alkylation (Scheme 3.10) of tosylate **144** was accomplished in the presence of sodium hydride and a large excess of propargyl alcohol in THF at reflux. Aqueous work-up followed by purification by column chromatography furnished the alkyne **145** in 98% yield. An upfield shift of the H-2'' signal in the ^{1}H NMR spectrum from δ_H 4.34 in tosylate **144** to δ_H 3.96 in **145** supported the displacement of the tosylate, while the ^{13}C NMR spectrum of compound **145** displayed signals for the alkyne carbons at δ_C 78.3 for C-2''' and δ_C 76.8 for C-3'''. As before, this sequence was preferred to direct propargylation of **143** with propargyl bromide.

3.4.1.2 Sonogashira coupling and final deprotection

Sonogashira coupling of 5'-*O*-benzoyl-5-iodo-d4U **60** with alkyne **145** using conditions previously described yielded the coupled product **146** in 70% yield (Scheme 3.11).

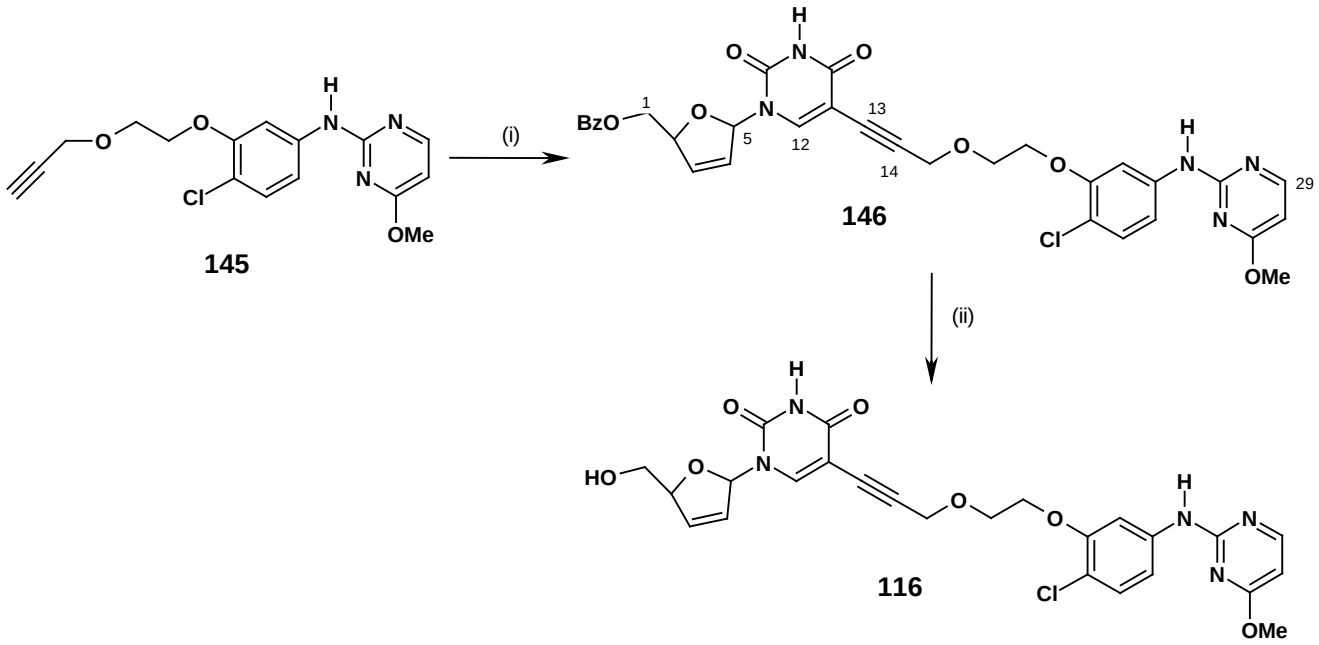

Scheme 3.11 *Reagents and conditions:* (i) 5'-Benzoyl-5-iodo-d4U, $Pd(PPh_3)_4$ (10%), CuI (50%), NEt_3 (2 eq), DMF/THF (1:2), rt, (70%); (ii) NaOMe, MeOH, rt, (51%).

The ^{1}H NMR spectrum of **146** showed the disappearance of the alkyne proton of **145** at δ_H 2.45. Some of the resonances for **146** derived from both **60** and **145** included a broad singlet at δ_H 7.66 (1H, H-12), a multiplet with allylic coupling at δ_H 6.76 (1H, H-5), a singlet at δ_H 3.91 (3H, OMe) and a doublet at δ_H 8.21 (1H, H-29). The ^{13}C NMR spectrum displayed diagnostic signals for the alkyne carbons at δ_C 84.3 (C-13) and δ_C 98.1 (C-14), as well as the anomeric carbon of the sugar (C-5) at δ_C 90.1.

Deprotection of the benzoyl group (Scheme 3.11) was achieved using sodium methoxide in methanol to give the deprotected target compound **116** in a moderate 51% yield. The reaction proceeds spot-to-spot on TLC and the low yield can only be attributed to compound loss during extractive work-up. The ^{1}H NMR spectrum of **116** (Fig. 3.13) exhibited an expected upfield shift for the diastereotopic H-1 protons to δ_H 3.61 in **116** from δ_H 4.49 in **146** as a result of the loss of the deshielding effect of the carbonyl group. Similarly, the ^{13}C NMR spectrum showed the disappearance of a carbonyl carbon at δ_C 165.6 and an upfield shift of C-1 from δ_C 65.2 in **146** to δ_C 64.8 in **116**. The deprotection was further confirmed by a broad band in the infrared spectrum at 3590 cm^{-1} for the hydroxyl group.

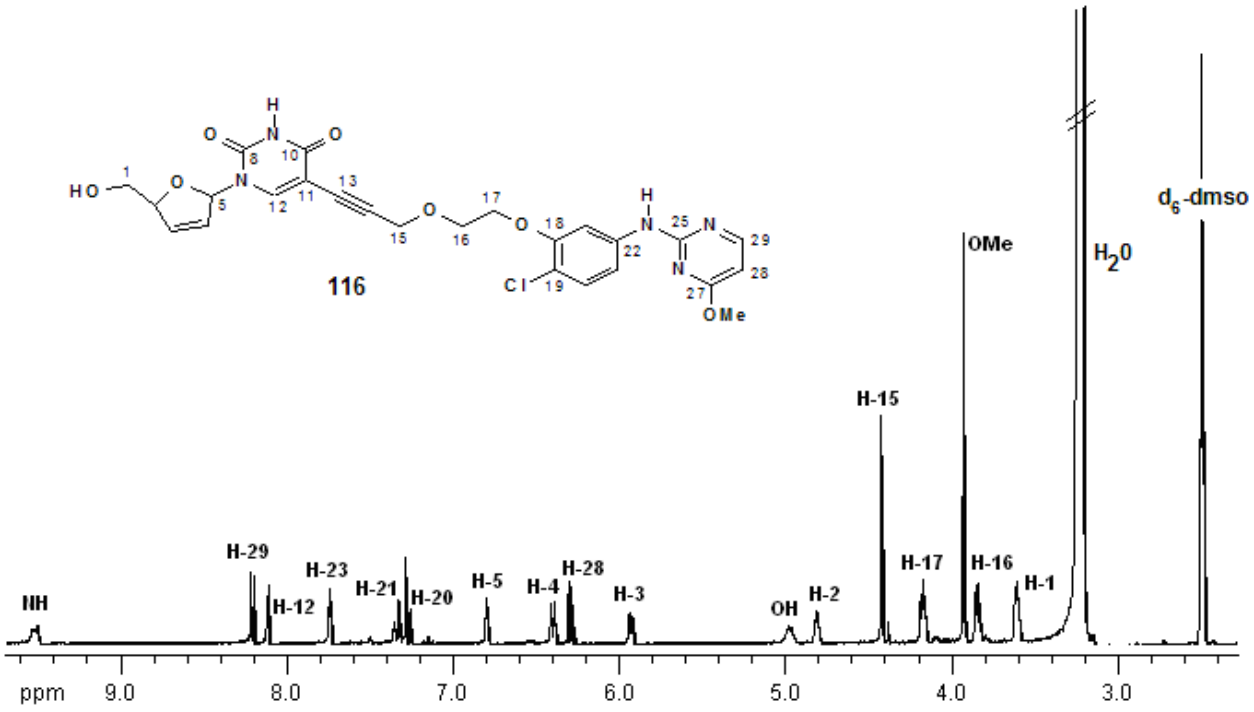

Figure 3.13 ^{1}H NMR spectrum of target **116**.

3.5 Biological evaluation and SAR interpretation

The inhibition of viral replication in HIV-infected cells of the 4-pyrimidinylarylamine derivatives (**128**-**134**), 2-pyrimidinylarylamine derivatives (**136**-**137** and **143**,**145**), as well as bifunctional targets **114**-**116** was measured against HIV-1 (IIIB) replication in MT-2 cell culture using an MTT assay (see Appendix I). None of the 2- or 4-pyrimidinylarylamine derivatives or the bifunctional targets synthesized (Table 3.3) showed any anti-HIV activity, i.e. they all had an EC_{50} = not active (N/A). CC_{50} values measuring cytotoxicity of normal cells had generally high micromolar values.

Table 3.3 Anti-HIV results of compounds tested in cell-culture.

Compound	EC_{50} (µM)[a]	CC_{50} (µM)[b]
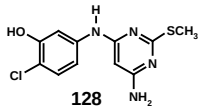 **128**	inactive	29
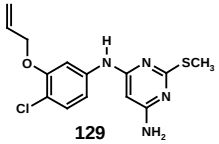 **129**	inactive	17

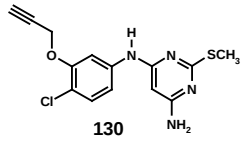 **130**	inactive	23
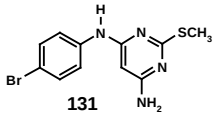 **131**	inactive	8
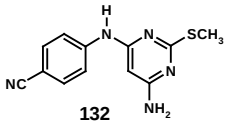 **132**	inactive	30
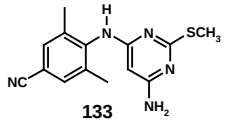 **133**	inactive	16
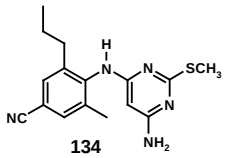 **134**	inactive	7
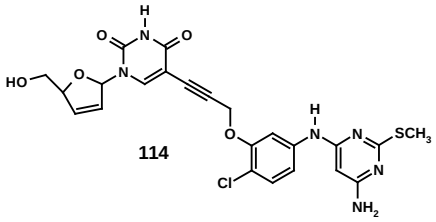 **114**	inactive	28
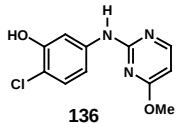 **136**	inactive	48
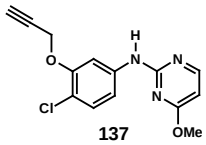 **137**	inactive	11
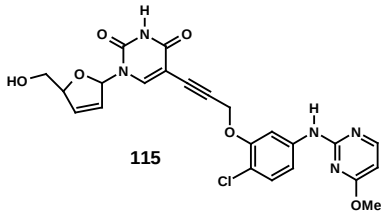 **115**	inactive	39
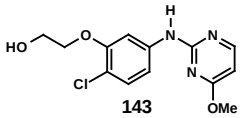 **143**	inactive	28

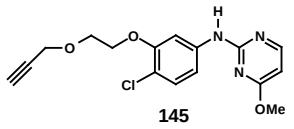 **145**	inactive	24
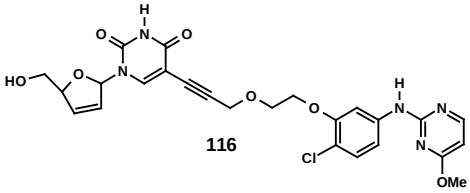 **116**	inactive	5.5

[a] Effective concentration that inhibits viral-mediated T-cell death by 50% and as an average of three results.
[b] Cytotoxicity = concentration that kills 50% of the T-cells and as an average of three results.

Once again, examination of the activity (or lack thereof) of these compounds offered important insight into the design of future bifunctional compounds, as well as offering valuable information regarding structure-activity relationships. Firstly, the *meta*-tethered 2-pyrimidinylarylamine derivatives (**137**, **143** and **145**) surprisingly were biologically inactive. In particular, a lack of activity for derivatives **136** and **137** was considered significant in view of Jorgensen's success with 2-pyrimidinylarylamines. A plausible explanation is that any *meta*-extension on the aryl component in the Het-NH-ArX motif other than the Jorgensen dimethylallyl (DMA) one, has weakened hydrophobic interactions with the Wing II residues. The mono-PEG-propyne derivatives **143** and **145**, as well as bifunctional targets **115** and **116** revealed that a spacer extension from the *meta*-position of the 2-substituted aromatic component attached to the pyrimidine was definitely not the correct connection point for a bifunctional synthesis.
Secondly, the fact that 4-pyrimidinylarylamine derivatives **128**-**134** were inactive also, including the prototype [d4U]-propyne-[4-pyrimidinylarylamines] bifunctional **114** does not necessarily mean that the spacer extention point on the aryl component in the Het-NH-ArX motif (whether *meta* or *ortho*) was incorrect, but could imply that the C-2 position of the pyrimidine (Het) moiety needs to be also substituted with an aryl component as in the potent DAPY derivatives such as TMC120 or TMC125. The lack of this vital C-2 pyrimidine linkage (which gives rise to important Wing II hydrophobic interactions with Lys101 and Tyr318) could have caused the NNRTI portion of the heterodimer not to bind tightly and specifically to the NNRTI-BP (or in our case not bind at all) with resulting lack of biological activity. Therefore, this structural study proved to be of great value in depicting how important every component of the potent DAPY compounds were in trying to achieve maximum biological activity.

Thus, these results allowed the following conclusions regarding rational drug design changes to be made in the next and final phase of the thesis:

(i) A full DAPY would have to be synthesized;

(ii) The best attachment point for the tether onto the NNRTI would be the *para*-position (2nd best *meta*-position) of the aromatic substituent attached to C-4 of the pyrimidine;

(iii) Variable spacer sizes needed to be evaluated for optimal activity and their influence on the entropy of activation addressed;

(iv) The need for molecular modeling and its part in understanding and probing for synergy between the NRTI active site and the NNRTI-BP had become evident in trying to develop a predictive model to work with, and finally;

(v) To gain insight into the requirements at the NRTI, d4U would have to be substituted by and then compared with a more flexible and mono-phosphorylated ANP (acyclic nucleotide phosphonate).

SYNTHESIS OF NRTI-SPACER-TMC120 DOUBLE-DRUGS

4.1 Strategy for the synthesis of [NRTI]-spacer-[TMC120] bifunctionals

Following the synthesis of the d4U-spacer-pyrimidinylarylamines in Chapter 3, many conclusions were made with regards to a more rational drug design approach. It became apparent that a full diarylpyrimidine (DAPY) would have to be synthesized, incorporating a flexible spacer linked to not only the rigid d4U, but also an acyclic nucleotide phosphonate (ANP). The activation entropy ($\Delta S^{\#}$) was likely to be greater for an ANP compared to the pre-organized form of d4U, however in theory, the ANP moiety might be able to adopt conformations where its enthalpy of activation ($\Delta H^{\#}$) would be lower (due to cooperativity), resulting in an overall lower Gibbs activation free energy ($\Delta G^{\#}$) leading to a greater negative$\Delta G_{overall}$ (faster and tighter binding). However, it was decided not to completely abandon d4U, but rather retain it for a comparative study with the ANP.

At the onset of this new strategy in 2007, collaborative work between Professors Roger Hunter (University of Cape Town), Karen Anderson and William Jorgenson (both Yale University) led the groups in search of a new target structure, this time an anti-HIV double-drug of the general formula [NRTI]-spacer-[TMC120]. Variation on the NRTI would cover both d4U and an ANP. Unlike in Chapter 3, a TMC120 (dapivirine) NNRTI template was chosen in which the Br and NH_2 groups in the pyrimidine ring are absent (Fig. 4.1). TMC120 is based on the clinically approved TMC125 (etravirine) belonging to the family of highly potent diarylpyrimidines (DAPY's), while TMC278 is the most active NNRTI known to date against single- and double-point mutations.[72]

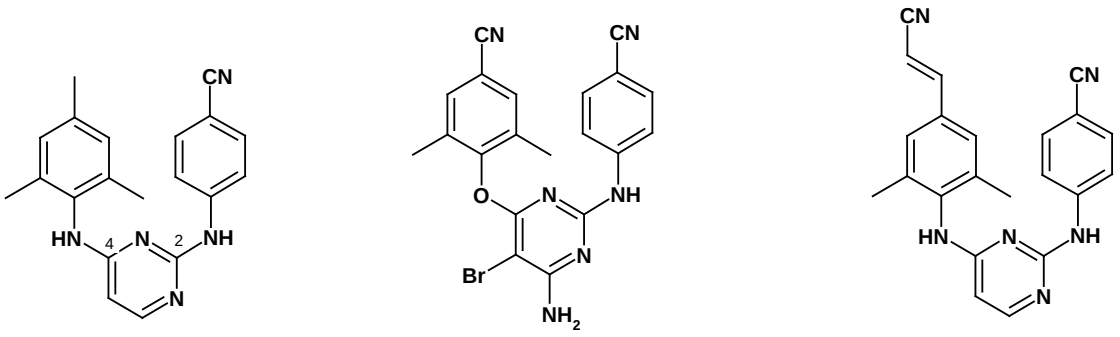

TMC120 **TMC125** **TMC278**

Figure 4.1 Structures of TMC120, TMC125 and TMC278 belonging to the family of DAPY's.

Before the start of any synthesis this time around, molecular modeling was used to extrapolate vital drug-design considerations. Thus, the Yale modeling group under supervision of Professor William Jorgenson came up with the following results.

4.2 Molecular modeling studies

4.2.1 Parameters for Molecular Modeling of d4U-n-PEG-TMC bound to HIV-1 RT:template:primer.

Since there was no crystal structure of RT complexed with both a NRTI and a NNRTI, a model was created starting from the crystal structures of the RT:template:primer complex from Huang *et al*.[184] (PDB entry 1rtd) and the Das *et al*. complex of the TMC120-R147681 NNRTI[90] (PDB entry 1s6q). First, both of these files were read into the UCSF Chimera program[185] and superimposed using the matchmaker utility. A composite protein was then created by combining residues 1a-92a, 108a-178a, 241a-554a, 3b-249b, the template, primer and the 4 Mg^{2+} ions from 1rtd and 93a-107a, 179a-240a, and the ligand from 1s6q.

The initial 3D structure of the bifunctional ligand (bf4) was created by drawing it in ChemDraw[186] and energy minimization using the MM2 force field in Chem3D[187] and writing as a PDB file. After reading this structure in Chimera, the nucleotide end of this molecule was superimposed to the dNTP of the composite protein created above, and a few of the dihedrals on the polyethylene glycol (PEG) spacer were manually changed to g+ or g- to superimpose as best as possible the NNRTI end to the TMC120 crystallographic ligand. The sidechain torsions $\chi 1$ and $\chi 2$ of Y188a were adjusted by -30 and +30° respectively to avoid a severe steric clash. Finally, the crystallographic dNTP and TMC120 were then removed and the resulting complex exported as a PDB file.

The creation of the model was completed by reading the PDB files created by Chimera in Schrödinger's Maestro 7.5[188] and adding the hydrogen atoms needed at protonation states appropriate to pH = 7. The following set of energy minimizations were sequentially run with the Impact program[189] using the OPLS 2001 force field with a distance-dependent dielectric $\varepsilon = 4r$, a 12 Å cutoff for non-bonded interactions, and the steepest descent algorithm. First, the newly created ligand and the segments of the protein chains originally from the 1s6q structure (93a-107a, 179a-240a) as well as all the residues within 4 Å of those were allowed to moved while the rest were kept fixed at their original positions during a 100-step optimization during which the total energy of the system decreased from 6.1×10^{14} to 927.0 kcal/mol. The resulting structure was checked for consistence, and a second run of 300 steps was restarted form this point using

the same degrees of freedom during which the energy decreased further to -187.2 kcal/mol. The entire system was then allowed to relax for successive optimizations of 100 and 300 steps reduced the total energy from 8,490.5 to -3,398.0 kcal/mol. The C^{α} rms deviation of the final structure to the initial 1rtd is only 0.27 Å which shows that there was relative little distortion created by the process.

4.2.2 Results from the molecular modeling

Molecular modeling suggested a 4-PEG spacer would be long enough to span the NNRTI binding pocket and the active site (Fig. 4.2 -A). This is the first ever modeling interpretation of a bifunctional entity complexed to HIV-1 RT as there are none in the literature. The 4-PEG spacer was identified as the minimum distance between the two sites, but the incorporation of longer PEG units would be very interesting from a SAR point of view. Very importantly, the modeling finally confirmed our earlier prediction, following a suggestion by Ruth and Cheng, that a C-5 connection to the base clearly 'exits' the substrate binding site with low interference to DNA base-pairing (Fig. 4.2 -B).[141]

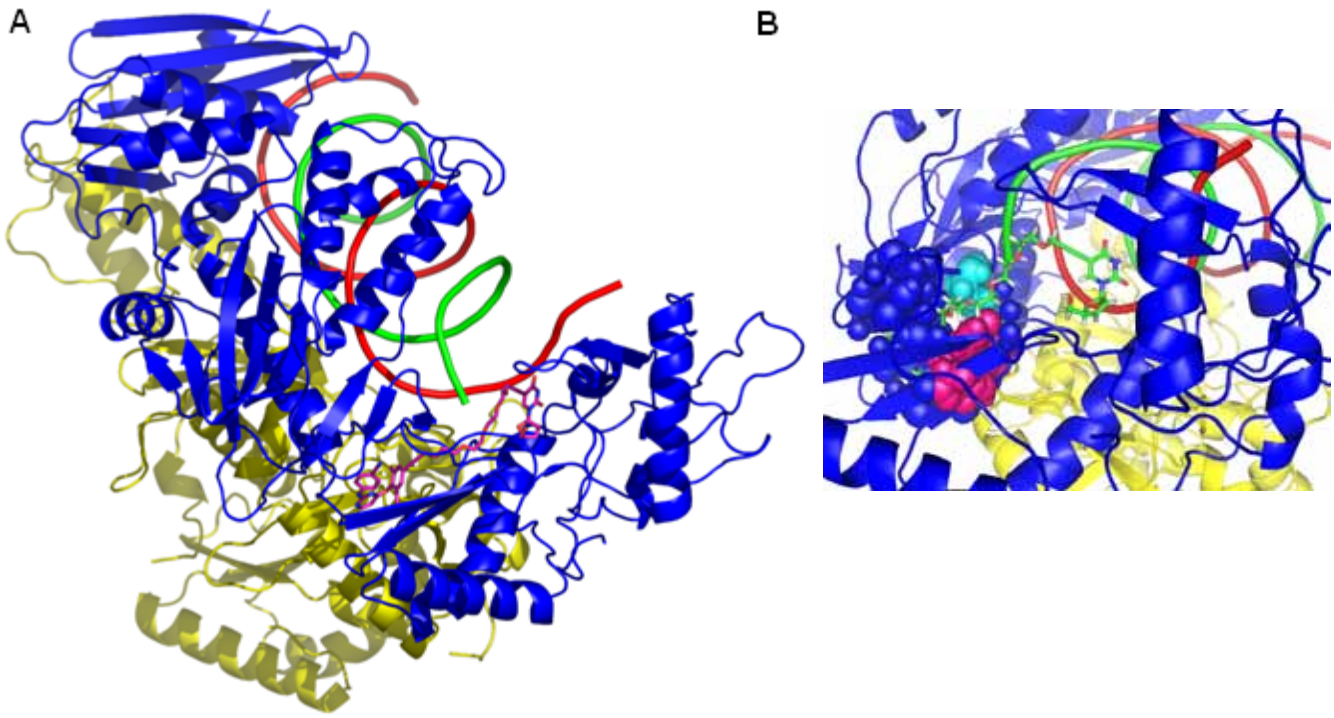

Figure 4.2 A) d4U-4PEG-TMC120 double drug bound to HIV-1 RT; B) NRTI position zoomed in, depicting the crucial C-5 spacer extension on the base moiety of the NRTI.

Most interestingly, the PEG spacer was predicted to protrude from the NNRTI binding pocket toward (Fig. 4.3 -D and E) the active site through a hydrophobic tunnel, similar to the tunnel identified in the TMC-278 (Fig. 4.2 -C) bound structure[77] (pdb ID: 2ZD1).

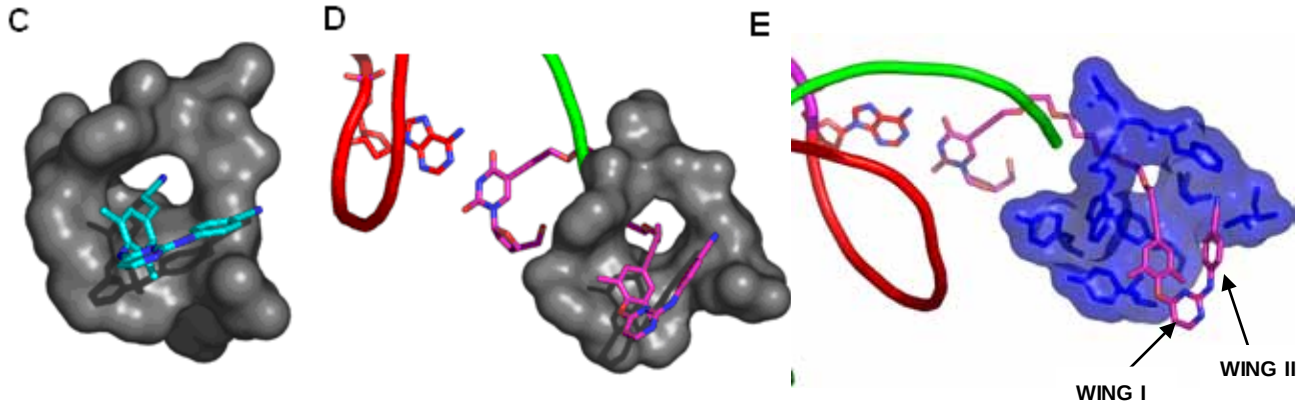

Figure 4.3 C) TMC278 bound to HIV-1 RT; D) The PEG spacer protruding from the NNRTI binding pocket toward the active site through a hydrophobic tunnel; E) Key amino acid residues highlighted in the NNRTI-BP.

As depicted in Figure 4.3 -E, the C-2 aromatic ring of the DAPY (see Figure 4.1 for numbering) is firmly embedded in the Wing II hydrophobic compartment of the RT NNRTI-BP, but the C-4 aryl ring is closer to residues near the 'exit tunnel' of interest, whilst the central pyrimidine unit binds strongly in the Wing I region. The *para*-position on the C-4 aromatic ring of the DAPY was identified as the optimal connection point for the spacer elongation (Fig. 4.3 -C/D). From the pictures generated, it was now evident that an *ortho*-extension on the C-4 aromatic ring would not work (as in Chapter 3), and that a *meta*-extension would probably not return any biological activity, but should definitely be synthesized and evaluated. These conclusions are in line with that made by Arnold and co-workers in his recent PNAS communication,[77] although his study did not include extensions to bifunctional entities.

Thus, it was decided to synthesize double-drugs of the general formula [NRTI]-spacer-[TMC120] using a *para*-connection to the spacer. The first such double-drugs would incorporate d4U as the NRTI. The bifunctional structures identified as possible targets are shown in Figure 4.4. Triphosphate **148** was identified for carrying out *in vitro* inhibition studies on RT directly in order to complement the cell-culture results.

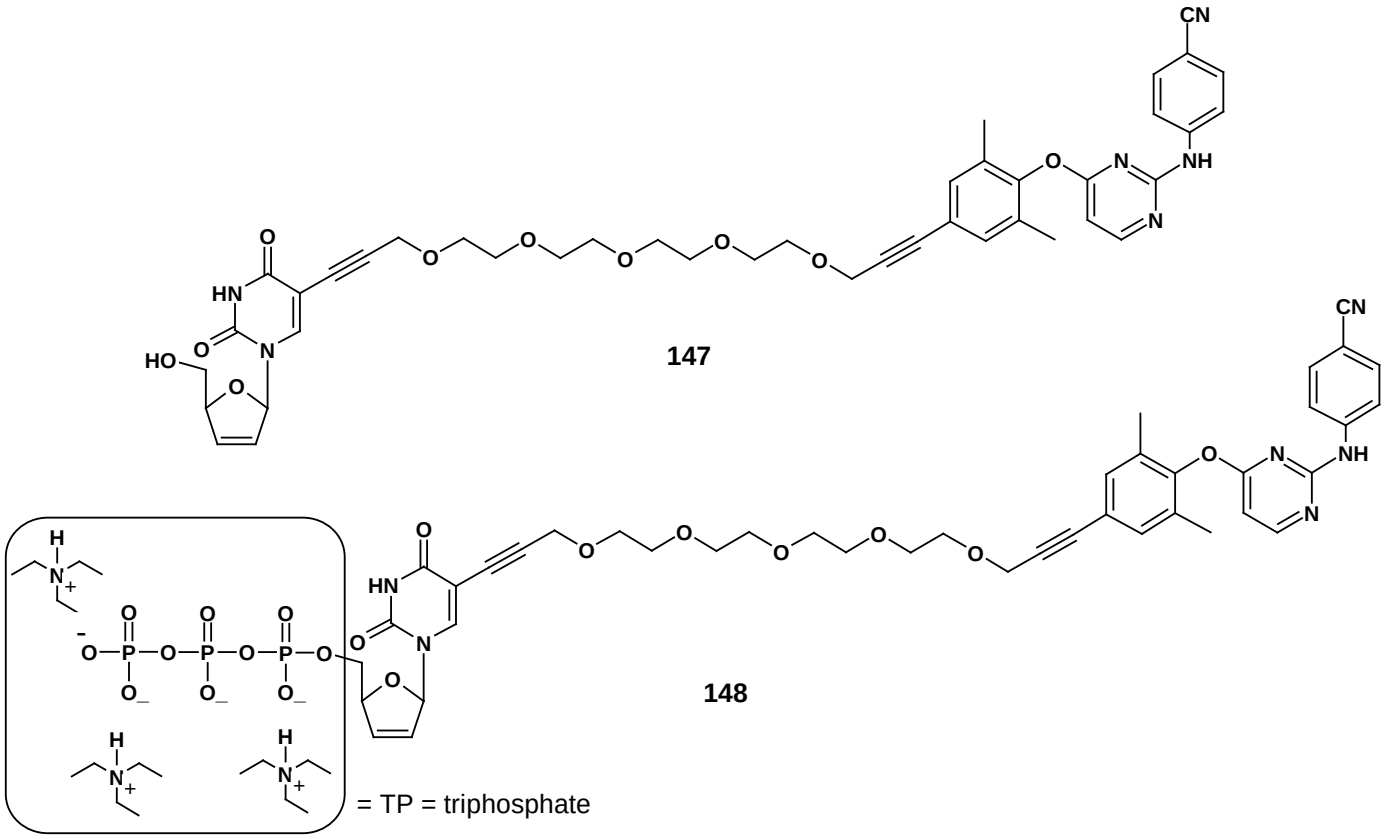

Figure 4.4 Target compounds identified from the molecular modeling.

4.3 Retrosynthetic analysis of [d4U-TP]-propyne-tetraPEG-propyne-[TMC120]

The total synthesis of target **147** was conceived using chemistry previously described *via* a convergent strategy involving the coupling of 5'-iodo d4U **60** to alkyne **149** followed by deprotection of the benzoyl group to render the target compound directly (Figure 4.5). This would be followed by a triphosphate salt incorporation to give the second target compound **148**. Alkyne **149** would in turn be formed from the propargylation of alcohol **150**, following tosylation and *in situ* generation of the propargyloxy anion from the reaction between propargyl alcohol and sodium hydride. Compound **150** would be tested for substituent effects in the HIV reverse transcriptase pocket, and could be obtained from the Sonogashira coupling of mono-propargylated tetraethylene glycol **151** and TMC120 derivative **152**.

TMC120 derivative **152** was anticipated to come from aryl coupling of appropriately substituted phenol **153** and key intermediate **154**. Key intermediate **154** could be obtained over three steps from commercially available 2-thiouracil **155** and 4-aminobenzonitrile **156**.

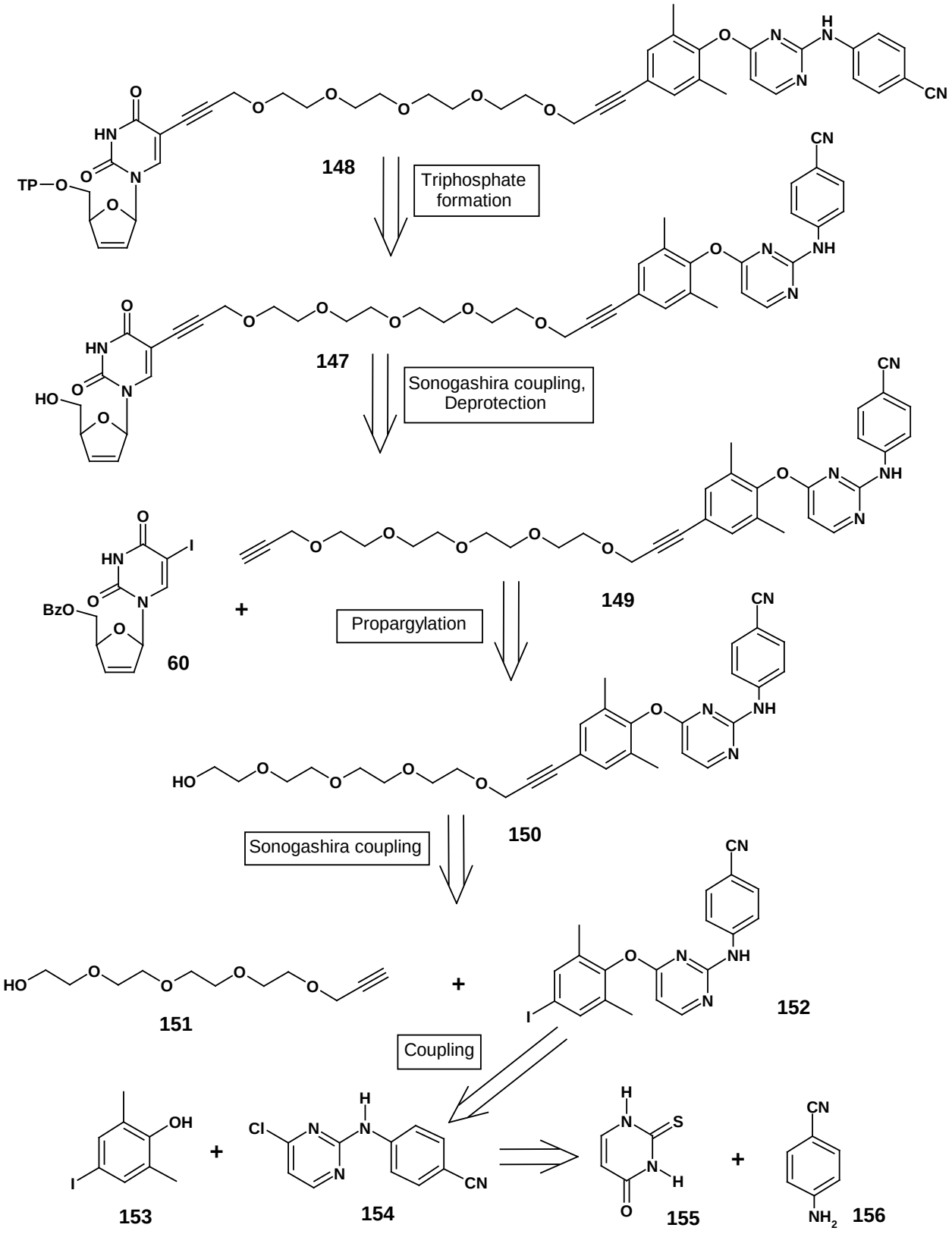

Figure 4.5 Retrosynthetic analysis of target compunds **147**-**148**.

4.4 Synthesis of [d4U-TP]-propyne-tetraPEG-propyne-[TMC120]

4.4.1 Synthesis of the tethered (propyne-tetraPEG-propyne)-TMC120 derivative

Our first challenge towards the synthesis of **147** and **148** was to access the very important Sonogashira coupling partner **152**. Intermediate **152** would be required in large quantities and thus a viable synthetic route needed to be explored. Isomura and co-workers published a report[190] in 1997 in which they synthesized **152** in a 72% overall yield over four steps (Scheme 4.1). To this end, commercially available 2-amino-4-chloro-1,3-pyrimidine **157** was di-protected at the C-2 amine using di-*tert*-butyldicarbonate and *N,N*-4-dimethylaminopyridine in THF at room temperature. An 85% yield was obtained after column chromatography.

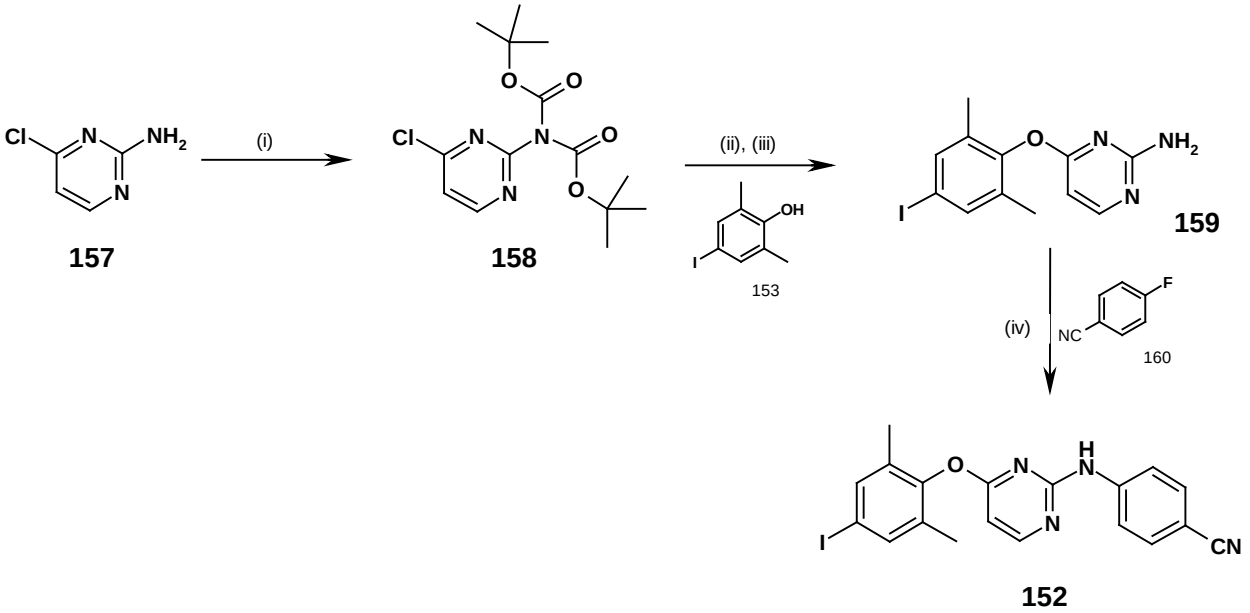

157 158 152

Scheme 4.1 *Reagents and conditions:* (i) $(Boc)_2O$ (2 eq), THF, DMAP (85%); (ii) **153**, Cs_2CO_3, DMF, 90 ^oC; (iii) CF_3CO_2H (10 eq), CH_2Cl_2, r.t (86% over two steps); (iv) **160**, *t*-BuOK, DMSO, 50 ^oC (45%).

This was followed by an addition-elimination type nucleophilic aromatic substitution reaction at the C-4 position of the pyrimidine using the iodophenol **153** and cesium carbonate in DMF at 90 ^oC. Subsequent filtration of excess cesium carbonate and removal of solvent under reduced pressure, followed by deprotection of the Boc-groups employing trifluoroacetic acid in dichloromethane at room temperature gave **159** in 86% yield over two steps. Finally, **152** was prepared by reacting **159** together with potassium tert-butoxide in DMSO at 50 ^oC, which after addition of arylamine **160** returned key TMC-intermediate **152** in a low 45% yield after column chromatography.

Not satisfied with the efficacy of this route, it was decided to develop an alternative based on a four-step procedure reported by Spychala[191] in 1997 regarding a facile preparation of N^2-

arylisocytosines. This approach required less column chromatography and made use of relatively cheap starting materials compared to the Isomura strategy. Thus, 2-thiouracil (Scheme 4.2) was subjected to sodium hydroxide dissolved in water and methyl iodide for 24 hrs at room temperature, which following acidification using acetic acid, rendered 2-(methylthio)pyrimidin-4(3*H*)-one **161** in 73% yield after crystallization from boiling ethanol. The ^{1}H NMR spectrum of **161** revealed only one NH signal present at δ_H 6.65, as well as the diagnostic thiomethyl singlet resonating at δ_H 2.43. The ^{13}C NMR spectrum confirmed formation of **161** with a singlet at δ_C 12.3 for the thiomethyl and a carbonyl peak at δ_C 164.1. The melting point of 188-189 ^{o}C was in full agreement with that reported in the literature (185-188 ^{o}C).

The next step (Scheme 4.2) involved treatment of **161** with a small excess of arylamine **156** in refluxing bis(2-methoxyethyl) ether (diglyme) resulting in precipitation of N^2-arylisocytosine **162** in a low yield of 36%. The yield was obtained after repeated crystallization of **162** from boiling methanol. Key diagnostic signals in the ^{1}H NMR spectrum of **162** were the new *AB* aromatic protons at δ_H 7.71 (d, *J* = 8.7 Hz, H-3') and δ_H 7.81 (d, *J* = 8.7 Hz, H-2'). The ^{13}C NMR spectrum of **162** validated this further with new aromatic signals at δ_C 101.7 (C-4'), δ_C 118.7 (C-3'), δ_C 132.7 (C-2') and δ_C 145.9 (C-1'), as well as the indicative CN singlet at δ_C 118.9. Once again, the melting point (260-261 ^{o}C) was in full agreement with literature reports (259-260 ^{o}C).

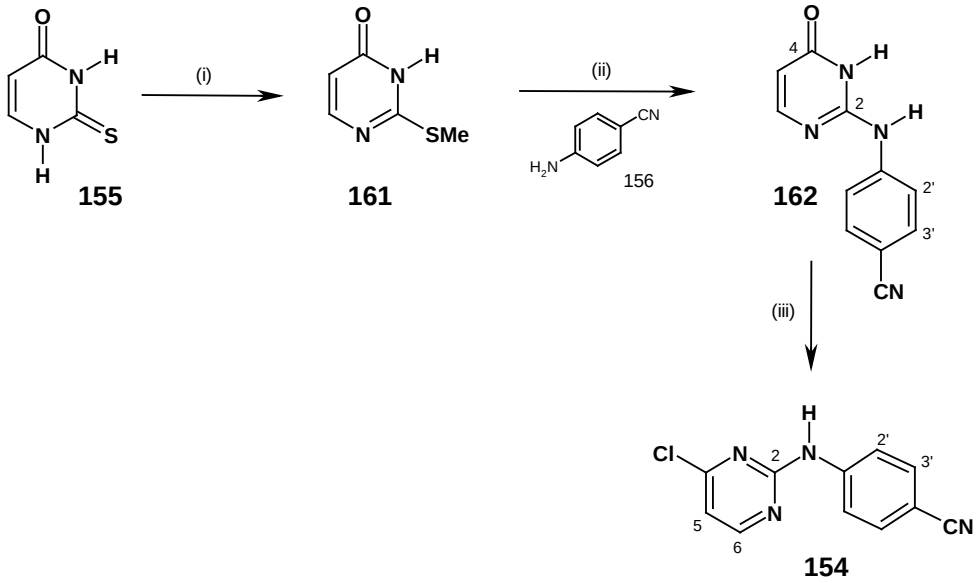

Scheme 4.2 *Reagents and conditions:* (i) CH_3I, NaOH, H_2O, CH_3CO_2H, r.t (73%); (ii) **156**, diglyme, Δ (36%); (iii) neat P_2O_5 (xs), 100 ^{o}C (90%).

Subsequent, chlorination of **162** using neat $POCl_3$ for 5 hrs at 100 ^{o}C gave compound **154** in 90% yield after column purification. The ^{1}H NMR spectrum of **154** displayed two AB doublet systems at δ_H 7.03 for H-5 and δ_H 8.49 for H-6 of the pyrimidine ring, as well as δ_H 7.73 for H-3'

and δ_H 8.06 for H-2' of the C-2 aromatic ring. The ^{13}C NMR spectrum of **154** revealed the disappearance of the carbonyl signal at δ_C 162.0 in **162** and the appearance of a singlet at δ_C 129.7 for the halogen-bearing carbon (C-4). Combustion microanalysis returned favorable data: Found C, 57.12; H, 3.09; N, 24.29; $C_{11}H_7N_4Cl$ requires C, 57.28; H, 3.06; N, 24.29.

Phenol **153** needed to be synthesized first for key intermediate **152** to be completed (Scheme 4.3). This was accomplished[192] using commercially available 2,6-dimethylphenol **163**, iodine and morpholine dissolved in diethyl ether, in which TLC confirmed reaction completion after 1½ hrs. Subsequent column purification returned the *para*-substituted phenol **153** in an excellent yield of 90%. The ^1H NMR spectrum of **153** displayed a free OH singlet at δ_H 4.62, as well as an aromatic proton singlet resonating at δ_H 7.31 integrating for two hydrogens. The ^{13}C NMR spectrum of **153** revealed the C-4 singlet for C-I at δ_C 82.3.

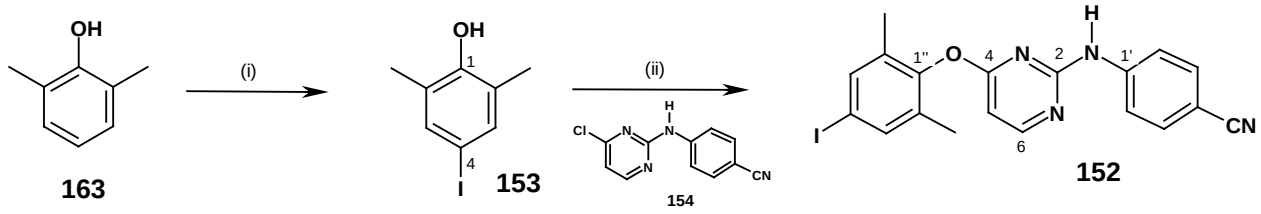

Scheme 4.3 *Reagents and conditions:* (i) I_2, morpholine, diethyl ether (90%); (ii) **154**, Cs_2CO_3, DMF, 90 ^oC (99%).

Successful coupling of phenol **153** to pyrimidine **154** was attained using identical conditions to that of Isomura, making use of cesium carbonate as base in hot DMF.[193] TMC-derivative **152** was obtained after 1 hr in 99% yield following silica-gel purification. The ^1H NMR spectrum of **152** revealed the absence of the free OH at δ_H 4.62 in **153**. The ^{13}C NMR spectrum of **152** displayed vital resonances at δ_C 159.0 (C-2), δ_C 168.0 (C-4), δ_C 144.4 (C-1') and δ_C 149.5 (C-1''). Finally, a correct HRMS evaluation (*m/z* HRMS (ES) 443.0348 $[M+H]^+$, $C_{19}H_{16}N_4OI$ requires *m/z* 443.0369 $[M+H]^+$), confirmed the structure of **152** as shown in Figure 4.3.

With the TMC-derivative **152** now in hand, our attention shifted to the synthesis of the spacer. The overall synthetic scheme for the initial phase of the spacer incorporation is shown in Scheme 4.4. Thus, propargylation of commercially available tetraethylene glycol[194] **164** (1.0 eq.) was achieved using sodium hydride (1.0 eq.) and propargyl bromide (1.1 eq.) in THF at room temperature in 42% yield after column purification. The ^1H NMR spectrum of **151** displayed the key alkyne proton at δ_H 2.42 (t, J = 2.4 Hz). The propargyl methylene signal resonated at δ_H 4.17

(d, J = 2.4 Hz). The ^{13}C NMR spectrum of **151** displayed characteristic alkyne resonances at δ_C 58.0 (C-9), δ_C 74.4 (C-11) and δ_C 79.3 (C-10).

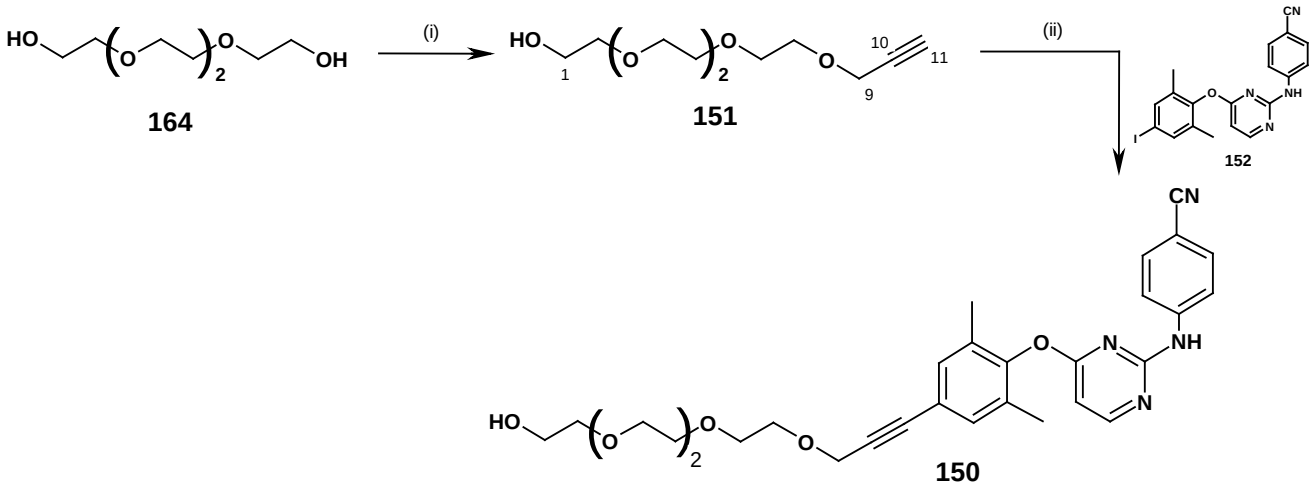

Scheme 4.4 *Reagents and conditions:* (i) propargyl bromide, NaH, THF, r.t (42%); (ii) **152**, $Pd(PPh_3)_4$ (10%), CuI (50%), NEt_3 (2 eq), DMF/THF (1:2), r.t (75%).

The Sonogashira coupling of TMC-derivative **152** with the 4-PEG alkyne **151**, using identical conditions to those described in Chapters 2 and 3, was carried out and the 4-PEG-elongated TMC120 derivative **150** isolated after silica-gel purification in a good yield of 75% (Scheme 4.4). Compound **150** was the first derivative in this series synthesized for anti-HIV probing. Of note, was that hydroxyl group protection was unnecessary, which greatly reduced the number of steps.

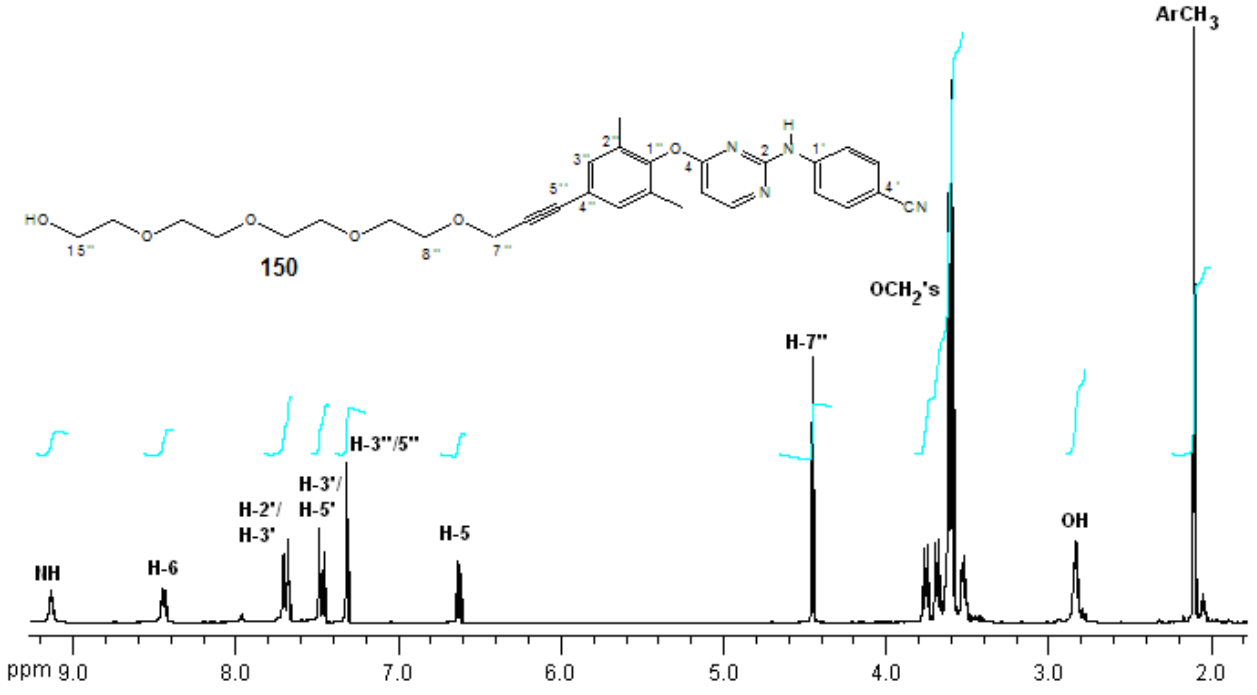

Figure 4.6 ^{1}H NMR spectrum of **150**.

The ^{1}H NMR spectrum of **150** (Fig. 4.6) revealed resonances for both moieties in a 1:1 ratio, key being the disappearance of an alkyne proton at δ_H 2.42. The ^{13}C NMR spectrum of **150** returned the correct number of resonances, i.e. 30 and was assigned using 2-D techniques such as HSQC and HMBC.

In anticipation of a second Sonogashira coupling of the end of the spacer (in **150**) to 5'-*O*-benzoyl-5-iodo-d4U **60**, the two-step conversion developed previously was necessary as depicted in Scheme 4.5. Thus, the hydroxyl group of **150** was converted to its tosylate **165** in 93% yield by reacting it with *p*-toluenesulfonyl chloride in the presence of triethylamine and a catalytic amount of DMAP in dichloromethane. The ^{1}H NMR spectrum of **165** displayed aromatic protons with AB coupling (J_{AB} = 8.6 Hz) resonating at δ_H 7.45 and δ_H 7.62 as well as a methyl singlet at δ_H 2.08. The presence of additional aromatic signals in the ^{13}C NMR spectrum further confirmed the presence of a tosylate group.

Substitution of tosylate **165** was accomplished in the presence of sodium hydride and a large excess of propargyl alcohol in THF at reflux as described for the UC-781 work. Aqueous work-up followed by purification by column chromatography furnished the alkyne **149** in 86% yield. The ^{1}H NMR spectrum of **149** displayed the characteristic alkyne signal at δ_H 2.42, while its ^{13}C NMR spectrum displayed signals for the alkyne carbons at δ_C 79.7 for C-17'' and δ_C 74.4 for C-18''.

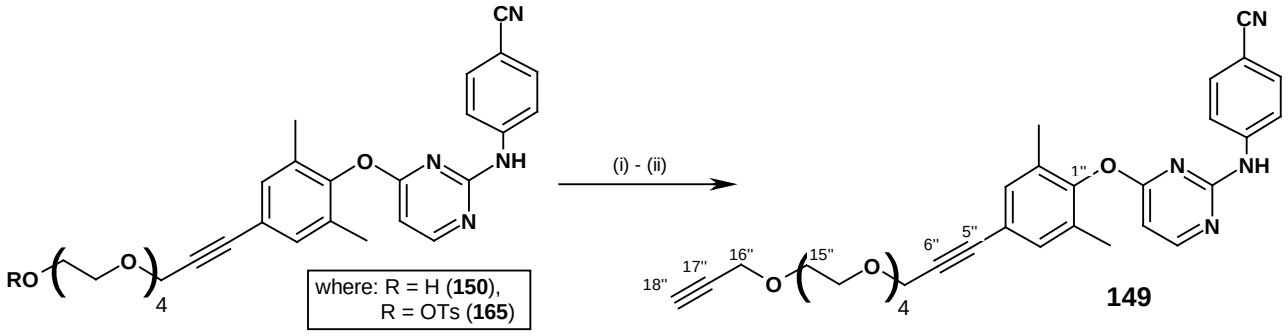

Scheme 4.5 *Reagents and conditions:* (i) *p*-TsCl, NEt_3, CH_2Cl_2, DMAP (cat) (93%); (ii) propargyl alcohol, NaH, THF, Δ (86%).

From a SAR point of view, the C-4 aromatic ring attached to the pyrimidine still needed to be extended from the meta-position. It was expected that such a derivative would have little to no biological activity, but this exploration would definitely validate the molecular modeling studies carried out at the onset of this part of the project. To this end, commercially available tetraethylene glycol **164** was mono-protected as its monobenzyl ether **166** in 39% yield with benzyl bromide and sodium hydride in THF after column chromatography (Scheme 4.6). The presence of a benzyl group in the product was confirmed by the ^{1}H NMR spectrum of **166**, which

revealed aromatic protons integrating for 5 protons resonating at δ_H 7.34 as well as methylene protons resonating at δ_H 4.56. The ^{13}C NMR spectrum displayed a methylene carbon at δ_C 73.1.
Treatment of alcohol **166** with carbon tetrabromide in dichloromethane (Scheme 4.6) rendered the bromide **167** in 95% yield. Work-up involved evaporating the solvent and purifying the crude product directly by column chromatography. The ^{1}H NMR spectrum of bromide **167** revealed the absence of a hydroxyl proton at δ_H 2.80, while its ^{13}C NMR spectrum revealed an upfield shift of the carbon at C-1 from δ_C 61.6 in alcohol **166** to δ_C 30.2, thus confirming that substitution by bromine had taken place.

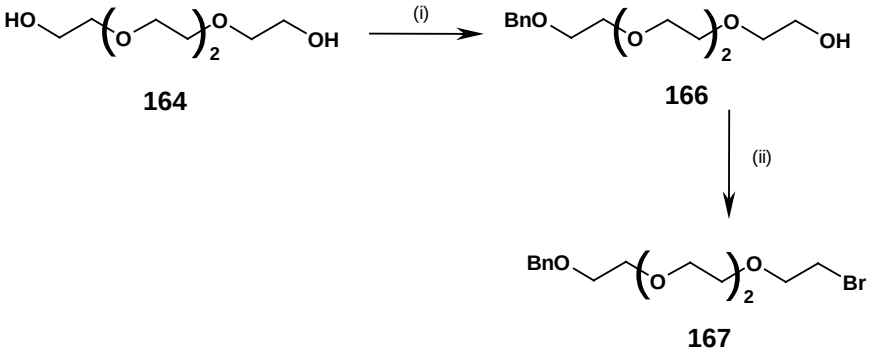

164 **166** **167**

Scheme 4.6 *Reagents and conditions:* (i) BnBr, NaH, THF, reflux, 20 hrs (39%); (ii) PPh_3, CBr_4, CH_2Cl_2, 0 ^oC, 30 min (88%).

The next step (Scheme 4.7) involved coupling of pyrimidine **154** to arylamine **119b** (prepared previously - see Chapter 3) using *p*-toluenesulfonic acid in 1,4-dioxane at 100^{o}C to yield DAPY **168** quantitatively. The ^{1}H NMR spectrum of **168** displayed the appearance of two independent NH signals at δ_H 9.43 and δ_H 10.02, as well as an OH singlet at δ_H 9.66. Finally, a correct HRMS evaluation (*m/z* HRMS (ES) 337.0738 [M^+], $C_{17}H_{12}N_5OCl$ requires *m/z* 337.0738 [M^+]), confirmed the structure of **168**.
Subsequent nucleophilic substitution of the bromide **167** by DAPY intermediate **168** was achieved using potassium carbonate as a base in acetonitrile at 50 ^{o}C to afford the desired compound **169** in 100% isolated yield. The ^{1}H NMR spectrum of **169** revealed a downfield shift of the protons α to bromine at δ_H 3.45 for the bromide **167** to δ_H 4.10 in **169** as a result of the deshielding effect of the phenoxy group, as well as the presence of signals for the phenolic moiety, thus confirming that the alkylation had occurred.
Catalytic hydrogenation of **169** (Scheme 4.7) using palladium-on-carbon catalyst in ethanol and THF furnished **170** in 70% yield as a more polar spot on TLC. The appearance of a hydroxyl proton as a broad singlet resonating at δ_H 3.04 and the absence of the characteristic benzylic

methylene singlet at δ_H 4.45 for **169** provided sufficient evidence that debenzylation had taken place.

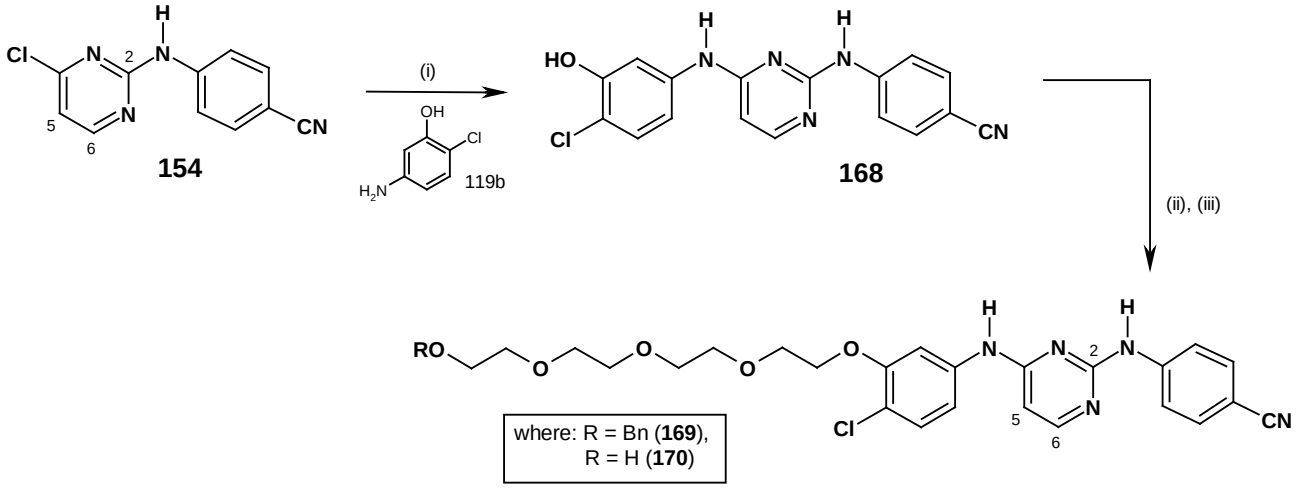

Scheme 4.7 *Reagents and conditions:* (i) **119b**, *p*-TsOH, 1,4-dioxane, 100 ^oC (100%); (ii) **167**, K_2CO_3, CH_3CN, 50 ^oC (100%); (iii) H_2, Pd/C, EtOH/THF (1:1), r.t (30%).

4.4.2 Sonogashira coupling and final deprotection

For bifunctional generation, the elongated TMC120-derivative **149** (see Figure 4.5) was subjected to a Sonogashira reaction with 5'-*O*-benzoyl-5-iodo-d4U **60**, under similar conditions as described before (Scheme 4.8). The coupling afforded **171** in 59% yield. The ^1H NMR spectrum data for **171** revealed signals for both the alkynyl **149** and d4U moieties in the ratio of 1:1. A successful coupling was further confirmed by the absence of a terminal alkyne proton at around δ_H 2.42. The ^{13}C NMR spectrum of **171** displayed diagnostic resonances at δ_C 143.6 (C-12), 90.6 (C-5), 59.0 (C-15) thus confirming the presence of both the nucleoside and the alkyne. The structure was further analyzed by 2D NMR in a satisfactory manner (see experimental for assignments).

Finally, **171** was deprotected with sodium methoxide in methanol to furnish **147** in 94% yield following neutralization with a few drops of acetic acid, evaporation of methanol and direct flash chromatography using DCM/MeOH (95:5). The ^1H NMR spectrum of **147** (Fig. 4.7) revealed resonances for both inhibitors, notably the d4U double bond signals and the H-12 uracil singlet at δ_H 8.34, as well as a characteristic set of aromatic and heteroaromatic signals for the DAPY unit. Its ^{13}C spectrum returned the correct number of singlets (42) and 2D-NMR techniques (HSQC, HMBC) were utilized to make a full structural assignment. Finally, a correct HRMS evaluation (*m/z* HRMS (EI) 793.3204 $[M+H]^+$, $C_{23}H_{22}N_6O_5SCl$ requires *m/z* 793.3191 $[M+H]^+$), confirmed the structure of **147** as shown in Scheme 4.8.

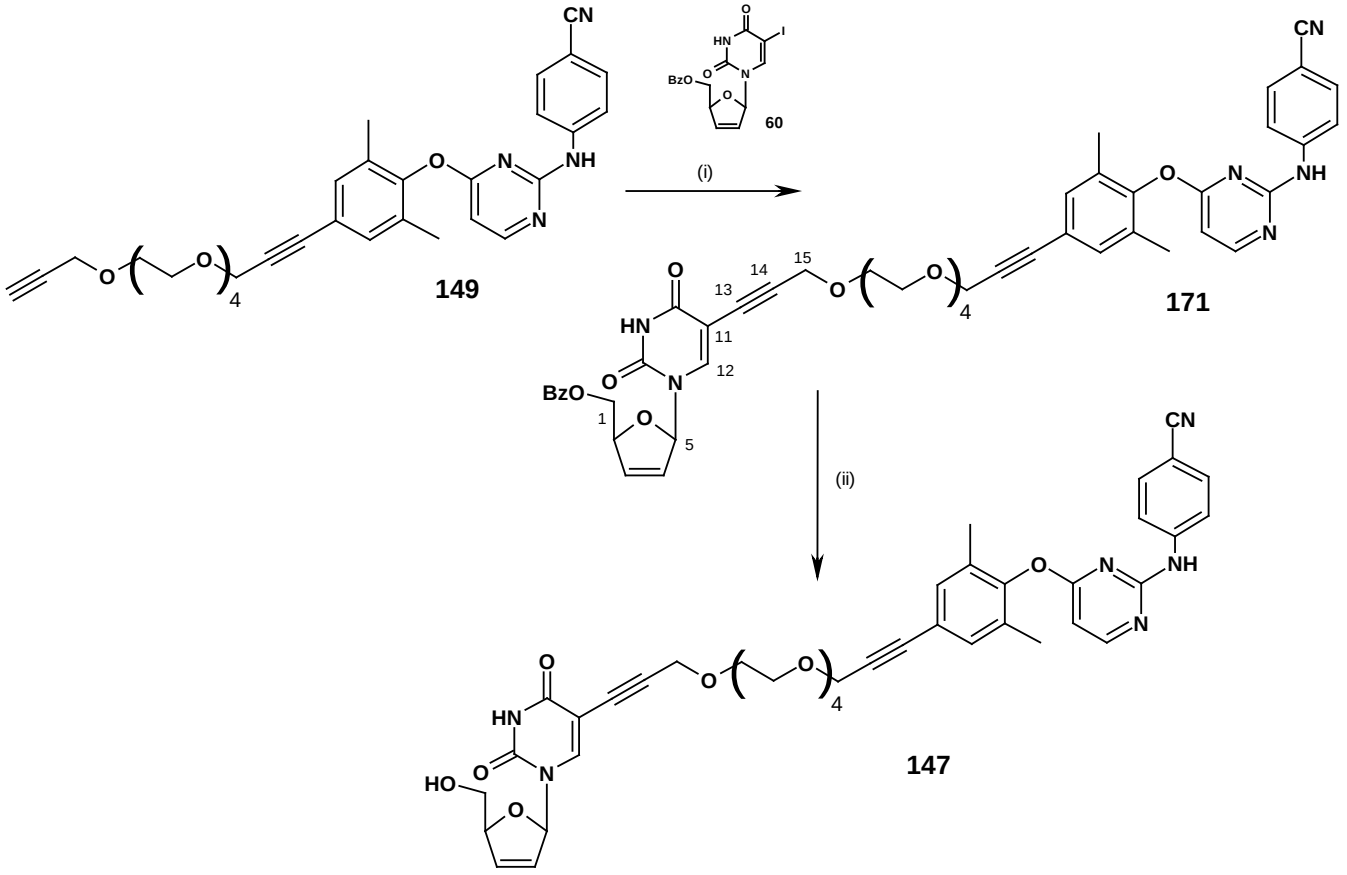

Scheme 4.8 *Reagents and conditions:* (i) 5'-Benzoyl-5-iodo-d4U, $Pd(PPh_3)_4$ (20%), CuI (50%), NEt_3 (3 eq), DMF/THF (1:2), rt, (59%); (ii) NaOMe, MeOH, rt, (94%).

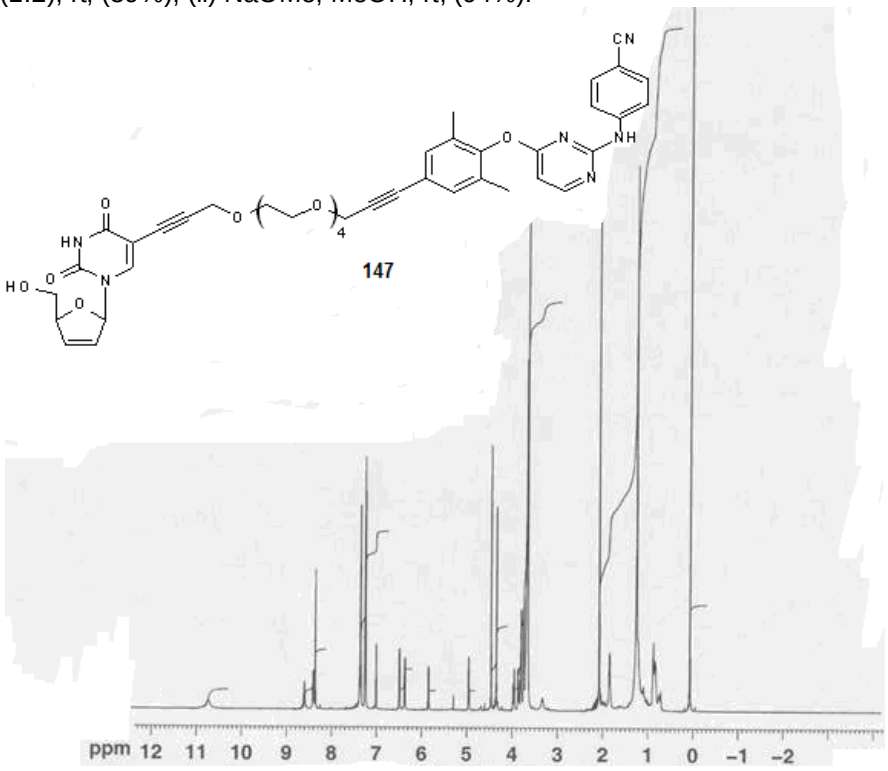

Figure 4.7 ^{1}H NMR spectrum of **147**.

4.4.3 Biological evaluation and SAR interpretation

The inhibition of viral replication in HIV-infected cells of the TMC-derivatives **150** and **170**, as well as bifunctional target **147** was measured against HIV-1 (IIIB) replication in MT-2 cell cultures using an MTT assay (see Appendix I). The results are summarized in Table 4.1 below.

Table 4.1 Anti-HIV results of compounds tested in MT-2 cell cultures using MTT assay.

Compound	*EC_{50} (nM)*	*CC_{50} (nM)*
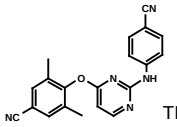 TMC120	2	100
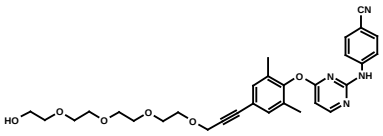 150	20	125
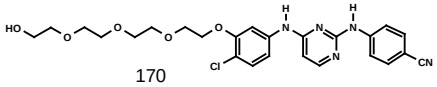 170	inactive	25
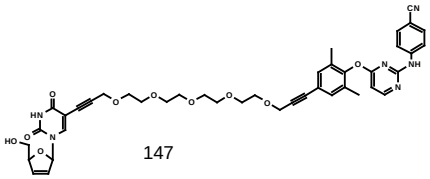 147	100	1200

The results above were fascinating. By probing the effect of the spacer elongation onto the NNRTI (**150**), a 20 nM activity for **150** (as a 10-fold reduction from TMC120) was obtained suggesting that the correct attachment point was chosen. As predicted, no anti-HIV activity was displayed by derivative **170**. This validated the molecular modeling studies and also depicts how extremely sensitive drug-design strategies are to error, i.e. moving from a *para*-elongated system to a *meta*-derivative defines the border between activity and no-activity in this case. The bifunctional **147** gave an impressive 100 nM activity, as a 50-fold reduction from TMC120 in the cell culture assay. Although this was a hugely encouraging result, the activity was still not comparable to that of the individual NNRTI (i.e. TMC120), thus indicating that a truly mixed-site inhibitor was not being realized. At this point, the question of whether the nucleoside was being phosphorylated by cellular kinases presented itself. Therefore, to establish whether the

bifunctional was being 'switched on' for incorporation into the growing DNA chain, it was decided to perform RT enzyme studies on the compounds tested above, as well as synthesize and test a triphosphorylated nucleotide form of **147**.

4.4.4 Triphosphate generation

In 1989, Eckstein[195] reported a four-step protocol for effective triphosphorylation of the 5'-hydroxyl group of a nucleoside. His procedure involved formation of a triethylammonium triphosphate salt which was useful as a water soluble metabolite required for cell-culture testing. Thus, subsequent treatment of nucleoside **147** (Scheme 4.9) with 2-chloro-1,3,2-benzodioxaphosphorin-4-one, pyridine and DMF at 0 ^{o}C DMF, followed by bis(tributylammonium) pyrophosphate, iodine and TEAB yielded triphosphate **148** in 37% yield after chromatography on a Sephadex ion-exchange (DEAE) column using aq. TEAB (triethylammonium bicarbonate) as the mobile phase. The bifunctional triphosphate eluted at around 0.6 M. TLC's were evaluated on amine-impregnated silica-gel plates using TEAB/MeOH = 3.5/6.5). The reaction proceeds *via* formation of a mixed phosphite, which is substituted by pyrophosphate and oxidized (at phosphorus one) by iodine.

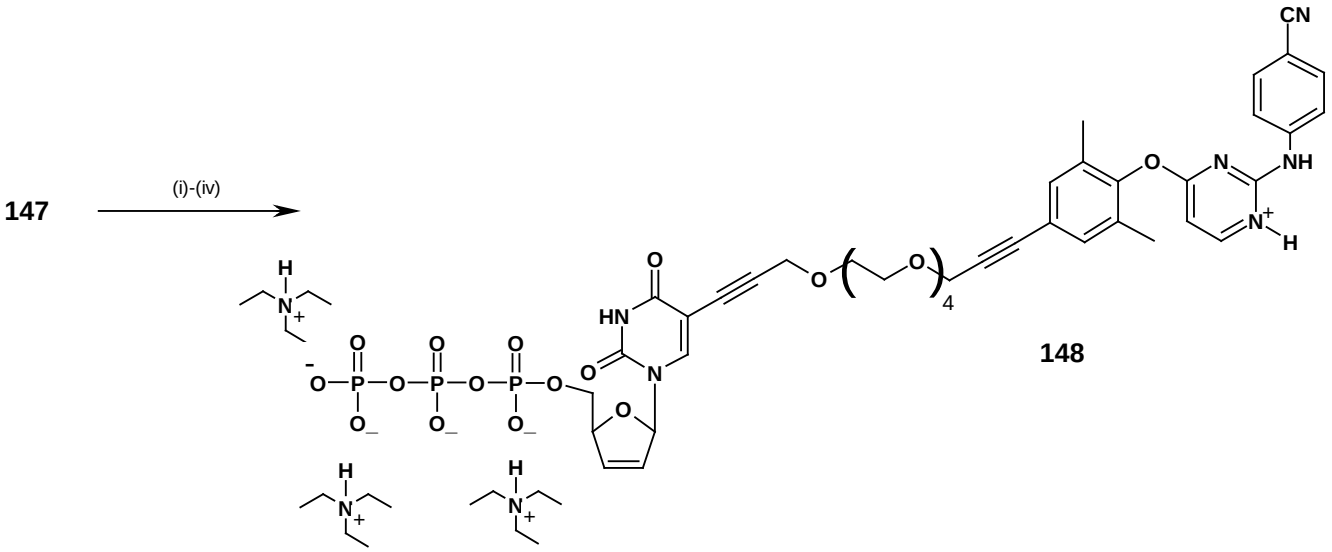

Scheme 4.9 *Reagents and conditions:* (i) 2-Chloro-1,3,2-benzodioxaphosphorin-4-one, pyr, DMF, 0 ^{o}C-r.t; (ii) bis(tributylammonium) pyrophosphate, NEt_3, DMF; (iii) I_2, pyr/H_2O; (iv) TEAB, DMF/THF, r.t (37% over 4 steps).

The bifunctional [d4U-TP]-propyne-4-PEG-propyne-[TMC120] **148** was further analyzed by high-pressure liquid chromatography (HPLC) on a DNA Pac PA-100 analytical column (Dionex, Sunnyvale, CA) using the following conditions: mobile phase A, 0.05 M triethylammonium bicarbonate (TEAB), pH 8.0; mobile phase B, 0.5 M TEAB, pH 8.0. Mobile phase flow rate was 1 mL / min using a gradient of 100% A to 50% A/50% B for ten minutes and then to 100% B for

five minutes. The mobile phase flow rate was 1 mL / min using a gradient of 100% A to 50% A / 50% B for ten minutes and then to 100% B for five minutes. Absorbance was measured at 260 nm. The HPLC trace is presented in Figure 4.8, displaying purity in the appearance of a single peak with a retention time of 22 min under these conditions.

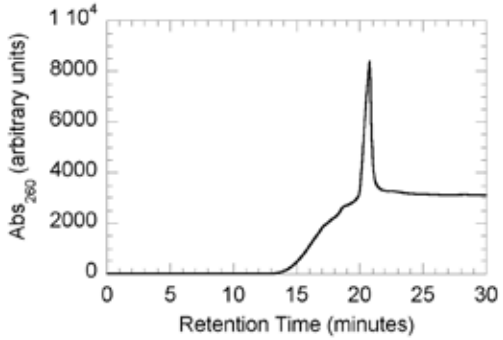

Figure 4.8 HPLC trace of [d4U-TP]-4PEG-[TMC120] **148**.

The ^{1}H NMR spectrum of **148** revealed the absence of an OH signal at δ_H 3.48 and the appearance of 27 protons resonating at δ_H 1.25 for the three triethylammonium moieties. The fourth cation for the triphosphate is presumably provided by a protonated pyrimidinium ion. Its ^{13}C NMR spectrum further supported TP incorporation in **148** with peaks at δ_C 9.1 and δ_C 47.2 for the triethylammonium moieties. However, clear-cut evidence was provided in the ^{31}P NMR spectrum of **148** (Fig. 4.9), displaying the necessary two-doublet / triplet set of signals resonating at δ_P -8.9 (d, *J* = 20.2 Hz), δ_P -9.8 (d, *J* = 20.2 Hz) and δ_P -22.1 (t, *J* = 20.2 Hz) for the two terminal phosphates and central one respectively. Finally, a correct HRMS evaluation (*m/z* HRMS (EI) 1031.2035 $[M+H]^+$, $C_{42}H_{48}N_6O_{19}P_3$ requires *m/z* 1031.2036 $[M+H]^+$), confirmed the structure of **148** as a triphosphoric acid.

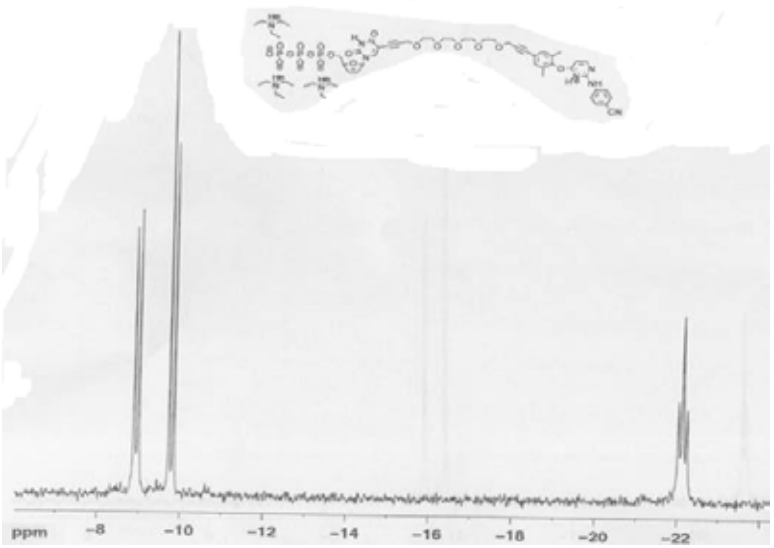

Figure 4.9 ^{31}P NMR of [d4U-TP]-propyne-4-PEG-propyne-[TMC120] **148**.

4.4.5 Biological evaluation and SAR interpretation

For the *in vitro* RT inhibition assays, dTTP and dGTP were purchased from GE Biosciences. Oligonucleotide primers and template were synthesized at the Keck Facility at Yale University and were purified using 20% denaturing gel-electrophoresis. The DNA primer template used in this study was as follows: D23 (5'-TCA GGT CCC TGT TCG GGC GCC AC -3'), D24 (5'-TCA GGT CCC TGT TCG GGC GCC ACT-3') for the primer, and D36 (5'-TCT CTA GCA GTG GCG CCC GAA CAG GGA CCT GAA AGC-3') for the template. Labeling and annealing of primer/templates were performed as described by Anderson.[196]

Expression and Purification of HIV-1 RT. C-terminal histidine tagged heterodimeric p66/p51 wild-type HIV-1 RT was expressed and purified as described previously[197] using a clone generously provided by Stephen Hughes, Paul Boyer, and Andrea Ferris (Fredrick Cancer Research and Development Center, Fredrick, MD).

IC_{50} determination. 8 nM RT (active sites based on pre-steady state active site determination) was pre-incubated for at least 15 minutes with 1 μM 5'-labeled primer/template prior to mixing with appropriate concentrations of inhibitor and allowed to incubate for a minimum of 15 additional minutes on ice. DMSO concentrations were kept constant at less than 2%. DMSO alone was added as a no inhibitor control for each set of experiments. Reactions were initiated with the addition of 5 μM dNTP and 10 mM $MgCl_2$ and were quenched after 15 minutes at 37° C with 0.3 M EDTA. All concentrations represent final concentrations after mixing. Reaction products were subjected to 20% denaturing polyacrylamide gel-electrophoresis and quantitated on a Bio-Rad Molecular Imager FX. Product formation was plotted as a function of inhibitor concentration and fitted to a hyperbola to generate IC_{50} curves. IC_{50} values are defined as the concentration of inhibitor that inhibits steady-state single nucleotide incorporation by 50%.

Incorporation Assays. Incorporation experiments were performed under single turnover conditions; 50 μM d4U-TP-4PEG-TMC and 10 mM $MgCl_2$ were mixed with 250 nM RT (active sites) and 50 nM 5'-labeled primer/template to initiate the reaction. Negative controls were performed under identical conditions without $MgCl_2$. The reaction was allowed to proceed for 30 minutes at 37° C, after which the reaction was quenched with 0.3 M EDTA. Reaction products were subjected to 20% denaturing polyacrylamide gel- electrophoresis and analyzed on a Bio-Rad Molecular Imager FX.

The results are summarized in Table 4.2.

Table 4.2 Anti-HIV results of compounds tested in the RT enzyme assay vs cell-culture results.

Compound	*IC_{50} (nM)*	*EC_{50} (nM)*
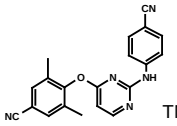 TMC120	9 ± 3	2
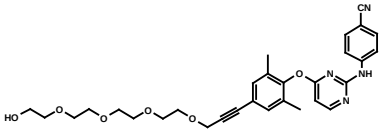 150	56 ± 6	20
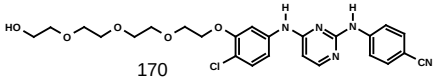 170	inactive	inactive
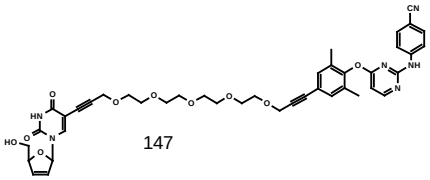 147	14 ± 2 18 ± 3	100
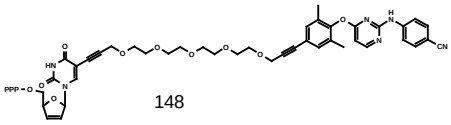 148	3 ± 2	not applicable

The RT inhibition assay involved measuring the interference of dTTP uptake into the DNA primer of the primer/template (both short DNA strands) as catalysed by RT, by competing uptake of the inhibitor, i.e. the nucleoside portion of the bifunctional entity. DNA products were quantified using gel-electrophoresis. Quite interestingly, the results revealed a drop in activity for TMC120 and compound **150** compared to the cell-culture assay. As suspected, no anti-HIV activity was displayed by derivative **170**. Impressively, though, a 14 nM activity was obtained for bifunctional **147** in the enzyme assay, compared to the 100 nM activity in the cell-culture assay (Table 4.1). The higher activity of the free bifunctional nucleoside **147** *in vitro* over cell-culture, was credited to the instability of **147** in cell-culture as well as permeability issues. The low IC_{50} (close to that of the NNRTI) *in vitro* suggests some level of mixed-site interaction, possibly involving H-bonding at the substrate site. Most significant, however, was that triphosphate **148** returned an outstanding 3 ± 2 nM activity in the enzyme assay, as a 3-fold increase in activity compared to

TMC120. This finally offered us a proof of principle of the existing synergy between the active site and the NNRTI-BP. However, proof beyond doubt would require an X-ray crystal structure, which has been elusive up till now.

It was now important to validate the incorporation of **148** into the primer. To this end, the incorporation of triphosphate **148** into the primer strand of a D23/D36 (correct base-pairing) primer/template was studied, as well as the incorporation into a D24/D36 (mismatch base-pairing) primer/template as schematically represented in Figure 4.10. In theory, triphosphate **148** was expected to be better recognized in the D23/D36 case than the mismatch case. This is because the nucleotide portion of the bifunctional **148**, resembling a C-5 elongated thymidine-triphosphate, was expected to compete better against dTTP uptake (with an A coding in the template strand) than against dGTP uptake in the mismatch experiment where a C in the template demands a G uptake in the primer.

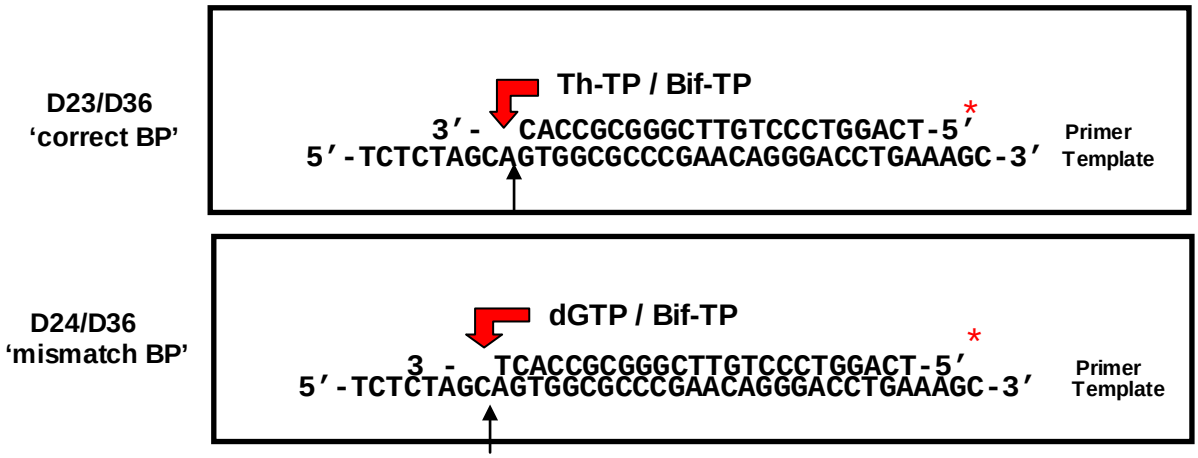

Figure 4.10 Schematic representation of correct vs mismatch base-pairing experiments for **148**.

Pleasingly a polyacrylamide gel-electrophoresis revealed excellent incorporation of triphosphate **148** into the D23 primer of the D23/D36 BP experiment (Figure 4.11).

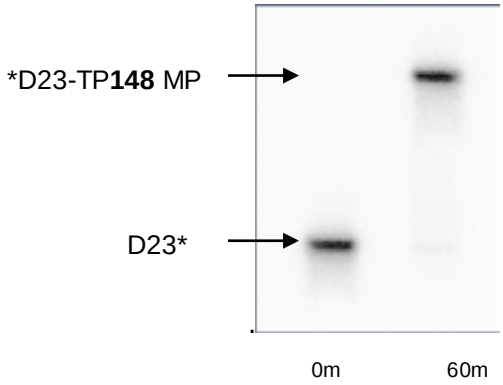

Figure 4.11 Bifunctional TP **148** incorporation as shown in a gel-electrophoresis experiment.

The huge increment by which the D23-TP**148** monophosphate (MP) band shifts relative to the D23 primer can be attributed to the increase in size of the DNA fragment now coupled to a large bifunctional entity.

The *in-vitro* RT results for the correct and mismatch BP assay are summarized in Table 4.3. The results revealed that all the compounds listed in Table 4.3 showed better activity for the 'correct BP' compared to the 'mismatch BP' assay. Most importantly, the activity of triphosphate **148** (38.1 nM) was effectively the same for the mismatch experiment as the free bifunctional nucleoside **147** (35.0 nM), providing compelling evidence that the nucleotide of bifunctional **148** in the matched experiment is getting incorporated, with a remarkable 1.7 nM activity. The fact that nucleotides only inhibit at low µM concentration and that the bifunctional nucleotide-TP **148** returned a lower nM activity IC_{50} than the NNRTI alone (5.2 nM), provides convincing evidence for *in vitro* synergy in a mixed-site fashion.

Table 4.3 Correct vs mismatch BP results for *in vitro* RT assay

Compound	**IC_{50} (nM) Correct BP (D23/D36)**	**IC_{50} (nM) Mismatch BP (D24/D36)**
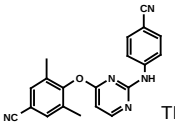 TMC120	5.2 ± 3.3	17.3 ± 11.2
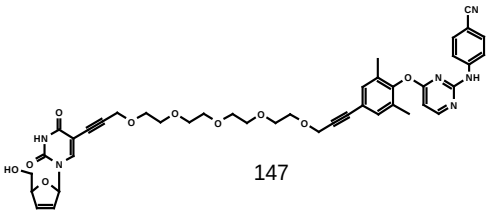 147	15.4 ± 3.6	35.0 ± 9.1
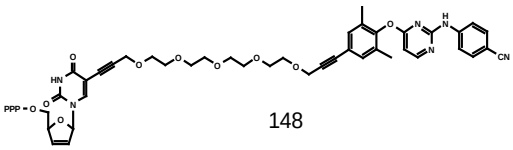 148	1.7 ± 1.0	38.1 ± 6.8

Although the inhibition results of the bifunctionals **147** and **148** were hugely encouraging, the overall conclusion was that the lower activity of the bifunctional **147** compared to TMC120 in cell-culture (50-times less active) implied a lack of *in vitro* phosphorylation. Therefore, it was decided to replace d4U by a phosphonate NRTI-prodrug in order to bring in a pronucleotide approach.

4.5 Synthesis of [ANP]-propyne-*n*-PEG-propyne-[TMC120]: where n = 4 and 6

A major feature of design of the bifunctional inhibitors described up to date was the incorporation of the rigid, non-flexible d4U as the NRTI portion of the heterodimer. The overall free energy demand on binding such a large non-cleavable entity could be somewhat attenuated with the aid of a more flexible inhibitor. For this reason, it was decided to change d4U to an acyclic nucleotide phosphonate (ANP). The prodrug would incorporate a phosphonate entity and this would circumvent the first intracellular kinase phosphorylation step increasing the likelihood of activation to the active 5'-triphosphate metabolite.

The ANP model chosen had uracil as its Watson-Crick base pair as opposed to cytosine used in the clinically approved cidofovir ANP. This choice of ANP was mainly influenced by having available the uracil chemistry required for the synthesis as well as the fact that 5'-fluorouracil acyclic nucleotide was known to be active with an EC_{50} of 34 μM (Fig. 4.12).[198-200] The uracil acyclic nucleotide was chosen as a prototype phosphonate that was considered relatively simple to synthesize under the time constraints. Its main objective was to study how such an entity might respond biologically, before embarking on a more elaborate tenofovir or cidofovir ANP synthesis.

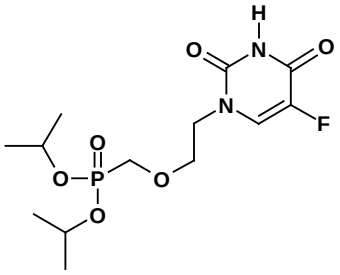

Figure 4.12 Known 5'-fluoro uracil acyclic nucleotide.

4.5.1 Retrosynthetic analysis of [ANP]-propyne-*n*-PEG-propyne-[TMC120]

Synthesis of the ANP incorporated bifunctionals **172** and **173** were envisaged as being achievable *via* a convergent Sonogashira coupling of elongated TMC-derivatives **149** (or **174**) and pyrimidine-tethered phosphonate **175b** (Fig. 4.13). Phosphonate **175b** would be generated from CAN iodination of **175a,** which in turn would be prepared from ^{1}N-alkylation of unprotected uracil to a modified two carbon tethered phosphonate of type **A**. The latter was envisaged as available *via* alkylation of protected alcohol **140** by phosphonate **176**. Known chemistry in the form of the Pudovik reaction would be employed for the synthesis of **176**. This new strategy was proposed on the back of the more divergent approach used in Chapter 3 for ANP formation.

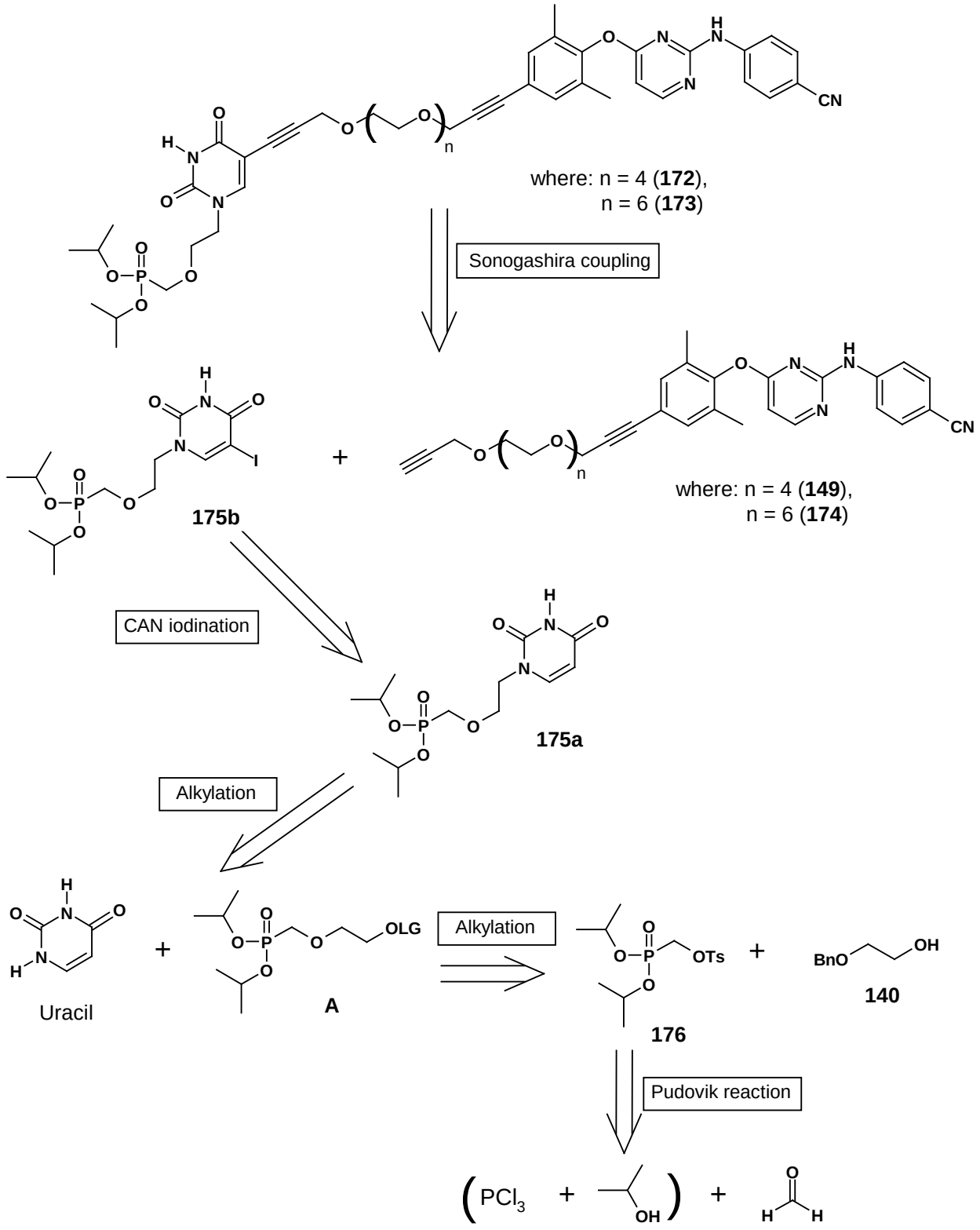

Figure 4.13 Retrosynthetic analysis of ANP incorporated bifunctionals **172** and **173**.

4.5.2 Synthesis of the ANP moiety

The synthesis towards 5-iodo-ANP **175b** began with large-scale (10 g) esterification of phosphorus trichloride with three equivalents of isopropanol (IPA) using two equivalents of sodium hydride in THF as outlined in a publication in 2004 by Fakhraian and co-workers[201] (Scheme 4.10). Diisopropyl hydrogen phosphonate **177** (DAHP) was isolated in 98% yield after an aqueous work-up using ammonium chloride and evaporation of solvent, without the need of any column chromatography. It was judged by ^{1}H NMR spectroscopy to be pure enough for taking to the next step without purification. The mechanism of the reaction (Fig. 4.14) reveals the importance of only adding two equivalents of base. Three equivalents of HCl are produced during the course of the reaction (step 1), of which only two equivalents can be mopped up by the base. The remaining equivalent of HCl is used in the protonation of the phosphorus of the trialkylphosphite, which rearranges to the more stable pentavalent phosphorus in the form of the desired dialkyl hydrogen phosphonate (DAHP) *via* an Arbuzov-type dealkylation. In the case of adding three equivalents of base, no DAHP is produced, but only the phosphite. The reaction can also be performed under base-free conditions, but this means having to neutralize large quantities of HCl in the work-up. The ^{1}H NMR spectrum of **177** revealed the characteristically large P-H coupling for the hydrogen attached to phosphorus at δ_H 6.77 (1H, d, J_{HP} = 687.0 Hz) proving a phosphonate structure rather than a hydroxyphosphite isomer.

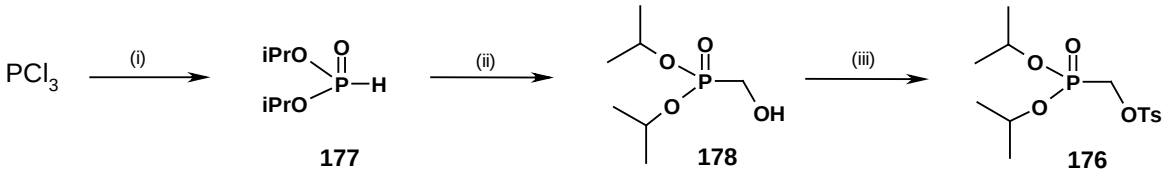

Scheme 4.10 *Reagents and conditions:* (i) IPA (3eq), NaH (2eq), THF, r.t (98%); (ii) $(H_2CO)_n$, K_2CO_3, IPA, 60 ^oC (98%); (iii) *p*-TsCl, NEt_3, CH_2Cl_2, DMAP (cat), r.t (92%).

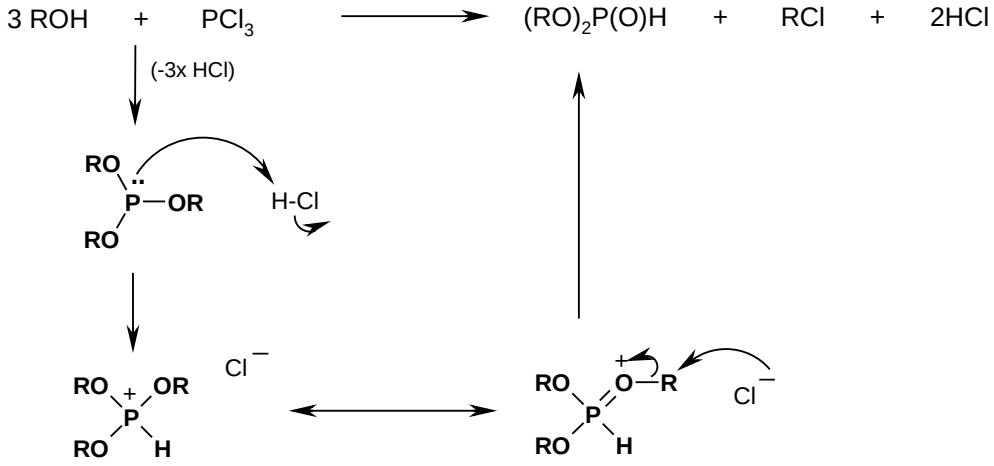

Figure 4.14 Mechanism pathway proposed for production of DAHP.[201]

The diisopropyl α-hydroxymethylphosphonate **178** was synthesized by reacting **177** with paraformaldehyde and anhydrous potassium carbonate as a catalyst in IPA at 60 °C, in a reaction better known as the Pudovik reaction (Fig. 4.15).[202] Carbonates are commonly used in heterogeneous phase as a non-nucleophilic solid 'soft' base because they are easy to handle and to eliminate by filtration at the end of the reaction. Therefore, the α-hydroxymethylphosphonate **178** was isolated in 98% yield without the need for silica-gel chromatography.

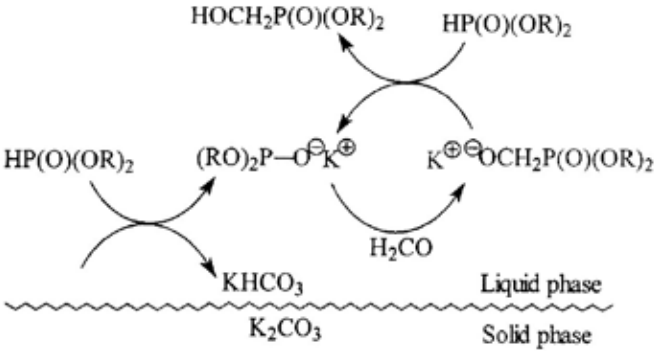

Figure 4.15 Proposed mechanism of the Pudovik reaction in heterogeneous conditions.[202]

The ^{1}H NMR spectrum of **178** revealed a diagnostic OH singlet at δ_H 2.15, as well as a methylene signal at δ_H 3.82 (2H, d, J_{HP} = 6.6 Hz, CH_2P). Its ^{31}P NMR spectrum displayed a characteristic signal at δ_P 22.9, exactly as reported in the literature.[202]

Subsequent tosylation of alcohol **178** (Scheme 4.10) using *p*-toluenesulfonyl chloride in the presence of triethylamine and a catalytic amount of DMAP in dichloromethane, returned the desired tosylate **176** uneventfully in 92% yield after column chromatography. The ^{1}H NMR spectrum of **176** displayed aromatic protons with AB coupling (J_{AB} = 8.0 Hz) resonating at δ_H 7.36 and δ_H 7.80 as well as a methyl singlet at δ_H 2.46. The presence of additional aromatic signals in the ^{13}C NMR spectrum further confirmed the presence of a tosylate group.

With **176** now in hand, our next challenge was to incorporate a two carbon tether (Scheme 4.11). This was accomplished through the use of mono-benzyl ether **140** and sodium hydride in THF at reflux, to obtain tethered phosphonate **179** in 72% yield after column purification. The ^{1}H NMR spectrum of **179** revealed an upfield shift of methylene protons α to phosporus at δ_H 4.12 (d, J_{HP} = 10.0 Hz, CH_2P) for the tosylate **176** to δ_H 3.82 in **179**, as well as the presence of the benzylic methylene protons at δ_H 4.54. Its ^{31}P NMR spectrum returned a single peak at δ_H 19.7. Finally, a correct HRMS evaluation (*m/z* HRMS (ES) 331.16681 $[M+H]^+$, $C_{16}H_{28}O_5P$ requires *m/z* 331.1674 $[M+H]^+$), confirmed the structure of **179**.

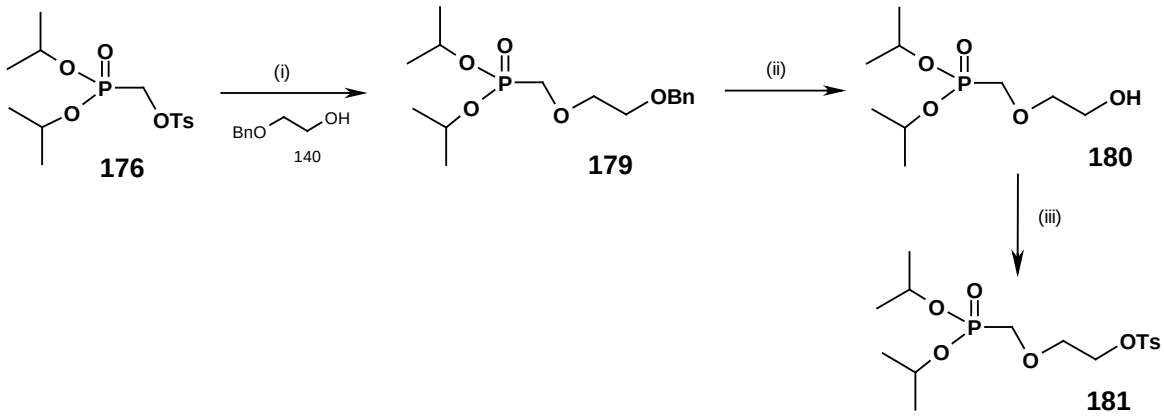

Scheme 4.11 *Reagents and conditions:* (i) **140**, NaH, THF, Δ (72%); (ii) H_2, Pd/C, MeOH:THF (1:1), r.t (77%); (iii) *p*-TsCl, NEt_3, CH_2Cl_2, DMAP (cat), r.t (90%).

Catalytic hydrogenation of **179** using palladium-on-carbon catalyst in methanol/THF (1:1) furnished **180** in 77% yield (Scheme 4.11). The appearance of a hydroxyl proton as a broad singlet resonating at δ_H 2.52 and the absence of the characteristic benzylic methylene singlet at δ_H 4.54 for **180** provided further evidence that debenzylation had taken place.

The hydroxyl group of **180** was subsequently converted to tosylate **181** in 90% yield by reacting it with *p*-toluenesulfonyl chloride in the presence of triethylamine and a catalytic amount of DMAP in dichloromethane (Scheme 4.11). The ^{1}H NMR spectrum of **181** displayed aromatic protons with AB coupling (J_{AB} = 8.3 Hz) resonating at δ_H 7.33 and δ_H 7.78 as well as a methyl singlet at δ_H 2.43. The presence of additional aromatic signals in the ^{13}C NMR spectrum further confirmed the presence of a tosylate group. The ^{31}P NMR spectrum returned a singlet peak at δ_P 18.6 for the phosphonate.

The final part in the synthesis of the ANP involved coupling of the modified tethered phosphonate **181** (Scheme 4.12) *via* ^{1}N-alkylation of uracil and was carried out using cesium carbonate in DMF at 100 ^{o}C. ANP **175a** was isolated following aqueous work-up and purification by column chromatography in a moderate 56% yield. The ^{1}H NMR spectrum of **175a** displayed two doublets at δ_H 5.62 (d, *J* = 7.9 Hz) and δ_H 7.34 (d, *J* = 7.9 Hz) for the H-5 and H-6 protons respectively. An upfield shift of the H-1' signal in the ^{1}H NMR spectrum from δ_H 4.14 in tosylate **181** to δ_H 3.93 in **175a** supported the displacement of the tosylate. The ^{13}C NMR spectrum of compound **175a** displayed signals for the ANP at δ_C 66.1 (d, $J_{C\text{-}P}$ = 168.4 Hz, C-3'), δ_C 48.3 (C-1'), δ_C 101.5 (C-5) and δ_C 145.8 (C-6). Its ^{31}P NMR spectrum displayed the diagnostic phosphonate singlet at δ_P 19.8.

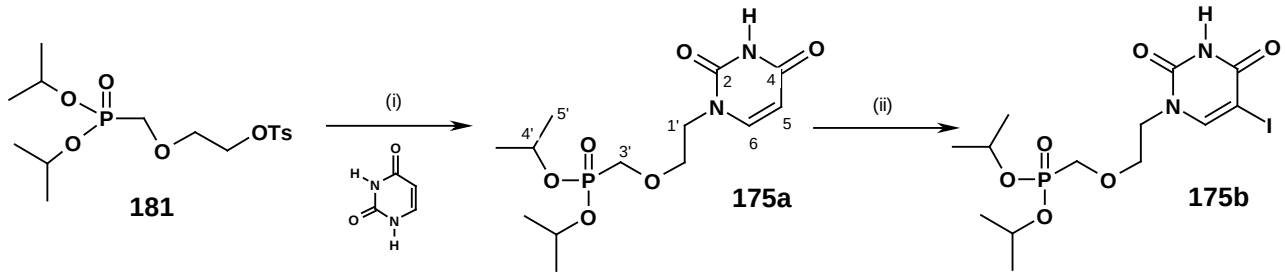

Scheme 4.12 *Reagents and conditions:* (i) Cs_2CO_3, DMF, 100 ^oC (56%); (ii) I_2, CAN, CH_3CN, 35 ^oC, 2 hrs (63%).

Finally, compound **175a** was iodinated (Scheme 4.12) using elemental iodine and cerium ammonium nitrate (IV) at 35 ^oC. TLC confirmed reaction completion after 2 hrs and **175b** was obtained in 63% yield after column chromatography. The ^1H NMR spectrum of **175b** (Fig. 4.16) supported iodination revealing the absence of a doublet at δ_H 5.62 for H-5 and a downfield shift in H-6 from δ_H 7.34 (a doublet) in **175a** to δ_H 8.04 (now a singlet) in **175b**. Its ^{13}C NMR spectrum also displayed a large upfield shift for C-5 from δ_C 101.5 in **175a** to δ_C 67.3 in **175b**. The ^{31}P NMR spectrum of **175b** revealed a singlet at δ_P 20.1. Combustion microanalysis returned favorable data: Found C, 33.71; H, 4.88; N, 6.01; $C_{13}H_{22}N_2O_6PI$ requires C, 33.93; H, 4.82; N, 6.09.

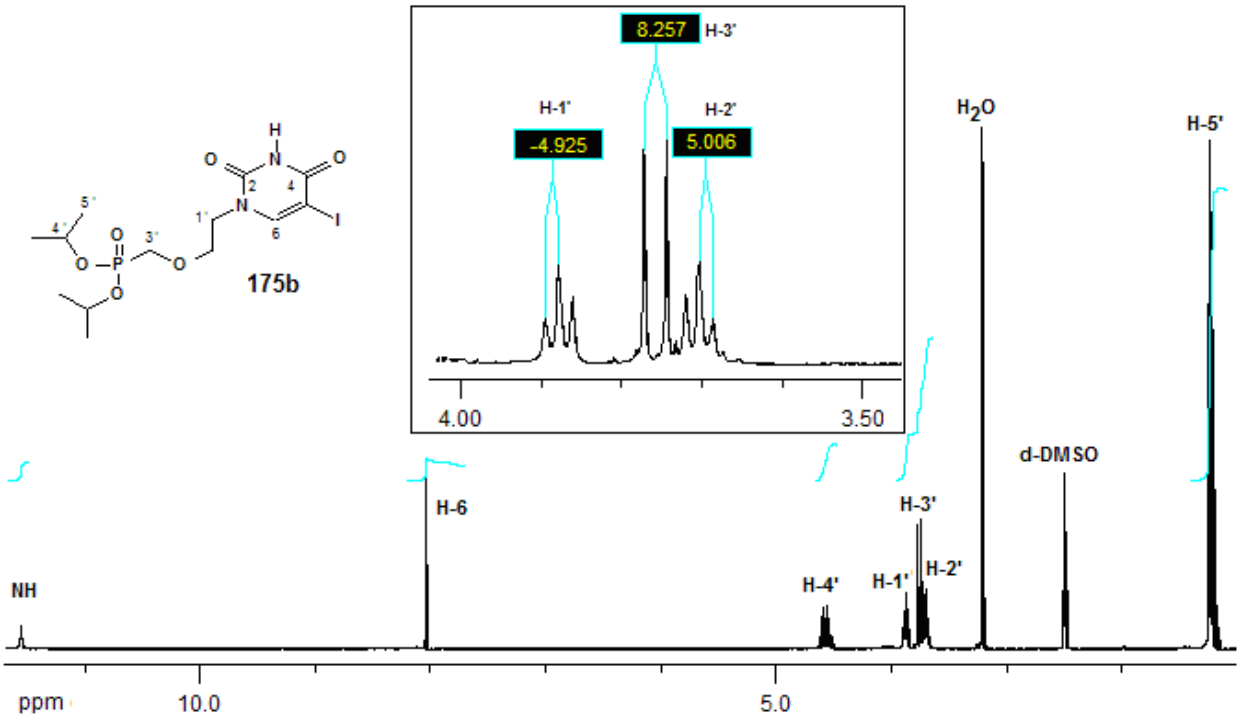

Figure 4.16 ^1H NMR spectrum of 5-iodo-ANP **175b**.

4.5.3 Synthesis of [ANP]-propyne-*tetra*PEG-propyne-[TMC120]

The final reaction carried out in this part of the project was a Sonogashira coupling of a 5-iodo-ANP derivative **175b** to the 4-PEG alkyne **149** (Scheme 4.13).

The standard Sonogashira coupling reaction conditions were used involving adding triethylamine and reactants to a mixture of dimethylformamide and tetrahydrofuran (1:2, v/v), which was thoroughly degassed before addition of catalysts in order to avoid unwanted oxidation of the palladium(0) catalyst. Introduction of the catalyst combination of Pd(0) / CuI in the form of solids resulted in product **172** formation after 3 hrs in 60% yield after column chromatography. Key spectroscopic indicators in the ^{1}H NMR spectra (Fig. 4.17) of **172** were the ANP uracil proton (H-6) at δ_H 7.87, the absence of an alkyne signal at δ_H 2.42 as well as the characteristic aromatic signals for the TMC120 moiety. The ^{13}C NMR spectrum of **172** returned the correct number of resonances of 46. Its ^{31}P NMR spectrum displayed the definitive phosphonate resonance at δ_P 23.2. All carbon resonances could be identified and assigned using 2D-NMR techniques. Finally, a correct HRMS evaluation (*m/z* HRMS (ES) 917.3848 $[M+H]^+$, $C_{46}H_{58}N_6O_{12}P$ requires *m/z* 917.3850 $[M+H]^+$), confirmed the structure of **172**.

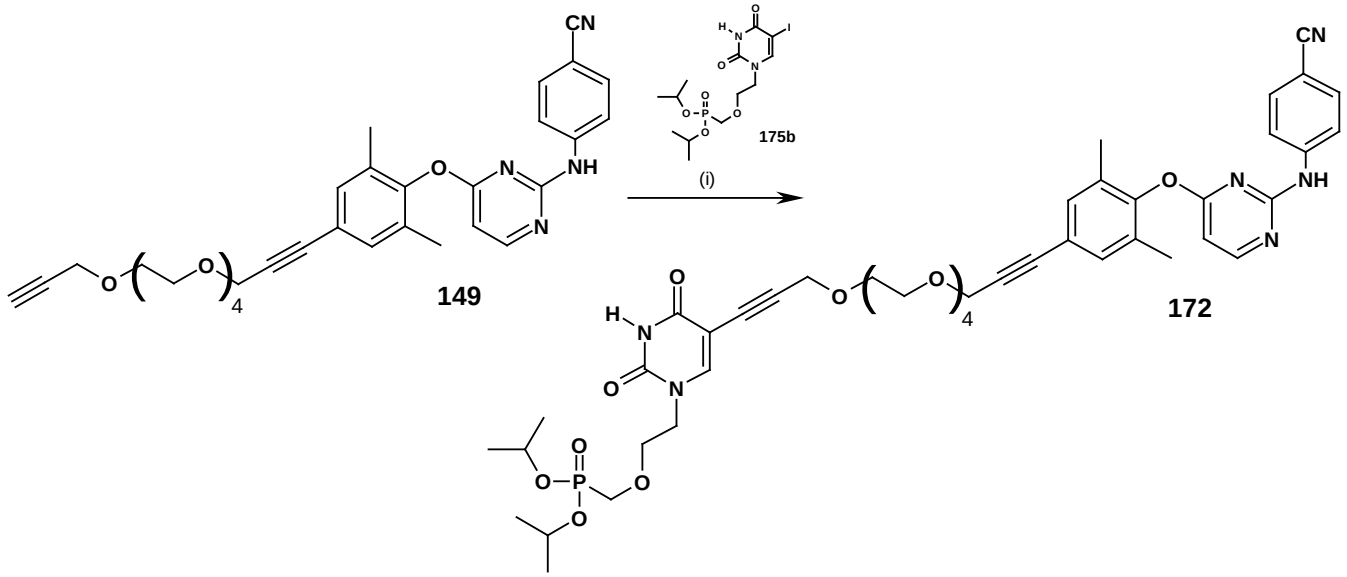

Scheme 4.13 *Reagents and conditions:* (i) 5-iodo-ANP, $Pd(PPh_3)_4$ (10%), CuI (50%), NEt_3 (2 eq), DMF/THF (1:2), rt, (60%).

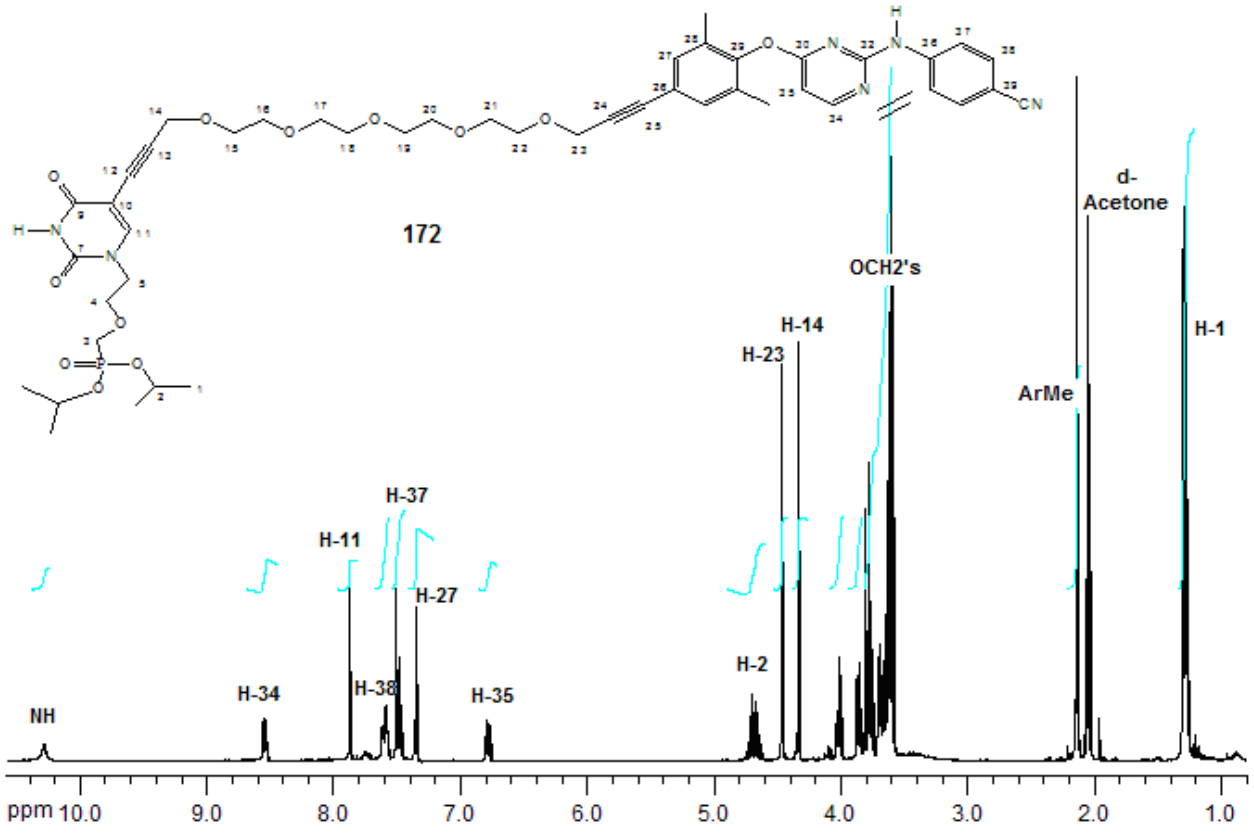

Figure 4.17 ^{1}H NMR spectrum of bifunctional **172**.

4.5.4 Synthesis of [ANP]-propyne-*hexa*PEG-propyne-[TMC120]

The next target chosen was one with a longer spacer (6-PEG) in order to explore SAR. Time constraints precluded making all members of the set so it was decided to go 'longer' than 'shorter', especially in view of the parameters set by the modeling. The overall synthetic scheme for the 6-PEG spacer incorporation is shown in Scheme 4.14, and is identical to that used for the 4-PEG. Thus, propargylation of commercially available hexaethylene glycol **182** was achieved using sodium hydride and propargyl bromide in THF at room temperature in 53% yield after column purification. The ^{1}H NMR spectrum of **183** displayed the key alkyne proton at δ_H 2.43 (t, J = 2.4 Hz). The propargyl methylene signal resonated at δ_H 4.15 (d, J = 2.4 Hz). The ^{13}C NMR spectrum of **183** displayed characteristic alkyne resonances at δ_C 58.2 (C-13), δ_C 74.4 (C-15) and δ_C 79.5 (C-14).

The Sonogashira coupling of TMC-derivative **152** with the 6-PEG alkyne **183**, using identical conditions to that described above, was carried out and the 6-PEG-elongated TMC120 derivative **184** isolated after silica-gel purification in a moderate 46% yield (Scheme 4.14). The ^{1}H NMR spectrum of **184** revealed resonances for both moieties in a 1:1 ratio, key being the

disappearance of an alkyne proton at δ_H 2.43. The ^{13}C NMR spectrum of **184** returned the correct number of resonances, i.e. 34 and was assigned using 2-D techniques such as HSQC and HMBC.

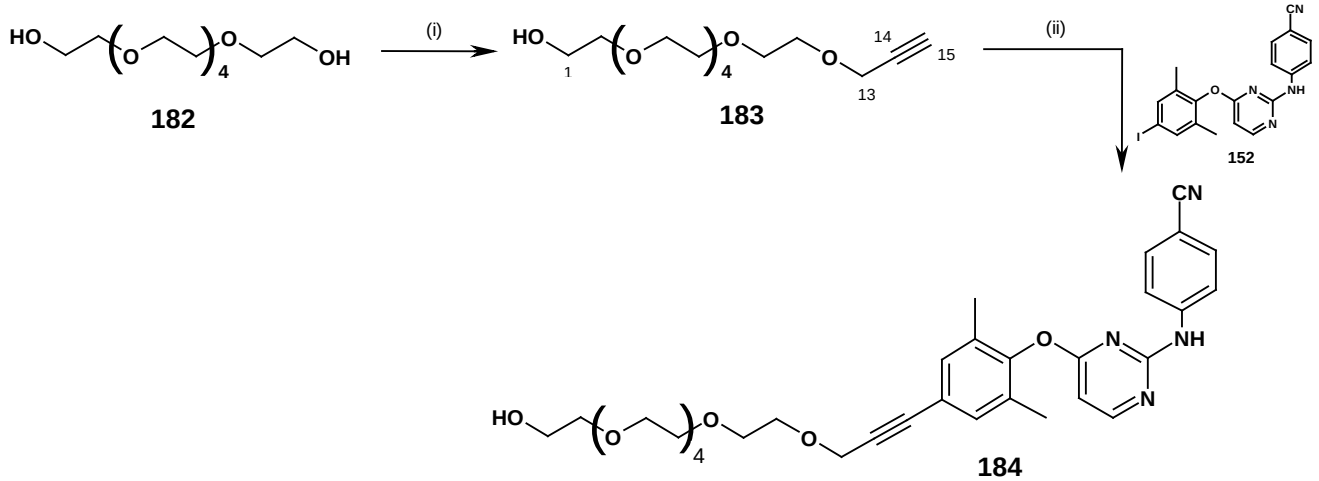

Scheme 4.14 *Reagents and conditions:* (i) propargyl bromide, NaH, THF, r.t (53%); (ii) **152**, $Pd(PPh_3)_4$ (10%), CuI (50%), NEt_3 (2 eq), DMF/THF (1:2), r.t (46%).

In anticipation of a second Sonogashira coupling to the free hydroxyl end of the spacer (in **184**) to 5-iodo-ANP, a two step conversion was necessary depicted in Scheme 4.15. Thus, the hydroxyl group of **184** was converted to the tosylate **185** in 57% yield by reacting it with *p*-toluenesulfonyl chloride in the presence of triethylamine and a catalytic amount of DMAP in dichloromethane. The ^1H NMR spectrum of **185** displayed aromatic protons with AB coupling (J_{AB} = 8.4 Hz) resonating at δ_H 7.46 and δ_H 7.81 as well as a methyl singlet at δ_H 2.45. The presence of additional aromatic signals in the ^{13}C NMR spectrum of **185** further confirmed the presence of a tosylate group.

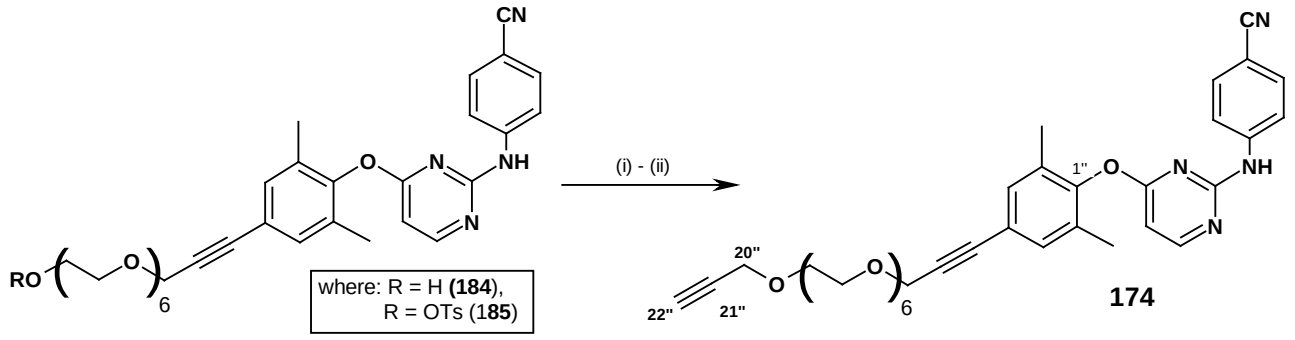

Scheme 4.15 *Reagents and conditions:* (i) *p*-TsCl, NEt_3, CH_2Cl_2, DMAP (cat) (57%); (ii) propargyl alcohol, NaH, THF, Δ (89%).

Alkylation of tosylate **185** was accomplished using sodium hydride and a large excess of propargyl alcohol in THF at reflux. Aqueous work-up followed by purification by column

chromatography furnished the alkyne **174** in 89% yield. The ^{1}H NMR spectrum of **174** displayed the characteristic alkyne signal at δ_H 2.89. The ^{13}C NMR spectrum of **174** displayed signals for the alkyne carbons at δ_C 80.2 for C-22'' and δ_C 75.1 for C-21''.

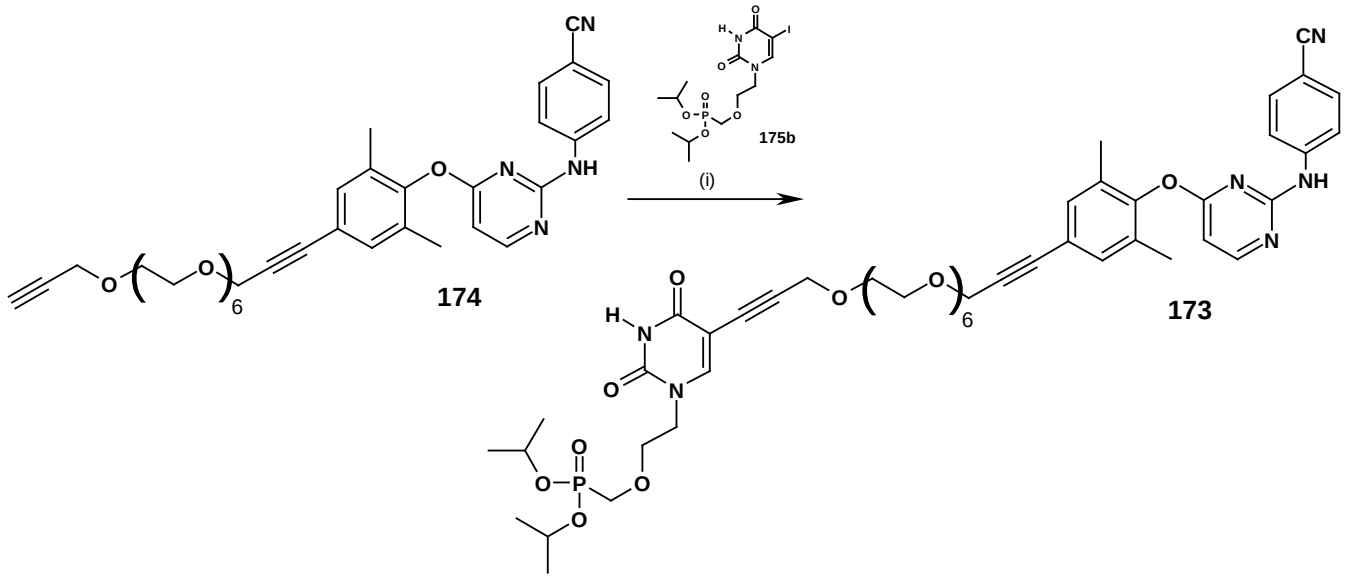

Scheme 4.16 *Reagents and conditions:* (i) 5-iodo-ANP, $Pd(PPh_3)_4$ (10%), CuI (50%), NEt_3 (2 eq), DMF/THF (1:2), rt, (70%).

Once again, a Sonogashira reaction was carried out to secure the synthesis of the double-drug. To this end, alkyne **174** was subjected to a Sonogashira reaction with the nucleotide reverse transcriptase inhibitor derivative, 5-iodo-ANP **175b**, to afford bifunctional **173** (Scheme 4.16). As expected, under the identical conditions as mentioned above, the reaction progressed smoothly and **173** was isolated in 70% yield after column chromatography. The ^{1}H NMR spectral data for **173** revealed signals for both the alkynyl **174** and 5-iodo-ANP moieties in the ratio of 1:1 (Fig. 4.18). A successful coupling was further confirmed by the absence of a terminal alkyne proton at around δ_H 2.89 ppm. The ^{13}C NMR spectrum of **173** displayed diagnostic resonances at δ_C 64.7 (d, $J_{C\text{-}P}$ = 150.1 Hz, C-3), δ_C 66.9 (C-4), δ_C 119.2 (C≡N) and δ_C 149.6 (C-11) thus confirming the presence of both the nucleotide and the alkyne. The structure was further confirmed by 2D NMR.

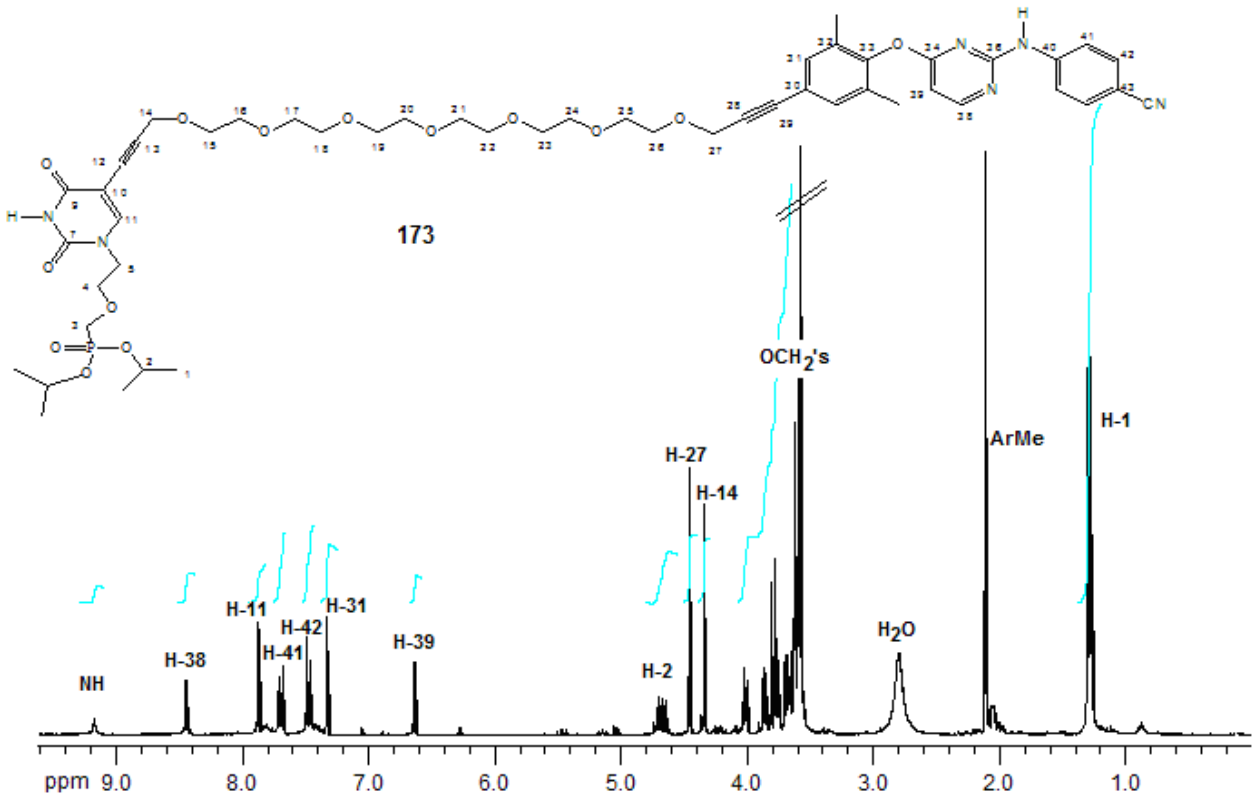

Figure 4.18 ^{1}H NMR spectrum of bifunctional **173**.

4.5.5 Biological evaluation and SAR interpretation

The inhibition of viral replication in HIV-infected cells of the bifunctional targets **172** and **173** was measured against HIV-1 (IIIB) replication in MT-2 cell culture using an MTT assay (see Appendix I). The results are summarized in Table 4.4 below.

Table 4.4 Anti-HIV results of bifunctionals **172** and **173** in cell-culture.

Compound	EC_{50} (nM)[a]	CC_{50} (nM)[b]	TI[c]
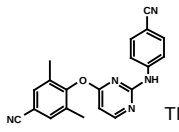 TMC120	2	9	4.5
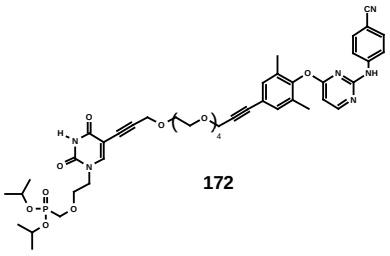 **172**	120	1800	15

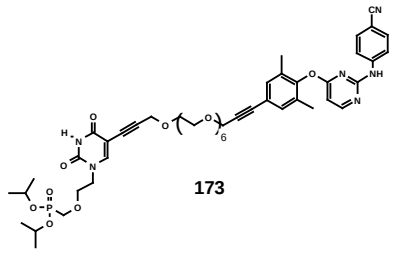 **173**	120	2100	17.5

[a] Effective concentration that inhibits viral-mediated T-cell death by 50% and as an average of three results.
[b] Cytotoxicity = concentration that kills 50% of the T-cells and as an average of three results.
[c] *In vitro* therapeutic index (CC_{50} /EC_{50})

The results revealed that the membrane-permeable, stable ANP phosphonate bifunctionals **172** and **173**, although more flexible than d4U, were still not able to give comparable activity to TMC120 in cell-culture testing. The best one, ANP 4-PEG derivative **172** showed a 60-fold decrease in activity compared to TMC120 and, more importantly was slightly less active than its 4-PEG d4U counterpart (100 nM). The results once again revealed a lack of *in vitro* phosphorylation, even with the incorporation of a membrane-permeable phosphonate. A possible reason for this could be the stability of the isopropyl ester protecting groups towards hydrolysis needed for conversion first to the acid as precursor for further phosphorylation. In addition, even assuming hydrolysis to the acid, the EC_{50} result (120 nM) suggests that further phosphorylation is not occurring as a result of poor substrate recognition. The fact that the d4U 4-PEG counterpart **147** gave a 100 nM activity, compared to the 120 nM activity for the ANP, also rendered compelling evidence in support of the notion that some degree of *in vitro* phosphorylation for the d4U bifunctional does take place in order to achieve this level of activity. Moreover, the results for **172** and **173** certainly suggest that the debate over the correct attachment point for spacer elongation has finally been resolved. The 120 nM activity of the 6-PEG derivative **173** is extremely interesting as normally one sees a significant reduction of activity for longer PEGS. This result not only suggests significant binding of both drugs (NRTI and NNRTI) to compensate a large entropy penalty, but also suggests, as hoped, that the longer PEG still allows NtRTI binding because of greater flexibility in the ANP NtRTI. This suggests that ANP-type structures are worthwhile pursuing in the future as the NtRTI component. CC_{50} values showed modest TI (SI) values, revealing high toxicity.

From all this, it can be concluded that the synthetic and biological work in this thesis has shown the way forward towards realizing synergy between the substrate binding site and NNRTI-BP. This promise certainly stands out in the enzyme assay work as reflected in outstanding results in the cell-culture assay for such large molecules, with nM activity being achieved regularly. This is

in contrast to earlier studies involving: (i) linkage of a spacer to Trovirdine by Ladurée and co-workers[120] which led to dimer formation with no anti-HIV activity; (ii) the linkage of AZT and TSAO-T inhibitors *via* a polymethylene spacer between the N-3 of the thymine base of both compounds by Camarasa and co-workers[126-129] which yielded moderate anti-HIV activity and; (iii) work by Monneret and co-workers[132] in synthesizing a variety of (N-3 and C-5) AZT-HEPT bifunctional conjugates displaying anti-HIV activity ranging between 2-5 μM. None of these cases reported any formal evidence of employing a rational drug-design strategy involving the use of extensive crystal structure analysis of the site of interest, or molecular modelling for assisting with choices in the attachment points to both the NRTI and the NNRTI moieties of the bifunctional entity. Hence, no proof of synergy was obtained.

The results of this thesis have thus developed and established a new level of rational drug-design for bifunctional HIV-drugs.

Final Conclusions

The following points may be concluded for future work in this field:

i) The correct attachment point for spacer elongation to TMC120 has been settled, and a four PEG spacer seems to be the optimal length for connecting the active site and the NNRTI-BP when using d4U as the NRTI. The data on the NRTI-PEG-TMC bifunctionals in conjunction with molecular modeling strongly supports the idea that the two sites link through a tunnel exiting the 'back' of the pocket close to W229. Such a linking would imply that the NNRTI "slides in" through the back from the substrate DNA side, rather than the NRTI exiting through the back of the pocket. This discovery is a new innovation contrasting with the alternative of linking the two sites *via* exiting the 'front' of the NNRTI pocket. ANP-PEG-TMC bifunctionals hold promise for accommodating more flexibility in the spacer. The correct choice of NtRTI might provide even better results.

ii) Bifunctional NRTI phosphorylation to an active triphosphorylated substrate appears to be a limitation for the concept of bifunctional NRTI/NNRTI HIV double-drugs. Future work could involve changing the relatively robust isopropyl ester groups of the ANP derivatives (**172** and **173**) described into inherently labile pivaloyloxymethyl (POM) or pivaloyloxymethylcarbonyl (POC) phosphonate-masking groups, which can also penetrate into cells *via* passive diffusion. D4U could also be converted to a *cyclo*Sal prodrug, which is well known to give the desired parent-nucleotide-MP intracellularly at physiological pH. This pronucleotide approach could also be extended to a phosphoramidate prodrug of

d4U. A full change-over to a clinically known ANP such as Tenofovir or Cidofovir would be worthwhile pursuing for hopefully overcoming the phosphorylation limitations.

iii) Finally, computational modeling has shown how rational drug-design strategies can and should be employed for developing double-drug entities on the basis of a predictive model.

CONCLUSION

The results of this thesis have developed and established a new level of rational drug-design for the synthesis of bifunctional HIV-drugs. It displays an evolution in ideas for development of double-drug entities starting from extensive crystal structure analysis of individual inhibitors to innovative molecular modeling to extrapolate vital drug-design considerations. This work is in contrast to earlier studies involving for example: (i) linkage of a spacer to Trovirdine by Ladurée and co-workers[120] which led to dimer formation with no anti-HIV activity; (ii) the linkage of AZT and TSAO-T inhibitors *via* a polymethylene spacer between the N-3 of the thymine base of both compounds by Camarasa and co-workers[126-129] which yielded moderate anti-HIV activity and; (iii) work by Monneret and co-workers[132] in synthesizing a variety of (N-3 and C-5) AZT-HEPT bifunctional conjugates displaying anti-HIV activity ranging between 2-5 μM. None of these cases reported any formal evidence of employing a rational drug-design strategy involving the use of extensive crystal structure analysis of the site of interest, or molecular modelling for assisting with choices in the attachment points to both the NRTI and the NNRTI moieties of the bifunctional entity.

This thesis describes its origin with a UC-781/d4U bifunctional synthesis in which a second-generation NNRTI was employed. A drawback in this synthesis was the inability to thiate the UC-781 amide which led us to progress our ideas to a more sophisticated second-generation NNRTI in the form of a pyrimidinylarylamine motif.

Further development of this system, steered by biological activity in conjunction with a structural-activity relationship study, ultimately culminated in a highly potent TMC120/d4U bifunctional synthesis. Biological results indicated the d4U-4-PEG-TMC120 bifunctional to have the lowest EC_{50} (100 nM) anti-HIV activity of any NRTI-spacer-NNRTI bifunctional inhibitor synthesized to date. The NRTI was also triphosphorylated and the product evaluated in an *in vitro* RT inhibition assay, to establish whether the bifunctional was being 'switched on' for incorporation into the growing DNA chain, which culminated in a 'proof of principle' of synergy existing between the substrate site and the allosteric binding pocket.

Exchanging d4U for a more flexible uracil-base ANP was attempted to address *in vitro* phosphorylation issues. The results suggested significant binding of both drugs (NRTI and NNRTI) to compensate a large entropy penalty, but also suggests, as hoped, that the longer 6-PEG still allows NtRTI binding because of greater flexibility in the ANP NtRTI. This suggests that ANP-type structures are worthwhile pursuing in the future as the NtRTI component. Future work could involve known ANP prodrugs such as Cidofovir or Tenofovir.

EXPERIMENTAL SECTION

6.1 General procedures

All solvents were freshly distilled. Diethyl ether and tetrahydrofuran were dried over sodium wire with benzophenone and distilled under nitrogen. Dichloromethane was distilled from phosphorus pentoxide under nitrogen. Other reagents were purified according to standard procedures. All commercial chemicals were purchased from Aldrich, Merck or Saarchem and were used as such.

Unless otherwise stated, reactions were run under an atmosphere of argon and monitored by thin-layer chromatography (TLC) using pre-coated silica gel 60 F_{254} sheets (0.2 mm layer) purchased from Merck. A 50:50 mixture (v/v) of 10% H_2SO_4 and 5% p-anisaldehyde were used to spray TLC plates and compounds were detected by UV absorption at 254 nm.
Column chromatography was effected by using Merck Kieselgel 60 silica-gel (0.040-0.063 mm). All products were dried on a nitrogen pump before yields were determined.

Nuclear Magnetic Resonance spectra were recorded on a Varian Unity 400 MHz (100 MHz for ^{13}C) or Varian Mercury 300 MHz (75 MHz for ^{13}C) and were carried out in chloroform-*d* unless otherwise stated. Chemical shifts (δ) were recorded using residual chloroform (δ 7.26 in ^{1}H NMR and δ 77.00 in ^{13}C NMR). All chemical shifts are reported in ppm, ^{1}H resonances to two decimal places and ^{13}C ones to one.

Optical rotations were obtained using a Perkin Elmer 141 polarimeter at 20°C. The concentration *c* refers to g/100ml. Melting points were obtained using a Reichert Jung Thermovar hot-stage microscope and are uncorrected. Elemental analyses were performed using a Fisons EA 1108 CHN elemental analyser. Infrared spectra were recorded on a Perkin-Elmer Paragon 1000 FT-IR spectrometer in either dichloromethane or chloroform. These spectra were recorded from 4000 to 600 cm^{-1} on sodium chloride plates. High-resolution mass-spectrometry was performed at the mass-spectrometry unit of the University of Witwatersrand using a VG70-SEQ micromass spectrometer or at The School of Chemistry, University of Stellenbosch on an API Q-TOF Ultima machine. All spectra were recorded in Electron Ionisation mode, unless otherwise stated.

6.2 Compounds synthesized

5-Benzyloxy-1-pentanol (90b)

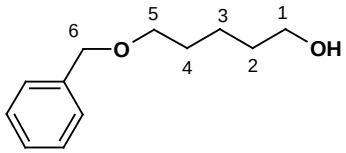

Sodium hydride (60%, 3.04 g, 76 mmol) was suspended in dry THF (250 mL) at 0°C (ice slurry), and to the solution was added 1,5-pentanediol (8.0 g, 76 mmol) portionwise. Once gas evolution had subsided, benzyl bromide (9.03 mL, 76 mmol) was added slowly. The ice bath was then removed and the mixture refluxed. TLC confirmed completion of the reaction after 20 hrs. The reaction mixture was cooled to room temperature, diluted with H_2O (150 mL) and extracted with diethyl ether (3 × 100 mL). The combined organic fractions were washed with brine (150 mL) before being dried over $MgSO_4$ and the solvent removed under reduced pressure. Purification by chromatography using a silica-gel column (70 g; EtOAc/hexane, 5:5) afforded product **90b** as a colourless oil, (7.90 g, 53%). ν_{max} /cm^{-1} ($CHCl_3$): 3617b (O-H, free), 2871s + 2941s (C-H, aliphatic), 1508s (C=C, aromatics); ^{1}H NMR ($CDCl_3$, 400 MHz) δ_H 1.42 (2H, m, H-3), 1.57 (2H, m, H-4), 1.65 (2H, m, H-2), 3.49 (2H, t, *J* = 6.5 Hz, H-5), 3.62 (2H, t, *J* = 6.5 Hz, H-1), 4.50 (2H, s, H-6), 7.33 (5H, m, Ar-H); ^{13}C NMR ($CDCl_3$, 100 MHz) δ_C 22.4 (C-3), 29.4 (C-2), 32.4 (C-4), 62.7 (C-1), 70.3 (C-5), 72.9 (C-6), 127.5 (Ar-*p*), 127.6 (Ar-*o*), 128.3 (Ar-*m*), 138.5 (Ar-*i*); HRMS (EI): *m/z* 194.13228 [M^+]. Calculated for $C_{12}H_{18}O_2$, 194.13068 [M^+].

5-Benzyloxypentanal (90a)

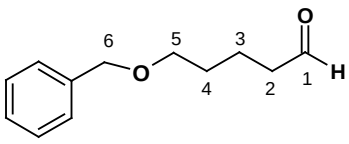

To a mixture of dimethyl sulfoxide (6.60 mL, 92 mmol) in dichloromethane (200 mL) at -78°C (dry-ice in acetone), was added oxalyl chloride (4.05 mL, 46.4 mmol) and the reaction mixture stirred for 15 min under a constant argon purge. Subsequent dropwise addition of alcohol **90b** (6.0 g, 31 mmol) was followed by stirring for a further 20 min. Triethylamine (22 mL, 155 mmol) was then added and the reaction allowed to warm to room temperature. TLC suggested

completion after 15 min. The reaction mixture was then diluted with aqueous $NaHCO_3$ (150 mL) and extracted with dichloromethane (3 × 150 mL). The organic extract was dried over $MgSO_4$ and removed under reduced pressure to give a viscous yellow oil. Purification by chromatography on a silica-gel column (70 g; EtOAc/hexane, 2:8) afforded aldehyde **90a** as a light yellow oil, (5.90 g, 99%). ν_{max} /cm^{-1} ($CHCl_3$): 2940s + 2872s (C-H, aliphatic), 1710s (C=O, aldehyde), 1495w (C=C, aromatic); ^{1}H NMR ($CDCl_3$, 400 MHz) δ_H 1.61 (2H, m, H-3), 1.70 (2H, m, H-4), 2.43 (2H, t, *J* = 6.5 Hz, H-2), 3.47 (2H, t, *J* = 6.5 Hz, H-5), 4.50 (2H, s, H-6), 7.33 (5H, m, Ar-H), 9.85 (1H, s, CHO); ^{13}C NMR ($CDCl_3$, 100 MHz) δ_C 19.2 (C-4), 29.4 (C-3), 43.8 (C-2), 69.9 (C-5), 73.2 (C-6), 127.8 (Ar-*p*), 127.8 (Ar-*o*), 128.6 (Ar-*m*), 139.0 (Ar-*i*), 202.1 (CHO); HRMS (EI): *m/z* 192.25812 [M$^+$]. Calculated for $C_{12}H_{16}O_3$, 192.25820 [M$^+$].

Methyl *E/Z* 2-(6-Benzyloxy-1-hexenyl)-3-furoate (92d)

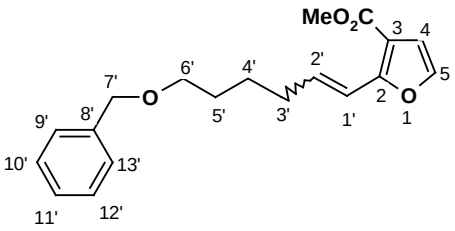

The methyl furanylphosphonium salt **90** (4.56 g, 9.50 mmol) was dissolved in a mixture of dry methanol (30 mL) and sodium methoxide (4.63 M, 2.27 mL, 10.5 mmol) added *via* syringe under nitrogen at 0^{o}C (ice-water slurry). Aldehyde **90a** (1.82 g, 9.50 mmol) was slowly added and the reaction mixture stirred at room temperature. The reaction mixture turned an immediate dark-red colour that progressively faded to a light-orange colour as it went to completion within 3 hrs. The reaction mixture was then diluted with brine (200 mL) and extracted with EtOAc (3 × 200 mL). The organic extract was dried over $MgSO_4$ and removed under reduced pressure. A yellow powder was obtained which was subjected to column chromatography using a silica-gel column (120 g; EtOAc/hexane, 0.3:9.7) to afford product **92d** (both *E*-and *Z*-stereoisomers in a 1:1 ratio) as a colourless oil, (2.70 g, 91%). ν_{max} /cm^{-1} ($CHCl_3$): 2928m + 2867s (C-H, aliphatic), 1715s (C=O, ester), 1649m (C=C, alkene), 1567m (C=C, aromatic); ^{1}H NMR of ***E*-isomer** ($CDCl_3$, 400 MHz) δ_H 1.60 (2H, m, H-4'), 1.69 (2H, m, H-5'), 2.29 (2H, qd, *J* = 7.5, 1.7 Hz, H-3'), 3.50 (2H, t, *J* = 6.4 Hz, H-6'), 3.83 (3H, s, CO_2Me), 4.50 (2H, s, H-7'), 6.51 (1H, dt, *J* = 16.0, 7.1 Hz, H-2'), 6.71 (1H, d, *J* = 2.0 Hz, H-4), 6.96 (1H, dt, *J* = 16.0, 1.6 Hz, H-1'), 7.29 (1H, d, *J* = 2.0 Hz, H-5), 7.33 (5H, m, Ar-H); ^{1}H NMR of ***Z*-isomer** ($CDCl_3$, 400 MHz) δ_H 1.60 (2H, m, H-4'), 1.69 (2H, m,

H-5'), 2.62 (2H, qd, *J* = 7.2, 1.3 Hz, H-3'), 3.50 (2H, t, *J* = 6.4 Hz, H-6'), 3.83 (3H, s, CO_2Me), 4.50 (2H, s, H-7'), 5.84 (1H, dt, *J* = 12.0, 7.6 Hz, H-2'), 6.67 (1H, d, *J* = 2.0 Hz, H-4), 6.90 (1H, dt, *J* = 12.0, 1.7 Hz, H-1'), 7.23 (1H, d, *J* = 2.0 Hz, H-5), 7.33 (5H, m, Ar-H); ^{13}C NMR of ***E/Z* isomers** (75 MHz, $CDCl_3$) δ_C 25.6/26.1 (C-4'), 29.8/29.4 (C-5'), 29.4/32.8 (C-3'), 51.3/51.4 (CO_2*Me*), 70.1/70.2 (C-6'), 72.8/72.9 (C-7'), 111.3/111.4 (C-4), 112.2 (C-3), 116.0/118.0 (C-1'), 127.4 (C-11'), 127.5/127.6 (C-9'/C-13'), 128.3 (C-10'/C-12'), 135.8/136.8 (C-2'), 138.6/138.7 (C-8'), 140.6/140.8 (C-5), 157.0/157.6 (C-2), 163.9/164.0 (*C*O_2Me); HRMS (EI): *m/z* 314.15111 [M^+]. Calculated for $C_{19}H_{22}O_4$, 314.15181 [M^+].

Methyl 2-(6-hydroxyhexyl)-3-furoate (94)

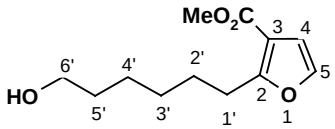

The furan ester **92d** (1.46 g, 4.64 mmol) was dissolved in absolute ethanol (10 mL) and stirred at room temperature. Subsequent addition of palladium-on-carbon (10%, 494 mg, 0.46 mmol) was followed by careful placement of a hydrogen gas balloon over the reaction flask. TLC confirmed reaction completion after 1 hr. The reaction mixture was filtered through a Celite-packed sintered funnel and washed with EtOAc (50 mL). Purification of the residue following solvent evaporation by chromatography using a silica-gel column (70 g; EtOAc/hexane, 1:9) afforded product **94** as a colourless oil, (983 mg, 94%). ν_{max} /cm^{-1} ($CHCl_3$): 3472b (O-H, free), 2940s + 2839s (C-H, aliphatic), 1720s (C=O, ester), 1612s (C=C, aromatic); ^{1}H NMR ($CDCl_3$, 400 MHz) δ_H 1.38 (4H, m, H-3', H-4'), 1.48 (1H, bs, OH), 1.63 (4H, m, H-2', H-5'), 3.00 (t, *J* = 7.6 Hz, H-1'), 3.61 (2H, t, *J* = 6.5 Hz, H-6'), 3.81 (3H, s, CO_2Me), 6.61 (1H, d, *J* = 2.0 Hz, H-4), 7.21 (1H, d, *J* = 2.0 Hz, H-5); ^{13}C NMR ($CDCl_3$, 75.5 MHz) δ_C 24.1 (C-3'), 27.9 (C-1'), 28.0 (C-4'), 28.1 (C-2'), 29.1 (C-5'), 51.2 (CO_2*Me*), 70.5 (C-6'), 110.6 (C-4), 112.8 (C-3), 140.5 (C-5), 162.9 (C-2), 164.7 (*C*O_2Me); HRMS (EI): *m/z* 226.12047 [M^+]. Calculated for $C_{13}H_{20}O_4$, 226.12051 [M^+].

Methyl 2-(6-*p*-toluenesulfonyloxyhexyl)-3-furoate (95)

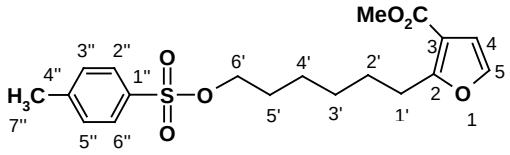

Compound **94** (622 mg, 2.75 mmol) was dissolved in dichloromethane (15 mL). Triethylamine (0.77 mL, 5.50 mmol) was added at 0°C followed by a catalytic amount of DMAP (17 mg, 0.12 mmol) to the reaction mixture. *p*-Toluenesulfonyl chloride (787 mg, 4.10 mmol) was then added dropwise and the solution left to stir at room temperature. TLC confirmed completion of the reaction after 2½ hrs. The reaction mixture was diluted with brine (50 mL) and extracted with dichloromethane (3 × 50 mL). The organic fractions were dried with $MgSO_4$ and removed under reduced pressure. Purification by chromatography using a silica-gel column (50 g; EtOAc/hexane, 1:9) afforded product **95** as a colourless oil, (974 mg, 94%). ν_{max} /cm^{-1} ($CHCl_3$): 2937s + 2864s (C-H, aliphatic), 1715s (C=O, ester), 1599s (C=C, aromatic), 1369s + 1177s (-SO_2-O-); ^{1}H NMR ($CDCl_3$, 300 MHz) δ_H 1.32 (4H, m, H-3', H-4'), 1.61 (4H, m, H-2', H-5'), 2.42 (3H, s, H-7''), 2.93 (2H, t, *J* = 7.6 Hz, H-1'), 3.79 (3H, s, CO_2Me), 3.99 (3H, t, *J* = 6.5 Hz, H-6'), 6.62 (1H, d, *J* = 2.0 Hz, H-4), 7.21 (1H, d, *J* = 2.0 Hz, H-5), 7.34 (2H, d, *J* = 7.9 Hz, H-3'', H-5''), 7.76 (2H, d, *J* = 7.9 Hz, H-2'', H-6''); ^{13}C NMR ($CDCl_3$, 75.5 MHz) δ_C 21.6 (C-7''), 24.9 (C-3'), 27.3 (C-1'), 27.6 (C-4'), 28.4 (C-2'), 28.7 (C-5'), 51.2 (CO_2*Me*), 70.5 (C-6'), 110.6 (C-4), 112.9 (C-3), 127.8 (C-2'', C-6''), 129.7 (C-3'', C-5''), 133.3 (C-4''), 140.4 (C-5), 144.6 (C-1''), 162.9 (C-2), 164.3 (*C*O_2Me); HRMS (EI): *m/z* 380.42675 [M$^+$]. Calculated for $C_{19}H_{24}O_6$, 380.42679 [M$^+$].

2-(6-Propargyloxyhexyl)furan-3-carboxylic acid (97)

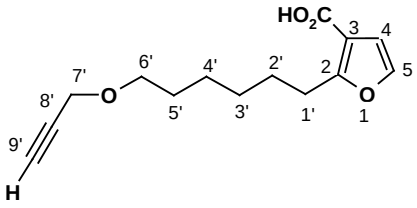

To a sodium hydride (60%, 464 mg, 11.6 mmol) suspension in THF (30 mL) at 0°C, was added propargyl alcohol (0.9 mL, 14.5 mmol) slowly whilst stirring. To this was added tosylate **95** (1.1 g, 2.9 mmol) and the reaction mixture refluxed. After 1 hr, 1M NaOH (10 drops) was added and the reaction mixture refluxed for a further hour. TLC confirmed completion after a total of 2 hrs. The

reaction mixture was diluted with 1M HCl (100 mL) and extracted with EtOAc (2 × 100 mL). The organic fractions were dried with $MgSO_4$ and removed under reduced pressure. Purification by chromatography using a silica-gel column (100 g; EtOAc/hexane, 1:9) afforded product **97** as a colourless oil, (822 mg, 98%). ν_{max} /cm^{-1} ($CHCl_3$): 3157b (O-H, H-bonded), 2935s + 2865s (C-H, aliphatic), 2254s (C≡C, alkyne), 1683s (C=O, carboxylic acid), 1596s (C=C, aromatic); ^{1}H NMR ($CDCl_3$, 300 MHz) δ_H 1.38 (4H, m, H-3', H-4'), 1.60 (2H, m, H-2'), 1.69 (2H, m, H-5'), 2.41 (1H, t, *J* = 2.4 Hz, H-9'), 3.02 (2H, t, *J* = 7.4 Hz, H-1'), 3.51 (2H, t, *J* = 6.6 Hz, H-6'), 4.13 (2H, d, *J* = 2.4 Hz, H-7'), 6.68 (1H, d, *J* = 2.0 Hz, H-4), 7.26 (1H, d, *J* = 2.0 Hz, H-5); ^{13}C NMR ($CDCl_3$, 75.5 MHz) δ_C 25.7 (C-3'), 27.5 (C-1'), 27.7 (C-4'), 28.9 (C-2'), 29.3 (C-5'), 57.9 (C-7'), 70.1 (C-6'), 74.0 (C-9'), 80.0 (C-8'), 110.8 (C-4), 112.6 (C-3), 140.6 (C-5), 164.7 (C-2), 169.6 (*CO*$_2$H); HRMS (EI): *m/z* 250.12053 [M$^+$]. Calculated for $C_{14}H_{18}O_4$, 250.12051 [M$^+$].

2-(6-Propargyloxyhexyl)furan-3-carboxylic acid [4-chloro-3-(3-methyl-but-2-enyl-1-oxy)-phenyl]-amide (99)

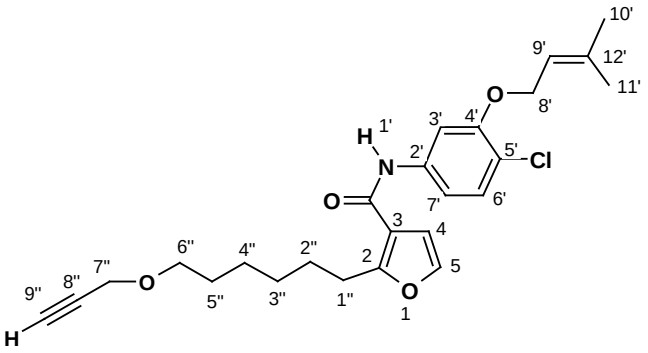

The acid **97** (108 mg, 0.32 mmol) was dissolved in thionyl chloride (1 mL) and the mixture heated to 40^{o}C under nitrogen for 1 hr with constant stirring. The excess thionyl chloride was then reduced on a vacuum pump and the resulting oil dissolved in dichloromethane (3 mL). Subsequent addition of pyridine (0.08 mL, 0.96 mmol) at 0^{o}C was followed by the arylamine **61** (68 mg, 0.32 mmol) and the reaction mixture stirred at room temperature. TLC (EtOAc/hexane, 3:7; R_f = 0.35) confirmed completion of the reaction after 30 min. The reaction mixture was diluted with EtOAc (50 mL) and extracted with 1M HCl (4 × 15 mL). The organic fractions were dried with $MgSO_4$ and removed under reduced pressure. Purification by chromatography using a silica-gel column (10 g; EtOAc/hexane, 1.5:8.5) afforded product **99** as a yellow oil, (133 mg, 78%). ν_{max} /cm^{-1} ($CHCl_3$): 3304s + 3440 m (N-H, amide), 2935s + 2864s (C-H, aliphatic), 2253s (C≡C, alkyne), 1674s (C=O, amide), 1595s (N-H and C-N stretching), 1513s + 1492s (C=C, aromatic); ^{1}H NMR (400 MHz, $CDCl_3$) δ_H 1.37 - 1.59 (8H, m, H-2'',3'',4'',5''), 1.74 + 1.78 (6H, 2 ×

s, H-10',11'), 2.39 (1H, t, *J* = 2.4 Hz, H-9''), 3.04 (2H, t, *J* = 7.6 Hz, H-1''), 3.48 (2H, t, *J* = 6.6 Hz, H-6''), 4.10 (2H, d, *J* = 2.4 Hz, H-7''), 4.58 (2H, d, *J* = 7.3 Hz, H-8'), 5.50 (1H, tq, *J* = 6.6, 1.5 Hz, H-9'), 6.53 (1H, d, *J* = 2.2 Hz, H-4), 6.88 (1H, dd, *J* = 8.8, 2.2 Hz, H-7'), 7.26 (1H, d, *J* = 8.8 Hz, H-6'), 7.30 (1H, d, *J* = 2.2 Hz, H-5), 7.46 (1H, s, H-1'), 7.58 (1H, d, *J* = 2.2 Hz, H-3'); ^{13}C NMR (75 MHz, $CDCl_3$) δ_C 18.2 (*C*H_3), 25.7 (*C*H_2), 25.8 (*C*H_3), 27.4 (C-1''), 27.8 (*C*H_2), 28.9 (*C*H_2), 29.3 (*C*H_2), 57.9 (C-7''), 66.1 (C-8'), 70.0 (C-6''), 74.0 (C-9''), 80.0 (C-8''), 106.1 (C-3'), 107.9 (C-4), 112.4 (C-7'), 115.5 (C-3), 118.0 (C-5'), 119.0 (C-9'), 129.9 (C-6'), 137.6 (C-2'), 138.6 (C-12'), 140.6 (C-5), 154.6 (C-4'), 161.8 (C-2), 161.9 (*C*ONH); HRMS (EI): *m/z* 443.17863 [M^+]. Calculated for $C_{25}H_{30}O_4NCl$, 443.17917 [M^+].

2-(6-Propargyloxyhexyl)furan-3-carbothioic acid [4-chloro-3-(3-methyl-but-2-enyloxy)-phenyl]-amide (100)

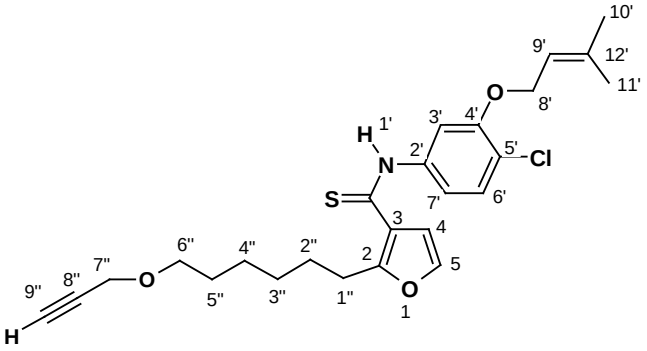

The amide **99** (40 mg, 0.10 mmol) was dissolved in toluene (2 mL) and to this was added Lawesson's reagent (73 mg, 0.18 mmol) and sodium hydrogen carbonate (84 mg, 1 mmol) with constant stirring. The reaction mixture was then slowly heated to 90^{o}C. TLC on neutral alumina (EtOAc/hexane, 3:7; R_f = 0.66) confirmed completion of the reaction after 4 hrs. The reaction mixture was filtered, washed with EtOAc (20 mL) and the solvent removed under reduced pressure. Purification by chromatography using a neutral alumina column (7 g; EtOAc/hexane, 0.8:9.2) afforded product **100** as a yellow oil, (27 mg, 59%). ν_{max} /cm^{-1} ($CHCl_3$): 3234m (N-H, thioamide), 2858s (C-H, aliphatic), 2270s (C≡C, alkyne), 1618s (C=C, aromatic), 1162s + 1389s (C=S stretches), 1550s + 1453s (C=C, aromatic); ^{1}H NMR (400 MHz, C_6D_6) δ_H 1.24 - 1.46 (8H, m, H-2'',3'',4'',5''), 1.45 + 1.51 (6H, 2 × s, H-10',11'), 2.02 (1H, t, *J* = 2.4 Hz, H-9''), 3.00 (2H, t, *J* = 7.6 Hz, H-1''), 3.28 (2H, t, *J* = 6.4 Hz, H-6''), 3.83 (2H, d, *J* = 2.4 Hz, H-7''), 4.41 (2H, d, *J* = 6.1 Hz, H-8'), 5.47 (1H, tq, *J* = 6.2, 1.4 Hz, H-9'), 6.13 (1H, d, *J* = 1.9 Hz, H-4), 6.38 (1H, d, *J* = 7.5 Hz, H-7'), 6.82 (1H, d, *J* = 7.5 Hz, H-6'), 7.15 (1H, d, *J* = 1.9 Hz, H-5), 7.98 (1H, s, H-1'), 8.17 (1H, s, H-3'); ^{13}C NMR (75 MHz, C_6D_6) δ_C 17.9 (*C*H_3), 25.5 (*C*H_2), 25.9 (*C*H_3), 27.9 (C-1'' + *C*H_2),

29.1 (*C*H_2), 29.5 (*C*H_2), 57.8 (C-7''), 66.1 (C-8'), 69.8 (C-6''), 73.9 (C-9''), 80.5 (C-8''), 106.1 (C-3'), 108.1 (C-4), 109.4 (C-7'), 115.7 (C-3), 119.7 (C-5'), 120.6 (C-9'), 130.1 (C-6'), 138.2 (C-2'), 138.7 (C-12'), 141.1 (C-5), 154.8 (C-4'), 157.3 (C-2), 160.0 (*C*SNH); HRMS (EI): *m/z* 459.16343 [M^+]. Calculated for $C_{25}H_{30}O_3NSCl$, 459.16349 [M^+].

5-{10-[3-(4-chloro-3-(3-methyl-but-2-enyl-1-oxy)phenylcarbamoyl)-furan-2-yl]-4-oxa-1-decynyl}-uridine-2',3'-didehydro-2',3'-dideoxy-5'-O-benzoate (101)

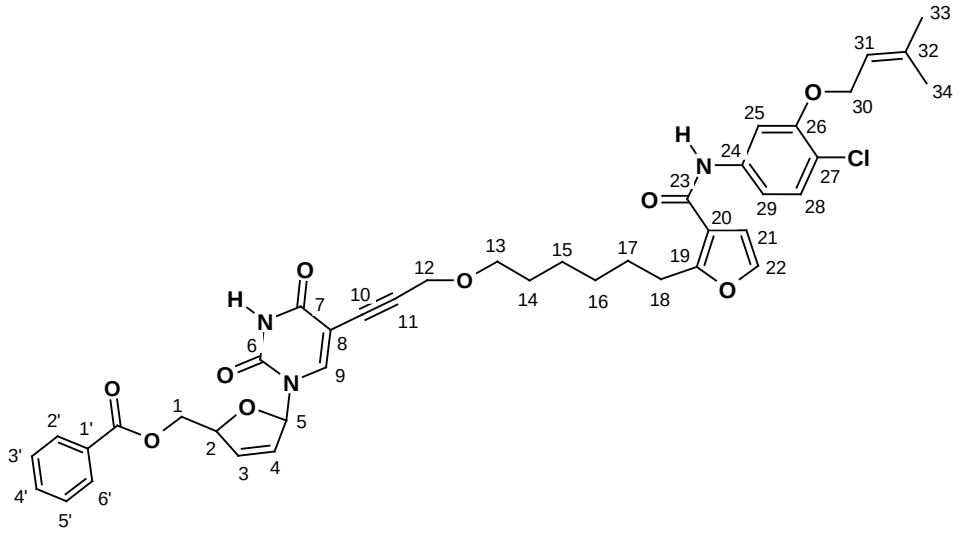

Amide **99** (50 mg, 0.09 mmol) was added together with the 5-iodo-d4U benzoate **60** (41 mg, 0.094 mmol) and the mixture dried carefully on a vacuum pump. A mixture of degassed DMF:THF (1:2 (v/v), 1 mL) was then added to the reaction vessel whilst the mixture stirred at room temperature under nitrogen. Subsequent addition of triethylamine (0.03 mL, 0.20 mmol) was followed by addition of copper(I) iodide (8.95 mg, 0.05 mmol) and tetrakistriphenylphosphinepalladium (10.9 mg, 0.01 mmol) respectively. The reaction was stirred continuously at room temperature and TLC (EtOAc/hexane, 3:7; R_f = 0.24) confirmed completion of the reaction after 2 hrs. The reaction mixture was diluted with a 5% EDTA solution (30 mL) and extracted with chloroform (3 × 20 mL). The organic fractions were dried with $MgSO_4$ and removed under reduced pressure. Purification by chromatography using a silica-gel column (10 g; EtOAc/hexane, 3:7) afforded product **101** as a clear oil, (48 mg, 61%). $[\alpha]_D$ -16.1° (*c* = 1.13, $CHCl_3$); ν_{max} /cm^{-1} ($CHCl_3$): 2932s (C-H, aliphatic), 2254s (C≡C, alkyne), 1720s (C=O, ester), 1693s (C=O, amide), 1599s (N-H and C-N stretching), 1514s + 1492s (C=C, aromatic); ^{1}H NMR (400 MHz, $CDCl_3$) δ_H 1.30 - 1.35 (8H, m, H-14,15,16,17), 1.73 - 1.77 (6H, 2 × s, H-33,34), 3.03 (2H, t, *J* = 7.7 Hz, H-18), 3.40 (2H, t, *J* = 6.7 Hz, H-13), 4.07 (2H, s, H-12), 4.58 (4H, m, H-1, H-30), 5.18 (1H, m, H-2), 5.50 (1H, tq, *J* = 6.8, 1.4 Hz, H-31), 5.95 (1H, dt, *J* = 5.7, 1.9 Hz, H-3),

6.38 (1H, dt, *J* = 5.7, 1.6 Hz, H-4), 6.56 (1H, d, J_{AB} = 2.2 Hz, H-21), 6.93 (2H, m, H-5, H-29), 7.26 (1H, m, H-28), 7.30 (1H, d, J_{AB} = 2.2 Hz, H-22), 7.41 - 7.57 (5H, m, H-2',3',4'), 7.67 (1H, s, H-9), 7.73 (1H, s, NH), 8.00 (1H, s, H-25), 8.73 (1H, bs, NH); ^{13}C NMR (75 MHz, $CDCl_3$) δ_C 18.3 (C-33/C-34), 25.7 (C-33/C-34), 25.8 (*C*H_2), 27.4 (C-18), 27.8 (*C*H_2), 28.9 (*C*H_2), 29.4 (*C*H_2), 58.8 (C-12), 64.9 (C-1), 66.1 (C-30), 70.0 (C-13), 75.3 (C-8), 75.9 (C-10), 85.0 (C-2), 90.6 (C-5), 102.2 (C-11), 105.9 (C-25), 108.0 (C-21), 112.4 (C-29), 115.4 (C-20), 117.9 (C-27), 119.1 (C-31), 127.0 (C-4), 128.7 (C-3', C-5'), 129.3 (C-1'), 129.8 (C-2', C-6'), 129.9 (C-28), 133.5 (C-3), 133.6 (C-4'), 137.6 (C-24), 138.5 (C-32), 140.6 (C-22), 144.0 (C-9), 150.0 (C-6), 154.6 (O*CO*C_6H_5), 154.6 (C-26), 159.6 (C-19), 161.9 (*CO*NH), 162.5 (C-7).

5-{10-[3-(4-chloro-3-(3-methyl-but-2-enyl-1-oxy)phenylcarbamoyl)-furan-2-yl]-4-oxa-1-decynyl}-2',3'-didehydro-2',3'-dideoxyuridine (102)

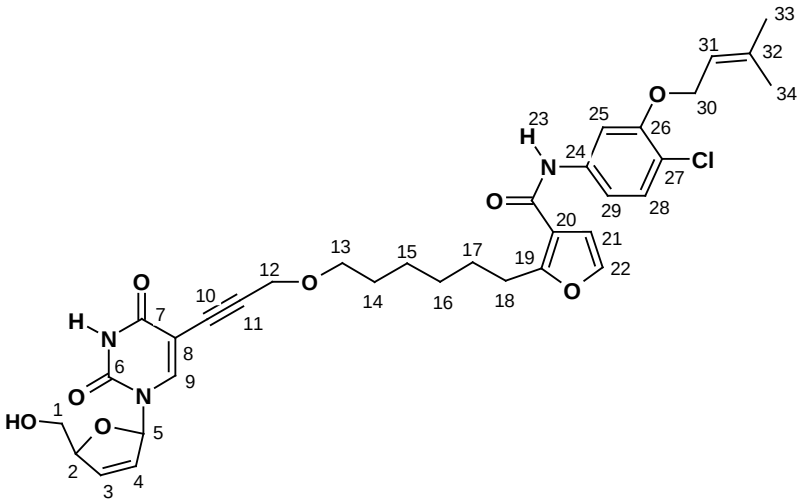

Sodium methoxide (4.63 M, 0.02 mL, 0.09 mmol) was added together with methanol (1.5 mL) at 0^{o}C. This was followed by addition of **101** (56 mg, 0.08 mmol) at 0^{o}C and the reaction mixture left to stir at room temperature. TLC (EtOAc/hexane, 6:4; R_f = 0.12) confirmed completion of the reaction after 1 hr. The reaction mixture was diluted with saturated NH_4Cl (20 mL) and extracted with EtOAc (3 × 20 mL). The organic fractions were dried with $MgSO_4$ and removed under reduced pressure. Purification by chromatography using a silica-gel column (5 g; EtOAc/hexane, 8:2) afforded product **102** as a clear oil, (26 mg, 51%). $[\alpha]_D$ -15.7° (*c* = 1.03, $CHCl_3$); ν_{max} /cm^{-1} ($CHCl_3$): 3592b (O-H, free), 2932s (C-H, aliphatic), 2254s (C≡C, alkyne), 1720s (C=O, ester), 1693s (C=O, amide), 1599s (N-H and C-N stretching), 1514s + 1492s (C=C, aromatic); ^{1}H NMR (400 MHz, $CDCl_3$) δ_H 1.24 - 1.33 (8H, m, H-14,15,16,17), 1.73 - 1.79 (6H, 2 × s, H-33, H-34), 2.80 (1H, s, OH), 3.03 (2H, t, *J* = 7.6 Hz, H-18), 3.46 (2H, t, *J* = 6.8 Hz, H-13), 3.78 (1H, dd, *J* =

12.4, 3.0 Hz, H-1), 3.88 (1H, dd, *J* = 12.4, 3.0 Hz, H-1), 4.21 (2H, s, H-12), 4.59 (2H, d, *J* = 6.5 Hz, H-30), 4.91 (1H, m, H-2), 5.51 (1H, tq, *J* = 6.8, 1.4 Hz, H-31), 5.83 (1H, m, H-3), 6.32 (1H, m, H-4), 6.56 (1H, d, J_{AB} = 2.2 Hz, H-21), 6.96 (2H, m, H-5, H-29), 7.26 (1H, m, H-28), 7.30 (1H, d, J_{AB} = 2.2 Hz, H-22), 7.53 (1H, s, H-9), 7.74 (1H, s, NH), 8.05 (1H, s, H-25), 9.0 (1H, s, NH); ^{13}C NMR (75 MHz, $CDCl_3$) δ_C 18.3 (C-33/34), 25.6 (C-33/34), 25.8 (*C*H_2), 27.2 (C-18), 27.7 (*C*H_2), 28.7 (*C*H_2), 29.2 (*C*H_2), 58.7 (C-12), 63.0 (C-1), 66.2 (C-30), 70.2 (C-13), 76.8 (C-8), 76.8 (C-10), 87.6 (C-2), 90.3 (C-5), 99.5 (C-11), 106.4 (C-25), 108.2 (C-21), 112.7 (C-29), 115.6 (C-20), 118.0 (C-27), 119.1 (C-31), 125.9 (C-4), 129.9 (C-28), 135.0 (C-3), 137.7 (C-24), 138.6 (C-32), 140.6 (C-22), 144.4 (C-9), 149.7 (C-6), 154.5 (C-26), 159.9 (C-19), 161.8 (*C*ONH), 162.2 (C-7).

5-Bromo-1-pentanol (104a)

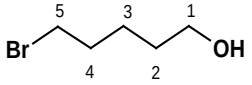

To a solution of 1,5-pentanediol (5.40 g, 50 mmol) in toluene (150 mL) was added HBr in ether (6.75 mL, 60 mmol), under a constant argon purge whilst stirring. The mixture was then refluxed at 110^{o}C for 10 hrs by which time TLC confirmed reaction completion (EtOAc/hexane, 3:7; R_f = 0.45). The reaction mixture was cooled to room temperature and then carefully diluted with aqueous $NaHCO_3$ (2 × 50 mL), until fizzing subsided. The mixture was shaken in a separating funnel (care), the toluene layer collected, which was washed with brine (40 mL). The organic extract was then dried over $MgSO_4$ and the solvent removed under reduced pressure. Purification by chromatography using a silica-gel column (70 g; EtOAc/hexane, 1:1) afforded product **104a** as a clear yellow oil, (4.30 g, 52%). ^{1}H NMR (400 MHz, $CDCl_3$) δ_H 1.48-1.67 (4H, m, H-3, H-4), 1.89 (2H, q, *J* = 6.8 Hz, H-2), 3.41 (2H, t, *J* = 6.8 Hz, H-5), 3.64 (2H, t, *J* = 6.8, H-1).

1-(5-Bromopentyl-1-oxy)-4-methoxybenzene (104c)

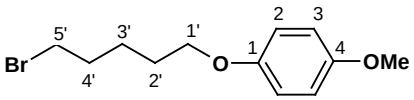

To a solution of **104a** (334 mg, 2.0 mmol) dissolved in dry THF (10 mL) was added *p*-methoxyphenol (261 mg, 2.1 mmol) and triphenylphosphine (577 mg, 2.2 mmol) under a constant argon gas flow, whilst stirring. DIAD (0.453 mL, 2.3 mmol) was added last and the solution turned an immediate yellow colour and was left to stir at room temperature for 3 hrs. TLC confirmed the completion of the reaction (pure hexane, R_f = 0.15). No work up was

performed and the reaction mixture was simply reduced in volume under pressure. Purification by chromatography using a silica-gel column (12 g; EtOAc/hexane, 2:8) afforded product **104c** as a viscous yellow oil, (304 mg, 56%). ν_{max} /cm^{-1} ($CHCl_3$): 3004s (C-H, aromatic), 2837m + 2870m + 2945s (C-H, aliphatic), 1508s + 1591s (C=C, aromatic); ^{1}H NMR (300 MHz, $CDCl_3$) δ_H 1.62 (2H, m, H-3'), 1.79 (2H, q, *J* = 6.9 Hz, H-4'), 1.94 (2H, q, *J* = 7.3 Hz, H-2'), 3.44 (2H, t, *J* = 6.9 Hz, H-5'), 3.77 (3H, s, O*Me*), 3.92 (2H, t, *J* = 7.3 Hz, H-1'), 6.83 (4H, s, Ar-*H*); HRMS (EI): *m/z* 272.04191 [M$^+$- H]. Calculated for $C_{12}H_{17}O_2Br$, 272.04119 [M$^+$- H].

5-(4-Methoxyphenoxy)-1-pentanol (104d)

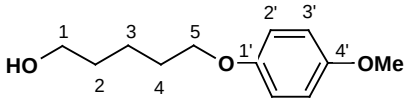

The methods (i) and (ii) below, relate to studying different solvents for the reaction.

(i) Sodium hydride (60%, 322 mg, 8.05 mmol) was suspended in dry THF (10 mL) at 0^{o}C (ice slurry), and to the solution was added *p*-methoxyphenol (1.0 g, 8.05 mmol) portionwise. Once gas evolution had subsided, 5-bromo-1-pentanol **104a** (1.34 g, 8.05 mmol) was added slowly. The ice bath was then removed and the mixture refluxed. TLC confirmed completion of the reaction (EtOAc/hexane 3:7; R_f = 0.24) after 20 hrs. The reaction mixture was cooled to room temperature, diluted with H_2O (30 mL) and extracted with EtOAc (2 × 30 mL). The organic fractions were washed with brine (30 mL) before being dried over $MgSO_4$ and the solvent removed under reduced pressure. Purification by chromatography using a silica-gel column (50 g; EtOAc/hexane, 6:4) afforded product **104d** as a colourless solid, (765 mg, 46%). The product was recrystallized from diethyl ether and petroleum ether before being submitted for spectral analysis.

(ii) Sodium hydride (60%, 988 mg, 24.7 mmol) was suspended in dry DME (10 mL) at 0^{o}C (ice slurry), and to the solution was added *p*-methoxyphenol (3.80 g; 30.6 mmol) portionwise. Once gas evolution had subsided, 5-bromo-1-pentanol **104a** (3.93 g, 23.5 mmol) was added slowly. The ice bath was then removed and the mixture refluxed. TLC confirmed completion of the reaction (EtOAc/hexane 3:7; R_f = 0.24) after 24 hrs. The reaction mixture was cooled to room temperature and diluted with H_2O (30 mL) and extracted with EtOAc (2 × 30 mL). The organic fractions were washed with brine (30 mL) before being dried over $MgSO_4$ and the solvent

removed under reduced pressure. Purification by chromatography using a silica-gel column (70 g; EtOAc/hexane, 1:1) afforded product **104d** as a colourless solid, (3.19 g, 69%). The product was recrystallized from diethyl ether and petroleum ether before being submitted for spectral analysis. M.p. 53 - 56°C; ν_{max} /cm^{-1} ($CHCl_3$): 3617b (O-H, free), 2871s + 2941s (C-H, aliphatic), 1508s (C=C, aromatics); ^{1}H NMR (400 MHz, $CDCl_3$) δ_H 1.53 (2H, m, H-3), 1.64 (2H, q, *J* = 7.0 Hz, H-2), 1.79 (2H, q, *J* = 6.8 Hz , H-4), 3.67 (2H, m, H-1), 3.76 (3H, s, O*Me*), 3.92 (2H, t, *J* = 6.8 Hz, H-5), 6.82 (4H, s, Ar-*H*); ^{13}C NMR (100 MHz, $CDCl_3$) δ_C 22.4 (C-3), 29.1 (C-4), 32.4 (C-2), 55.7 (O*Me*), 62.8 (C-1), 68.5 (C-5), 114.7 + 115.4 (C-2',3'), 153.2 (C-1'), 154.0 (C-4'); HRMS (EI): *m/z* 210.12436 [M$^+$]. Calculated for $C_{12}H_{18}O_3$, 210.12559 [M$^+$]; C, H, N Microanalysis found: C, 68.54; H, 8.64%; $C_{12}H_{18}O_3$ requires C, 68.54; H, 8.63%.

Methanesulfonic acid 5-(4-methoxyphenoxy)-1-pentyl ester (104e)

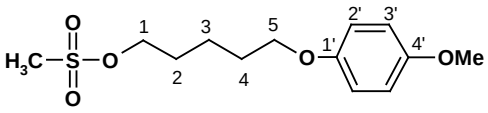

Alcohol **104d** (3.15 g, 15.0 mmol) was added to pyridine (2.42 mL, 30.0 mmol) at 0°C (ice slurry) and under a constant argon purge while stirring. Dichloromethane (20 mL) was added to the mixture, followed by the dropwise addition of methanesulfonyl chloride (1.74 mL, 22.5 mmol) and the reaction left to stir. TLC confirmed completion of the reaction (EtOAc/hexane, 3:7; R_f = 0.20) after 1½ hrs. To the reaction mixture was then added EtOAc (50 mL) and the organic fraction extracted with 1M HCl (2 × 30 mL). The organic fraction was finally washed with brine (30 mL), dried over $MgSO_4$ and removed under reduced pressure. Purification by chromatography using a silica-gel column (70 g; EtOAc/hexane, 3:7) afforded mesylate **104e** as a colourless oil, (4.02 g, 93%). ν_{max} /cm^{-1} ($CHCl_3$): 2950s + 2871m (C-H, aliphatic), 1508s (C=C, aromatic), 1356s + 1175s (-SO_2-O-); ^{1}H NMR (400 MHz, $CDCl_3$) δ_H 1.60 (2H, m, H-2), 1.81 (4H, m, H-3, H-4), 3.00 (3H, s, C*H*$_3$$SO_2$), 3.76 (3H, s, O*Me*), 3.92 (2H, t, *J* = 6.1 Hz, H-5), 4.26 (2H, t, *J* = 6.6 Hz, H-1), 6.82 (4H, s, Ar-*H*); HRMS (EI): *m/z* 288.10257 [M$^+$]. Calculated for $C_{13}H_{20}O_5S$, 288.10315 [M$^+$].

1-{5-[2-Benzyloxyethoxy)-2-ethoxy]-1-pentyloxy}-4-methoxybenzene (105a)

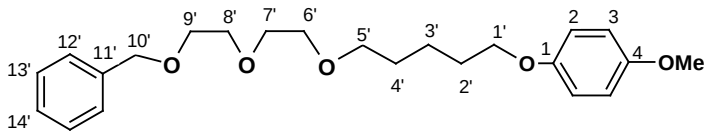

Three reactions were carried out varying the electrophilic alkylating agent as bromide or mesylate, as well as solvent (THFor DME):

(i) Sodium hydride (60%, 30 mg, 0.75 mmol) was dissolved in dry THF (3 mL) at 0^{o}C (ice slurry) while stirring. This was followed by the dropwise addition of **103** (99 mg, 0.5 mmol) and **104c** (137 mg, 0.5 mmol) respectively. The ice slurry was then removed and the mixture refluxed. The reaction was stopped after 2 hrs and TLC suggested product formation (EtOAc/hexane, 1:9; R_f = 0.13). After cooling to room temperature, the reaction mixture was then diluted with H_2O (30 mL) and extracted with EtOAc (3 × 30 mL). The organic fractions were then washed with brine (20 mL), dried over $MgSO_4$ and the solvent removed under reduced pressure. Purification by chromatography using a silica-gel column (5 g; EtOAc/hexane, 1:9) afforded product **105a** as a colourless oil, (71 mg, 37%).

(ii) Sodium hydride (60%, 48 mg, 1.20 mmol) was dissolved in dry THF (5 mL) at 0^{o}C (ice slurry) while stirring. This was followed by dropwise addition of **103** (157 mg, 0.80 mmol), and the mesylate **104e** (230 mg, 0.80 mmol) added after gas evolution had subdued. The ice slurry was then removed and the mixture refluxed. The reaction was complete after 20 hrs and TLC suggested product formation (EtOAc/hexane, 1:9; R_f = 0.13). After cooling to room temperature, the reaction mixture was then diluted with H_2O (30 mL) and extracted with EtOAc (3 × 30 mL). The organic fractions were then washed with brine (20 mL), dried over $MgSO_4$ and the solvent removed under reduced pressure. Purification by chromatography using a silica-gel column (10 g; EtOAc/hexane, 1:9) afforded product **105a** as a colourless oil, (222 mg, 72%).

(iii) Sodium hydride (60%, 624 mg, 15.6 mmol) was dissolved in dry DME (20 mL) at 0^{o}C (ice slurry) while stirring. This was followed by dropwise addition of **103** (2.04 g, 10.4 mmol), and the mesylate **104e** (3.0 g, 10.4 mmol) added after gas evolution had subdued. The ice slurry was then removed and the mixture refluxed. The reaction was complete after 5 hrs and TLC suggested product formation (EtOAc/hexane, 1:9; R_f = 0.13). After cooling to room temperature, the reaction mixture was then diluted with H_2O (30 mL) and extracted with EtOAc (3 × 40 mL).

The organic fractions were then washed with brine (20 mL), dried over $MgSO_4$ and the solvent removed under reduced pressure. Purification by chromatography using a silica-gel column (70 g; EtOAc/hexane, 1:9) afforded product **105a** as a colourless oil, (2.96 g, 74%). ν_{max} /cm^{-1} ($CHCl_3$): 2940s + 2869s (C-H, aliphatic), 1591m + 1591s (C=C, aromatic); ^{1}H NMR (400 MHz, $CDCl_3$) δ_H 1.52 (2H, m, H-2'), 1.66 (2H, quin, *J* = 7.0 Hz, H-3'), 1.78 (2H, quin, *J* = 7.0 Hz, H-4'), 3.50 (2H, t, *J* = 6.6 Hz, H-5'), 3.66 (8H, m, H-6',7',8',9'), 3.76 (3H, s, O*Me*), 3.90 (2H, t, *J* = 6.4 Hz, H-1'), 4.57 (2H, s, H-10'), 6.82 (4H, s, H-2,3), 7.35 (5H, m, H-12',13',14') ^{13}C NMR (75 MHz, $CDCl_3$): δ_C 22.6 (C-4'), 29.1 (C-3'), 29.3 (C-2'), 55.6 (O*Me*), 68.4 (C-9', C-1'), 69.4 (C-6'), 70.1 + 70.6 (C-7', C-8'), 71.2 (C-5'), 73.1 (C-10'), 114.5 (C-2/C-3), 115.3 (C-2/C-3), 127.4 + 127.6 + 128.2 (C-12',13',14'), 138.2 (C-11'), 153.2 (C-1), 153.6 (C-4); HRMS (EI): *m/z* 388.22540 [M$^+$]. Calculated for $C_{23}H_{32}O_5$, 388.22497 [M$^+$].

5-[2-Benzyloxyethoxy)-2-ethoxy]-1-pentanol (106)

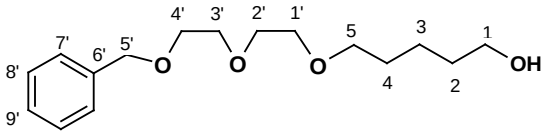

The *p*-methoxyphenyl ether **105a** (2.29 g, 5.88 mmol) was added to a mixture of acetonitrile (16 mL) and water (4 mL). The mixture was brought to 0^{o}C and cerium(IV) ammonium nitrate (16.1 g, 29.4 mmol) added portionwise. The solution turned an immediate dark-red colour and the reaction was complete after 10 min, as indicated by TLC (EtOAc/Hex, 1:1; R_f = 0.12). The reaction mixture was diluted with H_2O (30 mL) and extracted with dichloromethane (2 × 30 mL). The organic fractions were then washed with brine (30 mL), dried with $MgSO_4$ and the solvent removed under reduced pressure. Purification by chromatography using a silica-gel column (70 g; EtOAc/hexane, 6:4) afforded product **106** as an orange oil, (1.75 g, 86%). ν_{max} /cm^{-1} ($CHCl_3$): 3472b (O-H, free), 2938s + 2867s (C-H, aliphatic), 1496w + 1454s (C=C, aromatics); ^{1}H NMR (400 MHz, $CDCl_3$) δ_H 1.40 (2H, m, H-3), 1.58 (4H, m, H-2, H-4), 1.96 (1H, s, OH), 3.46 (2H, t, *J* = 6.6 Hz, H-5), 3.62 (10H, m, H-1,1',2',3',4'), 4.55 (2H, s, H-5'), 7.32 (5H, m, Ar-*H*); ^{13}C NMR (75 MHz, $CDCl_3$) δ_C 22.2 (C-3), 29.2 + 32.4 (C-2, C-4), 62.5 (C-1), 69.4 (C-4'), 70.0 + 70.6 + 71.2 (C-1',2',3'), 70.5 (C-5), 73.2 (C-5'), 127.5 (C-9'), 127.6 (C-7'), 128.3 (C-8'), 138.2 (C-6'); HRMS (EI): *m/z* 83.19020 [M$^+$ + H]. Calculated for $C_{16}H_{26}O_4$, 283.19093 [M$^+$ + H].

5-[2-Benzyloxyethoxy)-2-ethoxy]pentanal (107)

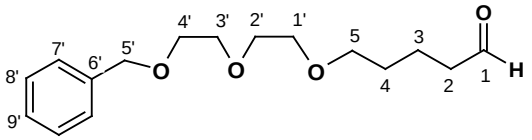

To a mixture of dimethyl sulfoxide (1.24 mL, 17.5 mmol) in dichloromethane (30 mL) at -78^{o}C (dry-ice in acetone), was added oxalyl chloride (0.76 mL, 8.75 mmol) and the reaction mixture stirred for 15 min under a constant argon purge. Subsequent dropwise addition of alcohol **106** (1.65 g, 5.83 mmol) was followed by stirring for a further 20 min. Triethylamine (4.06 mL, 29.2 mmol) was then added and the reaction allowed to warm to room temperature. TLC suggested completion after 15 min (EtOAc/hexane, 4:6; R_f = 0.54). The reaction mixture was then diluted with aqueous $NaHCO_3$ (50 mL) and extracted with dichloromethane (3 × 30 mL). The organic extract was dried over $MgSO_4$ and the solvent removed under reduced pressure, to give a viscous yellow oil. Purification by chromatography on a silica-gel column (70 g; EtOAc/hexane, 3:7) afforded aldehyde **107** as a yellow oil, (1.60 g, 98%). ν_{max} /cm^{-1} ($CHCl_3$): 2940s + 2872s (C-H, aliphatic), 1710s (C=O, aldehyde), 1495w (C=C, aromatic); ^{1}H NMR (300 MHz, $CDCl_3$) δ_H = 1.64 (4H, m, H-3,4), 2.43 (2H, td, *J* = 7.0, 1.4 Hz, H-2), 3.47 (2H, t, *J* = 6.2 Hz, H-5), 3.64 (8H, m, H-1',2',3',4'), 4.56 (2H, s, H-5'), 7.32 (5H, m, Ar-*H*), 9.73 (1H, d, *J* = 1.4 Hz, H-1).

Methyl *E/Z* 2-{6-[2-Benzyloxyethoxy)-2-ethoxy]-1-hexenyl}-3-furoate (108)

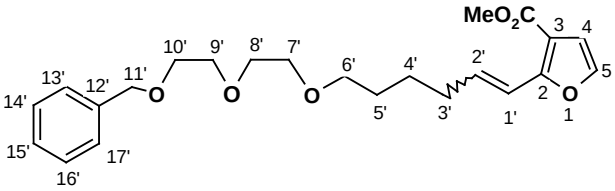

The methyl furanylphosphonium salt **90** (2.68 g, 5.57 mmol) was dissolved in a mixture of dry methanol (30 mL) and sodium methoxide (4.63 M, 1.32 mL, 6.12 mmol) was added *via* syringe under nitrogen at 0^{o}C (ice-water slurry). Aldehyde **107** (1.56 g, 5.57 mmol) was slowly added and the reaction mixture stirred at room temperature. The reaction mixture turned an immediate dark-red colour that progressively faded to a light-orange colour as it went to completion within 3 hrs. The reaction mixture was then diluted with brine (50 mL) and extracted with EtOAc (3 × 30 mL). The organic extract was dried over $MgSO_4$ and the solvent removed under reduced

pressure. A yellow powder was obtained which was subjected to column chromatography using a silica-gel column (70 g; EtOAc/hexane, 1.5:8.5) to afford product **108** as a mixture of *E*- and *Z*-stereoisomers in a 3:2 ratio and as a colourless oil, (1.73 g, 81%). ν_{max} /cm^{-1} ($CHCl_3$): 2928m + 2867s (C-H, aliphatic), 1715s (C=O, ester), 1649m (C=C, alkene), 1567m (C=C, aromatic); ^{1}H NMR of ***E*-isomer** ($CDCl_3$, 400 MHz) δ_H 1.54 (2H, m, H-4'), 1.64 (2H, m, H-5'), 2.28 (2H, qd, *J* = 7.2, 1.3 Hz, H-3'), 3.48 (2H, t, *J* = 6.4 Hz, H-6'), 3.58-3.67 (8H, m, H-7'-H-10'), 3.82 (3H, s, CO_2Me), 4.56 (2H, s, H-11'), 6.49 (1H, dt, *J* = 16.0, 7.1 Hz, H-2'), 6.69 (1H, d, *J* = 2.0 Hz, H-4), 6.94 (1H, dt, *J* = 16.0, 1.4 Hz, H-1'), 7.30 (1H, d, *J* = 2.0 Hz, H-5), 7.33 (5H, m, Ar-H); ^{1}H NMR of ***Z*-isomer** ($CDCl_3$, 400 MHz) δ_H 1.54 (2H, m, H-4'), 1.64 (2H, m, H-5'), 2.61 (2H, qd, *J* = 7.2, 1.3 Hz, H-3'), 3.48 (2H, t, *J* = 6.4 Hz, H-6'), 3.58-3.67 (8H, m, H-7'-H-10'), 3.82 (3H, s, CO_2Me), 4.56 (2H, s, H-11'), 5.82 (1H, dt, *J* = 12.0, 7.6 Hz, H-2'), 6.66 (1H, d, *J* = 2.0 Hz, H-4), 6.88 (1H, dt, *J* = 12.0, 1.7 Hz, H-1'), 7.21 (1H, d, *J* = 2.0 Hz, H-5), 7.33 (5H, m, Ar-H); ^{13}C NMR of ***E*/*Z* isomers** (75 MHz, $CDCl_3$) δ_C 25.5/26.0 (C-4'), 29.1/29.2 (C-5'), 29.4/32.8 (C-3'), 51.3/51.4 (CO_2*Me*), 69.5 (OCH_2), 70.1/70.2 (C-6'), 70.6 (OCH_2), 71.1 (OCH_2), 71.2 (OCH_2), 73.1 (C-11'), 111.2/111.3 (C-4), 112.2 (C-3), 115.9/117.9 (C-1'), 127.5 (C-15'), 127.6 (C-13'/C-17'), 128.3 (C-14'/C-16'), 136.0/136.9 (C-2'), 138.3 (C-12'), 140.7/140.8 (C-5), 157.0/157.6 (C-2), 163.9/164.0 (*C*O_2Me); HRMS (EI): *m/z* 402.20186 [M$^+$]. Calculated for $C_{23}H_{30}O_6$, 402.20424 [M$^+$].

Methyl 2-{6-[2-hydroxyethoxy)-2-ethoxy]-1-hexyl}-3-furoate (109)

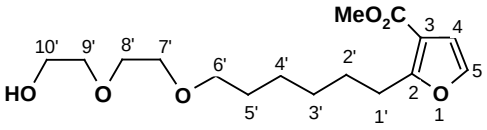

The furan ester **108** (660 mg, 1.64 mmol) was dissolved in absolute ethanol (5 mL) and stirred at room temperature. Subsequent addition of palladium on carbon 10% (175 mg, 0.164 mmol) was followed by careful placement of a hydrogen gas balloon over the reaction flask. TLC (EtOAc/hexane, 3:7; R_f = 0.10) confirmed completion of the reaction after 1 hr. The reaction mixture was filtered through a Celite packed sintered funnel with EtOAc. The organic solvent was then removed under reduced pressure. No purification was performed and the crude material was used in the next step.

Methyl 2-{6-[2-(*p*-toluenesulfonyloxyethoxy)-2-ethoxy]-1-hexyl}-3-furoate (110)

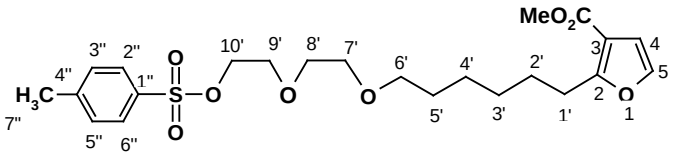

Compound **109** (478 mg, 1.52 mmol) was dissolved in dichloromethane (10 mL). Triethylamine (0.43 mL, 3.04 mmol) was added at 0°C followed by a catalytic amount of DMAP (10 mg, 0.076 mmol) to the reaction mixture. *p*-Toluenesulfonyl chloride (437 mg, 2.29 mmol) dissolved in dichloromethane (2 mL) was then added dropwise and the solution left to stir at room temperature. TLC (EtOAc/hexane, 3:7; R_f = 0.36) confirmed completion of the reaction after 1½ hrs. The reaction mixture was diluted with brine (30 mL) and extracted with dichloromethane (3 × 30 mL). The organic fractions were dried with $MgSO_4$ and the solvent removed under reduced pressure. Purification by chromatography using a silica-gel column (60 g; EtOAc/hexane, 1.5:8.5) afforded product **110** as a colourless oil, (540 mg, 76%). ν_{max} /cm^{-1} ($CHCl_3$): 2937s + 2864s (C-H, aliphatic), 1715s (C=O, ester), 1599s (C=C, aromatic), 1369s + 1177s (-SO_2-O-); ^{1}H NMR (400 MHz, $CDCl_3$) δ_H 1.33 (4H, m, H-3', H-4'), 1.53 (2H, m, H-2'), 1.67 (2H, m, H-5'), 2.41 (3H, s, H-7''), 2.97 (2H, t, *J* = 7.3 Hz, H-1'), 3.39 (2H, t, *J* = 6.6 Hz, H-6'), 3.49 (2H, m, H-7'), 3.55 (2H, m, H-8'), 3.68 (2H, m, H-9'), 3.80 (3H, s, CO_2CH_3), 4.15 (2H, m, H-10'), 6.62 (1H, s, H-4), 7.22 (1H, s, H-5), 7.31 + 7.79 (4H, 2 × d, J_{AB} = 8.4 Hz, H-2'', 3'', 5'', 6''); ^{13}C NMR (75 MHz, $CDCl_3$) δ_C 21.5 (C-7''), 25.7 + 27.8 + 28.9 + 29.4 (C-2',3',4',5'), 27.4 (C-1'), 51.2 (CO_2CH_3), 68.7 (C-9'), 69.2 (C-10'), 70.0 (C-7'), 70.7 (C-8'), 71.4 (C-6'), 110.5 (C-4), 112.8 (C-3), 127.9 (C-2'', C-6''), 129.7 (C-3'', C-5''), 133.1 (C-4''), 140.3 (C-5), 144.7 (C-1''), 163.2 (C-2), 164.4 (CO_2CH_3); HRMS (EI): *m/z* 468.18380 [M^+]. Calculated for $C_{23}H_{32}O_8S$, 468.18179 [M^+].

2-{6-[2-Propargyloxyethoxy)-2-ethoxy]-1-hexyl}furan-3-carboxylic acid (111)

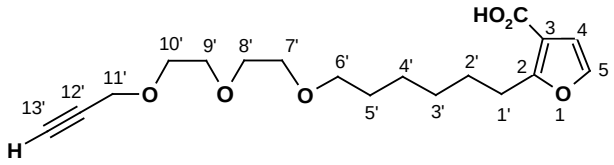

To a sodium hydride (60%, 69 mg, 1.72 mmol) suspension in THF (2 mL) at 0°C, was added propargyl alcohol (0.13 mL, 2.14 mmol) slowly whilst stirring. To this was added **110** (200 mg, 0.43 mmol) and the reaction mixture refluxed. After 1 hr 1M NaOH (4 drops) was added and the reaction mixture refluxed for a further hour. TLC (EtOAc/hexane, 3:7; R_f = 0.10) confirmed completion after a total of 2 hrs. The reaction mixture was diluted with 1M HCl (20 mL) and extracted with EtOAc (2 × 30 mL). The organic fractions were dried with $MgSO_4$ and the solvent removed under reduced pressure. Purification by chromatography using a silica-gel column (12 g; EtOAc/hexane, 3:7) afforded product **111** as a colourless oil, (138 mg, 95%). ν_{max} /cm^{-1} ($CHCl_3$): 3157b (O-H, H-bonded), 2935s + 2865s (C-H, aliphatic), 2254s (C≡C, alkyne), 1683s (C=O, carboxylic acid), 1596s (C=C, aromatic); ^{1}H NMR (400 MHz, $CDCl_3$) δ_H 1.36 (4H, m, H-3',4'), 1.57 (2H, quin, *J* = 6.9 Hz, H-2'), 1.70 (2H, quin, *J* = 7.3 Hz, H-5'), 2.41 (1H, t, *J* = 2.4 Hz, H-13'), 3.01 (2H, t, *J* = 7.4 Hz, H-1'), 3.45 (2H, t, *J* = 6.4 Hz, H-6'), 3.58 - 3.70 (8H, m, H-7',8',9',10'), 4.20 (2H, d, *J* = 2.4 Hz, H-11'), 6.67 (1H, d, *J* = 2.1 Hz, H-4), 7.26 (1H, d, *J* = 2.1 Hz, H-5); ^{13}C NMR (75 MHz, $CDCl_3$) δ_C 25.6 (CH_2), 27.4 (CH_2), 27.7 (CH_2), 28.7 (CH_2), 29.4 (CH_2), 58.4 (C-11'), 69.1 (OCH_2), 70.0 (OCH_2), 70.4 (OCH_2), 70.7 (C-6'), 71.3 (OCH_2), 74.4 (C-13'), 79.6 (C-12'), 110.9 (C-4), 112.6 (C-3), 140.6 (C-5), 164.4 (C-2), 168.5 (*C*O_2H); HRMS (EI): *m/z* 338.17678 [M^+]. Calculated for $C_{18}H_{26}O_6$, 338.17294 [M^+].

2-{6-[2-Propargyloxyethoxy)-2-ethoxy]-1-hexyl}furan-3-carboxylic acid [4-chloro-3-(3-methylbut-2-enyloxy)phenyl]amide (112)

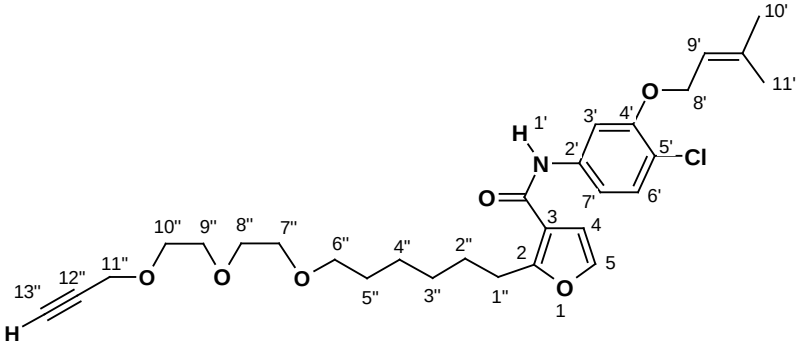

The acid **111** (108 mg, 0.32 mmol) was dissolved in thionyl chloride (1 mL) and the mixture heated to 40^{o}C under nitrogen for 1 hr with constant stirring. The excess thionyl chloride was then reduced on a vacuum pump and the resulting oil dissolved in dichloromethane (3 mL). Subsequent addition of pyridine (0.08 mL, 0.96 mmol) at 0^{o}C was followed by the arylamine **61** (68 mg, 0.32 mmol) and the reaction mixture stirred at room temperature. TLC (EtOAc/hexane, 3:7; R_f = 0.35) confirmed completion of the reaction after 30 min. The reaction mixture was diluted with EtOAc (50 mL) and extracted with 1M HCl (4 × 15 mL). The organic fractions were dried with $MgSO_4$ and the solvent removed under reduced pressure. Purification by chromatography using a silica-gel column (10 g; EtOAc/hexane, 1.5:8.5) afforded product **112** as a yellow oil, (133 mg, 78%). ν_{max} /cm^{-1} ($CHCl_3$): 3304s + 3440 m (N-H, amide), 2935s + 2864s (C-H, aliphatic), 2253s (C≡C, alkyne), 1674s (C=O, amide), 1595s (N -H and C-N stretching), 1513s + 1492s (C=C, aromatic); ^{1}H NMR (400 MHz, $CDCl_3$) δ_H 1.34 - 1.69 (8H, m, H-2'',3'',4'',5''), 1.74 + 1.78 (6H, 2 × s, H-10',11'), 2.39 (1H, t, *J* = 2.4 Hz, H-13''), 3.02 (2H, t, *J* = 7.5 Hz, H-1''), 3.41 (2H, t, *J* = 6.8 Hz, H-6''), 3.55 - 3.67 (8H, m, H-7'',8'',9'',10''), 4.17 (2H, d, *J* = 2.4 Hz, H-11''), 4.58 (2H, d, *J* = 6.6 Hz, H-8'), 5.51 (1H, tq, *J* = 6.6, 1.4 Hz, H-9'), 6.55 (1H, d, *J* = 2.1 Hz, H-4), 6.91 (1H, dd, *J* = 8.7, 2.4 Hz, H-7'), 7.25 (1H, d, *J* = 8.7 Hz, H-6'), 7.29 (1H, d, *J* = 2.1 Hz, H-5), 7.54 (1H, d, *J* = 2.4 Hz, H-3'), 7.58 (1H, s, NH); ^{13}C NMR (75 MHz, $CDCl_3$) δ_C 18.1 × 2 (CH_3), 25.8 (CH_2), 27.2 (C-1''), 27.4 (CH_2), 29.0 (CH_2), 29.5 (CH_2), 58.3 (C-11''), 66.1 (C-8'), 66.2 (OCH_2), 69.2 (OCH_2), 70.2 (C-6''), 70.7 (OCH_2), 71.5 (OCH_2), 74.5 (C-13''), 79.6 (C-12''), 106.2 (C-3'), 107.9 (C-4), 112.5 (C-7'), 115.5 (C-3), 117.9 (C-5'), 119.2 (C-9'), 129.9 (C-6'), 137.6 (C-2'), 138.3 (C-12'), 140.5 (C-5), 154.6 (C-4'), 161.9 (C-2), 161.9 (*C*ONH); HRMS (EI): *m/z* 531.24061 [M^{+}]. Calculated for $C_{29}H_{38}O_6NCl$, 531.23877 [M^{+}].

5-{16-[3-{4-chloro-3-(3-methyl-but-2-enyl-1-oxy)phenylcarbamoyl)furan-2-yl]-4,7,10-trioxahexadeca-1-ynyl}uridine-2',3'-didehydro-2',3'-dideoxy-5'-O-benzoate (113)

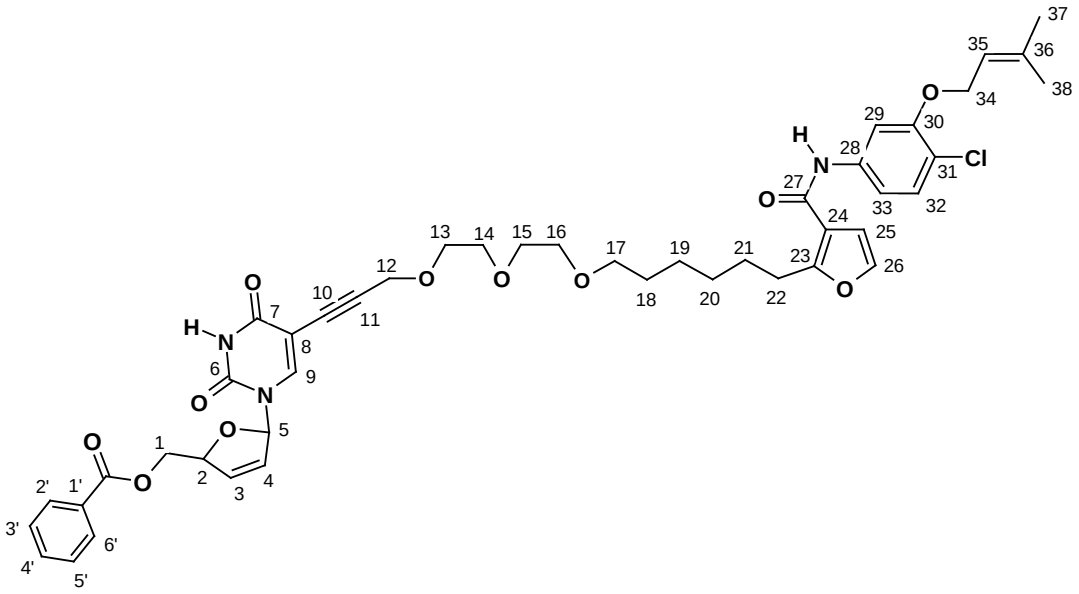

Amide **112** (50 mg, 0.09 mmol) was added together with the 5-iodo-d4U benzoate **60** (41 mg, 0.094 mmol) and the mixture dried carefully on a vacuum pump. A mixture of degassed DMF:THF (1:2 (v/v), 1 mL) was then added to the reaction vessel whilst the mixture stirred at room temperature under nitrogen. Subsequent addition of triethylamine (0.03 mL, 0.20 mmol) was followed by addition of copper(I) iodide (8.95 mg, 0.05 mmol) and tetrakistriphenylphosphinepalladium (10.9 mg, 0.01 mmol) respectively. The reaction was stirred continuously at room temperature and TLC (EtOAc/hexane, 3:7; R_f = 0.24) confirmed completion of the reaction after 2 hrs. The reaction mixture was diluted with a 5% EDTA solution (30 mL) and extracted with chloroform (3 × 20 mL). The organic fractions were dried with $MgSO_4$ and the solvent removed under reduced pressure. Purification by chromatography using a silica-gel column (10 g; EtOAc/hexane, 3:7) afforded product **113** as a clear oil, (48 mg, 61%). ν_{max} /cm^{-1} ($CHCl_3$): 2932s (C-H, aliphatic), 2254s (C≡C, alkyne), 1720s (C=O, ester), 1693s (C=O, amide), 1599s (N-H and C-N stretching), 1514s + 1492s (C=C, aromatic); ^{1}H NMR (400 MHz, $CDCl_3$) δ_H 1.35 - 1.69 (8H, m, H-18,19,20,21), 1.74 (3H, s, H-37/H-38), 1.79 (3H, s, H-37/H-38), 3.04 (2H, t, *J* = 7.7 Hz, H-22), 3.42 (2H, t, *J* = 6.6 Hz, H-17), 3.65 (8H, m, H-13,14,15,16), 4.24 (2H, s, H-12), 4.60 (4H, m, H-1, H-34), 5.20 (1H, s, H-2), 5.51 (1H, tq, *J* = 6.6, 1.4 Hz, H-35), 5.99 (1H, d, J_{AB} = 5.8 Hz, H-3), 6.41 (1H, d, J_{AB} = 5.8 Hz, H-4), 6.55 (1H, d, J_{AB} = 1.4 Hz, H-25), 6.89 (1H, m, H-33), 6.93 (1H, s, H-5), 7.26 (1H, m, H-32), 7.30 (1H, d, J_{AB} = 1.4 Hz, H-26), 7.45 - 7.55 (5H, m, H-2',3',4'), 7.77 (1H, s, H-9), 8.01 (1H, m, H-29), 8.03 (1H, s, NH), 8.63 (1H, bs, NH); ^{13}C NMR

(75 MHz, $CDCl_3$) δ_C 18.3 (C-37/C-38), 25.7 (C-37/C-38), 25.8 (CH_2), 27.4 (C-22), 27.8 (CH_2), 28.9 (CH_2), 29.4 (CH_2), 58.8 (C-12), 64.9 (C-1), 66.1 (C-34), 68.1 (OCH_2), 69.3 (OCH_2), 70.3 (C-17), 70.6 (OCH_2), 71.3 (OCH_2), 71.3 (C-8), 75.3 (C-10), 85.0 (C-2), 90.6 (C-5), 101.0 (C-11), 106.2 (C-29), 108.0 (C-25), 112.4 (C-33), 115.4 (C-24), 117.9 (C-31), 119.1 (C-35), 127.0 (C-4), 128.7 (C-3', C-5'), 129.3 (C-1'), 129.8 (C-2', C-6'), 129.9 (C-32), 133.5 (C-3), 133.6 (C-4'), 137.6 (C-28), 138.5 (C-36), 140.6 (C-26), 144.0 (C-9), 150.0 (C-6), 154.6 (C-30), 159.6 (C-23), 161.9 (*CO*NH), 162.0 (C-7), 166.3 (O*CO*C_6H_5).

Uridine-2',3',5'-trimesylate (83)[138]

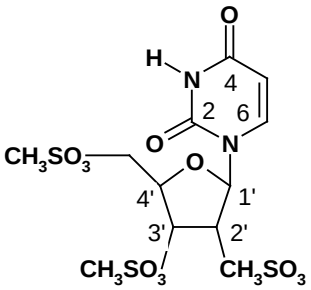

Methanesulfonyl chloride (8.7 mL, 113 mmol) was added to a cold and stirring solution of uridine (6.1 g, 25 mmol) in pyridine (35 mL) at 0°C. The reaction mixture was stirred at 0°C for 5 hrs and then poured into an ice-water slurry (250 mL) with stirring. The resulting mixture was then stirred for a further 10 min. The precipitate formed was collected by filtration and washed with water (3 × 100 mL) and dried to give **83** as a white solid (12.1 g, 100%). Mp: 170-171 °C (lit. 184-186°C); ^{1}H NMR (400 MHz, DMSO-d_6) δ_H 3.22 (3H, s, O_3SCH_3), 3.33 (3H, s, O_3SCH_3), 3.35 (3H, s, O_3SCH_3), 4.46 (2H, m, H-5'), 4.53 (1H, m, H-4'), 5.35 (1H, t, *J* = 5.3 Hz, H-3'), 5.60 (1H, t, *J* = 5.3 Hz, H-2'), 5.69 (1H, m, *J* = 1.5, 8.0 Hz, H-5), 5.97 (1H, d, *J* = 4.4 Hz, H-1'), 7.69 (1H, d, = 8.0 Hz, H-6); ^{13}C NMR (75 MHz, DMSO-d_6) δ_C 36.9 (O_3SCH_3), 37.9 (O_3SCH_3), 37.9 (O_3SCH_3), 67.3 (C-5'), 74.0 (C-3'), 76.0 (C-2'), 78.5 (C-4'), 88.7 (C-1'), 102.3 (C-5), 141.5 (C-6), 150.3 (C-2), 162.9 (C-4).

5'-O-Benzoyl-3'-O-methanesulfonyl-2'-anhydrouridine (84)[138]

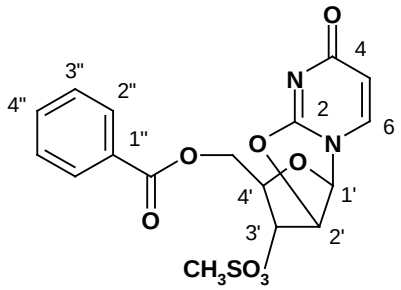

Trimesylate **83** (3.0 g, 6.3 mmol) was added to a stirred slurry of sodium benzoate (3.16 g, 21.9 mmol) in acetamide (25 g) at 115 ^{o}C. The reaction mixture was stirred at 115 ^{o}C for 65 min and then poured into an ice-water slurry (600 mL). The mixture was stirred at 0 ^{o}C for 15 min. The white solid was filtered, washed with water and dried to afford **84** (1.93, 75%) as colourless needles. Mp: 243-244 ^{o}C (lit. 226-227 ^{o}C); ^{1}H NMR (400 MHz, DMSO-d_6) δ_H 3.43 (3H, s, O_3SCH_3), 4.22 (1H, dd, *J* = 7.4, 12.1 Hz, H-5'), 4.33 (1H, dd, *J* = 4.8, 12.1 Hz, H-5'), 4.77 (1H, m, H-4'), 5.62 (1H, d, *J* = 2.4 Hz, H-3'), 5.69 (1H, d, *J* = 5.6 Hz, H-2'), 5.87 (1H, d, *J* = 7.6 Hz, H-5), 6.45 (1H, d, *J* = 5.6 Hz, H-1'), 7.49 (2H, t, *J* = 7.8 Hz, H-3'', H-5''), 7.65 (1H, m, H-4''), 7.89 (3H, m, H-6, H-2'', H-6''); ^{13}C NMR (75 MHz, DMSO-d_6) δ_C 37.5 (O_3SCH_3), 62.5 (C-5'), 80.9 (C-3'), 82.1 (C-4'), 86.0 (C-2'), 89.7 (C-1'), 109.0 (C-5), 128.7 (C-3'', C-5''), 128.9 (C-1''), 129.2 (C-2'', C-6''), 133.5 (C-4''), 136.5 (C-6), 159.2 (C-2), 165.1 (C-4), 170.6 (C=O).

5'-O-Benzoyl-2'-bromo-3'-O-methanesulfonyl-2'-deoxyuridine (85)[138]

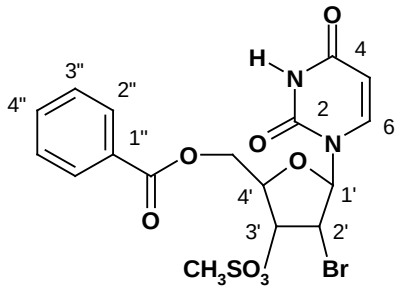

Acetyl bromide (2.5 mL, 33.9 mmol) was added dropwise to a stirring mixture of 5'-O-Benzoyl-3'-O-methanesulfonyl-2'-anhydrouridine **84** (1.90 g, 4.8 mmol) in EtOAc (50 mL) and MeOH (5 mL). The mixture was refluxed for 1 hr and then cooled. To the reaction mixture was added EtOAc (3 × 50 mL) and the organic layer washed with aq. $NaHCO_3$ (50 mL) followed by brine (50 mL). The organic layer was dried over $MgSO_4$ and the solvent removed under reduced pressure. The crude product was recrystallized from EtOAc/pet. ether to afford **85** as a white solid (2.23 g, 97%). ^{1}H NMR (400 MHz, $CDCl_3$) δ_H 3.18 (3H, s, O_3SCH_3), 4.65 (3H, m, H-4', H-5'), 4.74 (1H, m, H-2'), 5.27 (1H, m, H-3'), 5.60 (1H, d, *J* = 8.1 Hz, H-5), 6.12 (1H, d, *J* = 5.4 Hz, H-1'), 7.31 (1H,

d, *J* = 8.1 Hz, H-6), 7.46 (2H, m, H-3'', H-5''), 7.60 (1H, m, H-4''), 8.01 (2H, m, H-2'', H-6''), 9.49 (1H, brs, NH); ^{13}C NMR (75 MHz, $CDCl_3$) δ_C 38.8 (O_3SCH_3), 47.2 (C-2'), 62.2 (C-5'), 75.6 (C-3'), 80.7 (C-4'), 91.9 (C-1'), 103.4 (C-5), 128.7 (C-3'', C-5''), 129.0 (C-1''), 129.6 (C-2'', C-6''), 133.8 (C-4''), 139.6 (C-6), 150.0 (C-2), 162.8 (C-4), 165.9 (C_6H_5*OCO*).

5'-O-Benzoyl-2',3'-didehydro-2',3'-dideoxyuridine (86)[138]

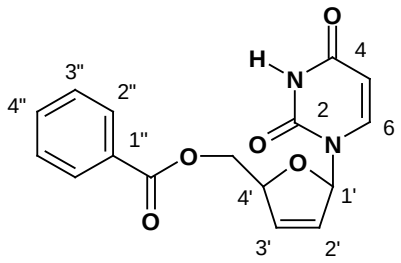

Acetic acid (0.25 mL) and zinc dust (0.50 g, 7.69 mmol) were added to a suspension of **85** (2.19 g, 4.61 mmol) in a mixture of EtOAc (40 mL) and MeOH (13 mL) at 18 ^{o}C. After 3.5 hrs, the excess zinc was removed by filtration and the cake was washed with a 3:1 mixture of EtOAc/MeOH (2 × 20 mL). The solvent was removed under reduced pressure and more 3:1 mixture of EtOAc/MeOH (6 mL) added. To this solution was then added water (75 mL) and the solution stirred for 30 min. The resulting precipitate was filtered and the product washed with water and dried (over P_2O_5) to afford **86** as colourless crystals (1.14 g, 83%). Mp: 141-142 ^{o}C (lit. 138.5-139 ^{o}C); ^{1}H NMR (400 MHz, $CDCl_3$) δ_H 4.53 (1H, dd, *J* = 2.9, 12.7 Hz, H-5'), 4.70 (1H, dd, *J* = 3.6, 12.7 Hz, H-5'), 5.16 (1H, m, H-4'), 5.33 (1H, d, *J* = 8.3 Hz, H-5), 5.89 (1H, dq, *J* = 1.4, 5.9 Hz, H-2'), 6.39 (1H, dt, *J* = 1.7, 5.9 Hz, H-3'), 7.00 (1H, m, H-1'), 7.34 (1H, d, *J* = 8.3 Hz, H-6), 7.46 (2H, m, H-3'', H-5''), 7.60 (1H, m, H-4''), 7.99 (2H, m, H-2'', H-6''), 9.10 (1H, brs, NH); ^{13}C NMR (75 MHz, $CDCl_3$) δ_C 64.5 (C-5'), 84.8 (C-4'), 89.8 (C-1'), 102.7 (C-5), 127.2 (C-2'), 128.6 (C-3'', C-5''), 129.6 (C-2'', C-6''), 135.6 (C-3'), 133.6 (C-4''), 133.8 (C-1''),139.8 (C-6), 150.6 (C-2), 163.0 (C-4), 166.1 (C_6H_5*OCO*).

5'-O-Benzoyl-2',3'-didehydro-2',3'-dideoxyuridine (60)[138]

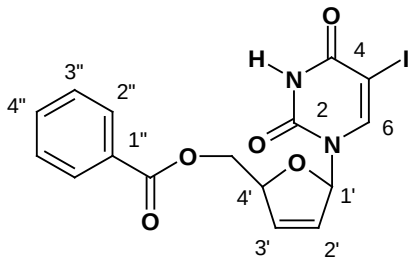

Cerium ammonium nitrate (IV) (0.77 g, 1.4 mmol) and iodine (0.43 g, 1.68 mmol) were added to a solution of 5'-O-Benzoyl-2'-3'-didehydro-2'3'-dideoxyuridine **86** (0.88 g, 2.8 mmol) in CH_3CN (40 mL). The mixture was stirred at 35 ^oC for 4 hrs. EtOAc (170 mL) was added to the residue and the solid product formed was removed by filtration. The filtrate was washed with a solution of $NaHSO_3$ (2 × 100 mL), water (2 × 100 mL), the organic layer dried over $MgSO_4$ and the solvent removed under reduced pressure. Recrystallization using CH_2Cl_2/pet. ether gave **60** as white needles (1.05 g, 85%). Mp: 141-142 ^oC (lit. 138.5-139 ^oC); ^1H NMR (400 MHz, Acetone-d_6) δ_H 4.57 (1H, dd, *J* = 3.2, 12.3 Hz, H-5'), 4.63 (1H, dd, *J* = 4.4, 12.3 Hz, H-5'), 5.25 (1H, m, H-4'), 6.16 (1H, dq, *J* = 1.1, 6.1 Hz, H-2'), 6.60 (1H, dt, *J* = 1.7, 6.1 Hz, H-3'), 6.88 (1H, m, H-1'), 7.53 (2H, m, H-3'', H-5''), 7.64 (1H, m, H-4''), 7.86 (1H, s, H-6), 8.04 (2H, m, H-2'', H-6''), 10.37 (1H, brs, NH); ^{13}C NMR (75 MHz, Acetone-d_6) δ_C 65.0 (C-5'), 68.9 (C-5), 85.1 (C-4'), 90.6 (C-1'), 127.1 (C-2'), 128.8 (C-3'', C-5''), 129.3 (C-1''), 129.8 (C-2'', C-6''), 133.5 (C-3'), 133.5 (C-4''), 144.1 (C-6), 150.2 (C-2), 159.9 (C-4), 166.4 (C_6H_5*OCO*).

2-Chloro-5-nitrophenol (119a)

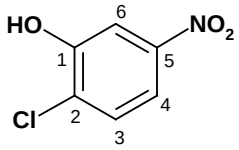

A reaction flask was charged with conc. HCl (20 mL) at 0 ^oC. To this was slowly added a mixture of 2-amino-5-nitrophenol (6.56 g, 42.6 mmol) and sodium nitrite (3.32 g, 48.2 mmol) in H_2O (7.5 mL). The reaction mixture was stirred for 3 hrs at 0^oC, after which sulfamic acid (0.15 g) was added slowly. The resulting mixture was then carefully added to a vigorously stirring 20% HCl solution (5 mL) containing copper(I)chloride (0.85 g, 85.8 mmol) over 1hr. TLC confirmed reaction completion after stirring at r.t. for a further 1 hr. The reaction mixture was diluted with 1M HCl (60 mL) and extracted EtOAc (3 × 100 mL), the organic layer dried over $MgSO_4$ and the solvent removed under reduced pressure. Purification by chromatography using a silica-gel column (100 g; EtOAc/hexane, 2:8) afforded product **119a** as a yellow precipitate, (4.61 g, 70%). Mp. 102-103 ^oC; ν_{max} /cm^{-1} ($CHCl_3$): 1629s (C=C, aromatic), 1523s + 1346s (N-O, aromatic nitro), 738s (C-Cl, halogen); ^1H NMR (Acetone-D_6, 400 MHz) δ_H 7.63 (1H, d, *J* = 8.8 Hz, H-3), 7.74 (1H, dd, *J* = 8.8, 2.6 Hz, H-4), 7.84 (1H, d, *J* = 2.6 Hz, H-6), 9.73 (1H, bs, OH); ^{13}C NMR (Acetone-D_6, 100 MHz) δ_C 111.3 (C-6), 115.5 (C-4), 127.9 (C-3), 130.9 (C-2), 148.1 (C-5), 153.8 (C-1); HRMS (EI): *m/z* 172.98877 [M^+]. Calculated for $C_6H_4O_3NCl$, 172.98846 [M^+]; C, H, N Microanalysis found: C, 41.56; H, 2.50; N, 7.72%; $C_6H_4O_3NCl$ requires C, 41.52; H, 2.38; N, 8.07%.

5-Amino-2-chlorophenol (119b)

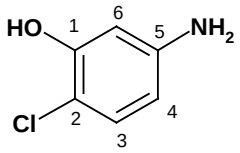

Iron mesh (1.20 g, 20 mmol) was added to a mixture of ethanol (5 mL), H_2O (1 mL) and HCl (0.2 mL), and the reaction heated. The reaction flask was fitted with a dropping funnel containing 2-chloro-5-nitrophenol **119a** dissolved in ethanol (1 mL), and upon refluxing of the reaction mixture the contents of the funnel was dropped in slowly. TLC confirmed reaction completion after 2 hrs. The solution was cooled, filtered through a Celite pad and washed with hot ethanol (10 mL). The solvent was removed under reduced pressure. Purification by chromatography using a silica-gel column (80 g; EtOAc/hexane, 6:4) afforded product **119b** as a white precipitate, (0.60 g, 73%). Mp. 97-99 ^{o}C; ν_{max} /cm^{-1} ($CHCl_3$): 3387s + 3321s (NH, primary amine), 1632s (C=C, aromatic), 815m (C-Cl, halogen); ^{1}H NMR (Acetone-D_6, 400 MHz) δ_H 4.62 (2H, bs, NH_2), 6.19 (1H, dd, *J* = 8.8, 2.6 Hz, H-4), 6.34 (1H, d, *J* = 2.6 Hz, H-6), 6.94 (1H, d, *J* = 8.8 Hz, H-3), 8.06 (1H, bs, OH); ^{13}C NMR (Acetone-D_6, 100 MHz) δ_C 102.7 (C-6), 107.6 (C-4), 107.8 (C-2), 129.9 (C-3), 149.0 (C-5), 153.4 (C-1); HRMS (EI): *m/z* 143.01377 [M^+]. Calculated for $C_6H_6N_3ClO$, 143.01379 [M^+]; C, H, N Microanalysis found: C, 50.69; H, 4.17; N, 9.24%; $C_6H_6N_3ClO$ requires C, 50.69; H, 4.21; N, 9.76%.

4-Chloro-3-(3-methyl-but-2-enyl-1-oxy)nitrobenzene (119c)

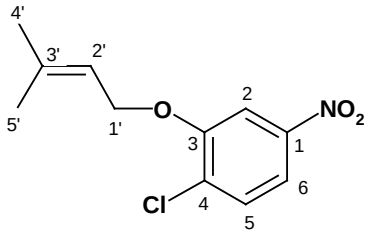

To a solution of 2-chloro-5-nitrophenol **119a** (5.09 g, 29 mmol) dissolved in methyl ethyl ketone (25 mL) was added both K_2CO_3 (4.50 g, 32.5 mmol) and *tetra*-butylammonium iodide (500 mg). Finally, 4-bromo-2-methyl-2-butene (4 mL, 35 mmol) was added and the reaction mixture stirred at r.t overnight. The solution was diluted with H_2O (100 mL) and extracted with EtOAc (3×100 mL). The combined organic extracts were then washed with brine (100 mL), dried over $MgSO_4$ and the solvent removed under reduced pressure. Purification by chromatography using a silica-gel column (70 g; EtOAc/hexane, 0.1:99.9) afforded product **119c** as a white precipitate, (6.7 g, 94%). Mp. 90-93 ^{o}C; ν_{max} /cm^{-1} ($CHCl_3$): 2978m + 2930m (CH, aliphatic), 1638s (C=C, aromatic), 1528s + 1352s (N-O, nitro aromatic), 738s (C-Cl, halogen); ^{1}H NMR ($CDCl_3$, 400 MHz) δ_H 1.80

(3H, d, *J* = 1.5 Hz, H-5'), 1.81 (3H, d, *J* = 1.5 Hz, H-4'), 4.70 (2H, d, *J* = 7.0 Hz, H-1'), 5.49 (1H, tsep, *J* = 7.0, 1.5 Hz, H-2'), 7.50 (1H, d, *J* = 8.8 Hz, H-5), 7.78 (1H, dd, *J* = 8.8, 2.6 Hz, H-6), 7.79 (1H, d, *J* = 2.6 Hz, H-2); ^{13}C NMR ($CDCl_3$, 100 MHz) δ_C 18.3 (C-4'), 25.9 (C-5'), 66.6 (C-1'), 108.2 (C-2), 116.0 (C-6), 118.8 (C-2'), 130.4 (C-5), 130.5 (C-4), 140.7 (C-3'), 148.2 (C-1), 155.8 (C-3); HRMS (EI): *m/z* 241.05048 [M^+]. Calculated for $C_{11}H_{12}NO_3Cl$, 241.05057 [M^+]; C, H, N Microanalysis found: C, 54.62; H, 5.10; N, 5.81%; $C_{11}H_{12}NO_3Cl$ requires C, 54.67; H, 5.01; N, 5.79%.

4-Chloro-3-(3-methyl-but-2-enyloxy)aniline (61)

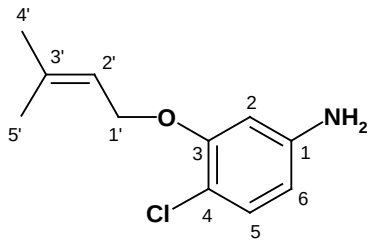

Iron mesh (3.27 g, 58.5 mmol) was added to a mixture of ethanol (10 mL), H_2O (2 mL) and HCl (0.23 mL), and the reaction heated. The reaction flask was fitted with a dropping funnel containing 4-chloro-3-(3-methyl-but-2-enyl-1-oxy)nitrobenzene **119c** (4.03 g, 16.7 mmol) dissolved in ethanol (5 mL), and upon refluxing of the reaction mixture the contents of the funnel were slowly dropped in. TLC confirmed reaction completion after 3½ hrs. The solution was cooled, filtered through a Celite pad and washed with hot ethanol (200 mL). The solvent was removed under reduced pressure. Purification by chromatography using a silica-gel column (100 g; EtOAc/hexane, 0.5:9.5) afforded product **61** as a white precipitate, (3.10 g, 88%). Mp. 82-85 ^{o}C; ν_{max} /cm^{-1} ($CHCl_3$): 3387s + 3321s (NH, primary amine), 2978m + 2930m (CH, aliphatic), 1638s (C=C, aromatic), 738s (C-Cl, halogen); ^{1}H NMR ($CDCl_3$, 300 MHz) δ_H 1.73 (3H, d, *J* = 1.5 Hz, H-5'), 1.78 (3H, d, *J* = 1.5 Hz, H-4'), 3.63 (2H, bs, NH_2), 4.53 (2H, d, *J* = 7.0 Hz, H-1'), 5.50 (1H, tsep, *J* = 7.0, 1.5 Hz, H-2'), 6.21 (1H, dd, *J* = 8.8, 2.6 Hz, H-6), 6.27 (1H, d, *J* = 2.6 Hz, H-2), 7.09 (1H, d, *J* = 8.8 Hz, H-5); ^{13}C NMR ($CDCl_3$, 75.5 MHz) δ_C 18.2 (C-4'), 25.7 (C-5'), 65.9 (C-1'), 101.5 (C-2), 107.9 (C-6), 112.1 (C-4), 119.5 (C-2'), 130.4 (C-5), 137.8 (C-3'), 146.2 (C-1), 154.9 (C-3); HRMS (EI): *m/z* 211.07668 [M^+]. Calculated for $C_{11}H_{14}NOCl$, 211.07652 [M^+]; C, H, N Microanalysis found: C, 62.44; H, 6.77; N, 6.64%; $C_{11}H_{14}NOCl$ requires C, 62.41; H, 6.67; N, 6.62%.

4-Chloro-3-propargyloxyaniline (120)

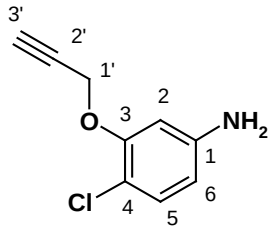

To a solution of **119b** (200 mg, 1.40 mmol) dissolved in acetone (7 mL) was added anhydrous K_2CO_3 (207 mg, 1.50 mmol) at room temperature. Propargyl bromide (0.15 mL, 1.7 mmol) was slowly added to this mixture followed by *tetra*-butylammonium iodide (30 mg, cat.). The reaction mixture was left to react at room temperature. After 5 hrs, the mixture was diluted with H_2O (50 mL) and extracted with EtOAc (3 × 50 mL), the organic layer dried over $MgSO_4$ and the solvent removed under reduced pressure. Purification by chromatography afforded product **120** as a red viscous oil, (200 mg, 79%). ν_{max} /cm^{-1} ($CHCl_3$): 3387s + 3321s (NH), 2253s (C≡C), 1632s (C=C, Ar), 815m (C-Cl); ^{1}H NMR ($CDCl_3$, 300 MHz) δ_H 2.54 (1H, t, *J* = 2.4 Hz, H-3'), 3.75 (2H, bs, NH_2), 4.71 (2H, d, *J* = 2.4 Hz, H-1'), 6.25 (1H, dd, *J* = 8.8, 2.6 Hz, H-6), 6.42 (1H, d, *J* = 2.6 Hz, H-2), 7.11 (1H, d, *J* = 8.8 Hz, H-5); ^{13}C NMR ($CDCl_3$, 75 MHz) δ_C 56.8 (C-1'), 76.0 (C-3'), 78.2 (C-2'), 101.9 (C-2), 109.0 (C-6), 112.3 (C-4), 130.6 (C-5), 146.3 (C-1), 153.7 (C-3). HRMS (EI): *m/z* 182.0376 $[M+H]^+$. Calculated for C_9H_9NOCl, 182.0373 $[M+H]^+$.

[2-(Triphenylphosphoniummethyl)-6-methylnitrobenzene] bromide (122)

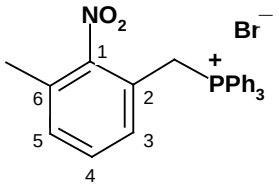

Triphenylphosphine (3.8 g, 14.4 mmol) and 2-(bromomethyl)-6-methylnitrobenzene **121** (3.3 g, 14.4 mmol) were dissolved in toluene (100 mL) and the solution refluxed for 12 hrs. The salt was filtered-off and washed with EtOAc (100 mL), affording product **122** as a white precipitate, (2.5 g, 78%). Mp. = 165 – 168^{o}C; ν_{max} /cm^{-1} ($CHCl_3$): 2986s (CH, aliphatic), 1639s (C=C, aromatic); 1528s + 1375s (N-O, nitro aromatic); ^{1}H NMR ($CDCl_3$, 300 MHz) δ_H 2.15 (3H, s, $ArCH_3$), 5.21 (2H, d, J_{HP} = 15.0 Hz, CH_2P), 7.06 (1H, d, *J* = 7.8 Hz, H-3), 7.35 (1H, t, J = 7.8 Hz, H-4), 7.47 (1H, d, *J* = 7.8 Hz, H-5), 7.65-7.74 (12H, m, Ph), 7.90 (3H, m, Ph); ^{13}C NMR ($CDCl_3$, 75.5 MHz) δ_C 17.4 ($ArCH_3$), 25.7 (d, J_{CP} = 38 Hz, CH_2P), 116.7 (C-2), 117.5 (Ph_q), 120.9 (C-6), 130.1 (Ph_m), 131.1 (C-3/C-5), 131.3 (C-4), 132.3 (C-3/C-5), 133.9 (Ph_o), 135.2 (Ph_p), 150.5 (C-1); HRMS (EI):

m/z 491.06439 [M^+]. Calculated for $C_{26}H_{23}O_2NPBr$, 491.06491 [M^+]; C, H, N Microanalysis found: C, 63.17; H, 4.70; N, 2.74%; $C_{26}H_{23}O_2NPBr$ requires C, 63.17; H, 4,75; N, 2.85%.

4-Bromo-2,6-dimethylaniline (124)

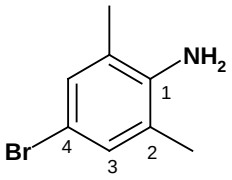

2,6-Dimethylaniline (2.0 g, 16.5 mmol) was dissolved in AcOH (20 mL). The temperature of the solution was lowered to 0^{o}C and ammonium bromide (1.9 g, 20 mmol) added. After stirring for 5 min, H_2O_2 (1.14 mL, 20 mmol) was carefully dropped into the mixture and the reaction allowed to warm to room temperature. The solution was diluted with aq. $NaHCO_3$ (200 mL) and extracted with EtOAc (3 × 200 mL), dried over $MgSO_4$ and the solvent removed under reduced pressure. Purification by chromatography using a silica-gel column (100 g; EtOAc/hexane, 1:9) afforded product **124** as a dark-red oil, (1.6 g, 49%). ν_{max} /cm^{-1} ($CHCl_3$): 3491s + 3379s (NH, primary amine), 2965m + 2939m (CH, aliphatic), 1639s (C=C, aromatic); 794m (C-Br, halogen); ^{1}H NMR ($CDCl_3$, 300 MHz) δ_H 2.14 (6H, s, $ArCH_3$), 4.11 (2H, bs, NH_2), 7.17 (2H, s, H-3); ^{13}C NMR ($CDCl_3$, 75.5 MHz) δ_C 17.1 ($ArCH_3$), 113.7 (C-4), 121.3 (C-2), 131.9 (C-3), 147.2 (C-1); HRMS (EI): *m/z* 198.99959 [M^+]. Calculated for $C_8H_{10}BrN$, 198.99966 [M^+].

4-Cyano-2,6-dimethylaniline (126)

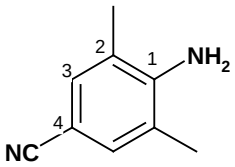

4-Bromo-2,6-dimethylaniline **124** (1.2 g, 5.8 mmol) was dissolved in DMF (10 mL) and CuCN (0.63 g, 7.0 mmol) added. The mixture was refluxed for 6 hrs after which TLC confirmed reaction completion. The reaction mixture was then poured into a freshly prepared aqueous ferric chloride solution (2.4 g) in conc. HCl (6 mL), H_2O (40 mL). The resulting mixture was heated to 70^{o}C and stirred vigorously for 20 min. After cooling, the mixture was extracted with diethyl ether (3 × 100 mL). The combined organic fractions were washed again with HCl (100 mL), H_2O (100 mL) and 10% NaOH (100 mL), dried over $MgSO_4$ and the solvent removed under reduced pressure. Purification by chromatography using a silica-gel column (75 g; EtOAc/hexane, 3:7) afforded product **126** as a light orange precipitate, (0.40 g, 47%). Mp. 108-111 ^{o}C; ν_{max} /cm^{-1}

($CHCl_3$): 3495s + 3389s (NH, primary amine), 2961m + 2931m (CH, aliphatic), 2209s (C-N, nitrile), 1633s (C=C, aromatic); ^{1}H NMR ($CDCl_3$, 300 MHz) δ_H 2.14 (6H, s, $ArCH_3$), 4.11 (2H, bs, NH_2), 7.17 (2H, s, H-3); ^{13}C NMR ($CDCl_3$, 75.5 MHz) δ_C 17.1 ($ArCH_3$), 99.1 (C-4), 120.4 (CN), 121.3 (C-2), 131.9 (C-3), 147.2 (C-1); HRMS (EI): *m/z* 146.08409 [M^+]. Calculated for $C_9H_{10}N_2$, 146.08440 [M^+]; C, H, N Microanalysis found: C, 73.90; H, 7.06; N, 19.16%; $C_9H_{10}N_2$ requires C, 73.94; H, 6.89; N, 19.16%.

2-Methyl-6-propylaniline (123)

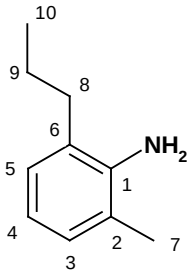

The alkene **122b** (1.30 g, 9.1 mmol) was dissolved in absolute ethanol (10 mL) and THF (10 mL) and stirred at room temperature. Subsequent addition of palladium-on-carbon (10%, 0.97 g, 0.90 mmol) was followed by careful placement of a hydrogen gas balloon over the reaction flask. TLC confirmed completion of the reaction after 1 hr. The reaction mixture was filtered through a Celite-packed sintered funnel with EtOAc (50 mL). The organic solvent was then removed under reduced pressure. Purification by chromatography using a silica-gel column (60 g; EtOAc/hexane, 0.5:9.5) afforded product **123** as a clear oil, (1.01 g, 74%). ν_{max} /cm^{-1} ($CHCl_3$): 3407s + 3391s (NH, primary amine), 2978m + 2930m (CH, aliphatic), 1661s (C=C, aromatic); ^{1}H NMR ($CDCl_3$, 400 MHz) δ_H 1.05 (3H, t, *J* = 7.3 Hz, H-10), 1.71 (2H, sext, *J* = 7.7 Hz, H-9), 2.22 (3H, s, H-7), 2.53 (2H, t, *J* = 7.3 Hz, H-8), 3.61 (2H, s, NH_2), 6.71 (1H, t, *J* = 7.3 Hz, H-4), 6.98 (2H, d, *J* = 7.3 Hz, H-3, H-5); ^{13}C NMR ($CDCl_3$, 100 MHz) δ_C 14.3 (C-10), 17.8 (C-7), 21.9 (C-9), 33.7 (C-8), 118.0 (C-4), 122.4 (C-2/C-6), 126.8 (C-2/C-6), 127.4 (C-3/C-5), 128.2 (C-3/C-5), 143.1 (C-1); HRMS (EI): *m/z* 149.12033 [M^+]. Calculated for $C_{10}H_{15}N$, 149.12045 [M^+].

4-Bromo-2-methyl-6-propylaniline (125)

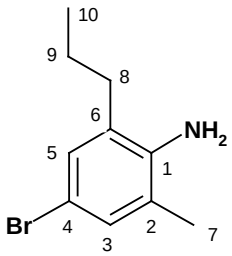

2-Methyl-6-propylaniline **123** (1.0 g, 6.7 mmol) was dissolved in AcOH (20 mL). The temperature of the solution was lowered to 0°C and ammonium bromide (0.80 g, 8.0 mmol) added. After stirring for 5 min, H_2O_2 (0.5 mL, 8.0 mmol) was carefully dropped into the mixture and the reaction gradually allowed to warm to ambient temperature. The solution was diluted with $NaHCO_3$ (100 mL) and extracted with EtOAc (3×100 mL), dried over $MgSO_4$ and the solvent removed under reduced pressure. Purification by chromatography using a silica-gel column (100 g; EtOAc/hexane, 1:9) afforded product **125** as a dark red oil, (0.83 g, 53%). ν_{max} /cm^{-1} ($CHCl_3$): 3491s + 3379s (NH, primary amine), 2965m + 2939m (CH, aliphatic), 1639s (C=C, aromatic); 794m (C-Br, halogen); ^{1}H NMR ($CDCl_3$, 300 MHz) δ_H 0.98 (3H, t, *J* = 7.8 Hz, H-10), 1.62 (2H, sext, *J* = 7.8 Hz, H-9), 2.13 (3H, s, H-7), 2.42 (2H, t, *J* = 7.8 Hz, H-8), 4.19 (2H, bs, NH_2), 7.15 (2H, s, H-3, H-5); ^{13}C NMR ($CDCl_3$, 75.5 MHz) δ_C 13.7 (C-10), 17.2 (C-7), 20.9 (C-9), 32.7 (C-8), 112.9 (C-4), 121.6 (C-2/C-6), 125.4 (C-2/C-6), 130.9 (C-3/C-5), 131.6 (C-5/C-5), 146.8 (C-1); HRMS (EI): *m/z* 227.03089 [M$^+$]. Calculated for $C_{10}H_{14}BrN$, 227.03096 [M$^+$].

4-Cyano-2-methyl-6-propylaniline (127)

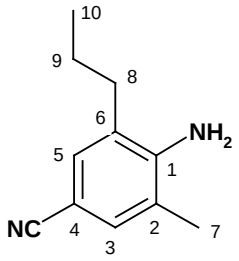

4-Bromo-2-methyl-6-propylaniline **125** (0.60 g, 2.6 mmol) was dissolved in DMF (7 mL) and CuCN (0.28 g, 3.2 mmol) added. The mixture was refluxed for 6 hrs after which TLC confirmed reaction completion. The reaction mixture was then poured into a freshly prepared aqueous ferric chloride solution (1.04 g) in conc. HCl (3 mL), H_2O (20 mL). The resulting mixture was heated to 70°C and stirred vigorously for 20 min. After cooling, the mixture was extracted with diethyl ether (3 × 100 mL). The combined organic fractions were washed again with HCl (100 mL), H_2O (100 mL) and 10% NaOH (100 mL), dried over $MgSO_4$ and the solvent removed under reduced pressure. Purification by chromatography using a silica-gel column (50 g; EtOAc/hexane, 1:9) afforded product **127** as a light-orange precipitate, (0.38 g, 84%). Mp. 112-113 °C; ν_{max} /cm^{-1} ($CHCl_3$): 3495s + 3389s (NH, primary amine), 2961m + 2931m (CH, aliphatic), 2209s (C-N, nitrile), 1633s (C=C, aromatic); ^{1}H NMR ($CDCl_3$, 300 MHz) δ_H 0.98 (3H, t, *J* = 7.8 Hz, H-10), 1.62 (2H, sext, *J* = 7.8 Hz, H-9), 2.13 (3H, s, H-7), 2.42 (2H, t, *J* = 7.8 Hz, H-8), 4.19 (2H, bs, NH_2), 7.15 (2H, s, H-3, H-5); ^{13}C NMR ($CDCl_3$, 75.5 MHz) δ_C 13.7 (C-10), 17.2 (C-7),

20.9 (C-9), 32.7 (C-8), 98.8 (C-4), 120.6 (C-11), 121.6 (C-2/C-6), 125.4 (C-2/C-6), 130.9 (C-3/C-5), 131.6 (C-3/C-5), 146.8 (C-1); HRMS (EI): *m/z* 174.11577 [M^+]. Calculated for $C_{11}H_{14}N_2$, 174.11570 [M^+]; C, H, N Microanalysis found: C, 75.81; H, 8.95; N, 16.05%; $C_{11}H_{14}N_2$ requires C, 75.82; H, 8.10; N, 16.08%.

4-(4-Bromophenylamino)-6-amino-2-methylthio-1,3-pyrimidine (131)

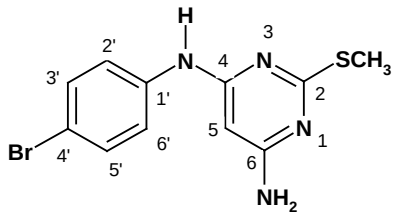

A reaction vessel was charged with 4-amino-6-chloro-2-(methylthio)pyrimidine (0.20 g, 1.14 mmol) and *p*-bromoaniline (0.39 g, 2.30 mmol) under a stream of argon gas. The two solids were heated to a melt at 160 ^oC without any use of solvent. TLC confirmed reaction completion after 2 hrs. The reaction mixture was diluted with aq. $NaHCO_3$ (50 mL) and extracted with EtOAc (3 × 50 mL), the organic layer dried over $MgSO_4$ and the solvent removed under reduced pressure. Purification by chromatography using a silica-gel column (20 g; EtOAc/hexane, 4:6) afforded product **131** as a white solid, (0.10 g, 28%). Mp. 125-126 ^oC; ν_{max} /cm^{-1} ($CHCl_3$): 3548s + 3439s (N-H, primary amine), 1639s (C=C, aromatic), 794m (C-Br, halogen); ^1H NMR (DMSO-D_6, 400 MHz) δ_H 2.39 (3H, s, SCH_3), 5.50 (1H, s, H-5), 6.38 (2H, bs, NH_2), 7.40 (2H, d, *J* = 8.8 Hz, H-2', H-6'), 7.49 (2H, d, *J* = 8.8 Hz, H-3', H-5'), 9.01 (1H, bs, NH); ^{13}C NMR (DMSO-D_6, 100 MHz) δ_C 14.1 (SCH_3), 82.1 (C-5), 113.2 (C-4'), 121.9 (C-3', C-5'), 131.9 (C-2', C-6'), 140.9 (C-1'), 160.8 (C-6), 164.3 (C-4), 170.1 (C-2); HRMS (EI): *m/z* 309.98892 [M^+]. Calculated for $C_{11}H_{11}N_4BrS$, 309.98878 [M^+]; C, H, N Microanalysis found: C, 42.49; H, 3.66; N, 17.75; S, 10.27%; $C_{11}H_{11}N_4BrS$ requires C, 42.45; H, 3.56; N, 18.00; S, 10.30%.

4-(4-Cyanophenylamino)-6-amino-2-methylthio-1,3-pyrimidine (132)

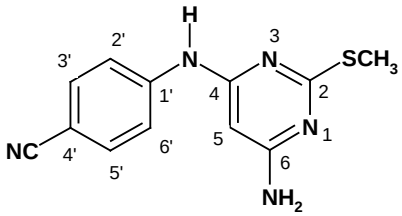

A reaction vessel was charged with 4-amino-6-chloro-2-(methylthio)pyrimidine (0.40 g, 2.28 mmol) and 4-aminobenzonitrile (0.64 g, 2.72 mmol) under a stream of argon gas. The two solids were heated to a melt at 160 ^oC without any use of solvent. TLC confirmed reaction completion

after 1 hr. The reaction mixture was diluted with aq. $NaHCO_3$ (50 mL) and extracted with EtOAc (3 × 50 mL), the organic layer dried over $MgSO_4$ and the solvent removed under reduced pressure. Purification by chromatography using a silica-gel column (30 g; EtOAc/hexane, 4:6) afforded product **132** as a bright yellow solid, (0.20 g, 35%). Mp. 130-133 ^oC; ν_{max} /cm^{-1} ($CHCl_3$): 3398s + 3439s (N-H, primary amine), 2223m (C-N, nitrile), 1633s (C=C, aromatic); ^1H NMR (DMSO-D_6, 400 MHz) δ_H 2.41 (3H, s, SCH_3), 5.60 (1H, s, H-5), 6.54 (2H, bs, NH_2), 7.65 (2H, d, *J* = 8.8 Hz, H-2', H-6'), 7.75 (2H, d, *J* = 8.8 Hz, H-3', H-5'), 9.46 (1H, bs, NH); ^{13}C NMR (DMSO-D_6, 100 MHz) δ_C 14.1 (SCH_3), 83.2 (C-5), 102.5 (C-4'), 119.2 (C-3', C-5'), 120.2 (*CN*), 133.7 (C-2', C-6'), 146.1 (C-1'), 160.2 (C-6), 164.7 (C-4), 170.5 (C-2); HRMS (EI): *m/z* 257.07333 [M^+]. Calculated for $C_{12}H_{11}N_5S$, 257.07352 [M^+]; C, H, N Microanalysis found: C, 55.93; H, 4.46; N, 26.70; S, 12.38%; $C_{12}H_{11}N_5S$ requires C, 56.01; H, 4.31; N, 27.22; S, 12.46%.

4-(4-Cyano-2,6-dimethylphenylamino)-6-amino-2-methylthio-1,3-pyrimidine (133)

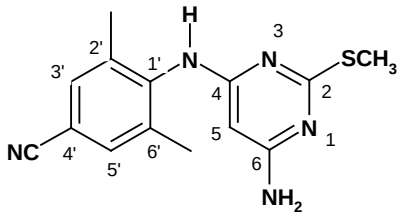

A reaction vessel was charged with 4-amino-6-chloro-2-(methylthio)pyrimidine (0.10 g, 0.68 mmol) and 4-cyano-2,6-dimethylaniline (0.12 g, 0.68 mmol) under a stream of argon gas. The two solids were heated to a melt at 200 ^oC without any use of solvent. TLC confirmed reaction completion after 3 hrs. The reaction mixture was diluted with $NaHCO_3$ (50 mL) and extracted with EtOAc (3 × 50 mL), the organic layer dried over $MgSO_4$ and the solvent removed under reduced pressure. Purification by chromatography using a silica-gel column (15 g; EtOAc/hexane, 2:8) afforded product **133** as a white solid, (0.07 g, 35%). Mp. 120-121 ^oC; ν_{max} /cm^{-1} ($CHCl_3$): 3411s (N-H, primary amine), 2251m (C-N, nitrile), 1633s (C=C, aromatic); ^1H NMR (DMSO-D_6, 400 MHz) δ_H 2.07 (6H, s, Ar*CH*$_3$), 2.39 (3H, s, SCH_3), 5.50 (2H, bs, NH_2), 6.16 (1H, s, H-5), 7.18 (2H, s, H-3', H-5'), 7.22 (1H, bs, NH); ^{13}C NMR (DMSO-D_6, 100 MHz) δ_C 13.3 (SCH_3), 17.4 ($ArCH_3$), 95.9 (C-4'), 98.5 (C-5), 120.9 (C-2', C-6'), 129.2 (*CN*), 131.4 (C-3', C-5'), 149.8 (C-1'), 158.4 (C-6), 165.2 (C-4), 172.1 (C-2); C, H, N Microanalysis found: C, 60.09; H, 6.51; N, 24.30; S, 9.86%; $C_{14}H_{15}N_5S$ requires C, 58.92; H, 5.29; N, 24.54; S, 11.23%.

4-(4-Cyano-2-propyl-6-methylphenylamino)-6-amino-2-methylthio-1,3-pyrimidine (134)

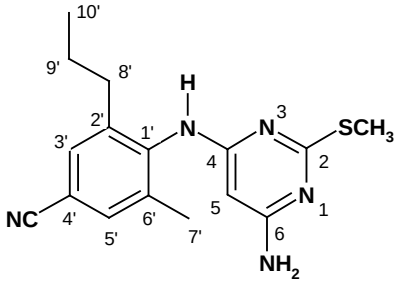

A reaction vessel was charged with 4-amino-6-chloro-2-(methylthio)pyrimidine (0.10 g, 0.57 mmol) and 4-cyano-2-propyl-6-methylaniline (0.20 g, 1.14 mmol) under a stream of argon gas. The two solids were heated to a melt at 200 ^{o}C without any use of solvent. TLC confirmed reaction completion after 3 hrs. The reaction mixture was diluted with aq. $NaHCO_3$ (50 mL) and extracted with EtOAc (3 × 50 mL), the organic layer dried over $MgSO_4$ and the solvent removed under reduced pressure. Purification by chromatography using a silica-gel column (15 g; EtOAc/hexane, 2:8) afforded product **134** as a white solid, (0.10 g, 35%). Mp. 121-124 ^{o}C; ν_{max} /cm^{-1} ($CHCl_3$): 3411s (N-H, primary amine), 2251m (C-N, nitrile), 1633s (C=C, aromatic); ^{1}H NMR (DMSO-D_6, 400 MHz) δ_H 0.96 (3H, t, *J* = 7.80 Hz, H-10'), 1.60 (2H, sext, *J* = 7.8 Hz, H-9'), 2.11 (3H, s, H-7'), 2.38 (3H, s, SCH_3), 2.45 (2H, t, *J* = 7.8 Hz, H-8'), 5.56 (2H, bs, NH_2), 6.14 (1H, s, H-5), 7.15 (2H, s, H-3', H-5'), 7.25 (1H, bs, NH); ^{13}C NMR (DMSO-D_6, 100 MHz) δ_C 13.5 (C-10'), 13.9 (SCH_3), 17.4 (C-7'), 20.5 (C-9'), 32.6 (C-8'), 99.1 (C-4'), 99.6 (C-5), 120.6 (*CN*), 121.4 (C-6'), 125.4 (C-2'), 130.3 (C-5'), 130.9 (C-3'), 151.7 (C-1'), 160.5 (C-6), 166.8 (C-4), 172.1 (C-2); HRMS (EI): *m/z* 313.13761 [M^+]. Calculated for $C_{16}H_{19}N_5S$, 313.13612 [M^+].

4-(3-Hydroxy-4-chlorophenylamino)-6-amino-2-methylthio-1,3-pyrimidine (128)

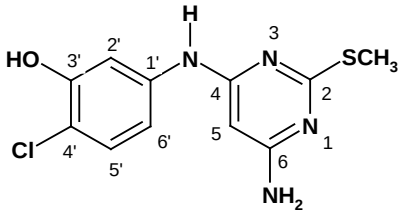

To a solution of 4-amino-6-chloro-2-(methylthio)pyrimidine (0.10 g, 0.57 mmol) and 3-hydroxy-4-chloroaniline (0.084 g, 0.57 mmol) dissolved in 1,4-dioxane (3 mL) was added anhydrous TsOH (98 mg, 0.57 mmol) at room temperature. The reaction mixture was heated to 100 ^{o}C and TLC confirmed reaction completion after 2 hrs. The reaction mixture was diluted with H_2O (50 mL) and extracted with EtOAc (3 × 50 mL), the organic layer dried over $MgSO_4$ and the solvent removed under reduced pressure. Purification by chromatography using a silica-gel column (20 g; EtOAc/hexane, 4:6) afforded product **128** as a brown precipitate, (74 mg, 47%). Mp. 157 ^{o}C;

ν_{max} /cm^{-1} ($CHCl_3$): 3434s (N-H, primary amine), 1657m (C=C, aromatic), 824m (C-Cl, halogen); ^{1}H NMR (Acetone-D_6, 300 MHz) δ_H 2.43 (3H, s, SCH_3), 5.65 (1H, s, H-5), 5.76 (2H, bs, NH_2), 7.01 (1H, dd, *J* = 8.8, 3.0 Hz, H-6'), 7.18 (1H, d, *J* = 8.8 Hz, H-5'), 7.37 (1H, d, *J* = 3.0 Hz, H-2'), 8.08 (1H, bs, NH), 8.58 (1H, bs, OH); ^{13}C NMR (Acetone-D_6, 75.5 MHz) δ_C 13.4 (SCH_3), 81.3 (C-5), 108.4 (C-2'), 112.1 (C-6'), 112.5 (C-4'), 129.6 (C-5'), 140.6 (C-1'), 153.0 (C-3'), 160.2 (C-6), 163.8 (C-4), 169.7 (C-2); HRMS (ES): *m/z* 282.03339 [M$^+$]. Calculated for $C_{11}H_{11}N_4OSCl$, 282.03336 [M$^+$]; C, H, N Microanalysis found: C, 47.77; H, 4.14; N, 19.39; S, 9.86%; $C_{11}H_{11}N_4OSCl$ requires C, 47.72; H, 3.92; N, 19.82; S, 10.34%.

4-(3-Allyloxy-4-chlorophenylamino)-6-amino-2-methylthio-1,3-pyrimidine (129)

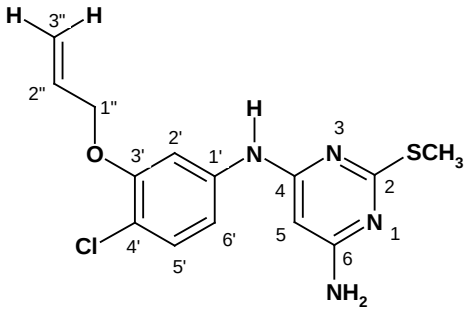

To a solution of **128** (0.03 g, 0.10 mmol) dissolved in acetone (3 mL) was added anhydrous K_2CO_3 (17 mg, 0.12 mmol) at room temperature. Allyl bromide (0.01 mL, 0.13 mmol) was slowly added to this mixture followed by *tert*-butylammonium iodide (4 mg, cat.). The reaction mixture was left to react at room temperature and TLC confirmed reaction completion after 6 hrs. The reaction mixture was diluted with H_2O (50 mL) and extracted with EtOAc (3 × 50 mL), the organic layer dried over $MgSO_4$ and the solvent removed under reduced pressure. Purification by chromatography using a silica-gel column (5 g; EtOAc/hexane, 6:4) afforded product **129** as a brown viscous oil, (28 mg, 46%). Mp.151-153 ^{o}C; ν_{max} /cm^{-1} ($CHCl_3$): 3464s (N-H, primary amine), 1751s (C=C, alkene), 1657m (C=C, aromatic), 830m (C-Cl, halogen); ^{1}H NMR (Acetone-D_6, 300 MHz) δ_H 2.45 (3H, s, SCH_3), 4.65 (2H, m, H-1''), 5.28 (1H, d, J_{cis} = 10.7 Hz, H-3''), 5.50 (1H, d, J_{trans} = 16.6 Hz, H-3''), 5.67 (1H, s, H-5), 5.79 (2H, bs, NH_2), 6.12 (1H, m, H-2''), 7.06 (1H, dd, *J* = 8.8, 2.9 Hz, H-6'), 7.26 (1H, d, *J* = 8.8 Hz, H-5'), 7.55 (1H, d, *J* = 2.9 Hz, H-2'), 8.19 (1H, bs, NH); ^{13}C NMR (Acetone-D_6, 75.5 MHz) δ_C 13.1 (SCH_3), 69.5 (C-1''), 81.4 (C-5), 106.4 (C-2'), 112.8 (C-6'), 115.0 (C-4'), 117.1 (C-3''), 129.8 (C-5'), 133.4 (C-2''), 141.1 (C-1'), 154.3 (C-3'), 160.8 (C-6), 164.3 (C-4), 170.5 (C-2); HRMS (ES): *m/z* 323.0732 [M+H]$^+$. Calculated for $C_{14}H_{16}N_4OSCl$, 323.0735 [M+H]$^+$.

4-(4-Chloro-3-propargyloxyphenylamino)-6-amino-2-methylthio-1,3-pyrimidine (130)

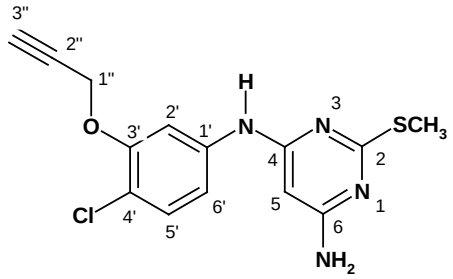

To a solution of 4-amino-6-chloro-2-(methylthio)pyrimidine (0.12 g, 0.68 mmol) and 4-chloro-3-prop-2-ynyloxyaniline (0.16 g, 0.68 mmol) dissolved in 1,4-dioxane (3 mL) was added anhydrous *p*-TsOH (0.12 mg, 0.68 mmol) at room temperature. The reaction mixture was heated to 100 ^{o}C and TLC confirmed reaction completion after 6 hrs. The reaction mixture was diluted with H_2O (50 mL) and extracted with EtOAc (3 × 50 mL), the organic layer dried over $MgSO_4$ and the solvent removed under reduced pressure. Purification by chromatography using a silica-gel column (15 g; EtOAc/hexane, 5:5) afforded product **130** as a brown precipitate, (105 mg, 49%). Mp.167-168,ν_{max} /cm^{-1} ($CHCl_3$): 3434s (N-H, primary amine), 2253s (C≡C, alkyne), 824m (C-Cl, halogen); ^{1}H NMR (Acetone-D_6, 300 MHz) δ_H 2.46 (3H, s, SCH_3), 2.46 (1H, t, *J* = 2.4 Hz, H-3''), 4.86 (2H, d, *J* = 2.4 Hz, H-1''), 5.69 (1H, s, H-5), 5.80 (2H, bs, NH_2), 7.18 (1H, dd, *J* = 8.8, 3.0 Hz, H-6'), 7.29 (1H, d, *J* = 8.8 Hz, H-5'), 7.58 (1H, d, *J* = 3.0 Hz, H-2'), 8.21 (1H, bs, NH); ^{13}C NMR (Acetone-D_6, 75.5 MHz) δ_C 13.8 (SCH_3), 56.9 (C-1''), 76.4 (C-3''), 77.9 (C-2''), 80.4 (C-5), 108.8 (C-2'), 112.7 (C-6'), 115.8 (C-4'), 130.6 (C-5'), 138.5 (C-1'), 153.5 (C-3'), 160.7 (C-6), 163.3 (C-4), 172.1 (C-2); HRMS (ES): *m/z* 321.0576 $[M+H]^+$. Calculated for $C_{14}H_{14}N_4OSCl$, 321.0577 $[M+H]^+$.

5-{3-[5-(6-Amino-2-thiomethyl-1,3-pyrimidin-4-yl)amino-2-chlorophenoxy]prop-1-ynyl}uridine-2',3'-didehydro-2',3'-dideoxy-5'-O-benzoate (135)

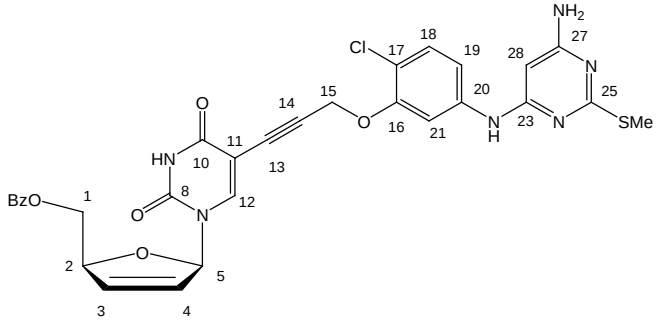

Alkyne **130** (80 mg, 0.22 mmol) was added together with 5-iodo-d4U 5'-benzoate (88 mg, 0.19 mmol) and the mixture dried carefully on a vacuum pump. A mixture of degassed DMF:THF (1:2

(v/v), 3 mL) was then added to the reaction vessel whilst the mixture stirred at room temperature under nitrogen. Subsequent addition of triethylamine (0.05 mL, 0.38 mmol) was followed by addition of copper(I) iodide (19 mg, 0.10 mmol) and tetrakis(triphenylphosphine)palladium (22 mg, 0.02 mmol) respectively. The reaction was stirred continuously at room temperature and TLC confirmed completion of the reaction after 2 hrs. The reaction mixture was diluted with a 5% EDTA solution (30 mL) and extracted with chloroform (3 × 20 mL). The organic fractions were dried with $MgSO_4$ and the solvent removed under reduced pressure. Purification by chromatography using a silica-gel column afforded product **135** as a colourless solid, (100 mg, 83%). $[\alpha]_D$ +12.2° (*c* = 1.03, acetone); ν_{max} /cm^{-1} (Acetone): 2254s (C≡C), 1720s (C=O, ester), 1693s (C=O, pyrimidine), 1599s (C-N stretching), 1514s + 1492s (C=C, aromatic); ^{1}H NMR (300 MHz, Acetone-D_6): δ_H 2.45 (3H, s, SCH_3), 4.56 (1H, dd, *J* = 12.4, 3.0 Hz, H-1), 4.57 (1H, dd, *J* = 12.4, 4.4 Hz, H-1), 4.85 (2H, s, H-15), 5.25 (1H, m, H-2), 5.74 (1H, s, H-28), 5.82 (2H, bs, NH_2), 6.10 (1H, m, H-3), 6.58 (1H, dt, *J* = 6.0, 1.7 Hz, H-4), 6.81 (1H, m, H-5), 7.17 (1H, dd, *J* = 8.6, 2.3 Hz, H-19), 7.26 (1H, d, *J* = 8.6 Hz, H-18), 7.45-7.60 (4H, m, H-21, OBz), 7.80 (1H, s, H-12), 8.00 (2H, m, OBz), 8.20 (1H, bs, N-H), 10.40 (1H, bs, N-H); ^{13}C NMR (75 MHz, Acetone-D_6): δ_C 13.2 (SCH_3), 57.3 (C-15), 65.5 (C-1), 79.7 (C-11), 81.4 (C-28), 85.2 (C-2), 87.6 (C-13), 90.9 (C-5), 98.8 (C-14), 106.9 (C-21), 113.9 (C-19), 115.3 (C-17), 126.9 (C-3), 128.9 (C-Bz), 129.7 (C-18), 130.1 (C-Bz), 132.1 (C-Bz), 133.5 (C-Bz), 134.0 (C-4), 140.9 (C-20), 144.1 (C-12), 149.8 (C-8), 153.5 (C-16), 160.8 (C-27), 161.1 (C-10), 164.3 (C-23), 166.0 ($OCOC_6H_5$), 170.8 (C-25); HRMS (ES): *m/z* 633.1315 $[M+H]^+$. Calculated for $C_{30}H_{26}N_6O_6SCl$, 633.1323 [M+H].

5-{3-[5-(6-Amino-2-thiomethyl-1,3-pyrimidin-4-yl)amino-2-chlorophenoxy]prop-1-ynyl}-2',3'-didehydro-2',3'-dideoxyuridine (114)

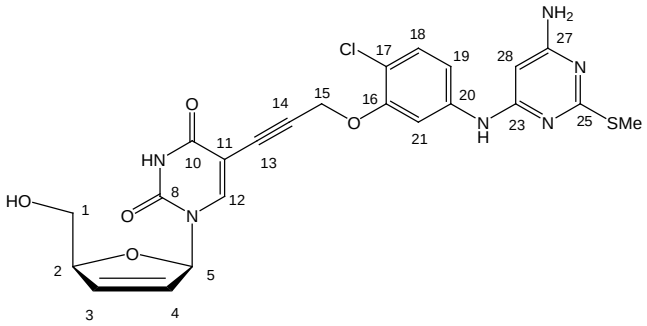

Sodium methoxide in methanol (1.97 M, 1 drop, cat.) was added to methanol (3 mL) at 0°C. This was followed by addition of **135** (35 mg, 0.05 mmol) at 0°C and the reaction mixture was left to stir at room temperature. After 1 hr, the reaction mixture was diluted with dichloromethane (2mL) and flash chromatography performed directly affording product **114** as a clear oil, (21 mg, 76%).

$[\alpha]_D$ +13.4° (*c* = 1.21, acetone); ν_{max} /cm^{-1} (Acetone): 3592b (O-H), 2254 (C≡C), 1693 (C=O, pyrimidine), 1599 (C-N stretching), 1514 + 1492 (C=C, aromatic); ^{1}H NMR (300 MHz, Acetone-D_6): δ_H 2.45 (3H, s, SCH_3), 3.82 (2H, m, H-1), 4.29 (1H, bs, OH), 4.87 (1H, m, H-2), 5.00 (2H, s, H-15), 5.75 (1H, s, H-28), 5.81 (2H, bs, NH_2), 5.95 (1H, m, H-3), 6.42, (1H, m, H-4), 6.92 (1H, m, H-5), 7.24 (1H, dd, *J* = 8.6, 2.3 Hz, H-19), 7.26 (1H, d, *J* = 8.6 Hz, H-18), 7.50 (1H, d, *J* = 2.3 Hz, H-21), 8.19 (1H, bs, N-H), 8.28 (1H, s, H-12), 10.24 (1H, s, N-H); ^{13}C NMR (75 MHz, Acetone-D_6): δ_C 13.1 (SCH_3), 57.3 (C-15), 62.7 (C-1), 80.3 (C-11), 81.3 (C-28), 87.0 (C-13), 88.1 (C-2), 90.2 (C-5), 97.9 (C-14), 107.0 (C-21), 114.0 (C-19), 115.3 (C-17), 126.1 (C-3), 130.1 (C-18), 135.6 (C-4), 140.9 (C-20), 146.1 (C-12), 149.9 (C-8), 153.5 (C-16), 160.8 (C-27), 161.5 (C-10), 164.4 (C-23), 171.0 (C-25); HRMS (ES): *m/z* 529.1073 $[M+H]^+$. Calculated for $C_{23}H_{22}N_6O_5SCl$, 529.1061 [M+H].

2-(3-Hydroxy-4-chlorophenylamino)-4-methoxy-1,3-pyrimidine (136)

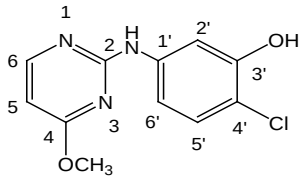

To a solution of 2-chloro-4-methoxypyrimidine (440 mg, 3.00 mmol) dissolved in 1,4-dioxane (7 mL) was added anhydrous *p*-TsOH (430 mg, 2.50 mmol) at room temperature. To this mixture was added 3-amino-6-chlorophenol **119b** (364 mg, 2.50 mmol) and the reaction mixture was heated to 100 °C. TLC confirmed reaction completion after 12 hrs. The reaction mixture was diluted with aq. $NaHCO_3$ (50 mL) and extracted with EtOAc (3 × 50 mL), the organic layer dried over $MgSO_4$ and the solvent removed under reduced pressure. Purification by chromatography using a silica-gel column (40 g; EtOAc/hexane, 3:7) afforded product **136** as a white solid, (600 mg, 95%). Mp. 154-155 °C; ν_{max} /cm^{-1} ($CHCl_3$): 3387s + 3321s (NH), 2978m + 2930m (CH, aromatic), 1638s (C=C, aromatic), 738s (C-Cl, halogen); ^{1}H NMR (Acetone-D_6, 400 MHz) δ_H 2.85 (1H, bs, OH), 3.93 (3H, s, OCH_3), 6.23 (1H, d, *J* = 5.7 Hz, H-5), 7.21 (1H, d, *J* = 8.7 Hz, H-5'), 7.27 (1H, dd, *J* = 8.7, 2.4 Hz, H-6'), 7.72 (1H, d, *J* = 2.4 Hz, H-2'), 8.16 (1H, d, *J* = 5.7 Hz, H-6), 8.46 (1H, bs, NH); ^{13}C NMR (Acetone-D_6, 100 MHz) δ_C 53.3 (OCH_3), 99.2 (C-5), 107.8 (C-2'), 111.7 (C-6'), 113.0 (C-4'), 129.6 (C-5'), 141.0 (C-1'), 152.6 (C-3'), 158.3 (C-6), 160.0 (C-4), 170.2 (C-2); HRMS (ES): *m/z* 252.0544 $[M+H]^+$. Calculated for $C_{11}H_{11}N_3O_2Cl$, 252.0540 $[M+H]^+$; C, H, N Microanalysis found: C, 52.82; H, 4.07; N, 16.37%; $C_{11}H_{10}N_3O_2Cl$ requires C, 52.50; H, 4.01; N, 16.70%.

2-(3-Propargyloxy-4-chlorophenylamino)-4-methoxy-1,3-pyrimidine (137)

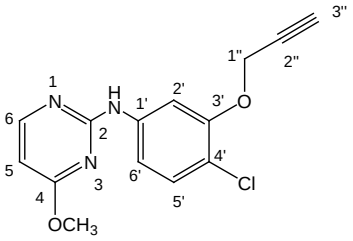

To a solution of 2-chloro-4-methoxypyrimidine (1.10 g, 7.60 mmol) dissolved in 1,4-dioxane (20 mL) was added anhydrous *p*-TsOH (1.10 g, 6.30 mmol) at room temperature. To this mixture was added substituted aniline **120** (1.15 g, 6.30 mmol) and the reaction mixture was heated to 100 ^{o}C. TLC confirmed reaction completion after 12 hrs. The reaction mixture was diluted with aq. $NaHCO_3$ (50 mL) and extracted with EtOAc (3 × 50 mL), the organic layer dried over $MgSO_4$ and the solvent removed under reduced pressure. Purification by chromatography using a silica-gel column (70 g; EtOAc/hexane, 2:8) afforded product **137** as a white solid, (1.32 g, 73%). Mp. 123-124 ^{o}C; ν_{max} /cm^{-1} ($CHCl_3$): 3377s + 3339s (NH, amine), 2259s (C≡C), 1627s (C=C, aromatic), 725s (C-Cl, halogen); ^{1}H NMR (Acetone-D_6, 400 MHz) δ_H 3.10 (1H, t, *J* = 2.40 Hz, H-3''), 3.98 (3H, s, OCH_3), 4.87 (1H, d, *J* = 2.4 Hz, H-1''), 6.26 (1H, d, *J* = 5.7 Hz, H-5), 7.30 (1H, d, *J* = 8.7 Hz, H-5'), 7.45 (1H, dd, *J* = 8.7, 2.4 Hz, H-6'), 7.96 (1H, d, *J* = 2.4 Hz, H-2'), 8.19 (1H, d, *J* = 5.7 Hz, H-6), 8.71 (1H, bs, NH); ^{13}C NMR (Acetone-D_6, 100 MHz) δ_C 53.6 (OCH_3), 56.6 (C-1''), 76.8 (C-3''), 78.7 (C-2''), 99.5 (C-5), 105.9 (C-2'), 112.8 (C-6'), 114.1 (C-4'), 129.9 (C-5'), 140.8 (C-1'), 153.8 (C-3'), 158.4 (C-6), 160.0 (C-4), 170.4 (C-2); HRMS (ES): *m/z* 290.0703 [M+H]$^{+}$. Calculated for $C_{14}H_{13}N_3O_2Cl$, 290.0696 [M+H]$^{+}$; C, H, N Microanalysis found: C, 58.00; H, 4.40; N, 14.64%; $C_{14}H_{12}N_3O_2Cl$ requires C, 58.04; H, 4.17; N, 14.50%.

5-{3-[5-(4-Methoxy-1,3-pyrimidin-2-yl)amino-2-chlorophenoxy]prop-1-ynyl}uridine-2',3'-didehydro-2',3'-dideoxy-5'-O-benzoate (138)

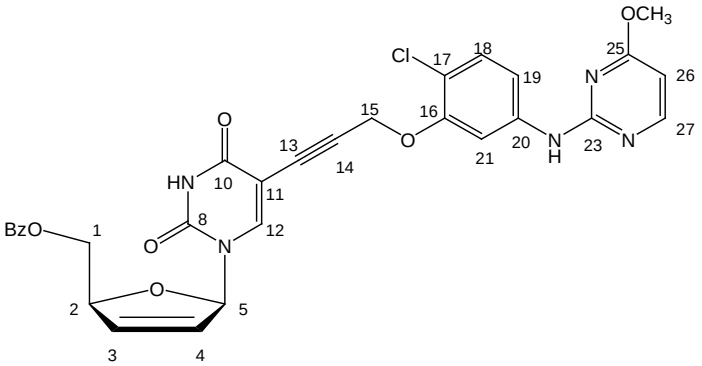

Alkyne **137** (140 mg, 0.48 mmol) was added together with 5-iodo-d4U 5'-benzoate (195 mg, 0.44 mmol) and the mixture dried carefully on a vacuum pump. A mixture of degassed DMF:THF (1:2 (v/v), 3 mL) was then added to the reaction vessel whilst the mixture stirred at room temperature under nitrogen. Subsequent addition of triethylamine (0.13 mL, 0.88 mmol) was followed by addition of copper(I) iodide (42 mg, 0.22 mmol) and tetrakis(triphenylphosphine)palladium (51 mg, 0.04 mmol) respectively. The reaction was stirred continuously at room temperature and TLC confirmed completion of the reaction after 5 hrs. The reaction mixture was diluted with a 5% EDTA solution (30 mL) and extracted with chloroform (3 × 20 mL). The organic fractions were dried with $MgSO_4$ and the solvent removed under reduced pressure. Purification by chromatography using a silica-gel column afforded product **138** as a colourless solid, (145 mg, 55%). $[\alpha]_D$ +10.9° (*c* = 1.01, acetone); ν_{max} /cm^{-1} (Acetone): 2255s (C≡C), 1723s (C=O, ester), 1688s (C=O, pyrimidine), 1598s (C-N stretching), 1516s + 1488s (C=C, aromatic), 726s (C-Cl, halogen); Mp. 99–102 ^{o}C; ^{1}H NMR (DMSO-D_6, 300 MHz) δ_H 3.92 (3H, s, OCH_3), 4.45 (2H, d, *J* = 3.9 Hz, H-1), 4.85 (2H, s, H-15), 5.13 (1H, s, H-2), 6.05 (1H, m, H-3), 6.28 (1H, d, *J* = 5.7 Hz, H-26), 6.46 (1H, dt, *J* = 6.0, 1.6 Hz, H-4), 6.72 (1H, m, H-5), 7.26 (1H, d, *J* = 8.7 Hz, H-18), 7.34 (1H, dd, *J* = 8.7, 2.2 Hz, H-19), 7.46 (2H, t, *J* = 7.3 Hz, Bz-m), 7.58 (1H, t, *J* = 7.3 Hz, Bz-p), 7.65 (1H, s, H-12), 7.85 (2H, d, *J* = 7.3 Hz, Bz-o), 7.89 (1H, d, *J* = 2.2 Hz, H-21), 8.19 (1H, d, *J* = 5.7 Hz, H-27), 9.61 (1H, bs, NH), 11.67 (1H, bs, NH); ^{13}C NMR (DMSO-D_6, 75.5 MHz) δ_C 53.2 (OCH_3), 56.9 (C-15), 65.2 (C-1), 79.3 (C-11), 84.3 (C-13), 87.2 (C-2), 90.3 (C-5), 97.7 (C-14), 98.8 (C-26), 105.0 (C-21), 112.4 (C-19), 113.3 (C-17), 126.3 (C-3), 128.7 (Bz-m), 129.0 (Bz-o), 129.1 (Bz-p), 129.4 (C-18), 133.2 (Bz-i), 133.7 (C-4), 140.6 (C-20), 143.8 (C-12), 149.4 (C-8), 152.4 (C-16), 158.2 (C-27), 159.4 (C-25), 161.2 (C-10), 165.4 (O*C*OC_6H_5), 169.4 (C-23); HRMS (ES): *m/z* 602.1449 $[M+H]^+$. Calculated for $C_{30}H_{25}N_5O_7Cl$, 602.1443 $[M+H]^+$; C, H, N Microanalysis found: C, 59.58; H, 4.38; N, 11.43%; $C_{30}H_{24}N_5O_7Cl$ requires C, 59.86; H, 4.02; N, 11.63%.

5-{3-[5-(4-Methoxy-1,3-pyrimidin-2-yl)amino-2-chlorophenoxy]prop-1-ynyl}-2',3'-didehydro-2',3'-dideoxyuridine (115)

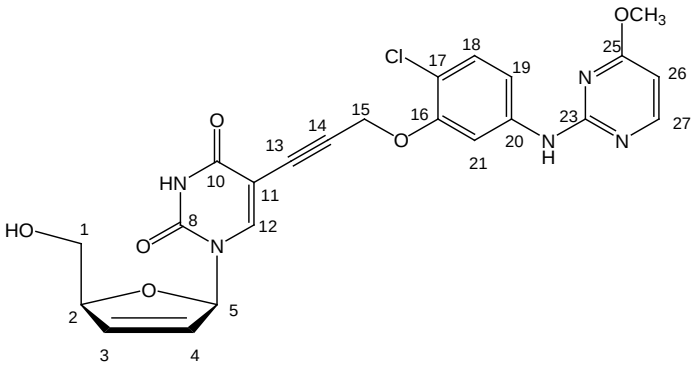

Sodium methoxide (1.97 M) in methanol (0.05 mL, 0.08 mmol) was added to methanol (5 mL) at 0°C. This was followed by addition of **138** (50 mg, 0.08 mmol) at 0°C and the reaction mixture was left to stir at room temperature. After 2 hr, the reaction mixture was diluted with dichloromethane (2mL) and flash chromatography performed directly affording product **115** as a white solid, (35 mg, 88%). Mp. 102-106°C; $[\alpha]_D$ +11.9° (*c* = 1.02, acetone); ν_{max} /cm^{-1} (Acetone): 3590b (O-H), 2248 (C≡C), 1692 (C=O, pyrimidine), 1599 (C-N stretching), 1510 + 1472 (C=C, aromatic), 720s (C-Cl, halogen); ^{1}H NMR (DMSO-D_6, 300 MHz) δ_H 3.64 (2H, m, H-1), 4.01 (3H, s, OCH_3), 4.86 (1H, m, H-2), 5.04 (1H, bs, OH), 5.06 (2H, s, H-15), 5.96 (1H, m, H-3), 6.36 (1H, d, *J* = 5.7 Hz, H-26), 6.45 (1H, m, H-4), 6.83 (1H, m, H-5), 7.35 (1H, d, *J* = 8.7 Hz, H-18), 7.42 (1H, dd, *J* = 8.7, 2.2 Hz, H-19), 7.93 (1H, d, *J* = 2.2 Hz, H-21), 8.17 (1H, s, H-12), 8.27 (1H, d, *J* = 5.7 Hz, H-27), 9.60 (1H, bs, NH), 11.65 (1H, bs, NH); ^{13}C NMR (DMSO-D_6, 75.5 MHz) δ_C 53.3 (OCH_3), 57.0 (C-15), 61.8 (C-1), 79.7 (C-11), 86.8 (C-13), 87.6 (C-2), 89.5 (C-5), 97.0 (C-14), 98.8 (C-26), 105.1 (C-21), 112.5 (C-19), 113.3 (C-17), 125.4 (C-3), 129.4 (C-18), 135.4 (C-4), 140.5 (C-20), 145.4 (C-12), 149.6 (C-8), 152.5 (C-16), 158.2 (C-27), 159.4 (C-25), 161.3 (C-10), 169.4 (C-23); HRMS (ES): *m/z* 498.1184 $[M+H]^+$. Calculated for $C_{23}H_{21}N_5O_6Cl$, 498.1180 $[M+H]^+$; C, H, N Microanalysis found: C, 55.47; H, 3.56; N, 14.71%; $C_{23}H_{20}N_5O_6Cl$ requires C, 55.48; H, 4.05; N, 14.09%.

2-Benzyloxyethanol (140)

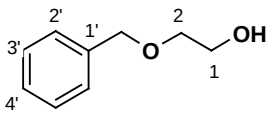

Benzyl bromide (7.60 mL, 64.4 mmol) was added dropwise to a suspension of NaH (60%, 1.55 g, 64.4 mmol) and 1,2-ethanediol (10.80 mL, 193.4 mmol) in THF (40 mL). After 20 hrs the

mixture was diluted with EtOAc (60 mL) and washed with aq. NH_4Cl (40 mL) and H_2O (2 × 40 mL), the organic layer dried over $MgSO_4$ and the solvent removed under reduced pressure. The crude product was purified by distillation [bp: 102 ^oC/0.7 mm Hg (lit. 90-95 ^oC/0.7 mm Hg)] to give product **140** as a colourless oil, (5.19 g, 53%). ^1H NMR ($CDCl_3$, 300 MHz) δ_H 2.52 (1H, s, OH), 3.58 (2H, t, *J* = 4.6 Hz, H-1), 3.74 (2H, t, *J* = 4.6 Hz, H-2), 4.56 (2H, s, ArC*H*$_2$O), 7.34 (5H, m, ArH); ^{13}C NMR ($CDCl_3$, 75.5 MHz) δ_C 61.8 (C-1), 71.5 (C-2), 73.3 (Ar*C*H$_2$O), 127.8, 128.4, 128.7 (Ar*C*H), 138.0 (C-1').

(2-Bromoethoxymethyl)benzene (141)

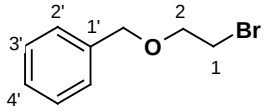

To a solution of the alcohol **140** (2.00 g, 13.1 mmol) and PPh_3 (4.14 g, 15.8 mmol) in CH_2Cl_2 (20 mL) was added CBr_4 (5.23 g, 15.8 mmol) at 0 ^oC. The reaction mixture was stirred at 0 ^oC for 30 min and the solvent removed under reduced pressure. Purification by chromatography afforded product **141** as a colourless oil, (2.68 g, 95%). ^1H NMR ($CDCl_3$, 300 MHz) δ_H 3.50 (2H, t, *J* = 6.2 Hz, H-1), 3.80 (2H, t, *J* = 6.2 Hz, H-2), 4.60 (2H, s, ArC*H*$_2$O), 7.36 (5H, m, ArH); ^{13}C NMR ($CDCl_3$, 75.5 MHz) δ_C 30.4 (C-1), 70.0 (C-2), 73.1 (Ar*C*H$_2$O), 127.7, 127.8, 128.5 (Ar*C*H), 137.8 (C-1').

2-[3-(2-Benzyloxyethoxy)-4-chlorophenylamino]-4-methoxy-1,3-pyrimidine (142)

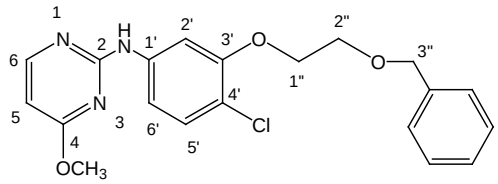

To a solution of **136** (500 mg, 2.00 mmol) dissolved in acetone (20 mL) was added anhydrous K_2CO_3 (550 mg, 4.00 mmol) at room temperature. 1-(2-Bromoethoxy)benzyl ether **141** (1.30 g, 6.00 mmol) was slowly added to this mixture followed by *tetra*-butylammonium iodide (50 mg, cat.). The reaction mixture was left to react at room temperature. After 16 hrs the mixture was diluted with H_2O (100 mL) and extracted with EtOAc (3 × 100 mL), the organic layer dried over $MgSO_4$ and the solvent removed under reduced pressure. Purification by chromatography afforded product **142** as a white solid, (791 mg, 100%). Mp. 121–122^oC; ν_{max} /cm^{-1} (Acetone): 2928m + 2867s (C-H, aliphatic), 1649m (C=C, alkene), 1567m (C=C, aromatic), 725s (C-Cl,

halogen); ^{1}H NMR (Acetone-D_6, 300 MHz) δ_H 3.90 (2H, t, *J* = 4.8 Hz, H-2''), 3.95 (3H, s, OCH_3), 4.29 (2H, t, *J* = 4.8 Hz, H-1''), 4.67 (2H, s, H-3''), 6.25 (1H, d, *J* = 5.7 Hz, H-5), 7.25-7.42 (7H, m, H-5', H-6', Ph), 7.88 (1H, d, *J* = 2.2 Hz, H-2'), 8.18 (1H, d, *J* = 5.7 Hz, H-6), 8.61 (1H, bs, NH); ^{13}C NMR (Acetone-D_6, 75.5 MHz) δ_C 53.2 (OCH_3), 68.5 (C-2''), 68.9 (C-1''), 72.9 (C-3''), 99.4 (C-5), 105.2 (C-2'), 112.1 (C-6'), 114.7 (C-4'), 127.5 (Bn-m), 127.6 (Bn-p), 128.4 (Bn-o), 129.7 (C-5'), 139.1 (Bn-i), 140.9 (C-1'), 154.6 (C-3'), 158.4 (C-6), 160.1 (C-4), 170.3 (C-2); HRMS (ES): *m/z* 386.1261 $[M+H]^+$. Calculated for $C_{20}H_{21}N_3O_3Cl$, 386.1271 $[M+H]^+$; C, H, N Microanalysis found: C, 62.38; H, 5.95; N, 10.80%; $C_{20}H_{20}N_3O_3Cl$ requires C, 62.26; H, 5.22; N, 10.89%.

2-[3-(2-Hydroxyethoxy)-4-chlorophenylamino]-4-methoxy-1,3-pyrimidine (143)

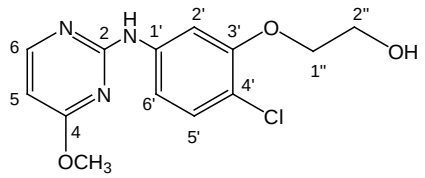

The benzyl ether **142** (750 mg, 1.94 mmol) was dissolved in absolute ethanol (10 mL) and stirred at room temperature. Subsequent addition of palladium-on-carbon (10%, 200 mg, 0.19 mmol) was followed by careful placement of a hydrogen gas balloon over the reaction flask. The reaction never went to completion even after 2 days of stirring. The reaction mixture was filtered through a Celite-packed sintered funnel and washed with EtOAc (100 mL). Purification by chromatography using a silica-gel column (20 g; EtOAc/hexane, 5:5) afforded product **143** as a colourless oil, (401 mg, 70%). ν_{max} /cm^{-1} (Acetone): 3594b (O-H), 3377s + 3339s (NH, amine), 1514 + 1492 (C=C, aromatic), 723s (C-Cl, halogen); ^{1}H NMR (Acetone-D_6, 400 MHz) δ_H 3.93 (2H, t, *J* = 4.8 Hz, H-2''), 3.96 (3H, s, OCH_3), 4.17 (2H, t, *J* = 4.8 Hz, H-1''), 6.26 (1H, d, *J* = 5.7 Hz, H-5), 7.26 (1H, d, *J* = 8.7 Hz, H-5'), 7.39 (1H, dd, *J* = 8.7, 2.3 Hz, H-6'), 7.86 (1H, d, *J* = 2.3 Hz, H-2'), 8.18 (1H, d, *J* = 5.7 Hz, H-6), 8.62 (1H, bs, NH); ^{13}C NMR (Acetone-D_6, 100 MHz) δ_C 53.9 (OCH_3), 60.8 (C-2''), 70.9 (C-1''), 99.4 (C-5), 104.7 (C-2'), 112.1 (C-6'), 114.7 (C-4'), 130.2 (C-5'), 140.9 (C-1'), 154.7 (C-3'), 158.3 (C-6), 161.0 (C-4), 170.6 (C-2); HRMS (ES): *m/z* 296.0812 $[M+H]^+$. Calculated for $C_{13}H_{15}N_3O_3Cl$, 296.0802 $[M+H]^+$.

2-[3-(2-(4-Methylbenzenesulfonyloxyethoxy)-4-chlorophenylamino]-4-methoxy-1,3-pyrimidine (144)

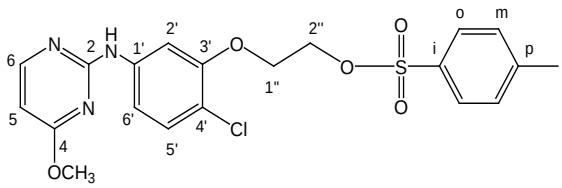

Alcohol **143** (150 mg, 0.51 mmol) was dissolved in dichloromethane (5 mL). Triethylamine (0.10 mL, 0.51 mmol) was added at 0^{o}C followed by a catalytic amount of DMAP (0.60 mg, 0.005 mmol) to the reaction mixture. *p*-Toluenesulfonyl chloride (145 mg, 0.76 mmol) in dichloromethane (2 mL) was then added dropwise and the solution left to stir at room temperature. TLC confirmed completion of the reaction after 4hrs. The reaction mixture was diluted with brine (50 mL) and extracted with dichloromethane (3 × 50 mL). The organic fractions were dried with $MgSO_4$ and removed under reduced pressure. Purification by chromatography using a silica-gel column (10 g; EtOAc/hexane, 5:5) afforded product **144** as a white solid, (160 mg, 70%). Mp. 118-122^{o}C; ν_{max} /cm^{-1} (Acetone): 3377s + 3339s (NH, amine), 1514 + 1492 (C=C, aromatic), 1369s + 1177s (-SO_2-O-), 723s (C-Cl, halogen); ^{1}H NMR (Acetone-D_6, 400 MHz) δ_H 2.43 (3H, s, ArCH_3), 3.94 (3H, s, OCH_3), 4.34 (2H, t, *J* = 4.4 Hz, H-2''), 4.46 (2H, t, *J* = 4.4 Hz, H-1''), 6.25 (1H, d, *J* = 5.7 Hz, H-5), 7.26 (1H, d, *J* = 8.7 Hz, H-5'), 7.38 (1H, dd, *J* = 8.7, 2.2 Hz, H-6'), 7.45 (2H, d, *J* = 8.6 Hz, Ar-m), 7.79 (1H, d, *J* = 2.2 Hz, H-2'), 7.84 (2H, d, *J* = 8.6 Hz, Ar-o), 8.18 (1H, d, *J* = 5.7 Hz, H-6), 8.61 (1H, bs, NH); ^{13}C NMR (Acetone-D_6, 100 MHz) δ_C 20.8 (Ar-CH_3), 53.3 (OCH_3), 66.8 (C-2''), 68.7 (C-1''), 99.4 (C-5), 105.3 (C-2'), 112.6 (C-6'), 114.8 (C-4'), 128.0 (Ar-o), 129.9 (C-5'), 130.1 (Ar-m), 133.6 (Ar-p), 140.9 (C-1'), 145.5 (Ar-i), 154.2 (C-3'), 158.3 (C-6), 160.3 (C-4), 170.2 (C-2); HRMS (ES): *m/z* 450.0876 [M+H]$^{+}$. Calculated for $C_{20}H_{21}N_3SO_5Cl$, 450.0890 [M+H]$^{+}$; C, H, N Microanalysis found: C, 53.24; H, 4.73; N, 9.42; S, 6.98%; $C_{20}H_{20}N_3SO_5Cl$ requires C, 53.39; H, 4.48; N, 9.34; S, 7.13%.

2-[3-(2-Propargyloxyethoxy)-4-chlorophenylamino]-4-methoxy-1,3-pyrimidine (145)

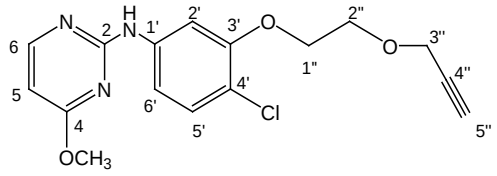

To a suspension of sodium hydride (60%, 50 mg, 1.24 mmol) suspension in THF (7 mL) at 0°C, was added propargyl alcohol (0.11 mL, 1.87 mmol) slowly whilst stirring. To this was added tosylate **144** (140 mg, 0.31 mmol) and the reaction mixture refluxed. TLC confirmed completion after a total of 20 hrs. The reaction mixture was diluted with aq. NH_4Cl (50 mL) and extracted with EtOAc (3 × 50 mL). The organic fractions were dried with $MgSO_4$ and removed under reduced pressure. Purification by chromatography using a silica-gel column (10 g; EtOAc/hexane, 4:6) afforded product **145** as a colourless oil, (822 mg, 98%). ν_{max} /cm^{-1} (Acetone): 3365s + 3340s (NH, amine), 2251 (C≡C), 1517 + 1450 (C=C, aromatic), 723s (C-Cl, halogen); ^{1}H NMR ($CDCl_3$, 300 MHz) δ_H 2.45 (1H, t, J = 2.4 Hz, H-5''), 3.95 (3H, s, OCH_3), 3.96 (2H, t, *J* = 4.9 Hz, H-2''), 4.23 (2H, t, *J* = 4.9 Hz, H-1''), 4.32 (2H, d, *J* = 2.4 Hz, H-3''), 6.22 (1H, d, *J* = 5.7 Hz, H-5), 7.01 (1H, dd, *J* = 8.6, 2.4 Hz, H-6'), 7.14 (1H, bs, NH), 7.26 (1H, d, *J* = 8.6 Hz, H-5'), 7.58 (1H, d, *J* = 2.4 Hz, H-2'), 8.13 (1H, d, *J* = 5.7 Hz, H-6); ^{13}C NMR ($CDCl_3$, 100 MHz) δ_C 53.7 (OCH_3), 56.1 (C-3''), 61.1 (C-2''), 70.8 (C-1''), 76.8 (C-5''), 78.3 (C-4''), 99.4 (C-5), 105.9 (C-2'), 112.2 (C-6'), 114.2 (C-4'), 129.8 (C-5'), 140.2 (C-1'), 153.8 (C-3'), 158.2 (C-6), 160.9 (C-4), 170.0 (C-2); HRMS (ES): *m/z* 333.0875 [M^+]. Calculated for $C_{16}H_{16}N_3O_3Cl$, 333.0880 [M^+].

5-{6-[5-(4-Methoxy-1,3-pyrimidin-2-yl)amino-2-chlorophenoxy]hexa-4-oxa-1-ynyl}uridine-2',3'-didehydro-2',3'-dideoxy-5'-O-benzoate (146)

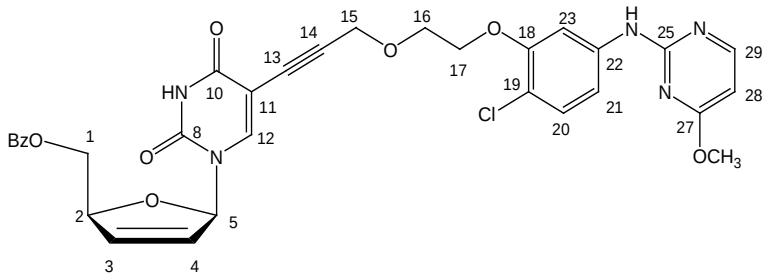

Alkyne **145** (55 mg, 0.16 mmol) was added together with 5-iodo-d4U 5'-benzoate (66 mg, 0.15 mmol) and the mixture dried carefully on a vacuum pump. A mixture of degassed DMF:THF (1:2 (v/v), 3 mL) was then added to the reaction vessel whilst the mixture stirred at room temperature under nitrogen. Subsequent addition of triethylamine (0.04 mL, 0.30 mmol) was followed by addition of copper(I) iodide (14 mg, 0.08 mmol) and tetrakis(triphenylphosphine)palladium (17 mg, 0.02 mmol) respectively. The reaction was stirred continuously at room temperature and TLC confirmed completion of the reaction after 4 hrs. The reaction mixture was diluted with a 5% EDTA solution (30 mL) and extracted with chloroform (3 × 20 mL). The organic fractions were dried with $MgSO_4$ and the solvent removed under reduced pressure. Purification by chromatography using a silica-gel column afforded product **146** as a colourless oil, (68 mg, 70%). $[\alpha]_D$ +9.4° (*c* = 1.01, acetone); ν_{max} /cm^{-1} (Acetone): 2254s (C≡C), 1720s (C=O, ester), 1693s (C=O, pyrimidine), 1599s (C-N stretching), 1514s + 1492s (C=C, aromatic); ^{1}H NMR (DMSO-D_6, 400 MHz) δ_H 3.77 (2H, t, *J* = 4.6 Hz, H-16), 3.91 (3H, s, OCH_3), 4.14 (2H, t, *J* = 4.6 Hz, H-17), 4.26 (2H, s, H-15), 4.49 (2H, s, H-1), 5.15 (1H, m, H-2), 6.09 (1H, m, H-3), 6.29 (1H, d, *J* = 5.7 Hz, H-28), 6.52 (1H, m, H-4), 6.76 (1H, m, H-5), 7.26 (1H, d, *J* = 8.7 Hz, H-20), 7.33 (1H, dd, *J* = 8.7, 2.1 Hz, H-21), 7.54 (2H, t, *J* = 8.0 Hz, Bz-m), 7.62 (1H, t, *J* = 8.0 Hz, Bz-p), 7.66 (1H, s, H-12), 7.75 (1H, d, *J* = 2.1 Hz, H-23), 7.93 (2H, d, *J* = 8.0 Hz, Bz-o), 8.21 (1H, d, *J* = 5.7 Hz, H-29), 9.59 (1H, bs, NH), 11.70 (1H, bs, NH); ^{13}C NMR (DMSO-D_6, 100 MHz) δ_C 53.4 (OCH_3), 58.3 (C-15), 65.2 (C-1), 67.4 (C-16), 67.8 (C-17), 77.7 (C-11), 84.3 (C-13), 88.8 (C-2), 90.1 (C-5), 98.1 (C-14), 98.7 (C-28), 104.6 (C-23), 111.8 (C-21), 113.2 (C-19), 126.2 (C-3), 128.5 (Bz-m), 129.3 (Bz-p), 131.8 (Bz-o), 132.2 (Bz-i), 133.3 (C-20), 133.6 (C-4), 140.5 (C-22), 143.0 (C-12), 149.5 (C-8), 153.4 (C-18), 156.2 (C-29), 159.3 (C-27), 161.3 (C-10), 165.6 ($OCOC_6H_5$), 169.4 (C-25); HRMS (ES): *m/z* 645.1630 [M^+]. Calculated for $C_{32}H_{28}N_5O_8Cl$, 645.1626 [M^+].

5-{6-[5-(4-Methoxy-1,3-pyrimidin-2-yl)amino-2-chlorophenoxy]hexa-4-oxa-1-ynyl}-2',3'-didehydro-2',3'-dideoxyuridine (116)

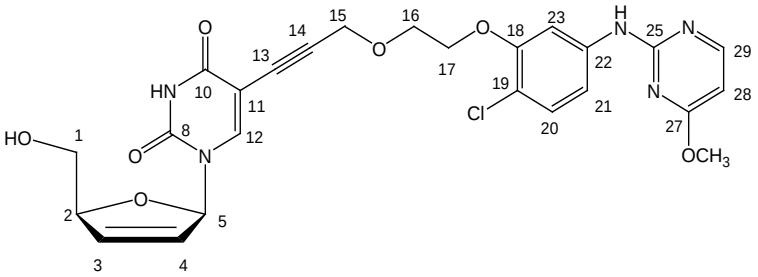

Sodium methoxide (1.97 M) in methanol (0.02 mL, 0.04 mmol) was added to methanol (3 mL) at 0°C. This was followed by addition of **146** (25 mg, 0.04 mmol) at 0°C and the reaction mixture was left to stir at room temperature. After 2 hr, the reaction mixture was diluted with dichloromethane (2mL) and flash chromatography performed directly affording product **116** as a clear oil, (11 mg, 51%). $[\alpha]_D$ +8.3° (*c* = 1.24, acetone); ν_{max} /cm^{-1} (Acetone): 3590b (O-H), 2248 (C≡C), 1692 (C=O, pyrimidine), 1599 (C-N stretching), 1510 + 1472 (C=C, aromatic), 720s (C-Cl, halogen); ^{1}H NMR (DMSO-D_6, 300 MHz) δ_H 3.61 (2H, m, H-1), 3.84 (2H, t, *J* = 4.5 Hz, H-16), 3.93 (3H, s, OCH_3), 4.17 (2H, t, *J* = 4.5 Hz, H-17), 4.42 (2H, s, H-15), 4.82 (1H, m, H-2), 4.97 (1H, bs, OH), 5.94 (1H, m, H-3), 6.29 (1H, d, *J* = 5.7 Hz, H-28), 6.40 (1H, m, H-4), 6.79 (1H, m, H-5), 7.26 (1H, d, *J* = 8.7 Hz, H-20), 7.35 (1H, dd, *J* = 8.7, 2.2 Hz, H-21), 7.74 (1H, d, *J* = 2.2 Hz, H-23), 8.11 (1H, s, H-12), 8.22 (1H, d, *J* = 5.7 Hz, H-29), 9.52 (1H, bs, NH), 11.54 (1H, bs, NH); ^{13}C NMR (DMSO-D_6, 75.5 MHz) δ_C 52.1 (OCH_3), 57.9 (C-15), 64.8 (C-1), 66.5 (C-16), 66.7 (C-17), 76.2 (C-11), 83.5 (C-13), 87.7 (C-2), 89.2 (C-5), 97.2 (C-14), 97.5 (C-28), 103.6 (C-23), 110.9 (C-21), 112.5 (C-19), 125.1 (C-3), 132.4 (C-20), 132.2 (C-4), 139.7 (C-22), 142.1 (C-12), 148.5 (C-8), 152.8 (C-18), 157.8 (C-29), 158.3 (C-27), 160.0 (C-10), 168.9 (C-25); HRMS (ES): *m/z* 542.1459 $[M+H]^+$. Calculated for $C_{25}H_{25}N_5O_7Cl$, 542.1443 $[M+H]^+$.

2-(Methylthio)-1,3-pyrimidin-4(3*H*)-one (161)[191]

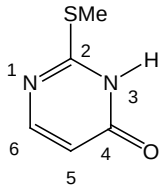

To a solution of sodium hydroxide (16 g, 390 mmol) in water (140 mL) was added 2-thiouracil (25.63 g, 200 mmol). This was followed by methyl iodide (14 mL) and the reaction mixture stirred for 24 hrs at room temperature. The mixture was finally acidified using acetic acid (11 mL) and

the precipitate collected after being washed several times with cold water (3 × 50 mL). Drying over P_2O_5 afforded compound **161** as a white solid, (20.7 g, 73%). Mp. 185-188 ^oC (lit. = 188-189 ^oC); ν_{max} /cm^{-1} (Acetone): 1687 (C=O, pyrimidine), 1600 (C-N stretching), 1512 + 1493 (C=C, aromatic); ^1H NMR (DMSO-D_6, 400 MHz) δ_H 2.43 (3H, s, SCH_3), 6.05 (1H, d, *J* = 6.5 Hz, H-5), 6.65 (1H, bs, NH), 7.82 (1H, d, *J* = 6.5 Hz, H-6); ^{13}C NMR (DMSO-D_6, 100 MHz) δ_C 12.8 (SCH_3), 109.1 (C-5), 153.5 (C-6), 164.0 (C-2), 164.1 (C-4); HRMS (ES): *m/z* 143.0276 $[M+H]^+$. Calculated for $C_5H_7N_2OS$, 143.0279 $[M+H]^+$.

2-[(4-Cyanophenyl)amino]-1,3-pyrimidin-4(3*H*)-one (162)[191]

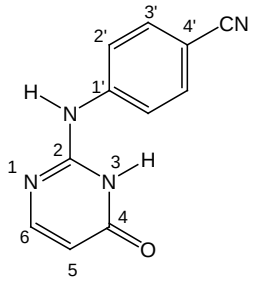

2-(Methylthio)pyrimidin-4(3*H*)-one **161** (5.00 g, 35.2 mmol) was dissolved in diglyme (25 mL) and to this was added 4-aminobenzonitrile (5.00 g, 42.0 mmol). The mixture was refluxed for 18 hrs according to the known procedure, where after cooling, diethyl ether (20 mL) was added and the desired compound precipitated. The precipitate was filtered and after recrystallization from boiling methanol (10 mL) afforded product **162** as a yellow solid, (2.65 g, 36%). Mp. 260-261 ^oC (lit. = 259-260 ^oC); ν_{max} /cm^{-1} (Acetone): 2210s (C-N, nitrile), 1687 (C=O, pyrimidine), 1600 (C-N stretching), 1512 + 1493 (C=C, aromatic); ^1H NMR (DMSO-D_6, 400 MHz) δ_H 6.00 (1H, d, *J* = 6.3 Hz, H-5), 6.08 (1H, bs, NH), 6.60 (1H, s, NH), 7.36 (1H, d, *J* = 6.3 Hz, H-6), 7.71 (2H, d, *J* = 8.7 Hz, H-3'), 7.81 (2H, d, *J* = 8.7 Hz, H-2'); ^{13}C NMR (DMSO-D_6, 100 MHz) δ_C 101.7 (C-4'), 108.9 (C-5), 118.7 (C-3'/C-5'), 118.9 (C≡N), 132.7 (C-2'/C-6'), 145.9 (C-1'), 153.3 (C-6), 160.0 (C-2), 162.0 (C-4); HRMS (ES): *m/z* 213.0778 $[M+H]^+$. Calculated for $C_{11}H_9N_4O$, 213.0776 $[M+H]^+$.

2-[(4-Cyanophenyl)amino]-4-chloro-1,3-pyrimidine (154)

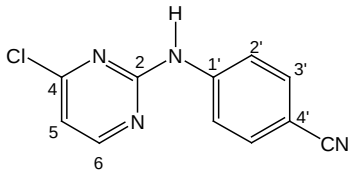

2-[(4-Cyanophenyl)amino]pyrimidin-4(3*H*)-one **162** (500 mg, 2.30 mmol) was dissolved in neat phosphorus oxychloride (5 mL, excess) and the reaction mixture heated to 100 ^{o}C. TLC confirmed reaction completion after 5 hrs. The mixture was cooled to 0 ^{o}C and diluted with H_2O (10 mL), aq. $NaHCO_3$ (50 mL) and extracted with EtOAc (3 × 50 mL), the organic layer dried over $MgSO_4$ and the solvent removed under reduced pressure. Purification by chromatography afforded product **154** as a yellow solid, (480 mg, 90%). Mp. 161-162 ^{o}C; ν_{max} /cm^{-1} (Acetone): 2209s (C-N, nitrile), 1517 + 1481 (C=C, aromatic), 720s (C-Cl, halogen); ^{1}H NMR (Acetone-D_6, 300 MHz) δ_H 7.03 (1H, d, *J* = 5.3 Hz, H-5), 7.73 (2H, d, *J* = 9.0 Hz, H-3'), 8.06 (2H, d, *J* = 9.0 Hz, H-2'), 8.49 (1H, d, *J* = 5.3 Hz, H-6), 9.39 (1H, bs, NH); ^{13}C NMR (Acetone-D_6, 75.5 MHz) δ_C 102.1 (C-4'), 113.7 (C-5), 118.7 (C-3'/C-5'), 119.0 (C≡N), 129.7 (C-4), 133.3 (C-2'/C-6'), 142.6 (C-1'), 158.9 (C-6), 159.1 (C-2); HRMS (ES): *m/z* 231.0433 $[M+H]^+$. Calculated for $C_{11}H_8N_4Cl$, 231.0437 $[M+H]^+$; C, H, N Microanalysis found: C, 57.12; H, 3.09; N, 24.29; $C_{11}H_7N_4Cl$ requires C, 57.28; H, 3.06; N, 24.29.

4-[(4-Chloro-3-hydroxyphenyl)amino]-2-[(4-cyanophenyl)amino]-1,3-pyrimidine (168)

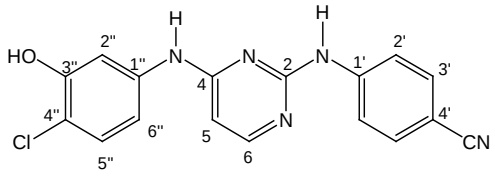

To a solution of 2-[(4-cyanophenyl)amino]-4-chloro-1,3-pyrimidine **154** (120 mg, 0.51 mmol) dissolved in 1,4-dioxane (10 mL) was added anhydrous *p*-TsOH (18 mg, 0.10 mmol) at room temperature. To this mixture was added substituted aniline **119b** (54 mg, 0.36 mmol) and the reaction mixture was heated to 100 ^{o}C. TLC confirmed reaction completion after 12 hrs. The reaction mixture was diluted with aq. $NaHCO_3$ (50 mL) and extracted with EtOAc (3 × 50 mL), the organic layer dried over $MgSO_4$ and the solvent removed under reduced pressure. Purification by chromatography using a silica-gel column (10 g; EtOAc neat) afforded product **168** as a clear oil, (174 mg, 100%). ν_{max} /cm^{-1} ($CHCl_3$): 3574b (O-H), 3381s + 3333s (NH, amine), 2209s (C-N, nitrile), 1521 + 1492 (C=C, aromatic), 726s (C-Cl, halogen); ^{1}H NMR (DMSO-D_6, 300 MHz) δ_H 6.32 (1H, d, *J* = 5.8 Hz, H-5), 7.11 (1H, d, *J* = 2.1 Hz, H-2''), 7.25 (1H, d, *J* = 8.6 Hz, H-5''), 7.30 (1H, dd, *J* = 8.6, 2.10 Hz, H-6''), 7.65 (2H, d, *J* = 9.0 Hz, H-3'), 7.94 (2H, d, *J* = 9.0 Hz, H-2'), 8.08 (1H, d, *J* = 5.8 Hz, H-4), 9.43 (1H, s, NH), 9.66 (1H, s, OH), 10.02 (1H, s, NH); ^{13}C NMR (DMSO-D_6, 75.5 MHz) δ_C 99.9 (C-5), 101.7 (C-4'), 108.7 (C-2''), 112.5 (C-6''), 113.4 (C-4''), 118.2 (C-2'/C-6'), 119.5 (C≡N), 129.4 (C-5''), 132.7 (C-3'/C-5'), 139.2 (C-1''),

145.1 (C-1'), 152.9 (C-3''), 155.9 (C-4), 158.7 (C-6), 160.4 (C-2); HRMS (ES): *m/z* 337.0738 [M^+]. Calculated for $C_{17}H_{12}N_5OCl$, 337.0738 [M^+].

2-[2-Benzyloxyethoxy)-2-ethoxy)-2-ethoxy]ethanol (166)

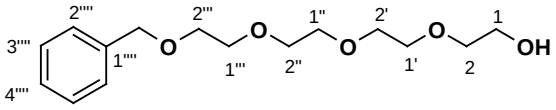

Benzyl bromide (3.06 mL, 25.7 mmol) was added dropwise to a suspension of NaH (60%, 1.03 g, 25.7 mmol) and tetraethylene glycol (4.44 mL, 25.7 mmol) in THF (50 mL). After 20 hrs the mixture was diluted with EtOAc (3 × 50 mL) and washed with aq. NH_4Cl (50 mL) and H_2O (2 × 50 mL), the organic layer dried over $MgSO_4$ and the solvent removed under reduced pressure. Purification by chromatography afforded product **166** as a colourless oil, (2.88 g, 39%). ^{1}H NMR ($CDCl_3$, 300 MHz) δ_H 2.80 (1H, brs, OH), 3.58 (2H, t, *J* = 4.8 Hz, H-1), 3.66 (14H, m, 7 × CH_2O), 4.56 (2H, s, Ar*C*H_2O), 7.34 (5H, m, ArH); ^{13}C NMR ($CDCl_3$, 75.5 MHz) δ_C 61.6 (C-1), 69.3 (CH_2O), 70.2 (CH_2O), 70.5 (2 × CH_2O), 70.6 (2 × CH_2O), 72.4 (CH_2O), 73.1 (Ar*C*H_2O), 127.4 (C-4''''), 127.6 (C-3'''', C-5''''), 128.2 (C-2'''', C-6''''), 138.2 (C-1'''').

2-[2-Benzyloxyethoxy)-2-ethoxy)-2-ethoxy]-1-bromoethane (167)

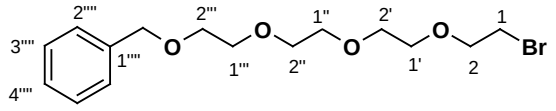

To a solution of the alcohol **166** (2.50 g, 8.79 mmol) and PPh_3 (2.77 g, 10.5 mmol) in CH_2Cl_2 (20 mL) was added CBr_4 (3.50 g, 10.5 mmol) at 0 ^{o}C. The reaction mixture was stirred at 0 ^{o}C for 30 min and the solvent removed under reduced pressure. Purification by chromatography afforded product **167** as a colourless oil, (2.69 g, 88%). ^{1}H NMR ($CDCl_3$, 300 MHz) δ_H 3.45 (2H, t, *J* = 6.3 Hz, H-1), 3.67 (12H, m, 6 × CH_2O), 3.80 (2H, t, *J* = 6.3 Hz, CH_2O), 4.57 (2H, s, ArCH_2O), 7.28 (1H, m, ArH), 7.35 (4H, m, ArH); ^{13}C NMR ($CDCl_3$, 75.5 MHz) δ_C 30.2 (C-1), 69.4 (CH_2O), 70.4 (CH_2O), 70.5 (2 × CH_2O), 70.6 (2 × CH_2O), 71.1 (CH_2O), 73.1 (Ar*C*H_2O), 127.5 (C-4''''), 127.6 (C-3'''', C-5''''), 128.2 (C-2'''', C-6''''), 138.2 (C-1'''').

4-[3-(2-Benzyloxyethoxy)-2-ethoxy)-2-ethoxy)-2-ethoxy)-4-chlorophenylamino]-2-[(4-cyano phenyl)amino]-1,3-pyrimidine (169)

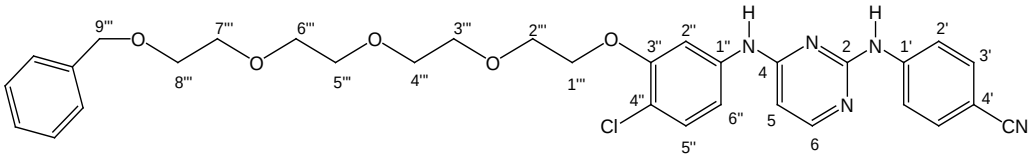

To a solution of DAPY **168** (120 mg, 0.36 mmol) dissolved in acetonitrile (10 mL) was added anhydrous K_2CO_3 (75 mg, 0.54 mmol) at room temperature. Tether **167** (135 mg, 0.40 mmol) was slowly added to this mixture and the reaction mixture heated to 50 ^oC. After 12 hrs the mixture was diluted with H_2O (100 mL) and extracted with EtOAc (3 × 100 mL), the organic layer dried over $MgSO_4$ and the solvent removed under reduced pressure. Purification by chromatography afforded product **169** as a white solid, (218mg, 100%). Mp. 183-185 ^oC; ν_{max} /cm^{-1} (Acetone): 3381s + 3333s (NH, amine), 2209s (C-N, nitrile), 1521 + 1492 (C=C, aromatic), 726s (C-Cl, halogen); ^1H NMR (DMSO-D_6, 400 MHz) δ_H 3.40-3.60 (12H, m, H-3''' - H-8'''), 3.75 (2H, t, *J* = 4.6 Hz, H-2'''), 4.10 (2H, t, *J* = 4.6 Hz, H-1'''), 4.45 (2H, s, H-9'''), 6.33 (1H, d, *J* = 5.8 Hz, H-5), 7.26-7.35 (8H, m, H-2'' + H-5'' + H-6'' + Ph), 7.65 (2H, d, *J* = 8.9 Hz, H-3'), 7.93 (2H, d, *J* = 8.9 Hz, H-2'), 8.10 (1H, d, *J* = 5.8 Hz, H-6), 9.55 (1H, bs, NH), 9.70 (1H, bs, NH); ^{13}C NMR (DMSO-D_6, 100 MHz) δ_C 59.6 (OCH_2), 60.1 (OCH_2), 68.3 (OCH_2), 68.6 (OCH_2), 69.0 (OCH_2), 69.7 x 2 (OCH_2), 70.0 (OCH_2), 71.9 (C-9'''), 100.1 (C-5), 101.8 (C-4'), 106.2 (C-2''), 113.2 (C-6''), 114.6 (C-4''), 118.3 (C-2'/C-6'), 119.5 (C≡N), 127.2 (Bn-*p*), 127.4 (Bn-*m*), 128.0 (Bn-*o*), 129.5 (C-5''), 132.7 (C-3'/C-5'), 138.3 (Bn-*i*), 139.7 (C-1''), 145.1 (C-1'), 153.7 (C-3''), 156.0 (C-6), 158.7 (C-4), 160.3 (C-2); HRMS (ES): *m/z* 604.2344 $[M+H]^+$. Calculated for $C_{32}H_{35}N_5O_5Cl$, 604.2327 $[M+H]^+$; C, H, N Microanalysis found: C, 63.65; H, 5.98; N, 11.58; $C_{32}H_{34}N_5O_5Cl$ requires C, 63.62; H, 5.67; N, 11.59.

4-[4-Chloro-3-(2-hydroxyethoxy)-2-ethoxy)-2-ethoxy)-2-ethoxy)phenylamino]-2-[(4-cyanophenyl)amino]-1,3-pyrimidine (170)

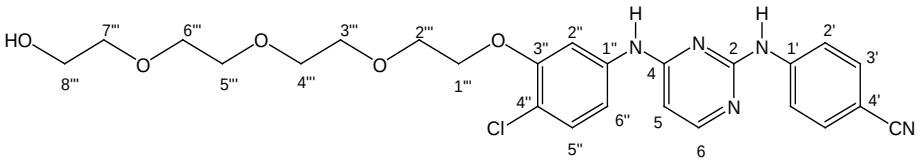

The benzyl ether **169** (250 mg, 0.40 mmol) was dissolved in absolute ethanol/THF (1:1) (4mL) and stirred at room temperature. Subsequent addition of palladium-on-carbon (10%, 220 mg, 0.20 mmol) was followed by careful placement of a hydrogen gas balloon over the reaction flask. The reaction failed to go to completion even after 2 days of stirring. The reaction mixture was

filtered through a Celite-packed sintered funnel and washed EtOAc (100 mL). Purification by chromatography using a silica-gel column (20 g; EtOAc neat) afforded product **170** as a colourless oil, (60 mg, 30%). ν_{max} /cm^{-1} (Acetone): 3577b (O-H), 3363s + 3336s (NH, amine), 2213s (C-N, nitrile), 1541 + 1422 (C=C, aromatic), 722s (C-Cl, halogen); ^{1}H NMR (Acetone-D_6, 300 MHz) δ_H 3.04 (1H, bs, OH), 3.49-3.70 (12H, m, H-3''' + H-8'''), 3.85 (2H, t, *J* = 4.76 Hz, H-2'''), 4.17 (2H, t, *J* = 4.7 Hz, H-1'''), 6.40 (1H, d, *J* = 5.8 Hz, H-5), 7.29 (2H, m, H-5'' + H-6''), 7.46 (1H, m, H-2''), 7.63 (2H, d, *J* = 9.0 Hz, H-3'), 8.00 (2H, d, *J* = 9.0 Hz, H-2'), 8.09 (1H, d, *J* = 5.8 Hz, H-6), 8.80 (1H, bs, NH), 8.89 (1H, bs, NH); ^{13}C NMR (Acetone-D_6, 75.5 MHz) δ_C 61.3 (OCH_2), 69.1 (OCH_2), 69.5 (OCH_2), 70.4 (OCH_2), 70.5 x 2 (OCH_2), 70.9 (OCH_2), 72.8 (OCH_2), 100.3 (C-5), 103.4 (C-4'), 107.3 (C-2''), 114.1 (C-6''), 116.3 (C-4''), 118.8 (C-2'/C-6'), 119.4 (C≡N), 129.9 (C-5''), 132.9 (C-3'/C-5'), 139.9 (C-1''), 145.4 (C-1'), 154.7 (C-3''), 156.5 (C-6), 159.4 (C-4), 161.2 (C-2); HRMS (ES): *m/z* 514.1860 $[M+H]^+$. Calculated for $C_{25}H_{29}N_5O_5Cl$, 514.1857 $[M+H]^+$.

4-Iodo-2,6-dimethylphenol (153)[192]

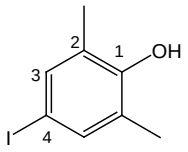

To 2,6-dimethylphenol **163** (2.50 g, 20.4 mmol), in diethyl ether (100 mL) was added morpholine (7.20 mL, 81.6 mmol), followed by iodine (5.20 g, 20.4 mmol) in diethyl ether (50 mL) with rapid stirring at room temperature. TLC confirmed reaction completion after 1½ hrs. The reaction precipitate was filtered off and the filtrate extracted into diethyl ether (3 × 100 mL) following addition of 1M HCl (100 mL). The combined organic extracts were dried over $MgSO_4$ and the solvent removed under reduced pressure. Purification by chromatography using a silica-gel column afforded product **153** as a light yellow solid, (4.60 g, 90%). Mp. 93-95 ^{o}C (Mp. Lit. 94-95 ^{o}C); ν_{max} /cm^{-1} (Acetone): 3573b (O-H), 1514s + 1492s (C=C, aromatic), 721s (C-I, halogen); ^{1}H NMR ($CDCl_3$, 300 MHz) δ_H 2.19 (6H, s, $ArCH_3$), 4.62 (1H, bs, OH), 7.31 (2H, s, H-3, H-5); ^{13}C NMR ($CDCl_3$, 75.5 MHz) δ_C 15.4 ($ArCH_3$), 82.3 (C-4), 125.7 (C-2), 137.0 (C-3), 152.1 (C-1); HRMS (ES): *m/z* 246.9635 $[M-H]^+$. Calculated for C_8H_9OI, 246.9620 $[M-H]^+$; C, H, N Microanalysis found: C, 38.63; H, 3.93; C_8H_7OI requires C, 38.73; H, 3.66.

Tetraethylene glycol monopropargyl ether (151)

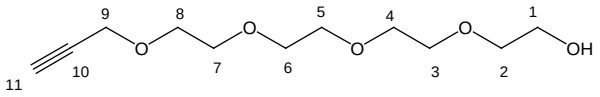

Sodium hydride (60%, 1.10 g, 25.7 mmol) was suspended in dry THF (50 mL) at 0°C (ice slurry), and to the solution was added tetraethylene glycol (4.40 mL, 25.7 mmol) portionwise. Once gas evolution had subsided, propargyl bromide (2.50 mL, 28.3 mmol) was added slowly. The ice bath was then removed and the mixture stirred at room temperature. TLC confirmed completion of the reaction after 6 hrs. The reaction mixture was diluted with water (100 mL) and extracted with EtOAc (3 × 100 mL), the organic layer dried over $MgSO_4$ and the solvent removed under reduced pressure. Purification by chromatography using a silica-gel column (80 g, MeOH/EtOAc, 0.5:9.5) afforded product **151** as a clear oil, (2.50 g, 42%). ν_{max} /cm^{-1} (Acetone): 2940s + 2872s (C-H, aliphatic), 2251s (C≡C); ^{1}H NMR ($CDCl_3$, 400 MHz) δ_H 2.42 (1H, t, *J* = 2.4 Hz, H-11), 2.79 (1H, bs, OH), 3.57-3.63 (16H, m, H-1 - H8), 4.17 (2H, d, *J* = 2.4 Hz, H-9); ^{13}C NMR ($CDCl_3$, 100 MHz) δ_C 58.0 (C-9), 61.2 (OCH_2), 68.7 (OCH_2), 69.7 (OCH_2), 69.9 (OCH_2), 70.1 (OCH_2), 70.2 (OCH_2), 70.3 (OCH_2), 72.2 (OCH_2), 74.4 (C-11), 79.3 (C-10); HRMS (ES): *m/z* 233.1385 $[M+H]^+$. Calculated for $C_{11}H_{21}O_5$, 233.1389 $[M+H]^+$.

Hexaethylene glycol monopropargyl ether (183)

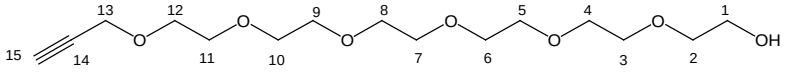

Sodium hydride (60%, 284 mg, 7.08 mmol) was suspended in dry THF (50 mL) at 0°C (ice slurry), and to the solution was added hexaethylene glycol (2.00 g, 7.08 mmol) portionwise. Once gas evolution had subsided, propargyl bromide (0.70 mL, 7.80 mmol) was added slowly. The ice bath was then removed and the mixture stirred at room temperature. TLC confirmed completion of the reaction after 5 hrs. The reaction mixture was diluted with water (100 mL) and extracted with EtOAc (3 × 100 mL), the organic layer dried over $MgSO_4$ and the solvent removed under reduced pressure. Purification by chromatography using a silica-gel column (30 g; MeOH/EtOAc, 2:8) afforded product **183** as a clear oil, (1.20 g, 53%). ν_{max} /cm^{-1} (Acetone): 2940s + 2872s (C-H, aliphatic), 2251s (C≡C); ^{1}H NMR ($CDCl_3$, 300 MHz) δ_H 2.43 (1H, t, *J* = 2.4 Hz, H-15), 2.78 (1H, bs, OH), 3.61-3.65 (24H, m, H-1 - H-12), 4.15 (2H, d, *J* = 2.4 Hz, H-13); ^{13}C NMR ($CDCl_3$, 75.5 MHz) δ_C 58.2 (C-13), 61.4 (OCH_2), 68.9 (OCH_2), 70.3 x 3 (OCH_2), 70.4 x 6

(OCH_2), 72.6 (OCH_2), 74.4 (C-15), 79.5 (C-14); HRMS (ES): *m/z* 321.1927 $[M+H]^+$. Calculated for $C_{15}H_{29}O_7$, 321.1913 $[M+H]^+$.

4-(4-Iodo-2,6-dimethylphenoxy)-2-[(4-cyanophenyl)amino]-1,3-pyrimidine (152)

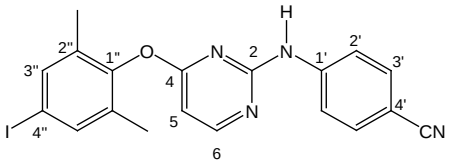

To a solution of cesium carbonate (840 mg, 2.60 mmol) and 4-iodo-2,6-dimethylphenol **153** (470 mg, 1.90 mmol) in DMF (8 mL), was added 2-[(4-Cyanophenyl)amino]-4-chloro-1,3-pyrimidine **154** (400 mg, 1.72 mmol) and the mixture heated to 90 ^oC. TLC confirmed reaction completion after 1 hr. The reaction mixture was diluted with brine (100 mL) and extracted with EtOAc (3 × 100 mL), the organic layer dried over $MgSO_4$ and the solvent removed under reduced pressure. Purification by chromatography using a silica-gel column (35 g; EtOAc/hexane, 5:5) afforded product **152** as a yellow solid, (758 mg, 99%). Mp. 218-220 ^oC; ν_{max} /cm^{-1} (Acetone): 3381s + 3333s (NH, amine), 2211s (C-N, nitrile), 1516s + 1489s (C=C, aromatic), 723s (C-I, halogen); ^1H NMR (DMSO-D_6, 300 MHz) δ_H 2.02 (6H, s, $ArCH_3$), 6.61 (1H, d, *J* = 5.6 Hz, H-5), 7.46 (2H, d, *J* = 8.9 Hz, H-3'), 7.56 (2H, d, *J* = 8.9 Hz, H-2'), 7.58 (2H, s, H-3'', H-5''), 8.43 (1H, d, *J* = 5.6 Hz, H-6), 9.99 (1H, bs, NH); ^{13}C NMR (DMSO-D_6, 75.5 MHz) δ_C 15.4 ($ArCH_3$), 90.4 (C-4''), 99.0 (C-5), 102.4 (C-4'), 118.2 (C-2'/C-6'), 119.3 (C≡N), 132.4 (C-3'/C-5'), 133.2 (C-2''/C-6''), 137.0 (C-3''/C-5''), 144.4 (C-1'), 149.5 (C-1''), 159.0 (C-2), 160.3 (C-6), 168.0 (C-4); HRMS (ES): *m/z* 443.0348 $[M+H]^+$. Calculated for $C_{19}H_{16}N_4OI$, 443.0369 $[M+H]^+$; C, H, N Microanalysis found: C, 52.18; H, 3.82; N, 12.96; $C_{19}H_{15}N_4OI$ requires C, 51.60; H, 3.62; N, 12.67.

4-[3-(2-Hydroxyethoxy)-2-ethoxy)-2-ethoxy)-2-ethoxy)prop-1-ynyl)-2,6-dimethylphenoxy)]-2-[(4-cyanophenyl)amino]-1,3-pyrimidine (150)

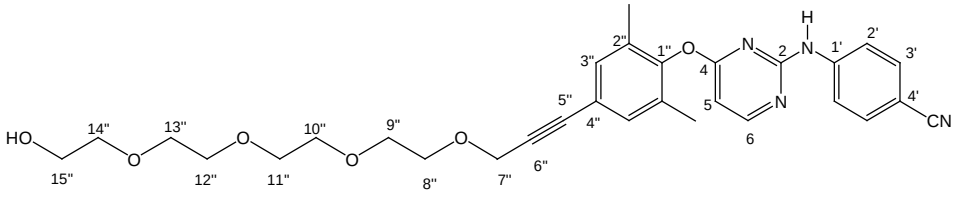

Alkyne **151** (231 mg, 1.00 mmol) was added together with DAPY **152** (485 mg, 1.10 mmol) and the mixture dried carefully on a vacuum pump. A mixture of degassed DMF:THF (1:2 (v/v), 6 mL) was then added to the reaction vessel whilst the mixture stirred at room temperature under

nitrogen. Subsequent addition of triethylamine (0.30 mL, 2.20 mmol) was followed by addition of copper(I) iodide (104 mg, 0.55 mmol) and tetrakis(triphenylphosphine)palladium (127 mg, 0.11 mmol) respectively. The reaction was stirred continuously at room temperature and TLC confirmed completion of the reaction after 30 min. The reaction mixture was diluted with a 5% EDTA solution (50 mL) and extracted with chloroform (3 × 100 mL). The organic fractions were dried with $MgSO_4$ and the solvent removed under reduced pressure. Purification by chromatography using a silica-gel column afforded product **150** as a clear oil, (450 mg, 75%). ν_{max} /cm^{-1} (Acetone): 3577b (O-H), 3353s + 3340s (NH, amine), 2253s (C≡C), 2208s (C-N, nitrile), 1541 + 1428 (C=C, aromatic); ^{1}H NMR (Acetone-D_6, 300 MHz) δ_H 2.11 (6H, s, $ArCH_3$), 2.81 (1H, s, OH), 3.52-3.62 (12H, m, H-9'' - H-14''), 3.69 (2H, m, H-15''), 3.76 (2H, m, H-8''), 4.45 (2H, s, H-7''), 6.64 (1H, d, *J* = 5.6 Hz, H-5), 7.32 (2H, s, H-3''/H-5''), 7.48 (2H, d, *J* = 8.8 Hz, H-3'/H-5'), 7.71 (2H, d, *J* = 8.8 Hz, H-2'/H-6'), 8.45 (1H, d, *J* = 5.6 Hz, H-6), 9.13 (1H, bs, NH); ^{13}C NMR (Acetone-D_6, 75.5 MHz) δ_C 15.7 ($ArCH_3$), 58.6 (C-7''), 61.3 (OCH_2), 69.2 (OCH_2), 70.4 x 2 (OCH_2), 70.6 x 3 (OCH_2), 72.9 (OCH_2), 85.4 (C-6''), 85.7 (C-5''), 99.4 (C-5), 104.0 (C-4'), 118.6 (C-2'/C-6'), 119.2 (C≡N), 120.4 (C -4''), 131.7 (C-2''/C-6'')), 132.1 (C-3'/C-5'), 132.8 (C-3''/C-5''), 144.8 (C-1'), 150.5 (C-1''), 159.8 (C-2), 160.4 (C-6), 169.1 (C-4); HRMS (ES): *m/z* 547.2604 $[M+H]^+$. Calculated for $C_{30}H_{35}N_4O_6$, 546.2624 $[M+H]^+$.

4-[3-(2-(4-Methylbenzenesulfonyloxyethoxy)-2-ethoxy)-2-ethoxy)-2-ethoxy)prop-1-ynyl)-2,6-dimethylphenoxy)]-2-[(4-cyanophenyl)amino]-1,3-pyrimidine (165)

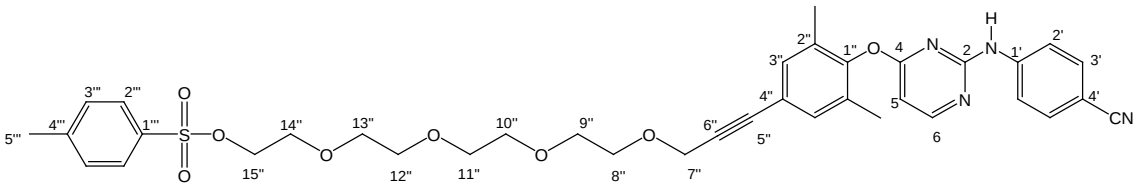

DAPY alcohol **150** (390 mg, 0.71 mmol) was dissolved in THF (10 mL). Triethylamine (0.14 mL, 1.00 mmol) was added at 0^{o}C followed by a catalytic amount of DMAP (18.0 mg, 0.14 mmol) to the reaction mixture. *p*-Toluenesulfonyl chloride (210 mg, 1.00 mmol) dissolved in THF (2 mL) was then added dropwise and the solution left to stir at room temperature. TLC confirmed completion of the reaction after 10 hrs. The reaction mixture was diluted with brine (50 mL) and extracted with EtOAc (3 × 50 mL). The organic fractions were dried with $MgSO_4$ and the solvent removed under reduced pressure. Purification by chromatography using a silica-gel column (30 g; EtOAc/hexane, 5:5) afforded product **165** as a clear oil, (463 mg, 93%). ν_{max} /cm^{-1} (Acetone):

3353s + 3340s (NH, amine), 2253s (C≡C), 2208s (C-N, nitrile), 1541 + 1428 (C=C, aromatic), 1372s + 1180s (-SO_2-O-); ^{1}H NMR (Acetone-D_6, 400 MHz) δ_H 2.08 (3H, s, H-5'''), 2.09 (6H, s, $ArCH_3$), 3.61 (12H, m, H-9'' - H-14''), 3.73 (2H, m, H-8''), 3.79 (2H, m, H-15''), 4.43 (2H, s, H-7''), 6.61 (1H, d, *J* = 5.6 Hz, H-5), 7.32 (2H, s, H-3''/H-5''), 7.45 (2H, d, *J* = 8.6 Hz, H-3'''/H-5'''), 7.48 (2H, d, *J* = 8.8 Hz, H-3'/H-5'), 7.62 (2H, d, *J* = 8.6 Hz, H-2'''/H-6'''), 7.69 (2H, d, *J* = 8.8 Hz, H-2'/H-6'), 8.44 (1H, d, *J* = 5.6 Hz, H-6), 9.11 (1H, bs, NH); ^{13}C NMR (Acetone-D_6, 100 MHz) δ_C 15.6 ($ArCH_3$), 20.7 (C-5'''), 58.6 (C-7''), 64.1 (OCH_2), 68.6 (OCH_2), 69.3 (OCH_2), 69.8 (OCH_2), 70.0 (OCH_2), 70.5 (OCH_2), 70.6 x 2 (OCH_2), 85.3 (C-6''), 85.7 (C-5''), 99.3 (C-5), 104.0 (C-4'), 118.6 (C-2'/C-6'), 119.2 (C≡N), 120.5 (C-4''), 125.4 (C-4'''), 128.0 (C-2'''/C-6'''), 129.8 (C-3'''/C-5'''), 130.1 (C-1'''), 131.7 (C-2''/C-6''), 132.1 (C-3'/C-5'), 132.8 (C-3''/C-5''), 144.8 (C-1'), 150.5 (C-1''), 159.7 (C-2), 160.4 (C-6), 169.0 (C-4); HRMS (ES): *m/z* 701.2693 $[M+H]^+$. Calculated for $C_{37}H_{41}N_4O_8S$, 701.2712 $[M+H]^+$.

4-[3-(2-Propargyloxyethoxy)-2-ethoxy)-2-ethoxy)-2-ethoxy)prop-1-ynyl)-2,6-dimethyl-phenoxy)]-2-[(4-cyanophenyl)amino]-1,3-pyrimidine (149)

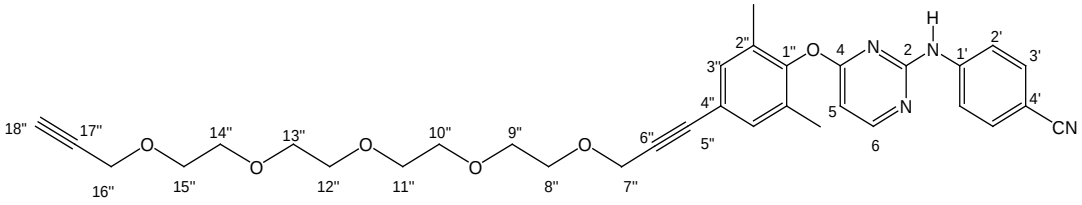

To a suspension of sodium hydride (60%, 100 mg, 2.50 mmol) suspension in THF (20 mL) at 0^{o}C, was added propargyl alcohol (0.21 mL, 3.60 mmol) slowly whilst stirring. To this was added DAPY tosylate **165** (420 mg, 0.60 mmol) and the reaction mixture refluxed. TLC confirmed completion after a total of 20 hrs. The reaction mixture was diluted with aq. NH_4Cl (100 mL) and extracted with EtOAc (3 × 100 mL). The organic fractions were dried with $MgSO_4$ and removed under reduced pressure. Purification by chromatography using a silica-gel column (50 g; EtOAc/hexane, 9:1) afforded product **149** as a colourless oil, (301 mg, 86%). ν_{max} /cm^{-1} (Acetone): 3353s + 3340s (NH, amine), 2253s (C≡C), 2208s (C-N, nitrile), 1541 + 1428 (C=C, aromatic); ^{1}H NMR ($CDCl_3$, 400 MHz) δ_H 2.10 (6H, s, $ArCH_3$), 2.42 (1H, t, *J* = 2.4 Hz, H-18''), 3.67 (12H, m, H-9'' - H-14''), 3.75 (2H, m, H-15''), 3.80 (2H, m, H-8''), 4.20 (2H, d, *J* = 2.4 Hz, H-16''), 4.46 (2H, s, H-7''), 6.49 (1H, d, *J* = 5.7 Hz, H-5), 7.26 (2H, d, *J* = 8.8 Hz, H-3''/H-5''), 7.41 (4H, m, H-2'/H-6' + H-3'/H-5'), 8.34 (1H, d, *J* = 5.7 Hz, H-6); ^{13}C NMR ($CDCl_3$, 100 MHz) δ_C 16.1 ($ArCH_3$), 58.2 (C-7''), 59.2 (C-16''), 69.2 (OCH_2), 70.6 x 7 (OCH_2), 74.4 (C-18''), 79.7 (C-17''), 85.1 (C-6''), 85.6 (C-5''), 99.4 (C-5), 104.6 (C-4'), 118.1 (C-2'/C-6'), 119.3 (C≡N), 120.2 (C-4''),

131.2 (C-2''/C-6'), 132.1 (C-3'/C-5'), 133.0 (C-3''/C-5''), 143.3 (C-1'), 150.0 (C-1''), 159.1 (C-2), 159.6 (C-6), 169.0 (C-4); HRMS (ES): *m/z* 585.2732 $[M+H]^+$. Calculated for $C_{33}H_{37}N_4O_6$, 585.2713 $[M+H]^+$.

5-{19-[4-(2-(4-Cyanophenylamino)-1,3-pyrimidine-4-oxy)-3,5-dimethylphenyl]-(4,7,10,13,16-pentaoxanonadecadi-1,18-ynyl)}uridine-2',3'-didehydro-2',3'-dideoxy-5'-O-benzoate (171)

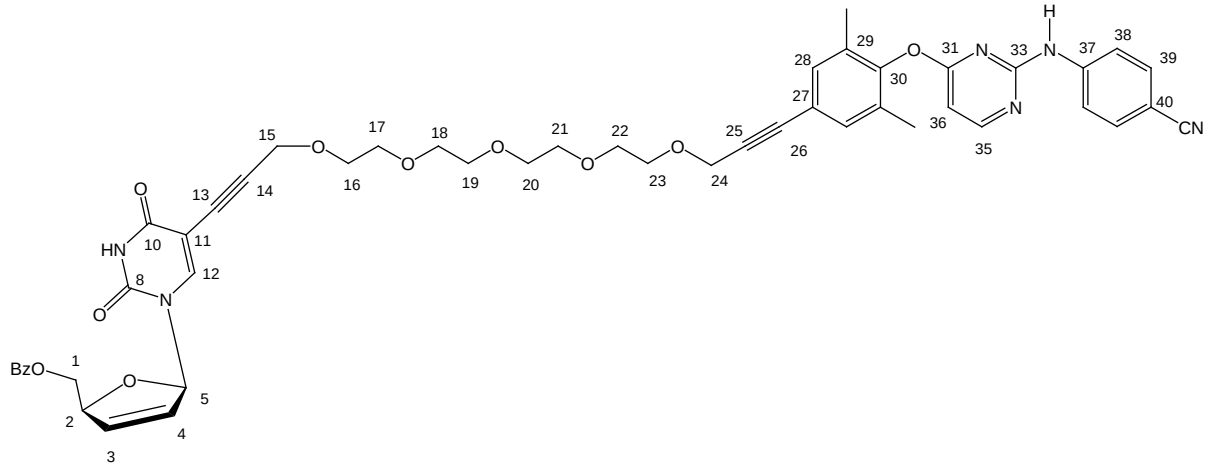

A mixture of (tetrakis)triphenylphosphinepalladium (0) (30.0 mg, 0.026 mmol) and copper (I) iodide (30.0 mg, 0.16 mmol) was added rapidly to a solution of 5-iodo-5´-benzoyl-d4U **60** (110 mg, 0.25 mmol) and alkyne **149** (99.0 mg, 0.17 mmol) in a degassed mixture of THF and DMF (6 ml, 2:1) at room temperature under nitrogen. TLC indicated reaction to a more polar product to be complete after 3 hours with complete consumption of alkyne. Work-up involved adding EDTA solution (20 ml, 5%) and extracting the product into EtOAc (3 x 50 ml). Drying (Na_2SO_4) and evaporation of solvent followed by column chromatography of the residue on silica-gel using EtOAc / hexane mixtures as eluent furnished the bifunctional compound **171** (91.0 mg, 59%). ^{1}H-NMR ($CDCl_3$, 500 MHz) δ_H 2.06 (6H, s, $ArCH_3$), 3.58-3.80 (16H, m, H-16 - H-23), 4.20 (2H, s, H-15), 4.43 (2H, s, H-24), 4.49 (1H, dd, *J* = 3.0, 10.0 Hz, H-1), 4.67 (1H, dd, *J* = 4.5, 10.0 Hz, H-1), 5.19 (1H, m, H-2), 5.96 (1H, m, H-3), 6.39 (1H, m, H-4), 6.47 (1H, d, *J* = 5.7 Hz, H-36), 6.94 (1H, m, H-5), 7.22 (2H, s, H-28), 7.32 (4H, m, H-38, H-39), 7.43 (2H, m, Bz-m), 7.56 (1H, m, Bz-p), 7.67 (1H, s, H-12), 7.99 (2H, m, Bz-o), 8.42 (1H, d, *J* = 5.7 Hz, H-35), 8.95 (1H, s, NH), 11.82 (1H, s, NH); ^{13}C-NMR ($CDCl_3$, 500 MHz) δ_C 16.2 ($ArCH_3$), 59.0 (C-24), 59.2 (C-15), 65.0 (C-1), 69.2 x 2 (OCH_2), 70.3 (OCH_2), 70.4 (OCH_2), 70.5 x 2 (OCH_2), 70.6 (OCH_2), 77.0 (OCH_2), 85.1 (C-14), 85.2 (C-25), 85.6 (C-2), 90.1 (C-5), 90.6 (C-26), 99.0 (C-13), 100.2 (C-36), 104.2 (C-40), 118.2 (C-11), 119.5 (C-38/C-42), 120.2 (CN), 120.8 (C-27), 126.8 (C-3), 128.7 (Bz-m), 129.1 (Bz-o), 129.7 (Bz-p), 131.2 (C-29), 132.1 (C-39/C-41), 132.8 (C-28), 133.4 (Bz-i), 133.7 (C-4),

142.5 (C-12), 143.6 (C-37), 150.1 (C-8), 150.3 (C-35), 158.9 (C-30), 159.0 (C-33), 162.2 (C-10), 166.2 (O*C*OC_6H_5), 169.2 (C-31); HRMS (EI): *m/z* 897.3464 $[M+H]^+$. Calculated for $C_{49}H_{48}N_6O_{11}$, 897.3453 $[M+H]^+$.

5-{19-[4-(2-(4-Cyanophenylamino)-1,3-pyrimidine-4-oxy)-3,5-dimethylphenyl]-(4,7,10,13,16-pentaoxanonadecadi-1,18-ynyl)}-2',3'-didehydro-2',3'-dideoxyuridine (147)

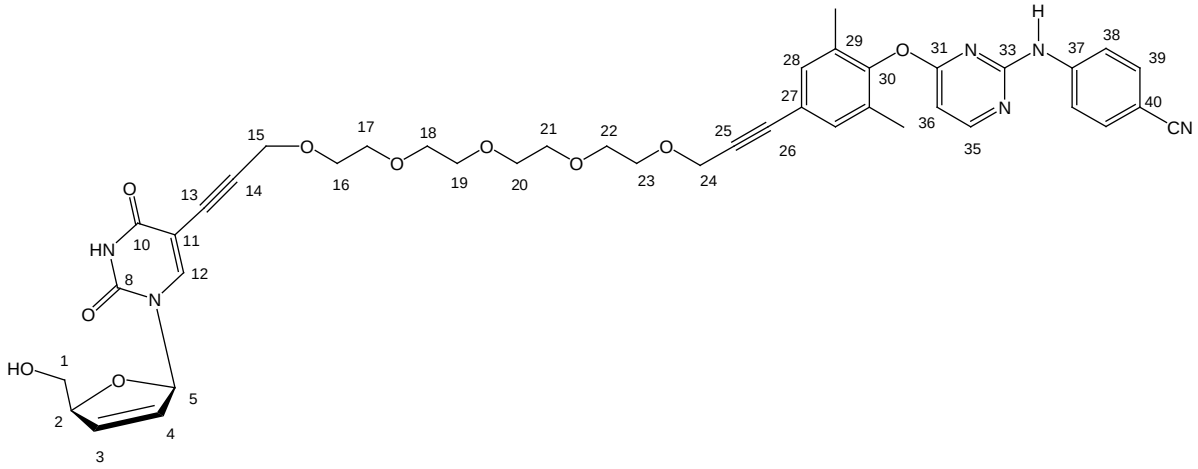

To a solution of benzoate **171** (38.0 mg, 0.042 mmol) dissolved in methanol (3 mL) at 0°C was added a solution of sodium methoxide in methanol (0.5 M, 0.1 mL). After 2 h, the solution was allowed to warm to rt. Once TLC indicated the complete consumption of starting material, acetic acid was added (3.0 mg, 0.05 mmol) and the methanol removed on the rotoevaporator. The residue was immediately chromatographed on silica-gel using EtOAc/ MeOH mixtures to obtain nucleoside **147** (31.5 mg, 94%) as a colourless oil. ^{1}H-NMR ($CDCl_3$, 500 MHz) δ_H 2.06 (6H, s, $ArCH_3$), 3.48 (1H, brs, OH), 3.60-3.80 (16H, m, H-16 - H-23), 3.84 (1H, dd, *J* = 2.0, 11.2 Hz, H-1), 3.94 (1H, dd, *J* = 3.0, 11.2 Hz, H-1), 4.32 (2H, s, H-15), 4.44 (2H, s, H-24), 4.94 (1H, m, H-2), 5.82 (1H, d, *J* = 5.8 Hz, H-3), 6.34 (1H, d, *J* = 5.8 Hz, H-4), 6.47 (1H, d, *J* = 5.2 Hz, H-36), 6.98 (1H, m, H-5), 7.22 (2H, s, H-28), 7.33 (4H, m, H-38, H-39), 8.34 (1H, s, H-12), 8.38 (1H, d, *J* = 5.2 Hz, H-35), 8.88 (1H, bs, NH), 11.54 (1H, bs, NH); ^{13}C-NMR ($CDCl_3$, 500 MHz) δ_C 16.3 ($ArCH_3$), 59.2 (C-24), 59.2 (C-15), 62.7 (C-1), 69.0 (OCH_2), 69.2 (OCH_2), 70.3 (OCH_2), 70.4 (OCH_2), 70.4 (OCH_2), 70.5 x 3 (OCH_2), 77.9 (C-14), 85.0 (C-25), 85.7 (C-2), 89.1 (C-5), 90.1 (C-26), 99.0 (C-13), 99.4 (C-36), 104.2 (C-40), 118.3 (C-11), 119.5 (C-38/C-42), 120.1 (CN), 120.8 (C-27), 126.0 (C-3), 131.3 (C-29), 132.1 (C-39/C-41), 132.8 (C-28), 135.0 (C-4), 143.6 (C-12), 145.2 (C-37), 150.2 (C-8), 150.5 (C-35), 158.9 (C-30), 159.1 (C-33), 162.4 (C-10), 169.2 (C-31); HRMS (EI): *m/z* 793.3204 $[M+H]^+$. Calculated for $C_{42}H_{44}N_6O_{10}$, 793.3191 $[M+H]^+$.

5-{19-[4-(2-(4-Cyanophenylamino)-1,3-pyrimidine-4-oxy)-3,5-dimethylphenyl]-(4,7,10,13,16-pentaoxanonadecadi-1,18-ynyl)}uridine-2',3'-didehydro-2',3'-dideoxy-5'-O-triphosphate (148)

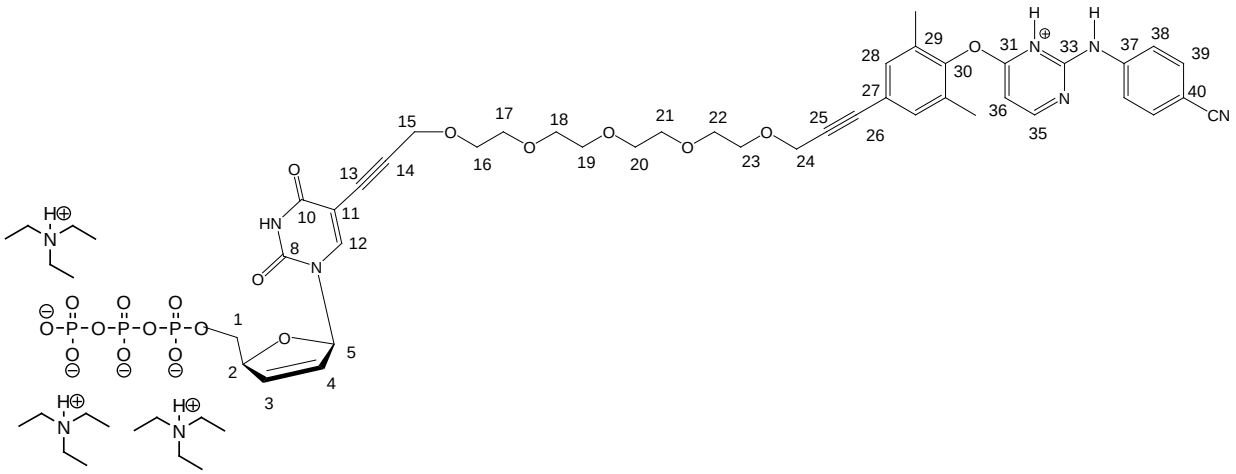

The bifunctional nucleoside **147** (95.0 mg, 0.120 mmol) was dissolved in a 1:1 mixture of DMF/Pyridine (1.0 ml) and the flask cooled to -20°C. 2-Chloro-1,3,2-benzodioxaphosphorin-4-one (30.0 mg, 0.148 mmol) dissolved in THF (0.5 mL) was added slowly and the reaction left to warm to rt. After 60 mins, bis(tributylammonium) pyrophosphate (92.0 mg, 0.168 mmol) in DMF (0.5 ml) was added followed by triethylamine (0.5 ml) and the solution left stirring for 1 h. I_2 (43.0 mg, 0.170 mmol) dissolved in pyridine/water (2 ml, 98:2) was then added, and the solution left stirring for 15 min before being quenched by aq. $Na_2S_2O_3$ (0.5 M, 0.5 ml). TEAB (1 M, 3.0 ml) was immediately added and the solution left stirring for 2h at rt. The solution was then evaporated to dryness before being chromatographed on a Sephadex ion-exchange (DEAE) column (3.0 g) using aq. TEAB as the mobile phase. The bifunctional triphosphate eluted at around 0.6 M. Fractions identified from TLC (amine-impregnated silica-gel plates using TEAB/MeOH = 3.5/6.5) were combined and the solvent evaporated. Following several additions of methanol with pumping, the tris(tiethylammonium) triphosphate **148** (60.0 mg, 0.045 mmol, 37 %) was obtained as a colourless oil. ^{1}H-NMR (CD_3OD, 500 MHz) δ_H 1.25 (27H, bs, $NCH_2\mathit{CH_3}$), 2.04 (6H, s, $ArCH_3$), 3.13 (18H, bs, $N\mathit{CH_2}CH_3$), 3.54 – 3.74 (16H, m, H-16 - H-23), 4.12 (2H, m, H-1), 4.32 (2H, s, H-15), 4.42 (2H, s, H-24), 5.02 (1H, m, H-2), 5.88 (1H, m, H-3), 6.55 (2H, m, H-36, H-4), 6.85 (1H, m, H-5), 7.23 (2H, s, H-28), 7.33 (2H, m, H-38), 7.43 (2H, m, H-39), 7.78 (1H, s, H-12), 8.32 (1H, m, H-35); ^{13}C-NMR (CD_3OD, 75 MHz) δ_C 9.1 ($NCH_2\mathit{CH_3}$), 16.4 ($ArCH_3$), 47.2 ($N\mathit{CH_2}CH_3$), 59.7 (C-24), 59.8 (C-15), 68.4 (C-1), 70.2 x 2 (OCH_2), 71.4 (OCH_2), 71.5 x 5 (OCH_2), 86.0 (C-14), 86.6 (C-25), 87.5 (C-2), 90.9 (C-5), 91.8 (C-26), 100.1 (C-13), 100.5 (C-36), 104.6 (C-40), 119.6 (C-11), 120.4 (CN), 121.5 (C-38/C-42), 120.8 (C-27), 126.5 (C-3), 132.8 (C-29), 133.1 (C-39/C-41), 133.7 (C-28), 136.6 (C-4), 145.4 (C-12), 145.9 (C-37), 151.6 (C-8),

151.8 (C-35), 160.8 (C-30), 161.2 (C-33), 164.1 (C-10), 170.4 (C-31); ^{31}P-NMR (CD_3OD, 202.4 MHz) δ_P -8.9 (d, *J* = 20.2 Hz), -9.8 (d, *J* = 20.2 Hz), -22.1 (t, *J* = 20.2 Hz); HRMS (EI): *m/z* 1031.2035 $[M-H]^+$. Calculated for the tetraphosphoric acid $C_{42}H_{46}N_6O_{19}P_3$, 1031.2036 $[M-H]^+$.

Diisopropyl 5-{19-[4-(2-(4-cyanophenylamino)-1,3-pyrimidine-4-oxy)-3,5-dimethylphenyl]-(4,7,10,13,16-pentaoxanonadecadi-1,18-ynyl)}pyrimidin(2H)-2,4-dioxo-3,4-dihydro-1-yl-(2-ethoxy) methylphosphonate (172)

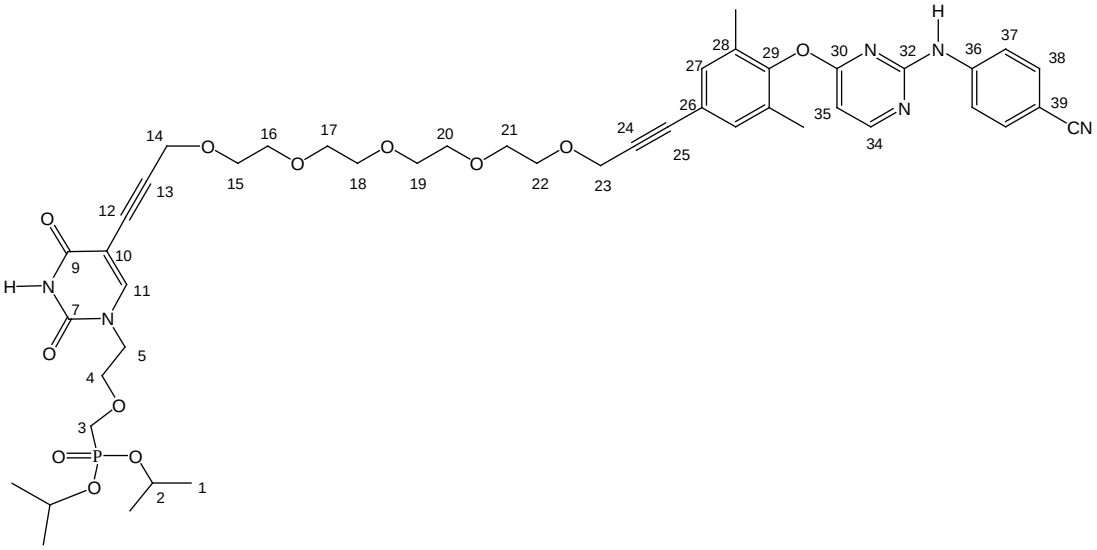

DAPY alkyne **149** (140 mg, 0.24 mmol) was added together with acyclic phosphonate **175b** (100 mg, 0.22 mmol) and the mixture dried carefully on a vacuum pump. A mixture of degassed DMF:THF (1:2 (v/v), 3 mL) was then added to the reaction vessel whilst the mixture stirred at room temperature under nitrogen. Subsequent addition of triethylamine (0.07 mL, 0.48 mmol) was followed by addition of copper(I) iodide (23 mg, 0.12 mmol) and tetrakis(triphenylphosphine)palladium (28 mg, 0.02 mmol) respectively. The reaction was stirred continuously at room temperature and TLC confirmed completion of the reaction after 1½ hrs. The reaction mixture was diluted with a 5% EDTA solution (50 mL) and extracted with chloroform (3 × 50 mL). The organic fractions were dried with $MgSO_4$ and the solvent removed under reduced pressure. Purification by chromatography using a silica-gel column afforded product **172** as a yellow solid, (121 mg, 60%). Mp.113-115 ^oC; $[\alpha]_D$ +15.7° (*c* = 1.31, acetone); ν_{max} /cm^{-1} (Acetone): 3353s + 3340s (NH, amine), 2253s (C≡C), 2208s (C-N, nitrile), 1725s (C=O, ester), 1691s (C=O, pyrimidine), 1538 + 1430 (C=C, aromatic); ^{1}H NMR (Acetone-D_6, 300 MHz) δ_H 1.29 (12H, m, H-1), 2.14 (6H, s, $ArCH_3$), 3.59-3.80 (18H, m, H-16 - H-21, H-3 -H-5), 3.85 (2H, t, *J* = 4.9 Hz, H-15), 4.01 (2H, t, *J* = 4.92 Hz, H-22), 4.33 (2H, s, H-14), 4.46 (2H, s, H-23), 4.68 (2H, sept, *J* = 6.2 Hz, H-2), 6.78 (1H, d, *J* = 5.7 Hz, H-35), 7.35 (2H, s, H-27), 7.50 (2H, m, H-37, H-

41), 7.61 (2H, m, H-38, H-40), 7.87 (1H, s, H-11), 8.54 (1H, d, *J* = 5.65 Hz, H-34), 10.28 (1H, bs, NH); ^{13}C NMR (Acetone-D_6, 75.5 MHz) δ_C 16.1 ($ArCH_3$), 23.9 (C-1), 48.3 (C-5), 58.9 (C-23), 59.1 (C-14), 66.1 (d, J_{C-P} = 148.3 Hz, C-3), 66.8 (C-4), 69.2 (OCH_2), 69.4 (C-2), 70.6 x 7 (OCH_2), 78.7 (C-13), 85.3 (C-24), 86.0 (C-25), 89.1 (C-12), 99.5 (C-35), 104.7 (C-39), 111.1 (C-10), 119.0 (C-37/C-41), 119.1 (C≡N), 120.8 (C-26), 131.9 (C-28), 132.2 (C-38/C-40), 132.8 (C-27), 137.8 (C-11), 143.8 (C-36), 149.5 (C-34), 150.4 x 2 (C-7 + C-29), 157.5 (C-32), 162.1 (C-9), 170.0 (C-30); ^{31}P NMR (Acetone-D_6, 121.5 MHz) δ_P 23.2; HRMS (ES): *m/z* 917.3848 $[M+H]^+$. Calculated for $C_{46}H_{58}N_6O_{12}P$, 917.3850 $[M+H]^+$.

4-{4-[3-(2-Hydroxyethoxy)-2-ethoxy)-2-ethoxy)-2-ethoxy)-2-ethoxy)-2-ethoxy)prop-1-ynyl)]-2,6-dimethylphenoxy}-2-[(4-cyanophenyl)amino]-1,3-pyrimidine (184)

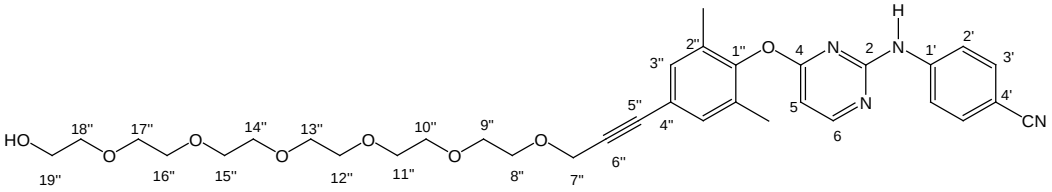

Alkyne **183** (197 mg, 0.62 mmol) was added together with DAPY **152** (300 mg, 0.67 mmol) and the mixture dried carefully on a vacuum pump. A mixture of degassed DMF:THF (1:2 (v/v), 3 mL) was then added to the reaction vessel whilst the mixture stirred at room temperature under nitrogen. Subsequent addition of triethylamine (0.20mL, 1.34 mmol) was followed by addition of copper(I) iodide (64 mg, 0.34 mmol) and tetrakis(triphenylphosphine)palladium (77 mg, 0.07 mmol) respectively. The reaction was stirred continuously at room temperature and TLC confirmed completion of the reaction after 3 hrs. The reaction mixture was diluted with a 5% EDTA solution (50 mL) and extracted with chloroform (3 × 100 mL). The organic fractions were dried with $MgSO_4$ and the solvent removed under reduced pressure. Purification by chromatography using a silica-gel column afforded product **184** as a clear oil, (180 mg, 46%). ν_{max} /cm^{-1} (Acetone): 3577b (O-H), 3353s + 3340s (NH, amine), 2253s (C≡C), 2208s (C-N, nitrile), 1541 + 1428 (C=C, aromatic); ^{1}H NMR (Acetone-D_6, 300 MHz) δ_H 2.11 (6H, s, $ArCH_3$), 3.53-3.63 (20H, m, H-9'' - H-18''), 3.70 (2H, m, H-19''), 3.77 (2H, m, H-8''), 4.46 (2H, s, H-7''), 6.63 (1H, d, *J* = 5.6 Hz, H-5), 7.32 (2H, s, H-3''/H-5''), 7.46 (2H, d, *J* = 8.8 Hz, H-3'/H-5'), 7.68 (2H, d, *J* = 8.8 Hz, H-2'/H-6'), 8.44 (1H, d, *J* = 5.6 Hz, H-6), 9.12 (1H, bs, NH); ^{13}C NMR (Acetone-D_6, 75.5 MHz) δ_C 15.6 ($ArCH_3$), 58.6 (C-7''), 61.2 (OCH_2), 69.1 (OCH_2), 70.4 x 4 (OCH_2), 70.5 x 5 (OCH_2), 72.7 (OCH_2), 85.3 (C-6''), 85.7 (C-5''), 99.3 (C-5), 104.1 (C-4'), 118.6 (C-2'/C-6'), 119.2 (C≡N), 120.4 (C -4''), 131.7 (C-2''/C-6''), 132.1 (C-3'/C-5'), 132.8 (C-3''/C-5''),

144.9 (C-1'), 150.7 (C-1''), 159.8 (C-2), 160.4 (C-6), 169.3 (C-4); HRMS (ES): *m/z* 635.3089 $[M+H]^+$. Calculated for $C_{34}H_{43}N_4O_8$, 635.3081 $[M+H]^+$.

4-{4-[3-(2-(4-Methylbenzenesulfonyloxyethoxy)-2-ethoxy)-2-ethoxy)-2-ethoxy)-2-ethoxy)-2-ethoxy)prop-1-ynyl)]-2,6-dimethylphenoxy}-2-[(4-cyanophenyl)amino]-1,3-pyrimidine (185)

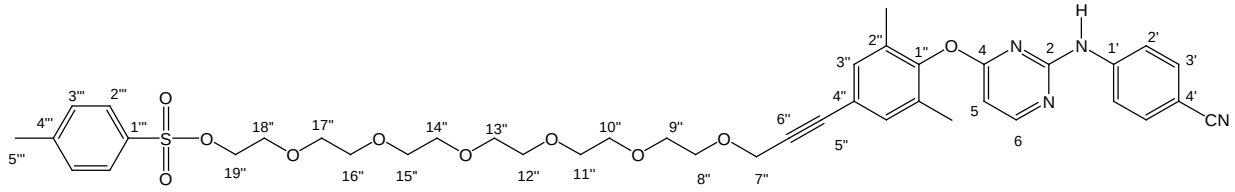

DAPY alcohol **184** (290 mg, 0.47 mmol) was dissolved in THF (10 mL). Triethylamine (0.08 mL, 0.56 mmol) was added at 0^{o}C followed by a catalytic amount of DMAP (12.0 mg, 0.09 mmol) to the reaction mixture. *p*-Toluenesulfonyl chloride (131 mg, 0.70 mmol) in THF (2 mL) was then added dropwise and the solution left to stir at room temperature. TLC confirmed completion of the reaction after 12 hrs. The reaction mixture was diluted with brine (100 mL) and extracted with EtOAc (3 × 100 mL). The organic fractions were dried with $MgSO_4$ and the solvent removed under reduced pressure. Purification by chromatography using a silica-gel column (30 g; MeOH/EtOAc, 0.5:9.5) afforded product **185** as a clear oil, (210 mg, 57%). ν_{max} /cm^{-1} (Acetone): 3353s + 3340s (NH, amine), 2253s (C≡C), 2208s (C-N, nitrile), 1541 + 1428 (C=C, aromatic), 1372s + 1180s (-SO_2-O-); ^{1}H NMR (Acetone-D_6, 400 MHz) δ_H 2.11 (6H, s, $ArCH_3$), 2.45 (3H, s, H-5'''), 3.57-3.67 (20H, m, H-9'' - H-18''), 3.75 (2H, m, H-8''), 4.16 (2H, m, H-19''), 4.45 (2H, s, H-7''), 6.63 (1H, d, *J* = 5.6 Hz, H-5), 7.31 (2H, s, H-3''/H-5''), 7.45 (2H, d, *J* = 8.8 Hz, H-3'/H-5'), 7.46 (2H, d, *J* = 8.4 Hz, H-3'''/H-5'''), 7.69 (2H, d, *J* = 8.8 Hz, H-2'/H-6'), 7.81 (2H, d, *J* = 8.4 Hz, H-2'''/H-6'''), 8.44 (1H, d, *J* = 5.6 Hz, H-6), 9.09 (1H, bs, NH); ^{13}C NMR (Acetone-D_6, 100 MHz) δ_C 15.7 ($ArCH_3$), 20.9 (C-5'''), 58.6 (C-7''), 68.6 (OCH_2), 69.3 (OCH_2), 70.0 (OCH_2), 70.4 x 3 (OCH_2), 70.5 x 3 (OCH_2), 70.6 x 3 (OCH_2), 85.3 (C-6''), 85.7 (C-5''), 99.3 (C-5), 104.0 (C-4'), 118.6 (C-2'/C-6'), 119.2 (C≡N), 120.4 (C-4''), 125.6 (C-4'''), 128.1 (C-2'''/C-6'''), 130.2 (C-3'''/C-5'''), 131.7 (C-1'''), 131.7 x 2 (C-2''/C-6''), 132.1 (C-3'/C-5'), 132.8 (C-3''/C-5''), 144.8 (C-1'), 150.2 (C-1''), 159.8 (C-2), 160.4 (C-6), 169.1 (C-4); HRMS (ES): *m/z* 789.3163 $[M+H]^+$. Calculated for $C_{41}H_{49}N_4O_{10}S$, 789.3169 $[M+H]^+$.

4-{4-[3-(2-Propargyloxyethoxy)-2-ethoxy)-2-ethoxy)-2-ethoxy)-2-ethoxy)-2-ethoxy)prop-1-ynyl)]-2,6-dimethylphenoxy}-2-[(4-cyanophenyl)amino]-1,3-pyrimidine (174)

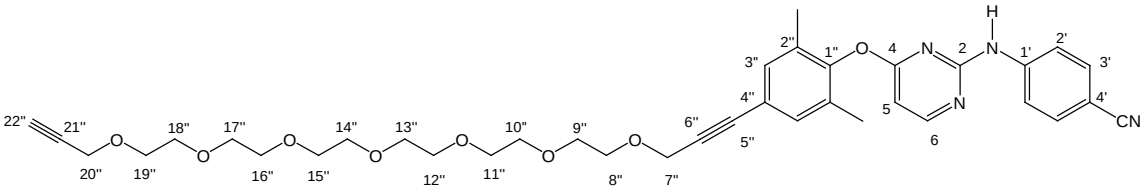

To a suspension of sodium hydride (60%, 32 mg, 0.80 mmol) suspension in THF (8 mL) at 0^{o}C, was added propargyl alcohol (0.07 mL, 1.20 mmol) slowly whilst stirring. To this was added DAPY tosylate **185** (160 mg, 0.20 mmol) and the reaction mixture refluxed. TLC confirmed completion after a total of 20 hrs. The reaction mixture was diluted with water (50 mL) and extracted with EtOAc (3 × 50 mL). The organic fractions were dried with $MgSO_4$ and the solvent removed under reduced pressure. Purification by chromatography using a silica-gel column (40 g; MeOH/EtOAc, 0.5:9.5) afforded product **174** as a colourless oil, (120 mg, 89%). ν_{max} /cm^{-1} (Acetone): 3353s + 3340s (NH, amine), 2253s (C≡C), 2208s (C-N, nitrile), 1541 + 1428 (C=C, aromatic); ^{1}H NMR (Acetone-D_6, 400 MHz) δ_H 2.11 (6H, s, $ArCH_3$), 2.89 (1H, t, *J* = 2.4 Hz, H-22''), 3.57-3.60 (20H, m, H-9'' - H-18''), 3.68 (2H, m, H-19''), 3.75 (2H, m, H-8''), 4.17 (2H, d, *J* = 2.4 Hz, H-20''), 4.45 (2H, s, H-7''), 6.63 (1H, d, *J* = 5.6 Hz, H-5), 7.31 (2H, s, H-3''/H-5''), 7.48 (2H, d, *J* = 8.8 Hz, H-3'/H-5'), 7.71 (2H, d, *J* = 8.8 Hz, H-2'/H-6'), 8.44 (1H, d, *J* = 5.6 Hz, H-6), 9.09 (1H, bs, NH); ^{13}C NMR (Acetone-D_6, 100 MHz) δ_C 15.6 ($ArCH_3$), 57.9 (C-7''), 58.6 (C-20''), 69.2 (OCH_2), 70.6 x 11 (OCH_2), 75.1 (C-22''), 80.2 (C-21''), 85.3 (C-6''), 85.9 (C-5''), 99.3 (C-5), 104.0 (C-4'), 118.5 (C-2'/C-6'), 119.3 (C≡N), 120.6 (C-4''), 131.6 (C-2''/C-6''), 132.1 (C-3'/C-5'), 132.7 (C-3''/C-5''), 144.7 (C-1'), 150.7 (C-1''), 159.8 (C-2), 160.3 (C-6), 169.1 (C-4); HRMS (ES): *m/z* 673.3210 $[M+H]^+$. Calculated for $C_{37}H_{45}N_4O_8$, 673.3237 $[M+H]^+$.

Diisopropyl 5-{25-[4-(2-(4-cyanophenylamino)-1,3-pyrimidine-4-oxy)-3,5-dimethylphenyl]-(4,7,10,13,16,19,22-heptaoxapentadecadecadi-1,24-ynyl)}pyrimidin(2H)-2,4-dioxo-3,4-dihydro-1-yl-(2-ethoxy) methylphosphonate (173)

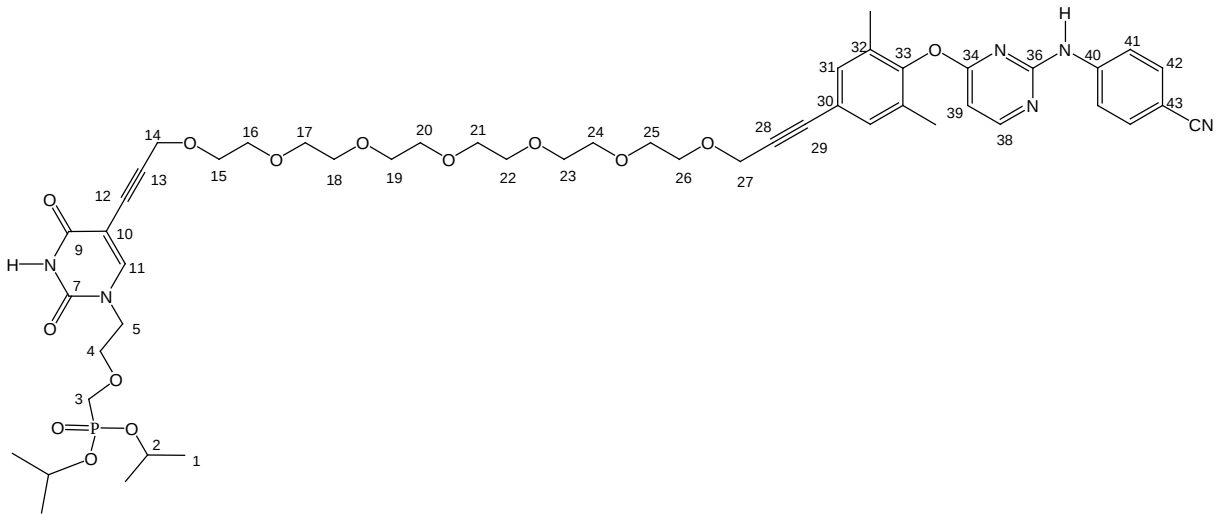

DAPY alkyne **174** (65 mg, 0.10 mmol) was added together with acyclic phosphonate **175b** (41 mg, 0.09 mmol) and the mixture dried carefully on a vacuum pump. A mixture of degassed DMF:THF (1:2 (v/v), 3 mL) was then added to the reaction vessel whilst the mixture stirred at room temperature under nitrogen. Subsequent addition of triethylamine (0.03 mL, 0.20 mmol) was followed by addition of copper(I) iodide (10 mg, 0.05 mmol) and tetrakis(triphenylphosphine)palladium (12 mg, 0.01 mmol) respectively. The reaction was stirred continuously at room temperature and TLC confirmed completion of the reaction after 3 hrs. The reaction mixture was diluted with a 5% EDTA solution (50 mL) and extracted with chloroform (3 × 50 mL). The organic fractions were dried with $MgSO_4$ and the solvent removed under reduced pressure. Purification by chromatography using a silica-gel column afforded product **173** as a yellow oil, (70 mg, 70%). $[\alpha]_D$ +14.7° (*c* = 1.04, acetone); ν_{max} /cm^{-1} (Acetone): 3353s + 3340s (NH, amine), 2253s (C≡C), 2208s (C-N, nitrile), 1725s (C=O, ester), 1691s (C=O, pyrimidine), 1538 + 1430 (C=C, aromatic); ^{1}H NMR (Acetone-D_6, 300 MHz) δ_H 1.28 (12H, m, H-1), 2.11 (6H, s, $ArCH_3$), 3.57-3.80 (26H, m, H-16 - H25 + H-3 - H-5), 3.85 (2H, t, *J* = 4.9 Hz, H-15), 4.01 (2H, t, *J* = 4.9 Hz, H-26), 4.34 (2H, s, H-14), 4.46 (2H, s, H-27), 4.67 (2H, sept, *J* = 6.2 Hz, H-2), 6.63 (1H, d, *J* = 5.7 Hz, H-39), 7.32 (2H, s, H-31), 7.47 (2H, d, *J* = 8.9 Hz, H-42), 7.68 (2H, d, *J* = 8.9 Hz, H-41), 7.87 (1H, s, H-11), 8.43 (1H, d, *J* = 5.7 Hz, H-38), 9.17 (1H, bs, NH); ^{13}C NMR (Acetone-D_6, 75.5 MHz) δ_C 15.6 ($ArCH_3$), 23.6 (C-1), 48.3 (C-5), 58.6 (C-27), 61.6 (C-14), 64.7 (d, J_{C-P} = 150.1 Hz, C-3), 66.9 (C-4), 66.1 (OCH_2), 69.2 (OCH_2), 69.5 (OCH_2), 69.7 (OCH_2), 70.0 (OCH_2), 70.3 (OCH_2), 70.5 x 3 (OCH_2), 70.6 x 3 (OCH_2), 70.6 x 2 (C-2), 78.2 (C-13), 85.3 (C-28),

85.7 (C-29), 88.9 (C-12), 99.3 (C-39), 104.0 (C-43), 111.0 (C-10), 118.6 (C-41), 119.2 (C≡N), 120.4 (C-30), 131.7 (C-32), 132.1 (C-42), 132.8 (C-31), 144.8 (C-40), 149.6 (C-11), 150.4 (C-7), 150.5 (C-33), 159.8 (C-36), 160.3 (C-38), 162.1 (C-9), 169.1 (C-34); ^{31}P NMR (Acetone-D_6, 121.5 MHz) δ_P 23.3; HRMS (ES): *m/z* 1005.4344 $[M+H]^+$. Calculated for $C_{50}H_{66}N_6O_{14}P$, 1005.4375 $[M+H]^+$.

Diisopropyl hydrogen phosphonate (177)[201]

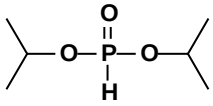

Isopropanol (5.24 g, 68.82 mmol) was added dropwise to a suspension of NaH (60% in mineral oil, 1.84 g, 45.88 mmol) in THF (60 mL) and the mixture was stirred for 15 min at 0 ^oC. Phosphorus trichloride (2.00 mL, 22.94 mmol) was added dropwise and then the mixture was warmed to rt with stirring for 1h. The reaction was quenched using aqueous NH_4Cl (10 mL). The mixture was diluted with EtOAc (80 mL), washed with aq NH_4Cl (50 mL), water (2 × 40 mL), dried over $MgSO_4$ and the solvent was evaporated under reduced pressure to give the product **177** without purification as a colourless oil (11.20 g, 98%). ^{1}H NMR (300 MHz, $CDCl_3$) δ_H 1.28 and 130 (2 × 6H, 2 × d, CH*(CH$_3$)$_2$*), 4.67 (2H, m, *CH*$(CH_3)_2$), 6.77 (1H, d, J_{HP} = 687.0 Hz, H-P=O); ^{31}P NMR ($CDCl_3$) δ_P 4.6.

Diisopropyl hydroxymethylphosphonate (178)[202]

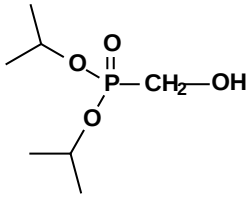

To a solution of diisopropyl hydrogen phosphonate **177** (5.00 g, 30.10 mmol), paraformaldehyde (1.05 g, 36.12 mmol) in isopropanol (20 mL) was added anhydrous potassium carbonate (0.21 g, 1.51 mmol). The mixture was stirred vigorously for 1h at 60 ^oC, filtered through Celite and the solvent was evaporated in *vacuum* to give the product **178** as a colourless oil (5.81 g, 98%) pure enough for the next step. ^{1}H NMR (300 MHz, $CDCl_3$) δ_H 1.32 (12H, d, *J* = 6.3 Hz, CH*(CH$_3$)$_2$*), 2.15 (1H, brs, OH), 3.82 (2H, d, J_{HP} = 6.6 Hz, CH_2P), 4.73 (2H, m, *CH*$(CH_3)_2$); ^{31}P NMR ($CDCl_3$) δ_p 22.9.

Diisopropyl *p*-toluenesulphonyloxymethylphosphonate (176)

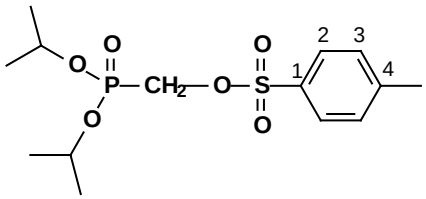

To a solution of diisopropyl hydroxymethyl phosphonate **178** (5.00 g, 25.49 mmol) in dry CH_2Cl_2 (30 mL), were added triethylamine (4.26 mL, 30.59 mmol) and *p*-toluenesulfonyl chloride (5.81 g, 30.59 mmol) followed by DMAP (0.02 g). The reaction mixture was stirred at rt for 16h. The mixture was diluted with CH_2Cl_2 (120 mL), washed with aq NH_4Cl (60 mL), water (70 mL), dried over $MgSO_4$ and solvent was removed under reduced pressure. Purification by column chromatography using EtOAc / pet ether (6 / 4) gave a colourless oil **176** (8.20 g, 92%). ν_{max} /cm^{-1} (Chloroform): 2986 (C-H), 1252 (P=O), 1176 (O-SO_2-), 1003 (P-O) cm^{-1}; ^{1}H NMR (400 MHz, $CDCl_3$) δ_H 1.29 and 1.33 (2 × 6H, 2 × d, *J* = 6.2 Hz, CH(*CH*$_3$)$_2$), 2.46 (3H, s, ArCH_3), 4.12 (2H, d, J_{HP} = 10.0 Hz, CH_2P), 4.73 (2H, m, *CH*(CH_3)$_2$), 7.36 (2H, d, *J* = 8.0 Hz, H-3, H-5), 7.80 (2H, d, *J* = 8.0 Hz, H-2, H-6); ^{13}C NMR (100 MHz, $CDCl_3$) δ_C 23.7 (d, J_{CP} = 4.6 Hz, CH(*CH*$_3$)$_2$), 23.9 (d, J_{CP} = 3.8 Hz, CH(*CH*$_3$)$_2$), 61.9 (d, J_{CP} = 169.1 Hz, CH_2P), 72.3 (d, J_{CP} = 6.1 Hz, *CH*(CH_3)$_2$), 128.1 (C-2, C-6), 129.9 (C-3, C-5), 131.8 (C-4), 145.3 (C-1); ^{31}P NMR ($CDCl_3$) δ_P 13.3; HRMS (ES): *m/z* 351.1044 $[M+H]^+$. Calculated for $C_{14}H_{24}O_6SP$, 351.1031 $[M+H]^+$.

Diisopropyl (2-benzyloxyethoxy)methylphosphonate (179)

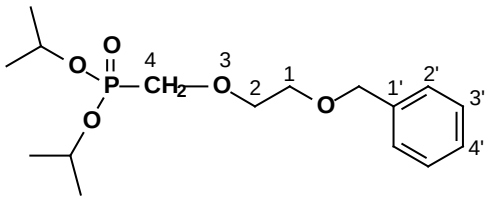

2-Benzyloxyethanol **140** (2.09 g, 13.70 mmol) was added dropwise to a suspension of NaH (60% mineral oil, 0.69 g, 17.13 mmol) in THF (60 mL) at 0 ^oC. The mixture was stirred for 30 min and the tosylate **176** (4.00 g, 11.42 mmol) was added. The mixture was heated at reflux for 3 h. The crude mixture was added to EtOAc (80 mL), which washed with aqueous NH_4Cl (50 mL), water (2 × 40 mL), dried over $MgSO_4$ and the solvent was evaporated under reduced pressure. The crude product was purified by column chromatography employing EtOAc / pet ether (7 / 3) to give compound **179** as a colourless oil (2.70 g, 72%). ν_{max} /cm^{-1} (Chloroform): 2986, 2935 (C-H), 1241 (P=O), 999 (P-O) cm^{-1}; ^{1}H NMR (400 MHz, $CDCl_3$) δ_H 1.31 and 1.33 (2 × 6H, 2 × d, *J* =

6.3 Hz, CH*(CH$_3$)$_2$*), 3.66 (2H, t, *J* = 4.7 Hz, H-1), 3.79 (2H, t, *J* = 4.7 Hz, H-2), 3.82 (2H, d, J_{HP} = 8.4 Hz, H-4), 4.54 (2H, s, ArCH$_2$O), 4.76 (2H, m, *CH*(CH$_3$)$_2$), 7.29 (1H, m, H-4'), 7.31 (4H, m, ArH); ^{13}C NMR (100 MHz, CDCl$_3$) δ_C 24.0 (m, CH*(CH$_3$)$_2$*), 66.1 (d, J_{CP} = 165.9 Hz, C-4), 69.4 (C-1), 71.0 (d, J_{CP} = 6.6 Hz, *C*H(CH$_3$)$_2$), 72.5 (d, J_{CP} = 10.5 Hz, C-2), 73.2 (Ar*C*H$_2$O), 127.5 (C-4'), 127.6 (C-3', C-5'), 128.3 (C-2', C-6'), 138.2 (C-1'); ^{31}P NMR (CDCl$_3$) δ_P 19.7; HRMS (ES): *m/z* 331.1668 [M+H]$^+$. Calculated for $C_{16}H_{28}O_5P$, 331.1674 [M+H]$^+$.

Diisopropyl (2-hydroxyethoxy)methylphosphonate (180)

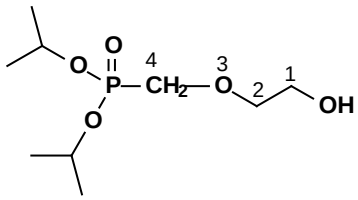

Hydrogen gas was introduced at atmospheric pressure to compound **179** (2.00 g, 6.05 mmol) and a suspension of 10% palladium-on-carbon (0.65 g, 0.61 mmol) in MeOH:THF (1:1) (15 mL). The mixture was stirred at room temperature for 6h. The catalyst was filtered through a pad of Celite, washed with MeOH (2 × 15 mL) and the filtrate evaporated in *vacuo* to give the product **180** as a colourless oil pure enough for the next step (1.12 g, 77%). ν_{max} /cm^{-1} (Chloroform): 3200 (OH), 2986 (C-H), 1234 (P=O), 996 (P-O) cm^{-1}: ^{1}H NMR (300 MHz, CDCl$_3$) δ_H 1.33 (12H, d, *J* = 6.2 Hz, CH*(CH$_3$)$_2$*), 2.52 (1H, brs, OH), 3.72 (4H, m, H-1, H-2), 3.79 (2H, d, J_{HP} = 7.8 Hz, H-4), 4.75 (2H, m, *CH*(CH$_3$)$_2$); ^{13}C NMR (75 MHz, CDCl$_3$) δ_C 23.9 (m, CH*(CH$_3$)$_2$*), 61.5 (C-1), 66.0 (d, J_{HP} = 167.3 Hz, C-4), 71.2 (d, J_{CP} = 6.6 Hz, *C*H(CH$_3$)$_2$), 75.0 (d, J_{CP} = 9.5 Hz, C-2); ^{31}P NMR (CDCl$_3$) δ_P 20.2.

Diisopropyl (2-*p*-toluenesulphonyloxyethoxy)methylphosphonate (181)

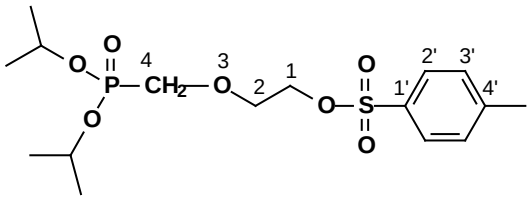

p-Toluenesulfonyl chloride (1.05 g, 5.50 mmol) was added to a stirring solution of the alcohol **180** (1.10 g, 4.58 mmol) containing triethylamine (0.77 mL, 5.50 mmol), and a catalytic a mount of DMAP in dry CH_2Cl_2 (20 mL) at 0 ^{o}C. The reaction mixture was stirred at rt for 16 h. The mixture was diluted with CH_2Cl_2 (80 mL), washed with aq NH_4Cl (25 mL), water (30 mL), dried

over $MgSO_4$ and the solvent removed under reduced pressure. Purification by column chromatography using EtOAc / pet ether (9 / 1) gave a colourless oil **181** (1.63 g, 90%). ν_{max} /cm^{-1} (Chloroform): 2986 (C-H), 1234 (P=O), 1176 (O-SO_2), 999 (P-O) cm^{-1}: ^{1}H NMR (300 MHz, $CDCl_3$) δ_H 1.28 and 1.31 (2 × 6H, 2 × d, J = 6.0 Hz, CH(*CH_3*)$_2$); 2.43 (3H, s, ArCH_3), 3.69 (2H, J_{HP} = 8.4 Hz, H-4), 3.77 (2H, t, J = 4.8 Hz, H-2), 4.14 (2H, t, J = 4.8 Hz, H-1), 4.71 (2H, m, *CH*$(CH_3)_2$), 7.33 (2H, d, J = 8.3 Hz, H-3', H-5'), 7.78 (2H, d, J = 8.3 Hz, H-2', H-6'); ^{13}C NMR (75 MHz, $CDCl_3$) δ_C 21.5 (d, J_{CP} = 3.7 Hz, Ar*C*H_3), 24.0 (m, CH(*C*H_3)$_2$), 66.1 (d, J_{CP} = 166.5 Hz, C-4), 68.7 (C-1), 70.4 (d, J_{CP} = 11.0 Hz, C-2), 71.2 (d, J_{CP} = 6.6 Hz, *C*H$(CH_3)_2$), 127.9 (C-2', C-6'), 129.8 (C-3', C-5'), 132.9 (C-4'), 144.8 (C-1'); ^{31}P NMR ($CDCl_3$) δ_P 18.6; HRMS (ES): *m/z* 395.1297 $[M+H]^+$. Calculated for $C_{16}H_{28}O_7PS$, 395.1293 $[M+H]^+$.

Diisopropyl [2-(2,4-dioxo-3,4-dihydro-2H-pyrimidin-1-yl)ethoxy]methylphosphonate (175a)

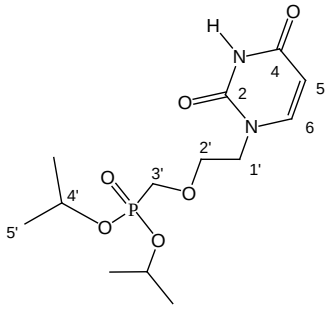

To a solution of cesium carbonate (815 mg, 2.50 mmol) and uracil (572 mg, 5.00 mmol) in DMF (10 mL), was added tosylate **181** (1.00 g, 2.50 mmol) and the mixture heated to 100 ^oC. TLC confirmed reaction completion after 6 hr. The reaction mixture was diluted with brine (100 mL) and extracted with EtOAc (3 × 100 mL), the organic layer dried over $MgSO_4$ and the solvent removed under reduced pressure. Purification by chromatography using a silica-gel column (70 g; MeOH/EtOAc, 1:9) afforded product **175a** as a clear oil, (471 mg, 56%). ν_{max} /cm^{-1} (Acetone): 1720s (C=O, ester), 1693s (C=O, pyrimidine), 721 (C-I, halogen); ^{1}H NMR ($CDCl_3$, 400 MHz) δ_H 1.32 (12H, m, H-5'), 3.71 (2H, d, J_{H-P} = 8.4 Hz, H-3'), 3.80 (2H, t, J = 4.6 Hz, H-2'), 3.93 (2H, t, J = 4.6 Hz, H-1'), 4.71 (2H, sept, J = 6.2 Hz, H-4'), 5.62 (1H, d, J = 7.9 Hz, H-5), 7.34 (1H, d, J = 7.9 Hz, H-6), 9.06 (1H, bs, NH); ^{13}C NMR ($CDCl_3$, 100 MHz) δ_C 23.9 (C-5'), 48.3 (C-1'), 66.1 (d, J_{C-P} = 168.4 Hz, C-3'), 71.1 (d, J_{C-P} = 11.0 Hz, C-2'), 71.2 (d, J_{C-P} = 6.3 Hz, C-4'), 101.5 (C-5), 145.8 (C-6), 150.8 (C-2), 163.6 (C-4); ^{31}P NMR (Acetone-D_6, 121.5 MHz) δ_P 19.8; HRMS (ES): *m/z* 335.1362 $[M+H]^+$. Calculated for $C_{13}H_{24}N_2O_6P$, 135.1372 $[M+H]^+$.

Diisopropyl [2-(5-iodo-2,4-dioxo-3,4-dihydro-2H-pyrimidin-1-yl)ethoxy]methylphosphonate (175b)

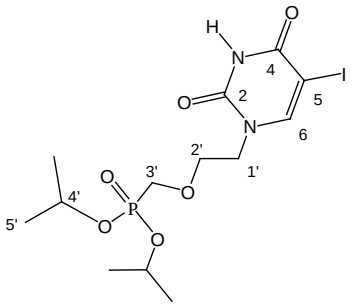

Cerium ammonium nitrate (IV) (492 mg, 0.90 mmol) and iodine (274 mg, 1.10 mmol) were added to a solution of phosphonate **175a** (600 mg, 1.80 mmol) in CH_3CN (20 mL). The reaction mixture was cooled to room temperature and diluted with sodium thiosulphate (50 mL) and extracted with EtOAc (3 × 50 mL), the organic layer dried over $MgSO_4$ and the solvent removed under reduced pressure. Purification by chromatography using a silica-gel column (50 g; EtOAc neat) afforded product **175b** as a yellow solid, (520 mg, 63%). Mp. 91-92 ^{o}C; ν_{max} /cm^{-1} (Acetone): 1720s (C=O, ester), 1693s (C=O, pyrimidine), 1599s (C-N stretching); ^{1}H NMR (DMSO-D_6, 400 MHz) δ_H 1.21 (12H, m, H-5'), 3.70 (2H, t, J_{H-P} = 8.4 Hz, H-3'), 3.75 (2H, d, J = 5.0 Hz, H-2'), 3.87 (2H, t, J = 5.0 Hz, H-1'), 4.57 (2H, sept, J = 6.2 Hz, H-4'), 8.04 (1H, s, H-6), 11.50 (1H, bs, NH); ^{13}C NMR (DMSO-D_6, 75.5 MHz) δ_C 23.5 x 4 (C-5'), 47.1 (C-1'), 64.8 (d, J_{C-P} = 163.9 Hz, C-3'), 67.3 (C-5), 69.6 (d, J_{C-P} = 11.3 Hz, C-2'), 70.0 (d, J_{C-P} = 6.4 Hz, C-4'), 150.1 (C-6), 150.4 (C-2), 160.7 (C-4); ^{31}P NMR (Acetone-D_6, 121.5 MHz) δ_P 20.1; HRMS (ES): *m/z* 461.0333 $[M+H]^+$. Calculated for $C_{13}H_{23}N_2O_6PI$, 461.0339 $[M+H]^+$; C, H, N Microanalysis found: C, 33.71; H, 4.88; N, 6.01; $C_{13}H_{22}N_2O_6PI$ requires C, 33.93; H, 4.82; N, 6.09.

Parts of this thesis have been published and presented at conferences:

RESEARCH OUTPUTS

The publication list below includes full references (i.e. authors, title, year, name of journal/publisher, volume and page numbers). Conference proceedings, technical reports, patents, etc, are reported.

JOURNAL PUBLICATIONS:

(i) Mohamed, E.; Hunter, R. *et al.* New Methodology for 2-alkylation of 3-furoic acids: application to the synthesis of tethered UC-781/d4T bifunctional HIV reverse-transcriptase inhibitors, *Tetrahedron Letters*, **2005,** *46*, 4023-4026.

(ii) Hunter, R. and Mohamed, E. Synthesis of a prototype [d4U]-spacer-[APY] bifunctional NRTI/NNRTI HIV-1 reverse-transcriptase inhibitor, *Afinidad*, **2007**, *64*, 231-236**.**

CONFERENCE PROCEEDINGS:

Oral and poster presentation (2006) – 9th Frank Warren Conference in Cape Town, South Africa.
Talk entitled: Synthesis Towards Tethered Bifunctional HIV-1 Reverse Transcriptase Inhibitors as Novel Antiretroviral Agents.

International poster presentation (2008) – 1st International Conference on Drug Design and Discovery (ICDDD'08) in Dubai.
Poster entitled: Probing the HIV Reverse-Transcriptase Enzyme: Synthesis and Biological Evaluation of Novel Bifunctional NRTI/NNRTI HIV-1 Reverse-Transcriptase Inhibitors.

Poster presentation (2008) – Bi-national Organic Chemistry Conference (BOCC'08) in Kruger National Park, South Africa.
Poster entitled: Synthesis and Biological Evaluation of Novel Bifunctional NRTI/NNRTI HIV-1 Reverse-Transcriptase Inhibitors.

PATENTS:

None as yet.

Appendix I

The Tetrazolium-based colorimetric (MTT) assay

Since its first description 20 years ago, the tetrazolium-based colorimetric (MTT) assay using MT-2 or MT-4 cells for the detection of anti-HIV compounds has been widely used. The replication is normally monitored over 5 days after infection; therefore this protocol can be divided into three steps: the infection (at day 0), an incubation period (5 days) and the evaluation (at day 5). Exact details are summarized below.

1×10^5 MT-2 cells per millilitre were infected with HIV-1 IIIB at 0.1 multiplicity of infection (MOI). 100 µL of this solution was mixed with each serial dilution of inhibitor in triplicate on a 96-well plate. Mock infected cells were also mixed with inhibitor in a similar manner. After 5 days of incubation, a cell-permeable tetrazolium dye (MTT) was added. The MTT reaction was stopped after 5 hrs by adding acidified isopropanol. The plates were gently shaken overnight, quantified on a plate reader and the absorbance measured at 595 nm. The absorbance values were then plotted versus inhibitor concentration to generate EC_{50} and CC_{50} values. The 50% effective concentration (EC_{50}) and 50% cytotoxic concentration (CC_{50}) of the test compounds were defined as the compound concentrations required to inhibit cell viability (MT-2) by 50% the number of viable cells in mock-infected cell cultures, respectively.

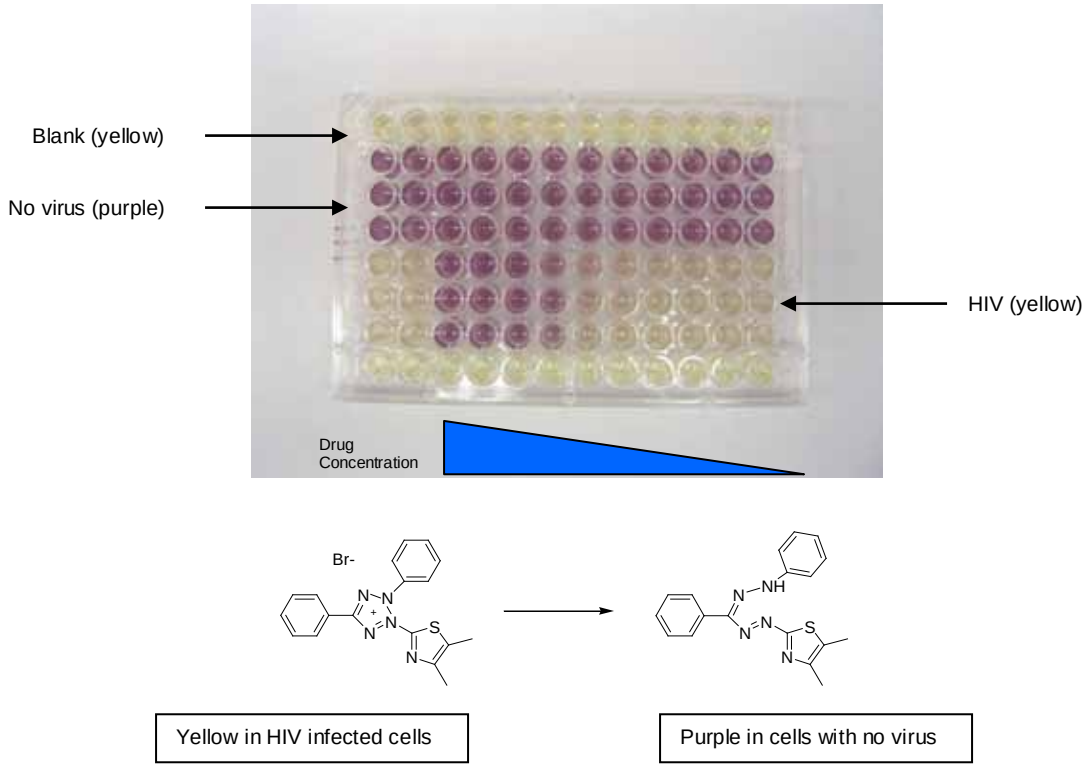

REFERENCES

1. Barre-Sinoussi, F.; Chermann, J.C.; Rey, F.; Nugeyre, M.; Charmart, S.; Gruest, J.; Dauguent, C.; Axlar-Blin, C.; Venzinet-Brun, F.; Rounzioux, C.; Rozenbaum, W.; Montagnier, L. *Science* **1983**, 220, 868-871.
2. Weiss, R. A. *Trop. Med. Int. Health* **2000**, 5, A-10-A15.
3. Aiken, C.; Trono, D. *J.Virol* **1995**, 69, 5048-5056.
4. Nomaguchi, M.; Fujita, M.; Adachi, A.; *Microbes and Infections* **2008**, 10, 960-967
5. AIDS/ HIV information from AVERT.org (available at http://www.avert.org/virus.htm).
6. (a) UNAIDS/WHO Epidemiological Fact Sheets on HIV/AIDS and Sexually Transmitted Infections, 2007 Epidemic Update: December **2007**. (b) UNAIDS/WHO Epidemiological Fact Sheets on HIV/AIDS and Sexually Transmitted Infections, 2008 Epidemic Update: July **2008.**
7. De Clercq, E. *Nature Rev*. **2007**, 6, 1001-1018.
8. De Clercq, E. *Biochem. Pharmocol.* **1994**, 47, 155-169.
9. Kwong, P. D.; Wayatt, R.; Robinson, J.; Sweet, R.W.; Sodroski, J.; Hendrickson, W. A. *Nature* **1998**, 393, 448.
10. Wyatt, R.; Kwong. P. D.; Desjardins, E.; Sweet, R. W.; Robinson. J.; Hendrickson, W. A.; Sodroski, J. G. *Nature* **1998**, 280, 705
11. Rizzuto, C. D.; Wyatt, R.; Hernandenz-Ramos, N.; Sun, Y.; Kwong, P. D.; Hendrickson, W. A.; Sodroski, *J. Science* **1998**, 280, 1949.
12. Borkow, G.; Lapaidot, A. *J. Infect.Dis.* **2005,** 5, 3-15.
13. De Clerq, E. *Int. J. Biochem. Cell Biol.* **2004**, 36, 1800-1822.
14. Ren, J.; Esnouf, R. M.; Hopkins, A. L.; Warren, J.; Balzarini, J.; Stuart, D. I.; Stammers, D. K. *Biochemistry*, **1998**, 37, 14394-14403.
15. Monini, P.; Sgadari, C.; Toschi, E.; Barilliari, G, Ensoli, B. *Nature Rev.* **2004,** 4, 861.
16. (a) Gottlieb, M. S.; Schroff, R.; Schanker, H. M. *New Engl. J. Med.* **1981**, 305, 1425-1431. (b) Scott, K.; Blankson, J. N. *Hopkins HIV Report*, **2007**, 19, 2, 10-12.
17. Budner, M.; Falzone, C.; Lantz, C.; Uy, J. HIV and AIDS: The Biochemistry Behind the Disease, 2002 (available at http://www.denison.edu/chem/DCS/journal/budnerv1n1.html).
18. Jacobo-Molina, A.; Ding, J.; Nanni, R. G.; Clark Jr.; A. D.; Lux, X.; Tantillo, C.; Willians, R. L.; Kamer, G.; Ferris, A. L; Clark. P. *Proc. Natl. Acad. Sci. USA*, **1993,** 90, 6320.
19. Pata, J. *et al. Proc Natl. Acad. Sci. USA,* **2004**, 101, 10548-10553.
20. Kohlstaedt, L. A; Wang, J.; Friedman, J. M.; Rice, P. A.; Steitz, T. A. *Science,* **1992**, 256, 1783-1790.
21. Zhou, Z.; Lin, X.; Madura, J. *J. Infect.Dis.* **2006**, 6, 391.
22. Sluis-Cremer, N.; Tachedjian, G. *Virus Res.* **2008,** 134, 147-156.
23. De Clercq, E. *Curr. Med. Chem.* **2001**, 8, 1543-1572.
24. Henry, K.; Erice, A.; Tierney, C.; Balfour, H. H. Jr.; Fischl, M. A.; Kmack, A.; Liou, S-H.;

Kenton, A.; Hirsch, M. S.; Phair, J.; Martinez, A.; Kahn, J. O. *J. Acquir. Immun. Defic. Syndr. Hum. Retrovirol*. **1998**, 19, 339-349.

25. Bisset, L. R.; Cone, R. W.; Huber, W.; Battegay, M.; Vernazza, P. L.; Weber, R.; Grob, P. J.; Opravil, M. *AIDS*, **1998**, 12, 2115-2123.
26. Woods II, M. L.; MacGinley, R.; Eisen, D. P.; Allworth, A. M. *AIDS*, **1998**, 12, 1491-1494.
27. Mitsuya, H.; Weinhold, K. J.; Furman, P. A.; St Clair, M. H.; Nusonoff-Iehrman, S.; Gallo, R. C.; Bolognesi, D. P.; Barry, D. W.; Broder, S. *Proc. Natl. Acad. Sci. USA*. **1985**, 82, 7096-7100.
28. Coates, J. A. V.; Cammack, N. S.; Jenkinson, H. J.; Jowett, A. J.; Jowett, M. I.; Pearson, B. A.; Pen, C. R.; Rouse, P. L.; Viner, K. C.; Cameron, J. M. *Antimicrob. Agents Chemother.* **1992**, 36, 733-739.
29. Ahluwalia, G.; Cooney, D. A.; Mitsuya, H.; Fridland, A.; Flora, K. P.; Hao, Z.; Dalal, M.; Broder, S.; Johns, D. G. *Biochem. Pharmacol*. **1986**, 35, 3797-3800.
30. Cooney, D. A.; Dalal, M.; Mitsuya, H.; McMahon, J. B.; Nadkarni, M.; Balzarini, J.; Broder, S.; Johns, D. G. *Biochem. Pharmacol.* **1986**, 35, 2065-2068.
31. Balzarini, J.; Kang, G. J.; Dalal, M.; Herdewijn, P.; De Clercq, E.; Broder, S.; Johns, D. G. *Mol. Pharmacol.* **1987**, 32, 162-167.
32. Crimmins, M. T.; King, B. W.; *J. Org. Chem.* **1996**, 61, 4192-4193.
33. (a) Liotta, D. G.; Choi, W. -B. *PCT Int. Appl. WO* 91252418, **1991**. (b) Liotta, D. C.; Schinazi, R. F.; Choi, W. -B. PCT *Int. Appl. WO* 9214743, **1992**.
34. (a) De Clercq, E. *Clin. Microbiol. Rev.* **1995**, 8, 200-239. (b) McComsey, G. A. et al. *Clin. Infect. Dis.* **2008**, 46, 1290–1296.
35. Meyer, P. R.; So, A. G.; Scott, W. A. *Proc. Natl. Acad. Sci. USA*. **1998**, 95, 13471-13476.
36. Miller, M. D.; Margot, N. A.; Hertogs, K.; Larder, B.; Miller, V. *Nucleos. Nucleot. Nucleic Acids* **2001**, 20, 1025-1028.
37. De Clercq, E. *Expert Opin. Emerging Drugs* **2005**, 10, 241-274.
38. De Clercq, E. *Nature Rev. Drug Discov.* **2002**, 1, 13-25.
39. (a) Hurwitz, S. J.; Otto, M. J. *Antiviral Chem. Chemother.* **2005**, 16, 117-127. (b) Feng, J. Y.; Junxing, S.; Schinazi, R. F.; Anderson, K. S. *FASEB*, **1999**, 13, 1511-1517.
40. De Clercq, E. *Antiviral Res.* **2007**, 75, 1-13.
41. De Clercq, E. *Biochem. Pharmacol.* **2007**, 73, 911-922.
42. Holy, A. *Antiviral Res.* **2006**, 71, 248-253.
43. Tantillo, C.; Ding, J.; Jacobo-Molina, A.; Nanni, R. G.; Boyer, P. L.; Hughes, S. H.; Arnold, E. *Proc. Natl. Acad. Sci. USA* **1993**, 90, 6320-6324.
44. Pata, J. D.; Stirtan, W. G.; Goldstein, S. W.; Steitz. T. A. *Proc. Natl. Acad. Sci. USA* **2004**, 101, 10548-10553.
45. Marx, A.; Detmer, I.; Gaster, J.; Summerer, D. *Synthesis* **2004**, 1, 1-14.

46. Perigaud, C.; Aubertin, A. -M.; Benzaria, S.; Pelicano, H.; Girardet, J. -L.; Maury, G.; Gosselin, G.; Kirn, A.; Imbach, J. -L. *Biochem. Pharmacol.* **1994**, 48, 11-14.
47. McGuigan, C.; Tsang, H. -W.; Cahard, D.; Turner, K.; Velazquez, S.; Salgado, A.; Bidios, L.; Naesens, L.; De Clercq, E.; Balzarini, J. *Antoviral Res.* **1997**, 35, 195-204.
48. Siddiqui, A. Q.; Ballatore, C.; McGuigan, C.; De Clercq, E.; Balzarini, J. *J. Med. Chem.* **1999**, 42, 393-399.
49. Siddiqui, A. Q.; McGuigan, C.; Ballatore, C.; Zuccotto, F.; Gilbert, I. H.; De Clercq, E.; Balzarini, J. *J. Med. Chem.* **1999**, 42, 4122-4128.
50. Balzarini, J.; Karlsson, A.; Aquaro, S.; Perno, C. -F.; Cahard, D.; Naesens, L.; De Clercq, E.; McGuigan, C. *Proc. Natl. Acad. Sci. USA* **1996**, 93, 7295-7299.
51. Aquaro, S.; Wedgwood, O.; Yarnold, C.; Cahard, D.; Pathinara, R.; Velazquez, S.; McGuigan, C.; Calio, R.; De Clercq, E.; Balzarini, J.; Perno, C. F. *Antimicrob. Agents Chemother.* **2000**, 44, 173-177.
52. Meier, C.; Lorey, M.; De Clercq, E.; Balzarini, *J. Bioorg. Med. Chem. Lett*. **1997**, 7, 99-104.
53. Meier, C.; Knispel, T.; De Clercq, E.; Balzarini, J. *Bioorg. Med. Chem. Lett.* **1997**, 7, 1577-1582.
54. Meier, C.; Lorey, M.; De Clercq, E.; Balzarini, J. *J. Med. Chem.* **1998**, 41, 1417-1427.
55. Meier, C.; Knispel, T.; De Clercq, E.; Balzarini, J. *J. Med. Chem.* **1999**, 42, 1604-1614.
56. Albert, A. *Selective toxicity.* Chapman and Hall Editors London, 1951.
57. Anastasi, C.; Quelever, G.; Burlet, S.; Garino, C.; Souard, F.; Kraus, J. -L. *Curr. Med. Chem.* **2003**, 10, 1825-1843.
58. Meier, C. *Eur. J. Org. Chem.* **2006**, 1081-1102.
59. Wagner, C. R.; Iyer, V. V.; McIntee, E. J. *Med. Res. Rev.* **2000**, 20, 417-451.
60. Meier, C. *Synlett* **1998**, 233-242.
61. Khan, S. R.; Nowak, B.; Plunkett, W.; Farquhar, D. *Biochem. Pharmacol.* **2005**, 69, 1307-1313.
62. Meier, C. *Mini-Rev. Med. Chem.* **2002**, 2, 219-234.
63. Meier, C.; Ruppel, M. F. H.; Vukadinovic, D.; Balzarini, J. *Mini. Rev. Med. Chem.* **2004**, 4, 383-394.
64. De Clercq, E.; Holy, A. *Nat. Rev. Drug Discov.* **2005**, 4, 928-940.
65. De Clercq, E.; Holy, A.; Rosenberg, I.; Sakuma, T.; Balzarini, J.; Maudgal, P. C. *Nature* **1986**, 323, 464-467.
66. De Clercq, E.; Descamps, J.; De Somer, P.; Holy, A. *Science* **1978**, 200, 563-565.
67. Shafer, R. W. *Clin. Microbiol. Rev*. **2002**, 247-277.
68. Meyer, P. R.; Matsuura, S. E.; So, A. G.; Scott, W. A. *Proc. Natl. Acad. Sci USA* **1998**, 13471-13476.
69. De Clercq, E. *Antiviral Res.* **1998**, 38, 153-179.

70. Sluis-Cremer, N.; Temiz, N. P.; Bahar, I. *Curr. HIV Res.* **2004**, 2, 323-332.
71. Pauwels, R.; Andries, K.; Desmyter, J.; Schols, D.; Kukla, M. J.; Breslin, H. J.; Raeymaeckers, A.; Van Gelder, J.; Woestenborghs, R.; Heykants, J.; Schellekens, K.; Janssen, M. A. C.; De Clercq, E.; Janssen, P. A. J. *Nature* **1990**, 343, 470-474.
72. Janssen, P. A. J.; Lewi, P. J.; Arnold, E.; Daeyaerts, F.; de Jonge, M.; Heeres, J.; Koymans, L.; Vinkers, M.; Guillemont, J.; Pasquier, E.; Kukla, M.; Ludovici, D.; Andries, K.; de Bethune, M. -P.; Pauwels, R.; Das, K.; Clark, A. D.; Frenkel, Y. V.; Hughes, S. H.; Medaer, B.; De Knaep, F.; Bohets, H.; De Clercq, F.; Lampo, A.; Williams, P.; Stoffels, P. *J. Med. Chem.* **2005**, 48, 1901-1909.
73. Pauwels, R.; Andries, K.; Debyser, Z.; Daele, P. V.; Schols, D.; Stoffels, P.; Vreese, K. D.; Woestenborghs, R.; Vandamme, A.; Janssen, C. G. M.; Anne, J.; Cauwenbergh, G.; Desmyter, J.; Heykants, J.; Janssen, M. A. C.; De Clercq, E.; Janssen, P. A. J. *Proc. Natl. Acad. Sci. USA* **1993**, 90, 1711-1715.
74. Ludovici, D. W.; Kukla, M. J.; Grous, P. G.; Krishnan, S.; Andries, K.; de Bethune, M. -P.; Azijn, H.; Pauwels, R.; De Clercq, E.; Arnold, E.; Janssen, P. A. J. *Bioorg. Med. Chem. Lett.* **2001**, 11, 2225-2228.
75. Ludovici, D. W.; Kavash, R. W.; Kukla, M. J.; Ho, C. Y.; Ye, H.; De Corte, B. L.; Andries, K.; de Bethune, M. -P.; Azijn, H.; Pauwels, R.; Moereels, H. E.; Heeres, J.; Koymans, L. M.; de Jonge, M. R.; Van Aken, K. J.; Daeyaert, F. F.; Lewi, P. J.; Das, K.; Arnold, E.; Janssen, P. A. J. *Bioorg. Med. Chem. Lett.* **2001**, 11, 2229-2234.
76. Sankatsing, S.; Weverling, G.; van 't Klooster, G.; Prins, J.; Lange, J. 9th Conference on Retroviruses and Opportunistic Infections, Seattle, WA, February 24-28, 2002. Abstract 5.
77. Das, K.; Bauman, J. D.; Clark, A. D.; Frenkel, Y. D.; Lewi, P. J.; Shatlin, A. J.; Hughes, S. H.; Arnold, E. *Proc. Natl. Acad. Sci. USA* **2008**, 105, 1466-1471.
78. Hsiou, Y.; Ding, J.; Das, K.; Clark, A. D.; Hughes, S. H.; Arnold, E. *Structure* **1996**, 4, 853-860.
79. (a) Rodgers, D. W.; Gamblin, S. J.; Harris, B. A.; Ray, S.; Culp, J. S.; Hellmig, B.; Woolf, D. J.; Debouck, C.; Harrison, S. C. *Proc. Natl. Acad. Sci. USA* **1995**, 92, 1222-1226. (b) Esnouf, R.; Ren, J.; Ross, C.; Jones, Y.; Stammers, D.; Stuart, D. *Nat. Struct. Biol.* **1995**, 2, 303-308. (c) Esnouf, R. M.; Ren, J.; Garman, E. F.; Somers, D. O. N.; Ross, C. K.; Jones, E. Y.; Stammers, D. K.; Stuart, D. I. *Acta Crystallogr.* **1998**, D 54, 938-954. (d) Das, K.; Sarafianos, S. G.; Clark Jr., A. D.; Boyer, P. L.; Hughes, S. H.; Arnold, E. *J. Mol. Biol.* **2007**, 365, 77-89. (e) Spence, R. A.; Kati, W. M.; Anderson, K. S.; Johnson, K. A. *Science* **1995**, 267, 988-993. (f) Xia, Q.; Radzio, J.; Anderson, K. S.; Sluis-Cremer, N. *Protein Sci.* **2007**, 16, 1728-1737. (g) Ren, J.; Stammers, D. K. *Virus Res.* **2008**, 134, 157-170.
80. Smith, M. B. K.; Lamb, M. L.; Tirado-Rives, J.; Jorgensen, W. L.; Michejda, C. J.; Ruby, S. K.; Smith, Jr. R. H. *Protein Eng.* **2000**, 13, 413-421.

81. Madrid, M.; Jacobo-Molina, A.; Ding, J.; Arnold, E. *Proteins* **1999**, 35, 332-337.
82. Campiani, G.; Ramunno, A.; Maga, G.; Nacci, V.; Fattirusso, C.; Catalanotti, B.; Morelli, E.; Novellino, E. *Curr. Pharmaceut. Des.* **2002**, 8, 615-657.
83. Parniak, M. A.; Sluis-Cremer, N. *Adv. Pharmacol.* **2000**, 49, 67-109.
84. Tronchet, J. M.; Seman, M. *Curr. Topics Med. Chem.* **2003**, 3, 1496-1511.
85. Ding, J.; Das, K.; Moereels, H.; Koymans, L.; Andries, K.; Janssen, P. A.; Hughes, S. H.; Arnold, E. *Nature Struct. Biol.* **1995**, 2, 407-415.
86. Herrewege, Y. V.; Michiels, J.; Van Roey, J.; Fransen, K.; Kestens, L.; Balzarini, J.; Lewi, P.; Vanham, G.; Janssen, P. *Antimicrob. Agents Chemother.* **2004**, 48, 337-339.
87. Jorgensen, W. L.; Ruiz-Crux, J.; Tirado-Rives, J.; Basavapathruni, A.; Anderson, K. S.; Hamilton, A. D. *Bioorg. Med. Chem. Lett.* **2006**, 16, 663-667.
88. Das, K.; Lewi, P. J.; Hughes, S. H.; Arnold, E. *Progr. Biophys. Mol. Biol.* **2005**, 88, 209-231.
89. De Corte, B. L. *J. Med. Chem.* **2005**, 48, 1689-1696.
90. Das, K.; Clark, A. D.; Lewi, P. J.; Heeres, J.; de Jonge, M. R.; Koymans, L. M. H.; Vinkers, H. M.; Daeyaert, F.; Ludovici, D. W.; Kukla, M. J.; De Corte, B.; Kavash, R. W.; Ho, C. Y.; Ye, H.; Lichtenstein, M. A.; Andries, K.; Pauwels, R.; de Bethune, M. -P.; Boyer, P. L.; Clark, P.; Hughes, S. H.; Janssen, P. A. J.; Arnold, E. *J. Med. Chem.* **2004**, 47, 2550-2560.
91. Rodriguez-Barrios, F.; Balzarini, J.; Gago, F. *J. Am. Chem. Soc.* **2005**, 127, 7570.
92. Balzarini, J.; Karlsson, A.; Perez-Perez, M. J.; Camarasa, M. J.; Tarpley, W. G.; *et al. J. Virol.* **1993**, 67, 5353-5359.
93. Bacheler, L.; Jeffrey, S.; Hanna, G.; D'Aquila, R.; Wallace, L.; *et al. J. Virol.* **2001**, 75, 4999-5008.
94. Ren, J.; Milton, J.; Weaver, K. L.; Short, S. A.; Stuart, D. I. *et al. Struct. Folds Des.* **2000**, 8, 1089-1094.
95. Hsiou, Y.; Das, K.; Ding, J.; Clark, A. D.; Kleim, J. P. *et al. J. Mol. Biol.* **1998**, 284, 313-323.
96. Udier-Blagovic, M.; Watkins, E.K.; Tirado-Rives, J.; Jorgensen, W. L. *Bioorg. Med. Chem. Lett.* **2003**, 13, 3337-3340.
97. Das, K.; Ding, J.; Hsiou, Y.; Clark, A. D.; Moereels, H. *et al. J. Mol. Biol.* **1996**, 264, 1085-1100.
98. Ren, J.; Nichols, C.; Bird, L.; Chamberlain, P.; Weaver, K.; *et al. J. Mol. Biol.* **2001**, 312, 795-805.
99. Nanni, R. G.; Ding, J.; Jacobo-Molina, A.; Hughes, S. H.; Arnold, E. *Perspect. Drug. Dis. Des.* **1993**, 1, 129-150.
100. Muhanji, C.I.; Hunter, R. *Curr. Med. Chem.* **2007**, 14, 1207-1220.
101. Xia, Z.; Wiebe, L. I.; Miller, G. G.; Kanaus, E. E. *Arch. Der Pharmazie* **1999**, 332, 286-294.
102. Nudelman, A.; Rephaedli, A. *J. Med. Chem.* **2000**, 43, 2962-2966.
103. (a) Sharma, U.; Marquis, J. C.; Dinaut, A. N.; Hillier, S. M.; Fedeles, B.; Rye, P. T.;

Essigmann, J. M.; Croy, R. G. *Bioorg. Med. Chem. Lett*. **2004**, 14, 3829; (b) Mitra, K.; Marquis, J. C.; Hillier, S. M.; Rye, P. T.; Zayas, B.; Lee, A. S.; Essigmann, J. M.; Croy, R. G. *J. Am. Chem. Soc* **2002**, 124, 1862.

104. Rink, S. M.; Yarema, K. J.; Solomon, M. S.; Paige, L. A.; Tadayoni-Rebek, B. M.; Essigmann, J. M.; Croy, R. G. *Proc. Natl. Acad. Sci. USA* **1996**, 93, 15063.
105. Romeo, S.; Dell'Agli, M.; Parapini, S.; Rizzi, L.; Galli, G.; Mondani, M.; Sparatore, A.; Taramelli, D.; Bosisio, E. *Bioorg. Med. Chem. Lett.* **2004**, 14, 2931.
106. Biot, C.; Dessolin, J.; Grellier, P.; Davioud-Charvet, E. *Redox Rep*. **2003**, 8. 280.
107. Davioud-Charvet, E.; Delarue, S.; Biot, C.; Schwobel, Boehme, C. C.; Mussigbrodt, A.; Maes, L.; Sergheraert, C.; Grellier, P.; Schirmer, R. H.; Becker, K. *J. Med. Chem* **2001**, 44, 4268.
108. Nizir, E.; Adani, R.; Meshulam, H.; Amitai, G.; Brenner, T. *Neurosci. Lett.* **2005**, 46, 376.
109. Farias, G. G.; Godoy, J. A.; Vazquez, M. C.; Adani, R.; Meshulam, H.; Avila, J.; Amitai, G.; Inestrosa, N. C. *Neurobiol. Dis*. **2005**, 18, 176.
110. Bailey, K.; Tan, E. W. *Bioorg. Med. Chem*. **2005**, 18, 176.
111. Ackerley, N.; Brewster, A. G.; Brown, G. R.; Clarke, D. S.; Foubister, A. J.; Griffin, S. J.; Husdson, J. A.; Smithers, M. J.; Whittamore, P. R. O. *J. Med. Chem.* **1995**, 38, 1608.
112. Carroll, L. *Through the Looking Glass*. First published in 1871.
113. Wang, Z.; Bennett. E. M.; Wilson, D. J.; Salomon, C.; Vince, R. *J. Med. Chem.* **2007**, 50, 3416.
114. (a) Matsumoto, H.; Hamawaki, T.; Ota, H.; Kimura, T.; Goto, T.; Sano, K.; Hayashi, Y.; Kiso, Y. *Bioorg. Med. Chem. Lett.* **2000**, 10, 1227-1231. (b) Kimura, T.; Matsumoto, H.; Matsuda, T.; Hamawaki, T.; Akaji, K.; Kiso, Y. *Bioorg. Med. Chem. Lett.* **1999**, 9, 803-806.
115. Tamamura, H.; Omagri, A.; Hiramatsu, K.; Kanamoto, T.; Gotoh, K.; Kanbara, K.; Yamamoto, N.; Nakahima, H.; Otaka, A.; Fujii, N. *Bioorg. Med. Chem*. **2001**, 9, 2179.
116. Daoudi, J. M.; Greiner, J.; Aubertin, A. M.; Vierling, P. *Bioorg. Med. Chem. Lett.* **2004**, 14, 495-498.
117. Vliegher, P.; Clerc, T.; Pannecouque, C.; Witvrouw, M.; De Clercq, E.; Salles, J-P.; Kraus, J-L. *J. Med. Chem*. **2002**, 45, 1275.
118. Ijichi, K.; Fujiwara, M.; Mori, K.; Morozumi, M.; Machida, H.; Shigeta, S.; Konno, K.; Yokota, T.; Baba, M. *Antiviral Res*. **1996**, 31, 115.
119. (a) Mohamed, L. A.; Taourirte, M.; Rochdi, A.; Lazrek, H. B.; Vassuer, J. -J.; Engels, J. W.; Pannecouque, C.; De Clercq, E. *Nucleos. Nucleot. Nucleic Acids* **2003**, 22, 829-831. (b) Taourirte, M.; Mohamed, L. A.; Rochdi, A.; Vasseur, J. -J.; Fernandez, S.; Ferrero, M.; Gotor, V.; Pannecouque, C.; De Clercq, E.; Lazrek, H. B. *Nucleos. Nucleot. Nucleic Acids* **2004**, 23, 701-714.

120. Gavriliu, D.; Fossey, C.; Ciurea, A.; Delbederi, Z.; Sugeac, E.; Laduree, D.; Schmidt, S.; Laumond, G.; Aubertin, A. M. *Nucleos. Nucleot. Nucleic Acids* **2002**, 21, 505-533.

121. Sugeac, E.; Fossey, C.; Laduree, D.; Schmidt, S.; Laumond, G.; Aubertin, A. M. *J. Enzym. Inhib. Med. Chem.* **2003**, 18, 175-186.

122. Laduree, D.; Sugeac, E.; Fossey, C.; Schmidt, S.; Laumond, G.; Aubertin, A. M. *Nucleos. Nucleot. Nucleic Acids* **2003**, 22, 873-875.

123. Peterson, L.; Jørgensen, P. T.; Nielsen, C.; Hasen, T. H.; Nielsen, J.; Pederson, E. B. *J. Med. Chem*. **2005**, 48, 1211-1220.

124. Pėrigaud, C.; Gosselin, G.; Lefebvre, I.; Girardet, J-L.; Benzaria, S.; Barber, I.; Imbach, J-L. *Bioorg. Med. Chem. Lett*. **1993**, 3, 2521-2526.

125. Basavapathruni, A.; Bailey, C. M.; Anderson, K. S. *J. Biol. Chem.* **2004**, 279, 6221-6224.

126. (a) Velazquez, S.; Alvarez, R.; San-Felix, A.; Jimeno, M. L.; De Clercq, E.; Balzarini, J.; Camarasa, M. L. *J. Med. Chem.* **1995**, 38, 1641-1649. (b) Velazquez, S.; Tunon, V.; Jimeno, M. L.; Chamorro, C.; De Clercq, E.; Balzarini, J.; Camarasa, M. L. *J. Med. Chem.* **1999**, 42, 5188-5196.

127. McGuigan, C.; Devine, K. G.; O' Connor, T. J.; Galpin, S. A.; Jeffries, D. J.; Kirchington, D. *Antiviral Chem. Chemother.* **1990**, 1, 107-113.

128. Valazquez, S.; Lobaton, E.; De Clercq, E.; Koontz, D. L.; Mellors, J. W.; Balzarini, J.; Camarasa, M. L. *J. Med. Chem.* **2004**, 47, 3418-3426.

129. (a) Oberg, B. *Pharmacol. Ther.* **1989**, 40, 213-285. (b) Wagstaff, A. J.; Bryson, H. M. *Drugs* **1994**, 48, 199-226. (c) Chrisp, P.; Clissold, S. F. *Drugs* **1991**, 41, 104-129.

130. Fletcher, C. V.; Collier, A. C.; Rhame, F. S.; Bennet, D.; Para, M. F.; Beatty, C. C.; Jones, C. E.; Balfour, H. H. Jr. *Antimicrob. Agents Chemother.* **1994**, 38, 604-607.

131. Renoud-Grappin, M.; Fossey, C.; Fontaine, G.; Laduree, D.; Aubertin, A. M.; Kirn, A. *Antiviral Chem. Chemother.* **1998**, 9, 205-223.

132. Pontikis, R.; Dolle, V.; Guillaumel, J.; Dechaux, E.; Note, R.; Nguyen, C. H.; Legraverend, M.; Bisagni, E.; Aubertin, A. -M.; Grierson, D. S.; Monneret, C. *J. Med. Chem.* **2000**, 43, 1927-1939.

133. (a) Horwitz, J. P.; Chua, J.; Da Rooge, M. A.; Noel, M. *Tetrahedron Lett.* **1964**, 2725-2727. (b) Horwitz, J. P.; Chua, J.; Klundt, I. L.; Da Rooge, M. A.; Noel, M. *J. Am. Soc.* **1964**, 86, 1986. (c) Horwitz, J. P.; Chua, J.; Da Rooge, M. A.; Noel, M.; Klundt, I. L. *J. Org. Chem.* **1966**, 31, 205-211.

134. Mansuri, M. M.; Starrett, Jr. J. E.; Ghazzouli, I.; Hitchcock, M. J. M.; Sterzycki, R. Z.; Brankovan, V.; Lin, T-S.; August, E. M.; Prusoff, W. H.; Sommadossi, J-P.; Martin, J. C. *J. Med. Chem.* **1989**, 32, 461-466.

135. Skonezny, P. M.; Eisenreich, E.; Stark, D. R.; Boyhan, B. T.; Baker, S. R. *US Patent No.* 5,539,099, **1996**.

136. Joshi, B. V.; Rao, T. S.; Reese, C. B. *J. Chem. Soc. Perkin Trans 1* **1992**, 2537-2544.

137. Chen, B-C.; Quinlan, S. L.; Reid, J. G.; Spector, R. H. *Tetrahedron Lett.* **1998**, 39, 729-732.

138. Chen, B-C. ; Quinlan, S. L.; Stark, D. R.; Reid, G.; Audia, V. H.; George, J. G.; Eisenreich, E.; Brundidge, S. P.; Racha, S.; Spector, R. H. *Tetrahedron Lett.* **1995**, 36, 7957-7960.

139. *US Patent No.* 5,696,151.

140. De Corte, B.; de Jonge, M. R.; Heeres, J.; Ho, C. Y.; Janssen, P. A. J.; Kavash, R. W.; Koymans, L. M. H.; Kukla, M. J.; Ludovici, D. W.; Van Aken, K. J. A. *US Patent no.* 2003/0114472 A1, **2003**.

141. (a) Ruth, J. L.; Cheng, Y. C. *Mol. Pharmacol.* **1981**, 20, 415-422. (b) Ruth, J. L.; Cheng, Y. C. *J. Biol. Chem.* **1982**, 10261-10266.

142. Rong, F. G.; Soloway, A. H. *Nucleos. Nucleot.* **1994**, 13, 2021-2034.

143. Mao, C.; Sudbeck, E. A.; Venkatchalam, T. K.; Uckun, F. M. *Biochem. Pharm.* **2000**, 60, 1251-1265.

144. Sonogashira, K.; Todha, Y.; Hagihara, N. *Tetrahedron Lett.* **1975**, 16, 4467-4470.

145. Ciurea, A.; Fossey, C.; Benzaria, S.; Gavriliu, D.; Delbederi, Z.; Lelong, B.; Laduree, D.; Aubertin, A. M.; Kirn, A. *Nucleos. Nucleot. Nucleic Acids* **2001**, 20, 1655-1670.

146. De Clercq, E. *J. Clin. Virol.* **2004**, 30, 115-133.

147. Arnott, G.; Hunter, R.; Mbeki, L.; Mohamed, E. *Tetrahedron Lett.* **2005**, 4023-4026.

148. Agrofoglio, L. A.; Gillaizeau, I.; Saito, Y. *Chem. Rev.* **2003**, 103, 1875-1916.

149. Crisp, G.; Flynn, B. L. *J. Org. Chem.* **1993**, 58, 6614-6619.

150. Robins, M. J.; Barr, P. J. *J. Org. Chem.* **1983**, 48, 1854-1862.

151. Hobbs, F. W. Jr. *J. Org. Chem.* **1989**, 54, 3420-3422.

152. Robins, M. J.; Vinayak, R. S.; Wood, S. G. *Tetrahedron Lett.* **1990**, 31, 3731-3734.

153. Garg, N. K.; Woodroofe, C. C.; Lacenere, C. J.; Quake, S. R.; Stoltz, B. M. *Chem. Comm.* **2005**, 4551-4553.

154. Ciurea, A.; Fossey, C.; Gavriliu, D.; Delbederi, Z.; Sugeac, E.; Laduree, D.; Schmidt, S.; Laumond, G.; Aubertin, A. M. *J. Enzym. Inhib. Med. Chem.* **2004**, 19, 511-519.

155. Asakura, J.; Robins, M. J. *J. Org. Chem.* **1990**, 55, 4928-4933.

156. Prusoff, W. H.; Holmes, W. L.; Welch, A. D. *Cancer Res.* **1953**, 13, 221-225.

157. Dale, R. M. K.; Ward, D. C.; Livingston, D. C.; Martin, E. *Nucleic Acid Res.* **1975**, 2, 915-930.

158. (a) Van Altena, I. A.; Miller, D. A. *Aust. J. Chem.***1989**, *42*, 2181-2190; (b) Buttery, C. D.; Cameron, A. G.; Dell, C. P.; Knight, D. W. *J. Chem. Soc., Perkin Trans 1* **1990**, 1601-1610; (c) Tada, M.; Yamada, H.; Kanamori, A.; Chiba, K. *J. Chem. Soc., Perkin Trans 1* **1993**, 239-247; (d) Wang, F.; Chiba, K.; Tada, M. *Chem. Lett*. **1993**, *12*, 2117-2120; (e) Perry, P. J.; Pavlidis, V. H.; Hadfield, J. A.; Coutts, I. G. C. *J. Chem. Soc., Perkin Trans 1* **1995**, *9*, 1085-1087; (f) Mal, D.; Bandhyopadhyay, M.; Datta, K.; Murty, K. V. S. N. *Tetrahedron* **1998**, *54*, 7525-7538; (g) Kline, T.; Bowman, J.; Iglewski, B. H.; de Kievit, T.; Kakai, Y.; Passador, L. J.

Biorg. Med. Chem. Lett. **1999**, *9*, 3447-3452.

159. (a) Knight, D. W. *Tetrahedron. Lett*. **1979**, *20*, 469-472; (b) Knight, D. W.; Nott, A. P. *J. Chem. Soc., Perkin Trans 1* **1981**, 1125-1131.
160. Yu, S.; Beese, G.; Keay, B. A *J. Chem. Soc., Perkin Trans 1* **1992**, 2729-2731.
161. Tada, M.; Sugimoto, Y.; Takahashi, T. *Bull. Chem. Soc., Jpn*., **1980**, *53*, 2966-2970.
162. (a) Schweizer, E. E.; Creasy, W. S.; Light, K. K.; Shaffer, E.; T. *J. Org. Chem*. **1969**, *34,* 212-218; (b) Cooper, J. A.; Cornwall, P., Dell, C. P.; Knight, D. W. *Tetrahedron Lett.* **1988,** *29*, 2107-2110; (c) Hart, D. J.; Patterson, S.; Urich, J. P. *Synlett* **2003**, 1334-1338.
163. Khatuya, H. *Tetrahedron Lett*. **2001**, *42*, 2643-2644.
164. For an interesting stereoelective Birch reduction of 3-methyl-2-furoates as an entry into 2,5-dihydrofurans, see: Donohoe, T. J.; Raoof, A.; Freestone, G. C.; Linney, I. D.; Cowley, A.; Helliwell, M. *Org. Lett*. **2002**, *4*, 3059-3062.
165. Jesberger, M.; Davis, T. P.; Barner, L. *Synthesis* **2003**, 13, 1929-1958.
166. Chong, J. M.; Heuft, M. A.; Rabbat, P. *J. Org. Chem*. 2000, **65**, 5837-5838.
167. Clayden, J.; Greeves, N.; Warren, S.; Wothers, P. *Organic Chemistry*, Oxford University Press, Oxford, **2001**.
168. Wenseleers, R. *J. Phys. Chem. B.* 2002, **106**(27), 6860.
169. Fukuyama, T.; Laird, A. A.; Hotchkiss, L. M. *Tetrahedron Lett*. 1985, **26**(51), 6291-6292.
170. Petitou, M.; Duchaussoy, P.; Choay, J. *Tetrahedron Lett*. 1988, **29**(12), 1389-1390.
171. Hunter, R.; Mohamed, E. *Afinidad*, **2007**, 64, 231-236.
172. Thakur, V. V.; Kim, J. T.; Hamilton, A. D.; Bailey, C. M.; Domaoal, R. A.; Wang, L.; Anderson, K. S.; Jorgensen, W. L. *Bioorg. Med. Chem. Lett.* **2006**, 16, 5664-5667.
173. Ruiz-Caro, J.; Basavapathruni, A.; Kim, J. T.; Bailey, C. M.; Wang, L.; Anderson, K. S.; Hamilton, A. D.; Jorgensen, W. L. *Bioorg. Med. Chem. Lett.* **2006**, 16, 668-671.
174. Hunter, R.; Muhanji, C. I.; Hale, I.; Basavapathruni, A.; Bailey, C. M.; Anderson, K. S. *Bioorg. Med. Chem. Lett.* **2007**, 48, 1051-1058.
175. Sato, K.; Tsukase, M.; Shibata, T. *Eur. Pat. Applic.* 205983, 30 Dec. **1985**.
176. Taher, A.; Ladwa, S.; Rajan, S. T.; Weaver, G. W. *Tett. Lett.* **2000**, 41, 9893-9897.
177. Makhija, M. T. *et al. Bioorg. Med. Chem. Lett.* **2004**, 12, 2317-2333.
178. Krishna Mohan, K. V. V.; Narender, N.; Srinivasu, P.; Kulkarni, S. J.; Raghavan, K. V. *Synthetic Comm.* **2004**, 34 (12), 2143-2152.
179. Schareina, T.; Zapf, A.; Beller, M. *J. Org. Chem.* **2004**, 689, 4576-4583.
180. Weissman, S. A.; Zewge, D.; Chen, C. *J. Org. Chem.* **2005**, 70, 1508-1510.
181. Hatsuda, M.; Seki, M. *Tetrahedron* **2005**, 61, 9908-9917.
182. Lu, Z.; Mayr, A.; Cheung, K. *Inorganica Chimica Acta* **1999**, 284, 205-214.
183. Marshall, J. A.; Trometer, J. D.; Blough, B. E.; Crute, T. D. *J. Org. Chem.* **1988**, 53, 4274-4282.

184. Huang, H.; Chopra, R.; Verdine, G. L.; Harrison, S. C. *Science* **1998**, *282*, 1669-1674.
185. Pettersen, E.F.; Goddard, T.D.; Huang, C.C.; Couch, G.S.; Greenblatt, D.M.; Meng, E.C.; and Ferrin, T.E. *J. Comput. Chem.* **2004**, *25*, 1605-1612.
186. ChemDraw, version 6.0, CambridgeSoft Corporation, Cambridge, MA, 2000.
187. Chem3D, version 5.0, CambridgeSoft Corporation, Cambridge, MA, 2000.
188. Maestro, version 7.5, Schrödinger, LLC, New York, NY, 2006.
189. Impact, version 4.0, Schrödinger, LLC, New York, NY, 2006.
190. Isomura, Y. *Chem. Pharm. Bull.* **1997**, 45, 482-486.
191. Spychala, J. *Synthet. Comm.* **1997**, 27, 1943-1949.
192. Chabrier, M.; Seyden-Penne, J.; Fouace, A.M. *C. R. Acad. Sc.* **1957,** *245*, 174-175.
193. Zhang, Y. M.; Razler, T.; Jackson, P.F. *Tetrahedron Lett.* **2002**, *43*, 8235-8239.
194. Veciana, J.; Hernandez, E.; Galan, A.; Rovira, C. *Synthesis* **1992**, 1164-1169.
195. Eckstein, F.; Ludwig, J. *J. Org. Chem.* **1989**, *54*, 631-635.
196. Murakami, E.; Feng, J.Y.; Lee, H.; Hanes, J.; Johnson, K.A.; Anderson, K.S. *J. Biol. Chem.* **2003**, *278*, 36403-36409.
197. Kerr, S.G.; Anderson, K.S. *Biochemistry* **1997**, *36*, 14064-14070.
198. Holý, A. *Antiviral Res.* **2006**, 71, 248-253.
199. Hockova, D.; Holý, A.; Masojidkova, M.; Andrei, G.; Snoeck, R.; De Clercq, E.; Balzarini, J. *Bioorg. Med. Chem.* **2004**, *12*, 3197-3202.
200. Pomeisl, K.; Votruba, I.; Holý, A.; Pohl, R. *Coll. Czech. Chem. Comm.* **2006**, 71, 595-624.
201. Fakhraian, H.; Mirzaei, A. *Org. Proc. Res. Developm.* **2004**, 8, 401-404.
202. Jeanmaire, T.; Hervaud, Y.; Boutevin, B. *Phosphorus, Sulfur and Silicon*, **2002**, 177, 1137-1145.

PhD Corrections

PhD candidate: Ebrahim Mohamed
Student number: MHMEBR008

Supervisor: Professor Roger Hunter
Department: Chemistry (UCT)

Title of Thesis: Probing the HIV reverse transcriptase enzyme with novel bifunctional HIV-1 RT inhibitors of the general formula NRTI-spacer-NNRTI.

Chapter 1	Examiner	Recommendation	Action
1	CM1	P2 - spelling 'everyday'	corrected to 'every day'
		P5 - typo '400'	corrected to '400/'
		P6 - citation required for Fig. 1.5	corrected and cited reference 18
		P8 - mention fuzeon, raltegravir, maraviroc	corrected and included on P8
		P8 - 'nucleotides' to 'ANP'	corrected to acyclic nucleoside phosphonate
		P9 - mention RT in list	corrected and RT listed
		P10 - show stereochemistry of 3TC	ignored - stereochemistry correctly shown (Fig. 1.8)
		P10 - PI's worse for lipid disfunction	corrected - D4T changed to PI's and rephrased
		P11 - add 'viral replication' at end	corrected - viral replication added
		P11 - for AZT 2nd step rate limiting	corrected - 1st to 2nd step and rephrased
		P11 - esterase should read phosphatase	corrected - reads phosphatase
		P14 - preface by 'in most cases'	corrected - preface added
		P14 - *Cyclo* SAL mis-drawn	corrected - change one benzyl to phenyl phosphate
		P16 - phosphorylases to phosphatases	corrected - reads phosphatases
		P16 - carboxyesterase to enzymatic	corrected - reads enzymatic
		P17 - carboxylate to carboxyl	corrected - reads carboxyl
		P18 - 'OH-' is oddly drawn	corrected - redrawn and adjusted Fig. 1.15
		P19 - replace arrows (Fig. 1.16a)	corrected - solid arrows replaced by dotted arrows
		P21 - english unclear	corrected - rephrased english
		P23 - TSAO derivative oddly named	corrected - renamed to TSAO-N3Me
		P24 - use different arrow	ignored - is non-synthetic arrow
		P25 - change 'fold resistance' in header	corrected - header changed in Table 1.2
		P30 - say 'further studies', not toxicology	corrected - changed 'toxicology studies' to further...
		P32 - enormously crucial an overstatement	corrected - rephrased to just crucial
		P38 - add 'phosphorylated' after 'released'	corrected - phosphorylated added
		P39 - check stereochemistries	checked and correct
		P40 - add number of approved drugs/step	ignored - mentioned in other parts of this thesis
		P41 - rephrase 'considerable boost'	corrected - changed to simply 'boost'
		P41 - rephrase 'remarkable' to significant	corrected - changed to significant
		P48 - Isnt simultaneous binding the goal?	ignored - wording is OK as it corcerns a hypothesis
		P49 - give AZT data	corrected and data included (AZT = 6 nM)
	DC	P53 - paragraph needs reference	corrected - reference 132 cited

Examiner legend: Prof Chris McGuigan (CM1); Prof Chris Meier (CM2); Prof David Chu (DC)

Chapter 1	Examiner	Recommendation	Action
2	CM1	P60 - 'lead pass' unclear	corrected - lead past
		P61 - BVDU of 'limited' clinical use	corrected - added 'limited' to sentence
		P67 - spelling 'aas'	corrected - 'aas' to 'as'
		P76 - explain 'crystal argon'	corrected - high purity argon gas (> 99%)
		P77 - show thio attempts	ignored - mentioned in text
		P79 - 'is' to 'maybe' ; 'also' to 'may'	corrected as recommended
		P79 - comment on 100x reduction of 100	ignored - rationale requires a more in depth study
			with modelling. Sentence rephrased.
	DC	P77 - check if compound 102 correct	checked and correct
		P78 - correct last sentence	ignored - no errors found
		P83 - compound 104 missing	ignored - cmpd 104 is pentanediol on P81 (Sch 2.12)
		P91 - activity of 113 written somewhere?	corrected - noted 'no activity' on P92
		P92 - is compound 112 correct?	checked and correct as is
3	CM1	P96 - insert 'protected' before '5'-iodo	corrected - changed to 'protected 5'-iodo…'
		P100 - level of spectroscopic detail?	ignored - details required for proof of success
		P117 - elaborate on phosphorylation?	corrected and elaborated on P117
4	CM1/CM2	P146 - explain choice of isopropyl phosph-	corrected - prototype explained on P140
		ate protection?	
	CM1/CM2	P151 - proof of synergy?	corrected and worded accordingly on P151-152

Note: Professor Chris Meier's comments were noted and are highly appreciated. The comments were taken into account and were in sync with comments and corrections made for Professor Chris McGuigan. All comments were useful and will contribute to future publications.

Examiner legend: Prof Chris McGuigan (CM1); Prof Chris Meier (CM2); Prof David Chu (DC)